LEABHARLANN CHOLÁISTE NA TRÍONÓIDE, BAILE ÁTHA CLIATH | TRINITY COLLEGE LIBRARY DUBLIN
Ollscoil Átha Cliath | The University of Dublin

Terms and Conditions of Use of Digitised Theses from Trinity College Library Dublin

Copyright statement

All material supplied by Trinity College Library is protected by copyright (under the Copyright and Related Rights Act, 2000 as amended) and other relevant Intellectual Property Rights. By accessing and using a Digitised Thesis from Trinity College Library you acknowledge that all Intellectual Property Rights in any Works supplied are the sole and exclusive property of the copyright and/or other IPR holder. Specific copyright holders may not be explicitly identified. Use of materials from other sources within a thesis should not be construed as a claim over them.

A non-exclusive, non-transferable licence is hereby granted to those using or reproducing, in whole or in part, the material for valid purposes, providing the copyright owners are acknowledged using the normal conventions. Where specific permission to use material is required, this is identified and such permission must be sought from the copyright holder or agency cited.

Liability statement

By using a Digitised Thesis, I accept that Trinity College Dublin bears no legal responsibility for the accuracy, legality or comprehensiveness of materials contained within the thesis, and that Trinity College Dublin accepts no liability for indirect, consequential, or incidental, damages or losses arising from use of the thesis for whatever reason. Information located in a thesis may be subject to specific use constraints, details of which may not be explicitly described. It is the responsibility of potential and actual users to be aware of such constraints and to abide by them. By making use of material from a digitised thesis, you accept these copyright and disclaimer provisions. Where it is brought to the attention of Trinity College Library that there may be a breach of copyright or other restraint, it is the policy to withdraw or take down access to a thesis while the issue is being resolved.

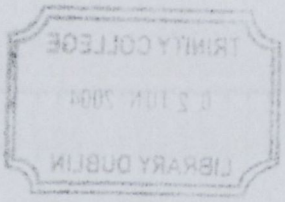
Access Agreement

By using a Digitised Thesis from Trinity College Library you are bound by the following Terms & Conditions. Please read them carefully.

I have read and I understand the following statement: All material supplied via a Digitised Thesis from Trinity College Library is protected by copyright and other intellectual property rights, and duplication or sale of all or part of any of a thesis is not permitted, except that material may be duplicated by you for your research use or for educational purposes in electronic or print form providing the copyright owners are acknowledged using the normal conventions. You must obtain permission for any other use. Electronic or print copies may not be offered, whether for sale or otherwise to anyone. This copy has been supplied on the understanding that it is copyright material and that no quotation from the thesis may be published without proper acknowledgement.

Immediate-Early-Gene (*IEG*) expression in Excitotoxicity

Thesis submitted to the
University of Dublin
for the Degree of
Doctor of Philosophy



by

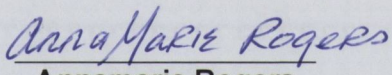
Annamarie Rogers
Department of Biochemistry
Trinity College
Dublin

August 2003

TRINITY COLLEGE
02 JUN 2004
LIBRARY DUBLIN
THOR S
~~7990~~
7520

Declaration

I certify that the work herein is entirely my own and has not been submitted for a degree at this, or any other, University. Joint experiments were described in Sections 4.2.7 and 4.2.8 of Chapter 4, where cell culture and exposure were performed at the University of St. Andrews, Scotland. The library at Trinity College, Dublin has my full permission to lend or copy this thesis upon request.



Annamarie Rogers

Acknowledgements

Firstly, I would like to thank Professor D. Clive Williams, Dr. Gabriele Schmuck, Dr. Gabriele Scholz and Dr. Dr. Ahr for their support, advice and encouragement throughout this project.

A huge thanks to Wibke Lofink for her invaluable support, for showing me the art of organisation and for just being Wibke.

I would like to thank Wolfgang "The Body" Hain for his critical interest in my work.

A special thanks goes to Tanja, Andreas and, of course my little woman, Nina, for introducing me to German beer festivals and for always making me feel at home.
Ronny, my second Mum, where would I have been without you? A special thanks.

A warm thanks goes to Jutta for her "concentration drops" and for the many acupuncture treatments.

Thanks to Daniela, Melanie, Hoai Son Tran, Ellen, Stefan and Doris for keeping up my spirits and for always making me laugh.

A special thanks goes to my Irish supporters, Aurdo, Joanne, Fiona (Noni), the Morris family, Aine and Daragh.

Thanks also to Dr. Peter and Erika Andrews for putting up with me for 4 years and for treating me like one of the family. I shall never forget the lovely summers in Gellertweg 2.

Most importantly, I would like to thank Mam, Dad, Alan, Jonathan, Brendan and Breda for always being there for me, for the many telephone calls and letters and for sharing the laughter and the tears.

Last but not least, I would like to thank Udi, who knows as much about *c-fos* at this stage as I do- thanks for being my rock and best friend and for either making or buying me dinner.

For Roisin

Table of Contents

Declaration 2

Acknowledgements 3

Table of Contents 5

Abbreviations 10

Abstract 14

Chapter 1 General Introduction 16

1.1 Cells of the nervous system 17

1.2 Ion channels and the action potential 19

1.3 Chemical communication of nerve cells at synapses 21

1.4 Glutamate Receptor Classification 23

1.4.1 NMDA receptors 24

1.4.2 Non-NMDA (Kainate and AMPA) receptors 26

1.4.3 Metabotropic receptors 27

1.5 Neurotransmitters 29

1.5.1 The role of the Type I neurotransmitters, Glu and Asp, in the CNS 29

1.6 Antagonists of the ionotropic Glu receptors 31

1.6.1 Antagonists of the NMDA subtype of Glu receptor 31

1.6.2 Antagonists of the KA and AMPA receptors 33

1.7 Excitotoxicity 33

1.7.1 Role of Ca^{2+} in Excitotoxicity 35

1.7.2 Role of Mitochondria in Excitotoxicity 37

1.8 *Immediate early genes* (*IEGs*) 39

1.8.1 What are oncogenes? 40

1.8.2 Induction of *immediate early genes* (*IEGs*) 41

1.9 Interaction between Fos and Jun 46

1.10 Regulation of immediate-early response in PC12 pheochromocytoma cells 48

1.11 Neurophysiological correlates of *IEG* induction 50

1.11.1 Ischaemic Cerebral cell death 50

1.11.2 Seizures 52

1.11.3 Kindling 53

1.11.4 Long-term potentiation 54
1.12 EAA induced *c-fos* expression is NMDA receptor mediated 54
1.13 Role for *c-fos* in excitotoxicity ? 55
1.14 Role for *fosB* in excitotoxicity ? 57
1.15 Is excitotoxic cell death apoptotic or necrotic? 58

Chapter 2 Materials and Methods 65

2.1 Materials 66
2.2 Primary neuronal cell culture 71
2.2.1 Preparation of primary cultures of mouse cerebellar granule cells (mCGCs) 71
2.2.2 Preparation of primary cultures of rat cortical neurons 72
2.3 Growth and treatment of permanent NIH 3T3 mouse fibroblasts 73
2.4 Neurotoxicity assays 73
2.4.1 MTT assay 73
2.4.2 Measurement of mitochondrial membrane potential ($\Delta\psi_m$) 74
2.4.3 ATP determination 75
2.4.4 Morphological observation of the neurons using the Giemsa stain 76
2.5 Isolation of total RNA from animal cells 76
2.5.1 Isolation of total RNA from primary cells with a Qiagen RNeasy 96 Kit 76
2.5.2 Isolation of total RNA from a mouse cell line with a Qiagen RNeasy Midi Kit 77
2.6 Quantitation and quality control of total RNA isolated from animal cells 78
2.6.1 Preparation of an RNA Standard curve 78
2.6.2 Total RNA quantitation 79
2.6.3 Quality control of total RNA isolated from animal cells 81
2.7 Reverse Transcription 81
2.8 Primer design 84
2.9 Real-time quantitative RT-PCR using SYBR® Green 84
2.10 RT-PCR data analysis using the Comparative CT method 88
2.11 Optimisation of primer concentrations using RT-PCR and SYBR® Green 90
2.12 Polymerase Chain Reaction (PCR) for primer control 91
2.13 Agarose gel electrophoresis and Ethidium Bromide staining 92
2.14 Preparation of an 18S standard curve for RT-PCR 92
2.15 Dissociation Curve 95

2.16 Relative Efficiency of Target and Reference 96

2.17 Gene Expression using Affymetrix GeneChip® Technology 98

2.17.1 Overview of Affymetrix microarray technology 98
2.17.2 First strand cDNA synthesis 99
2.17.3 Synthesis of double-stranded cDNA 99
2.17.4 Purification of the double-stranded cDNA 100
2.17.5 Synthesis of Biotin-Labeled cRNA 101
2.17.6 Purification of cRNA using an RNeasy Mini Kit 101
2.17.7 Precipitation of purified cRNA 102
2.17.8 Measurement of cRNA 102
2.17.9 Fragmentation of cRNA 103
2.17.10 Hybridisation of the cRNA samples onto the Affymetrix GeneChip® arrays 103
2.17.11 Washing and Staining of Affymetrix arrays 104
2.17.12 Data Analysis 106

Chapter 3 Characterisation of Two Different *In Vitro* Models for Excitotoxic Investigations 108

3.1 Introduction 109

3.2 Results 115

3.2.1 Concentration- and time-dependence of neuronal viability after EAA treatment 115
3.2.2 EAA-induced neurotoxicity in mCGCs is mediated through the NMDA receptor subtype of Glu receptors 121
3.2.3 Rapid reduction of intracellular ATP levels in mCGCs following EAA treatment 126
3.2.4 EAA-induced decreases in intracellular ATP levels of mCGCs are NMDA receptor mediated 131
3.2.5 Development of a primary cell culture system of rat cortical neurons 136
3.2.6 Rat cortical neurons develop increased EAA sensitivity in culture 139
3.2.7 Intracellular ATP concentrations as a measure of toxicity 144
3.2.8 Time-dependence of EAA-induced neurotoxicity in mature rat cortical neurons 151
3.2.9 EAA induced loss of mitochondrial membrane potential ($\Delta\psi_m$) in rat cortical neurons .. 157

3.3 Discussion 164

Chapter 4 Expression of Excitatory Amino Acid induced *IEGs* in Mouse Cerebellar Granule Cells. 169

4.1 Introduction 170

4.2 Results 177

4.2.1 Optimisation of *fos* and *jun* primers for RT-PCR gene expression analysis 177

4.2.2 *c-fos* expression profiles vary with time and Glu concentration 182

4.2.3 NMDA receptor specificity of Glu-induced *c-fos* mRNA expression 184

4.2.4 Asp changes *c-fos* mRNA expression in a time- and concentration-dependent manner 188

4.2.5 Receptor-specificity of Asp-induced changes in *c-fos* expression 188

4.2.6 Neither Ala nor paraquat induced *c-fos* expression in mature mCGCs 189

4.2.7 Can "toxicity-related" *c-fos* mRNA expression be used to predict excitotoxic properties of compounds? 196

4.2.8 Screening experiment using the original protocol 197

4.2.9 Screening experiment using a modified antagonist protocol in the *c-fos* assay ($Q^{240/30}$) test 202

4.2.10 Single laboratory experiments using the original protocol ! 206

4.2.11 *fosB* expression profiles vary with time and Glu concentration 208

4.2.12 NMDA receptor specificity of Glu-induced *fosB* mRNA expression 210

4.2.13 *FosB* expression profiles vary with Asp concentration 214

4.2.14 NMDA receptor specificity of Asp-induced *fosB* mRNA expression 216

4.2.15 Neither Ala nor paraquat induced *fosB* expression in mature mCGCs 216

4.2.16 *fra-1, fra-2* and 3 members of the *jun* family of *IEGs* are unaffected by EAAs 222

4.3 Discussion 237

Chapter 5 Expression of *IEGs* in Rat Cortical Neurons. 248

5.1 Introduction 249

5.2 Results 252

5.2.1 *c-fos* mRNA expression varies with time and Glu concentration 252

5.2.2 NMDA receptor specificity of Glu-induced *c-fos* mRNA expression 255

5.2.3 Asp induced changes in *c-fos* expression are time and concentration-dependent 259

5.2.4 Asp-induced *c-fos* mRNA expression is NMDA receptor specific 261

5.2.5 Neither Ala nor paraquat induce *c-fos* expression in primary rat cortical neurons 267

5.2.6 Changes in *fosB* expression are dependent on time and Glu concentration 267

5.2.7 NMDA receptor specificity of Glu-induced *fosB* mRNA expression 268

5.2.8 Changes in *fosB* expression as a function of time and Asp concentration 274

5.2.9 NMDA receptor specificity of Asp-induced *fosB* mRNA expression 275

5.2.10 Neither Ala nor paraquat induce *fosB* expression in rat cortical neurons 277

5.2.11 Assessment of the potential of *c-fos* and *fosB* as screens for excitotoxicity 283

5.2.12 Analysis of the effects of a wide range of compounds on *c-fos* expression 284

5.2.13 Analysis of the effects of a range of compounds on *fosB* expression 287
5.2.14 Effects of the excitotoxin, Glu, on the expression of other members of the *fos* and *jun* families of *IEGs* 288
5.3 Discussion 296

Chapter 6 Gene Expression Profiling: Potential markers for Excitotoxicity in two different *In Vitro* Models 302

6.1 Introduction 303
6.2 Results 311
6.2.1 Comparative analysis of hybridised mouse GeneChip® arrays 311
6.2.2 Glu induced changes in gene expression on mouse arrays 312
6.2.3 Several genes share the same expression profiles as *c-fos*, *fosB* and ATF3 319
6.2.4 K-Means cluster analysis of the 76 deregulated genes from the mouse arrays 329
6.2.5 Tile display of the 76 deregulated genes following K-means clustering 330
6.2.6 Analysis of micro-array data from rat cortical neurons treated with Glu 339
6.2.7 Gene expression changes in Glu stimulated rat cortical neurons 341
6.2.8 Search for genes with similar expression profiles to *c-fos*, *junB* and ATF3 346
6.2.9 K-Means cluster analysis of the 73 deregulated genes from the rat arrays 354
6.3 Discussion 363

Chapter 7 Concluding Remarks 375

References

Abbreviations

$1_{SR},3_{RS}$-ACPD	1-aminocyclopentane-1,3-dicarboxylic acid
5-HT	5-hydroxytryptamine
Ach	Acetylcholine
Acryl	Acrylamide
AD	Afterdischarge
ADP	Adenosine diphosphate
Affx	Affymetrix
AIDS	Acquired immunodeficiency syndrome
Ala	Alanine
AMPA	(RS)-α-amino-3-hydroxy-5-methyl-isoxazole-4-propionic acid
AP-1	Activator protein-1
AP5	D,L (±)-2-amino-5-phosphonopentanoic acid
AP7	D,L (±)-2-amino-7-phosphonoheptanoic acid
Asp	Aspartate
ASV-17	Avian sarcoma virus 17
ATF	Activating transcription factor
ATP	Adenosine triphosphate
(-)-Bicuc	(-)-Bicuculline
BSA	Bovine serum albumin
cAMP	Cyclic adenosine monophosphate
$[Ca^{2+}]_I$	Calcium ion concentration
$[Ca^{2+}]_R$	Resting internal calcium ion concentration
cDNA	Complementary DNA
CGCs	Cerebellar granule cells
cGMP	Cyclic guanosine monophosphate
CNQX	6-cyano-7-nitroquinoxaline-2,3-dione
CNS	Central nervous system
CPP	3-((±-2-carboxypiperazin-4-yl)-propyl-1-phosphonic acid
CRE	Calcium response element
C_T	Threshold cycle
CTF	Constitutive transcription factor
DAG	Diacylglycerol

D-HCA	D-Homocysteate
D-HCSA	D-Homocysteine sulphinate
DIV	Days *in vitro*
DMEM	Dulbecco's modified Eagle's medium
DMSO	Dimethyl sulphoxide
DNA	Deoxyribonucleic acid
DNQX	6,7-dinitroquinoxaline-2,3-dione
DSE	Dyad symmetry element
EAA	Excitatory amino acid
ECS	Electroconvulsive seizures
EGF	Epidermal growth factor
Em	Emission
EPSPs	Excitatory postsynaptic potentials
ESTs	Expressed sequence tags
Ex	Excitation
FBJ-MSV	Finkel-Biskis-Jinkins murine osteogenic sarcoma virus
FCS	Foetal calf serum
For	Forward
GABA	Gamma-amino-butyric acid
GDEE	Glutamic acid diethylester
GITC	Guanidine isothiocyanate
Glu	Glutamate
GluR	Glutamate receptor
G-proteins	GTP-binding proteins
HRP	High ratio proportion analysis
ID	Identification label
IEGs	*Immediate early genes*
IP_3	Inositol triphosphate
IPSPs	Inhibitory postsynaptic potentials
KA	Kainic acid
KCl	Potassium chloride
KDa	Kilodalton
KRE	Krox response elements
L-AP4	L-(+)-2-Amino-4-phosphonobutyric acid

L-CSA	L-Cysteine sulphinate
L-HCA	L-Homocysteate
L-HCSA	L-Homocysteine sulphinate
Lind	Lindane
L-SSC	*S*-Sulpho-L-cysteine
LTD	Long term depression
LTP	Long term potentiation
MAS5	Microarray Suite Version 5 of Affymetrix
MCGCs	Mouse cerebellar granule cells
$MgSO_4$	Magnesium sulphate
MGluR	Metabotropic glutamate receptors
min	Minute
MK-801	Dibenzocycloheptenеimine
mM	Millimolar
MM	Mismatch
MPP^+ Iodide	1-methyl-4-phenylpyridinium Iodide
MTT	3-[4,5-dimethylthiazol-2-yl]-2,5-diphenyltetrazolium bromide
mV	Millivolts
NaCN	Sodium cyanide
$NaHCO_3$	Sodium-hydrogencarbonate
NBQX	2,3-dihydroxy-6-nitro-7-sulfamoyl-benzo(F)quinoxaline
Neg	Negative
NGF	Nerve growth factor
Nimodip	Nimodipine
nM	Nanomolar
NMDA	N-Methyl-D-Aspartic acid
NR	NMDA receptor
NTC	Non-template control
PCP	Phencyclidine
PCR	Polymerase chain reaction
PDGF	Platelet-derived growth factor
PIP_2	L-3-phosphatidylmyoinositol-4,5-bisphosphate
PKA	Protein kinase A
PKC	Protein kinase C

PLC	Phospholipase C
PM	Perfect match
PNS	Peripheral nervous system
Pos	Positive
PTP	Permeability transition pore
PTZ	Pentylenetetrazole
QA	Quisqualic acid
Rev	Reverse
RNA	Ribonucleic acid
ROS	Reactive oxygen species
Rpm	Rounds per minute
RT	Reverse transcriptase
RT-PCR	Reverse transcription polymerase chain reaction
SAGE	Serial analysis of gene expression
SAPE	R-phycoerythrin streptavidin
s.d.	Standard deviation
SIE	c-Sis inducible element
SRE	Serum response element
SRF	Serum response factor
Tau	Taurine
TCP	N-[1-(1-thienyl-cyclohexyl)] piperidine
TE buffer	Tris/EDTA buffer
TF	Transcription factors
TG	(RS)-(Tetrazol-5-yl) glycine
TPA	12-*o*-tetradecanoylphorbol-13-ester
TRE	TPA-responsive elemnt
VSCC	Voltage-sensitive Ca^{2+} channels
UV	Ultra violet
Verat	Veratridine
Vpate	Valproate
$\Delta\psi_m$	Mitochondrial membrane potential
µM	Micromolar

Abstract

The mouse cerebellar granule cell system (mCGCs; Schousboe *et al.,* 1989) was established in this laboratory (Bayer AG, Germany) as a suitable cell culture model for excitotoxicity studies. Suitability was confirmed by MTT-based cytotoxicity, which was induced by glutamate (Glu) receptor agonists and inhibited by NMDA receptor antagonists (AP5), but not by antagonists of the non-NMDA receptor subtype (CNQX).

A rat cortical neuronal culture system, developed by Schmuck and Schlüter (1996), was established as an additional *in vitro* model for excitotoxic investigations. Its suitability for studying excitotoxicity was demonstrated by showing Glu receptor agonist induced cytotoxicity, which could be blocked by AP5 but not by CNQX. This excitotoxicity was dependent on the length of time the cells had been maintained in culture, presumably due to the time required for cells to express functional NMDA receptors. In contrast, paraquat sensitivity was not time-dependent, as expected for a Glu receptor–independent toxicity mechanism.

Primers were designed and shown by PCR to be suitable for examining mouse and rat *c-fos* mRNA expression. Additionally, primers were designed for the other members of the *fos* (*fosB*, *fra-1* and *fra-2*) and *jun* (*c-jun*, *junB* and *junD*) families of *immediate early genes* (*IEGs*). Quantitative, real-time RT-PCR measurements were made using a comparative C_T method in order to investigate the levels of *fos* and *jun* mRNAs as one measure of the expression of their respective protein products. The expression values of all genes measured were normalised to an internal control, 18S, prior to calculation of the fold induction values of all genes relative to the untreated, time matched controls.

For mCGCs, exposure to excitotoxic concentrations of Glu and aspartate (Asp) led to a changed time profile for mRNA expression, from a transient *c-fos* expression at 15 - 30 min to a delayed, elevated and sustained expression at later time-points. The results showed that the elevated and sustained expression of *c-fos* mRNA, induced by excitotoxic concentrations of Glu or Asp, was prevented by selective antagonism of the NMDA receptor but not of the AMPA/kainate receptor demonstrating that *c-fos* induction was mediated through the specific activation of the NMDA receptor subtype in mCGCs. The non-toxic compound alanine, or the toxic compound paraquat, did not induce *c-fos* mRNA expression.

The question as to whether *c-fos* expression changes could be used to predict excitotoxicity was addressed by testing the *c-fos* response of the cultures to several compounds at low (and therefore non-toxic) and high (toxic) concentrations at two suitable

time-points of exposure (30 and 240 min), in the presence and absence of NMDA and non-NMDA Glu receptor antagonists. The results suggested that the assay of delayed, elevated and sustained *c-fos* expression could be used to screen for excitotoxins at a reasonable throughput but that the test was not fully robust due to some variability in *c-fos* expression, responses to compounds and receptor antagonism.

Treatment of mCGCs with Glu and Asp at toxic concentrations led to concentration-dependent changes in the expression levels of *fosB* and slight increases in *fra-2*, but not *fra-1*, *c-jun*, *junB* or *junD*. This changed profile again appeared as a delayed, elevated and sustained expression. In addition, the levels of sustained *fosB* induction were much higher under excitotoxic conditions when compared to *c-fos*. The elevated and sustained expression of *fosB* mRNA, induced by toxic concentrations of Glu or Asp, was prevented by selective antagonism of the NMDA receptor but not of the non-NMDA receptors, showing that *fosB* expression was mediated by activation of the NMDA receptor subtype in mCGCs. For rat cortical neurons, exposure to excitatory amino acids at high, toxic concentrations showed a change in the *c-fos* mRNA expression profile to sustained elevated levels, with the increased levels being much higher than in the mCGCs. For the expression of the variants, there was increased, sustained expression of *fosB* and also to a lower extent, *fra-2*. The profile of *fosB* expression following treatment with excitotoxins showed a biphasic response, which was different to the response observed in mCGCs. Both *c-fos* and *fosB* expression, under excitotoxic conditions, were inhibited by AP5 but not CNQX.

As the rat is the preferred species in toxicological investigations, the rat cortical cell model was compared to the mCGC model, using *c-fos* and *fosB* mRNA expression, for suitability in prediction of the excitotoxic potential of chemicals by testing low and high concentrations of compounds at a single time-point of exposure, a method allowed by the high levels of expression of *c-fos* and *fosB* under excitotoxic conditions. It was concluded that both *c-fos* and *fosB* can be used as molecular biomarkers to predict the excitotoxic properties of compounds, despite both *IEGs* exhibiting different patterns of induction.

Altered gene expression in both culture systems was also measured using DNA micro-array methodology, confirming results from RT-PCR. The induction of several genes were found to be affected by excitotoxins in mouse (95 genes) and rat (73 genes). In particular, it was found that *c-fos*, *fosB* and ATF3 were up-regulated in mCGCs under excitotoxic conditions, while in the rat cortical system, *c-fos, junB* and ATF3 were up-regulated under excitotoxic conditions.

Chapter 1

General Introduction

1.1 Cells of the nervous system

The vertebrate nervous system comprises the *central nervous system* or *CNS* (that is, the brain together with the spinal cord; see Figure 1.1), and the *peripheral nervous system* or *PNS*, which relays impulses to and from the rest of the body.

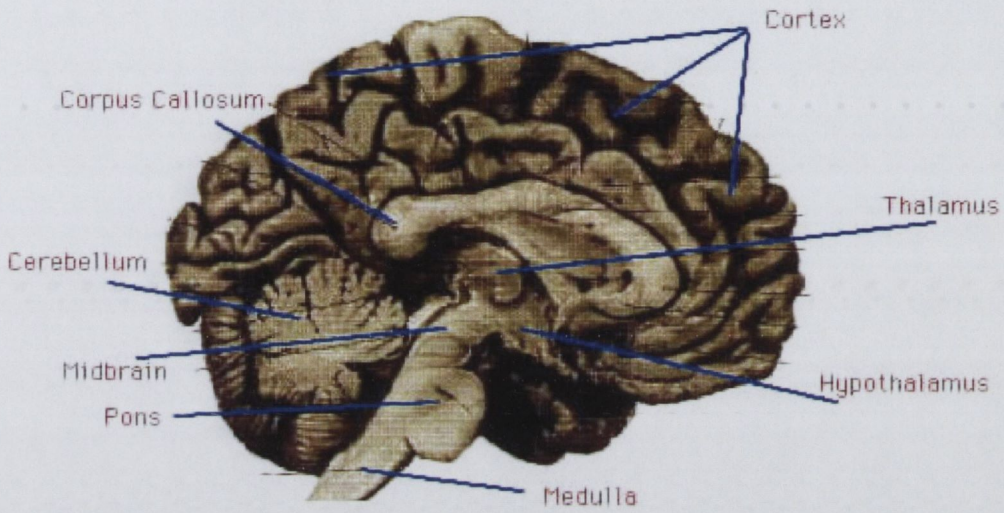


Figure 1.1: Illustration of the different regions of the brain
(Image taken from **ifcsun1.ifisiol.unam.mx/ Brain/nervsys.htm)**

Nervous tissue contains neurons (nerve cells) which are responsible for information transfer and processing, and glia, which are 10 times more numerous than neurons and whose diverse functions include transmitter and metabolite supply, support, insulation, axonal guidance during development and regulation of the ionic environment of the neurons. One of the unique characteristics of the nervous system is the capacity of nerve cells to communicate with each other and with other cells. In the 19th century, a controversy developed concerning how nerve cells interconnect and intercommunicate. The "reticular theory" suggested that there was a protoplasmic continuity between various nervous elements. A noted Spanish neuroanatomist, Santiago Ramon y Cajal (1852-1934), first proposed that nerve cells are contiguous but not continuous. In Cajal's "neuron theory" nerve cells were anatomical entities forming intercommunicating networks. After the birth of the neuron theory, modern techniques continued to verify that the central nervous system is composed of a variety of nerve cells and supporting glial elements. The nerve cells intercommunicate with each other via multiple processes and synaptic contacts.

The essential task of the neuron is to receive, conduct and transmit signals. Each neuron consists of a *cell body* or *soma* (containing the nucleus) from which a number of long, thin processes radiate outward. Usually there is one long axon, to conduct signals away from the cell body toward distant targets, and several shorter branching dendrites, which extend from the cell body like antennae and provide an enlarged surface area to receive signals from the axons of other nerve cells. Signals are also received on the cell body itself. The axon commonly divides at its far end into many branches and so can pass on its message to many target cells simultaneously. Likewise, the extent of branching of the dendrites can be very great - in some cases sufficient to receive as many as 100,000 inputs on a single neuron.

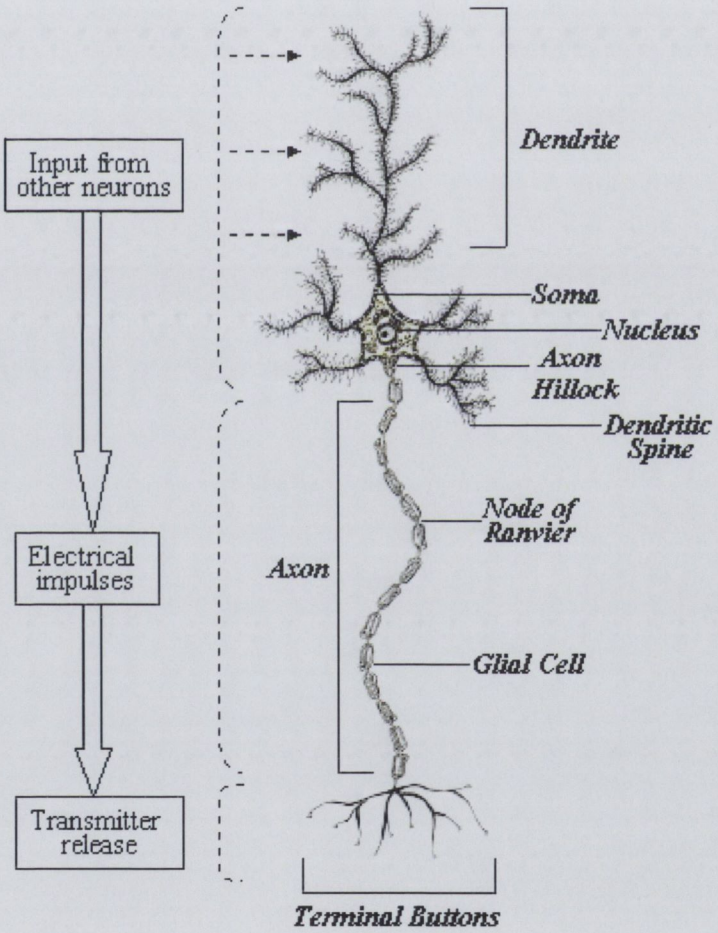


Figure 1.2: Illustration of a neuron

(Modified image taken from www-users.york.ac.uk/~scf104/ neuralmusic/neuron-work.html)

The significance of the signals carried by a neuron depends on the part played by the individual cell in the functioning of the nervous system as a whole. For example, in a *motor neuron* the signals represent commands for the contraction of a particular muscle, whereas, in a *sensory neuron* they represent the information that a specific type of stimulus, such as light or a chemical substance, is present at a certain site in the body. Despite the varied significance of the signals, their form is the same, consisting of changes in the electrical potential across the neurons plasma membrane. Communication occurs because an electrical disturbance produced in one part of the cell spreads to other parts. Such a disturbance becomes weaker with increasing distance from its source unless energy is expended to amplify it as it travels. Over small distances neurons can conduct their signals passively. However, larger neurons require an active signalling mechanism that involves the automatic amplification of the electrical signal and enables its propagation along the neuron's plasma membrane. This travelling wave of electrical excitation, known as an action potential or nerve impulse, can carry a message without attenuation from one end of a neuron to the other.

1.2 Ion channels and the action potential

An excess of positive charge on one side and a matching excess of negative charge on the other create the voltage gradient across the cell membrane, or membrane potential. Charge is traversed across the nerve cell membrane by small inorganic ions – sodium (Na^+), potassium (K^+), chloride (Cl^-) and calcium (Ca^{2+}) ions, that cross the lipid bilayer by passing through selective ion channels formed by specific transmembrane proteins. When the ion channels open or close, the charge distribution shifts and the membrane potential changes. Neuronal signalling thus depends on channels whose permeability is regulated – so-called "ion gated channels". Two classes of gated channels are of crucial importance: (a) voltage-gated channels (especially Na^+ channels) play a key role in the explosions of electrical activity by which action potentials are propagated along an axon, and (b) ligand-gated channels, which convert extracellular chemical signals into electrical signals.

When an axon is in the resting state, the membrane potential is uniformly negative, with the interior of the axon having a negative potential. An action potential is triggered when the membrane is momentarily depolarised beyond a certain threshold value. Such a depolarisation causes Na^+ channels to open, permitting an influx of Na^+ down its electrochemical gradient, which causes still further depolarisation and opening of Na^+ channels in a self-amplifying manner until the membrane reaches the Na^+ equilibrium

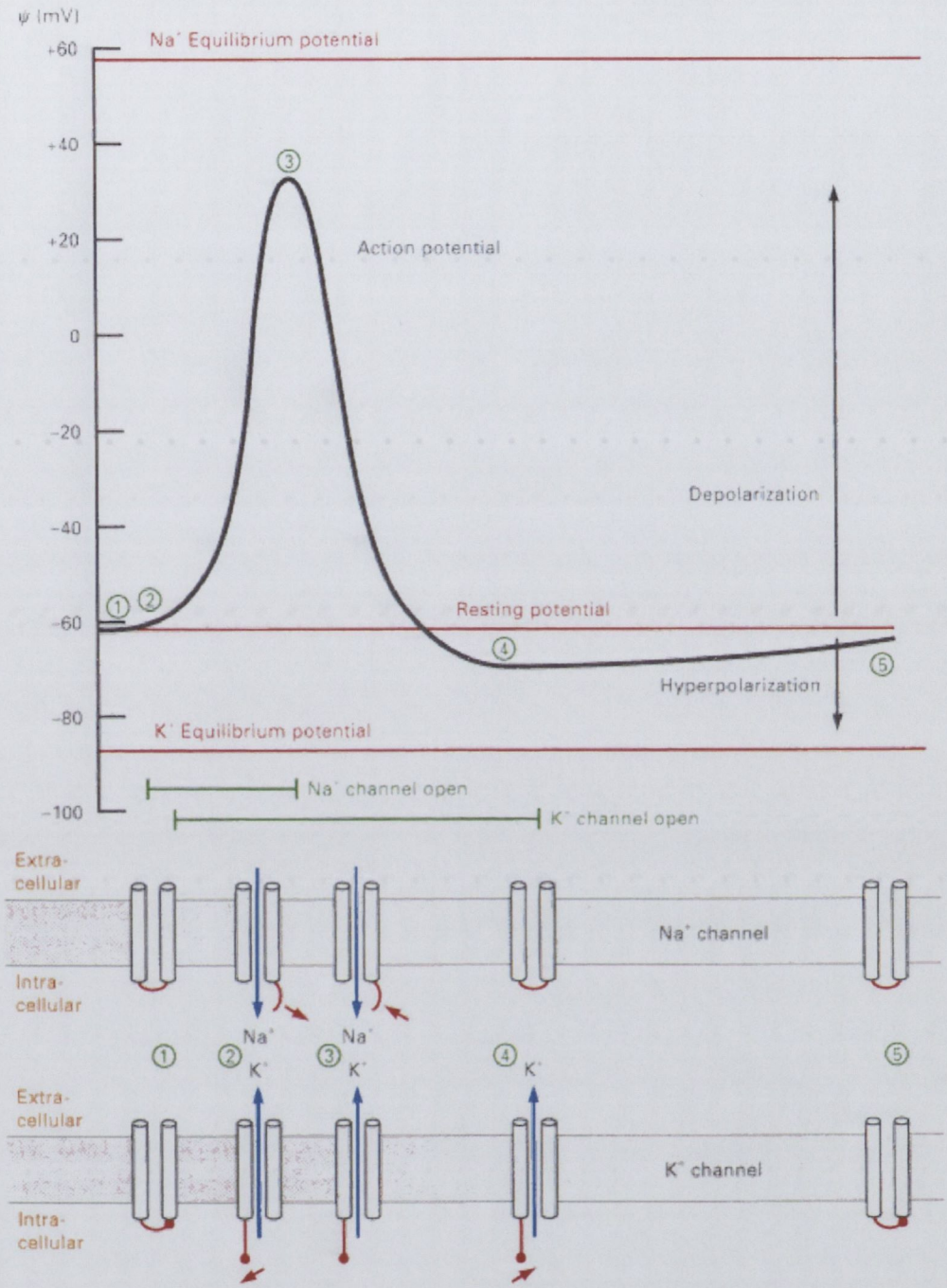


Figure 1.3: Neuronal action potential

When an axon is in the resting state, the membrane potential is uniformly negative. (1). An intra- or extracellular signal causes the Na^+ and K^+ channels to open. (2). The initial influx of Na^+ depolarises the membrane and triggers an action potential (depolarisation). (3) Simultaneously, Na^+ channels close and an efflux of K^+ occurs. (4) The Na^+ influx is overwhelmed by the efflux of K^+ (hyperpolarisation) and the membrane returns to its original negative potential.

potential that is, a positive membrane potential of +30-50 mV. On reaching the Na^+ equilibrium potential, two factors conspire to return the membrane to its original negative potential: the Na^+ channels spontaneously convert to a closed inactivated state while K^+ ions are pumped out of the cell (repolarisation). Once the K^+ channels are open, the Na^+ influx is overwhelmed by an efflux of K^+ and the membrane returns to its original negative potential. The repolarisation causes the K^+ channels to close again and allows the inactivated Na^+ channels to regain their original closed but activatable state. In this way, the membrane is prepared to fire another action potential in less than a millisecond. The action potential is propagated along the axon by the opening and closing of Na^+ channels until it reaches the chemical synapse where it opens voltage-gated Ca^{2+} channels, allowing an influx of Ca^{2+} to trigger the exocytic release of neurotransmitter from synaptic vesicles at a rate that increases rapidly with the free Ca^{2+} concentration. The neurotransmitter then diffuses across the synaptic cleft and binds to receptor proteins in the membrane of the post-synaptic cell. The increase of free Ca^{2+} concentration is short-lived because Ca^{2+}-binding proteins, Ca^{2+}-sequestering vesicles, and mitochondria rapidly take up the Ca^{2+} that has entered the axon terminal, while Ca^{2+} pumps in the plasma membrane, driven either by adenosine triphosphate (ATP) hydrolysis or by the Na^+ electrochemical gradient, pump it out of the cell.

1.3 Chemical communication of nerve cells at synapses

Neuronal signals are transmitted from cell to cell at specialised sites of contact known as synapses. At the end of each axon branch of the pre-synaptic neuron is a nerve terminal from which a chemical, known as a neurotransmitter, is released in response to Ca^{2+} entry triggered by the arrival of the action potential; some classes of neurons also release neurotransmitter from a series of swellings, known as varicosities or boutons, spaced along the branched axon. Most release of neurotransmitter occurs into the narrow synaptic cleft, which separates the pre-synaptic nerve terminal from the receptors present on the postsynaptic membrane of the subsequent neuron. The pre-synaptic membrane, synaptic cleft and post-synaptic membrane, together make up the synapse (see Figure 1.4).

After its release, the neurotransmitter has 3 possibilities. It can (a) diffuse away from the synapse and enter the circulation, (b) be actively removed from the cleft by uptake processes or (c) interact with neurotransmitter receptors.

The structure of synapses minimises the diffusion of the transmitter from the cleft under normal circumstances. This makes transmission more efficient by containing the transmitter within the limited area of the synaptic contact. The second general mechanism involves the active removal of the neurotransmitter by uptake processes located in both the pre-synaptic and post-synaptic cell membranes. Glutamate (Glu) and gamma-amino-butyric acid (GABA) are examples of neurotransmitters actively removed by an uptake process. The third fate of the neurotransmitter is to diffuse across the synaptic cleft and interact with various receptors on the post-synaptic membrane of the effector cell. The receptor is a transmembrane protein that has on its extracellular surface a selective binding site for the neurotransmitter. The binding energy of the neurotransmitter with the receptor is translated into a conformational change of the receptor. The conformational change brings about the transmembrane signalling of the information that was originally contained in the action potential of the pre-synaptic nerve.

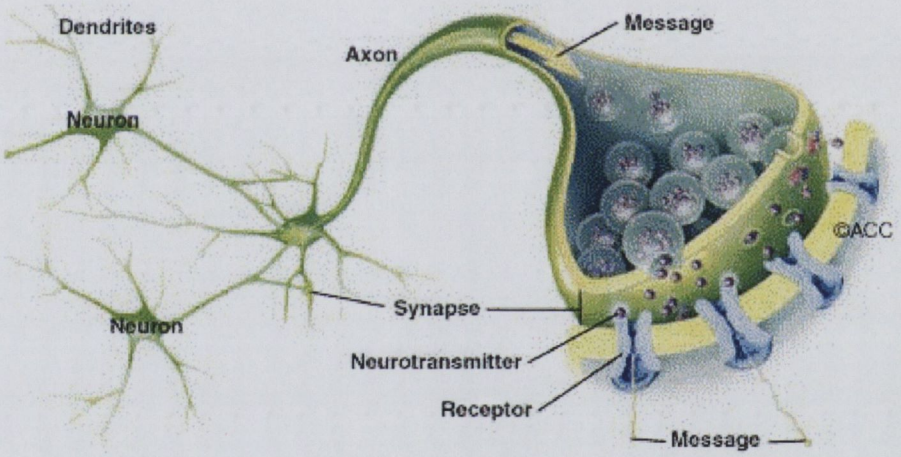


Figure 1.4: Neurons communicate with each other across a synapse

Incoming messages from the dendrites are passed to the axon where the nerve cell is stimulated to release neurotransmitters into the synapse. The neighbouring nerve cell receptors pick up these chemical messengers and effectively transmit the messages to other neighbouring nerve cells (modified image taken from **www.mayfieldclinic.com/PE/PE-PD.HTM**).

1.4 Glutamate Receptor Classification

Glu is the principal endogenous excitatory neurotransmitter in the mammalian CNS, subserving post-synaptic excitatory responses in many neuronal efferent systems. When glutamatergic terminals are depolarised, vesicular Glu is released into the synaptic cleft in a Ca^{2+}-dependent manner. Normally, this is triggered by action potential invasion of the pre-synaptic terminal with consequent depolarisation and influx of Ca^{2+} through non-inactivating voltage-sensitive Ca^{2+}-channels. Once released into the synaptic cleft, Glu interacts with several distinct families of receptors located principally on post-synaptic membranes.

The excitatory action of Glu is exerted via membrane receptors belonging to several subtypes. On the basis of pharmacological and electrophysiological studies, at least two distinct groups of receptors exist based on their signal transduction pathways: ionotropic and metabotropic receptors. The ionotropic excitatory amino acid (EAA) receptors are further divided into two groups, N-methyl-D-aspartate (NMDA) and non-NMDA receptors (kainate (KA) and (RS)-α-amino-3-hydroxy-5-methyl-isoxazole-4-propionic acid (AMPA)) and have been defined by the depolarising actions of selective agonists, that is, NMDA, KA and AMPA and their blockade by selective antagonists. In contrast to the ionotropic receptors, metabotropic Glu receptors (mGluR) belong to the family of receptors coupled to GTP-binding proteins (G-proteins) and have the potential to modulate a variety of intracellular events (Mac Dermott and Dale, 1987; Monaghan *et al.*, 1989). The NMDA and non-NMDA receptors (KA and AMPA) are ionotropic, opening a cation channel that allows the passage of Na^+ and K^+, thereby altering the membrane permeability. The NMDA receptor, in addition to allowing the passage of Na^+ and K^+ is a major Ca^{2+} ionophore (Mayer and Miller, 1990). This receptor differs from the other Glu receptors in being both ligand- and voltage-gated (that is, gating requires occupation of the NMDA/Glu binding site by an agonist and relief by depolarisation of the voltage-dependent Mg^{2+} block within the ion channel). The metabotropic receptors are coupled to G proteins and are linked to the activation of phospholipase C (PLC) and adenyl cyclases.

Excitatory transmission appears to involve actions mediated by one or more combinations of these receptors, even at single synapses. EAA receptors appear not only to mediate normal synaptic transmission along excitatory pathways, but also to participate in the modification of synaptic connections during development and changes in the efficacy of synaptic transmission throughout life (Kaczmarek *et al.,* 1997).

1.4.1 NMDA receptors

The NMDA receptors are believed to function as mediators of slow, Glu-mediated excitatory synaptic transmission in the CNS (Mayer and Miller, 1990). Slow, excitatory postsynaptic potentials mediated by transmitters acting at NMDA receptors are long in duration and have been recorded in a wide range of vertebrates and in many CNS areas (Dale *et al.*, 1986). These receptor ion channels have high conductances with permeability's to monovalent (Na^+ and K^+) and divalent (Ca^{2+}) cations and they desensitise relatively slowly (Mac Dermott *et al.*, 1986; Jahr and Stevens; 1987; Mayer *et al.*, 1989). NMDA receptors are heteromeric complexes formed by an NMDA receptor (NR) 1 subunit, and one or more NR 2 subunits designated NR 2 A - D (Michaelis, 1998). Their functional characteristics are determined by the receptor's specific combination of NR 1 and NR 2 A - D subunits. Desensitisation of NMDA receptors is regulated in a concentration-dependent manner by glycine, that is, the action of NMDA is selectively and dramatically potentiated by glycine (Johnson and Ascher, 1987). This was first discovered in electrophysiological studies in cultured cells, where addition of glycine was found to increase the opening probability of the NMDA-receptor associated ion channel at least 10-fold. This effect is not blocked by strychnine and is therefore distinct from the inhibitory strychnine-sensitive glycine receptor. The slow response of the NMDA receptors is thought to be as a consequence of physiological concentrations of Mg^{2+} (1 mM) present in the extracellular environment of neurons. Mayer *et al.* (1984) and Nowak *et al.* (1984) both reported that physiological concentrations of Mg^{2+} blocked ion channels linked to NMDA receptors, and that the blocking effect increased with hyperpolarisation. Thus, the three "elementary" properties of the individual cation channels opened by Glu (elementary conductance, mean open time and frequency of opening) are voltage-dependent. At membrane potentials near rest (-60 to -70 mV), the blocking action of Mg^{2+} is pronounced and progressive depolarisation produces a gradual alleviation of the channel blockade. Full activation of the NMDA receptors requires two events to occur simultaneously, that is, the removal of the Mg^{2+} blockade and the opening of the NMDA receptor channels, which allows the entry of Ca^{2+} and Na^+ into the dendritic spine. Because Mg^{2+} inhibition of the ion channels of NMDA receptors is a voltage-dependent phenomenon, the rapid activation of KA and/or AMPA receptors by Glu released into the synaptic cleft and the subsequent depolarisation of the postsynaptic membrane diminishes the inhibition of NMDA receptors by Mg^{2+} and leads to their activation. These events are likely to occur in neuronal synapses as both AMPA- and NMDA-sensitive receptors are localised in the vicinity of

nerve terminal contacts with the dendrites (Bekkers and Stevens, 1989; Jones and Baughman, 1991). Not only are both AMPA and NMDA receptors located in the immediate vicinity of synapses, but they are also co-localised under the same nerve terminals on the same neuritic processes. Activation of ionotropic EAA receptors can trigger Ca^{2+} influx into neurons through voltage-sensitive Ca^{2+} channels activated as a result of cell depolarisation and also directly via NMDA receptor-gated ion channels.

In addition to the transmitter recognition site, an array of other functional subcomponents of the NMDA receptor exists, each with discrete ligand binding domains (see Figure 1.5). Currently, there are at least five pharmacologically distinct sites through which compounds can alter the activity of this receptor. They include (a) a neurotransmitter binding site, which binds Glu, (b) a regulatory or co-activator site, which binds glycine, (c) a site within the channel that binds phencyclidine (PCP) and related compounds (Lodge *et al.*, 1982), (d) a voltage-dependent Mg^{2+} binding site, and (e) an inhibitory divalent cation site that can bind Zn^{2+}. In addition, ligand-binding analysis indicates that there are two distinct binding sites associated with the transmitter-binding site, one that preferentially binds agonists and one that preferentially binds antagonists (Monaghan *et al.*, 1989; Olverman *et al.*, 1988a; 1988b).

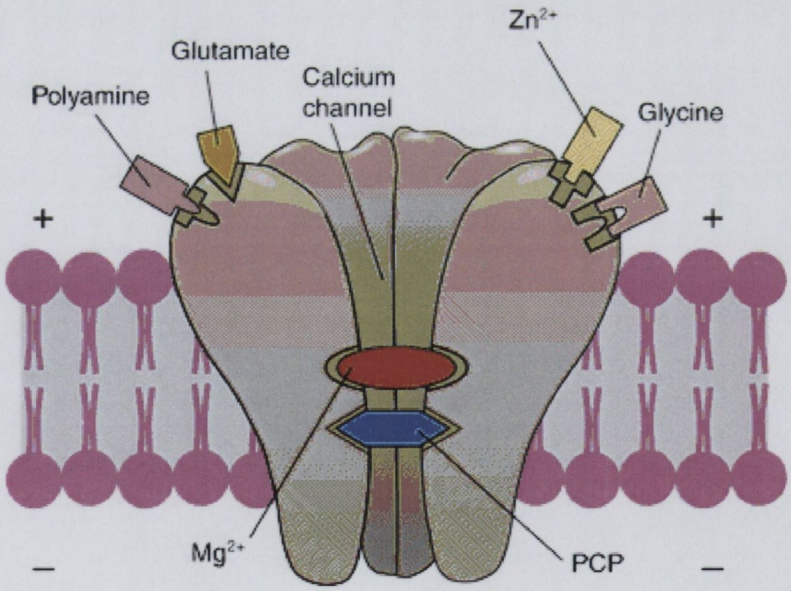


Figure 1.5: Illustration of the NMDA receptor

(modified image taken from homepage.psy.utexas.edu/ .../transmitters.html)

1.4.2 Non-NMDA (Kainate and AMPA) receptors

Kainate (KA)- and AMPA-sensitive receptors are ligand-gated ion channels and probably mediate most fast excitatory synaptic transmission in the CNS (Mayer and Westbrook, 1987). These channels are primarily permeable to monovalent cations such as Na^+ and K^+ and the synaptic currents mediated by them rise rapidly and decay fast. They are also characterised by rapid desensitisation (Jahr and Stevens, 1987; Partin *et al.*, 1993; Patneau *et al.*, 1993), a conformational transition to a close state in the continued presence of agonist. Desensitisation of ligand-gated ion channels shapes synaptic responses and provides a critical mechanism of protection at central synapses. AMPA receptors are known to rapidly desensitise in response to Glu (and AMPA) although the rate and degree of desensitisation is controlled in a number of ways, such as ribonucleic acid (RNA) editing, dependence on the flip/flop splice variant and on the molecular combination of receptor subunits. Cyclothiazide potentiates responses at AMPA receptors, at least in part by blocking the onset of desensitisation (Patneau *et al.*, 1993). In addition, cyclothiazide exhibits a very high degree of selectivity, acting exclusively on AMPA but not KA receptors (Partin *et al.*, 1993).

AMPA receptors are composed of Glu receptor (GluR) subunits 1 - 4 that determine their functional properties. The majority of AMPA receptors gate ion channels primarily permeable to monovalent cations; however, receptors lacking the GluR 2 subunit are freely permeable to Ca^{2+}. In fact, a single amino acid, arginine, in the second transmembrane domain of the GluR 2 subunit determines the Ca^{2+} permeability. Arginine is not encoded at the genomic level but a specific, developmentally controlled pre-mRNA editing mechanism ensures that GluR 2 subunits are Ca^{2+} impermeable (Burnashev *et al.*, 1992, 1996). Indeed, extensive data suggests that excess stimulation of non-NMDA receptors can suffice to destroy neurons (Rothman and Olney, 1987; Frandsen *et al.*, 1989). For example, Cebers *et al.* (1997) showed that even in the presence of NMDA receptor blockade, Glu in combination with cyclothiazide (to prevent AMPA receptor desensitisation) caused a significant enhancement of intracellular Ca^{2+} ion concentration in single cerebellar granule cells thus supporting a relationship between AMPA receptor-mediated neurotoxicity and increases in intracellular Ca^{2+} ion concentration. These observations of a strong relationship between AMPA receptor-mediated excitotoxicity in granule cells and increases in intracellular Ca^{2+} ion concentration are in agreement with the later results of Sinclair *et al.* (2003), who also reported the presence of Ca^{2+}-permeable AMPA receptors (GluR 5 - 7) in granule cells. Pharmacological studies indicate

that the KA and/or the AMPA receptors are responsible for the voltage-independent portion of the synaptic response in many neuronal pathways.

The AMPA receptors are believed to be involved in mediating all forms of fast glutamatergic neurotransmission. Much less is known about the physiological function of KA receptors. The main effect of either systemic or intrabrain KA treatment is neuronal damage (Sperk, 1994). In addition, KA also exerts a potent convulsive action when applied systemically into the cerebrospinal fluid or locally into limbic brain areas (Nadler *et al.*, 1980), leading to the use of KA in epilepsy research.

1.4.3 Metabotropic receptors

The metabotropic action of excitatory amino acids on phosphoinositide metabolism was first demonstrated by Sladeczek *et al.* (1985) in striatal neurons in culture with the relative potency quisqualate (QA) > Glu > NMDA, KA. Metabotropic Glu receptors (mGluRs) are members of the family of heptahelical proteins that are coupled to intracellular effector proteins (phospholipase C, adenylyl cyclase or cyclic guanosine monophosphate (cGMP) phosphodiesterase) or to ionic channels (K^+ or Ca^{2+} channels) via G proteins. Eight different subtypes of mGluRs (mGluR 1 - 8) have been cloned and characterised. They can be sub-classified into three groups, according to their sequence similarities, pharmacological properties and signalling cascades.

In the first group, mGluR 1 and mGluR 5 are positively coupled to phosphoinositide hydrolysis, which is a major biochemical mechanism of signal transduction in the central nervous system. MGluR 1 and mGluR 5 receptors are coupled either to pertussis toxin (PTX)-sensitive or insensitive G proteins (G_i/G_o or G_q; Nicoletti *et al.*, 1988; Suzdak *et al.*, 1993). Stimulation of these mGluRs activates phospholipase C (PLC) which catalyses the conversion of L-3-phosphatidylmyoinositol-4,5-bisphosphate (PIP_2) to inositol triphosphate (IP_3) and diacylglycerol (DAG) (Nicoletti *et al.*, 1986). IP_3 enhances the mobilisation of Ca^{2+} from intracellular stores, such as the endoplasmic reticulum (Murphy and Miller, 1988), while DAG is involved in the activation of protein kinase C (PKC), a kinase dependent on Ca^{2+} for activity, in neurons (Nicoletti *et al.*, 1990). For these receptors, that are coupled to PLC, QA is the most potent agonist followed by Glu, ibotenate and 1-aminocyclopentane-1,3-dicarboxylic acid ($1_{SR},3_{RS}$-ACPD) or its active isomer $1_S,3_R$-ACPD. Stimulation of different populations of mGluRs by a specific agonist $1_{SR},3_{RS}$-ACPD produces both excitatory and inhibitory effects.

The second group of mGluRs consists of mGluR 2 and mGluR 3 which stimulate adenylyl cyclases, following activation by $1_{SR},3_{RS}$-ACPD. Stimulation is not mediated by direct coupling of adenylyl cyclase to a G-protein (Schoepp and Conn, 1993) but by potentiation of responses from activation of other G-protein coupled receptors. Thus, a mGluR subtype exists that belongs to the growing family of receptor's that potentiate cAMP responses to G-protein-coupled receptor's. MGluR 2 and/or 3 modulate voltage-dependent Ca^{2+} channels. Activation of mGluR 2 and/or 3, acting either directly through receptor coupled G proteins or indirectly through stimulation of PKC, inhibit voltage gated L- and N - type Ca^{2+} channels and voltage-dependent and Ca^{2+}-activated K^+ channels (Koh *et al.*, 1992; Chavis *et al.*, 1994). However, there is also evidence to suggest that activation of mGluR subtypes enhance conductance through NMDA and AMPA receptors, which may selectively potentiate excitatory responses to high-intensity stimuli and facilitate induction of long-term potentiation. For example, in rat dorsal horn spinal neurons mGluR activation by $1_S,3_R$-ACPD increased currents and Ca^{2+} mobilisation induced by NMDA, AMPA and KA (Bleakman *et al.*, 1992). Potentiation of NMDA responses by mGluRs could therefore also contribute to Glu excitotoxicity. However, these responses depend to a large extent on the neuronal population that is being tested, suggesting considerable variability in the configuration of the mGluRs expressed by neurons in different brain regions. For example, $1_{SR},3_{RS}$-ACPD increases the activity of a large-conductance Ca^{2+}-dependent K^+ channel in cerebellar granule cells, and thereby reduces excitability of these cells. In contrast, mGluR activation by $1_{SR},3_{RS}$-ACPD depolarises hippocampal pyramidal cells and enhances their excitability by reducing the voltage-dependent K^+ conductance and the Ca^{2+}-dependent K^+ conductance. MGluRs also act indirectly through depolarisation and Ca^{2+} influx to induce the release of arachidonic acid (Dumuis *et al.*, 1990).

In contrast, the third group of mGluRs (mGluR 4, 6, 7 and 8) are negatively and directly coupled to adenylyl cyclases, inhibiting cAMP formation, via a transduction G protein-coupled receptor of the PTX-sensitive G_I/G_O subtype (Prezeau *et al.*, 1992, 1994). For these receptors, QA is the most potent agonist followed by Glu, KA and $1_{SR},3_{RS}$-ACPD or its active isomer $1_S,3_R$-ACPD.

While the effects of mGluR activation on ion channels vary between brain regions and cell types, a physiological effect of mGluR agonists that is consistent throughout the brain is a reduction of transmission at excitatory amino acid synapses. $1_{SR},3_{RS}$-ACPD or $1_S,3_R$-ACPD reduce evoked excitatory postsynaptic potentials (EPSPs) at glutamatergic synapses in the hippocampus, striatum, cerebellum and in primary cultures of mitral cells

from the olfactory bulb. In addition to reducing evoked EPSPs, $1_{SR},3_{RS}$-ACPD also reduces evoked inhibitory postsynaptic potentials (IPSPs) in the striatum and hippocampus (as reviewed by Schoepp and Conn, 1993). At present, the mechanisms by which mGluR agonists decrease Glu or GABA release are unknown.

Thus, the mGluRs may produce the most widespread physiological and biochemical effects on neurons of any of the EAA receptors.

1.5 Neurotransmitters

Neurotransmitters are synthesized and stored in concentrated form in small membrane bound vesicles in all nerve terminals. The vesicles are recycled from the nerve terminal membrane after exocytosis has occurred. The vesicles may also be transported from the cell body pre-packed with neurotransmitter, as is the case for larger peptides. Storage of the neurotransmitter in vesicles protects the transmitter from destruction by cytosolic, mitochondrial, or other enzymes and maintains the transmitter in a concentrated, rapidly releasable form.

Neurotransmitters are very diverse but have been divided into 3 categories. Type I neurotransmitters are simple amino acids such as Glu, Asp, which are present in high concentrations in the mammalian brain (approx. 10 and 4 mmol/L respectively), GABA and glycine which may account for transmission at up to 90% of all CNS synapses and which are responsible for the fastest information transfer. Type II neurotransmitters include the "classical" transmitters acetylcholine (ACh), the catecholamines (dopamine, noradrenaline and to a lesser extent adrenaline) and 5-hydroxytryptamine (5-HT). Type II neurotransmitters are predominantly slow acting and play a modulatory role in the CNS. Type III neurotransmitters encompass a wide variety of neuropeptides which are characteristically present at very low concentrations. Neuropeptides act predominantly as neuromodulators controlling the activity of diffuse receptors rather than at purely synaptic sites.

1.5.1 The role of the Type I neurotransmitters, Glu and Asp, in the CNS

Hayashi first demonstrated in 1954 that a direct injection of monosodium Glu into the brain induces seizures and later Van Harreveld (1959) showed that its application on the cerebral cortex causes massive depolarisation and spreading depression. These early observations of a potential role for Glu as an excitatory agent in the CNS were soon followed by detailed electrophysiological studies of the depolarising effects of the EAAs,

Glu and Asp, on single neurons of the vertebrate CNS. For example, these two amino acids were applied to single neurons in spinal cord (Curtis and Watkins, 1963) and also to single neurons in the cerebral and cerebellar cortex (Krnjevic and Phillis, 1963), by iontophoresis, and were found to produce strong depolarisation of the neuronal membrane potential. Essentially all neurons in these different regions of the mammalian CNS responded to the application of the EAAs. The membrane depolarisation induced by the EAAs was shown to be primarily the result of increased Na^+ (Curtis *et al.*, 1972; Mac Donald and Wojtowiez, 1980) and/or Ca^{2+} ion permeability and an increase in potassium (K^+) ion conductance of the nerve membrane.

Curtis, Watkins and their colleagues (Curtis *et al.*, 1960; Curtis and Watkins, 1963; Johnston *et al.*, 1974; Davies *et al.*, 1979) showed clear evidence of molecular constraints for activity of Glu and Asp in triggering excitatory responses in spinal cord neurons. These studies, together with others that discovered selective antagonists, which inhibited the excitatory responses initiated by Glu and Asp in CNS neurons (Davies and Watkins, 1979; Davies *et al.*, 1981), were critical in identifying specific EAA receptors on neuronal membranes.

Following the discovery of EAA receptors, Nadler *et al.* (1976) and Hamberger *et al.* (1979) demonstrated that Glu and Asp are released from nerve endings upon depolarisation or from brain tissue upon excitation (Bliss *et al.*, 1986) in a Ca^{2+}-dependent manner. Specific, high affinity and high capacity transport systems in nerve endings and glial cells were shown to rapidly reduce the extracellular concentration of Glu and Asp following synaptic release (Logan and Snyder, 1972; Balcar and Johnston, 1972; Kanner and Sharon, 1978; Schousboe, 1981; Drejer *et al.*, 1982). Glu is removed from the synaptic cleft and extracellular space by Na^+-dependent, high-affinity monocarboxylic acid carriers located in both neurons and glia (Nicholls and Atwell, 1990). Efficient uptake of Glu (Eliasof and Werblin, 1993), possibly supplemented by its diffusion away from the synaptic cleft (Isaacson and Nicoll, 1993), contributes to the termination of Glu actions on synaptic receptors because there are no extracellular enzymes to degrade the transmitter signal. The presence of both a biosynthetic pathway for the synthesis of Glu in neurons (Balazs *et al.*, 1966) and an ATP-dependent transport system in synaptic vesicles, that is involved in the storage of Glu (Naito and Ueda, 1983), solidified the concept that Glu meets many of the criteria for a chemical neurotransmitter in the vertebrate CNS.

Beyond the function of Glu as a synaptic neurotransmitter, this amino acid also produces long-lasting changes in neuronal excitability, such as the long term potentiation (LTP) of

synaptic transmission in neurons of the hippocampus and visual cortex, suggesting that NMDA receptor subtypes of Glu receptors may be an important component of the processes involved in learning and long-term depression (LTD) in the cerebellum (Artola and Singer, 1987; Cotman *et al.*, 1988; Ito, 1989). Other demonstrations of long-lasting actions of Glu on neurons include the effects produced on developing neurons through the activation of EAA receptors. Glu is one of the stimuli for the initiation of neuronal migration in the developing cerebellar cortex (Rossi and Slater, 1993), regulation of neurite outgrowth, axonal growth and synaptic formation (Pearce *et al.*, 1987; Mattson *et al.*, 1988; Mattson and Kater, 1989; Brewer and Cotman, 1989; Baird *et al.*, 1996) and survival of neurons in culture (Balazs *et al.*, 1988).

1.6 Antagonists of the ionotropic Glu receptors

Antagonists are important research tools. By their use it has been possible to differentiate certain pathways and physiological functions as dependent on either NMDA or other subtypes of EAA receptors. Antagonists offer advantages in receptor investigations primarily because they are often more specific for discrete types of receptor than the corresponding agonists. Furthermore, antagonists are important because of their considerable potential as new centrally acting drugs.

1.6.1 Antagonists of the NMDA subtype of Glu receptor

The glutamic acid diethylester (GDEE) was the first compound considered as a Glu antagonist (Haldeman and Lennon, 1972). It is active at the AMPA-preferring receptor but also affects other membrane properties and other types of neurotransmission including cholinergic. A year later another compound, a pyridine analogue, HA 966, was shown to possess some Glu blocking action (Davies and Watkins, 1973). However, more potent antagonists were identified through the systemic study of analogues of Glu *in vitro* (Davies *et al.*, 1981). The most potent and selective antagonists of excitatory amino acids are longer chain analogues of Glu and Asp with the ω-carboxyl group substituted by a phosphono, especially D,L (±)-2-amino-5-phosphonopentanoic acid (AP5) and D,L (±)-2-amino-7-phosphonoheptanoic acid (AP7). In both cases, the D-isomer possesses the greater activity. Both compounds were tested in the spinal cord and cerebral cortex and were found as highly selective antagonists of excitation at the NMDA receptor, with little activity at the KA or AMPA receptors. Thus, the antagonists AP5 and AP7 have been used as key compounds in identifying NMDA receptor action in a variety of CNS regions

in electrophysiological and biochemical assays. In addition, both antagonists when administered systemically are also effective against a variety of seizures induced by NMDA, and do not protect against seizures induced by KA (Czuczwar and Meldrum, 1982). Another generation of NMDA receptor antagonists were obtained by incorporation of the carbon backbone of AP5 and AP7 into heterocyclic ring derivatives. For example, 3-((±-2-carboxypiperazin-4-yl)-propyl-1-phosphonic acid (CPP), a derivative approximately five fold more potent than AP5 (Davies *et al.*, 1986; Lehmann *et al.*, 1987). All of the antagonists mentioned so far are antagonists of the NMDA receptor-binding site. However, antagonists also exist for the NMDA-glycine binding site and the NMDA receptor ion channel.

Kynurenate acts as a competitive glycine antagonist (Kessler *et al.*, 1989). By binding to the glycine site, kynurenate decreases the ability of Glu to open the channel associated with the NMDA receptor and thus behaves functionally as an NMDA receptor antagonist. Lodge *et al.* (1982) first reported that the dissociative anaesthetic ketamine and phencyclidine (PCP) are selective antagonists of the NMDA receptor ion channel. Without altering responses to KA or QA, ketamine and PCP completely blocked the actions of NMDA. Since those initial reports, PCP and related compounds have been found to inhibit NMDA receptor activity in a range of preparations, for example mouse hippocampal slices (Duchen *et al.*, 1985) and rat cerebral cortex slices (Harrison and Simmons, 1985; Lodge and Johnson, 1985). Further investigations reported the structurally related compounds 1-(1-thienyl-cyclohexyl) piperidine (TCP) and dibenzocycloheptenеimine (MK-801) as displaying greater potency and selectivity (Wong *et al.*, 1986). PCP, ketamine, TCP and MK-801 are non-competitive antagonists of NMDA induced responses, and attenuate NMDA receptor action by blocking the cation channel gated by the NMDA recognition site. It was also suggested that PCP-like compounds bind to a site within the open channel (Huettner and Bean, 1988). These observations formed the basis of a proposal that the receptor must be in the agonist-bound, open-channel state for the antagonist to bind or dissociate from a site within the receptor-gated channel. The partial voltage dependency of the block and its removal suggests that the PCP binding site is within the ion channel itself. The ability of Mg^{2+} to voltage-dependently prevent MK-801 blockade suggested that these two sites are very near to one another (Huettner *et al.*, 1988).

1.6.2 Antagonists of the KA and AMPA receptors

The most potent AMPA and KA antagonists are the quinoxaline derivatives, 6,7-dinitroquinoxaline-2,3-dione (DNQX) and 6-cyano-7-nitroquinoxaline-2,3-dione (CNQX) reported by Honoré and colleagues (1988). A third quinoxaline was also reported, 2,3-dihydroxy-6-nitro-7-sulfamoyl-benzo(F)quinoxaline (NBQX) as an antagonist of the AMPA receptor (Fletcher *et al.,* 1988; Sheardown *et al.*, 1990). These compounds were shown to selectively block the excitatory action of AMPA and KA (Honoré *et al.*, 1988; Drejer and Honoré, 1988). Schild analysis indicated that both KA and AMPA antagonism was competitive (Drejer and Honoré, 1988).

The two structurally related 2,3-benzodiazepines GYKI 52466 and GYKI 53655 are the best antagonists in terms of discriminating between AMPA and KA receptors because they selectively inhibit the AMPA receptors without altering the activity of KA receptors (Donevan *et al.*, 1994; Osipenko *et al.*, 1994). However, high concentrations of these antagonists can produce a weak block of KA receptor responses (Partin and Mayer, 1996). GYKI 52466 is a non-competitive antagonist of AMPA receptors, but it does not alter the extent or kinetics of onset of desensitisation nor does it act as an open channel blocker. This distinguishes GYKI 52466 from other non-competitive inhibitors of AMPA receptors such as the Joro spider toxin, which acts as an open channel inhibitor that preferentially blocks AMPA receptors (Akaike *et al.*, 1987). Partin and Mayer, (1996) reported that both antagonists act through negative allosteric modulation of the receptor. 2,3-benzodiazepines have anticonvulsant activity in seizure paradigms, presumably through attenuation of AMPA receptor-mediated excitatory synaptic transmission, which makes these compounds potentially useful as therapeutic anticonvulsants (Donevan *et al.*, 1994).

1.7 Excitotoxicity

The potential for Glu to act as a mediator of neuropathologic events was realised at the same time that its activity as an excitatory neurotransmitter was being established. Coincident with the early characterisation of Glu as the most prevalent excitatory neurotransmitter in CNS synapses by Curtis and Watkins (1960; 1963), Lucas and Newhouse (1957) described the neurodegeneration of the inner neural layers of the retina produced by the systemic injections of Glu to immature mice. These observations remained in relative obscurity until they were reproduced by Olney twelve years later, who confirmed the retino-toxicity of Glu and, in addition, showed that systemically administered

Glu destroys neurons by acute necrosis in the brains of newborn mice, rats or monkeys (Olney, 1969; Olney *et al.*, 1971, 1978). It was further reported that the structurally related compounds Glu and KA produced brain lesions in immature animals that did not possess a fully developed blood-brain barrier. Since Glu was being used liberally as a flavour additive in baby foods, concern was raised that neurons in vulnerable regions of the immature human brain might be destroyed. It was also proposed, in light of the high concentrations of Glu found in the brain, that endogenous Glu might play a role in human neurodegenerative diseases. Interest in and support for this hypothesis increased dramatically when the neuronal pathology induced by various excitotoxins was found to be similar to that associated with a wide spectrum of neurological insults. For example, the characteristic dendrosomatotoxic/axon-sparing dendritic lesions produced by the EAA agonists, Glu, Asp and NMDA, are similar to the neuronal damage found in anoxia, ischaemia, hypoglycemia and epilepsy (Olney, 1969; Rothman, 1984; Auer *et al.*, 1984; Griffiths *et al.*, 1983 and Olney *et al.*, 1986). Olney coined the term "excitotoxicity" which hypothesises that Glu neurotoxicity is mediated by a prolonged depolarising action of Glu at its postsynaptic dendrosomal receptor sites, an action assumed to result in pathological membrane permeability changes and impaired ion homeostasis. Excitotoxicity has also been considered as a major mechanism in seizure-induced neuropathology, where excessive amounts of Glu are released into the extracellular space and are toxic to neurons (Meldrum, 1985; Meldrum, 1994), and chronic neurodegeneration associated with Alzheimer's disease (Mattson *et al.*, 1999), Huntington's disease (Koh *et al.*, 1986; Alexi *et al.*, 2000) and amyotropic lateral sclerosis (Plaitakis *et al.*, 1982; Plaitakis and Caroscio, 1987; Beal *et al.*, 1986; Rothstein, 1995). Thus, Glu and a variety of Glu analogues including KA, AMPA and NMDA are reported to be excitotoxins capable of intiating or potentiating neuronal cell death. The involvement of the EAA receptors in the underlying mechanisms of these pathological neurodegenerative diseases was strengthened by the dramatic illustration that EAA antagonists, particularly those of the NMDA subtype of Glu receptor, could block the neuronal death in experimental models of these neuropathological conditions. Thus administration of NMDA antagonists reduced the cell loss associated with anoxia, ischaemia (Simon *et al.*, 1984; Foster *et al.*, 1987) and hypoglycemia (Wieloch, 1985).

1.7.1 Role of Ca^{2+} in Excitotoxicity

Of obvious importance is the elucidation of the biochemical events in the excitotoxic process that occurs following excitatory receptor activation. Throughout the literature, high extracellular Glu is the prevalent, speculative trigger of excitotoxicity (Olney, 1969; Budd and Nicholls, 1996; Choi, 1987, 1988a, 1988b, 1992; Leist and Nicotera, 1998; Michaelis, 1998). Clearly, the exceptional diversity of Glu-operated ion channels, the complexity of their modulation, and the likely involvement of second messenger systems, provide opportunities for other damaging mechanisms to occur, in addition to direct actions of increased Glu levels on its receptors. Although the molecular basis of Glu-evoked neuronal excitotoxicity is uncertain, several experiments have identified an apparent ionic dependence of excitotoxicity. The initial event has been reported as an extensive inward current of Ca^{2+} and Na^{+} through the NMDA receptor, possibly supplemented by release of Ca^{2+} from intracellular stores (mitochondria and endoplasmic reticulum) subsequent to mGluR activation, leading to intracellular Ca^{2+} overload and culminating in necrotic or apoptotic cell death (Choi, 1987, 1995; Garthwaite and Garthwaite, 1986; Ankarcrona *et al.*, 1995; Siesjo *et al.*, 1995). The observations of Choi suggested two possible additive mechanisms of Glu-induced excitotoxic neuronal death, distinguished on the basis of differences in time course and ionic dependence. First, an acute, rapid swelling Na^{+}- and Cl^{-}-dependent component, and second, a delayed, Ca^{2+}-dependent component marked by delayed cell degeneration. The Na^{+}- and Cl^{-}-dependent neurotoxicity is due to cell swelling, initiated by acute Na^{+} influx which draws in Cl^{-} and water through the NMDA channels to maintain electroneutrality, and which culminates in cell lysis (Dessi *et al.*, 1994; Lysko *et al.*, 1994). Since Ca^{2+}-dependent damage can occur after only brief excitotoxic exposure, in the absence of swelling, Choi concluded that Ca^{2+} entry is the more significant cause of pathology following exposure to excitotoxins *in vivo*.

There are two other issues regarding excitotoxicity and Ca^{2+} ions that require discussion – the path of Ca^{2+} entry and the actual mechanism of Ca^{2+}-induced cell damage. The dynamics of Ca^{2+} regulation in central neurons is complex. The level of Ca^{2+} can increase in the neuronal cytoplasm through a variety of mechanisms, but nerve cells are equipped to cope with excessive Ca^{2+} entry and can dispose of large Ca^{2+} amounts. Extracellular Ca^{2+} can enter neurons through voltage-gated Ca^{2+} channels, transmitter-gated channels permeable to Ca^{2+} or through ion exchangers. Irrespective of the mechanism by which Ca^{2+} enters the cell, neurons have an intracellular Ca^{2+} concentration ($[Ca^{2+}]_i$) in the mM range, similar to the concentration of Ca^{2+} in the extracellular fluid (1 mM), yet they

maintain their resting $[Ca^{2+}]_R$ at around 100 nM. The difference between neuronal Ca^{2+} content ($[Ca^{2+}]_I$) and $[Ca^{2+}]_R$ is as a result of the majority of Ca^{2+} being sequestered into intracellular organelles, such as the mitochondria or endoplasmic reticulum. The electrochemical gradient across the cell membrane that drives Ca^{2+} into neurons is maintained by the low Ca^{2+} permeability of the membrane and by Ca^{2+} extrusion processes. Ca^{2+} efflux occurs via a high affinity Ca^{2+}-activated ATPase and a low affinity Na^+/Ca^{2+} exchanger driven by the plasma membrane Na^+ gradient (as reviewed by Small *et al.*, 1999). Following a brief excitotoxic exposure, neuronal $[Ca^{2+}]_R$ rises because of the impairment of energy-dependent membrane transport systems and the release of Ca^{2+} from internal stores. This is followed by a larger rise in $[Ca^{2+}]_R$ coincident with the depolarisation of the plasma membrane. Depolarisation triggers further Ca^{2+} influx through NMDA and Ca^{2+} channels, which contributes to the lethal Ca^{2+} concentration associated with cell damage. It is generally accepted that the NMDA subtype of Glu receptors plays a key role in mediating Ca^{2+}-induced cell damage, possibly owing to the ion channels associated with the receptor, which represent a major route of entry for this excessive Ca^{2+} influx (Choi, 1987; Choi *et al.*, 1987). Indeed, Sattler *et al.* (1998) reported that the entry of Ca^{2+} through the NMDA receptor, and not the Ca^{2+} load, was the main determinant of the neurotoxic potential of Ca^{2+} ions.

Ca^{2+} influx is critical for activity-dependent synaptic plasticity and, if excessive, is potentially damaging because it can over-stimulate Ca^{2+}-dependent enzymes such as phospholipases, proteases and endonucleases (Lipton and Rosenberg, 1994) and irreversibly damage mitochondria. Proteolysis of cellular proteins is an important component of neurodegeneration. Calpains I and II are found throughout the brain and are activated by Ca^{2+} at neutral pH. The endogenous inhibitor, calpastatin, which forms a complex with calpain limiting its proteolytic activity, also regulates calpain activity. Activated calpains hydrolyse peptide bonds in cytoskeletal and structural proteins (spectrin, actin, tubulin, tau, neurofilaments and microtubules), membrane proteins (Glu receptors and epidermal growth factor (EGF) receptors) and other regulatory and signalling proteins (protein kinase C, calcineurin and calmodulin-binding proteins). Uncontrolled proteolysis destroys the plasma membrane and kills the cell. In addition, transient changes in the concentration of intracellular Ca^{2+} ion concentration can trigger alterations in gene expression. Among the Ca^{2+}-regulated processes critical for the long-term structural and functional modification of neurons are changes in gene expression. Regulation of gene expression is an important component of the cellular response to

environmental cues, and involves integration of signals from many signal transduction pathways. Activation of either two types of Ca^{2+} channels – the NMDA subtype of Glu receptor and the voltage-gated L-type Ca^{2+} channel induces expression of the *c-fos* gene and other *immediate early genes (IEGs)*.

1.7.2 Role of Mitochondria in Excitotoxicity

Mitochondria from differing cell types vary widely in size, shape and number. Each mitochondrion has an outer membrane, which is freely permeable to molecules up to a size of 10 KDa and surrounds the mitochondrion and an inner membrane that is relatively impermeable and contains the electron transport enzyme complexes. The inner compartment of the mitochondrion, enclosed by the inner membrane, is the matrix in which the Krebs cycle takes place. NADH and $FADH_2$, generated from the Krebs cycle, donate electrons, which are carried through the series of transport enzymes of the inner mitochondrial membrane to ATP synthase, the last enzyme complex of the electron transport chain (Complex I - V). Concomitantly, ejection of protons across the inner mitochondrial membrane results in an electrochemical gradient, which stores potential energy. In the cells of higher animals, approximately 95% of the common cellular energy denominator, adenosine triphosphate (ATP), is produced by oxidative phosphorylation within mitochondria. Oxidative phosphorylation is the coupling of the transfer of reducing equivalents (electrons) to oxygen with the synthesis of ATP. Mitochondrial dysfunction has been suggested as a final common denominator in several chronic neurodegenerative disorders (Beal, 1992) and investigators have documented increased lactate levels in Huntington's disease, which may correlate with impaired mitochondrial ATP generation (Jenkins *et al.*, 1993). In addition, mitochondria have been implicated as targets for NMDA receptor-mediated injury (Nicholls and Budd, 1998; Reynolds, 1999).

Under physiological conditions, mitochondrial Ca^{2+} uptake via the mitochondrial Ca^{2+} uniporter is thought to up-regulate the activity of Krebs cycle enzymes to meet increased ATP demand during calcium signalling and cellular activities (Mc Cormack and Denton, 1994) and modulate increases in intracellular Ca^{2+} concentrations via rapid influx, which is energetically downhill, and slow efflux, which is energetically uphill, from the mitochondrial matrix (Babcock *et al.*, 1997). The resultant steady-state cycling of Ca^{2+} across the inner mitochondrial membrane allows the mitochondrion to regulate the extra-mitochondrial free Ca^{2+} concentration with a precision and flexibility that would not be possible with a single carrier and enhances the general function of mitochondria in the regulation of cytosolic

Ca^{2+} concentration. Limited Ca^{2+} uptake increase the availability of substrate molecules as well as the rate of electron transport (Mc Cormack and Denton, 1993). There is also some evidence that mitochondrial function plays a role in synaptic plasticity (Nguyen and Atwood, 1994).

Excessive stimulation of neurons, however, with Glu or NMDA leads to the overloading of mitochondria with Ca^{2+} (White and Reynolds, 1996, 1997; Peng *et al.*, 1998; Budd and Nicholls, 1996) and the subsequent compromise of its bioenergetic intergrity and/or the generation of free radicals (Dugan *et al.,* 1995; Reynolds and Hastings, 1995). Large increases in mitochondrial matrix Ca^{2+} interfere with mitochondrial ATP production by activating the non-selective permeability transition pore (PTP; Gunter *et al.*, 1994), a nuclear encoded protein in the inner mitochondrial membrane, which is closed in tightly coupled mitochondria. Activation of the pore results in mitochondrial depolarisation and swelling as all solutes and proteins smaller than 2 KDa move freely through the mitochondrial membrane (Bernardi *et al.*, 1994). The pore is regulated by various physiological signals, including adenosine nucleotides (in particular adenosine diphosphate (ADP)), Mg^{2+} and both matrix and cytosolic Ca^{2+} ions. Mitochondrial Ca^{2+} accumulaton sufficient to activate the PTP can, however, dissipate the mitochondrial membrane potential ($\Delta\psi_m$) and therefore ADP phosphorylation, irreversibly damaging the cells, even when mitochondrial respiration is stimulated initially by the Ca^{2+} uptake. The $\Delta\psi_m$ results from the asymmetric distribution of protons and other ions on both sides of the inner mitochondrial membrane, giving rise to a chemical (pH) and electrical gradient, which is essential for mitochondrial function. The inner side of the inner mitochondrial membrane is negatively charged (reviewed by Kroemer *et al.*, 1997). The electron transport chain normally maintains an electrochemical potential of 150 - 180 mV across the inner mitochondrial membrane by moving protons out of the matrix and into the cytosol (Gunter and Gunter, 1994). Therefore, mitochondria possess an enormous capacity to sequester Ca^{2+} whenever the free Ca^{2+} concentration in their environment exceeds 0.5 µM (Nicholls and Scott, 1980; Nicholls and Åkerman, 1982). The total electrochemical potential is the sum of the electrical ($\Delta\psi_m$) and the chemical (ΔpH) components. The relative contribution of these components to the electrochemical potential can vary, depending on the experimental conditions. For example, Ca^{2+} accumulation can result in an increased ΔpH with a corresponding decrease in $\Delta\psi_m$. Thus, above a critical accumulation threshold the matrix Ca^{2+}-phosphate complex can compromise mitochondrial function leading to a collapse of $\Delta\psi_m$, matrix acidification, ATP

hydrolysis and a catastrophic release of the cation – the permeability transition (Bernardi *et al.*, 1994). Although recovery of $\Delta\psi_m$ following Glu exposure is associated with apoptosis or necrosis (Ankarcrona *et al.*, 1995), the underlying relationships are unclear. Mitochondria are also the main source of ATP in the brain. As such, even a transient alteration in function resulting from excessive Glu stimulation could have damaging effects on energy-dependent processes such as maintenance of ionic gradients, biosynthesis, neurotransmission and intracellular transport.

1.8 *Immediate early genes* (*IEGs*)

In neuron-to-neuron signalling, the activation of neurotransmitter receptors by the primary neurotransmitter generates precise messages for the post-synaptic neurons, leading to functional modifications of regulatory processes located in plasma membranes, cytosol and nucleus. During long-term plastic changes of neuronal function, a co-ordinated change in the expression of a set of genes occurs. Neurons are often described as being "plastic" because they can show short- or long-lasting changes in their phenotype in response to different stimuli. Within minutes of neurotransmitter release, the expression of a family of genes termed *immediate early genes* (*IEGs*) is induced in the post-synaptic neuron. *IEGs* contain a number of phylogenetically conserved genes which have been identified as cellular homologs of retroviral transforming genes, termed proto-oncogenes, and which function in the transmission of information between and within cells. *IEGs* are thought to control physiological processes of development, growth and differentiation. Many *IEGs* encode transcription factors, which then induce subsequent waves of delayed response gene expression. Delayed response genes encode proteins that are likely to be determinants of neuronal plasticity. These proteins may include neurotransmitter-synthesizing enzymes, neurotransmitter receptors, neurotrophins as well as structural components of the synapse. The proto-typical *IEG* is *c-fos* (see Figure 1.6).

In non-neuronal cells, the *c-fos* proto-oncogene is of particular interest as it can be rapidly and transiently induced at the level of transcription by a variety of external stimuli (growth factors, mitogens, ionophores). In differentiated neuronal cells, synaptic signalling appears to be important in causing this induction and, thereby, increasing the nuclear content of the phosphoprotein encoded by the *c-fos* mRNA, c-Fos, suggesting that c-Fos may regulate gene expression. In fact, c-Fos appears to be involved in the transcriptional regulation of some genes, in as much as it interacts with other nuclear proteins, forming the transcription factor activator protein-1 (AP-1). It can be inferred that *c-fos* may co-

ordinately regulate the expression of cell-specific target genes encoding for proteins participating in various neuronal responses.

1.8.1 What are oncogenes?

Retroviral oncogenes were first defined as the genetic information responsible for the induction of cellular transformation by RNA tumor viruses. Subsequent studies revealed that they were derived from normal cellular genes, termed proto-oncogenes, by recombination with viruses (Bishop, 1983, 1985). The oncogenic potential of these cellular genes is realised either by mutagenesis or by deregulation of expression. Thus, oncogenesis can result from the aberrant or abnormal expression of normal cellular genes. The definition of oncogenes has now been expanded to include many classes of genes that are mutated or otherwise activated during tumorigenesis. Over the past few years, several retroviral oncogenes and their cellular counterparts, proto-oncogenes, have been identified and characterised. The main driving force behind this research was the hope that by investigating the molecular basis of virus-induced tumors more knowledge would be gained about human cancer. Indeed, several viral oncogenes, for example *ras*, have been found as mutated in human tumors. However, a second, but equally important, rationale argued that proto-oncogenes were likely to represent cellular genes that played critical roles in normal growth regulation. This led to a detailed analysis of the properties of the proteins encoded by proto-oncogenes. Such investigations revealed that proto-oncogenes are involved in several critical aspects of the regulation of cellular growth and differentiation. They were found to encode proteins that function as extracellular growth factors, cell-surface receptors, G-proteins, protein kinases, hormone receptors and transcription factors (Reddy *et al.*, 1988). Although the exact molecular function of each of these proteins can be varied, they share a common feature in that they participate in signal transduction processes, that is, in the transmission of information between and within cells. Thus, oncogenesis can be viewed as a breakdown of the molecular mechanisms involved in intracellular and intercellular communication (as reviewed by Curran and Morgan, 1995).

The interest in the proteins encoded by proto-oncogenes and related genes extend well beyond the field of oncology. Proto-oncogenes can be viewed simply as components of signal transduction pathways that operate in several cellular contexts. Indeed, they have been shown to function in critical aspects of differentiation and development in several species (Reddy *et al.*, 1988). It has also become apparent that proto-oncogenes have a

function in the adult nervous system. One example was the finding by Chao (1992) that the *trk* proto-oncogene encodes a protein tyrosine kinase that normally functions as the receptor for nerve growth factors (NGF).

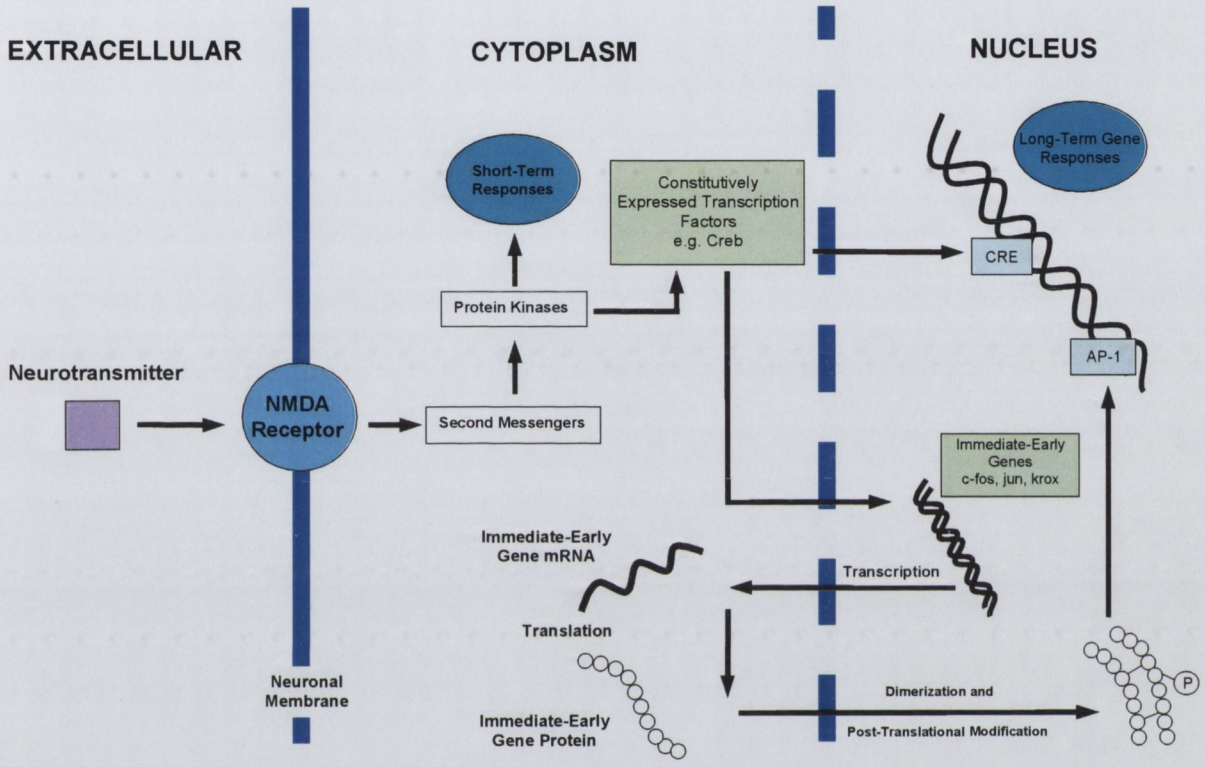


Figure 1.6: Signal-regulated transcription factors mediate long-term changes in gene expression within the neuron.

Short-term responses within the neuron are produced by activated protein kinases. Long-term responses within the neuron involve changes in neuronal gene expression. These changes in gene expression are controlled by signal-regulated transcription factors. Different families of signal-regulated transcription factors exist, for example, the CREB (post-translationally activated) and the *IEG* family (transcriptionally activated).

1.8.2 Induction of *immediate early genes* (*IEGs*)

The *fos* proto-oncogene was first described as the gene responsible for induction of bone tumors by the ***F***inkel-Biskis-Jinkins murine ***os***teogenic sarcoma virus (FBJ-MSV; Curran and Teich, 1982). Like many acutely oncogenic retroviruses, FBJ-MSV was driven by

recombination of retroviral sequences with cellular genetic information. The normal cellular sequence's from which the viral oncogene (v-*fos*) was derived is referred to as the *fos* proto-oncogene or *c-fos*. In the majority of cell types, the basal level of *c-fos* mRNA and protein expression is relatively low. One of the features of *c-fos* that suggested it might function in signalling processes was the discovery that its expression could be transiently induced to very high levels by serum and polypeptide growth factors (Muller *et al.*, 1984) as an immediate consequence of receptor stimulation. It is now established that many types of stimuli, some associated with the process of differentiation and some linked to neuronal excitation, elicit a very similar transient induction of *c-fos* mRNA and protein. The time-course of the induction is identical in most circumstances. Transcriptional activation occurs within 5 minutes (min) and continues for 15 - 30 min (Greenberg *et al.*, 1985). mRNA accumulates and reaches peak values at 30 - 45 min post-stimulation (Muller *et al.*, 1984), after which it declines with a relatively short half-life time of approximately 12 min. Synthesis of c-Fos protein follows mRNA expression. As the induction of *c-fos* transcription occurred in the presence of protein synthesis inhibitors, for example cycloheximide, it was suggested that the proteins required for expression are constitutively expressed in unstimulated cells and that they are activated by post-translational modification. This feature led to the classification of *c-fos* and other rapidly induced genes as cellular *immediate early genes* by analogy to the immediate-early genes of viruses (Curran and Morgan, 1987; Lau and Nathans, 1987), that is, they are rapidly synthesized following infection of a host cell, their transcription does not require protein synthesis, and they generally function in regulating expression of other viral genes.

Several regulatory elements located in the 5' untranslated region of *c-fos* have been shown to play a role in controlling the induction of expression (see Figure 1.7). The major DNA elements include, from 5' to 3', the SIE, TCF/ETS-E, an SRE, an E-box, an AP-1 site and a CRE site. (a) The first regulatory element to be defined operationally was the serum response element (SRE). This element is also known as the dyad symmetry element (DSE). The SRE is a 22 base pair segment that is located at -310 and contains the inner core sequence CCA/T-6-GG. This is similar to the CArG box, which is also present in some other *IEGS* such as *krox-20* and *krox-24*. The SRE functions as an inducible enhancer element in that it binds a 67 KDa nuclear phosphoprotein termed the serum response factor (SRF). The SRE mediates *c-fos* induction by phorbol esters, growth factors (EGF, platelet-derived growth factor (PDGF), insulin) and UV in either a PKC-dependent or –independent manner. However, it is not responsive to increases in

intracellular calcium or activation of protein kinase A (PKA). The SRF and its accessory protein, TCF/ELK-1, are the main transducers of SRE-mediated transactivation of *c-fos*. The TCF complex stabilises the binding of SRF to the SRE. PKC-dependent simulation of *c-fos* transcription requires ternary SRF-TCF-SRE complexation, whereas PKC-independent stimulation requires only an SRF-SRE binary complex. Two different signal cascades can phosphorylate TCF: JNKs phosphorylate TCF during the cellular stress response, whereas the ERK kinases activate the SRF/TCF complex following stimulation by growth factors and 12-*o*-tetradecanoylphorbol-13-ester (TPA). Different second messenger pathways activate the JNK and ERK kinases. (b) The c-Sis inducible element (SIE) is rapidly activated following cellular stimulation by PDGF and EGF. These growth factors cause rapid phosphorylation of the pre-existing nuclear protein SIF (c-Sis inducible factor) which then binds to and activates the SIE. (c) The 5' calcium response element (CRE) binds the CREB protein as well as c-Jun:c-Fos dimers (AP-1), and is the main site for NGF-mediated c-Fos expression in PC12 cells. c-Jun:c-Fos dimers bind to the CRE of *c-fos* and activate its transcription. The CRE also mediates the induction of *c-fos* by cAMP. (d) The levels of AP-1 binding activity increase after cells are treated with a variety of stimulatory agents including serum and NGF.

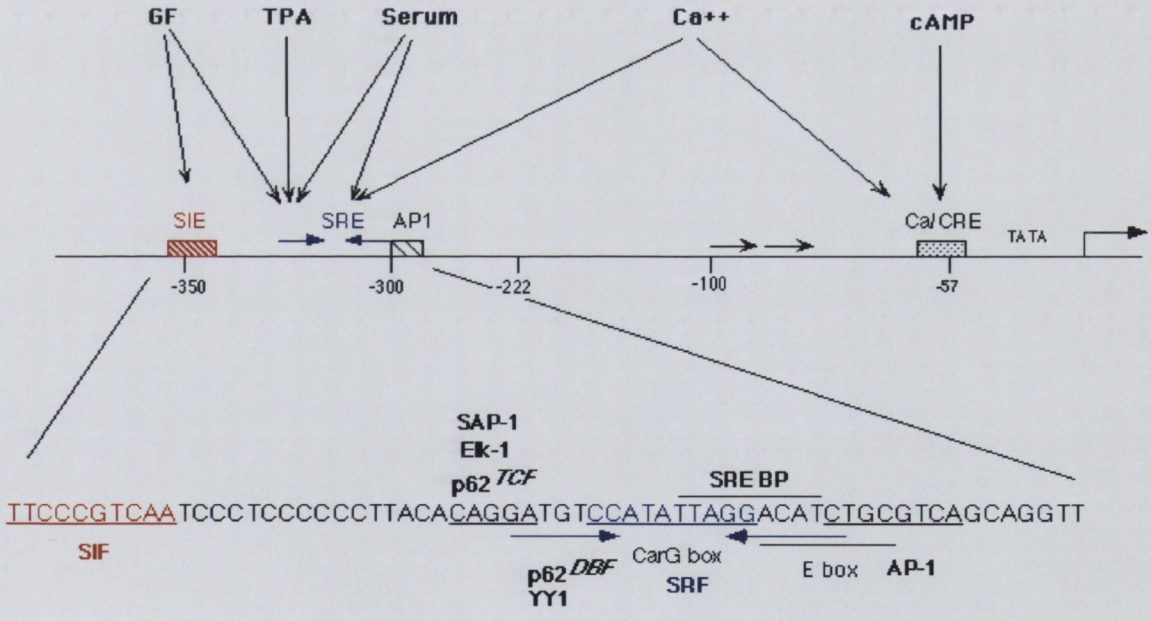


Figure 1.7: Illustration of the regulatory elements located in the 5' untranslated region of *c-fos*.

The major DNA elements, from 5' to 3', include the SIE, TCF/ETS-E, an SRE, an E-box, an AP1 site and a CRE site.

Thus, a single extracellular stimulus does not activate just one promoter element of one gene. Rather, it produces a shower of factors that act at several promoter elements. The convergence of second messenger pathways on the *c-fos* promoter includes those activated by neurotransmitters and hormones, and the Ras- and mitogen-stimulated pathways. AP-1 acting at the SRE can produce repression of *c-fos* transcription. In addition, c-Fos acting with Jun proteins can effectively repress *c-fos* transcription by binding to the CArG box in its own promoter (Sassone-Corsi *et al.*, 1988). This repressor function may be required for the rapid decline in immediate-early gene expression that follows induction as the shut-off process requires ongoing protein synthesis.

The *c-fos* gene encodes a 62 KDa nuclear protein, c-Fos, which undergoes extensive post-translational modification (Curran *et al.*, 1984). Most of the modification corresponds to serine and threonine phosphorylation. The phosphorylation of c-Fos is required to enhance its capacity for transcriptional activation (Bannister *et al.*, 1994) and to enable repression of transcription of its own gene promoter with a negative feedback loop. c-Fos participates in a nuclear protein complex with a cellular protein, Jun, previously termed as p39, the product of the *c-jun* oncogene (Rauscher *et al.*, 1988). This protein was routinely detected in immunoprecipitates of both *v-fos* and *c-fos* from non-denatured cellular extracts (Curran *et al.*, 1984, 1985). This finding was followed closely by the identification of several more putative *IEGs* by screening serum-inducible complementary DNA (cDNA) libraries for clones related in sequence to *c-fos* and *c-jun*. In this way, *junB* (Lau and Nathans, 1987; Ryder *et al.*, 1988), *junD* (Hirai *et al.*, 1989; Ryder *et al.*, 1989), *fra-1* (Cohen and Curran, 1988), *fosB* (Zerial *et al.*, 1989) and *fra-2* (Nishina *et al.*, 1990) were identified. Thus, the *fos* family consists of *c-fos*, *fosB*, *fra-1* and *fra-2* while the *jun* family of *IEGs* consists of *c-jun*, *junB* and *junD*. The protein products of the *fos* family of *IEGs* share several regions of homology, including the DNA-binding domain and, furthermore, all members of the *jun* family form complexes with the proteins encoded by the *fos* family (Rauscher *et al.,* 1988a). Cellular proto-oncogenes encode proteins at three major sites: the cell membrane, the cytosol and the nucleus.

The demonstration that c-Fos functions directly as a transcriptional regulator in co-operation with c-Jun through so-called activator-protein-1 (AP-1) regulatory elements (Lee *et al.*, 1988) was the culmination of several independent studies that led to the conclusion that the Fos and Jun proteins interact as a heterodimeric protein complex at the AP-1/TRE binding site. The initial observation was that of a sequence similarity between the predicted amino acid sequence of the *v-jun* oncogene and the DNA-binding domain of the

yeast transcription factor GCN4 (Vogt *et al.*, 1987). GCN4 induces transcription of several genes involved in amino acid biosynthesis and binds as a dimer to the target sequence ATGA(C/G)TCAT. A region of similarity in c-Jun can replace the binding domain of GCN4 to give a functional transcriptional activator (Struhl, 1988). The name *jun* was given to the oncogene carried by avian sarcoma virus 17 (ASV-17) because *ju-n*ana is the Japanese translation of 17 (Maki *et al.*, 1987). The core DNA sequence recognised by GCN4 is closely related to the mammalian regulatory element known as the AP-1/TRE binding site (Hill *et al.*, 1986; Lee *et al.*, 1987). Similarities between Jun and GCN4 stimulated an investigation of the relationship between Jun and AP-1. Transcription factor AP-1 was described initially as a DNA binding activity in HeLa cell extracts that specifically recognise the enhancer elements of SV40 and the human metallothionein IIA (hMIIA) gene (Lee *et al.*, 1987). AP-1 has subsequently been identified in the control regions of viral and cellular genes that are stimulated following treatment of the cells with a variety of stimulatory agents including serum, NGF, and the calcium ionophore A23187 (Curran and Franza, 1988; Franza *et al.*, 1988). These investigations suggested that AP-1 was involved in many aspects of gene regulation. Indeed, affinity-purified preparations of AP-1 contained several polypeptides in the 35 - 50 KDa range (Rauscher *et al.*, 1988b). The first of these proteins to be identified was the product of the *jun* proto-oncogene, Jun. The *c-jun* promoter contains binding sites for the transcription factor proteins TFIID, Sp1, CTF, AP-1, NF, a related SRF, CREB/ATF-1 and activating transcription factor (ATF) -2 proteins. (a) The TFIID site binds the related SRF, which can mediate the induction of *c-jun* by EGF, TPA and serum. (b) The 3' modified AP-1 motif (*jun 1*) is the main target of Fos:Jun and Jun:Jun dimers. In addition, the transcription of *c-jun* regulated by CREB *in vitro* occurs via the AP-1 site, CREB being an activator following PKA catalysed Ser-133 phosphorylation and a repressor following dephosphorylation. Also, a stable high affinity complex containing ATF-2 and c-Jun proteins can occupy AP-1. Thus, not only do the Jun, Fos and ATF-2 proteins have to compete for dimerisation but also their various dimers have to compete for a particular DNA binding site. (c) The CCAAT-box is recognised by CTFs. (d) The NF site is bound by the NF-Jun protein (nuclear factor-*jun*, a transcription factor with homology to NF-kB) after treatment with TPA, TNF or cycloheximide. (e) In the distal promoter region, a second AP-1-like site, *jun 2*, mediates TPA-induced transcription independently of, or in concert with the proximal *jun 1* site. The *jun 2* site also binds c-Jun:ATF-2 heterodimers tightly, inducing and auto-regulating *c-jun*'s expression and its activation following phosphorylation of ATF-2 and c-Jun via JNK/SAPK

kinases. However, ATF-2 cannot alone confer TPA-inducibility on *c-jun*, showing the requirement for pre-existing AP-1 proteins. Although the *jun 1* and *jun 2* sites differ in only two nucleotides the classical Fos:Jun dimers cannot bind to the *jun 2* response element. It was later found that many AP-1 complexes contained several peptides, which were related to Jun.

The observation by Distel *et al.* (1987) of a protein-DNA complex whose formation was inhibited by anti-Fos antibodies suggested that Fos interacts with a regulatory element of a gene specific for adipocyte differentiation. A combination of studies involving mutagenesis, competition analysis and DNA-affinity precipitation revealed that Fos binds to the AP-1 consensus recognition sequence (Franza *et al.*, 1988; Rauscher *et al.*, 1988c). Indeed, further investigations revealed the presence of several Fos- and Jun-related proteins (Fos-related antigens and p39) and some unrelated proteins in preparations of AP-1 DNA binding activity (Franza *et al.*, 1988). Thus, Fos, Jun and several related proteins were found to interact with a similar nucleotide sequence motif, the AP-1/TRE binding site. While these studies established a connection between Fos, Jun and Ap-1/TRE, it was the identification of p39, the Fos-associated protein, by Rauscher *et al.* (1988b) as the product of the *jun* proto-oncogene, that established the nature of the connection. Thus, it was postulated that Fos and Jun bound together forming a complex, previously identified as AP-1, which then associated with transcriptional control elements containing AP-1/TRE binding sites. Much has been discovered since these early studies and it is now clear that *fos* and *jun* are members of inducible gene families whose protein products form an array of homodimeric and heterodimeric complexes that function as transcriptional regulators by interacting with DNA sequences related to the AP-1 and CRE (ATF binding site) motifs.

1.9 Interaction between Fos and Jun

Neither c-Fos nor c-Jun contain domains previously associated with DNA-binding proteins, such as zinc fingers or helix-turn-helix motifs. Analysis of the DNA binding and dimerisation functions of c-Fos and c-Jun were thus simplified by the proposal of a leucine zipper structure (Landschulz *et al.*, 1988). The leucine zipper was first identified in the C/EBP transcription factor, and was suggested to mediate dimerisation by an interaction of leucine side chains, spaced seven amino acids apart on adjacent α helices. The leucine-zipper structure is found within proteins of the b-zip family. Transcription factors included in this family include Myc, GCN4 and CREB. Mutagenesis studies pointed to a

central role of the leucine zipper in the formation of Fos:Jun heterodimers (Bos *et al.*, 1989; Kouzarides and Ziff, 1988; Ransone *et al.*, 1989). It was found that dimerisation of Jun and Fos proteins occur via hydrophobic interactions between their so-called "leucine-zipper" regions. Studies on synthetic zipper peptides (O'Shea *et al.*, 1989) and comparison of the complementary effect of mutations in Fos and Jun (Gentz *et al.*, 1989) revealed that the zipper most likely represents a parallel association of α helices, somewhat like the coiled-coil structure. This parallel association results in juxtaposition of regions of each protein rich in basic amino acids, both of which contact DNA (Abate *et al.*, 1990). Dimerisation is necessary for DNA-binding activity, and a basic region from each protein is required. In addition to enabling dimerisation, the leucine zipper is believed to hold the basic amino-acid DNA contact surface in the correct three-dimensional orientation and to stabilise it.

There is a degree of specificity among zipper-containing proteins. All members of the Jun family (c-Jun, JunB and JunD) can form both heterodimeric and homodimeric complexes, which bind to the AP-1/TRE binding site. In contrast, c-Fos and Fos-related proteins (FosB, Fra-1 and Fra-2) do not associate with each other and therefore do not bind DNA by themselves. However, the Fos proteins can associate with any member of the Jun family to generate stable heterodimers (Cohen *et al.*, 1989). The transactivational abilities of the various dimers that form at the AP-1/TRE site differ markedly, depending upon their composition. The c-Jun and JunD homodimers bind to AP-1/TRE sites and weakly stimulate transcription (Suzuki *et al.*, 1991). JunB homodimers are almost inactive and only activate transcription from promoters containing multiple AP-1/TRE sites. Therefore, the binding of JunB protein to either c-Jun or JunD results in the formation of Jun heterodimers with lower transactivational ability than c-Jun:c-Jun and JunD:JunD homodimers. The presence of Fos in a Fos:Jun heterodimer increases the affinity of the complex for DNA by increasing the stability of the protein-DNA interaction (Rauscher *et al.*, 1988c; Suzuki *et al.*, 1991). Thus, *IEG* protein products do not act in a vacuum, but rather interact among themselves and with constitutively expressed proteins (such as CREB and members of the activating transcription factor (ATF) family). To summarise, in the case of the b-zip factors, the unstimulated cell has a complete complement of dimers composed of constitutively expressed b-zip proteins, some of which are relatively abundant. Following stimulation, additional b-zip proteins appear and dimerise among themselves and with the constitutive b-zip proteins. This can result in a potential alteration of the transcriptional activity of the complex as well as the DNA sequences that they bind

to. B-zip proteins exhibit varying degrees of cell and tissue specificity, that is, depending on the cell type, the somewhat stereotyped panel of *IEG* proteins interacts with a different cast of constitutive b-zip proteins.

1.10 Regulation of immediate-early response in PC12 pheochromocytoma cells

Rat adrenal PC12 pheochromocytoma cells were first used as a model to investigate the biochemical and molecular genetic events that accompany neuronal differentiation (Greene and Tischler, 1982). In the undifferentiated state, PC12 cells resemble their normal counterparts, neural crest-derived precursor cells. Upon NGF stimulation, PC12 cells undergo a diverse set of molecular and gross morphological changes and assume the phenotype of a sympathetic neuron, including extensive neuritic outgrowth. The process of NGF-induced differentiation is accompanied by alterations in gene expression, thereby raising the question of how the extracellular growth factor is coupled to the intracellular transcriptional machinery. This consideration led several groups to investigate the effects of NGF on cellular *IEG* expression. It was found that NGF elicited a rapid and transient induction of *c-fos* in PC12 cells (Curran and Morgan, 1985; Greenberg *et al.*, 1985; Milbrandt, 1986). These investigations paved the way for further research into *c-fos* and related *IEGs* in the nervous system. In addition to NGF, a diverse array of agents have been shown to induce *c-fos* expression in PC12 cells, including EGF, depolarising stimuli and cyclic AMP analogues (Greenbeg *et al.*, 1985; Morgan and Curran, 1986).

Although most of the initial studies concentrated on *c-fos* alone, immunoprecipitation analyses revealed that the levels of p39 (Jun) also transiently increased following treatment of PC12 cells with NGF. Thus, both *c-jun* and *c-fos* are transcriptionally activated shortly after application of NGF to PC12 cells.

These studies in PC12 cells led several groups to examine whether *IEGs* were expressed in the nervous system *in vivo* (Morgan *et al.*, 1987; Dragunow and Robertson, 1987). These and other studies established that cellular *IEGs* were naturally expressed in the CNS and that their expression could be dramatically increased following the application of various types of stimuli, ranging from surgical trauma, through seizures, to neuropharmacological interventions, sensory stimulation and behavioural challenges.

The earliest example of neurotransmitter–mediated induction of *c-fos* involved the opening of voltage-sensitive Ca^{2+} channels (VSCCs) after membrane depolarisation induced by nicotinic receptor activation in PC12 cells (Greenberg *et al.*, 1986). The resulting increase in intracellular Ca^{2+} was believed to lead to the increase in *c-fos* expression. Increased

intracellular Ca^{2+} produced by other methods also resulted in *c-fos* expression, suggesting that increases in the concentration of intracellular Ca^{2+} leads to the activation of cellular mechanisms that then regulate the expression of *IEGs* (Morgan and Curran, 1986). In contrast, NGF mediated induction of *c-fos* gene expression in PC12 cells does not require the entry of extracellular Ca^{2+} ions. The pathway from growth factor activation of its receptor to *c-fos* induction involves the activation of protein kinase C. Thus, at least three distinct second-messenger systems activate *c-fos* expression, namely those involving diacylglycerol-protein kinase C (Greenberg *et al.*, 1986), cyclic AMP (Greenberg *et al.*, 1985) and calcium-calmodulin (Morgan and Curran, 1986; see Figure 1.8).

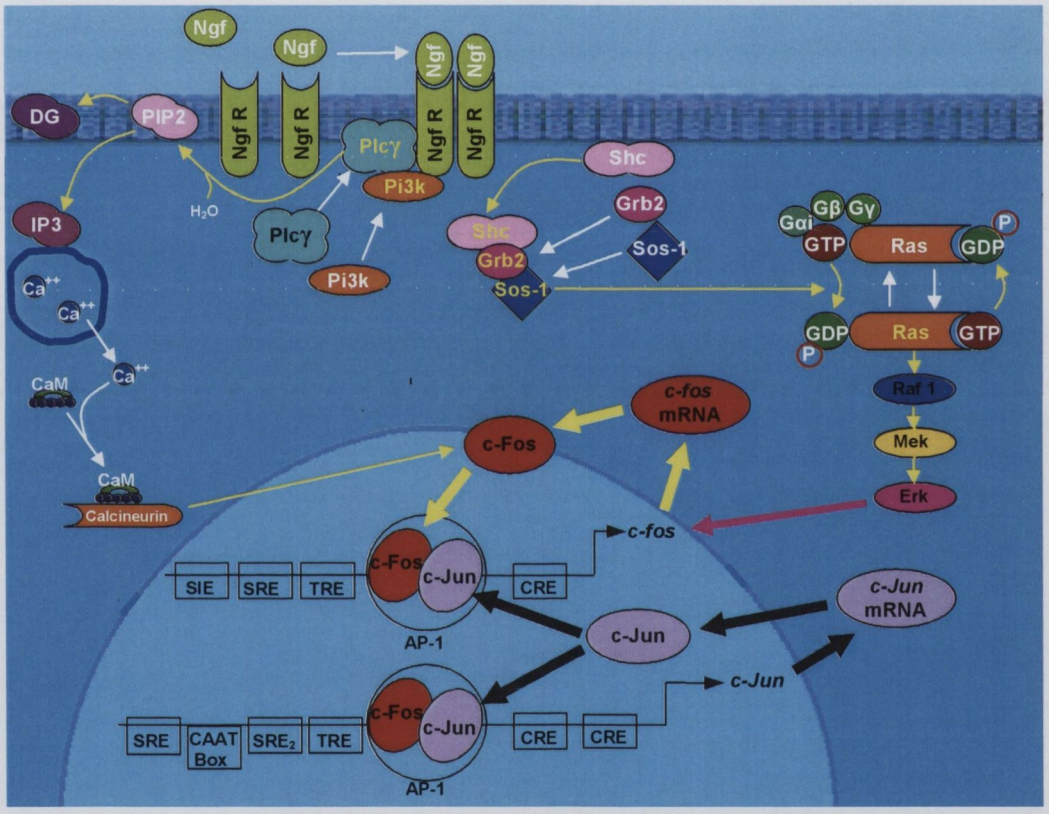


Figure 1.8: Diagram showing the effects of NGF on cellular *IEG* expression

NGF activates a number of second messenger systems whose end kinases phosphorylate pre-existing inducible transcription factors. The phosphorylated c-Fos and c-Jun transcription factors translocate to the nucleus and dimerise to form an AP-1 complex. The AP-1 complex binds to the AP-1 DNA binding site and induces the synthesis of further *IEG* mRNAs and/or initiates the ordered expression of various target genes.

1.11 Neurophysiological correlates of *IEG* induction

In the CNS, diverse physiological and pharmacological stimuli when presented once or on multiple occasions can alter the "normal" functioning of the brain in a permanent or semi-permanent fashion. In many cases, these same stimuli activate inducible transcription factors of the *IEG* family. Examples of pharmacological stimuli that lead to long-term changes are the highly addictive psychostimulant drugs amphetamine and cocaine. These drugs produce rapidly induced expression of *IEGs*, for example, *c-fos*, *junB* and *egr-1*, in what are believed to be the neural substrates of addiction (Beretta *et al.*, 1993; Nestler *et al.*, 1993; Moratalla *et al.*, 1993). In animal models of neuro-plasticity, such as ischaemia, seizures, kindling and long-term potentiation, activation of *IEG* transcription factors is observed following delivery of the inducing stimuli (Dragunow and Robertson, 1987a, 1987b; Hughes *et al.*, 1999; Dragunow *et al.*, 1989, 1992). *IEGs* are also activated by non-invasive stimuli, such as a simple light pulse, given to animals in a darkened environment. Animals housed in these darkened conditions can have their circadian rhythms shifted by exposing them to a light during their subjective night. These are some of the many examples, which illustrate the association between stimuli, which lead to changes in brain function, and the activation of *IEGs*, such as *c-fos*, in the CNS.

1.11.1 Ischaemic Cerebral cell death

In order to understand the patho-physiological mechanisms underlying stroke in man, two animal models of stroke have been developed to represent the two main types of ischaemic cell death, that is, global and focal ischaemia. In global ischaemia models, the lack of blood flow is transient (5 - 30 min) but complete. If blood flow is not restored within 30 min, pannecrosis occurs and there is no functional recovery of the tissue. Selective neuronal death of pyramidal neurons in the CA1 region of the hippocampus, cerebellar Purkinje neurons and medium-sized striatal neurons occurs following reperfusion within 30 min. The sensitivity of these neurons to ischaemia differs between brain regions, as does the time course of cell death (Pulsinelli *et al.*, 1982). CA1 pyramidal neurons are more sensitive to ischaemia than striatal neurons but after a severe global ischaemic insult (30 min), the more resistant striatal neurons begin to die after 3 to 12 hours of reperfusion whereas the more sensitive CA1 neurons remain viable for 2 to 3 days before succumbing to the insult. This model most closely represents the clinical situation of a cardiac arrest or near drowning.

The focal models are a closer representation of the clinical situation in which a localised and more prolonged ischaemic period occurs, resulting from the occlusion of an individual cerebral blood vessel. The pattern of focal ischaemia is not as severe as that of global ischaemia. There is a central core region, closest to the occluded vessel, which results in immediate pannecrosis if reperfusion does not occur within 60 min of the occlusion. Surrounding the edge of the core is a region referred to as the penumbra, which is hypoperfused and is at risk of dying but can be salvaged with increased perfusion and/or pharmacological intervention. In the absence of intervention, the penumbra begins to die within 3 to 4 hours of reperfusion. This cell loss is restricted to neurons; glial cells do not die (reviewed by Small *et al.*, 1999).

Within seconds of the onset of ischaemia, the decline in blood flow and the subsequent loss of oxygen supply result in the reduction of high-energy metabolites such as ATP and phosphocreatine (Hansen, 1985; Choi, 1990). The combination of ATP breakdown and compensatory activation of anaerobic glycolysis during ischaemia leads to an increase in the levels of inorganic phosphate, lactate and H^+ formation causing cellular acidification. The depletion of neuronal ATP also results in the loss of Na^+ gradients, normally maintained by the ATP-dependent membrane Na^+ - K^+ pump (Hansen, 1985). The resulting depolarisation triggers Ca^{2+} influx through voltage-sensitive Ca^{2+} channels that further depolarises the membrane and stimulates the release of excessive amounts of the excitatory neurotransmitter, Glu, into the extracellular space. Normally, neurons are exposed to only brief pulses of Glu because excess extracellular Glu is actively returned to presynaptic terminals and glial cells by the Glu uptake system (Drejer *et al.*, 1982). During ischaemia, however, the energy-dependent mechanisms responsible for Glu re-uptake are impaired; hence extracellular Glu can approach concentrations of up to 100 μM. The elevated extracellular Glu induces the excessive activation of Glu receptors, primarily the NMDA subtype of the ionotropic Glu receptors, stimulating the further influx of Ca^{2+}. Glu also induces Ca^{2+} influx through the activation of Ca^{2+} channels secondary to the transmitter-evoked depolarisation of the membrane. These events all occur during ischaemia and in the early period of reperfusion (as reviewed by Small *et al.*, 1999). In the hours to days following an ischaemic insult, there is a disruption of Ca^{2+} homeostasis that leads to the activation of a series of Ca^{2+}-dependent processes, activation of kinases, induction of *IEGs* and mitochondrial dysfunction. Both focal and global cerebral ischaemia rapidly and transiently increases the expression of the *IEGs c-fos*, *junB*, *c-jun* , *junD*, *Krox-20* and *krox 24* (Herdegen and Leah, 1988)

1.11.2 Seizures

The long-term responses of the brain to chemical and electrical stimulation have served as useful models to gain insight into the molecular mechanisms underlying neural plasticity. Different types of seizures are dynamic behavioural manifestations of excessive activation of distinct brain regions. Electroconvulsive seizures (ECS) depend on activation of the motor cortex, whereas most chemically induced seizures occur, at least initially, via activation of limbic structures (Mc Namara, 1994). A motor seizure is characterised by clonic jerking of major muscle groups of the body. In contrast to limbic seizures, which occur via activation of excitatory pathways in limbic brain structures (for example, the hippocampus and amygdala), motor seizures depend on activation of NMDA Glu receptor subtypes in the motor cortex. Increasing evidence suggests that chemically and electrically induced seizures rapidly increase the expression of *IEGs* in mouse and rat brain.

In the first two studies investigating chemically induced seizures, the convulsant drug pentylenetetrazole was found to induce *c-fos* mRNA and protein firstly in nuclei of neurons of the dentate gyrus, pyriform and, subsequently, throughout cortex, hippocampus and the limbic system (Morgan *et al.*, 1987; Dragunow and Robertson, 1987a). The time-course of *c-fos* mRNA induction *in vivo* was protracted compared with that in serum-stimulated fibroblasts and in PC12 cells treated with NGF. Induction of *c-fos* mRNA was refractory to additional seizure-mediated induction, whereas Fos-like protein immunoreactivity remained induced throughout the brain. Fos-like immunoreactivity was increased only in neurons and not glia (Morgan *et al.*, 1987).

Hiroi *et al.* (1998) reported that chronic ECS resulted in an increase of approximately 70% in AP-1 binding activity in rat frontal cortex. A FosB/ΔFosB antibody disrupted the chronic AP-1 complex, whereas antibodies directed against c-Fos, Fra-1 or Fra-2 were without effect. An anti-JunD antibody also disrupted the chronic AP-1 complex, whereas an anti-cJun antibody was without effect. An anti-JunB antibody produced a small but consistent decrement in levels of AP-1 binding. Thus, these results indicated that the chronic AP-1 complex was composed predominantly of a FosB/ΔFosB protein coupled to JunD, and to a lesser extent JunB. It was also reported by Hiroi *et al.* (1998) that a single acute (2 hours later) ESC induced four major Fos-like proteins, that is, c-Fos, FosB, Fra-1 or Fra-2 and ΔFosB.

1.11.3 Kindling

Kindling is produced by a series of repeated, sub-convulsive electrical stimuli that eventually results in the formation of a state whereby the same sub-convulsive stimulus elicits a fully generalised seizure. A notable aspect of this process is that once the kindled state is achieved, it is "permanent" in that the animal will continue to experience seizures in response to the initially sub-convulsive stimuli throughout its lifetime. Kindling is a useful animal model for human epilepsy and for studies of the development of hyperexcitability that underlies the generation and spread of seizures (Goddard *et al.*, 1969). Kindling has also been considered a model for learning and memory, and the mechanisms that underlie facilitation of synaptic transmission (Glanzman *et al.*, 1990). Focal electrical stimulation (usually to the amygdala or hippocampus) results in a brief focal seizure or electrically induced afterdischarge (AD). The AD is an absolute prerequisite for kindling to occur.

IEGs have been implicated in the coupling of neuronal excitation to changes in target gene expression and have been reported as being rapidly induced following relatively brief periods of neuronal excitation. It is believed that such gene changes may play a role in the development, but not necessarily the maintenance, of the kindling process since the responses seen are transient. Within the cerebral cortex, a single kindling AD results in the strong induction of *c-fos, c-jun* and *egr-1* (Duman *et al.*, 1992). Amygala kindling also induces increased expression of *c-fos* mRNA and c-Fos protein (Teskey *et al.*, 1991), *c-jun*, *junB*, *krox-24* mRNA and protein and Krox-20 protein (Hughes *et al.*, 1994). Labiner *et al.* (1993) reported that the presence of *c-fos* mRNA expression in hippocampal dentate granule cells 30 min following a seizure, which was selectively and markedly inhibited by the NMDA receptor antagonist, MK-801. The distribution of *IEG* expression depends upon the stage of kindling and the length of the AD (Teskey *et al.*, 1991). Because induction is transient, with basal levels reached for all *IEGs* investigated by 48 hours (Morgan and Curran, 1991; Dragunow *et al.*, 1992), the *IEGs* are thought to exert their effect by providing a link between brief periods of neuronal activation and adaptive/plasticity responses in the brain by altering the expression of other genes. For example, the expression of proteins believed to be involved in neuronal structure and function, such as GAP43, are induced by seizures (Bendotti *et al.*, 1993; Meberg *et al.*, 1993). In addition, it was demonstrated that the absence of a functional *c-fos* allele resulted in a reduction in mossy fiber sprouting and attenuated kindling (Watanabe *et al.*, 1996). This implied c-Fos as positively contributing to epileptogenesis, perhaps by facilitating sprouting.

1.11.4 Long-term potentiation

Long-term potentiation (LTP), first described in 1973 by Bliss and Lomo, refers to the long-lasting enhancement of synaptic efficacy that can be achieved by certain forms of pre-synaptic stimuli. The induction of LTP in the hippocampus requires activation of the NMDA subtype of Glu receptors (Collingridge and Bliss, 1987; Bliss and Collingridge, 1993). Upon binding Glu, Mg^{2+} dissociates from its binding state within the NMDA receptor channel, allowing the influx of both Na^{+} and Ca^{2+} ions into the dendritic spine (Ascher and Nowak, 1988). The consequent rise of intracellular Ca^{2+} is the critical trigger for LTP. Chelating intracellular Ca^{2+} with EGTA prevents the induction of LTP indicating that Ca^{2+} influx through the NMDA receptor is a necessary first step for this form of cellular plasticity (Lynch *et al.*, 1983; Malenka *et al.*, 1988). A similar requirement for NMDA receptor activation and calcium influx has been shown for the induction of LTP in cortical slices (Mooney *et al.*, 1993).

The mechanisms by which Ca^{2+} influx leads to long-term adaptive responses are not well understood. One attractive hypothesis is that brief periods of appropriate stimuli lead to the Ca^{2+}-dependent activation of novel patterns of gene expression, which ultimately alter the physiological state of the cell. Two lines of evidence suggest the possibility that gene expression is required for long-term adaptive responses. First, a number of stimuli that led to long-term changes in physiology or function in the nervous system also led to rapid changes in gene expression (Cole *et al.*, 1989). Second, there is evidence that learning-related phenomena also induce *IEG* formation in the brain (Kaczmarek, 1993a, 1993b). For example, hippocampal *c-fos* mRNA levels in rats are increased three-fold immediately after training to attain foot-shock-motivated brightness discrimination in a Y-maze. The elevated levels of *c-fos* mRNA had returned to basal levels after 2 hours. Apamin, a bee venom neurotoxin that can improve learning and memory retention, enhanced the learning induced increase in *IEG* expression within the hippocampus (Heurteaux *et al.*, 1993).

1.12 EAA induced *c-fos* expression is NMDA receptor mediated

The activation of EAA receptors sensitive to Glu was suggested to play a pivotal role in the development of trans-synaptically induced neuronal plasticity in both *in vivo* and *in vitro* models used to study learning and memory consolidation, where a role for Ca^{2+} and Ca^{2+}-dependent enzyme (such as PKC) signalling had been proposed. These observations prompted Szekely *et al.* (1989) to investigate whether the stimulation of specific Glu receptors induce the expression of the proto-oncogene, *c-fos*, in primary

cultures of rat cerebellar granule cells (CGCs). It was found that a brief exposure to low levels of Glu rapidly induced the expression of *c-fos* mRNA, which was transient in nature. It is probable that this transient expression was part of the gene regulation of adaptive neuronal change. In addition, this Glu-induced transient *c-fos* expression could be prevented by specific NMDA receptor antagonists, such as AP5, PCP and Mg^{2+} but was potentiated by glycine. Thus, these results indicated the activation of the NMDA-subtype of Glu receptor as being responsible for triggering the nuclear induction of *c-fos*.

1.13 Role for *c-fos* in excitotoxicity ?

As discussed previously, the NMDA subtype of Glu receptor is strongly associated with long term modification of neuronal function, including learning and memory (Morris *et al.*, 1986), and also with neuropathological processes such as seizure activity and excitotoxicity (Lipton and Rosenberg, 1994). EAA receptor-mediated "excitotoxic" cell death is thought to be the main cause of several human neuropathological disorders such as stroke, Parkinson's and Alzheimer's disease. Taken together, these observations and the fact that *c-fos* was also found in experimental models of chemically and electrically induced seizure activity suggested that *c-fos* may have a role in excitotoxic mechanisms of neuronal cell death. In support of this hypothesis, Smeyne *et al.* (1993) reported that following excitotoxic lesion, *c-fos* was continuously expressed preceding programmed cell death *in vivo*. In addition, a more delayed and prolonged phase of *IEG* expression was observed in CA1 pyramidal cells suffering irreversible neuronal injury (Dragunow *et al.*, 1994). In accordance with these findings of a continuous *c-fos* expression, Gorman *et al.* (1995), observed that exposure of primary cultures of mature mouse cerebellar granule cells (mCGCS) to toxic concentrations of Glu correlated with the appearance of a delayed and elevated expression of *c-fos* mRNA which was sustained for at least four hours. EAAs that did not exhibit toxicity in granule cells, for example AMPA, caused only a rapid, transient increase in *c-fos* mRNA levels (Griffiths *et al.*, 1997). Furthermore, the pharmacology of excitotoxin-induced, sustained increases in *c-fos* mRNA levels was examined and it was shown that selective antagonism of the NMDA receptor but not AMPA/KA receptors prevented excitotoxic cell death, underlining a strong NMDA receptor involvement in excitotoxicity. Thus, these findings indicated that excessive exposure results in a switch from transient to prolonged, and even delayed *c-fos* induction and implied that the measurement of *c-fos* mRNA could be used as a mechanistically relevant molecular biomarker for *in vitro* excitotoxic cell death.

Griffiths *et al.* (1997) extended this hypothesis by the proposal of a predictive test based on the different patterns of *c-fos* expression found in the non-excitotoxic versus excitotoxic state. Two time-points were chosen, 30 min (representing non-excitotoxic transient *c-fos* expression) and 240 min (representing the "excitotoxic" pattern of delayed, sustained and elevated *c-fos* mRNA expression), and a ratio ($Q^{240/30}$) of *c-fos* expression was used to predict the exitotoxic outcome. It was proposed that a $Q^{240/30} > 1$ correlated with excitotoxic cell death, whereas a $Q^{240/30} < 1$ correlated with non-excitotoxicity. The robustness of the ratio method as a predictive index of excitotoxicity was supported by a number of criteria (a) it was successfully applied to both mCGCs (Gorman *et al.*, 1995) and cortical neurons (Meredith *et al.*, 1996), (b) it gave a positive correlation with the known excitotoxic potentials of a number of EAAs (Glu, NMDA, KA and S-sulpho-L-cysteine (L-SSC)) and (c) a positive correlation was seen with the prevention of excitotoxicity in response to the selective NMDA receptor antagonist, AP5 (Griffiths *et al.*, 1997). Thus, the strong correlation found to exist between NMDA receptor-mediated excitotoxic cell death and the appearance of a delayed, elevated and sustained profile of *c-fos* mRNA expression was used to design an *in vitro* test, based on early response gene measurement, for the assessment of excitotoxicity. The *in vitro* test was based on the measurement of *c-fos* mRNA levels by Northern blot analysis. For the test to be accepted as a valid and robust predictor of an excitotoxic outcome three criteria were required to be satisfied (a) a presumed excitotoxic compound must exhibit an elevated *c-fos* mRNA 240/30 min ratio greater than 1 (b) neurotoxic but non-excitotoxic compounds, or compounds that were non-toxic, should give ratios less than 1 and (c) the excitotoxin induced elevation of the *c-fos* mRNA ratio should be prevented in the presence of a Glu receptor antagonist.

The fidelity of the test was further evaluated by the application of the test to a selection of compounds that were subdivided into four groups (excitotoxins (Group 1), neurotoxic but non-excitotoxic compounds (Group 2), neuroactive but non-toxic compounds (Group 3) and compounds that were toxic to other target organelles (Group 4)), based on their known or presumed actions (Griffiths *et al.*, 2000). The test was satisfied as only the excitotoxins exhibited elevated *c-fos* mRNA 240/30 min ratios under excitotoxic conditions with ratios less than 1 in the presence of the NMDA receptor antagonist, N-[1-(2-thienyl)cyclohexyl]-piperidine (TCP). The remaining three groups were classified correctly, according to the criteria of the test, as non-excitotoxic.

The role of the *c-fos* proto-oncogene in excitotoxicity is uncertain as is the reason behind the pattern of delayed, elevated and sustained expression of *c-fos* mRNA under excitotoxic conditions. It can only be speculated that the increase may be related to the Ca^{2+} perturbations in the process of excitotoxicity; indeed, increases in intracellular levels via L-type voltage-activated Ca^{2+} channels or following influx via the NMDA-receptor ion channel complex are known to be linked to the induction of *c-fos* through a variety of intracellular Ca^{2+}-dependent enzyme systems (Bading *et al.*, 1993; Ghosh and Greenberg, 1995). It was also reported by Griffiths *et al.* (1998) that the route of Ca^{2+} entry, via dihydropyridine-sensitive, non-inactivating L-type channels, is responsible for the altered temporal profile in steady-state *c-fos* mRNA measurements. It seems also that the induced *c-fos* mRNA and Fos protein may transcriptionally regulate or dysregulate other more specific delayed response genes, some of which might function as more toxic factors (Tatter *et al.*, 1995; Ginty, 1997).

1.14 Role for *fosB* in excitotoxicity ?

Up to now, considerable attention has focused on the involvement of *c-fos* and its product, the c-Fos protein, in EAA mediated excitotoxicity. However, several studies (Greenberg *et al.*, 1998; Lidwell *et al.*, 2000) have implicated *fosB*, another member of the *fos* family of *IEGs*, as being selectively expressed under excitotoxic conditions. Indeed, Hou *et al.* (1997) showed that stimulation of rat cerebellar granule cells with a cytotoxic concentration of NMDA, or AMPA in the presence of cyclothiazide (to prevent receptor desensitisation), was associated with the expression of the FosB protein, with Jun-D and c-Fos also being detected as components of AP-1 complexes under these conditions. Lidwell *et al.* (2000) reported that using gel supershift analysis of nuclear extracts derived from mCGCs, exposed to an excitotoxic concentration of Glu in the presence of the NMDA receptor antagonist TCP, anti-FosB antibody was unable to disrupt the AP-1 complex. TCP is a non-competitive antagonist of the NMDA receptor and acts to prevent Ca^{2+} influx by blocking the receptor-associated ion channel. Thus, these results imply a role for NMDA-receptor mediated Ca^{2+} influx in the regulation of *fosB* expression in cultured mCGCs and, furthermore, the involvement of *fosB* in excitotoxicity.

It has been established that two different forms of *fosB* mRNA can be generated by alternative splicing of the transcript from a single gene (Mumberg *et al.*, 1991; Yen *et al.*, 1991; Nakabeppu & Nathans, 1991). The longer transcript (*fosB*) codes for a protein of 338 amino acids in length, termed FosB (45 KDa), while the shorter transcript (*ΔfosB*)

encodes a truncated form of FosB known as ΔFosB (37 KDa). *ΔfosB* mRNA results from a deletion of 101 bases from the carboxy-terminus of the *fosB* transcript. This deletion shifts the reading frame by a single base, creating the in-frame stop codon TGA. As a result, ΔFosB is only 237 amino acids in length and lacks the last 101 amino acids found in FosB. Present within this truncated region is the major activating region of FosB. ΔfosB, therefore, lacks the potent transcriptional activating properties of FosB, although the DNA binding activity and the ability to dimerise with Jun proteins are retained.

1.15 Is excitotoxic cell death apoptotic or necrotic?

In addition to its vital role as a neurotransmitter, Glu at high levels is excitotoxic to neurons. Elevated extracellular Glu induces the excessive activation of Glu receptors on cell dendrites, primarily the NMDA subtype (and AMPA) of the ionotropic Glu receptors, which in turn leads both directly and indirectly to a sustained depolarisation and the influx of intracellular Ca^{2+}. Glu also induces Ca^{2+} influx through the activation of voltage sensitive Ca^{2+} channels secondary to the transmitter-evoked depolarisation of the membrane. Subsequently, the transmembrane flux of Ca^{2+} through both the NMDA receptor and voltage-activated Ca^{2+} channels results in an increased concentration of intracellular Ca^{2+} triggering a signalling cascade that culminates in transcriptional activation of *c-fos*. Following the excitotoxic insult, there is a disruption of the internal homeostasis that leads to cytoskeletal alterations, impaired Glu uptake, the activation of Ca^{2+}-dependent kinases, endonucleases and proteases, and mitochondrial dysfunction. These events occur before Glu-induced cell death in several neuronal cell types. However, the mode of cell death following injury induced by EAAs remains controversial. Overstimulation of neuronal Glu receptors typically leads to rapid, dramatic cell body and dendrite swelling, mediated by excessive Na^{+} and Ca^{2+} entry through Glu receptor gated channels, associated with Cl^{-} and water influx. Several lines of evidence suggest that cell death occurs by one of two general pathways, necrosis or apoptosis. Necrosis and apoptosis are distinct mechanisms of cell death with very different characteristics. Necrosis is associated with non-physiological conditions such as catastrophic toxic or traumatic events with passive cell swelling, uncontrolled Ca^{2+} overload, random DNA fragmentation, injury to cytoplasmic organelles including mitochondria, energy loss and rapid collapse of internal homeostasis, all of which are associated with excitotoxicity.

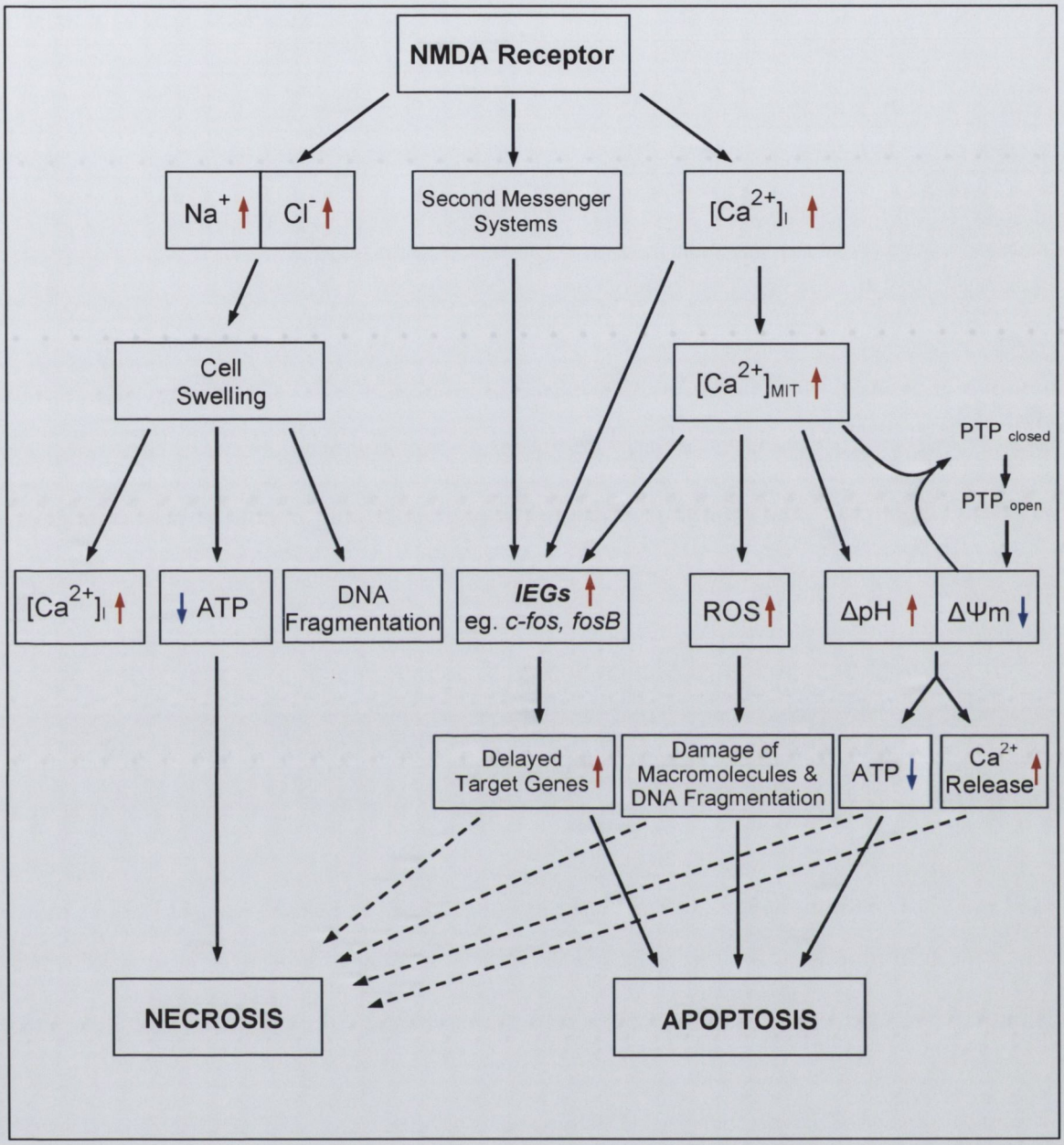


Figure 1.9: Over-activation of the NMDA receptor had detrimental consequences

Ionotropic NMDA-receptor mediated excitotoxicity, occurs across a continuum of insult-dependent injury involving apoptosis and necrosis. The "acute" necrotic phase, which is Na^+ and Cl^- dependent, results in the build-up of a sodium chloride intracellular pool leading to the movement of water, swelling of the cell and acute osmotic damage The delayed, apoptotic phase of neurodegeneration is Ca^{2+} dependent and is possibly mediated by a transmembrane influx of Ca^{2+} into neurons.

Necrosis terminates in membrane lysis, release of cellular contents and resulting inflammation (Kerr and Harmon, 1991; Schwartz *et al.*, 1993). In contrast, apoptosis is an active process of cell destruction and is characterised morphologically by cell shrinkage, membrane blebbing, and, if a nucleus is present, nuclear pyknosis, chromatin condensation and genomic fragmentation (see Figure 1.9; Kerr *et al.*, 1972; Choi and Rothman, 1990; Kerr and Harmon, 1991). Some forms of apoptosis require metabolic energy to synthesise de novo RNA and protein (Oppenheim, 1991), whereas other forms are produced by constitutively expressed proteins (Raff *et al.*, 1993; Eastman, 1993).

A biochemical hallmark of cells undergoing apoptosis is double strand DNA cleavage by activation of endonucleases to produce oligonucleosomal-length fragments, which are revealed as a DNA pattern on agarose gel electrophoresis. A major difference between the two types of cell death is the generalised involvement of neighbouring cells or synaptically connected neurons in the degeneration of wide expanses of neuronal circuits by necrosis. To prevent leakage of EAAs, proteolytic enzymes, DNA, and oxidised lipids with a pro-inflammatory response, apoptotic cells condense their chromatin, shrink, and in so-doing preserve their external and internal membranes until phagocytosis intervenes (Kerr and Harmon, 1991).

The idea that excitotoxin-induced neuronal death is necrotic rather than apoptotic had received support from various studies of neurons in culture. Dessi *et al.*, (1993) demonstrated the absence of either descriptive or interventional features of apoptosis in cultured mCGCs undergoing Glu-induced excitotoxic cell death. Didier *et al.*, (1996) found that excitotoxicity in mCGCs was associated with DNA damage progressing from single-strand breaks with low-grade excitotoxicity, to double-strand breaks with more intense excitotoxicity. Indeed, Gasull *et al.* (2000) reported that overactivation of the NMDA subtype of Glu receptor releases choline, by inhibition of phosphatidylcholine synthesis, which precedes and is directly related to excitotoxic necrotic neuronal death.

However, several other studies have suggested that exposure to excitotoxins can induce neuronal apoptosis. Some neurons degenerating after intraparenchymal injection of excitotoxins exhibit chromatin condensation and internucleosomal DNA fragmentation (Portera-Cailliau *et al.*, 1995; Pollard *et al.*, 1994; Filipkowski *et al.*, 1994). Additionally, caspases 1 and 8 (Culmsee *et al.*, 2001), and the pro-apoptotic proteins Par-4 (Mattson *et al.*, 2000; Culmsee *et al.*, 2001) and Bax (Eilers *et al.*, 1999), have been reported as being involved in Glu-induced apoptosis.

Bonofoco *et al.* (1995) reported that intense excitotoxic insults produced clear-cut necrosis, whereas milder excitotoxic insults induce some apoptotic changes, including internucleosomal DNA fragmentation. Consistent with this view, Choi (1996) reported that despite a lack of accompanying morphological or interventional features, internucleosomal DNA fragmentation was detected transiently during slowly triggered (but not rapidly triggered) excitotoxicity, reflecting incomplete triggering of apoptosis by lower levels of excitotoxic injury. Cheung *et al.* (1998) reported that at concentrations of Glu < 20 μM acute rapid swelling of neurons was not observed and death was exclusively by apoptosis, as shown by electrophoretic evidence of cycloheximide-sensitive DNA fragmentation and morphological evidence of neurite blebbing and cell shrinkage. However, necrosis began to occur in the presence of apoptosis at intermediate concentrations (20 – 50 μM) of Glu, and was eventually the sole death process as the insult became extreme (> 50 μM). Thus, these reports are indicative of ionotropic NMDA-receptor mediated neurotoxicity, subsequent to exposure to Glu, occurring across a continuum of insult-dependent injury involving apoptosis and necrosis.

Another factor, which may decide the mode of neuronal death, is the appearance of *IEG* encoded transcription factors and the subsequent formation of the AP-1 complex following EAA insult. Many, but not all, of the protein products of *IEGs* regulate gene expression by acting as DNA-binding transcription factors. *IEG* encoded transcription factors are expressed in a protein-synthesis-independent fashion after cell stimulation and therefore are induced rapidly and transiently. For example, following a brief exposure to non-toxic concentrations of Glu, *c-fos* is rapidly and transiently expressed in primary cultures of mCGCs, by activation of the NMDA subtype of Glu receptor (Szekely *et al.*, 1989; Malcolm *et al.*, 1997; Griffiths *et al.*, 1997). However, the shut-off of *c-fos* transcription requires new protein synthesis; a typical feature of apoptosis, which requires that energy must be expended by the neurons. Therefore, it can be speculated that the transient expression of *c-fos* under non-excitotoxic conditions could act as an initial event in the apoptotic suicide program. Furthermore, other members of the *fos* and *jun* families of *IEGs* have been implied in neuronal apoptosis. In cultured cortical neurons, in which apoptosis is induced by amyloid-β peptide, there is a strong expression of *c-jun*, *junB*, *c-fos* and *fosB*, but not of *fra-1* or *junD* (Herdegen and Leah, 1998). In NGF-deprived PC12 cells, degeneration is accompanied by a persisting expression of *c-jun*, but only a transient expression of *c-fos* and *krox-24* (Mesner *et al.*, 1995). Moreover, c-Jun

neutralising antibodies prevented NGF-deprived neurons from undergoing apoptosis (Estus *et al.*, 1994).

In contrast, exposure of mouse CGCs to toxic concentrations of Glu was found to correlate with a change in the kinetics of *c-fos* induction, from a transient expression to that of a more delayed, elevated and sustained *c-fos* expression, indicating a more intense role for *c-fos* or its product, Fos, in mediating necrotic cell death under excitotoxic conditions (Malcolm *et al.*, 1997; Griffiths *et al.*, 1997, 1998, 2000). In addition, continuous *c-fos* induction and the subsequent prolonged potentiation of AP-1 DNA binding have been reported *in vivo* following excitotoxic lesion initiated by treatment with KA (Smeyne *et al.*, 1993; Pennypacker *et al.*, 1994, 1995) or QA (Shan *et al.*, 1997).

The elevated and sustained nature of the excitotoxic *c-fos* response may reflect the dimerisation of the *c-fos* product, Fos, with the products of other members of the *jun* family of *IEGs*, thereby leading to a concomitant accumulation of AP-1 binding proteins which (a) activate the expression of late response target genes whose products are then thought to serve more specific effector functions in the excitotoxic neuronal response, and (b) maintain the continued expression of *c-fos*. In addition to *c-fos*, Lidwell *et al.* (2000) recently reported the FosB/JunD AP-1 transcription factor complex as having an exclusive role in mature cultures of murine CGCs undergoing Glu-mediated excitotoxicity, while c-Fos and c-Jun were detected under both excitotoxic and non-excitotoxic conditions.

The redox state, dimerisation partner and phosphorylation and/or dephosphorylation state of the *IEG* encoded transcription factors may be responsible for determining and regulating their actions. In addition, the necessity and sufficiency of a gene in mediating apoptotic or necrotic cell death is likely to depend on other factors such as the levels of kinases, peptides and phosphatases.

Aims of this study

Glu is the major excitatory neurotransmitter in the vertebrate CNS. The excitatory responses of this endogenous excitotoxin are mediated by a number of pharmacologically and functionally distinct cell-membrane receptors that are, the ionotropic NMDA, KA and AMPA receptors as well as the metabotropic receptors. Activation of Glu receptors has been linked to the establishment of synaptic networks, formation of associative and motor memory and induction of long-term potentiation. However, excessive activation of the NMDA subtype of Glu receptor, in particular, is thought to initiate the process of excitotoxicity, which is reported as having an important role in the pathophysiology of a number of neurodegenerative disorders, such as Huntington's, Parkinson's and Alzheimer's-disease.

Although the molecular basis of excitotoxic cell death remains elusive, studies of neurotoxicity in cultured neurons have established important roles for intracellular ionic changes caused by Glu, especially in the influx of Na^+ and Ca^{2+} ions, which in turn trigger a signalling cascade that culminates in the transcriptional activation of a number of *IEGs*. These genes encode nuclear proteins that, by interacting with regulatory DNA elements of neuronal target genes, can function as third messengers bringing about transcriptional activation or repression. Several studies have now shown that *c-fos* is transiently induced following NMDA receptor activation. Futhermore, Gorman *et al.* (1995) first reported that excessive excitotoxic activation of the NMDA receptor changes the profile of *c-fos* to that of an elevated and sustained expression. These results were later confirmed by Malcolm *et al.* (1995), Meredith *et al.* (1996), and Griffiths *et al.* (1997, 1998, 2000). Thus, *c-fos* may be an important and early component of the molecular mechanism that leads to excitoxicity.

All of the above studies employed the technique of Northern blot analysis, which does not allow a sensitive quantification of the relative levels of a particular transcript. Recent advances in the use of fluorescent DNA binding dyes, for example SYBR® Green, in conjunction with real-time RT-PCR have enabled the measurement of an accumulating PCR product in real-time. This allows the rapid generation of quantitative data showing changes in the levels of transcripts. In addition, Affymetrix high density, two-dimensional arrays, which contain synthetic oligonucleotides, enable the analysis of thousands of mRNA transcript levels from a single sample. This state-of-the-art design strategy uses an average of 16 - 20 pairs of 25-mer oligonucleotide probes to interrogate each target

sequence, resulting in highly specific, extremely sensitive, quantifiable gene expression data. The combination of these two methods therefore provides a more quantitative assessment of *c-fos* in excitotoxicity, and also may uncover other related and unrelated *IEGs* that could act as additional markers and endpoints in the mechanism of excitotoxicity. Thus, the aims of this project were

(1) To set up two different primary cell culture models, mouse cerebellar granule cells (mCGCs) and rat cortical neurons, and to show their suitability for studying excitotoxicity by characterising the excitotoxic effects of Glu, Asp and NMDA on cell viability, mitochondrial membrane potential and intracellular ATP levels.

(2) To investigate whether *c-fos* mRNA could be quantitatively measured in these models of mCGCs and rat cortical neurons using the technique of real-time RT-PCR in order to provide a non-radioactive, high throughput, lower animal usage model for *in vitro* testing of excitotoxins.

(3) To compare and contrast *c-fos* mRNA expression in the mouse and rat models.

(4) To use real-time RT-PCR, to investigate whether other members of the *fos* (*fosB, fra-1 and fra-2*) and *jun* (*c-jun, junB and junD*) families of *IEGs* may be involved in excitotoxicity.

(5) To confirm and enhance our findings of RT-PCR with an alternative independent method, that is, the use of high-density DNA microarrays, which contain oligonucleotide probes for thousands of genes including members of the *fos* and *jun* families of *IEGs*, and thereby also uncover other potential biomarkers important in the molecular mechanisms of neurotoxicity and excitotoxicity.

Chapter 2

Materials and Methods

2.1 Materials

The full names and addresses of the sources listed below are given at the end of the list.

ABI Prism Optical Adhesive Cover Starter Pack	Applied Biosystems
Acetylated Bovine Serum Albumin solution	Invitrogen Life Technologies
Agarose (Electrophoresis grade)	Invitrogen Life Technologies
Ammonium acetate (7.5 M)	Sigma
Antibody (IgG) Goat	Sigma
Anti-streptavidin antibody goat, biotinylated	Vector Laboratories
ATP Lite™-M kit	Packard Bioscience B.V.
B27	Invitrogen Life Technologies
Bovine serum albumin (BSA)	Sigma
Bromophenol blue–Xylene Cyanole dye	Sigma
Control Oligo B2 (30 nm)	Affymetrix Inc.
Cytosine arabinoside	Sigma
D-AP5	Tocris
D-glucose	Sigma
D-Homocysteic acid	Sigma
Dimethylsulfoxide (DMSO)	Sigma
DNA polymerase I	Invitrogen Life Technologies
DNAse	Sigma
dNTP (10 mM) mix	Invitrogen Life Technologies
Dulbecco's modified Eagle's medium	Invitrogen Life Technologies
Dulbecco's phosphate buffered saline (PBS)	Sigma
EDTA Disodium salt (0.5 M)	Sigma
ENZO® BIOarray™ HighYield™ RNA Transcript labelling Kit	Affymetrix Inc.
Ethidium Bromide	Sigma
Foetal calf serum (FCS)	Harlan Sera Lab.
Gamma-amino-butyric acid	Sigma
Gene Chip® Rat Expression Array	Affymetrix Inc.
Gene Chip® Mouse Expression Array	Affymetrix Inc.
GeneChip® Sample Cleanup Module	Affymetrix Inc.

Giemsa	Merck
Glutamine (200 mM)	Invitrogen Life Technologies
Glycine	Sigma
Glycogen (20 µg/µl)	Boehringer Ingelheim
HEPES	Sigma
Herring Sperm DNA	Sigma
Insulin	Sigma
Kainic acid	Sigma
L-Alanine	Sigma
L-Aspartic acid	Sigma
L-Cysteine sulphinate	Sigma
L-Glutamic acid	Sigma
L- Homocysteic acid	Sigma
L-Homocysteine sulphinate	Sigma
Magnesium acetate	Sigma
MES Free Acid Monohydrate Sigma Ultra	Sigma
MES Sodium Salt	Sigma
MicroAmp® Optical 96-Well Reaction Plate & Caps	Applied Biosystems
MPP^+ Iodide	Sigma
MTT	Sigma
N-methyl-D-aspartic acid	Sigma
Neurobasal™ culture medium	Invitrogen Life Technologies
Oligo (dT) 12-18 Primer	Invitrogen Life Technologies
p-Aminobenzoate	Sigma
Paraquat	Riedel-deHaën over Sigma
Penicillin-streptomycin (5000 U/ml)	Invitrogen Life Technologies
Phase-lock-gel microcentrifuge tubes	Eppendorf
Phenol Red	Sigma
Poly-D-Lysine coated culture plates	Biocoat Becton and Dickinson
Poly-D-Lysine	Sigma
Potassium acetate	Sigma
Quisqualic acid	Sigma
R-phycoerythrin-streptavidin (SAPE)	Molecular Probes
Ribogreen™RNA Quantitation kit	Molecular Probes

Ribogreen™RNA Quantitation reagent	Molecular Probes
RNA 6000 Labchip® Kit	Agilent Technologies
RNase-Free DNase Set	Qiagen
RNaseOUT™	Invitrogen Life Technologies
RNeasy Mini Kit	Qiagen
RNeasy® 96 kit	Qiagen
RNeasy® Midi kit	Qiagen
S-Sulpho-L-cysteine	Sigma
Sodiumhydrogencarbonate	Merck
Soybean trypsin inhibitor	Sigma
SSPE buffer (20X)	Ambion
Superscript™ Double-Stranded cDNA synthesis kit	Invitrogen Life Technologies
Superscript™ First-Strand synthesis system for RT-PCR	Invitrogen Life Technologies
Superscript™ II Rnase H^- RT	Invitrogen Life Technologies
SYBR® Green PCR and RT-PCR kit	Applied Biosystems
T7-d(T) 24 Oligo	Geneset Oligos
TAE (50X) buffer	Invitrogen Life Technologies
TE buffer	Molecular Probes
Tetramethylrhodamine dye	Molecular Probes
Tris/EDTA buffer (pH 8.0)	Sigma
Trizol	Invitrogen Life Technologies
Trypsin	Sigma
Tween 20 (10%)	BioRad

NIH 3T3 cells were kindly provided by Dr. Gabriele Scholz, Toxicology, Bayer AG. All PCR primers were synthesized by Invitrogen Life Technologies.

Addresses of suppliers

Affymetrix UK Limited, Voyager, Mercury Park, Wycombe Lane, Wooburn Green, High Wycombe, HP10 0HH, United Kingdom.

Agilent Technologies, Deutschland GmbH, Friedrichstraße 50, 10117 Berlin, Germany.

Ambion (Europe) Ltd, Spitfire Close, Ermine Business Park, Huntingdon, Cambridgeshire, PE29 6XY, United Kingdom.

Applied Biosystems, Applera GmbH, Brunnenweg 13, D-64331 Weiterstadt, Germany.

Becton Dickinson Labware Europe, Becton Dickinson France S.A., 11 rue Aristide Bergès, BP4, 38800 Le Pont De Claix, France.

BIO-RAD Laboratories GmbH, Heidemannstraße 164, D-80939 München, Germany.

Boehringer Ingelheim GmbH, 55216 Ingelheim, Germany.

Eppendorf Vertrieb Deutschland GmbH, Peter-Henlein Straße 2, 50389 Wesseling-Berzorf, Germany.

Geneset Oligos, Proligo France SAS, 1 rue Robert et Sonia Delaunay, 75011 Paris, France.

Harlan Sera-Ltd., Crawley Down, RH10 4FF, United Kingdom.

Invitrogen GmbH, Technologiepark Karlsruhe, Emmy-Noether Straße 10, 76131 Karlsruhe, Germany.

Merck KgaA, Frankfurter Straße 250, D-64293 Darmstadt, Germany.

Molecular Biologische Technologie, Mo Bi Tec, Wagenstieg 5, D-37077 Göttingen, Germany.

Qiagen GmbH, Max-Volmer Straße 4, 40724 Hilden, Germany.

Sigma-Aldrich GmbH, Kappelweg 1, D-91625 Schnelldorf, Germany.

Tocris, Eupener Straße 157, D-50933, Köln, Germany.

Vector Laboratories Inc., 30 Ingold Road, Burlingame, CA 94010, USA.

2.2 Primary neuronal cell culture

2.2.1 Preparation of primary cultures of mouse cerebellar granule cells (mCGCs)

This procedure is based on the technique developed by Messer (1977) and modified by Meier and Schousboe (1982), Drejer *et al.* (1983) and Schousboe *et al.* (1989). The basic strategy for the preparation of this type of neuronal culture is to take cerebella from the 7-day-old mice, that is, a developmental stage at which the other types of cerebellar neurons have reached the differentiation (post-mitotic) stage of development, whereas granule cells are still capable of undergoing mitosis (Hertz *et al.*, 1985). In addition, glial cells at this developmental stage are still in the mitotic phase, but this cell type can be eliminated from the cultures by treatment with cytosine arabinoside, a pyrimidine anti-metabolite that inhibits DNA synthesis. The advantage of this type of culture is that it consists of at least 90% granule cells, which are characterised as glutamatergic neurons, that is, they synthesize, store and release Glu and Asp upon stimulation (Schousboe *et al.*, 1985).

Solutions 1 - 4 (see below) were prepared immediately prior to the mCGC isolations. A small volume of *Solution 1* (1.5 ml), containing BSA (1.2%) and $MgSO_4$ (4.65 mM) dissolved in PBS buffer, was transferred to a sterile Petri-dish (35 mm) placed on ice. Under sterile conditions, the post-natal mice (7 days old) were sacrificed by decapitation. Whilst the head was secured with one pincer, a scissors was used to make two inclined cuts on each side of the head. The protective skin surrounding the brain matter meninges was then peeled back and the brain exposed. The cerebella were aseptically removed and placed into the Petri-dish, containing Solution 1, on ice. Following dissection, the cerebella were transferred, using a forceps, onto a sterile Teflon disc and the tissue finely sliced (using alternate perpendicular cuts) with a sharp blade. The fragmented tissue was transferred, using a sterile Pasteur pipette, into a tapered centrifuge tube (50 ml) containing a minimal volume of Solution 1. The tissue was triturated a number of times before a brief centrifugation at 1000 rpm for 60 s (200 g). Following centrifugation, the supernatant was gently removed and *Solution 2* (20 ml) containing trypsin (0.025% w/v) and DNase (0.004% w/v) dissolved in PBS buffer, used to suspend the pellet. The capped tube, containing the suspension, was placed in a shaking water-bath (37°C) for 15 min. During the incubation, the tube was inverted at regular intervals of 5 min. Immediately afterwards *Solution 4* (20 ml), containing DNase (0.004% w/v) and soybean trypsin inhibitor (0.052% w/v) dissolved in PBS buffer, was added to the cell suspension, the tube

was capped and slowly inverted (3 times). The tube was then centrifuged at 1000 rpm (200 g) for 5 min. Following centrifugation, the supernatant was discarded. *Solution 3*, containing DNase (0.004% w/v), soybean trypsin inhibitor (0.052% w/v) and $MgSO_4$ (1.5 mM), was added to the pellet (2 ml/10 cerebella) and the pellet was triturated (10 times) under pressure using a sterile glass pipette (the pipette tip was firmly pressed against the bottom of the centrifuge tube throughout). The suspension, which appeared cloudy, was allowed to stand for 5 min to allow for the sedimentation of clumps. The supernatant, containing the single dissociated cells, was then added with a Pasteur pipette into a centrifuge tube (50 ml) containing sterile Dulbecco's modified Eagle's medium (DMEM, 6 ml), supplemented with KCl (19 mM), D-glucose (34 mM), $NaHCO_3$ (26.2 mM), glutamine (0.8 mM), *p*-aminobenzoic acid (7.3 µM), insulin (4 ng/ml), Penicillin-Streptomycin (50 U/ml) and FCS (10% v/v, heat inactivated). The supplemented DMEM was referred to as N-DMEM. Any remaining clumps were re-suspended in a small volume of Solution 3 and triturated. The solutions of single cells were combined and centrifuged at 1000 rpm (200 g) for 5 min. Following centrifugation, the supernatant was discarded and sterile N-DMEM used to suspend the pellet (10 ml per 10 cerebella). A small volume (10 µl) of the cell suspension was removed in order to determine the cell density. The cell suspension was then diluted with sterile N-DMEM to the appropriate cell density. The cells were transferred at a cell density of 1×10^6 cells per well in a 24 well pre-coated poly-D-lysine plate (Becton and Dickenson), with a final volume of 1 ml per well, and cultured at 37°C in a humidified atmosphere of 5% CO_2/95% air. Cytosine arabinoside (20 µM final concentration) was added to the cultures 48 hours after seeding to prevent the proliferation of non-neuronal cells. The culture media was not changed during the period of culturing, which was normally 7 days. Cultures were used after 7 - 8 days *in vitro*, at which time they functionally represent mature cerebellar granule neurons (Hertz and Schousboe, 1987).

2.2.2 Preparation of primary cultures of rat cortical neurons

Pregnant Wistar rats were sacrificed by asphyxiation, the foetuses (E18 - E19) immediately removed from the uterus and placed in a Petri-dish on ice. Under sterile conditions, the foetuses were removed from their enveloping embryonic sacs and decapitated. Whilst the head was stabilised with one pincer, another pincer was used to remove the outer layers of protective cartilage surrounding the brain matter. The cortex was dissected from the whole brain tissue under a stereo-microscope (Leica MIO) with a

sterile pincer and subsequently ensheated from the cerebral membrane. The tissues were pooled in sterile Neurobasal medium (Gibco), supplemented with B27 (2%) and Penicillin-Streptomycin (50 U/ml). The isolation of single cells from the collective cortical tissues was performed by filtration of the neuronal cells through two Nylon meshes of different pore diameters (135 and 25 µm). The filtrate, consisting of a single-cell suspension of cortical neurons, was centrifuged for 5 min at 1000 rpm (200 g). The cell pellet was suspended in the culture medium (10 ml) and the cell number counted. The cells were plated onto 24 well pre-coated poly-D-lysine plates (Becton and Dickenson) at a cell concentration of 1×10^6 cells per well and a final volume of 1.5 ml. Since, initially, the optimal time in culture was unknown, the cells remained in culture for 7 to 13 days before testing. The cultures consisted of 90 - 95% neurons and 5 - 10% glial cells. These data were determined by immunohistochemistry (Schmuck and Schlüter, 1996) using NSE and GFAP antibodies.

2.3 Growth and treatment of permanent NIH 3T3 mouse fibroblasts

NIH 3T3 mouse fibroblasts were grown at 37°C under a humidified atmosphere of 5% CO_2/95% air in 75 cm^2 flasks containing DMEM medium supplemented with heat inactivated foetal calf serum (FCS; 10% v/v) and Penicillin-Streptomycin (50 U/ml). Confluent cultures were rendered quiescent by incubation for 12 - 18 hours in DMEM containing FCS (0.5% v/v, heat inactivated). The cells were then trypsinised, transferred to 100 mm sterile Petri-dishs and grown for 24 hours before treatment. The 3T3 cells were treated with either of 2 concentrations of 12-*o*-tetradecanoylphorbol-13-ester (TPA), 0.3 µM or 3 µM, over a time-course of 15 to 120 min. At the indicated times after stimulation, medium was aspirated and the cells lysed by the addition of lysis buffer (Qiagen).

2.4 Neurotoxicity assays

2.4.1 MTT assay

The 3-[4,5-dimethylthiazol-2-yl]-2,5-diphenyltetrazolium bromide (MTT) assay measures the viability of cells on the basis of mitochondrial dehydrogenase activity. MTT is yellowish in colour when dissolved in balance salt solution without phenol red. Mitochondrial dehydrogenases of viable cells selectively cleave the tetrazolium ring yielding blue/purple formazan crystals. The crystals are dissolved in acidified isopropanol and the resulting

colour read spectrophotometrically. A decrease in absorbance when compared to control cells provides a quantitative assessment of cell damage.

Primary cultures of mCGCs and rat cortical neurons were isolated and seeded at a density of 1×10^6 cells per well as described in Sections 2.2.1 and 2.2.2, respectively. Experiments were undertaken on cells at 7 days *in vitro* (DIV), in the case of mCGCs, and between 7 - 13 DIV in the case of the rat cortical neurons. For pharmacological investigations, the neurons were pre-incubated with a fixed concentration of AP5 (500 µM) or CNQX (10 µM), for 15 min before exposure to the test compounds. All compounds were initially prepared at 50X the final required concentration in HEPES (10 mM) or the appropriate solvent and adjusted to pH 7.4. The compounds were then adjusted to 25X in medium, so that a final volume of 40 µl added to 1 ml culture medium for mCGCs (or 60 µl added to 1.5 ml medium for rat cortical neurons) gave the required final concentration. Concurrent control wells were always on the same 24 well culture dish as treatments. Cells were then incubated at 37°C in a humidified atmosphere of 5% CO_2/95% air for the designated time period.

To assay for cytotoxicity, 100 µl of MTT solution (final concentration 0.5 mg/ml in PBS) was added to each well. The plate was incubated in the dark for 2 hours at 37°C in a humidified atmosphere. After the incubation period, the total solution of medium and MTT was carefully removed by aspiration. 500 µl of 0.04 M HCl in anhydrous iso-propanol was added to each well followed by 100 µl SDS (3% w/v). The plate was shaken for 15 min, to ensure solubilisation of the blue/purple formazan crystals, and then allowed to stand at room temperature for 15 min. Absorbance was measured at 570 nm and 630 nm in a spectrophotometer (Tecan Ultra). Results were expressed as the percentage of blue formazon absorbance compared with untreated control neurons, which were assumed as having 100% viability.

2.4.2 Measurement of mitochondrial membrane potential ($\Delta\psi_m$)

Mitochondrial membrane potential was assessed using the fluorescent dye tetramethylrhodamine (Molecular Probes). A decrease in fluorescence in comparison to control cells provides a quantitative assessment of loss of $\Delta\psi_m$.

Primary cultures of rat cortical neurons were isolated and seeded at a density of 1×10^6 cells per well (1.5 ml final volume) as described in Section 2.2.2. Experiments were undertaken on cells at 13 DIV. When pharmacology was tested, the neurons were pre-incubated with a fixed concentration of AP5 (500 µM) or CNQX (10 µM), for 15 min,

before exposure to the test compounds. All compounds were initially prepared at 50X the final required concentration in HEPES (10 mM) or the appropriate solvent and adjusted to pH 7.4. The compounds were then adjusted to 25X in medium so that a final volume of 60 µl added to 1.5 ml medium gave the required final concentration. Concurrent controls were run on the same 24 well culture plate as treatments. Cells were incubated at 37°C in a humidified atmosphere of 5% CO_2/95% air for 24h before being assayed for loss of $\Delta\psi_m$. Tetramethylrhodamine (final concentration 3.3 µM) was added to each well of the 24 well culture plate. The cells were incubated with the dye for 30 min at 37°C. Following incubation the cells were washed with PBS buffer. Following washing, a volume of PBS buffer was added to each well (200 µl per well) and the fluorescence measured using a multi-well spectroflurometer (Tecan Ultra) at an excitation wavelength of 555 nm and an emission wavelength of 585 nm.

2.4.3 ATP determination

ATP is a marker for cell viability because it is present in all metabolically active cells and the concentration declines very rapidly when the cells are damaged. The intracellular ATP concentration was determined with chemiluminescence using an ATPLite™-M kit (Packard Bioscience B.V). The ATPLite™-M assay system is based on the production of light caused by the reaction of ATP with added luciferase and D-luciferin. The assay is based on luciferases requirement for ATP in producig light and the emitted light is proportional to the ATP concentration.

Primary cultures of mCGCs and rat cortical neurons were isolated and seeded at a density of 1×10^6 cells per well as described in Sections 2.2.1 and 2.2.2, respectively. Experiments were undertaken on cells at 7 DIV, in the case of mCGCs, and between 10 - 13 DIV in the case of rat cortical neurons. When pharmacology was tested, the neurons were pre-incubated with a fixed concentration of AP5 (500 µM) or CNQX (10 µM), for 15 min, before exposure to the test compounds. All compounds were initially prepared at 50X the final required concentration in HEPES (10 mM) or the appropriate solvent and adjusted to pH 7.4. The compounds were then adjusted to 25X in medium so that a final volume of 40 µl added to 1 ml culture medium for mCGCs (or 60 µl added to 1.5 ml medium for rat cortical neurons) gave the required final concentration. Control wells were always present on the same 24 well culture plate as treatments.

The treated cells were incubated at 37°C in a humidified atmosphere of 5% CO_2/95% air for either 4 or 24 hours before the intracellular ATP concentration was measured.

Following incubation, the medium was carefully removed by aspiration. PBS (100 µl) followed by "Cell lysis solution" (50 µl, supplied in the kit) was added to each well in the plate. The plate was shaken for 2 min. The total solution of cells in PBS and lysis solution was pipetted into a white 96 well plate and "substrate solution" (50 µl; provided with the kit) added. The plate was incubated in the dark for 10 min at 37°C and then the luminescence measured in a plate-luminometer (Tecan Ultra).

2.4.4 Morphological observation of the neurons using the Giemsa stain

Staining experiments were performed on 7 DIV mCGCs and 13 DIV rat cortical neurons. All compounds were initially prepared at 50X the final required concentration in HEPES (10 mM) or the appropriate solvent and adjusted to pH 7.4. The compounds were then adjusted to 25X in medium so that a final volume of 40 µl added to 1 ml culture medium for mCGCs (or 60 µl added to 1.5 ml medium for rat cortical neurons) gave the required final concentration. Treated cells were then incubated at 37°C in a humidified atmosphere of 5% CO_2/95% air for 24 hours, before being stained with Giemsa.

The medium was firstly removed from the cells by snap-inversion. The cells were then fixed with methanol (200 µl per well) for 15 min. During the 15 min fixation period, the Giemsa solution was diluted (1/7) and filtered. The adherent cells were then coated with the dye (100 µl) and allowed to stand at room temperature for 13 min. The stained cells were washed with distilled water and allowed to dry before being observed under the light microscope (Leica Fluovert Fu) and photographed (Wild Leitz camera).

2.5 Isolation of total RNA from animal cells

2.5.1 Isolation of total RNA from primary cells with a Qiagen RNeasy 96 Kit

The isolation of total RNA from mouse and rat primary neurons was performed with the use of an RNeasy 96 Kit (Qiagen), according to the manufacturer's instructions. Cells were first lysed under highly denaturing conditions with guanidine isothiocyanate (GITC), which immediately inactivated any RNases and ensured the isolation of intact RNA. Ethanol was added to provide appropriate binding conditions and the samples were then applied to the wells of the RNeasy 96 well plate. Total RNA bound and contaminants were efficiently washed away. An on-column DNase step allowed digestion of any small amounts of residual DNA remaining on the columns. High-quality RNA was then eluted in

a small volume of water, ready for use in downstream RT-PCR or micro-array applications.

The RNase-Free DNase Kit (Qiagen) was used to prepare a DNase I solution (214 Kunitz units), immediately before the total RNA isolation, which was mixed by gentle inversion and maintained on ice.

Lysis buffer (350 µl), containing β-mercaptoethanol (0.145 M) to avoid RNA degradation, was added to the cells in each well of the cell culture plate (24 well plate) and the cells sheared by passage of the lysate, 5 - 10 times, through an 18 - 20 gauge needle fitted to an RNase-free syringe. Following shearing, ethanol (70%; 350 µl) was added to each lysate and mixed thoroughly by trituration (3x). The RNeasy 96 well plate was placed on top of a plastic collecting box and cell lysate in ethanol (maximum of 700 µl) applied to each well. The surface of the RNeasy plate was covered with adhesive tape and the plate centrifuged, at room temperature, for 4 min at 5600 g. The adhesive tape was removed after centrifugation and the DNase I mix (80 µl) was loaded directly onto the RNeasy membrane of each well in the RNeasy 96 plate. The plate was sealed and allowed to stand, on ice, for 15 min. RW1 buffer (800 µl) was then added to each well in the RNeasy plate, the tape reapplied and the plate centrifuged for 4 min at 5600 g. The RNeasy 96 plate was then placed on a fresh collecting block and the tape removed. RPE buffer with ethanol (100%, 800 µl) was added to each well and the tape reapplied. The plate was again centrifuged for 4 min at 5600 g. The flow-through was discarded and the tape removed. RPE buffer with ethanol (100%, 800 µl) was again added per well and the plate was centrifuged for 10 min at 5600 g. The flow-through was discarded.

In order to elute the total RNA, RNase-free water (50 µl) was added to each well of the RNeasy plate and the plate was allowed to stand, on ice, for 2 min. The plate was then centrifuged for 4 min at 5600 g. Following centrifugation, RNase-free water (50 µl) was again added and the plate centrifuged at 5600 g for 4 min. The total volume of RNA eluted was 100 µl and the eluted RNA was immediately placed on ice. Typically 3 replicate wells were pooled following total RNA isolation giving a total volume of 300 µl per sample with a concentration of 25 – 35 µg/ml. The isolated total RNA was stored at –80°C.

2.5.2 Isolation of total RNA from a mouse cell line with a Qiagen RNeasy Midi Kit

The isolation of total RNA from NIH 3T3 mouse fibroblasts was performed with the use of an RNeasy Midi Kit (Qiagen), according to manufacturer's instructions. An on-column DNase step allowed digestion of any small amounts of residual DNA remaining on the

columns and also genomic DNA. The RNase-Free DNase Kit (Qiagen) was used, according to the manufacturer's instructions, to prepare a DNase I stock solution (967.7 Kunitz units) immediately before the total RNA isolation, which was mixed gently by inversion and maintained on ice.

3T3 fibroblasts, grown in 35 mm cell-culture vessels, were lysed by the direct addition of lysis buffer (2 ml), containing β-mercaptoethanol (0.145 M). The cells were sheared by passage of the lysate, 5 - 10 times, through an 18 – 20 gauge needle fitted to an RNase-free syringe. Following shearing, 1 volume of ethanol (70%; 2 ml) was added to each lysate and mixed thoroughly by triturating 3 times. The lysates (plus ethanol) were then applied to RNeasy Midi spin columns, with one sample per column (maximum of 4 ml), the columns were capped and then centrifuged, at room temperature, for 5 min at 5000 g. RW1 buffer (2 ml) was added to each spin column and the columns were centrifuged at 5000 g to wash. The flow-through was discarded. An aliquot of the DNase I stock solution (20 µl) was diluted with RDD buffer (140 µl; provided in the RNase-Free DNase Kit) and applied directly onto each spin-column membrane. The columns were allowed to stand, at room temperature, for 15 min. After the incubation, RW1 buffer (2 ml) was added and the columns were centrifuged for 5 min at 5000 g. The flow-through was discarded and RPE buffer, containing 100% ethanol (2.5 ml) was added. The columns were centrifuged for 2 min at 5000 g and the flow-through was discarded. A second volume of RPE buffer (2.5 ml) in ethanol was added to each column and this time the columns were centrifuged for 10 min at 5000 g, to dry the spin-column membrane. The flow-through was discarded.

In order to elute the total RNA, the RNeasy columns were transferred to new RNase-free collection tubes (15 ml). RNase-free water (150 µl) was added directly onto each column membrane and the columns were allowed to stand, on ice, for 2 min. The columns were then centrifuged for 3 min at 5000 g. The elution step was repeated with a second volume of RNase-free water (150 µl) and the columns centrifuged at 5000 g for 3 min. The total volume of RNA eluted was 300 µl and the eluted RNA was immediately placed on ice. The isolated total RNA was stored at –80°C.

2.6 Quantitation and quality control of total RNA isolated from animal cells

2.6.1 Preparation of an RNA Standard curve

A 1X Tris EDTA (TE) buffer solution was first prepared by diluting the concentrated TE buffer (20X), provided in the Ribogreen™RNA Quantitation kit (Molecular Probes), with

RNase-free water. Ribogreen dye in anhydrous DMSO (1 ml; provided with the kit) was diluted by a factor of 200 with RNase-free water and covered with aluminium foil to protect from light, as Ribogreen is susceptible to photo-degradation.

A stock of 16S and 23S ribosomal RNA (100 µg/ml; provided with the kit) was thawed and used to prepare the RNA standards. This stock was diluted 1:50 with 1X TE buffer and used to prepare the following standards: 1.00 µg/ml, 0.50 µg/ml, 0.10 µg/ml, 0.02 µg/ml and 0.00 µg/ml (blank) according to the scheme below. These standards (100 µl) were pipetted, in triplicate, into a 96 well fluorometric plate and diluted 1:2 with the Ribogreen dye solution. The plate was shaken for 3 min in the dark before the fluorescence was measured using a fluorescence multi-well plate reader (CytoFluor™II) at an excitation wavelength of 535 nm and an emission wavelength of 485 nm (see Figure 2.1).

TE buffer (µl)	RNA (µl)	Ribogreen (µl)	Final RNA Conc. (200 µl)
0 µl	100 µl	100 µl	1 µg/ml
50 µl	50 µl	100 µl	0.5 µg/ml
90 µl	10 µl	100 µl	0.1 µg/ml
98 µl	2 µl	100 µl	0.02 µg/ml
100 µl	0 µl	100 µl	Blank

2.6.2 Total RNA quantitation

Solutions of isolated total RNA (see Section 2.5) were quantitated using the fluorescent nucleic acid stain, "Ribogreen" (as in section 2.6.1). An experimental RNA probe was serially diluted in 1X TE buffer on ice, with a final volume of 100 µl, and the dilution factor which compared the sample most to the standard curve was chosen for all the remaining probes. For both mCGCs and rat cortical neurons, seeded at 1×10^6 cells per well, a dilution factor of 1:100 was chosen.

Each experimental RNA sample (2 µl) was pipetted, in triplicate, into a 96 well fluorometric plate on ice, and diluted with 1X TE buffer (98 µl). The RNA standards (100 µl) were also pipetted, in triplicate, onto the same fluorometric plate. Ribogreen dye solution (100 µl) was added to all wells and the plate shaken for 3 min before the fluorescence was measured using a multi-well spectroflurometer at an excitation wavelength of 535 nm and an emission wavelength of 485 nm.

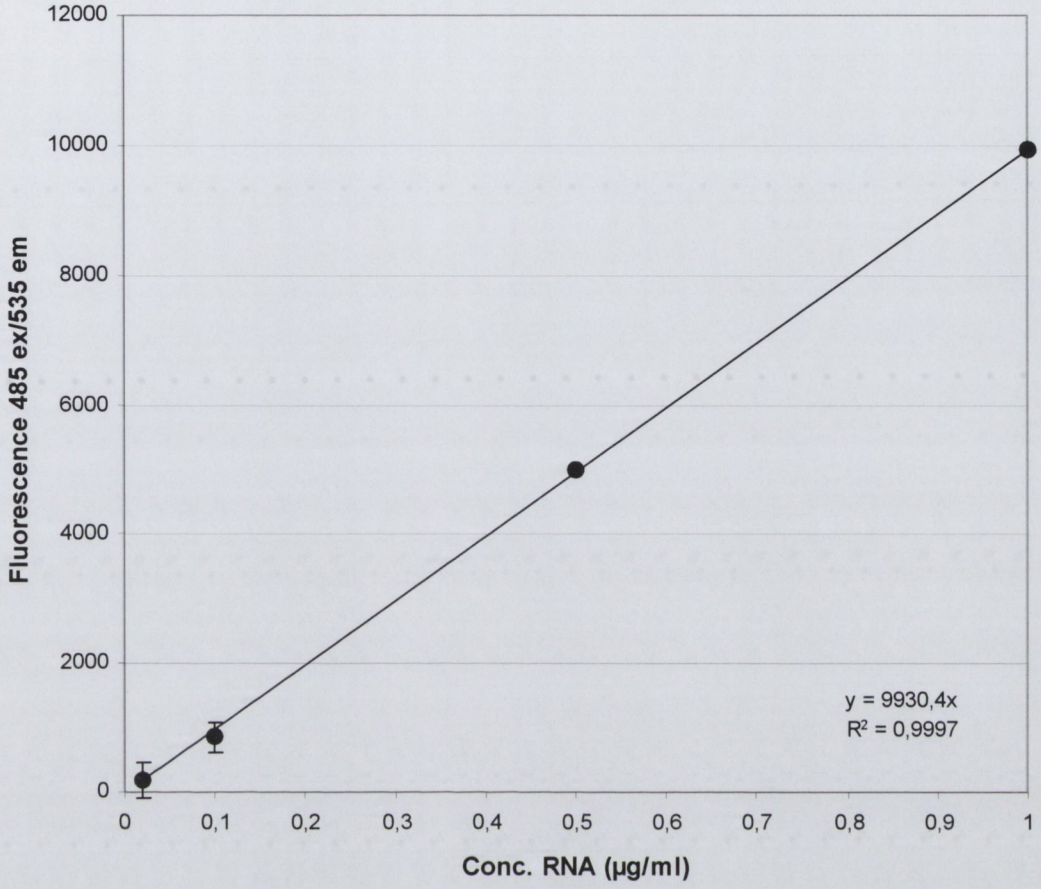


Figure 2.1: RNA standard curve

A stock of 16S and 23S ribosomal RNA (100 µg/ml) was diluted 1:50 with 1X TE buffer and used to prepare the following standards; 1.00 µg/ml, 0.50 µg/ml, 0.10 µg/ml, 0.02 µg/ml and 0.00 µg/ml (blank). These standards (100 µl) were pipetted, in triplicate, onto a 96 well fluorometric plate and diluted 1:2 with Ribogreen dye solution (see Section 2.6.1). The plate was shaken for 3 min in the dark before the fluorescence was measured using a multi-well spectrofluorometer at an excitation wavelength of 485 nm and an emission wavelength of 535 nm.

2.6.3 Quality control of total RNA isolated from animal cells

The quality of the experimental total RNA probes, isolated from animal cells as described in Section 2.5, was controlled using an RNA 6000 LabChip Kit (Agilent Technologies). An RNA LabChip contains an interconnected set of micro-channels that, when filled with a gel matrix, sieves nucleic acids by size as they are forced through it by means of electrophoresis. The RNA LabChip kit was used in correlation with the Agilent 2100 bio-analyser system.

A gel-dye solution was first prepared. RNA dye (4 µl) was added to an RNA gel matrix (400 µl) in a micro centrifuge tube (1.5 ml). The solution was vortexed and transferred to a spin filter. The solution was centrifuged at 1000 g for 10 min, the spin filter was removed and the gel-dye mix protected from light. The gel-dye mix was stored at 4°C for 4 weeks.

An RNA LabChip was placed on the chip priming station. The gel-dye mix (9 µl) was pipetted into the well-marked "G" on the chip. The priming station was then closed and the plunger on the station pressed down until held by the clip. The plunger was maintained in this position for 30 s and the clip released. The priming station was opened and the chip checked for air bubbles. The gel-dye mix (9 µl) was pipetted into the two top right-hand wells. Sample buffer (5 µl) was pipetted into the 12 sample wells followed by 1 µl of each experimental total RNA sample and 1 µl of an RNA ladder. The chip was vortexed for 1 min before being run in the Agilent 2100 bioanalyser. For successful quality control, using the RNA LabChip kit, each experimental total RNA sample must show 2 ribosomal peaks (18S and 28S).

2.7 Reverse Transcription

Synthesis of cDNA from total RNA is the first step in the two-step reverse transcription polymerase chain reaction (RT-PCR) gene expression quantification experiment. The Superscript™ First-Strand Synthesis kit (Invitrogen Life Technologies) was used in this study to produce single-stranded cDNA from total RNA.

Normally, for the relative quantitation of target genes to 18S, two separate reverse transcription (RT) master-mixes are required– one master-mix containing oligo dT primers to amplify the target of interest and a separate master-mix containing random hexamers to amplify 18S (the internal control). However, a new RT reaction was designed in this study, which contained the two primer sets, oligo dT primers and random hexamers, in the same reaction.

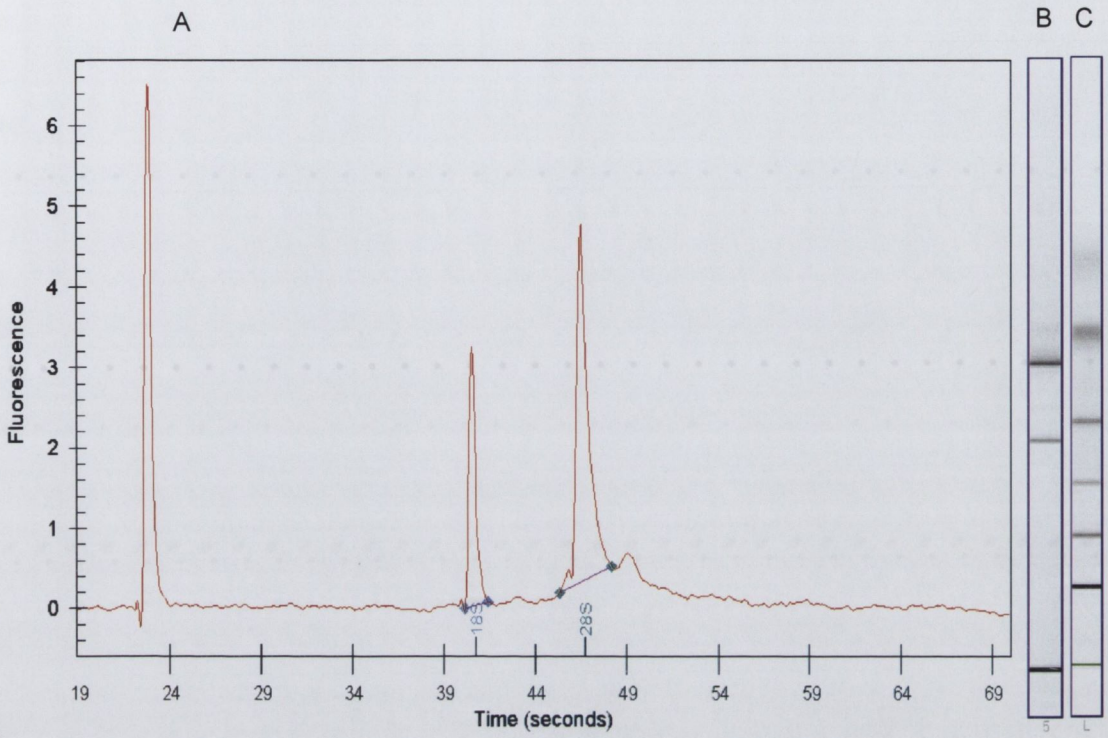


Figure 2.2: Quality control of experimental total RNA isolated from mCGCs

A. The electropherogram above shows two separate ribosomal peaks in a sample of total RNA isolated from mCGCs. The unmarked, first peak is representative of a low marker present in the RNA 6000 LabChip sample buffer. This peak has no influence on total RNA quality but serves as a quality control for the working of the chip. The next 2 peaks represent the amount of I8S and 28S, respectively, in the total RNA sample. The rRNA ratio of 28S concentration to 18S concentration was 2.04 in this case. B. The diagram shows the two peaks as bands in a gel. C represents the RNA 6000 ladder.

The oligo (dT) primers are specific and hybridise to 3' poly (A) tails, which are found in the vast majority of eukaryotic mRNAs. Since poly $(A)^+$ RNA constitutes approx. 1% to 2% of total RNA, the amount and complexity of cDNA is less than when random hexamers are used. When performing RT-PCR of a new mRNA target, the use of oligo (dT) is recommended by Invitrogen (Producer of the kit) rather than using random hexamers. Random hexamers are non-specific primers so all the RNAs in a population are templates for first-strand cDNA synthesis and the PCR primers provide the needed specificity during the PCR amplification reaction. However, in order to use the 18S as an internal control random hexamers must be used in the RT reaction.

The first-strand cDNA synthesis reaction was catalysed by Superscript™ II RNase H-Reverse Transcriptase. Typically, cDNA was prepared in batches of 30 samples and the incubations were performed in single micro-centrifuge tubes (0.5 ml), eliminating the possible risk of contamination. An RT "master-mix" was prepared according to the scheme below. The volumes were adjusted according to the number of samples in hand. A fixed volume of RT master-mix (12 µl) was added into each labelled micro-centrifuge tube on ice. A fixed concentration of each particular total RNA (125 ng/µl; normalised conditions) sample was then added into its corresponding micro-centrifuge tube, the tube was sealed and mixed briefly by vortexing. The tubes were centrifuged at 1000 g for 60 s and placed into a Thermocycler (Peltier Thermal Cycler (PTC) 200). The reactions were incubated according to the following thermal profile: 25°C for 10 min, 42°C for 30 min and 70°C for 15 min. The cDNA (50 ng/µl) was stored at -20°C.

RT Master-Mix

Components	(1x) Volume (µl)	Final Concentration (20 µl)
Total RNA	8	50 ng/µl
Oligo (dT) primer (0.5 µg/µl)	0.5	0.0125 µg/µl
Random Hexamer (50 ng/µl)	0.5	1.25 ng/µl
10X RT buffer	2	1 X
25mM $MgCl_2$	4	5 mM
10 mM dNTP mix	1	500 µM per dNTP
0.1 mM DTT	2	0.01 mM
RNaseOut™ (40 U/µl)	1	2 U/µl
Superscript II RT (50 U/µl)	1	2.5 U/µl
Total Volume	20	

2.8 Primer design

An important parameter for successful PCR is the design of primers. The primer sequence determines the length of the product, melting temperature and its ultimate yield. The primers for the genes under study, along with Genbank accession numbers and PCR conditions are shown in Table 2.1. The computer software Primer 3 was used to design all mouse and rat primer pairs (Rozen and Skaletsky, 1998) and is available at http://www-genome.wi.mit.edu/cgi-bin/primer/primer3_www.cgi. All PCR primers were synthesized by Invitrogen Life Technologies.

The primers were selected containing minimal internal structure (that is, hairpins and primer-dimer formation as determined by the software) and having a melting point temperature of 60 °C ± 1 °C. Primers were also selected that were between 18 – 24 bases in length with the G/C content between 20% and 70%. The chosen primers all had amplicons between 80 - 100 nucleotides in length and contained a maximum of 2 - 3 Gs or Cs among the last 5 bases of the 3' end. All chosen primers were searched for homologies with similar genes of the same species using the BLAST programme.

2.9 Real-time quantitative RT-PCR using SYBR® Green

Two types of quantitation are possible with the SYBR® Green reagents, namely, absolute and relative quantitation. Absolute quantification quantitates unknowns with a real quantity. Relative quantification quantitates a fold difference between samples.

Absolute quantitation involves the creation of a standard curve from a target of known quantity (that is, copy number). Unknowns are then compared to the standard curve and a value extrapolated. Absolute quantitation is useful for quantitating copy number of a certain target in genomic DNA samples. Relative quantitation involves the comparison of a sample(s) (for example *c-fos* mRNA in treated neurons) to another sample (calibrator) of significance (for example *c-fos* mRNA in untreated neurons). The quantity of the calibrator is not known and cannot be measured absolutely. Therefore, the calibrator and samples are firstly normalised to a housekeeping gene and then compared to each other to get a fold difference. Relative quantitation is useful for quantitating messenger RNA levels. In this study, relative quantitation of RT-PCR reactions was used.

The threshold cycle or C_T value is the cycle at which a statistically significant increase in product (ΔRn) is first detected and will always occur during the exponential phase. In Figure 2.3, the threshold cycle occurs when the Taqman sequence detector begins to detect the increase in signal associated with an exponential growth of PCR product.

Target Genes Sequence of Primers (5'to 3')	Oligo Start	Oligo Length (bp)	Product Length (bp)	GenBank Accession Number	Tm (°C)	RT-PCR Cycles
Mouse (and Rat) *junD*						
Left GACCCTCAAAAGCCAGAACA	927	20	97	J05205	60	40
Right GTTGACGTGGCTGAGGACTT	1023	20				
Mouse *junB*						
Left ATCCCTATCGGGGTCTCAAG	5673	20	97	U20735	60	40
Right CCTGTGTCTGATCCCTGACC	5769	20				
Mouse (and Rat) *fra-2*						
Left TTATCCCGGGAACTTTGACA	12	20	113	X83971	60	40
Right CAGGCATATCTACCCGGAACT	124	21				
Mouse *fra-1*						
Left ACCGAAGAAAGGAGCTGACA	567	20	101	U34245	60	40
Right CTGCTTCTGCAGCTCTTCAA	667	20				
Mouse *c-jun*						
Left AGTAGCCCCCAACCTCTTTG	2650	20	104	J04115	60	40
Right ACAGGGGACACAGCTTTCAC	2753	20				
Rat (and Mouse) *fosB*						
Left TCTTGCTGGAGCGCTTTATAC	218	21	70	C06882	60	40
Right GGGGGTCAATCCCATCC	287	17				
Rat (and Mouse) *c-fos*						
Left CCGACTCCTTCTCCAGCAT	235	19	93	X06769	60	40
Right TCACCGTGGGGATAAAGTTG	327	20				
Rat *fra-1*						
Left CAAGCATCAACGCTGTCAGT	347	20	94	NM_012953	60	40
Right TAGGTCAGAGGTCGGGGATA	440	20				
Rat *junB*						
Left CAGTTACTCCCCAGCCTCTG	549	20	99	NM_021836	60	40
Right GCATGTGGGAGGTAGCTGAT	647	20				
Rat *c-jun*						
Left CAGTTACTCCCCAGCCTCTG	629	20	107	X17163	60	40
Right GCATGTGGGAGGTAGCTGAT	735	20				
Mouse (and Rat 18S)						
Left CCCAGTAAGTGCGGGTCATA	1644	20	96	X00686	60	40
Right GGCCTCACTAAACCATCCAA	1739	20				

Table 2.1. Primer pairs, Genbank accession numbers and Product size

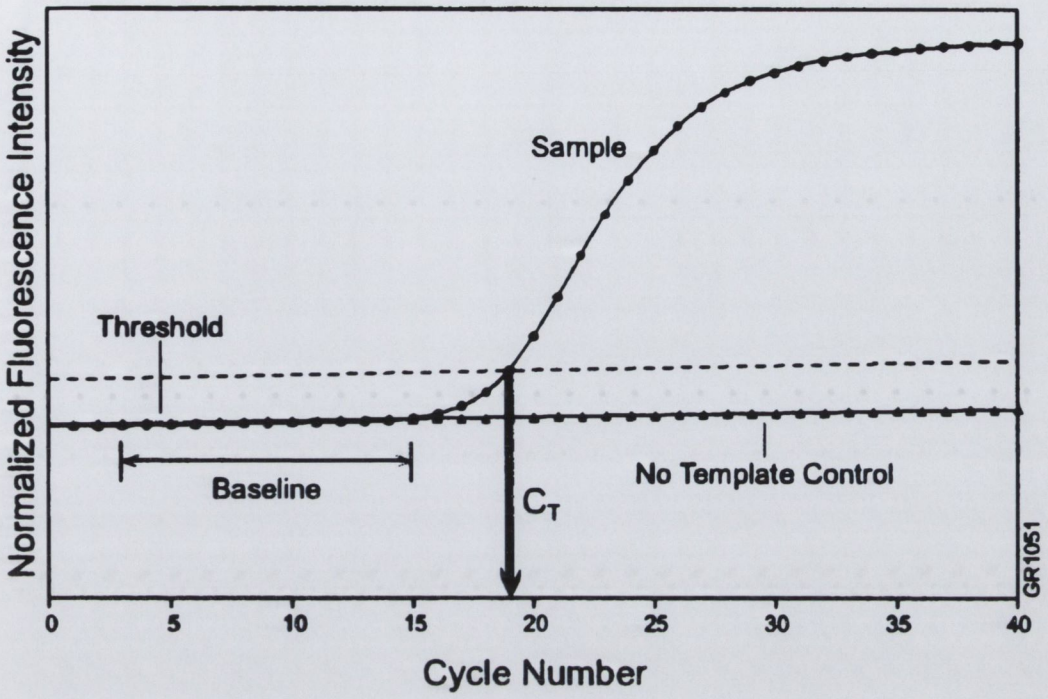


Figure 2.3: Real-time RT-PCR amplification plot

Illustration of a typical real-time RT-PCR amplification plot (modified image from www.AppliedBiosystems.com).

The fluorescent DNA binding dye SYBR® Green (Applied Biosystems) was used in all RT-PCR reactions. Typically, RT-PCR amplification and product analysis are separate, sequential procedures. If, however, a double stranded specific DNA binding dye is included in the reaction, amplicon amplification may be measured in real-time. In this study, 18S Ribosomal RNA was used as an active endogenous control to compensate for variations in RNA quality, initial quantitation errors and random well-to-well variation in RT and PCR reactions. For target gene and 18S quantification, separate SYBR® Green master-mixes were prepared, that is, one master-mix containing the forward and reverse primers for 18S and one containing the forward and reverse primers for the target gene, as outlined below. Each RT-PCR experiement contained a reference 18S standard curve to control for inter-assay variation, thus cDNA (untreated mCGC cDNA or untreated rat cortical neuronal cDNA; 2 µl) from each of the 3 "reference dilutions" (see section 2.14) was pipetted, in triplicate, onto a Taqman 96 well plate. Water (non-template control (NTC); 2 µl) was pipetted into 6 wells on the plate to check for any non-specific amplification by 18S or the target gene. The experimentally treated cDNA (2 µl; 50 ng/µl) samples were then pipetted, in triplicate, onto the plate. A fixed volume of the 18S master-

mix (20 µl) was added to each "dilution", while a fixed volume of the target gene master-mix (20 µl) was added to each of the experimental cDNA samples. The Taqman 96 well plate was sealed and centrifuged at 1000 g for 60 s. Following centrifugation, real-time quantitative RT-PCR was performed in an ABI Prism 7700 sequence detector (Applied Biosystems) using SYBR® Green detection. The thermal cycling parameters were as follows,

2 min at 50°C	AmpErase activation	
10 min at 95°C	"hot start" initial denaturation	
15 s at 95°C	denaturation	x 40 cycles
1 min at 60°C	annealing and extension	

The first step is required for AmpErase activation. The second "hot start" parameter is required for the activation of AmpliTaq Gold DNA Polymerase, which is provided in an inactive state and which becomes activated during a pre-PCR step of 10 min at 95°C. The third step is a melting step to separate the complementary strands of DNA. The fourth step is a primer annealing/extension step to allow hybridisation of the primers to the single stranded DNA, initiation of polymerisation and completion of primer extension.

A second plate was then run containing the same 18S "standard curve", NTC and experimental cDNA samples (2 µl; 50 ng/µl). However, 18S master-mix (20 µl) was added to all wells on the Taqman 96 well plate. The plate was sealed and real-time RT-PCR was performed using the same thermal cycling parameters as above. Data from the target gene RT-PCR was analysed using the Comparative C_T method (see Section 2.10).

SYBR® Green Master-mix

PCR Components	(1x) Volume (µl)	Final Concentration (22 µl)
cDNA (50 ng/µl)	2	9.1 ng/µl
10X SYBR® Green PCR buffer	2	0.9X
25 mM $MgCl_2$	2.4	2.73 mM
10 mM dNTP mix	1.6	0.73 mM
For primer (50 nM)	3	6.82 nM
Rev primer (50 nM)	3	6.82 nM
Amplitaq Gold (5 U/µl)	0.1	0.02 U/µl
AmpErase UNG (1 U/µl)	0.2	0.009 U/µl
RNase-free water	7.7	
Total Volume	22	

2.10 RT-PCR data analysis using the Comparative CT method

Relative quantitation of the target genes against the calibrator and normalised to the internal control, 18S, was used to measure all *immediate early gene* (*IEG*) expression levels. Variations in the initial concentration and quality of the total RNA, and in the conversion efficiency of the reverse transcription reaction were accounted for by the normalisation of all quantitations to 18S.

The endpoint used in the real-time PCR quantification, C_T, is defined as the PCR cycle at which a statistically significant increase in product is first detected. This point will always occur during the exponential phase of amplification. *IEG* expression was measured using the Comparative C_T ($2^{-\Delta\Delta CT}$) method (Applied Biosystems Sequence Detector User Bulletin #2, www.docs.appliedbiosystems.com/pebiodocs/04303859.pdf). The amount of target gene expression, for example *c-fos*, normalised to an endogenous reference (18S) and relative to a calibrator is given by $2^{-\Delta\Delta CT}$. The calibrator sample can be any sample (in this case, untreated mCGCs or rat cortical neurons) chosen to represent a 1X expression of the gene of interest. The calibrator sample is analysed on every assay plate with the unknown samples of interest.

Firstly, the ΔC_T was determined by subtracting the average 18S C_T value from the average *c-fos* C_T value. The standard deviation of the difference was calculated from the standard deviations of the 18S and *c-fos* values. The calculation of $\Delta\Delta C_T$ involved the subtraction of the control sample ΔC_T from all of the treated sample ΔC_Ts. As $\Delta\Delta C_T$ involved the subtraction of an arbitrary constant, the standard deviation of $\Delta\Delta C_T$ was the same as the standard deviation of ΔC_T. The expression values of the target genes, normalised to 18S and relative to the untreated, time-matched controls were then determined by evaluating the expression: $2^{-\Delta\Delta CT}$.

This formula is based on the assumption that the rate of C_T change versus the rate of target copy change is identical for the gene of interest and the housekeeping gene and that a doubling of target results in a 1 cycle decrease in the measured C_T. The $2^{-\Delta\Delta CT}$ method permits higher throughput than the standard curve method but requires two things,

(a) 100% efficiency of the reaction (slope = -3.3)

(b) identical slopes for each gene compared.

An example of a Comparative C_T calculation is shown below for the expression values of mCGCs treated with various concentrations of Glu for 240 min.

mCGC Sample	*c-fos* Mean C_T	s.d. of *c-fos* C_T	18S Mean C_T	s.d. of 18S C_T	ΔC_T (a) *c-fos*-18s	s.d. of ΔC_T	$\Delta\Delta CT$ (b) $\Delta C_{T\ treated} - \Delta C_{T\ control}$	$2^{-\Delta\Delta CT}$ (c) Fold Induction
control	21.33	0.10	13.15	0.09	**8.18**	0.14	**0**	**1.0**
500 µM	18.64	0.33	13.25	0.09	**5.39**	0.34	**-2.79**	**6.9**
250 µM	18.67	0.11	13.97	0.71	**4.71**	0.72	**-3.47**	**11.11**
100 µM	18.73	0.13	13.35	0.13	**5.39**	0.18	**-2.79**	**6.93**
25 µM	19.87	0.21	13.41	0.32	**6.45**	0.38	**-1.73**	**3.31**
2.5 µM	21.36	0.08	13.57	0.37	**7.79**	0.38	**-0.39**	**1.31**

(a) The ΔC_T value is determined by subtracting the average 18S C_T value from the average target gene (*c-fos*) C_T. The standard deviation of the difference is calculated from the standard deviation of the mean 18S s.d. and *c-fos* s.d. values, using the formula s.d. = $\sqrt{(S1)^2 + (S2)^2}$ where S1 = *c-fos* and S2 = 18S.

(b) The calculation of $\Delta\Delta C_T$ involves the subtraction of the calibrator ΔC_T (control ΔC_T) from all of the treated ΔC_Ts. $\Delta\Delta C_T$ involves the subtraction of an arbitrary constant so the standard deviation of $\Delta\Delta C_T$ is the same as the standard deviation of ΔC_T.

(c) The expression values of the target genes, relative to the control, are then determined by evaluating the expression: $2^{-\Delta\Delta CT}$.

2.11 Optimisation of primer concentrations using RT-PCR and SYBR® Green

All of the primer pairs were optimised to determine the minimum primer concentrations giving the maximum signal and minimum non-specific amplification. A 5 µM working stock solution of each primer pair was first prepared, from which the various primer compositions, outlined in the table below, were prepared with Tris/EDTA buffer (pH 8.0, Sigma).

Reverse Primer (nM)	Forward Primer (nM)		
	50	**300**	**900**
50	50/50	300/50	900/50
300	50/300	300/300	900/300
900	50/900	300/900	900/900

An RT-PCR "master-mix" was prepared according to the scheme below. The volumes were adjusted according to the number of samples in hand.

PCR Components	(1x) Volume (µl)	Final Concentration (22 µl)
10X SYBR® Green buffer	2	0.91X
25 mM $MgCl_2$	2.4	2.73 mM
10 mM dNTP mix	1.6	0.73 mM
Amplitaq Gold (5 U/µl)	0.1	0.023 U/µl
AmpErase UNG (1 U/µl)	0.2	0.0091U/µl
Total Volume	6.3	

A fixed volume of RT-PCR master-mix (6.3 µl) was pipetted into all wells of a Taqman 96 well plate. The plate was divided into 2 parts, the first half used to optimise primer concentrations and the second half used as a non-template control (NTC) to check for any non-specific amplification.

cDNA (2 µl) from untreated mCGCs, with a concentration of 50 ng/µl, was pipetted into every well of the first half of the plate, followed by a particular primer pair composition. The volumes in each well were made up to 22 µl with RNase-free water.

RNase-free water (2 µl, non-template control (NTC)) was pipetted into every well of the second half of the plate, followed by a particular primer pair composition. The volumes in

each well were made up to 22 µl with RNase-free water. The Taqman 96 well plate was sealed and centrifuged at 1000 g for 60 s. Following centrifugation the plate was transferred to an ABI Prism 7700 sequence detector (Applied Biosystems). The thermal cycling parameters were

2 min at 50°C	AmpErase activation	
10 min at 95°C	"hot start" initial denaturation	
15 s at 95°C	denaturation	x 40 cycles
1 min at 60°C	annealing and extension	

50 nM was chosen as the optimal primer concentration for both forward and reverse primers because a maximum signal was obtained and, in addition, no amplification occurred in the NTC with these concentrations.

2.12 Polymerase Chain Reaction (PCR) for primer control

NIH 3T3 mouse fibroblasts treated with 12-*o*-tetradecanoylphorbol-13-ester (TPA), are known to induce the expression of several immediate response genes including *c-fos* (Cano e*t al.*, 1995; Soh *et al.*, 1999) and were used, in this study, as a positive control to check for the sensitivity of the newly designed primers pairs.

NIH 3T3 mouse fibroblasts were grown as described in Section 2.3. Total RNA was isolated as described in Section 2.5.2, quantitated and checked for purity as described in Section 2.6. cDNA was prepared as outlined in Section 2.7. Aliquots of cDNA (50 ng/µl) were used to amplify target primers by PCR. A PCR "master-mix" was prepared according to the scheme below. The volumes were adjusted according to the number of samples in hand. A fixed volume of PCR master-mix (45 µl) was added into each labelled micro-centrifuge tube on ice. Separate PCR mastermixes containing forward and reverse primers were prepared for all genes of interest. Each particular cDNA sample (5 µl; 50 ng/µl) was then added into its corresponding micro-centrifuge tube to give a total volume of 50 µl. The tube were sealed and mixed briefly by vortexing. The tubes were then centrifuged at 1000 g for 60 s and placed into a Peltier Thermal Cycler (PTC) 200. The reactions were incubated according to the following thermal profile:

3 min at 94°C	ini	
45 s at 94°C	de	x 35 cycles
30 s at 59°C	annealing	x 35 cycles
150 s at 72°C	extension	
10 min at 72°C	final extension	

denaturaton
annealing
extension

The primers produced a single product of the desired length. In all experiments, the presence of possible contaminants was checked by control reactions in which amplification was carried out for 35 cycles on samples without reverse transcriptase.

PCR Master-mix

PCR Components	(1x) Volume (µl)	Final Concentration (50 µl)
cDNA (50 ng/µl)	5	5 ng/µl
10X PCR buffer	5	1X
25 mM $MgCl_2$	1	0.5 mM
10 mM dNTP mix	1.5	0.3 mM
Forward primer (50 nM)	2	2 nM
Reverse primer (50 nM)	2	2 nM
Taq DNA polymerase (5 U/µl)	0.5	0.05
RNase-free water	33	
Total Volume	50	

2.13 Agarose gel electrophoresis and Ethidium Bromide staining

Each PCR reaction product (from section 2.12) was visualised using agarose gel electrophoresis. An aliquot of each PCR sample (20 µl) was mixed with a tracker dye (4 µl). The products were elecrophoresed at 126 V for 2 hours in a 2 % agarose gel prepared with TAE running buffer (1X). The gels were incubated in an ethidium bromide (10 mg/ml in UPD water and diluted to 5 µg/ml with TAE buffer) solution for 5 min.

Following incubation, the gels were washed with normal water. Results were developed using an ImageMaster® VDS processor.

2.14 Preparation of an 18S standard curve for RT-PCR

Each RT-PCR experiment contained a reference 18S standard curve to control for inter-assay variation. A large batch of total RNA was isolated from untreated mouse or rat neuronal cells (50 ng/µl), reverse transcribed and used as a concurrent standard curve to control the efficiency and reproducibility of the reverse transcription and PCR reactions.

A 1:3 dilution series, with Tris/EDTA (TE) buffer, was prepared from the stock of untreated neuronal cDNA and 2 µl of each dilution was pipetted, in triplicate, onto a Taqman 96 well plate. An 18S RT-PCR SYBR® Green master-mix was prepared as outlined below and a

fixed volume (20 µl) was added to each dilution of untreated neuronal cDNA. The Taqman 96 well plate was sealed and centrifuged at 1000 g for 60 s. Real-time quantitative PCR was performed in an ABI Prism 7700 sequence detector (Applied Biosystems). The thermal cycling parameters were as described in Section 2.9.

PCR Components	**(1x) Volume (µl)**	**Final Concentration (22 µl)**
cDNA (50 ng/µl)	2	9.1 ng/µl
10X SYBR® Green PCR buffer	2	0.9X
25 mM $MgCl_2$	2.4	2.73 mM
10 mM dNTP mix	1.6	0.73 mM
18S For primer (50 nM)	3	6.82 nM
18S Rev primer (50 nM)	3	6.82 nM
Amplitaq Gold (5 U/µl)	0.1	0.02 U/µl
AmpErase UNG (1 U/µl)	0.2	0.009 U/µl
RNase-free water	7.7	
Total Volume	22	

The cDNA dilutions chosen to construct the 18S mouse standard curve were 1:9, 1:81 and 1:729, whereas 1:9, 1:81 and 1:2187 were chosen for the rat 18S standard curve.

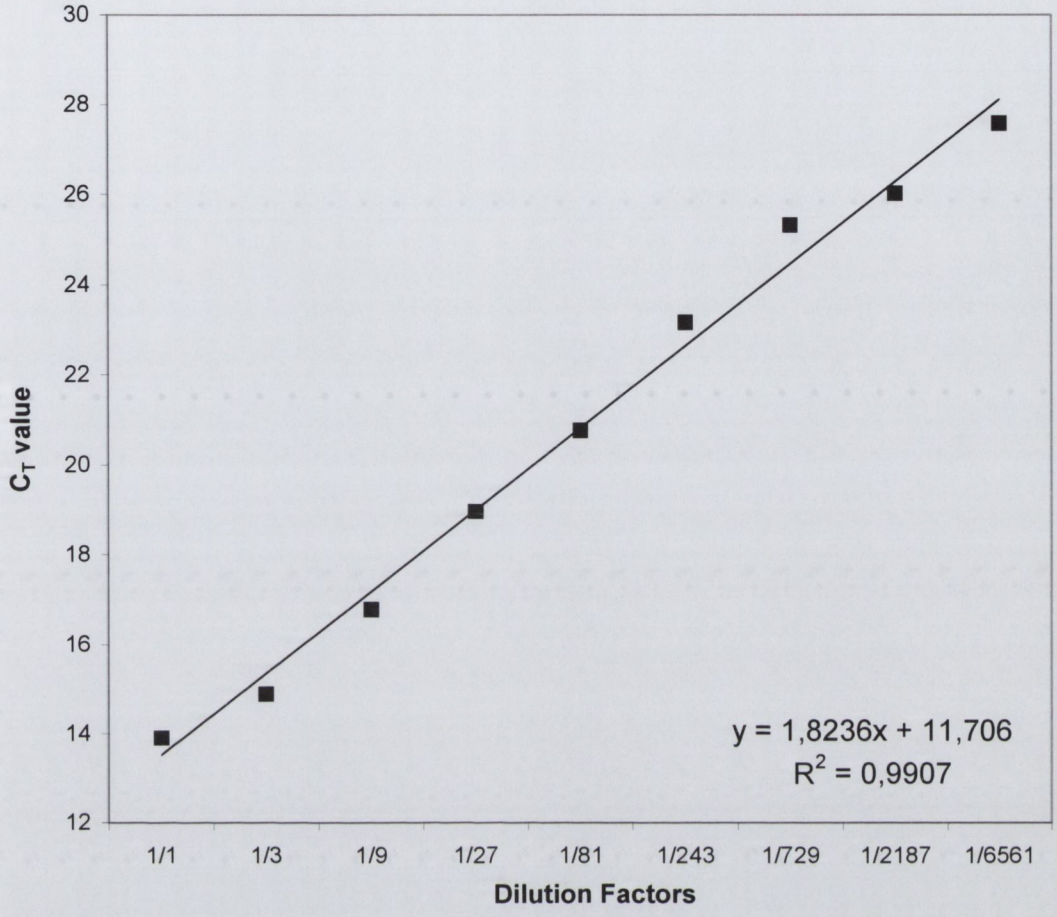


Figure 2.4: A reference 18S standard curve controls for inter-assay variation during a real-time RT-PCR assay

A 1:3 dilution series, with TE buffer, was prepared from the stock of untreated neuronal cDNA and 2 µl of each dilution pipetted, in triplicate, onto a Taqman 96 well plate. A 1/1 dilution factor represents undiluted neuronal cDNA (50 ng/µl). A fixed volume of the 18S master-mix (20 µl) was added to each dilution, the plate was sealed and centrifuged at 1000g for 60 s. Following centrifugation, RT-PCR was performed in an ABI Prism 7700 sequence detector (Applied Biosystems) with thermal cycling conditions as described in Section 2.9.

2.15 Dissociation Curve

Following the SYBR® Green RT-PCR reactions, characteristic dissociation-curves of the amplified products were obtained. A dissociation curve is a graph that displays dissociation data from the amplicons of quantitative PCR runs. During the double stranded DNA dissociation process, SYBR® Green is released, and a decrease in fluorescence occurs. Loss of fluorescence is then plotted against temperature to give a dissociation curve. Dissociation curves were used to detect non-specific amplification, including primer-dimers and were performed for all newly designed primer pairs.

Dissociation curves were obtained using an ABI Prism 7900 sequence detector (Perkin-Elmer Applied Biosystems). The thermal cycling parameters were 15 s at 95°C, 20 s at 60°C, 15 s at 95°C. Figure 2.5 shows a typical dissociation curve for *c-fos*.

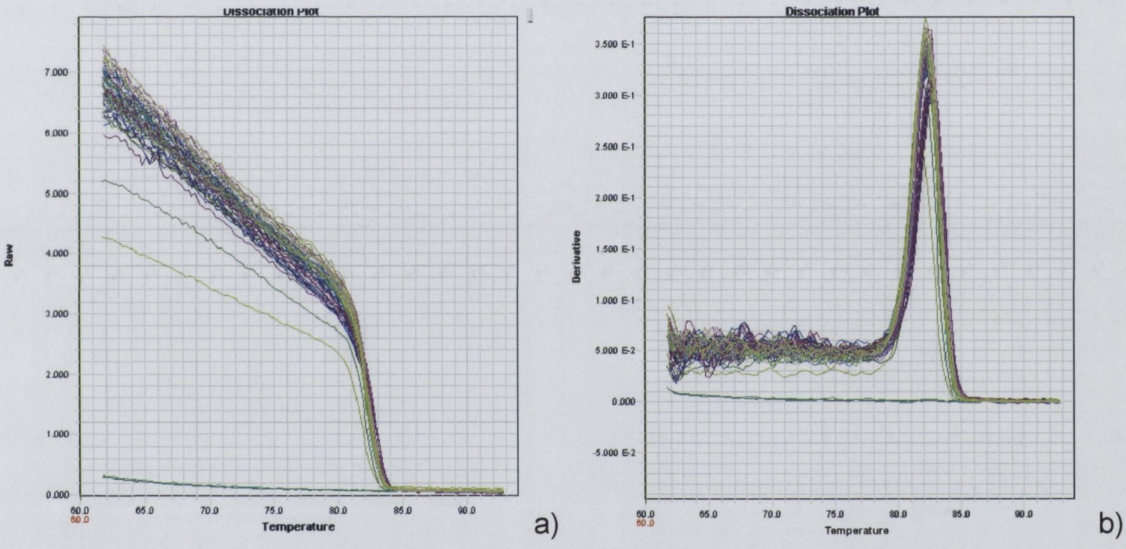


Figure 2.5: Dissociation curve of the *c-fos* product

The induction of *c-fos* following stimulation of mCGCs with various concentrations of Glu was investigated using a SYBR® Green RT-PCR reaction. Following RT-PCR, a characteristic dissociation-curve of the amplified product was detected using an ABI Prism 7900 sequence detector (Applied Biosystems). Figure 2.3 a) represents loss of fluorescence as a function of increasing temperature and b) represents the log of decreasing fluorescence as a function of increasing temperature and shows a single melting peak for the *c-fos* product. Dissociation curves were performed for all newly designed primer pairs.

2.16 Relative Efficiency of Target and Reference

The Comparative C_T method measures the amount of gene expression with the use of the arithmetical formula, $2^{-\Delta\Delta CT}$. For the $\Delta\Delta C_T$ calculation to be valid, the efficiency of the target amplification and the efficiency of the internal control must be approximately equal. A sensitive method for assessing if two PCR reactions have the same efficiency is to look at how ΔC_T varies with template dilution (Applied Biosystems Sequence Detector User Bulletin #2, www.docs.appliedbiosystems.com/pebiodocs/04303859.pdf). Real-time quantitative RT-PCR was performed in an ABI Prism 7700 sequence detector (Applied Biosystems) using SYBR® Green detection.

A 1:3 dilution series, with Tris/EDTA buffer (pH 8.0, Sigma), of cDNA was prepared (as Section 2.14) and 2 µl of each dilution was pipetted, in triplicate, onto a Taqman 96 well plate. Two RT-PCR SYBR® Green master-mixes were prepared, as described in Section 2.9, one containing the forward and reverse primers for 18S and one containing the forward and reverse primers for the target gene, in this case *c-fos*. A fixed volume of the 18S master-mix gene (20 µl) was added to each template dilution. The Taqman 96 well plate was sealed and centrifuged at 1000 g for 60 s. Real-time quantitative PCR was performed in an ABI Prism 7700 sequence detector (Perkin-Elmer Applied Biosystems). The thermal cycling parameters were as follows,

2 min at 50°C	AmpErase activation	
10 min at 95°C	"hot start" initial denaturation	
15 s at 95°C	denaturation	x 40 cycles
1 min at 60°C	annealing and extension	

A second plate was then run using the same cDNA dilution series. However, *c-fos* master-mix (20 µl) was added to all wells on the Taqman plate.

cDNA (ng/µl)	Log of cDNA	*cfos* Average C_T	*cfos* Std. Dev	18S Average C_T	18S Std. Dev	ΔC_T *c-fos*-18S	Std. Dev of ΔC_T
0.003	-2.545	33.89	0.414	26.38	0.240	7.517	0.48
0.01	-2.068	31.71	0.502	24.29	0.516	7.420	0.72
0.03	-1.590	30.86	0.597	23.24	0.076	7.620	0.60
0.8	-1.113	29.53	0.187	21.94	0.272	7.593	0.33
0.23	-0.636	27.31	0.311	19.80	0.558	7.510	0.64
0.69	-0.159	25.95	0.017	18.53	0.120	7.423	0.12

Table: 2.1 Average C_T values for *c-fos* and 18S with different input amounts

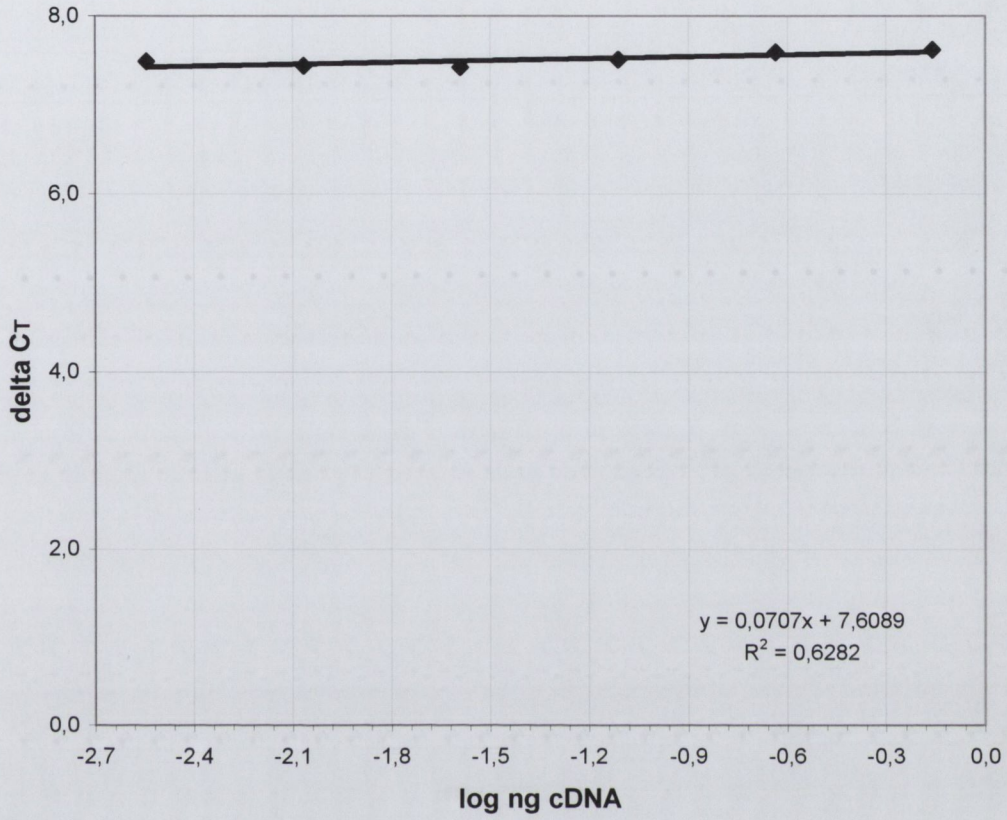


Figure 2.6: Relative Efficiency Plot of *c-fos* and 18S

Before using the $\Delta\Delta C_T$ method for quantitation, a validation experiment was performed (see Table 2.1) to demonstrate that efficiencies of target and reference amplification are approximately equal. The absolute value of the slope of log input amount versus ΔC_T should be < 0.1. The slope found in this case is 0.0707, which passes the test.

2.17 Gene Expression using Affymetrix GeneChip® Technology

2.17.1 Overview of Affymetrix microarray technology

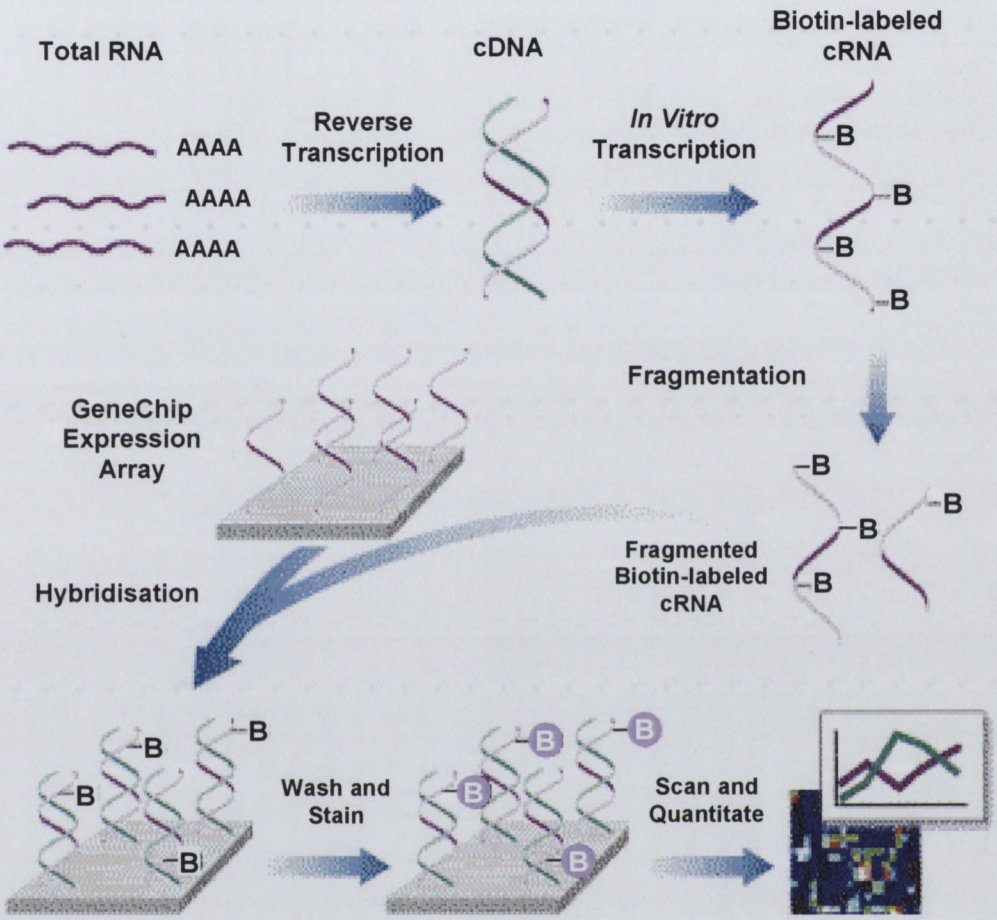


Figure 2.7: Schematic representation of expression monitoring using Affymetrix GeneChip® arrays

In this expression assay system, total RNA isolated from primary neurons was used for processing. The mRNA component was converted to biotinylated cRNA from oligo-dT-primed cDNA. Each sample is hybridised to a separate array. After hybridisation, biotin cRNA bound to the array is stained with a fluorophore conjugated to avidin and detected by laser scanning (modified image from Affymetrix Inc.).

2.17.2 First strand cDNA synthesis

Total RNA from mCGCs and/or rat cortical neurons was isolated, as described in Section 2.5.1, quantitated using the fluorescent nucleic acid stain, Ribogreen, and quality controlled (see Section 2.6). Samples with an absolute amount of 5 µg of total RNA were evaporated to dryness and then dissolved in a fixed volume of RNase-free water (11 µl). T7-oligo (dT) primer (100 pmol, Geneset Oligos) was added to each of the RNA samples, the micro-centrifuge tubes sealed and incubated for 10 min at 70°C (primer hybridisation). Following incubation, the tubes were centrifuged briefly and placed on ice. A First strand cDNA synthesis master-mix (components were from the Superscript™ Double-Stranded cDNA Synthesis kit, Invitrogen), minus reverse transcriptase, was prepared as outlined below and a fixed volume (7 µl) added to each micro-centrifuge tube and the tubes incubated for 2 min at 42°C (temperature adjustment).

Components	(1x) Volume (µl)	Final Concentration (20 µl)
First Strand buffer (5X)	4	1X
0.1 mM DTT	2	0.01 mM
10 mM dNTP	1	0.5 mM
Total Volume	7	

Following incubation SS™II RT (10 U/µl; Invitrogen) was added to each sample and mixed well. The samples were incubated for 1 hour at 42°C (first-strand synthesis) and then maintained on ice.

2.17.3 Synthesis of double-stranded cDNA

The Superscript™ Double-Stranded cDNA Synthesis kit (Invitrogen) was used to produce double-stranded cDNA. A "master-mix" was prepared according to the scheme below. The volumes were adjusted according to the number of samples in hand. A fixed volume of cDNA master-mix (130 µl) was added into each labelled micro-centrifuge tube containing the experimental first-strand cDNA (20 µl; from Section 2.17.2).

Components	(1x) Volume (µl)	Final Concentration (150 µl)
RNase-free water	91	
5X Second Strand buffer	30	1X
10 mM dNTP mix	3	200 µM
DNA Ligase (10 U/µl)	1	10 U
E. Coli DNA polymerase I (10 U/µl)	4	40 U
RNase H (2 U/µl)	1	2 U
Total Volume	130	

Each sample was carefully mixed and incubated for 2 hours at 16°C. Following incubation the samples were centrifuged briefly. T4 DNA polymerase (2µl; final amount 20 U; Invitrogen) was then added to each sample, mixed carefully and incubated for a further 5 min at 16°C. After the 5 min incubation, EDTA (10 µl; final concentration 0.03 M) was added to each sample to terminate the reaction. The samples were either stored at -20°C overnight or used as described in the subsequent section.

2.17.4 Purification of the double-stranded cDNA

Phase-lock micro-centrifuge tubes (Eppendorf) were centrifuged for 30 s at 16100 g. 1 volume of Trizol (162 µl; Sigma) and chloroform (65 µl) was added to each of the double-stranded cDNA samples (total volume 162 µl; from Section 2.17.3), mixed and pipetted into the phase-lock micro-centrifuge tubes. The phase-lock tubes were then centrifuged for 2 min at 16100 g. The supernatant (250 µl) was removed and added into a new set of labelled micro-centrifuge tubes (1.5 ml). A "wash" solution was prepared, according to the scheme below, and added to each of the supernatants. The volumes were adjusted according to the number of samples in hand.

Components	(1x) Volume (µl)	Final Concentration (1000.6 µl)
NH_4Acetate (7.5 M)	125	0.9 M
Ethanol (100%, -20°C)	625	
Glycogen (20 µg/µl)	0.6	(0.01 µg/µl)
Total Volume	750.6	

The micro-centrifuge tubes were vortexed and centrifuged, at room temperature, for 20 min at 16100 g. The supernatants were removed and discarded. The pellets were washed twice with 80% ethanol (0.5 ml) and then centrifuged at room temperature for 5 min at 16100 g. The supernatants were removed and discarded. The pellets were air-dried for approximately 30 min, suspended in RNase-free water (22 µl per pellet) and stored at -20°C.

2.17.5 Synthesis of Biotin-Labeled cRNA

The ENZO® BIOarray™ HighYield™ RNA Transcript labelling Kit (Enzo Diagnostics, distributed by Affymetrix Inc.) was used to produce biotin-labeled single-stranded copy RNA (cRNA) by *in vitro* transcription from bacteriophage T7 RNA polymerase promoters.
An RNA transcript labelling solution was prepared, according to the scheme below, as a master-mix and the volumes were adjusted according to the number of samples in hand.

RNA labeling Components	**(1x) Volume (µl)**
10X HY Reaction buffer	4
10X Biotin-labelled Ribonucleotide	4
10X DTT	4
Total Volume	12

The experimental cDNA (22 µl) samples, prepared in Section 2.17.4, were thawed on ice, and RNA labelling solution (12 µl) was added to each sample, followed by RNase inhibitor (10X; 4 µl) and T7 RNA polymerase (20X; 2 µl).
The samples (40 µl per sample total volume) were vortexed and the contents collected at the bottom of the tubes by short micro-centrifugation at room temperature. Following centrifugation, the samples were incubated for 4 - 5 hours at 37°C, with gentle tapping of the contents of the tubes every 30 min, followed by a short centrifugation.

2.17.6 Purification of cRNA using an RNeasy Mini Kit

Biotin-Labeled cRNA samples (40 µl, prepared in Section 2.17.5), were divided into two equal parts (2 x 20 µl). One part (20 µl) was purified with the use of an RNeasy Mini Kit (Qiagen), and the remaining part was stored at -20°C. RLT buffer (350 µl; provided with the kit) and RNase free water (80 µl) was added to each sample to be purified. The

samples were mixed with ethanol (100%; 250 µl), applied to RNeasy Mini spin-columns (one sample per column) and centrifuged, at room temperature, for 1 min at 16100 g. The flow-through was re-applied to the mini spin-columns and re-centrifuged for 1 min at 16100 g. The flow-through was discarded. RPE wash buffer (500 µl) was added to each spin-column and the columns were centrifuged for 1 min at 16100 g. A second volume of RPE buffer (500 µl) was added and the columns were centrifuged for 2 min at 16100 g. The flow-throughs were discarded. The mini spin-columns were transferred to new RNase-free micro-centrifuge tubes and RNase-free water (50 µl) was added directly onto each column membrane to elute the purified cRNA. The columns were allowed to stand on ice for 1 min and before being centrifuged for 1 min at 9300 g. The elution step was repeated with a second volume of RNase-free water (50 µl) and the first and second eluates were combined giving a total volume of approximately 100 µl cRNA.

2.17.7 Precipitation of purified cRNA

A "precipitation" solution was prepared, according to the scheme below, and added to each of the samples of purified cRNA (100 µl), from Section 2.17.6. The volumes were adjusted according to the number of samples in hand.

Components	(1x) Volume (µl)	Final Concentration (700.8 µl)
NH_4Acetate (7.5 M)	100	1.07 M
Ethanol (100%, -20°C)	500	
Glycogen (20 µg/l)	0.8	(0.02 µg/µl)
Total Volume	600.8	

The cRNA solutions were mixed by vortexing and incubated overnight at -20°C.

2.17.8 Measurement of cRNA

Following overnight precipitation at -20°C, the cRNA was pelleted at 4°C for 30 min at 16100 g. The supernatants were discarded and the pellets were washed with 2 volumes of ice-cold (500 µl; -20°C) ethanol (80%). The cRNA was then pelleted at 4°C for 5 min at 16100 g. The washed pellets were air-dried for approximately 30 min before being re-suspended in RNase-free water (30 µl) over 3 hours at 4°C. An aliquot of cRNA sample (2 µl) was diluted 1:100 in RNase-free water. 70 µl of the diluted cRNA sample was pipetted

into an RNase-free 384 well plate and the concentration of cRNA was determined by measurement of the absorbance at 260 nm in a spectrophotometer. The concentration of cRNA was calculated by the following formula,

$$\mathbf{A_{260} \times 40 \times dilution\ factor = \mu g/ml,}$$

as an absorbance of 1 unit at 260 nm corresponds to 40 µg of RNA per ml in aqueous solution. The purity of the cRNA was estimated by the ratio of the absorbance readings at 260 nm and 280 nm. Pure cRNA has a ratio between 1.9 and 2.1 and can therefore be used for hybridisation.

2.17.9 Fragmentation of cRNA

cRNA (see Section 2.17.7) was fragmented to a mean size of 50 – 100 nucleotides before being hybridised to the Affymetrix GeneChip® arrays. cRNA samples, with an absolute amount of 20 µg of RNA, were evaporated to dryness and then dissolved in a fixed volume of RNase-free water (32 µl). 5X Fragmentation buffer (8 µl; final concentration 40 mM Trisacetate, 6.4 µg/µl magnesium acetate and 9.8 µg/µl potassium acetate) was added to each cRNA sample giving a total volume of 40 µl. Thus, the cRNA samples had a final concentration of 0.5 µg/µl. The fragmented cRNA experimental samples were incubated for 40 min at 94°C.

2.17.10 Hybridisation of the cRNA samples onto the Affymetrix GeneChip® arrays

The Affymetrix RG_U34 (for rat neuronal samples) or MG_U74 (for mouse neuronal samples) arrays were removed from storage at 4°C and allowed to equilibrate at room temperature. The arrays were pre-hybridised with 1X MES buffer (200 µl: final concentration 100 mM MES, 1 M [Na^+], 20mM EDTA, 0.01% Tween) and equilibrated for 10 min at 45°C with rotation (60 rpm) in the GeneChip® hybridisation oven. Note that the chips were not filled to full volume with the pre-hybridisation buffer to allow for movement of the buffer over the array. The hybridisation buffer was prepared, according to the following scheme, and the volumes were adjusted according to the number of samples in hand. (The 20X Eukaryotic (Euk.) Hybridisation controls solution and the Control Oligo B2 were pre-warmed for 5 min at 65°C).

Components	(1x) Volume (µl)	Final Concentration (300 µl)
RNase-free water	84	
Control Oligo B2 (3 nM) 20X Euk. Hybridisation controls buffer (*bioB, bioC, bioD,cre*)	5 15	50 pM 1X (1.5, 5, 25 & 100 pM, respectively)
Herring Sperm (10 mg/ml)	3	0.1 mg/ml
Acetylated BSA (50 mg/ml)	3	0.5 mg/ml
2X MES buffer	150	1X
Total Volume	260	

Hybridisation buffer (260 µl) was added to each of the experimental samples of fragmented cRNA (40 µl: 0.5 µg/µl; see Section 2.17.9). The solutions were incubated for 5 min at 99°C and then for 5 min at 45°C. Following incubation, the solutions were centrifuged, at room temperature, for 5 min at 16100 g, to pellet any insoluble material from the hybridisation mixture.

Two pipette tips were used to fill the probe array cartridge; one for filling and emptying the probe array cartridge and the second to allow venting of air from the hybridisation chamber.

The 1X MES buffer was carefully removed and discarded. A cRNA-Hybridisation sample was pipetted into an Affymetrix array (200µl; one sample per chip) and the arrays were incubated for 16 – 17 hours at 45°C, with rotation (60 rpm), in the GeneChip® hybridisation oven.

2.17.11 Washing and Staining of Affymetrix arrays

Again, two pipette tips were used to fill the probe array cartridge; one for filling and emptying the probe array cartridge and the second to allow venting of air from the hybridisation chamber.

The cRNA-Hybridisation samples were removed from the chips and discarded. The chips were then filled with a non-stringent buffer, Buffer A (6X SSPE, 0.01% Tween 20), which was prepared immediately before use. An r-phycoerythrin streptavidin (SAPE; Molecular Probes) stain solution (light-sensitive) was prepared, according to the scheme below. 2 volumes of 600 µl of "SAPE" solution were required per chip and aliquots were stored in light-sensitive micro-centrifuge tubes.

Components	(1x) Volume (µl)	Final Concentration (1200 µl)
2X MES stain buffer	600	1X
RNase-free water	540	
Acetylated BSA (50 mg/ml)	48	2 mg/ml
SAPE (1 mg/ml)	12	10 µg/ml
Total Volume	1200	

An antibody master-mix was also prepared according to the scheme below, and 1 volume of antibody master-mix (600 µl) was required per chip.

Components	(1x) Volume (µl)	(Final Concentration (600 µl)
2X MES stain buffer	300	1X
Normal Goat anti-IgG (10 mg/ml)	6	0.1 mg/ml
Biotinylated antibody (0.5 mg/ml)	3.6	3 µg/ml
Acetylated BSA (50 mg/ml)	24	2 mg/ml
RNase-free water	266.4	
Total Volume	600	

The chips were washed and stained in an Affymetrix Fluidics station 450/250 according to protocol EukGE-WS2[a] in the Fluidics Station User's Guide (Affymetrix Inc). Buffer A (6X SSPE, 0.01% Tween 20) and Buffer B (100 mM MES, 0.1 M [Na^+], 0.01% Tween 20) were firstly prepared.

The arrays were inserted into the modules of the fluidics station while the cartridge lever was in the down, or eject, position. The cartridge was then returned to the up, or engaged, position. The arrays were washed with Buffer A and B. One vial containing streptavidin phycoerythrin (SAPE; 600 µl) solution mix was placed in the sample holder. After the first staining, the SAPE vial was removed and a vial containing anti-streptavidin biotinylated antibody (600 µl) was placed in the sample holder. The anti-streptavidin biotinylated antibody vial was removed and replaced with a second vial containing SAPE (600 µl). Following staining, the arrays were subjected to a final wash with Buffer A. The washing and staining procedure were as follows,

EukGE-WS2[a] Washing and Staining	Stages
Post Hyb Wash #1	10 cycles of 2 mixes/cycle with Wash Buffer A at 25°C
Post Hyb Wash #2	4 cycles of 15 mixes/cycle with Wash Buffer B at 50°C
Stain	Staining of probe array for 10 min in SAPE solution at 25°C
Post Stain Wash	10 cycles of 4 mixes/cycle with Wash Buffer A at 25°C
2nd Stain	Staining of probe array for 10 min in antibody solution at 25°C
3rd Stain	Staining of probe array for 10 min in SAPE solution at 25°C
Final Wash	15 cycles 4 mixes/cycle with Wash Buffer A at 30°C. The holding temperature was 25°C

Following washing and staining, the arrays were removed from the fluidics station and quality controlled to ensure the absence of air bubbles. Any air bubbles were removed by re-loading the chips into the fluidics station and subjecting them to a second "Final wash". The arrays were then scanned at room temperature in a GeneArray® scanner. The scanner was controlled by Affymetrix® Microarray suite and scanning was according to the instructions in the Microarray suite User's guide. The software defined the probe cells and computed an intensity for each cell. Each complete probe array image was stored in a separate data file and saved with a data image file (.dat) extension.

2.17.12 Data Analysis

Data was analysed using the Microarray suite Expression Analysis window. The .dat image was analysed for probe intensities and results were reported in a tabular and graphical format. Data was analysed according to the instructions in the, GeneData

Refiner (version 3.0.4.) and Analyst Software module of GD Expressionist Version 4.0.5 guides.

Following a quantitative scan of an array, a grid was aligned to the image using the known dimensions of the array and the corner control regions as markers. The image was reduced to a simple text file containing position and intensity using Affymetrix® Microarray suite. This text file was merged with another file, which contained information relating physical position on the array to probe sequence and RNA identification for which the oligonucleotide was designed. The quantitative analysis of the hybridisation results involves a simple form of pattern recognition based on the assumption that, in the presence of a specific RNA, the perfect match (PM) probes hybridise more strongly on average than their mismatch (MM) partners. The numbers of instances in which the PM hybridisation signal is larger than the MM signal is computed along with averages of the logarithm of the PM/MM ratios for each probe set. These values were used to determine the absence or presence of RNA. To determine the quantitative RNA abundance, the average of the differences (PM minus MM) for each probe family were calculated. The advantage of the difference method is that signals from random cross-hybridisation contribute equally to the PM and MM probes, while specific hybridisation contributes more to the PM probes. By averaging the pairwise differences, the real signals add constructively while the contributions from cross-hybridisation tend to cancel.

When the differences between two different RNA samples were assessed, the hybridisation signals from side-by-side experiments in identically synthesized arrays were compared directly. The magnitude of the changes in the average of the difference (PM-MM) values was interpreted by comparison with the signals observed for the internal standard bacterial and phage RNAs spiked into each sample at a known amount. The analysis programs, GeneData Refiner (version 3.0.4.) and Analyst Software module of GD Expressionist Version 4.0.5, perform these operations automatically.

Chapter 3

Characterisation of Two Different *In Vitro* Models for Excitotoxic Investigations

3.1 Introduction

Excitotoxins represent a group of neuroactive compounds characterised by their combined affinity for any of the brain Glu receptor subtypes and ability to excite and destroy neurons. Endogenous excitotoxins such as glutamate (Glu), aspartate (Asp), quinolinate and homocysteate are integral components of the biochemical machinery of the brain. Glu is the predominant excitatory amino acid (EAA) neurotransmitter in the mammalian central nervous system (CNS) and under normal circumstances plays a key role in neurological processes including neuronal survival and refinement of neuronal connections during brain development, learning and memory. However, over-activation of Glu receptors leads to neurodegeneration and this phenomenon, called *excitotoxicity,* has a role in a number of neuropathologies ranging from acute insults such as stroke, hypoglycaemia and epilepsy to chronic degenerative states such as Huntington's disease and the acquired immunodeficiency syndrome (AIDS) dementia complex (Lipton and Rosenberg, 1994).

The receptors for Glu are either ionotropic (ligand-gated ion channels for sodium and calcium) or metabotropic (the receptors being linked by G-proteins to a variety of intracellular messengers that mediate slower pre- and post-synaptic responses). The ionotropic Glu receptors are further classified, according to their interactions with non-physiological Glu analogues, as N-methyl-D-aspartate (NMDA), amino-3-hydroxy-5-methyl-4-isoxazolepropionic acid (AMPA) and kainate (KA) receptors. However, since neither agonist nor antagonist selectively differentiates AMPA from KA receptors these two receptor families are often denominated together as non-NMDA receptors (Pláteník *et al.*, 2000). NMDA receptor channels are permeable to both monovalent cations and Ca^{2+} ions (Mac Dermott *et al.*, 1986; Ascher and Nowak, 1988), whereas non-NMDA receptor channels are predominantly permeable to monovalent cations (Mayer *et al.*, 1987). Ionotropic Glu receptors have two known roles. They are responsible for the majority of excitatory neurotransmission and also for CNS pathology. The metabotropic receptors regulate the production of intracellular messengers.

The potential role of Glu toxicity in ischaemia and trauma is not fully understood, but there have been strong indications that several cell death pathways are involved. In localised cerebral infarcation, the neurons in the epicentre die rapidly, whereas those more distal remain viable for several hours (Siesjö, 1992). Multiple types of neuronal cell death have been identified in CNS primary cultures following exposure to toxic concentrations of Glu

(Choi, 1992). For example, it was reported by Ankarcrona *et al.* (1995) that a rapid necrotic phase is followed by a delayed apoptotic-like cell death in primary cultures of cerebellar granule cells exposed to Glu. The excessive interaction of EAAs with subtypes of Glu receptors alters intracellular ion concentrations, protein phosphorylation and energy metabolism (Martin *et al.*, 1998). This is the basis of the "excitotoxicity hypothesis" formulated by Olney *et al.* (1971), which proposed that injury is a direct consequence of excessive neuroexcitation.

Excessive activation of the NMDA receptor subtype by EAAs and the subsequent increase in intracellular calcium ion concentration ($[Ca^{2+}]_i$) is thought to be the main initiator in a cascade of events that ultimately results in irreversible neuronal cell death (Bonfoco *et al.*, 1995; Frandsen and Schousboe, 1993; Nicotera *et al.*, 1992, 1996). Excitotoxicity is defined as an excessive stimulation of the NMDA subtype of Glu receptors and may be due to excessive Glu release and/or lack of clearance. The excess Glu released activates a number of postsynaptic cell membrane receptors, which upon activation open their associated ion channel pore to produce ion influx or efflux. This leads to a disturbance of the intracellular ionic environment, the best-characterised feature of which is the influx of sodium (Na^+), chloride (Cl^-) and Ca^{2+} ions. As already mentioned, previous reports suggest that two phases may be involved in EAA-induced excitotoxicity, that is, an acute, necrotic phase and a delayed, apoptotic phase (Choi, 1987; Ankarcrona *et al.*, 1995). The "acute" phase, which is Na^+ and Cl^- dependent, causes cell depolarisation entailing a passive influx of Cl^- ions; since the distribution of Cl^- ions across the cell membrane follows the changes of membrane potential. The build-up of a sodium chloride intracellular pool leads to a movement of water, swelling of the cell and acute osmotic damage (Choi, 1987). This phase may be mediated via excessive activity of non-NMDA receptors, as neuronal swelling is eliminated when incubations are performed in Na^+ free culture media (Choi, 1987). The delayed, apoptotic phase of neurodegeneration is Ca^{2+} dependent and is possibly mediated by a transmembrane influx of Ca^{2+} into neurons. It is possible that the late phase of neurodegeneration is mediated through excessive activation of NMDA receptors as Choi reported in 1987, that NMDA receptor antagonists prevented this phase. Excitotoxic cell death, therefore, appears to be mediated via a precipitous increase in internal Ca^{2+} ion concentrations, and indeed, an elevation of Ca^{2+} has long been implicated in ischaemia-induced neuronal degeneration.

Leist and Nicotera suggested in 1998, that mitochondria may act as the deciding factor between helping cells to recover, accelerating their demise or triggering the execution

phase of cell death. Ankarcrona *et al.* (1996), reported that a decrease in the mitochondrial membrane potential ($\Delta\psi_m$) is an early event in apoptosis, an event which is associated with the opening of the permeability transition pore (PTP). In this Chapter, $\Delta\psi_m$ was measured as an important event in Glu-induced excitotoxicity. The PTP is a multiprotein complex, built up at the contact site between the mitochondrial inner and outer membranes. Under stressful conditions, this pore is permeable to compounds of molecular mass of 2 KDa and allows the equilibration of ions and respiratory substrates between mitochondrial matrix and cytosol. The mitochondrion is an important Ca^{2+} ion compartment, which responds rapidly to changes in intracellular Ca^{2+} concentrations ($[Ca^{2+}]_i$). Limited Ca^{2+} uptake increases the speed of electron transfer through the respiratory chain, providing a functional coupling between cell activation and adenosine triphosphate (ATP) production. Large increases in mitochondrial concentrations of Ca^{2+} ions activate intracellular Ca^{2+}-dependent signalling cascades which in turn activate enzymes such as proteases and lipases, induce the breakdown of phospholipids, generate reactive oxygen species (ROS), inhibit the respiratory chain and open the permeability pore. The interaction of high $[Ca^{2+}]_i$ and ROS may lead to a vicious circle, since stressed mitochondria, possibly with uncoupled respiratory chain, produce ROS as a consequence of NMDA receptor stimulation and Ca^{2+} overload. Massive loss in $\Delta\psi_m$ and the subsequent opening of the permeability transition pore can cause the activation of calcium ATPase leading to a collapse in ATP production (Ankarcrona *et al.*, 1996).

Mitochondria are essential in cellular function in that they are the major organelles which produce ATP within the cell. Neurons are particularly susceptible to mitochondrial dysfunction because they are highly active cells, which are dependent on ATP production by oxidative metabolism. Increases in mitochondrial concentrations of Ca^{2+} open the PTP causing the collapse of the $\Delta\psi_m$, which results in impaired respiration and ATP depletion. The availability of ATP seems to be the significant determinant of the mode of cell death. Indeed, Leist *et al.* (1997), reported that apoptosis is an energy-requiring process, whereas complete ATP depletion causes necrosis. It was also suggested that when cells sustain a toxic insult they are able to execute the apoptotic programme providing they have sufficient energy, whereas in situations of limiting ATP the same degree of toxic insult results in necrosis. It has been shown that Glu excitotoxicity can induce either apoptosis or necrosis depending on mitochondrial function. Ankarcrona *et al.* (1995), found that during and shortly after exposure to Glu, neurons that died by necrosis had

reduced mitochondrial membrane potential and swollen nuclei. In contrast, neurons that recovered $\Delta\psi_m$ and ATP levels subsequently underwent apoptosis.

Several research groups have examined the pharmacology of Glu toxicity in neuronal culture intensively and it has been demonstrated that this toxicity can be attenuated by NMDA receptor antagonists (Choi *et al.*, 1988a; Frandsen *et al.*, 1989; Goldberg *et al.*, 1987). In this study, the NMDA receptor antagonist D-(±)-2-amino-5-phosphonopentanoic acid (AP5) was used as a selective competitive antagonist at NMDA receptor binding sites and the quinoxalinedione, 6-cyano-7-nitroquinoxaline-2, 3-dione (CNQX) was used as a potent and selective competitive antagonist at non-NMDA receptors (Honoré *et al.*, 1988), although at high concentrations CNQX can additionally reduce NMDA-induced injury (Koh *et al.*, 1990) probably by displacement of glycine from the strychnine-insensitive site on the NMDA receptor complex (Kessler *et al.*, 1989; Johnson & Ascher, 1987).

In this Chapter, the stimulation of Glu receptors in primary neuronal cultures by EAAs was used to study the cellular events triggering neuronal death. Neurons in primary culture provide a homogeneous and reliable model system for pharmacological and electrophysiological investigations, bypassing the experimental difficulties associated with the use of CNS-tissue (Frandsen and Schousboe, 1987). Here, the mechanisms underlying the death of both mCGCs and cultured rat embryonic cortical neurons exposed to the excitatory amino acids, Glu, NMDA and Asp were investigated.

The cerebellar granule cell system used in this study is based on the technique developed by Messer (1977) and modified by Meier and Schousboe (1982), Drejer *et al.* (1983) and Schousboe *et al.* (1989). The basic strategy for the preparation of this type of neuronal culture is to take cerebella from 7 day old animals, that is, a developmental stage at which the other types of cerebellar neurons have reached the differentiating (postmitotic) stage of development, whereas the granule cells are still capable of undergoing mitosis (Hertz *et al.*, 1985). In addition, glial cells at this developmental stage are still in the mitotic phase, but this cell type can be eliminated from the cultures by treatment with cytosine arabinoside, a pyrimidine antimetabolite that inhibits DNA synthesis (Martin, 1990). The advantage of this type of culture is that it contains a virtually single cell population (Vaccarino *et al.*, 1987) that possesses NMDA-type channels (Schramm *et al.*, 1990) providing a good model to study the synaptic activity mediated by Glu receptors. Thus, in these cells, Glu toxicity can be exclusively attributed to the over-stimulation of Glu receptors, leading to Ca^{2+} ion overload (Schramm *et al.*, 1990).

The rat cortical cell culture method used in this study is based on the technique developed by Schmuck and Schlüter (1996) and Schmuck *et al.* (2000). It has been demonstrated in neuronal cultures that the composition of the culture medium and the *in vitro* age are two important factors that influence the expression of Glu receptor subunits and thus the functional properties of these receptors (Balazs *et al.*, 1992; Didier *et al.*, 1997; Brewer *et al.*, 1993). In this rat cortical cell system, a serum–free B27-Supplemented Neurobasal™ medium was used. This simple to use, quality-controlled, serum-free medium is superior to Dulbecco's modified Eagle's medium (DMEM) in that the concentration of glutamine is reduced and also the medium does not contain toxic ferrous sulphate. Glutamine is an agent, which encourages the growth of glial cells at high concentrations, and ferrous iron (II) is known as an initiator of lipid peroxidation (Konings, 1984).

Aims of this Chapter

The first aim of this Chapter was to establish primary cultures of mouse cerebellar granule cells in our laboratory.

The second aim was to confirm the suitability of the mCGCs as a model for investigating excitotoxicity induced by the EAAs, Glu, Asp and NMDA, and to compare these results with the results of the non-excitatory compound, Ala.

The third aim was to develop and optimise a novel rat cortical neuronal system.

Our fourth aim was to demonstrate that primary cultures of rat cortical neurons could be used to study excitotoxicity, which involved a comparison of excitatory (Glu and Asp), non-excitatory (alanine (Ala)) and a neurotoxic but non-excitotoxic compound (paraquat) on cell viability, intracellular ATP concentrations and mitochondrial membrane potential.

3.2 Results

3.2.1 Concentration- and time-dependence of neuronal viability after EAA treatment

Primary cultures of mCGCs were prepared from post-natal mice as described in Section 2.2.1 and by Meier and Schousboe (1982), Drejer *et al.* (1983) and Schousboe *et al.* (1989). The mCGCs were routinely cultured for 7 days before exposure to both excitatory (Glu, Asp and NMDA) and non-excitatory (Ala) compounds. The 3-[4,5-dimethylthiazol-2-yl]-2,5-diphenyltetrazolium bromide (MTT) toxicity test was used as an initial screen for general cytotoxicity. An investigation into cytotoxicity was performed by assaying for MTT activity in the neurons following 4 and 24 hour exposure periods. Cytotoxicity was assessed by the measurement of MTT activity in treated neurons when compared to control, untreated neurons (where MTT activity was 100 %).

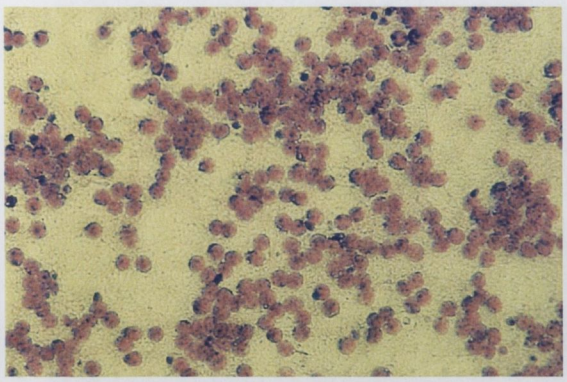
The cytotoxic actions of Glu, Asp and NMDA on mCGCs are shown in Figures 3.2 to 3.4 and can be compared to the non-cytotoxic action of Ala in Figure 3.5.

When mCGCs were exposed to various concentrations of Glu, Asp and NMDA for 4 and 24 hours, concentration-dependent decreases in cell viability were observed. The EC_{50} values for Glu, Asp and NMDA were 80 µM, 100 µM and > 300 µM, respectively, at 4 hours. At 24 hours, the EC_{50} values for Glu, Asp and NMDA were 60 µM, 70 µM and 300 µM, respectively. These findings are consistent with studies of Glu toxicity in similar cultures (Griffiths *et al.,* 1998, 2000), where EC_{50} values of approximately 50 µM were reported. Furthermore, reductions in MTT activity and therefore cell viability were more extensive in cultures exposed to Glu and Asp, with NMDA having a less toxic effect over the same concentration range.

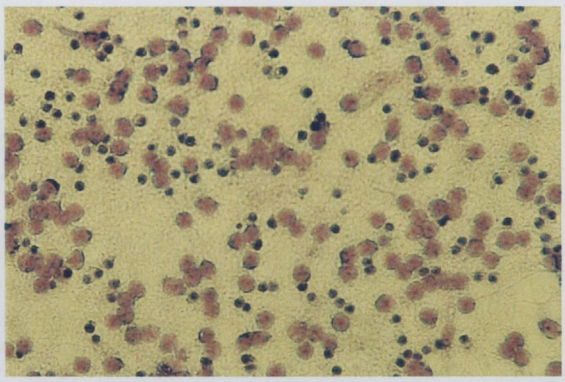
In the case of Glu and Asp, the decrease in cell viability seemed to plateau at approximately 20 %. This plateau of 20 % is consistent with the MTT activity of EAA-resistant astrocytic contamination of the mCGC cell culture system (Schousboe *et al.,* 1989).

Ala, the non-EAA, did not decrease cell viability at either 4 or 24 hours.

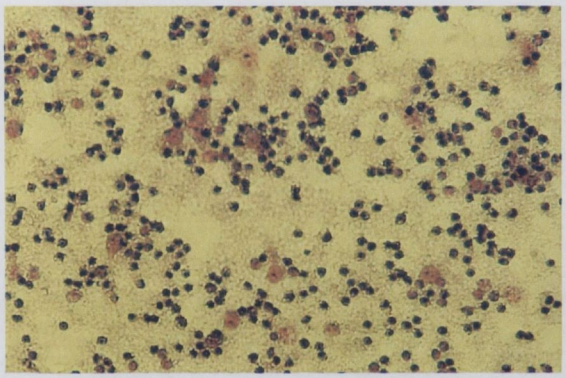
The cytotoxic effects of the EAAs were consistent with the appearance of the cell cultures when visually observed under the light microscope (see Figure 3.1). On day 7, untreated mCGCs appeared as a monolayer of small rounded bodies with extensive neurite complexes. Following treatment with Glu, at concentrations higher that 100 µM over 24 hours, the cell networks were completely disintegrated.



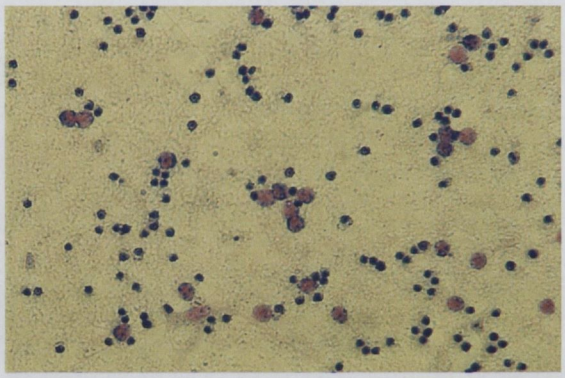
a) Untreated mCGCs



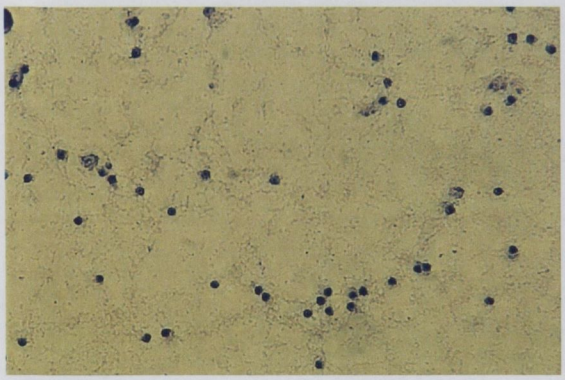
b) 25 µM Glu



c) 100 µM Glu



d) 250 µM Glu



e) 500 µM Glu



f) 1000 µM Glu

Figure 3.1: Glu cytotoxicity is concentration-dependent in mCGCs

Primary mCGCs were exposed to various concentrations of Glu for 24 hours before being stained with Giemsa and visually observed under the light microscope.

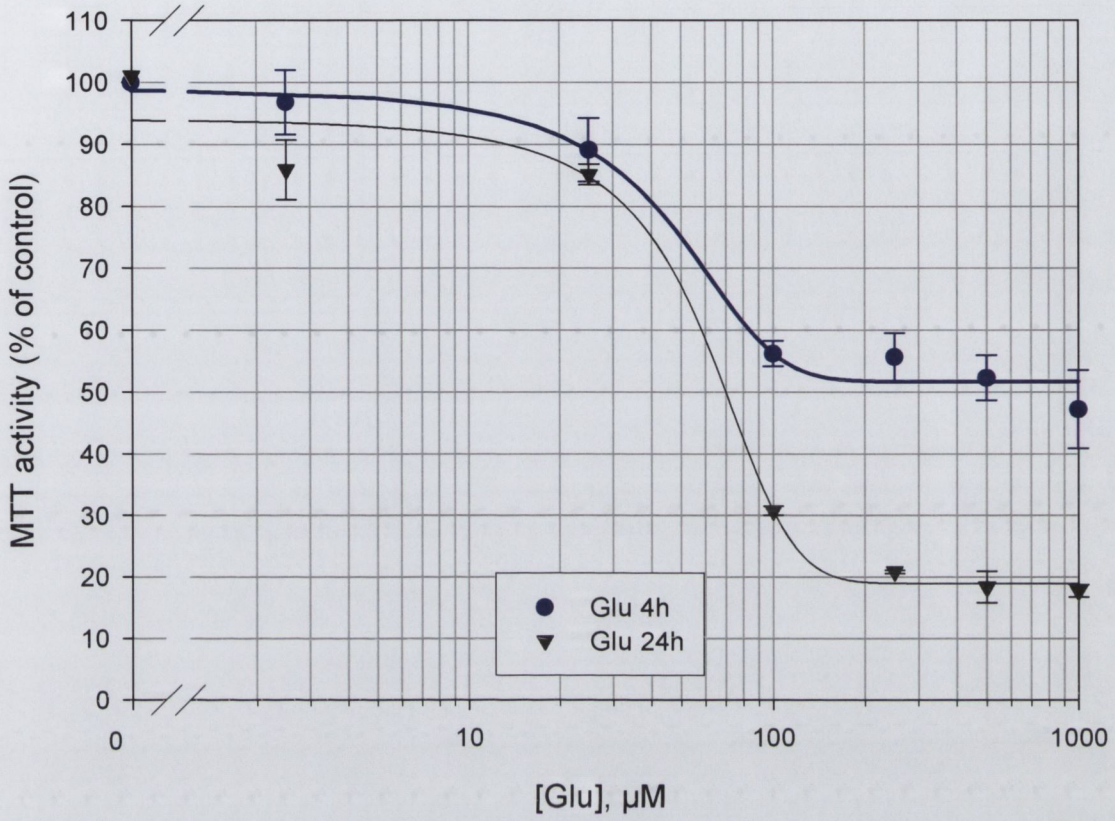


Figure 3.2: Concentration- and time-dependence of Glu on viability of mCGCs

Primary cultures of cerebellar granule cells, prepared from suspensions of dissociated cells from 7-day-old post-natal mouse cerebella, were maintained in culture for 7 days. Cells were then exposed for either 4 or 24 hours to various concentrations of Glu (added directly to the incubation medium) prior to assessment of cell viability by the MTT assay. The absorbance at 570 nm was expressed as a percentage of control (untreated) cells. Data represent mean ± s.d. values of triplicate MTT reactions derived from three separate experiments (n = 3).

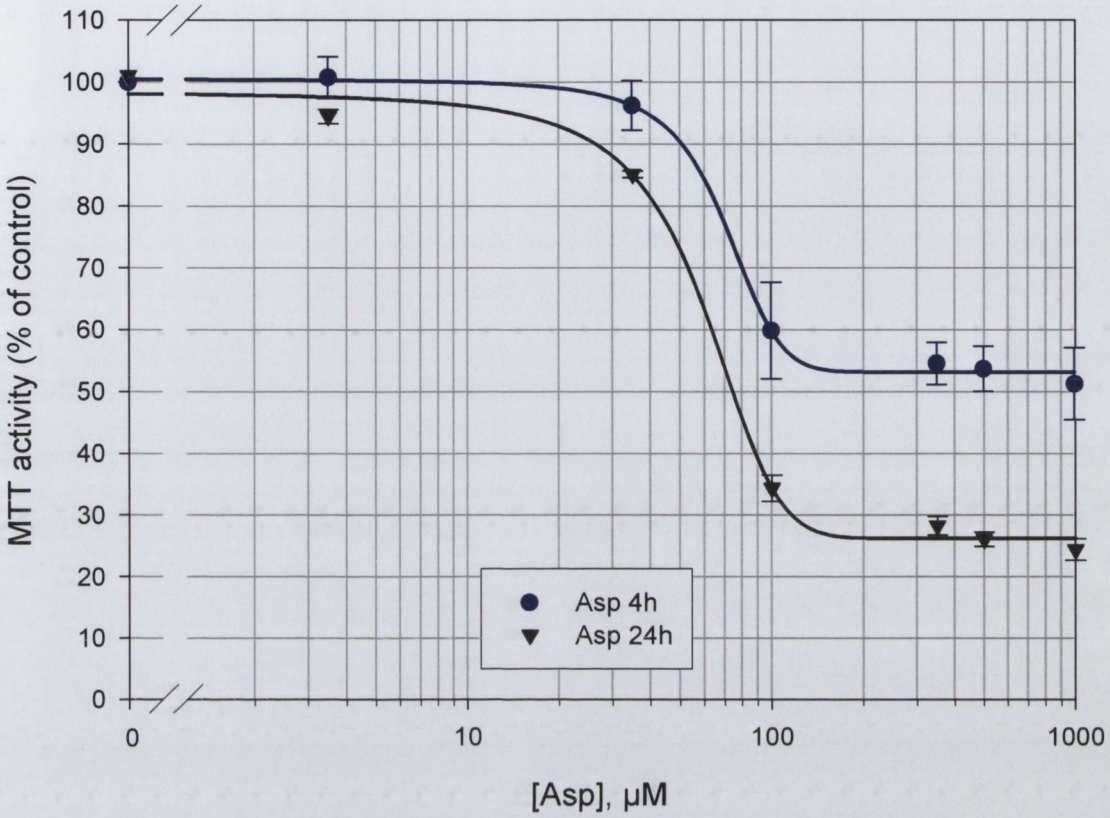


Figure 3.3: Concentration- and time-dependence of Asp on viability of mature mCGCs

Primary cultures of cerebellar granule cells, prepared from suspensions of dissociated cells from 7-day-old post-natal mouse cerebella, were maintained in culture for 7 days. Cells were then exposed for either 4 or 24 hours to various concentrations of Asp (added directly to the incubation medium) prior to assessment of cell viability by an MTT assay. The absorbance at 570 nm was expressed as a percentage of control (untreated) cells. Data represent mean ± s.d. values of triplicate MTT reactions derived from three separate experiments (n = 3).

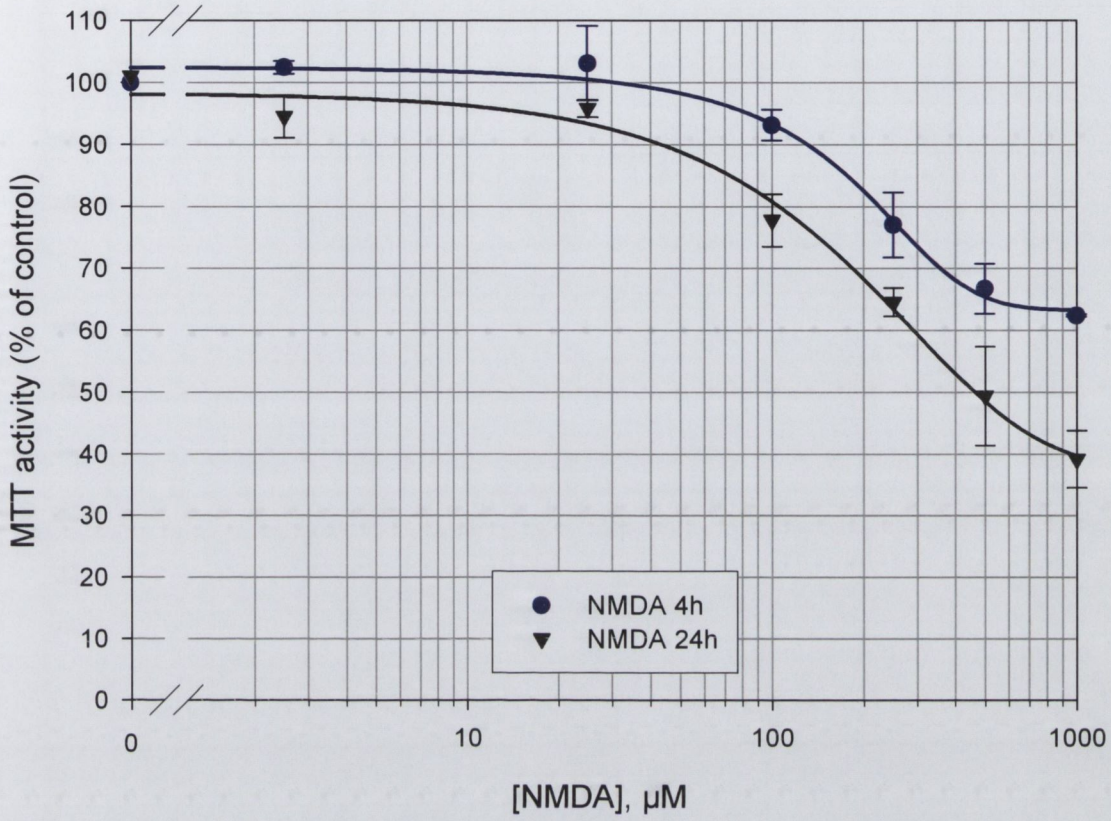


Figure 3.4: Concentration- and time-dependence of NMDA on viability of mCGCs

Primary cultures of cerebellar granule cells, prepared from suspensions of dissociated cells from 7-day-old post-natal mouse cerebella, were maintained in culture for 7 days. Cells were then exposed for either 4 or 24 hours to various concentrations of NMDA (added directly to the incubation medium) prior to assessment of cell viability by the MTT assay. The absorbance at 570 nm was expressed as a percentage of control (untreated) cells. Data represent mean ± s.d. values of triplicate MTT reactions derived from three separate experiments (n = 3).

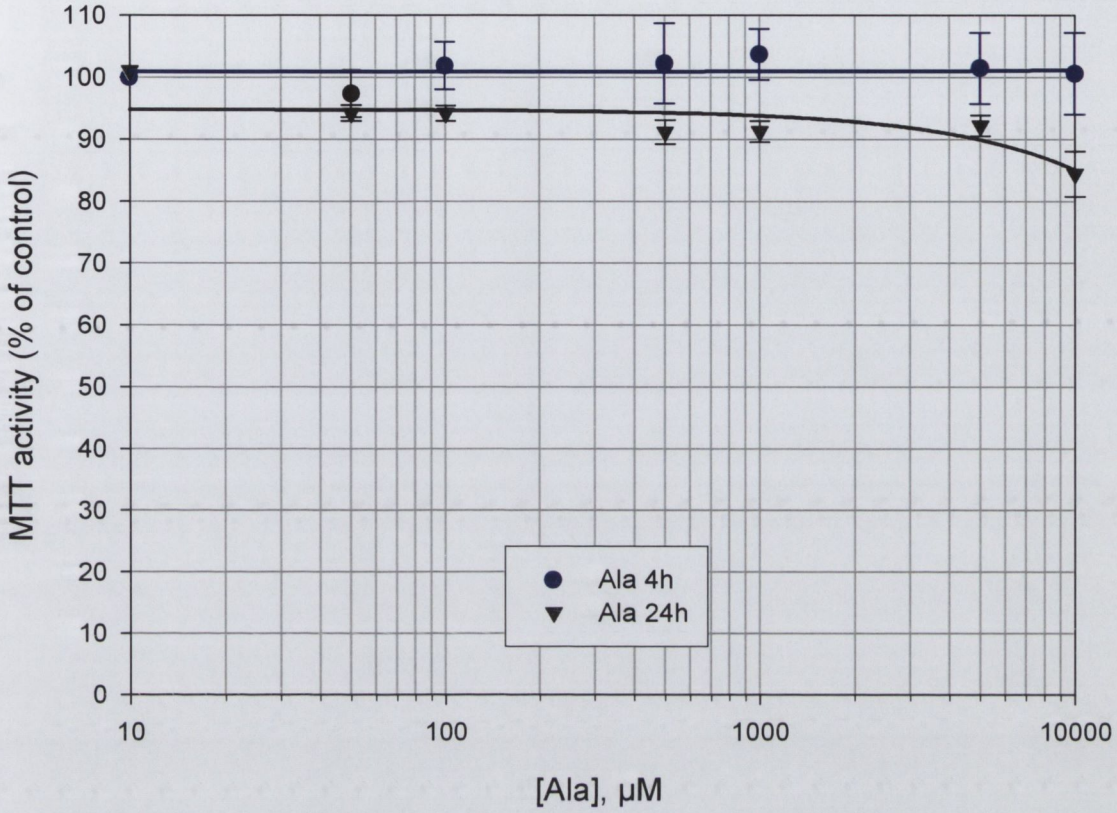


Figure 3.5: No decrease in viability of mCGCs treated with Ala

Primary cultures of cerebellar granule cells, prepared from suspensions of dissociated cells from 7-day-old post-natal mouse cerebella, were maintained in culture for 7 days. Cells were then exposed for either 4 hour or 24 hour time-periods to various concentrations of Ala (added directly to the incubation medium) prior to assessment of cell viability by the MTT assay. The absorbance at 570 nm was expressed as a percentage of control (untreated) cells. Data represent mean ± s.d. values of triplicate MTT reactions derived from three separate experiments (n = 3).

3.2.2 EAA-induced neurotoxicity in mCGCs is mediated through the NMDA receptor subtype of Glu receptors

In order to investigate whether EAA-induced cytotoxicity specifically involves NMDA receptors, the degree of protection offered by the selective, competitive NMDA receptor antagonist, AP5, was assessed in the presence of 3 known excitotoxins. The non-NMDA receptor antagonist, CNQX, was used for investigation of non-NMDA receptor activation. Primary cultures of mCGCs were prepared from post-natal mice as described in Chapter 2 (Section 2.2.1) and by Meier and Schousboe (1982), Drejer *et al.* (1983) and Schousboe *et al.* (1989) and were cultured for 7 days before exposure to both excitatory (Glu, Asp and NMDA) and non-excitatory (Ala) compounds. The mCGCs were pre-incubated with a fixed concentration of AP5 (500 µM) or CNQX (10 µM) for 15 min, before exposure to 3 different concentrations of the EAAs, Glu, Asp and NMDA, and the non-EAA, Ala. Cell viability was assessed by the MTT assay following 24 hour treatment; 24 hours was selected as the exposure time suitable to induce widespread neuronal degeneration.

When mCGCs were exposed to 25 µM Glu, a slight decrease in neuronal viability was observed. Antagonistic effects of either AP5 or CNQX were not apparent. Exposure of mCGCs to higher, toxic concentrations of Glu (100 µM and 250 µM) induced significant decreases in cell viability. Pre-treatment with AP5 effectively inhibited the Glu-induced cytotoxicity. Pre-treatment with CNQX had no protective effect (see Figure 3.6).

AP5 similarly antagonised Asp-induced decreases in neuronal viability, with CNQX having no effect (see Figure 3.7).

When mCGCs were exposed to 25 µM NMDA no real decrease in neuronal viability was observed. Thus, protective effects of either AP5 or CNQX were not apparent. However, exposure to higher, toxic concentrations of NMDA (100 µM and 250 µM) induced modest decreases in neuronal viability, which were antagonised by AP5. Pre-treatment with CNQX did not prevent the cytotoxic effects of NMDA (see Figure 3.8).

Thus, the results suggest that EAA-induced cytotoxicity is NMDA receptor mediated.

No difference was found between control neurons and neurons treated with Ala, with or without prior exposure to AP5 or CNQX (see Figure 3.9).

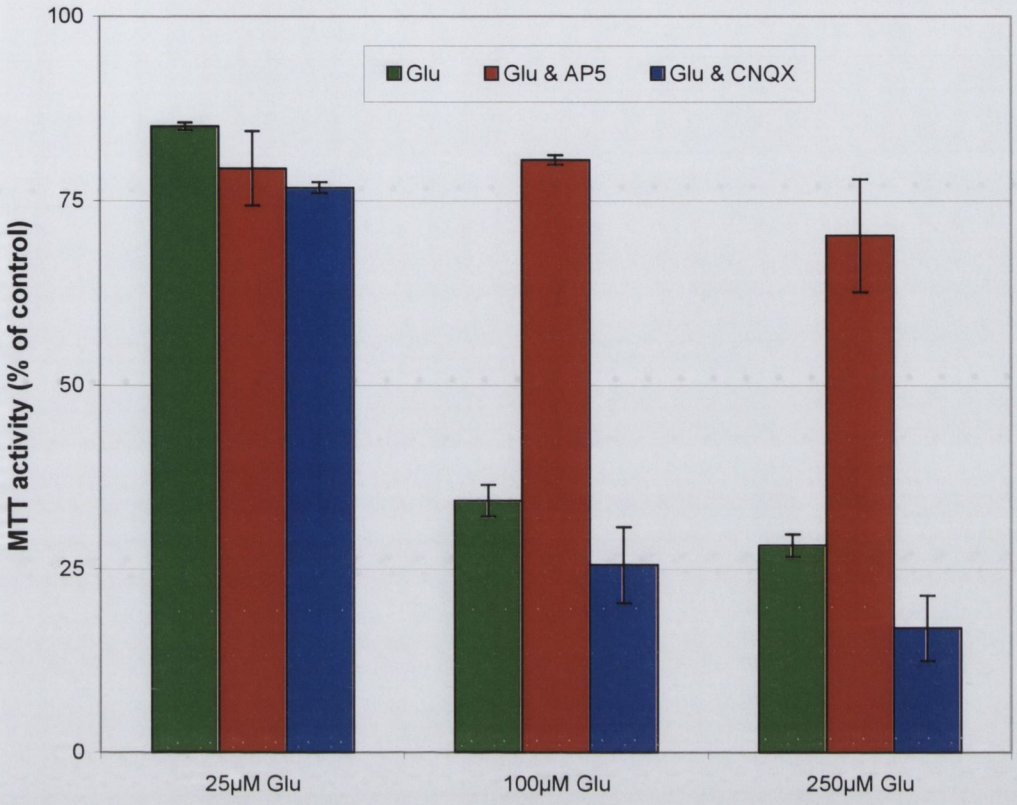


Figure 3.6: Glu-induced neurotoxicity is mediated through the NMDA receptor subtype in mature mCGCs

Primary cultures of mCGCs, prepared from suspensions of dissociated cells from 7-day-old post-natal mouse cerebella, were maintained in culture for 7 days before use. On the day of the experiment, cells were pre-incubated for 15 min with either AP5 (500 μM) or CNQX (10 μM) prior to co-exposure for 24 hours with 3 concentrations of Glu (25, 100 and 250 μM). Cell viability was assessed by the MTT assay. The absorbance at 570 nm was expressed as a percentage of control (untreated) cells. Data represent mean ± s.d. values of three separate experiments. Each column represents the mean ± s.d. values of 9 replicates.

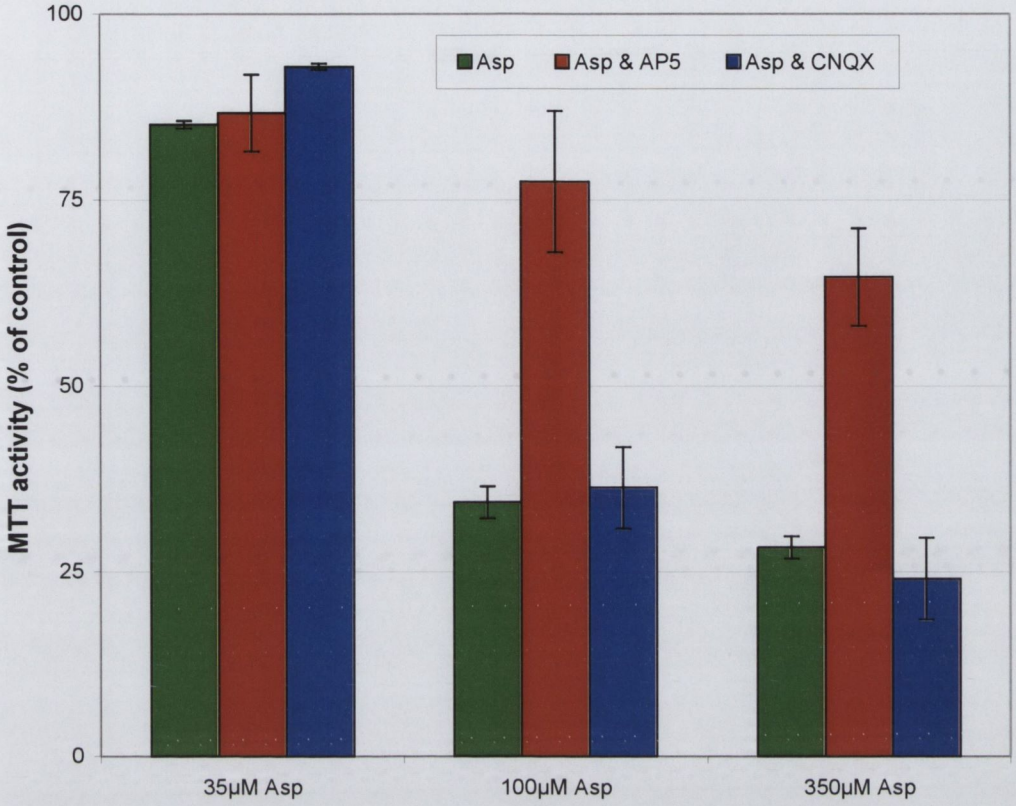


Figure 3.7: Asp-induced neurotoxicity in mCGCs is mediated through the NMDA receptor subtype.

Primary cultures of mCGCs, prepared from suspensions of dissociated cells from 7-day-old post-natal mouse cerebella, were maintained in culture for 7 days before use. On the day of the experiment, cells were pre-incubated for 15 min with either AP5 (500 μM) or CNQX (10 μM) prior to co-exposure for 24 hours with 3 concentrations (35, 100 and 350 μM) of Asp. Cell viability was assessed by the MTT assay. The absorbance at 570 nm was expressed as a percentage of control (untreated) cells. Data represent mean ± s.d. values of three separate experiments. Each column represents the mean ± s.d. values of 9 replicates.

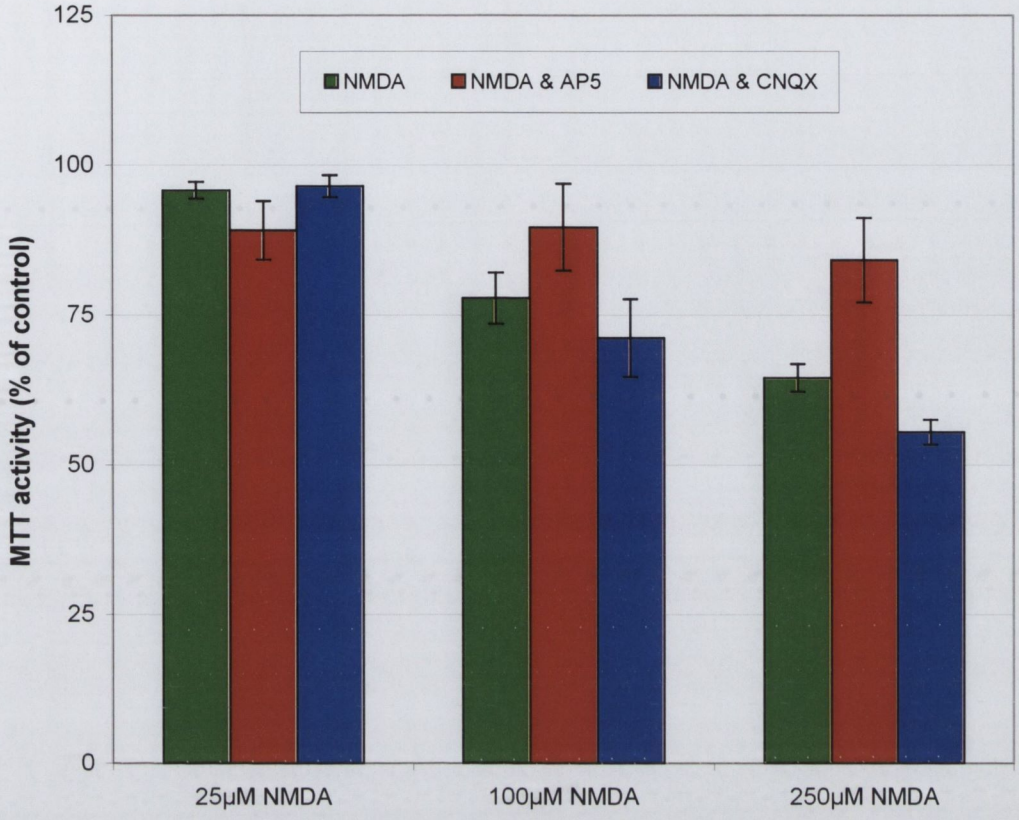


Figure 3.8: NMDA-induced neurotoxicity in mCGCs is mediated through the NMDA receptor subtype.

Primary cultures of mCGCs, prepared from suspensions of dissociated cells from 7-day-old post-natal mouse cerebella, were maintained in culture for 7 days before use. On the day of the experiment, cells were pre-incubated for 15 min with either AP5 (500 μM) or CNQX (10 μM) prior to co-exposure for 24 hours with 3 concentrations (25, 100 and 250 μM) of NMDA. Cell viability was assessed by the MTT assay. The absorbance at 570 nm was expressed as a percentage of control (untreated) cells. Data represent mean ± s.d. values of three separate experiments. Each column represents the mean ± s.d. values of 9 replicates.

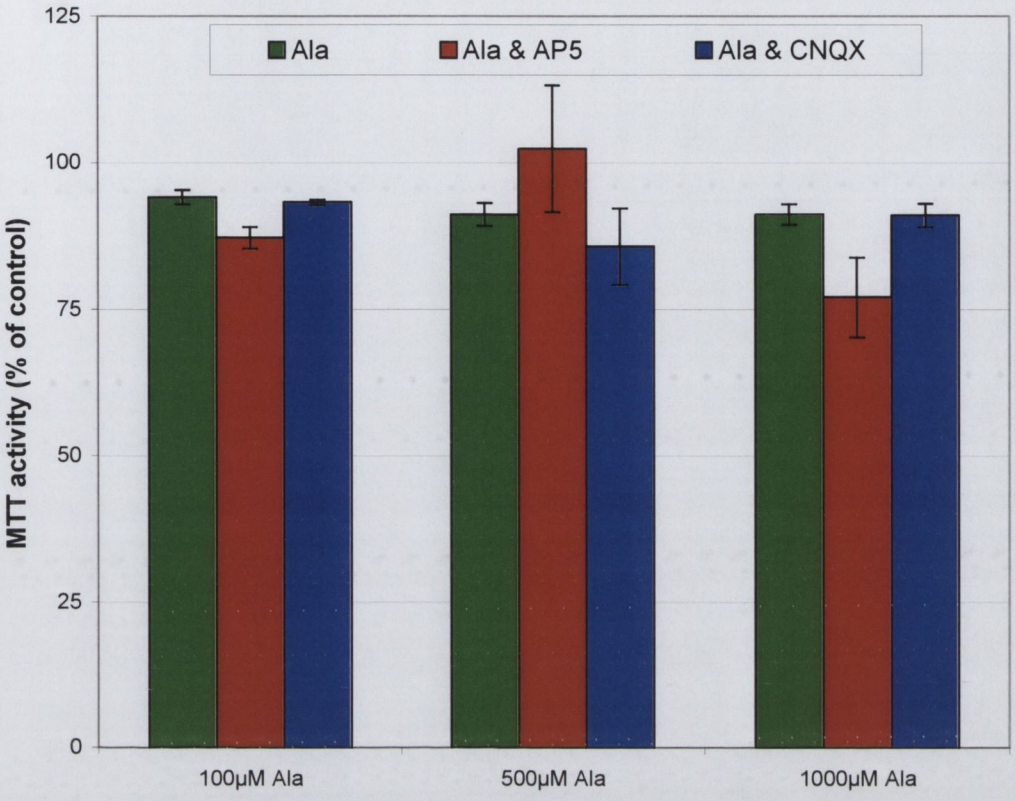


Figure 3.9: Ala does not induce neurotoxicity in mature mCGCs

Primary cultures of mCGCs, prepared from suspensions of dissociated cells from 7-day-old post-natal mouse cerebella, were maintained in culture for 7 days before use. On the day of the experiment, cells were pre-incubated for 15 min with either AP5 (500 μM) or CNQX (10 μM) prior to co-exposure for 24 hours with 3 concentrations (100, 500 and 1000 μM) of Ala. Cell viability was assessed by the MTT assay. The absorbance at 570 nm was expressed as a percentage of control (untreated) cells. Data represent mean ± s.d. values of three separate experiments. Each column represents the mean ± s.d. values of 9 replicates.

3.2.3 Rapid reduction of intracellular ATP levels in mCGCs following EAA treatment

Previous reports (Ankarcrona *et al.*, 1995, 1996) suggest that following EAA exposure, the mode of rat cerebellar granule cell death is dependent on intracellular ATP concentrations and mitochondrial function. Moreover, the intensity of the initial stimulus on intracellular ATP concentration decides the prevalence of either apoptosis or necrosis (Leist *et al.*, 1997). Primary cultures of mCGCs were prepared from post-natal mice as described in Section 2.2.1 and by Meier and Schousboe (1982), Drejer *et al.* (1983) and Schousboe *et al.* (1989). The mCGCs were cultured for 7 days before exposure to various concentrations of both excitotoxins (Glu, Asp and NMDA) and non-excitotoxins (Ala). Intracellular ATP concentrations were measured using the ATPLite™-M kit, a luminescent ATP detection assay. The toxic effects of Glu, Asp and NMDA on intracellular ATP levels are shown in Figures 3.10 to 3.12 and can be compared to the non-toxic action of Ala in Figure 3.13.

When mCGCs were exposed to various concentrations of Glu, Asp and NMDA, for 4 and 24 hours, rapid decreases in intracellular ATP levels were observed. These decreases were concentration-dependent. The EC_{50} values for Glu, Asp and NMDA at 4 hours were 37 µM, 65 µM and 90 µM, respectively. At 24 hours, the EC_{50} values for Glu, Asp and NMDA were 50 µM, 60 µM and 140 µM, respectively. The results reveal that following insult ATP concentration had decreased rapidly by 4 hours, with no further decrease in ATP concentration at 24 hours. These results are in contrast to the time-dependent decreases of neuronal viability induced by the EAAs (see Section 3.2.1).

Additionally, it was shown that both Glu and Asp had similar toxic effects on the cells while NMDA was less potent. In the case of Glu and Asp, the decrease in intracellular ATP concentration seemed to plateau at approximately 20 %. This plateau of 20 % implicates a residual amount of ATP in the neurons.

The non-EAA, Ala, had no effect on intracellular ATP concentrations (see Figure 3.13) and was thus non-toxic to the cells.

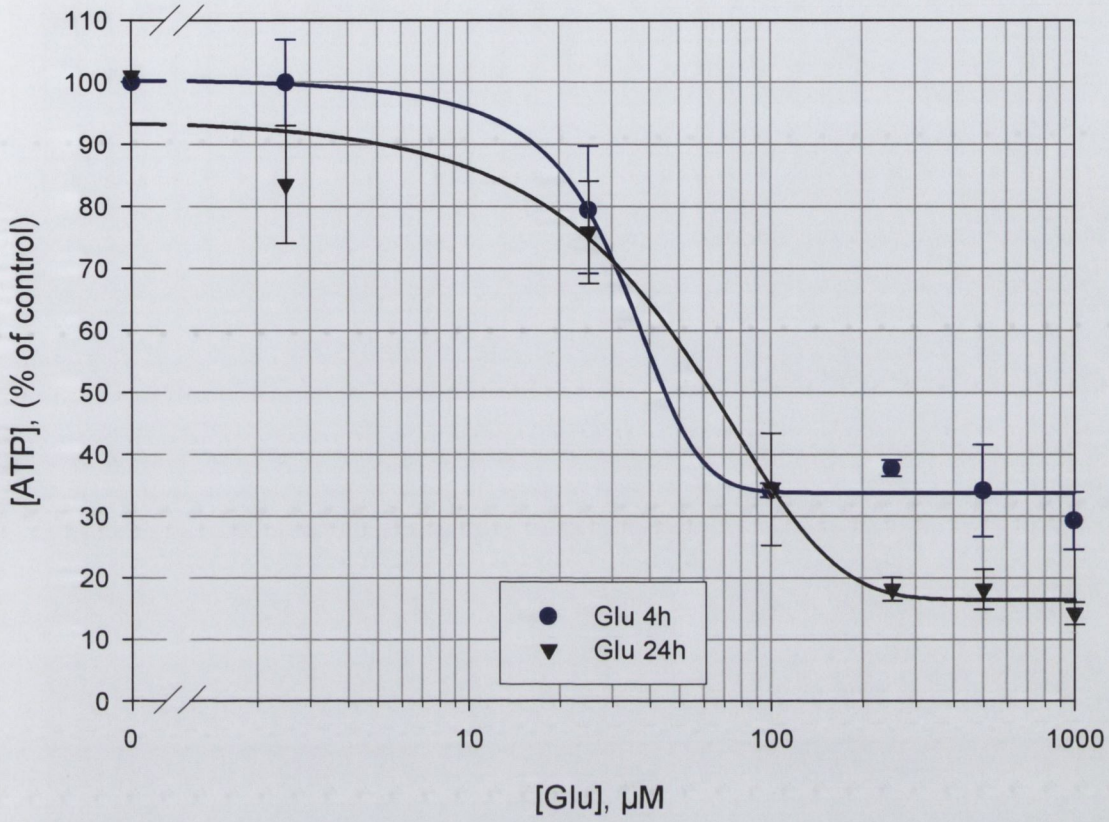


Figure 3.10: Glu rapidly decreases intracellular ATP concentrations in mCGCs

Primary cultures of cerebellar granule cells were maintained in culture for 7 days and were then exposed for either 4 or 24 hours to various concentrations of Glu (added directly to the incubation medium). ATP concentrations were then measured using the ATPLite™-M kit, a luminescent ATP detection assay. The luminescence values were expressed as a percentage of control (untreated) cells. Data represent mean ± s.d. values of triplicate ATP reactions derived from three separate experiments (n = 3).

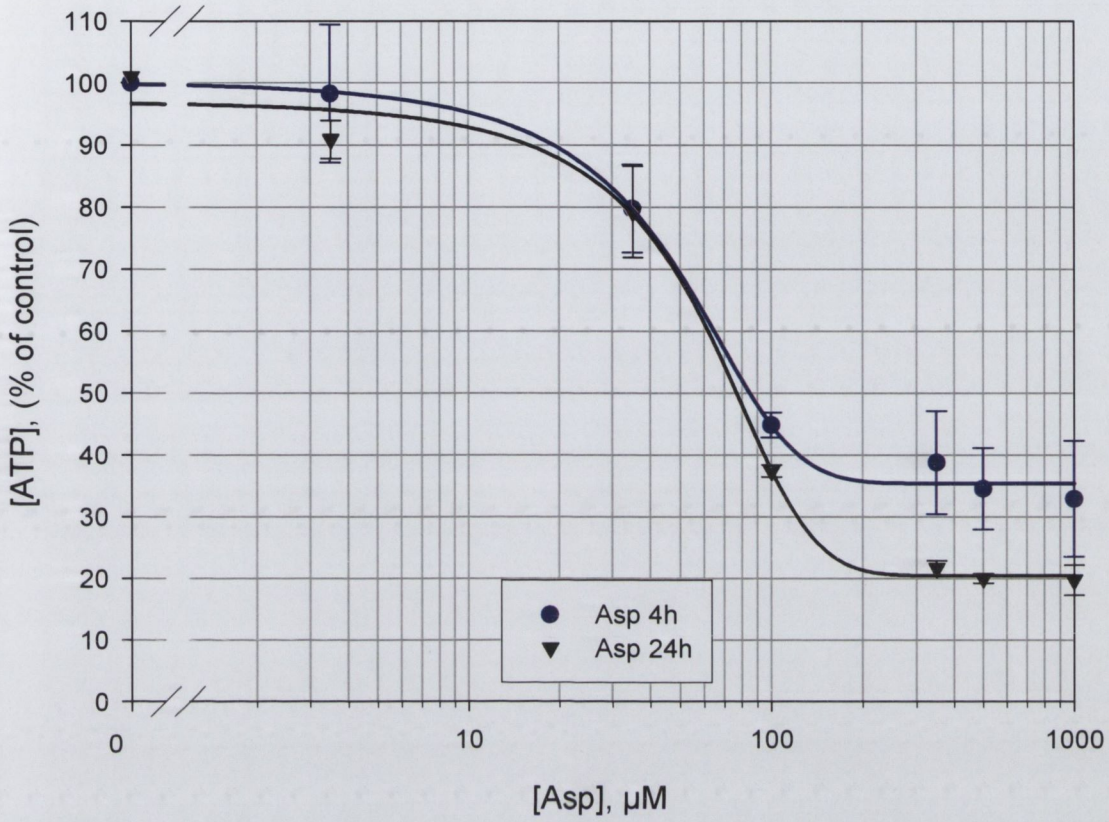


Figure 3.11: Asp rapidly decreases intracellular ATP concentrations in mCGCs

Primary cultures of mCGCs were maintained in culture for 7 days and were then exposed for either 4 or 24 hours to various concentrations of Asp (added directly to the incubation medium). ATP concentrations were then measured using the ATPLite™-M kit, a luminescent ATP detection assay. The luminescence values were expressed as a percentage of control (untreated) cells. Data represent mean ± s.d. values of triplicate ATP reactions derived from three separate experiments (n = 3).

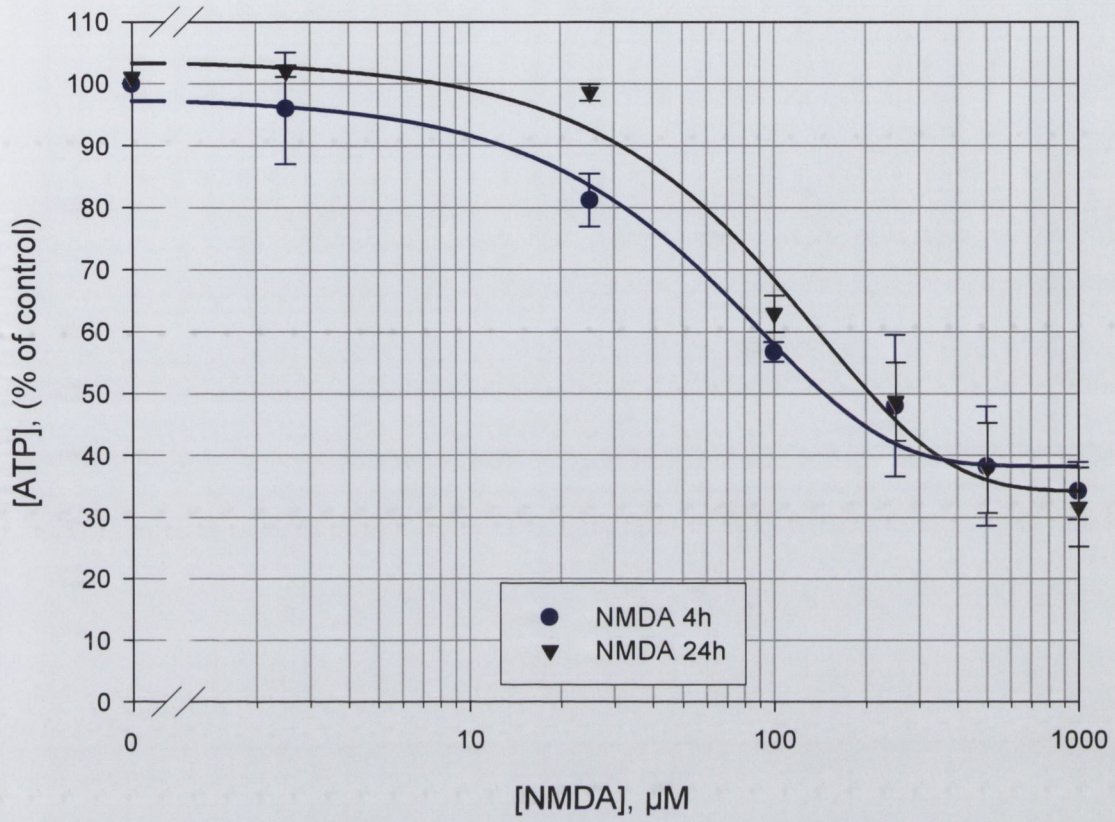


Figure 3.12: NMDA decreases intracellular ATP concentrations in mCGCs

Primary cultures of cerebellar granule cells were maintained in culture for 7 days and were then exposed for either 4 or 24 hours to various concentrations of NMDA (added directly to the incubation medium). ATP concentrations were then measured using the ATPLite™-M kit, a luminescent ATP detection assay. The luminescence values were expressed as a percentage of control (untreated) cells. Data represent mean ± s.d. values of triplicate ATP reactions derived from three separate experiments (n = 3).

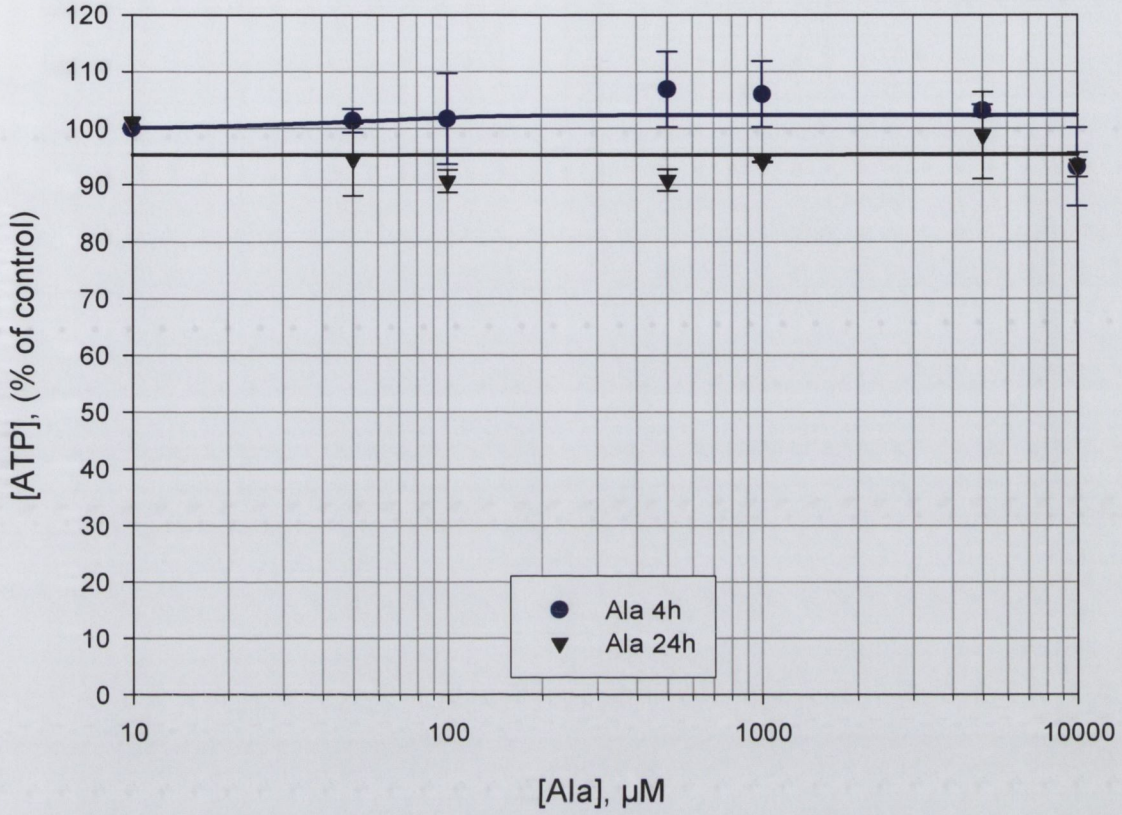


Figure 3.13: Ala has no effect on intracellular ATP concentrations in mCGCs

Primary cultures of cerebellar granule cells were maintained in culture for 7 days and were then exposed for either 4 or 24 hours to various concentrations of Ala (added directly to the incubation medium). ATP concentrations were then measured using the ATPLite™-M kit, a luminescent ATP detection assay. The luminescence values were expressed as a percentage of control (untreated) cells. Data represent mean ± s.d. values of triplicate ATP reactions derived from three separate experiments (n = 3).

3.2.4 EAA-induced decreases in intracellular ATP levels of mCGCs are NMDA receptor mediated

Previously, it was shown that AP5 effectively antagonised the cytotoxic effects of Glu, Asp and NMDA, while CNQX had no inhibitory effect (see Section 3.2.2). All 3 excitotoxins induced concentration-dependent decreases in intracellular ATP levels (Section 3.2.3), which were similar in profile to the decreases observed in cell viability (see Section 3.2.1). It was therefore of interest to investigate whether the NMDA receptor antagonist, AP5, could also protect against excitotoxin-induced loss of intracellular ATP. The non-NMDA receptor antagonist, CNQX, was used for comparison.

Primary cultures of mCGCs (7 DIV) were pre-treated with a fixed concentration of AP5 (500 µM) or CNQX (10 µM) for 15 min before exposure to 3 different concentrations of Glu, Asp and NMDA for 24 hours. The time-point of 24 hours was selected as a suitable assay time and also exposure time to induce intracellular ATP loss. The non-EAA, Ala, was used as a control compound. Intracellular ATP concentrations were measured using the ATPLite™-M kit, a luminescent ATP detection assay.

It was observed that AP5 fully protected against ATP loss induced by concentrations of Glu and Asp up to 100 µM. However, less protection by AP5 was observed in the presence of higher concentrations of Glu and Asp (250 and 350 µM, respectively), as would be expected for the competitive interaction of agonists and competitive antagonists (see Figures 3.14 and 3.15).

With all 3 concentrations of NMDA (25 µM, 100 µM and 250 µM), AP5 effectively protected the neurons against ATP loss (see Figure 3.16).

These results suggest that the protection of the cells by AP5, from excitotoxin–induced ATP loss, is a function of both the concentration of the excitotoxins used and their relative potencies.

With all concentrations of Glu, Asp and NMDA, pre-treatment of the neurons with CNQX offered no protective effect. Thus, excitotoxin-induced decreases in intracellular ATP concentrations are NMDA receptor mediated.

No difference was found between control neurons and neurons treated with Ala, with or without prior exposure to the antagonists (see Figure 3.17).

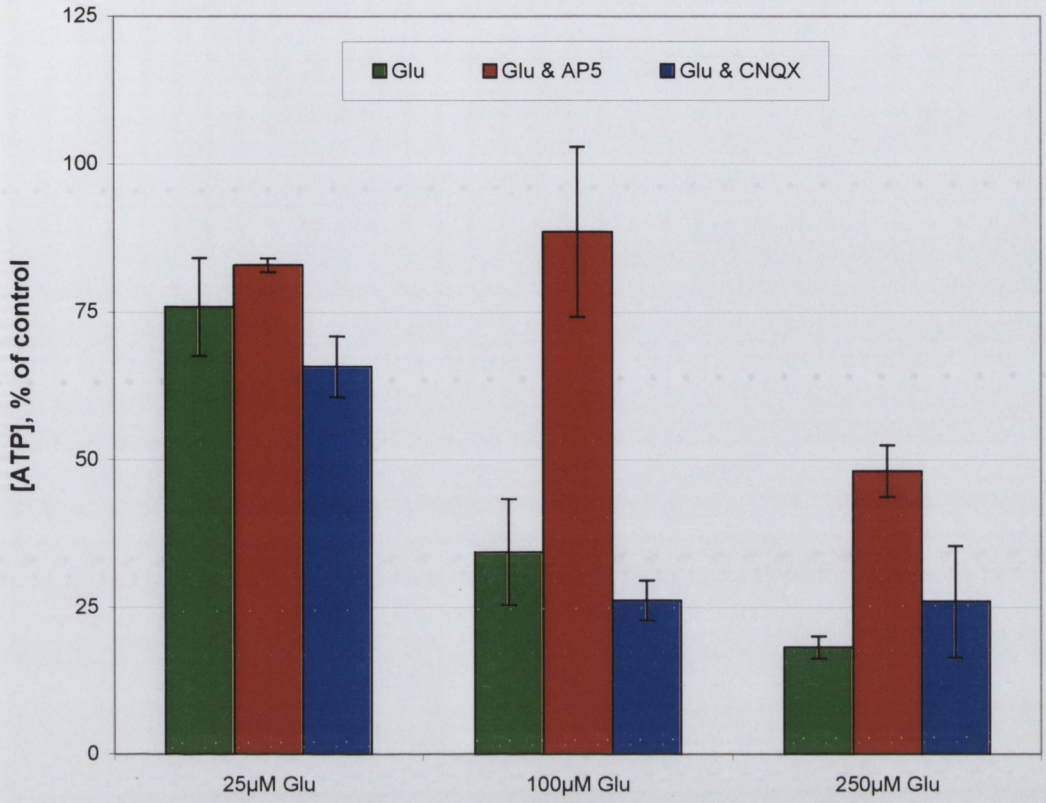


Figure 3.14: Glu-induced decreases in intracellular ATP concentration are NMDA receptor mediated in mCGCs

Primary cultures of cerebellar granule cells (7 DIV) were pre-incubated for 15 min with either AP5 (500 μM) or CNQX (10 μM) prior to co-exposure for 24 hours with 3 concentrations (25, 100 and 250 μM) of Glu (added directly to the incubation medium). ATP concentrations were then measured using the ATPLite™-M kit, a luminescent ATP detection assay. The luminescence values were expressed as a percentage of control (untreated) cells. Data represent mean ± s.d. values of three separate experiments. Each column represents the mean of 9 replicates.

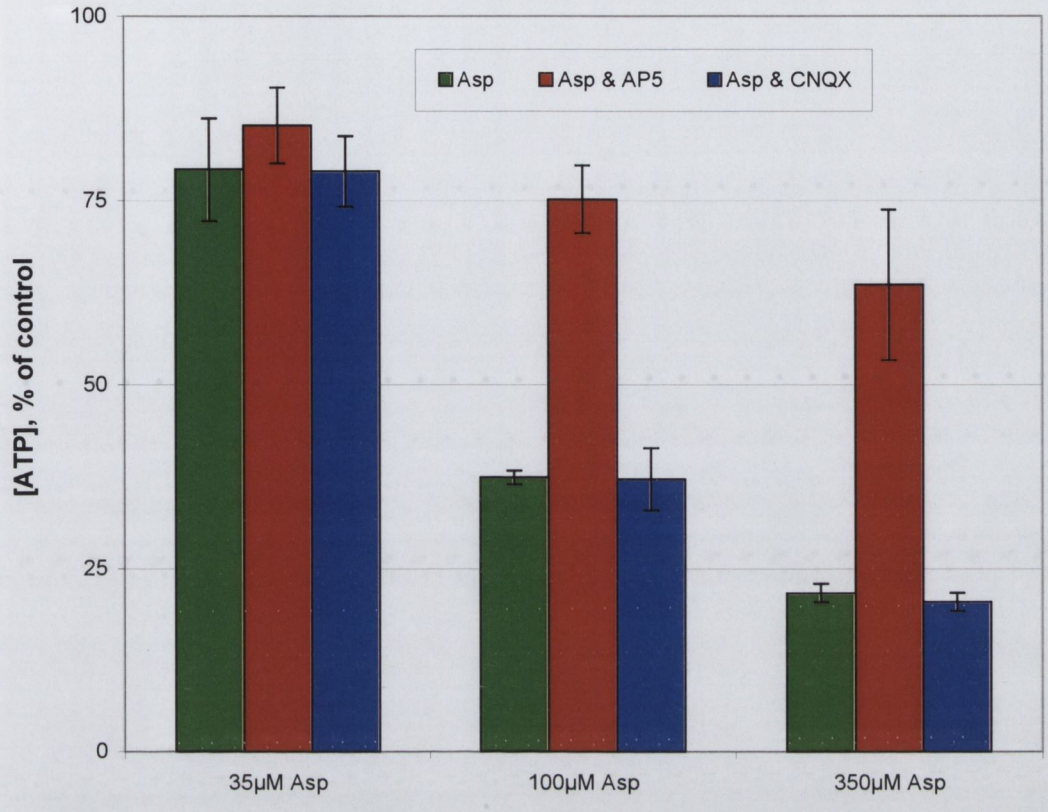


Figure 3.15: Asp-induced loss of intracellular ATP is mediated through the NMDA receptor subtype in mCGCs

Primary cultures of cerebellar granule cells (7 DIV) were pre-incubated for 15 min with either AP5 (500 μM) or CNQX (10 μM) prior to co-exposure for 24 hours with 3 concentrations of Asp (35, 100 and 350 μM; added directly to the incubation medium). ATP concentrations were then measured using the ATPLite™-M kit, a luminescent ATP detection assay. The luminescence values were expressed as a percentage of control (untreated) cells. Data represent mean ± s.d. values of three separate experiments. Each column represents the mean of 9 replicates.

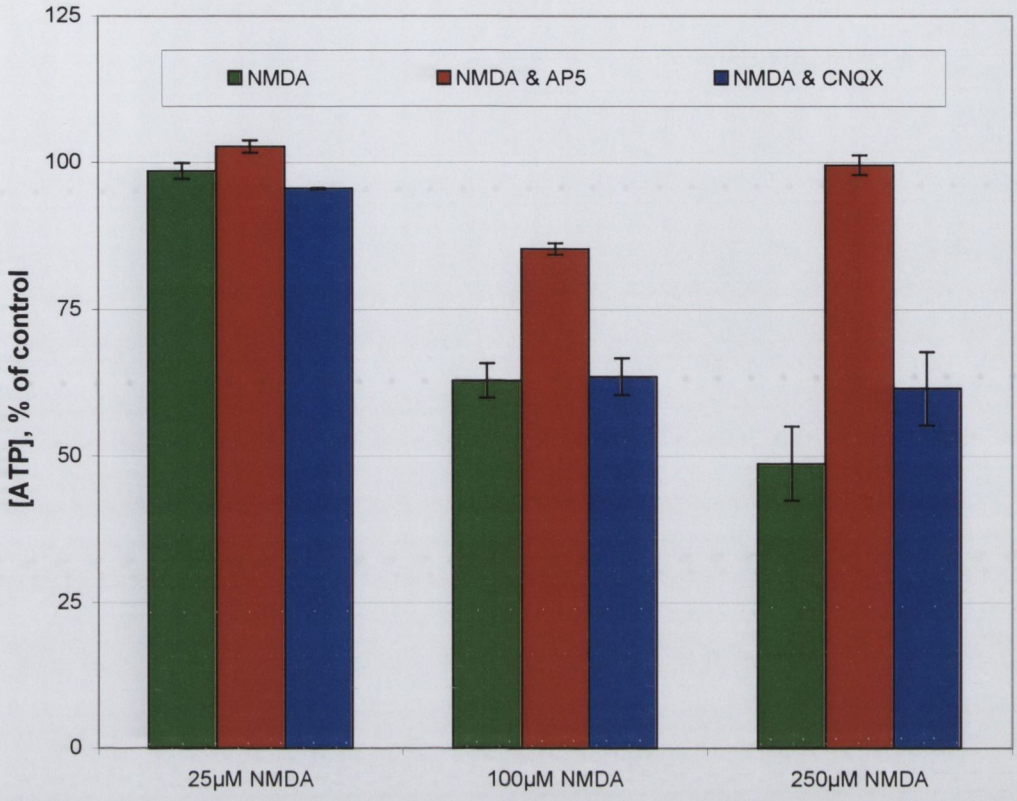


Figure 3.16: NMDA-induced decreases in intracellular ATP concentration are mediated through the NMDA receptor subtype in mCGCs

Primary cultures of cerebellar granule cells (7 DIV) were pre-incubated for 15 min with either AP5 (500 μM) or CNQX (10 μM) prior to co-exposure for 24 hours with 3 concentrations of NMDA (25, 100 and 250 μM; added directly to the incubation medium). ATP concentrations were then measured using the ATPLite™-M kit, a luminescent ATP detection assay. The luminescence values were expressed as a percentage of control (untreated) cells. Data represent mean ± s.d. values of three separate experiments. Each column represents the mean of 9 replicates.

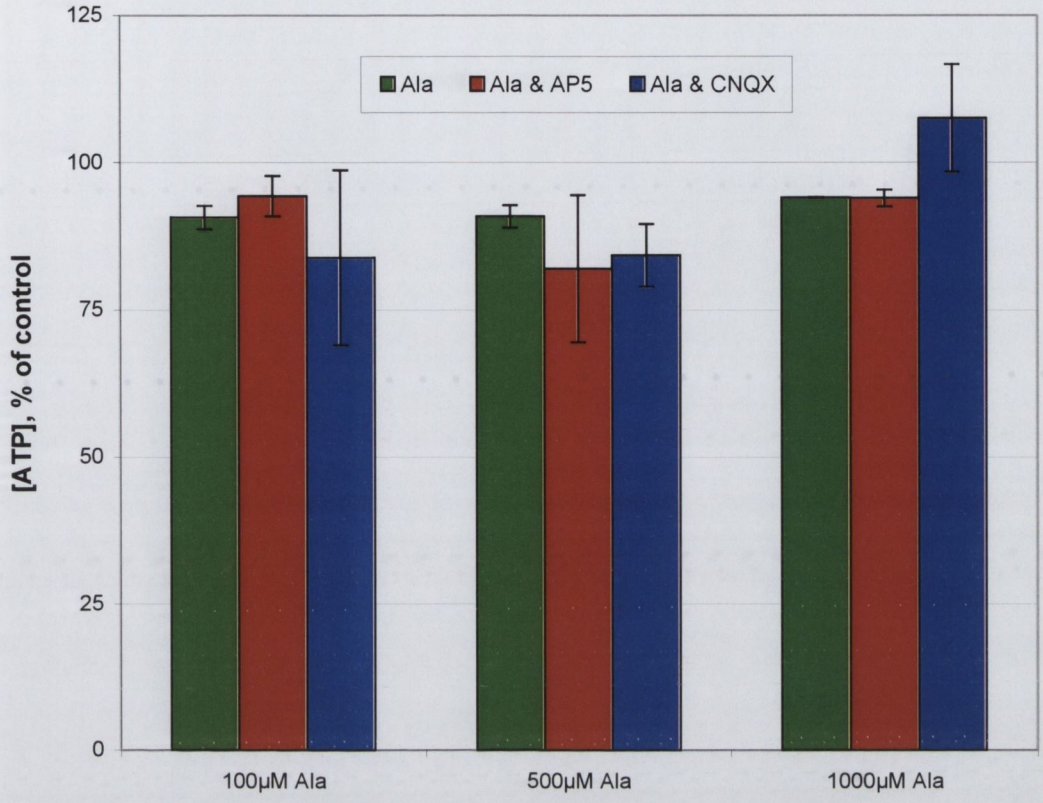


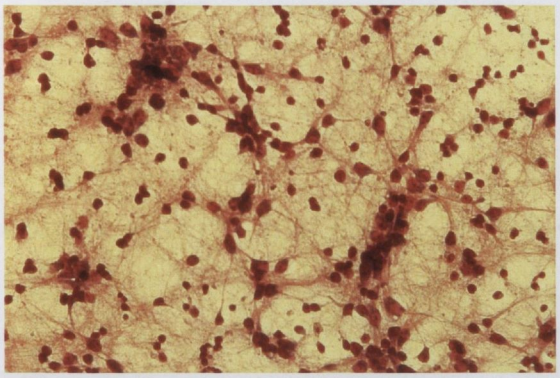
Figure 3.17: Ala treatment does not affect intracellular ATP levels of mCGCs

Primary cultures of cerebellar granule cells, prepared from suspensions of dissociated cells from 7-day-old post-natal mouse cerebella, were maintained in culture for 7 days before use. On the day of the experiment, cells were pre-incubated for 15 min with either AP5 (500 μM) or CNQX (10 μM) prior to co-exposure for 24 hours with 3 concentrations (100, 500 and 1000 μM) of Ala. ATP concentrations were then measured using the ATPLite™-M kit, a luminescent ATP detection assay. The luminescence values were expressed as a percentage of control (untreated) cells. Data represent mean ± s.d. values of three separate experiments. Each column represents the mean of 9 replicates.

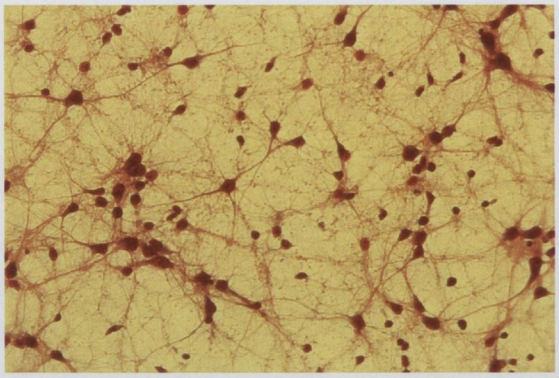
3.2.5 Development of a primary cell culture system of rat cortical neurons

Having established primary cultures of mCGCs in our laboratory as a suitable model for excitotoxic investigations, it was decided to develop an additional and alternative model of primary neurons from a different species and brain region. Like with mCGCs, the system should be robust, reproducible and contain a pure neuronal population. The rat cortical neuronal system reported by Schmuck and Schlüter (1996) and Schmuck *et al.* (2000) seemed to meet these criteria and even involved a serum-free media. The main disadvantage of using the mCGC system is the use of serum in the media used to culture the neurons. It has previously been reported (Schramm *et al.*, 1990) that the Glu component in serum causes neuronal death through activation of the NMDA subtype of Glu receptor. Another advantage in using the rat cortical model is that cultures maintained in serum-free media have a very low percentage of glia (Stefanis *et al.*, 1999).

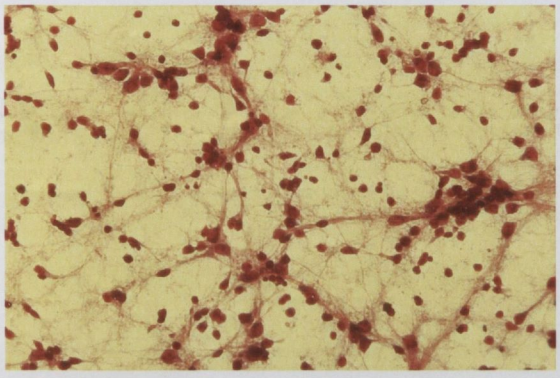
It was reported by Schubert *et al.* (2001) that the efficiency of toxic cell death is dependent on the length of time the neurons have been maintained in culture. Indeed, Balaz et al. (1988) reported that the expression of NMDA receptors by mCGCs is significantly delayed in serum-free as opposed to serum-containing medium. This is presumably attributable to the time required for the neurons to express functional ionotropic Glu receptors. A consistent finding is that "immature" cultures (2 DIV) of both mCGCs and rat cortical neurons exhibit no toxicity when exposed to high concentrations of Glu and other EAA agonists (Frandsen and Schousboe, 1990; Meredith *et al.*, 1996) even though functional EAA receptors are present at this stage in development (Balazs *et al.*, 1988). In order to investigate the efficiency of NMDA receptor-mediated neurotoxicity, rat cortical neurons were cultured from 7 to 13 days before exposure to the EAA, Glu (see Figure 3.19). It was found that cell viability following Glu exposure was not only proportional to the concentrations of Glu used but also to the length of time the neurons were maintained in culture. It was observed that 10 DIV and 13 DIV cultures of rat cortical neurons were the most sensitive to Glu stimulation (see Figure 3.19) and were therefore used in subsequent experiments. The cytotoxic effects of Glu were consistent with the appearance of the cell cultures when observed visually under the light microscope (see Figure 3.18). 13 DIV untreated rat cortical neurons appeared as a monolayer of small pyramidal bodies with extensive neurite complexes. Following treatment with Glu, at concentrations higher that 100 µM over 24 hours, the cell networks were completely disintegrated.



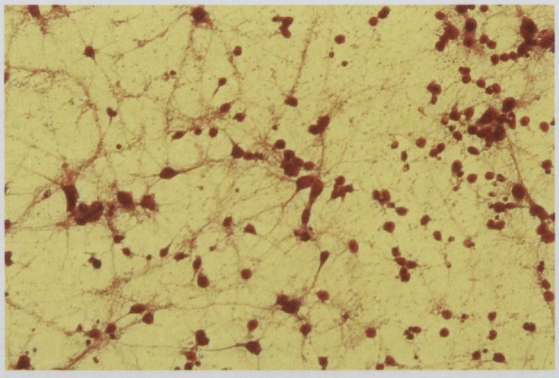
Untreated mCGCs



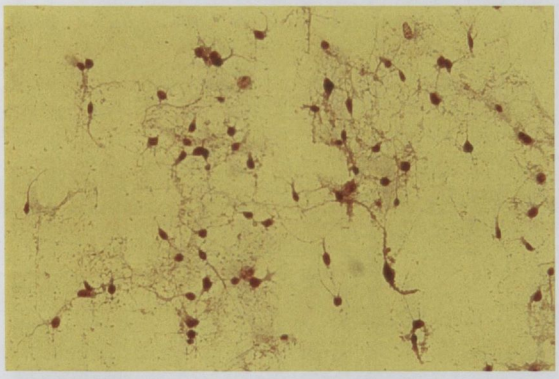
b) 25 µM Glu



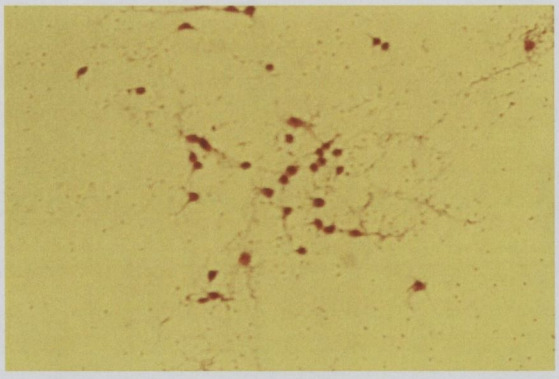
c) 100 µM Glu



d) 250 µM Glu



e) 500 µM Glu



f) 1000 µM Glu

Figure 3.18: Glu cytotoxicity is concentration-dependent in rat cortical neurons
Primary cultures of rat cortical neurons (13 DIV) were exposed to various concentrations of Glu for 24 hours before being stained with Giemsa and visually observed under the light microscope.

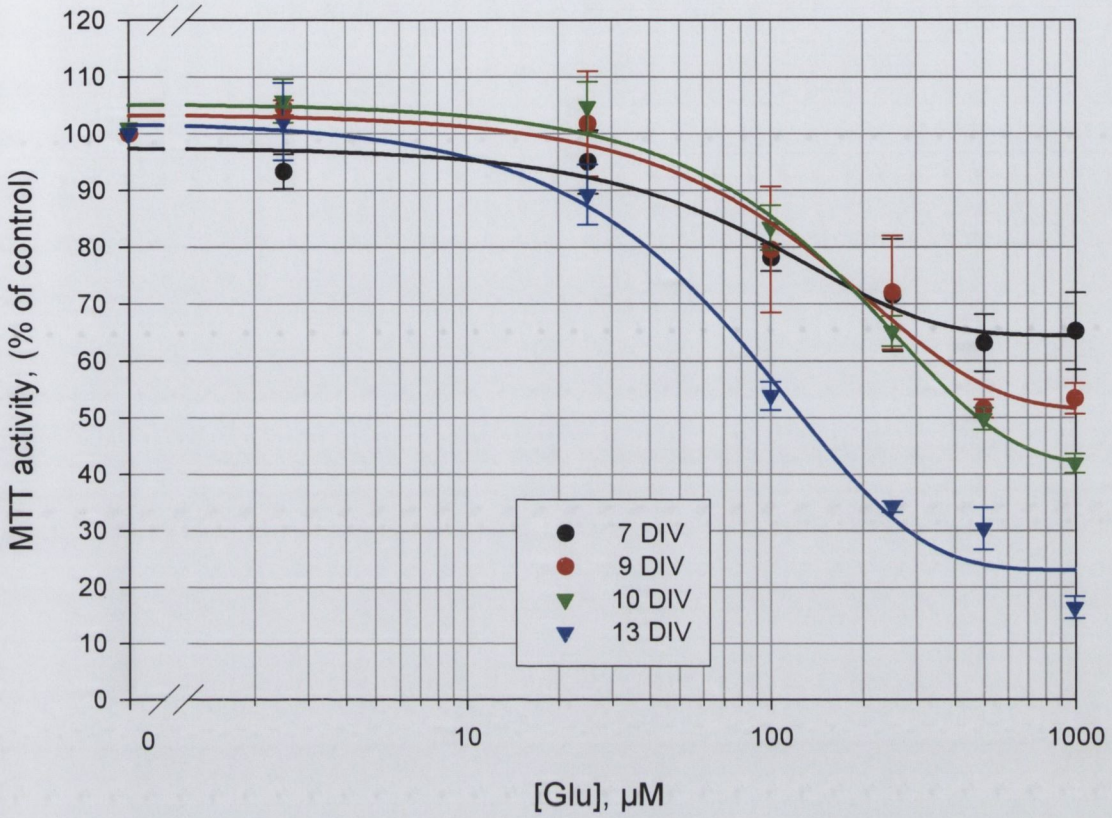


Figure 3.19: Glu-induced neurotoxicity in rat cortical neurons is dependent on both concentration and time in culture

Primary cultures of rat cortical neurons, prepared from suspensions of dissociated cells from fetal rats (E18), were maintained in culture from days 7 to 13. On each measurement day, cells were exposed for 24 hours to various concentrations of Glu (added directly to the incubation medium) prior to assessment of cell viability by the MTT assay. The absorbance at 570 nm was expressed as a percentage of control (untreated) cells. Data represent mean ± s.d. values of triplicate MTT reactions derived from three separate experiments (n = 3).

3.2.6 Rat cortical neurons develop increased EAA sensitivity in culture

From consideration of the results in the previous section, it was decided to investigate the effects of both excitatory (Glu and Asp) and non-excitatory (Ala and paraquat) compounds on 10 DIV and 13 DIV rat cortical neurons.

Primary cultures of rat cortical neurons were prepared from fetal rats (E18) as described in Section 2.2.2 and by Schmuck and Schlüter (1996) and Schmuck *et al.* (2000). Cytotoxicity was assessed by the measurement of MTT activity in treated neurons when compared to untreated neurons (where MTT activity was 100 %). The cytotoxic actions of Glu and Asp on rat cortical neurons after 24 hours are shown in Figures 3.20 and 3.21 and can be compared to the non-cytotoxic action of Ala in Figure 3.22. The cytotoxic actions of Paraquat are shown in Figure 3.23.

When rat cortical neurons were exposed to various concentrations of Glu and Asp for 24 hours, concentration-dependent decreases in cell viability were observed. In addition, the neurons were more sensitive to EAA stimulation at 13 DIV rather than at 10 DIV. The EC_{50} values for Glu and Asp in 10 DIV neurons were 280 µM and > 100 µM, respectively. For 13 DIV neurons, the EC_{50} values for Glu and Asp were 90 µM and 140 µM, respectively.

The non-excitatory amino acid, Ala, had no effect on cell viability in either 10 DIV or 13 DIV rat cortical cultures.

With paraquat, a concentration-dependent decrease in cell viability occurred in both 10 DIV and 13 DIV rat cortical neurons, which is in accordance with previous reports (Schmuck *et al.*, 2000). No real difference in sensitivity was observed between the 10 DIV (EC_{50} value of 160 µM) and 13 DIV (EC_{50} value of 200 µM) cortical cultures. These results suggest that the toxic response of the cells to paraquat is not dependent on time in culture. Furthermore, the results are demonstrative of the differences that exist in the mechanisms of EAA and paraquat neurotoxicity. The mechanism of paraquat neurotoxicity involves cyclic reduction/reoxidation resulting in NADPH consumption and radical formation (Corasanti *et al.*, 1998).

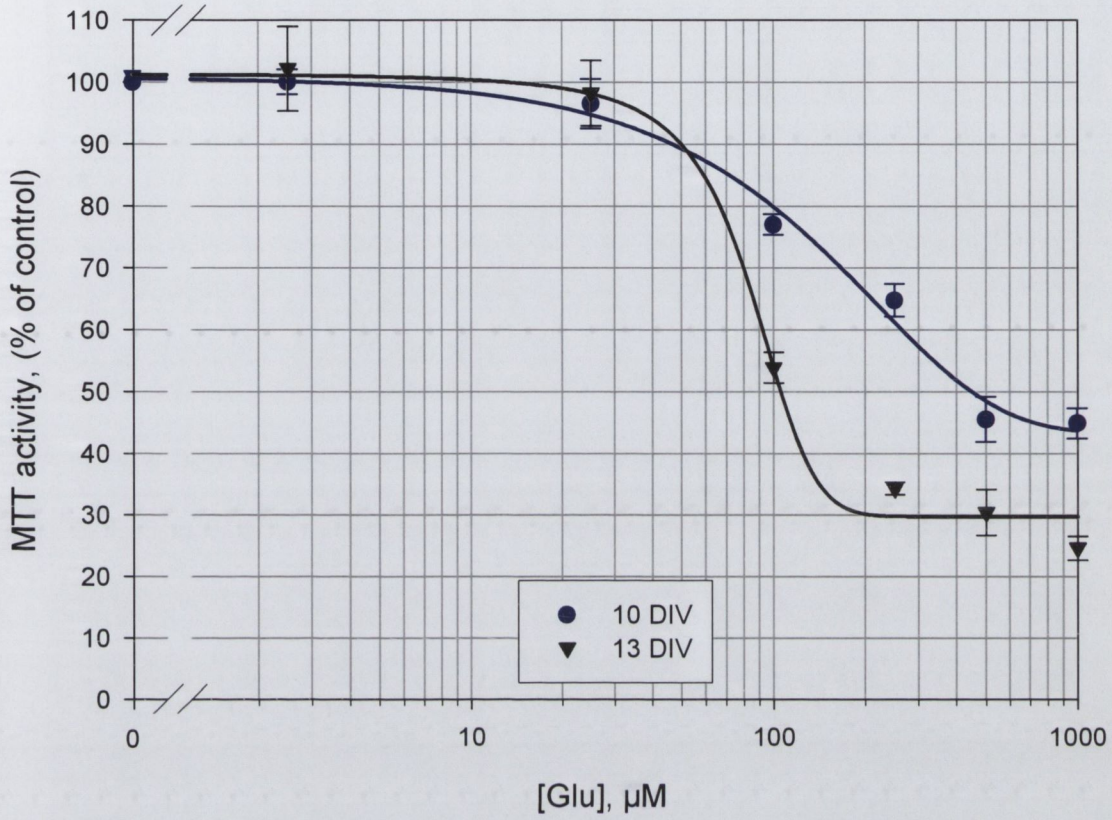


Figure 3.20: Concentration-dependence of Glu on cell viability in 10 DIV and 13 DIV rat cortical neurons

Primary cultures of rat cortical neurons, prepared from suspensions of dissociated cells from fetal rats (E18), were maintained in identical culture conditions for either 10 days or 13 days. 10 DIV and 13 DIV neurons were exposed for 24 hours to various concentrations of Glu (added directly to the incubation medium) prior to assessment of cell viability by the MTT assay. The absorbance at 570 nm was expressed as a percentage of control (untreated) cells. Data represent mean ± s.d. values of three separate experiments. Each point represents the mean of 9 replicates.

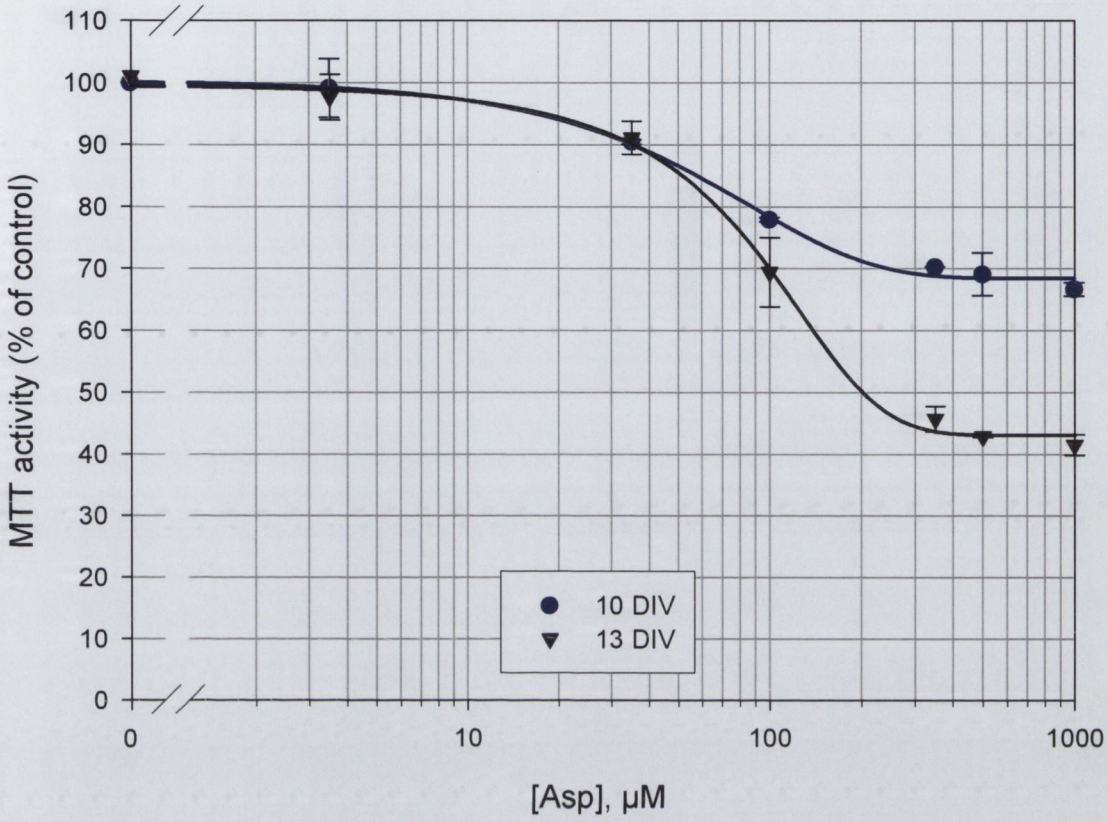


Figure 3.21: Concentration-dependence of Asp on cell viability in 10 DIV and 13 DIV rat cortical neurons

Primary cultures of rat cortical neurons, prepared from suspensions of dissociated cells from fetal rats (E18), were maintained in identical culture conditions for either 10 days or 13 days. 10 DIV and 13 DIV neurons were exposed for 24 hours to various concentrations of Asp (added directly to the incubation medium) prior to assessment of cell viability by the MTT assay. The absorbance at 570 nm was expressed as a percentage of control (untreated) cells. Data represent mean ± s.d. values of three separate experiments. Each point represents the mean of 9 replicates.

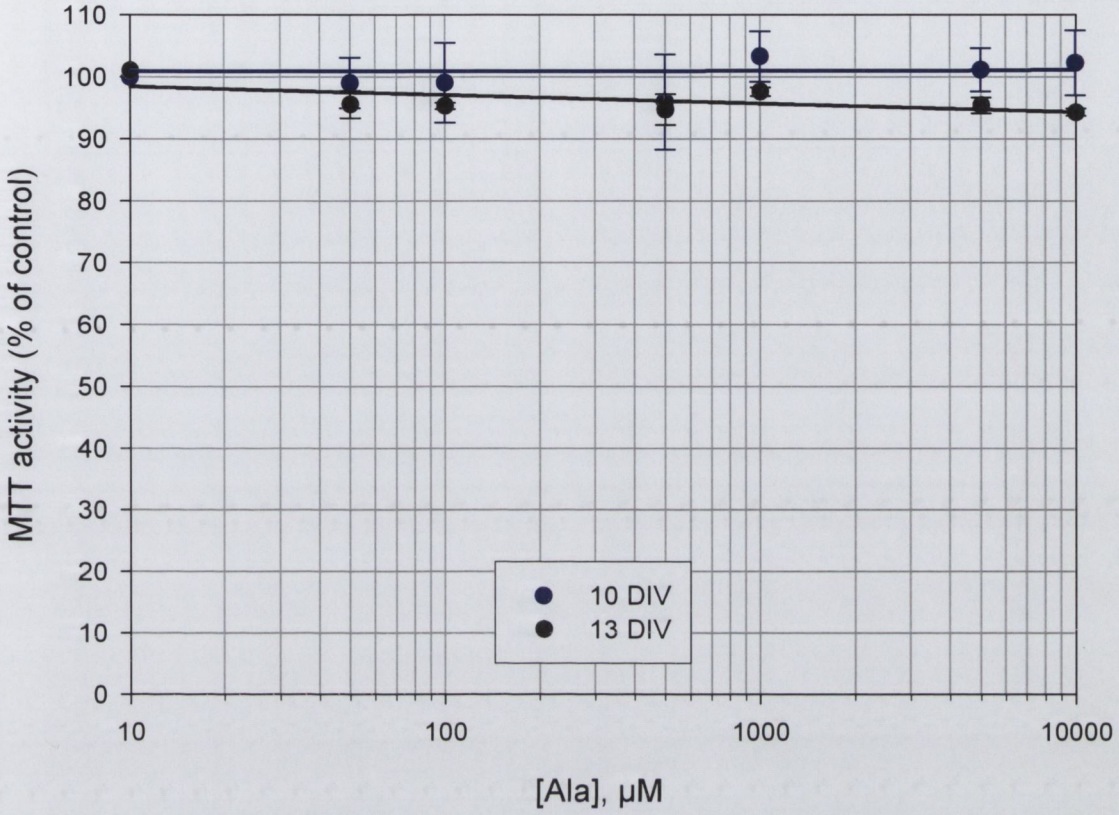


Figure 3.22: No effect of Ala on viability of rat cortical neurons

Primary cultures of rat cortical neurons, prepared from suspensions of dissociated cells from fetal rats (E18), were maintained in identical culture conditions for either 10 days or 13 days. 10 DIV and 13 DIV neurons were exposed for 24 hours to various concentrations of Ala (added directly to the incubation medium) prior to assessment of cell viability by the MTT assay. The absorbance at 570 nm was expressed as a percentage of control (untreated) cells. Data represent mean ± s.d. values of three separate experiments. Each point represents the mean of 9 replicates.

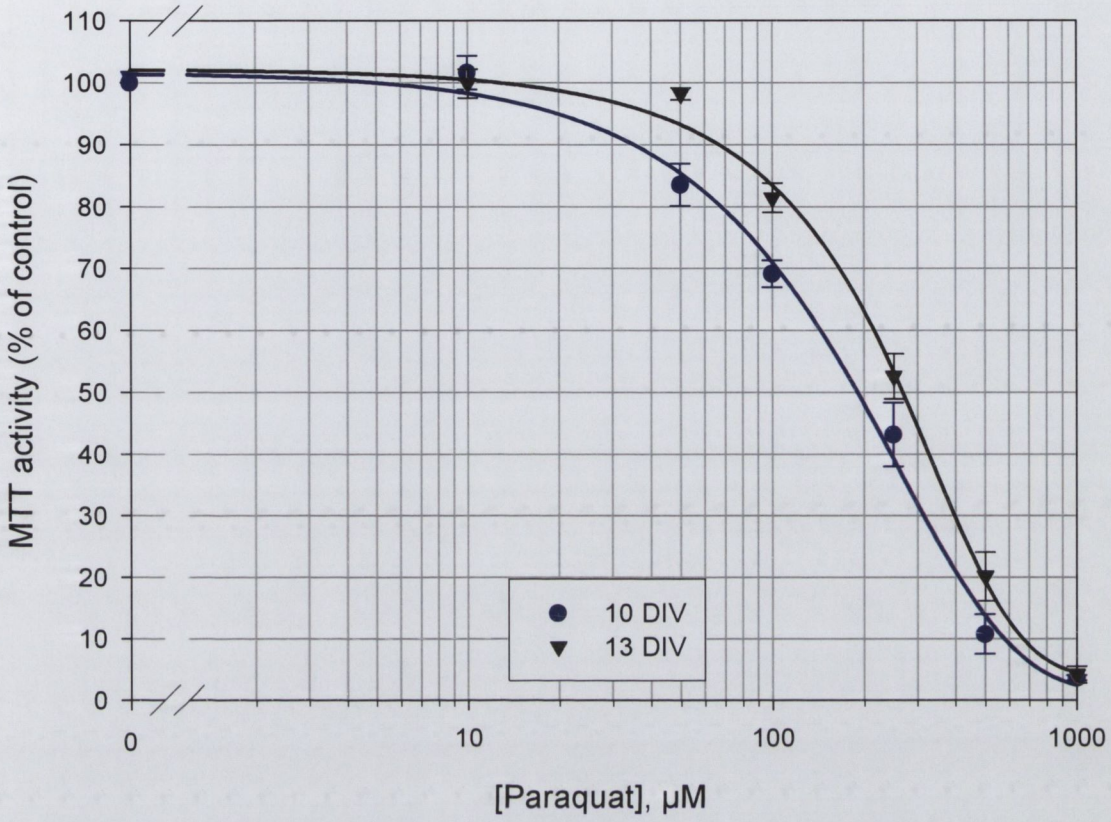


Figure 3.23: Paraquat toxicity does not show dependence for culture time

Primary cultures of rat cortical neurons, prepared from suspensions of dissociated cells from fetal rats (E18), were maintained in identical culture conditions for both 10 days and 13 days. 10 DIV and 13 DIV neurons were exposed for 24 hours to increasing concentrations of paraquat (added directly to the incubation medium) prior to assessment of cell viability by the MTT assay. The absorbance at 570 nm was expressed as a percentage of control (untreated) cells. Data represent mean ± s.d. values of three separate experiments. Each point represents the mean of 9 replicates.

3.2.7 Intracellular ATP concentrations as a measure of toxicity

Rat cortical neurons at both 10 and 13 DIV were exposed to two excitatory compounds, Glu and Asp, a non-excitatory compound, Ala, and a neurotoxic but non-excitotoxic compound, paraquat, for 24 hours. Intracellular ATP levels were measured using the ATPLite™-M kit, a luminescent ATP detection assay.

When rat cortical neurons were treated with various concentrations of Glu for 24 hours, concentration-dependent decreases in intracellular ATP levels were observed, which were similar in both 10 DIV (EC_{50} value of 170 µM) and 13 DIV cultures (EC_{50} value of 140 µM; see Figure 3.24).

When the cortical neurons were exposed to various concentrations of Asp it was observed that 10 DIV cultures were not as sensitive to energy loss when compared to 13 DIV cultures (see Figure 3.25). The difference in ATP loss between 10 DIV (EC_{50} value of 500 µM) and 13 DIV (EC_{50} value of 180 µM) cultures suggests Asp as being less potent in its excitatory action. Ala, the non-EAA, did not decrease intracellular energy levels in either 10 or 13 DIV cultures (see Figure 3.26).

In order to investigate the receptor specificity of the excitotoxin-induced decreases in ATP levels, the protective effects of the NMDA receptor antagonist, AP5, were compared to that of the non-NMDA receptor antagonist, CNQX. Rat cortical neurons, 13 DIV, were pre-incubated with a fixed concentration of AP5 (500 µM) or CNQX (10 µM), for 15 min, before exposure to various concentrations of Glu. When cortical neurons were pre-treated with AP5 before exposure to Glu, for either 4 or 24 hours, complete protection against loss of ATP concentration was obtained (up to 250 µM Glu; see Figure 3.27 and 3.28, respectively). At all concentrations of Glu, pre-treatment of the neurons with CNQX offered no protective effect. These results demonstrate that loss in ATP, following EAA treatment of rat cortical neurons, occurs as a result of NMDA receptor subtype activation.

It was observed that following exposure of the rat cortical neurons to paraquat for 24 hours concentration-dependent decreases in intracellular ATP levels occurred. It was found that at concentrations higher than 25 µM, a rapid and complete loss of ATP occurred in both 10 DIV (EC_{50} value of 80 µM) and 13 DIV cultures (EC_{50} value of 100 µM; Figure 3.29), demonstrating the non-specific toxicity of paraquat to all cell types in the culture.

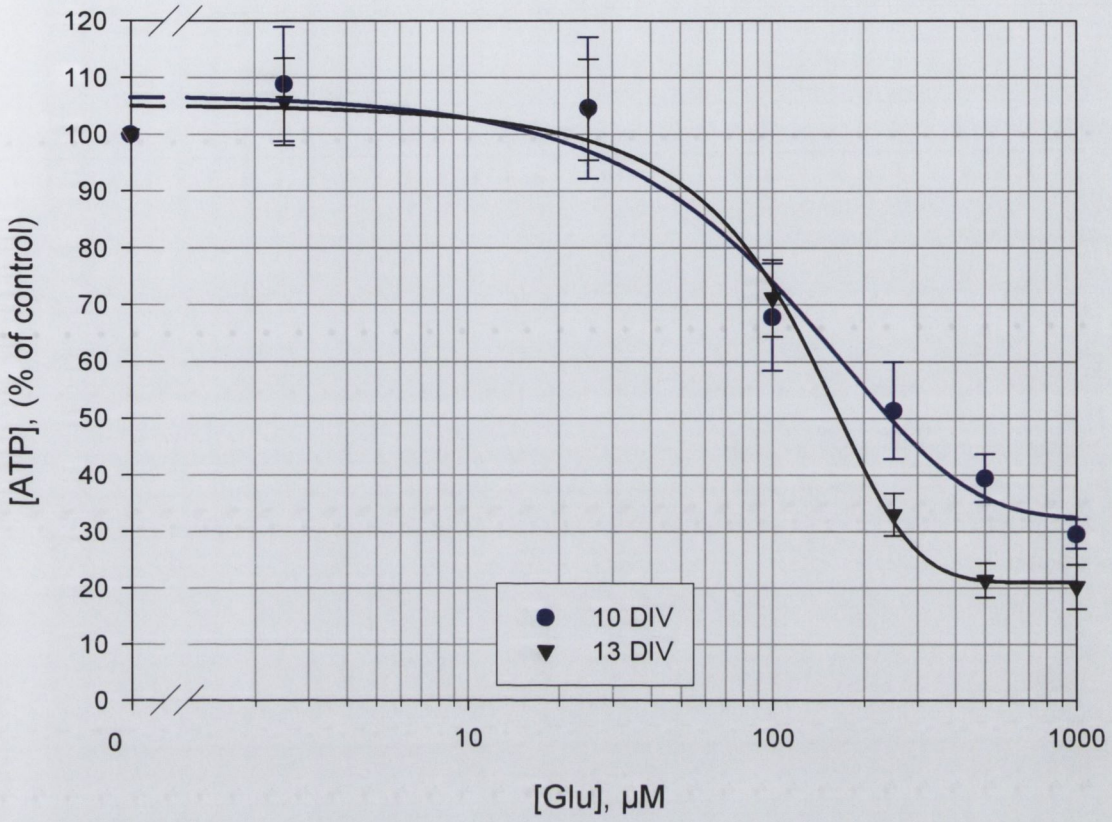


Figure 3.24: Glu rapidly decreases intracellular ATP concentrations in 10 DIV and 13 DIV rat cortical neurons.

Primary cultures of rat cortical neurons, prepared from suspensions of dissociated cells from fetal rats (E18), were maintained in identical culture conditions for both 10 and 13 days. 10 DIV and 13 DIV neurons were exposed for 24 hours to various concentrations of Glu (added directly to the incubation medium) prior to measurement of intracellular ATP. Intracellular ATP concentrations were measured using the ATPLite™-M kit, a luminescent ATP detection assay. The luminescence values were expressed as a percentage of control (untreated) cells. Data represent mean ± s.d. values of three separate experiments. Each point represents the mean of 9 replicates.

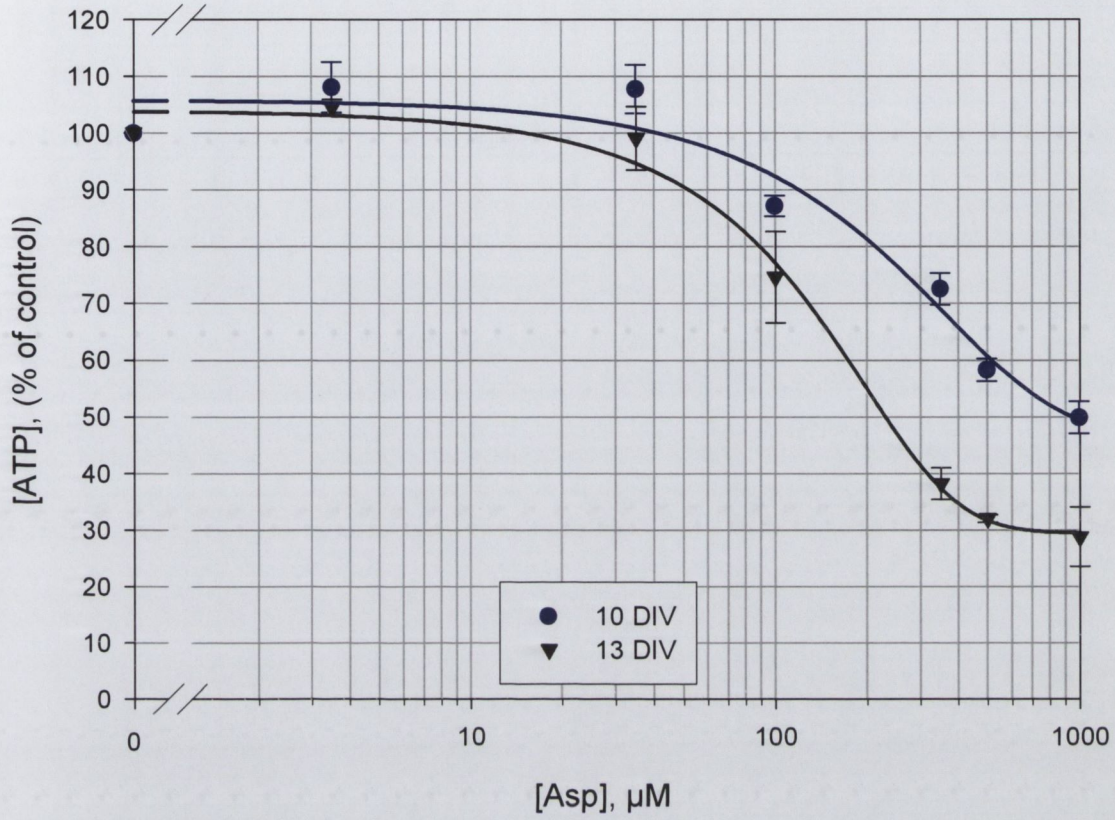


Figure 3.25: Asp rapidly decreases intracellular ATP concentrations in 10 DIV and 13 DIV rat cortical neurons.

Primary cultures of rat cortical neurons, prepared from suspensions of dissociated cells from fetal rats (E18), were maintained in identical culture conditions for both 10 and 13 days. 10 DIV and 13 DIV neurons were exposed for 24 hours to various concentrations of Asp (added directly to the incubation medium) prior to measurement of intracellular ATP. Intracellular ATP concentrations were measured using the ATPLite™-M kit, a luminescent ATP detection assay. The luminescence values were expressed as a percentage of control (untreated) cells. Data represent mean ± s.d. values of three separate experiments. Each point represents the mean of 9 replicates.

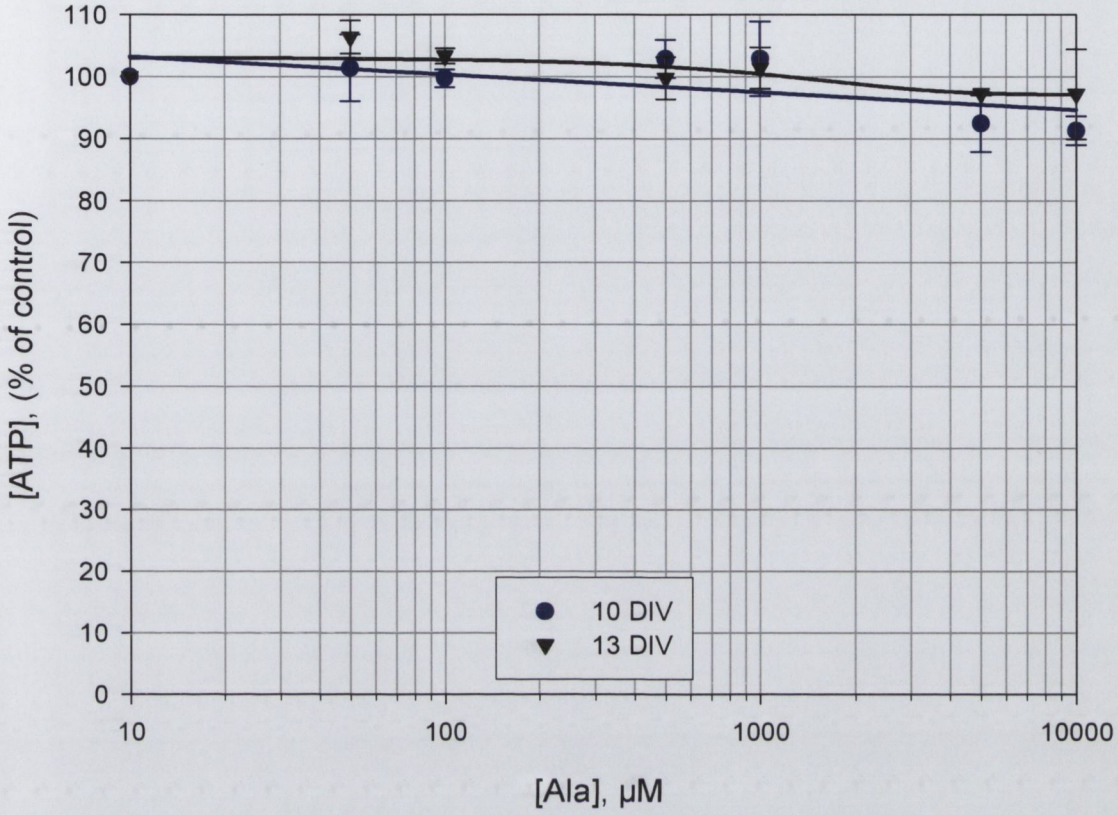


Figure 3.26: Ala does not decrease intracellular ATP levels in rat cortical neurons

Primary cultures of rat cortical neurons, prepared from suspensions of dissociated cells from fetal rats (E18), were maintained in identical culture conditions for both 10 and 13 days. 10 DIV and 13 DIV neurons were exposed for 24 hours to various concentrations of Ala (added directly to the incubation medium) prior to measurement of intracellular ATP. Intracellular energy concentrations were measured using the ATPLite™-M kit, a luminescent ATP detection assay. The luminescence values were expressed as a percentage of control (untreated) cells. Data represent mean ± s.d. values of three separate experiments. Each point represents the mean of 9 replicates.

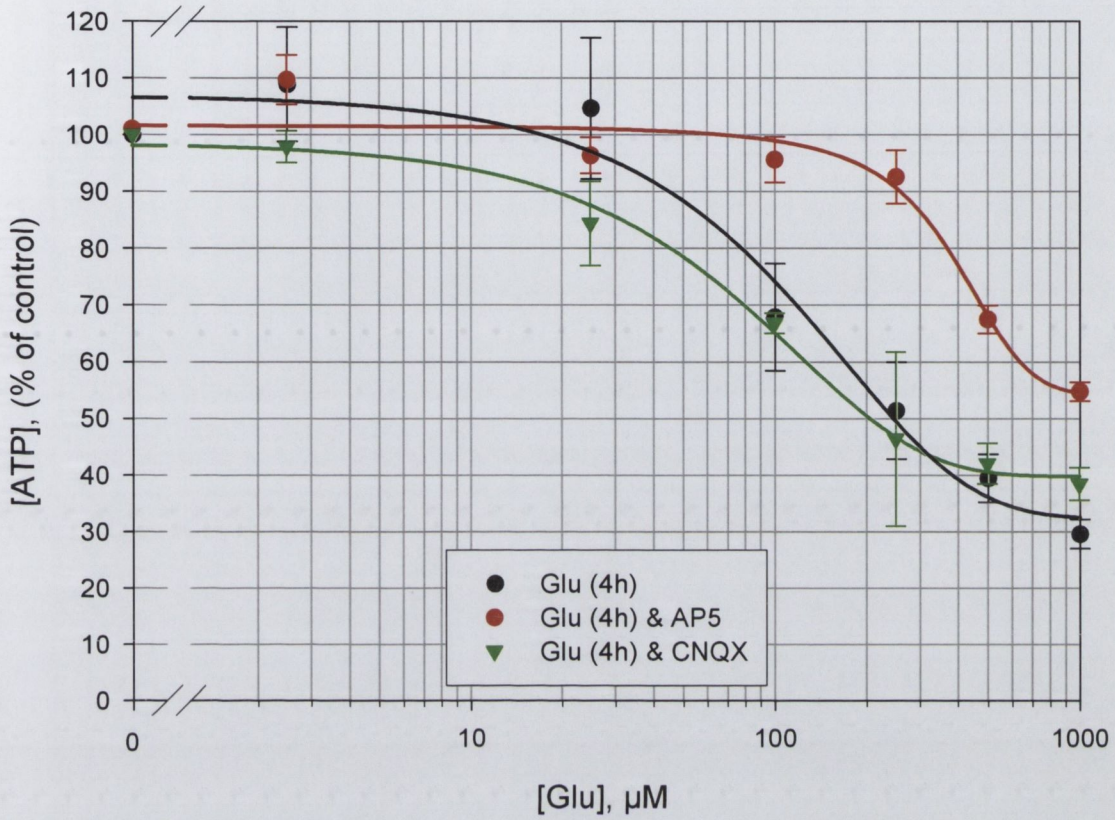


Figure 3.27: Glu-induced decreases in intracellular ATP concentrations are NMDA receptor mediated

Primary cultures of rat cortical neurons, prepared from suspensions of dissociated cells from fetal rats (E18), were maintained in culture for 13 days. On the day of the experiment, the cells were pre-incubated for 15 min with either AP5 (500 µM) or CNQX (10 µM) prior to co-exposure for 4 hours with various concentrations of Glu (added directly to the incubation medium). Intracellular energy concentrations were measured using the ATPLite™-M kit, a luminescent ATP detection assay. The luminescence values were expressed as a percentage of control (untreated) cells. Data represent mean ± s.d. values of three separate experiments. Each point represents the mean of 9 replicates.

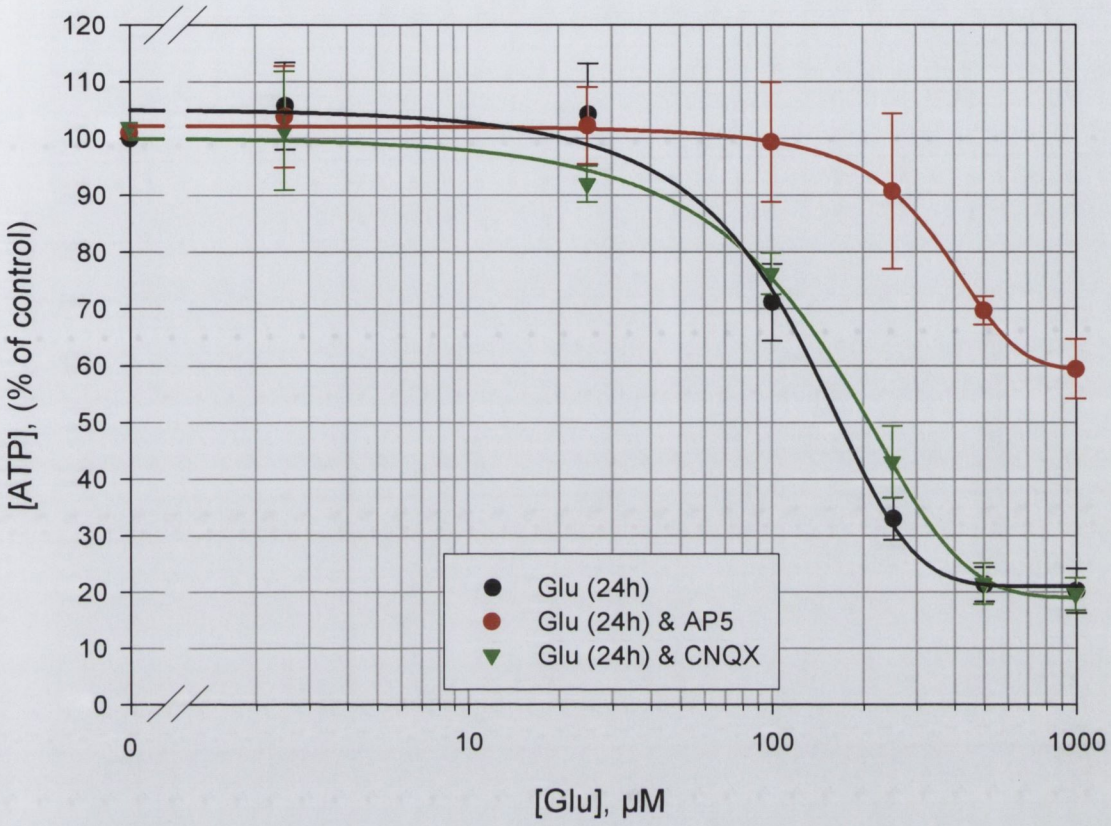


Figure 3.28: Decreases in intracellular ATP concentration, following 24 hours exposure to Glu, are NMDA receptor mediated

Primary cultures of rat cortical neurons, prepared from suspensions of dissociated cells from fetal rats (E18), were maintained in culture for 13 days. On the day of the experiment, the cells were pre-incubated for 15 min with either AP5 (500 µM) or CNQX (10 µM) prior to co-exposure for 24 hours with various concentrations of Glu (added directly to the incubation medium). Intracellular energy concentrations were measured using the ATPLite™-M kit, a luminescent ATP detection assay. The luminescence values were expressed as a percentage of control (untreated) cells. Data represent mean ± s.d. values of three separate experiments. Each point represents the mean of 9 replicates.

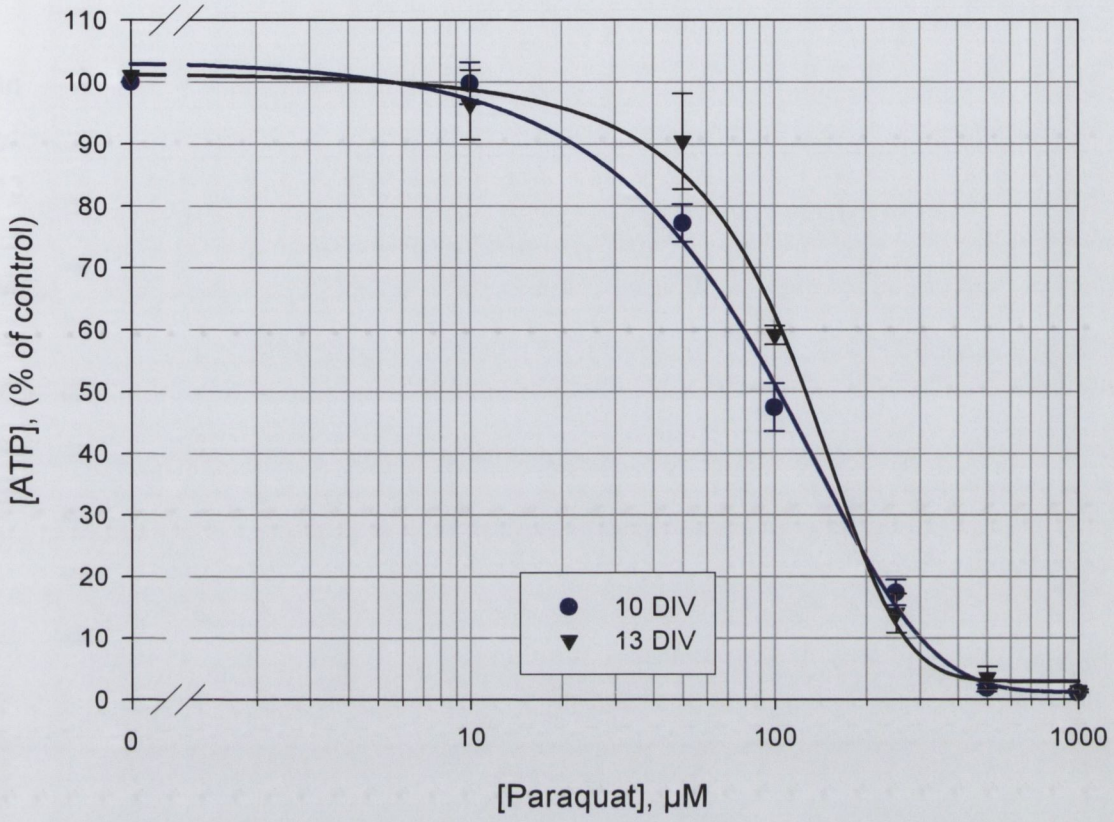


Figure 3.29: ATP concentrations decrease as a result of the non-specific toxicity of paraquat

Primary cultures of rat cortical neurons, prepared from suspensions of dissociated cells from fetal rats (E18), were maintained in identical culture conditions for both 10 days and 13 days. On day 10 (and later on day 13) cells were exposed for 24 hours to various concentrations of paraquat (added directly to the incubation medium) prior to measurement of cellular ATP. Cellular energy levels were then measured using the ATPLite™-M kit, a luminescent ATP detection assay. The luminescence values were expressed as a percentage of control (untreated) cells. Data represent mean ± s.d. values of three separate experiments. Each point represents the mean of 9 replicates.

3.2.8 Time-dependence of EAA-induced neurotoxicity in mature rat cortical neurons

On account of the results in Section 3.2.6, it was decided to investigate whether the cytotoxic effects of Glu and Asp are also time-dependent in mature rat cortical neurons (13 DIV). The cytotoxic actions of Glu and Asp after 4 and 24 hours are shown in Figures 3.30 and 3.31 and can be compared to the non-cytotoxic action of Ala (see Figure 3.32).

When rat cortical neurons (13 DIV) were incubated with various concentrations of Glu for 4 hours, a decrease in cell viability was observed. Exposure of the neurons to Glu for 24 hours induced a more pronounced decrease in cell viability, demonstrating a time-dependent cytotoxic response (EC_{50} value of 85 µM; see Figure 3.30).

With Asp, a similar pattern of time-dependent cytotoxicity occurred. In addition, it was observed that cytotoxicity was more extensive in cultures exposed to Glu, with Asp having a less toxic effect at 24 hours (EC_{50} value of 140 µM; see Figure 3.31), which is consistant with the results in Section 3.2.6.

The non-EAA, Ala, did not decrease cell viability in mature cortical neurons at either time-point (see Figure 3.32).

So as to demonstrate the NMDA receptor specificity of Glu-induced cytotoxicity at different time-points, the degree of protection offered by AP5 was assessed in the presence of Glu. The non-NMDA receptor antagonist, CNQX, was used for comparison. Rat cortical neurons (13 DIV) were pre-incubated with a fixed concentration of AP5 (500 µM) or CNQX (10 µM), for 15 min, before being exposed to various concentrations of Glu for either 4 or 24 hours.

It was observed that pre-treatment of the neurons with AP5 before exposure to Glu, for either 4 or 24 hours, completely protected against cytotoxicity (up to 250 µM; see Figures 3.33 and 3.34). Furthermore, protection of the neurons by AP5 was proportional to Glu concentration. With all concentrations of Glu, pre-treatment of the neurons with CNQX offered no protection.

Overall, the results show that EAA-mediated cytotoxicity occurs via the NMDA receptor.

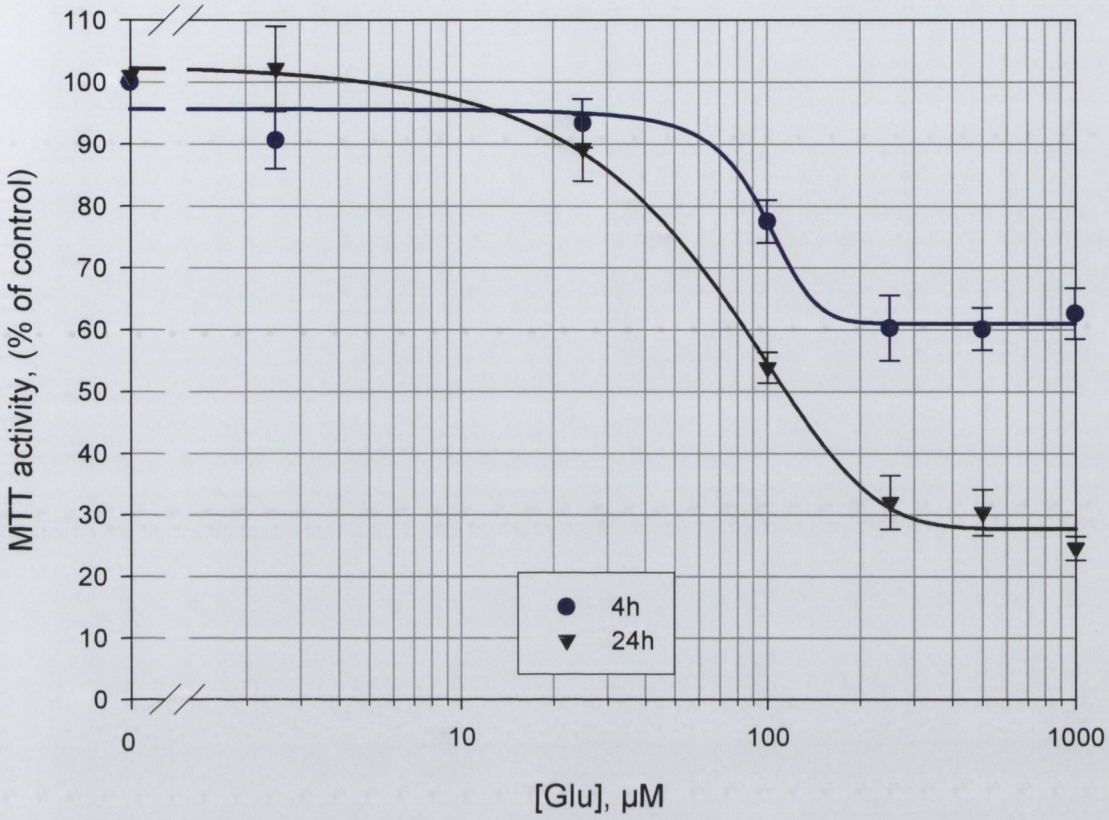


Figure 3.30: Concentration- and time-dependence of Glu on neuronal viability in mature rat cortical neurons (13 DIV)

Primary cultures of rat cortical neurons, prepared from suspensions of dissociated cells from fetal rats (E18), were maintained in culture for 13 days. On the day of the experiment, cells were exposed for either 4 hours or 24 hours to various concentrations of Glu (added directly to the incubation medium) prior to assessment of cell viability by the MTT assay. The absorbance at 570 nm was expressed as a percentage of control (untreated) cells. Data represent mean ± s.d. values of triplicate MTT reactions derived from three separate experiments (n = 3).

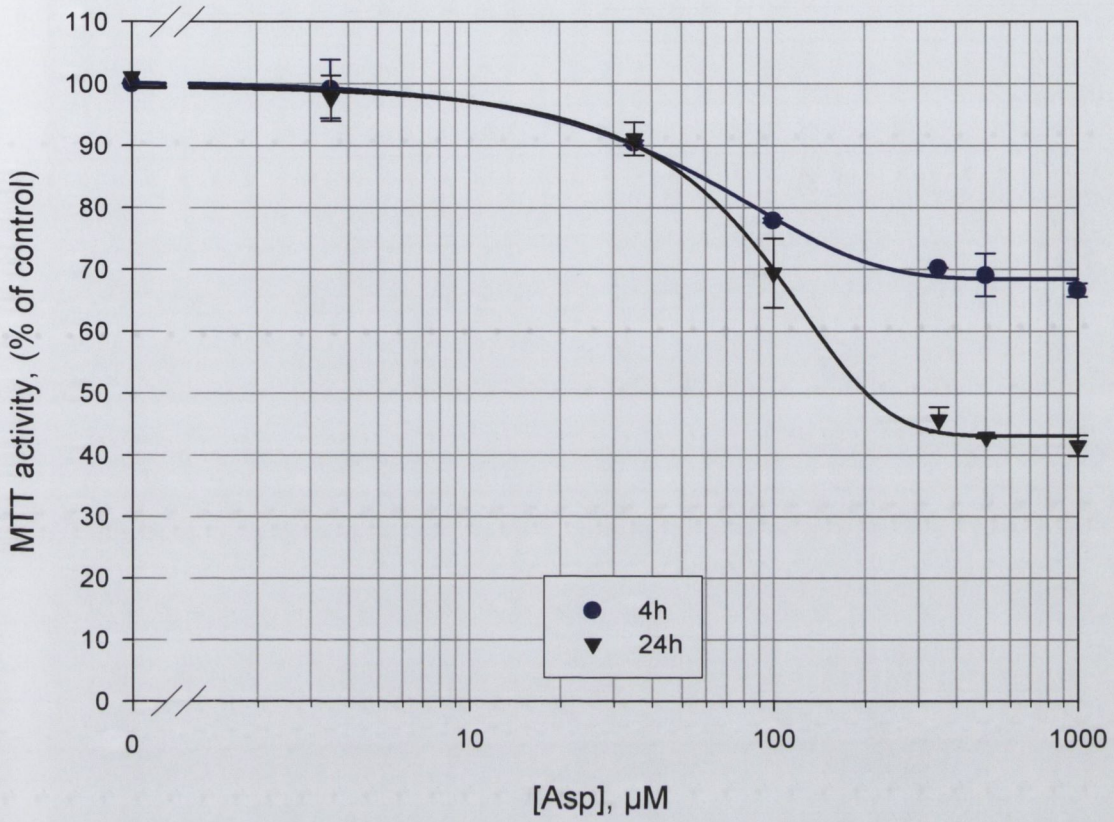


Figure 3.31: Concentration- and time-dependence of Asp treatment on neuronal viability in mature rat cortical neurons (13 DIV)

Primary cultures of rat cortical neurons, prepared from suspensions of dissociated cells from fetal rats (E18), were maintained in culture for 13 days. On the day of the experiment, cells were exposed for either 4 hours or 24 hours to various concentrations of Asp (added directly to the incubation medium) prior to assessment of cell viability by the MTT assay. The absorbance at 570 nm was expressed as a percentage of control (untreated) cells. Data represent mean ± s.d. values of triplicate MTT reactions derived from three separate experiments (n = 3).

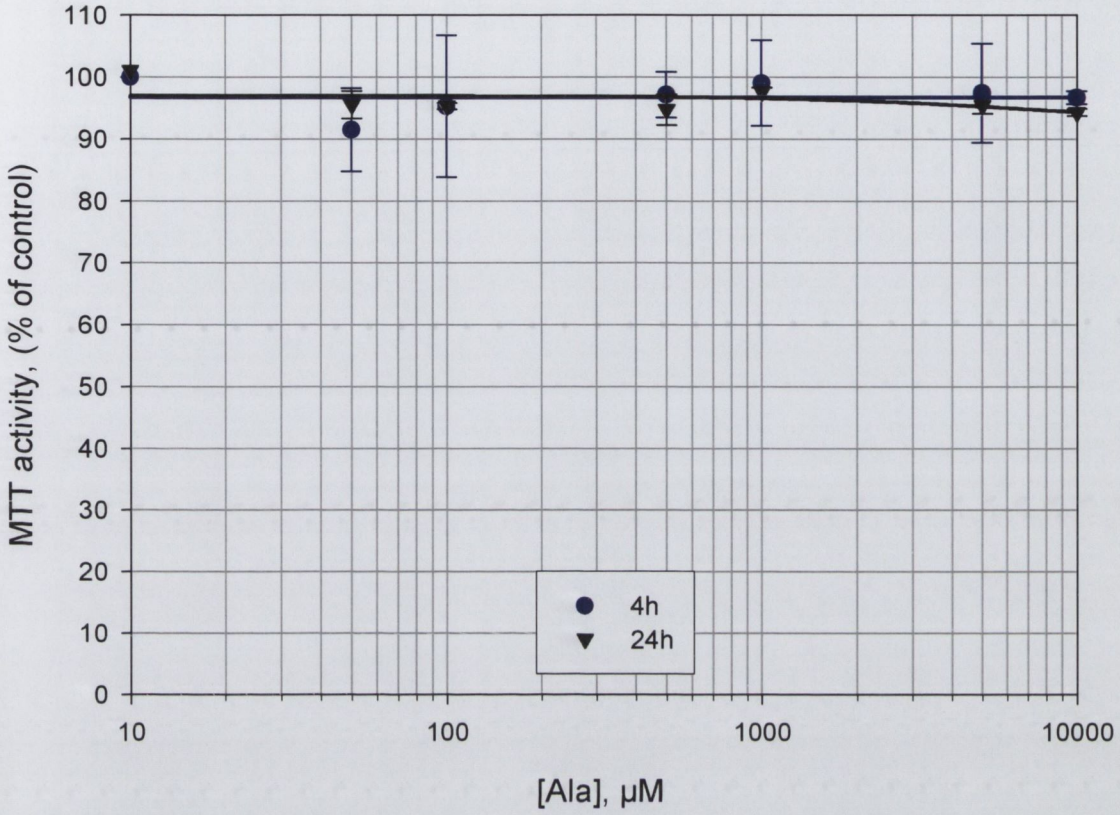


Figure 3.32: No effect of Ala on cell viability

Primary cultures of rat cortical neurons, prepared from suspensions of dissociated cells from fetal rats (E18), were maintained in culture for 13 days. On the day of the experiment, cells were exposed for either 4 hours or 24 hours to various concentrations of Ala (added directly to the incubation medium) prior to assessment of cell viability by the MTT assay. The absorbance at 570 nm was expressed as a percentage of control (untreated) cells. Data represent mean ± s.d. values of triplicate MTT reactions derived from three separate experiments (n = 3).

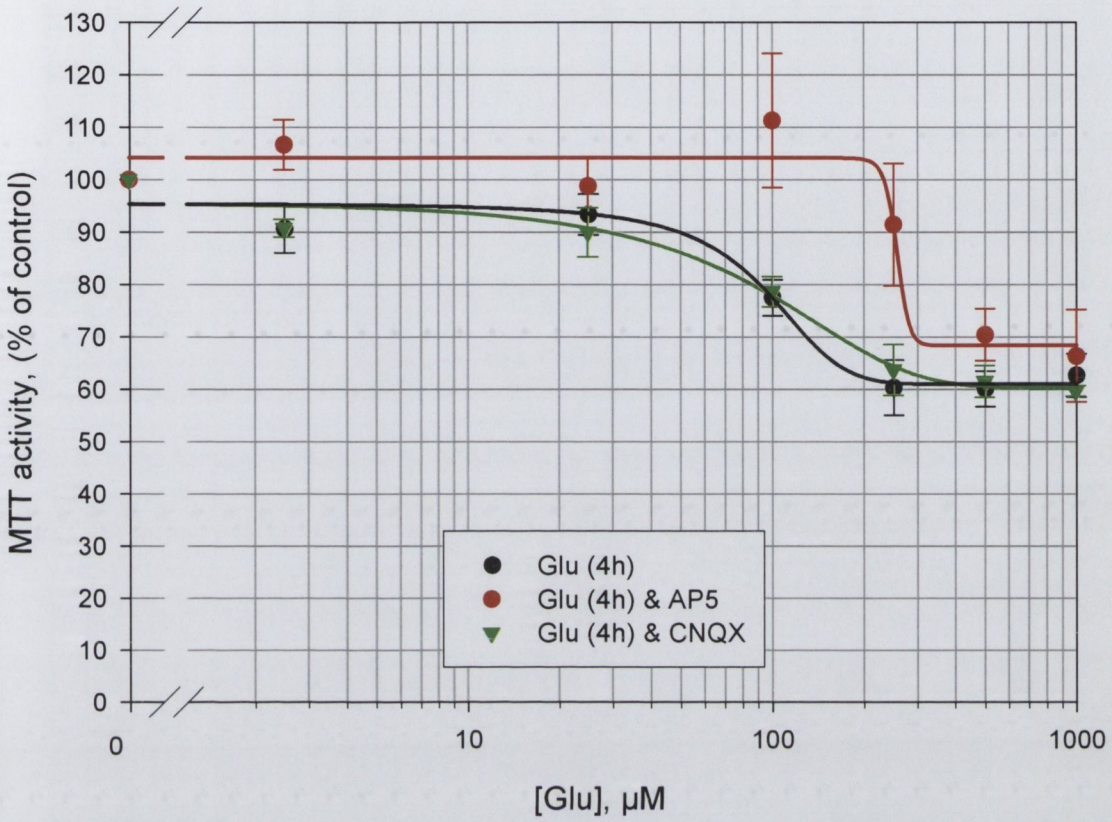


Figure 3.33: Glu-induced neurotoxicity is mediated through the NMDA receptor subtype in rat cortical neurons

Primary cultures of rat cortical neurons, prepared from suspensions of dissociated cells from fetal rats (E18), were maintained in culture for 13 days. On the day of the experiment, cells were pre-incubated for 15 min with either AP5 (500 µM) or CNQX (10 µM) prior to co-exposure for 4 hours with various concentrations of Glu (added directly to the incubation medium). Cell viability was measured by the MTT assay. The absorbance values at 570 nm were expressed as a percentage of control (untreated) cells. Data represent mean ± s.d. values of triplicate MTT reactions derived from three separate experiments (n = 3).

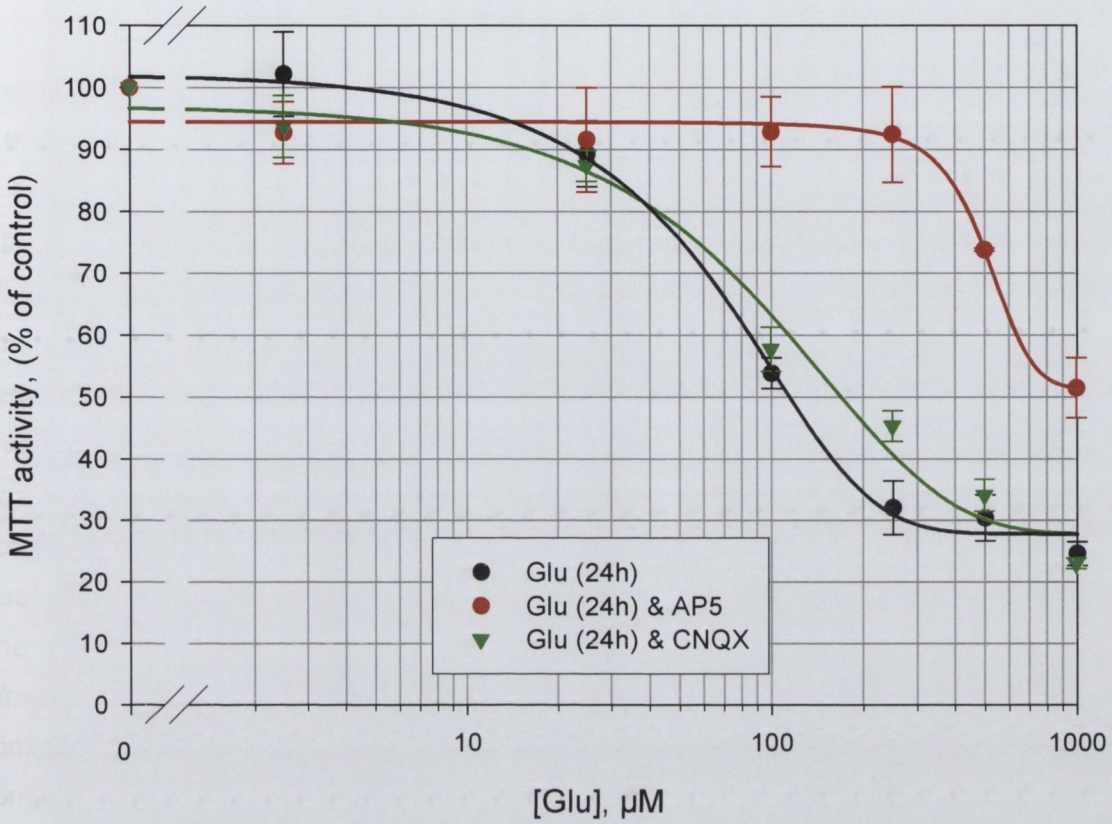


Figure 3.34: Glu-induced neurotoxicity is mediated through the NMDA receptor subtype in rat cortical neurons

Primary cultures of rat cortical neurons, prepared from suspensions of dissociated cells from fetal rats (E18), were maintained in culture for 13 days. On the day of the experiment, cells were pre-incubated for 15 min with either AP5 (500 µM) or CNQX (10 µM) prior to co-exposure for 24 hours with various concentrations of Glu (added directly to the incubation medium). Cell viability was measured by the MTT assay. The absorbance values at 570 nm were expressed as a percentage of control (untreated) cells. Data represent mean ± s.d. values of triplicate MTT reactions derived from three separate experiments (n = 3).

3.2.9 EAA induced loss of mitochondrial membrane potential ($\Delta\psi_m$) in rat cortical neurons

Another prominent feature associated with over-activation of the NMDA receptor subtype is the alteration of mitochondrial membrane potential ($\Delta\psi_m$).

In this Chapter, the fluorescent dye, tetramethylrhodamine, was used to investigate the $\Delta\psi_m$ of intact neurons (untreated) when compared to neurons impaired by EAA treatment.

When mature rat cortical neurons (13 DIV) were exposed to various concentrations of Glu and Asp for 24 hours, it was observed that the $\Delta\psi_m$ collapsed in a concentration-dependent manner.

The EC_{50} value following exposure of the cortical neurons to toxic concentrations of Glu was approximately 160 µM (see Figure 3.35).

Following exposure of the neurons to Asp, a similar pattern of concentration-dependent loss of $\Delta\psi_m$ was observed, with an EC_{50} value of 300 µM (see Figure 3.36).

The non-EAA, Ala, had no effect on the $\Delta\psi_m$ of the cortical neurons (see Figure 3.37).

When protection experiments were performed using the NMDA receptor antagonist, AP5 complete loss of $\Delta\psi_m$ was prevented following treatment of the cortical neurons with toxic concentrations of Glu (see Figure 3.38). CNQX offered no protection against loss of $\Delta\psi_m$ (also Figure 3.38), demonstrating that EAA-induced loss of $\Delta\psi_m$ is mediated via NMDA receptor subtype activation. Additionally, these results show that the voltage sensitive dye, tetramethylrhodamine, can be used as a marker to measure depolarisation of $\Delta\psi_m$ following NMDA receptor subtype activation.

When the cortical neurons were incubated with paraquat a rapid concentration-dependent collapse of $\Delta\psi_m$ occurred, with an EC_{50} value of 100 µM (see Figure 3.39) demonstrating the very toxic effect of paraquat on mitochondria.

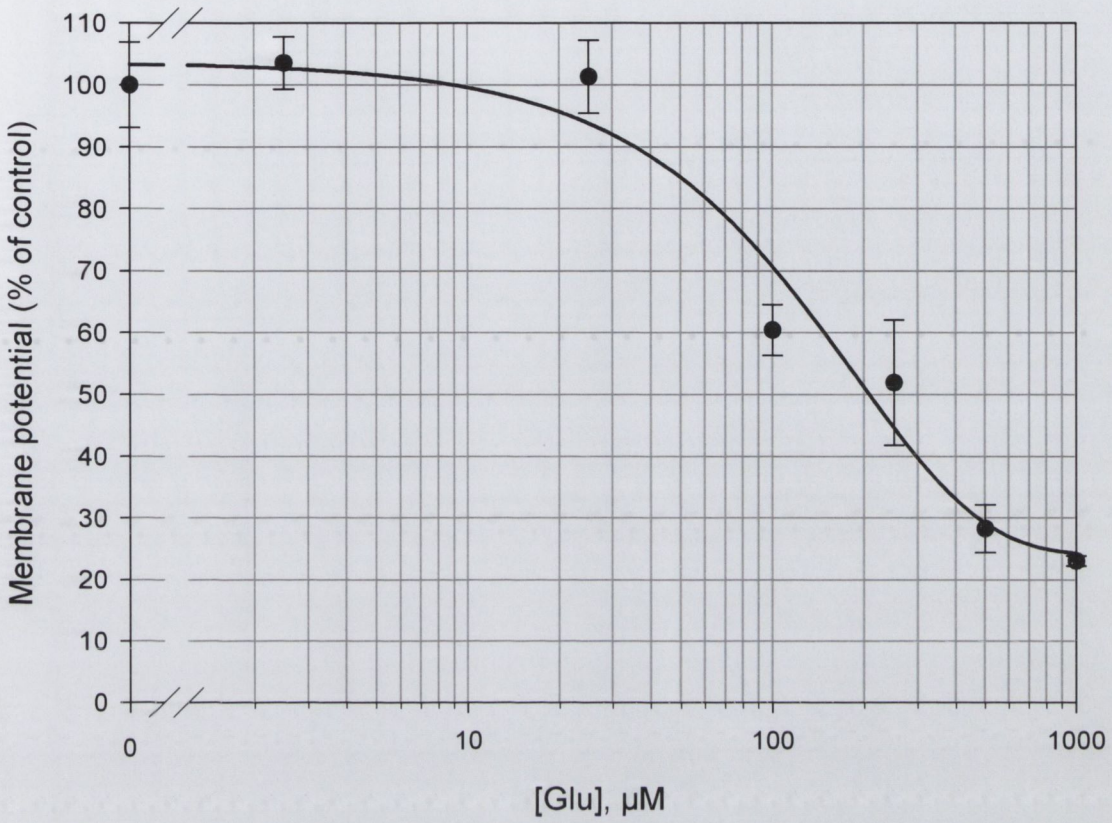


Figure 3.35: The mitochondrial membrane potential ($\Delta\psi_m$) of rat cortical neurons (13 DIV) decreases rapidly following treatment with Glu

Primary cultures of rat cortical neurons, prepared from suspensions of dissociated cells from fetal rats (E18), were maintained in identical culture conditions for 13 days. On the day of the experiment, the neurons were exposed for 24 hours to various concentrations of Glu (added directly to the incubation medium) prior to measurement of the mitochondrial membrane potential. The fluorescence values were expressed as a percentage of control (untreated) neurons. Data represent mean ± s.d. values of triplicate reactions derived from three separate experiments (n = 3).

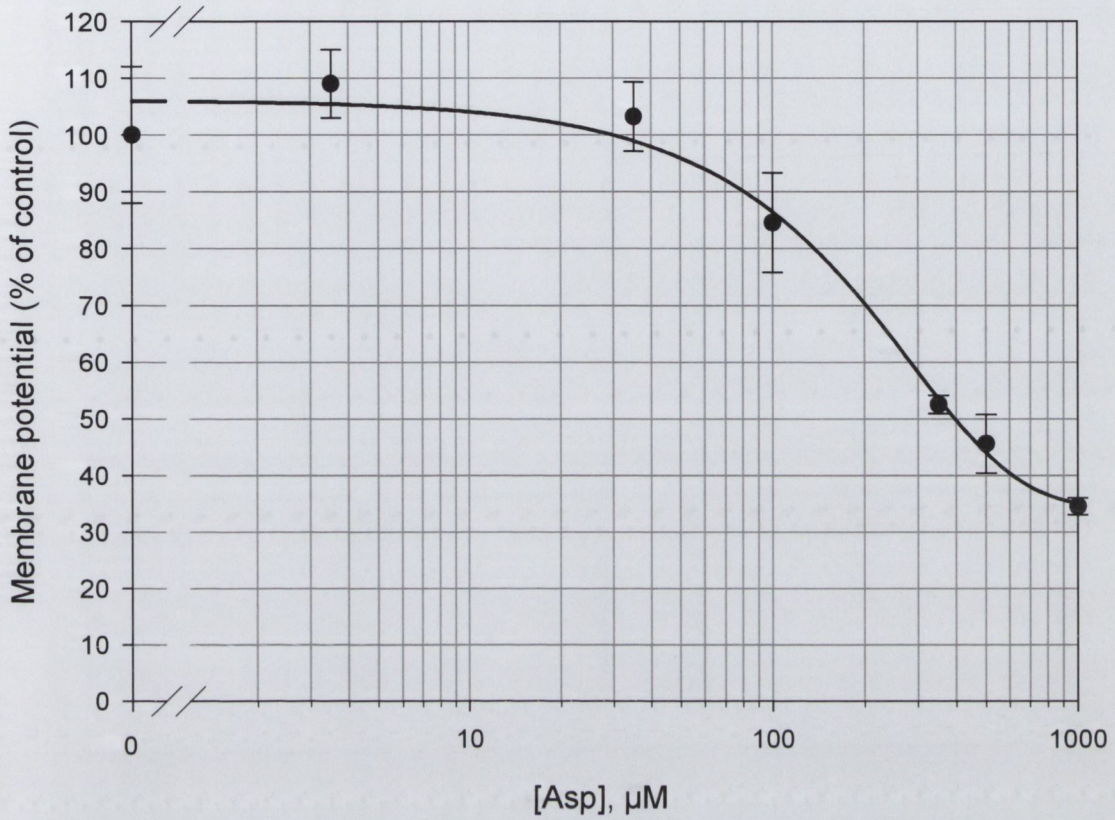


Figure 3.36: The $\Delta\psi_m$ of rat cortical neurons (13 DIV) decreases rapidly following treatment with Asp

Primary cultures of rat cortical neurons, prepared from suspensions of dissociated cells from fetal rats (E18), were maintained in identical culture conditions for 13 days. On the day of the experiment, the neurons were exposed for 24 hours to various concentrations of Asp (added directly to the incubation medium) prior to measurement of the mitochondrial membrane potential. The fluorescence values were expressed as a percentage of control (untreated) neurons. Data represent mean ± s.d. values of triplicate reactions derived from three separate experiments (n = 3).

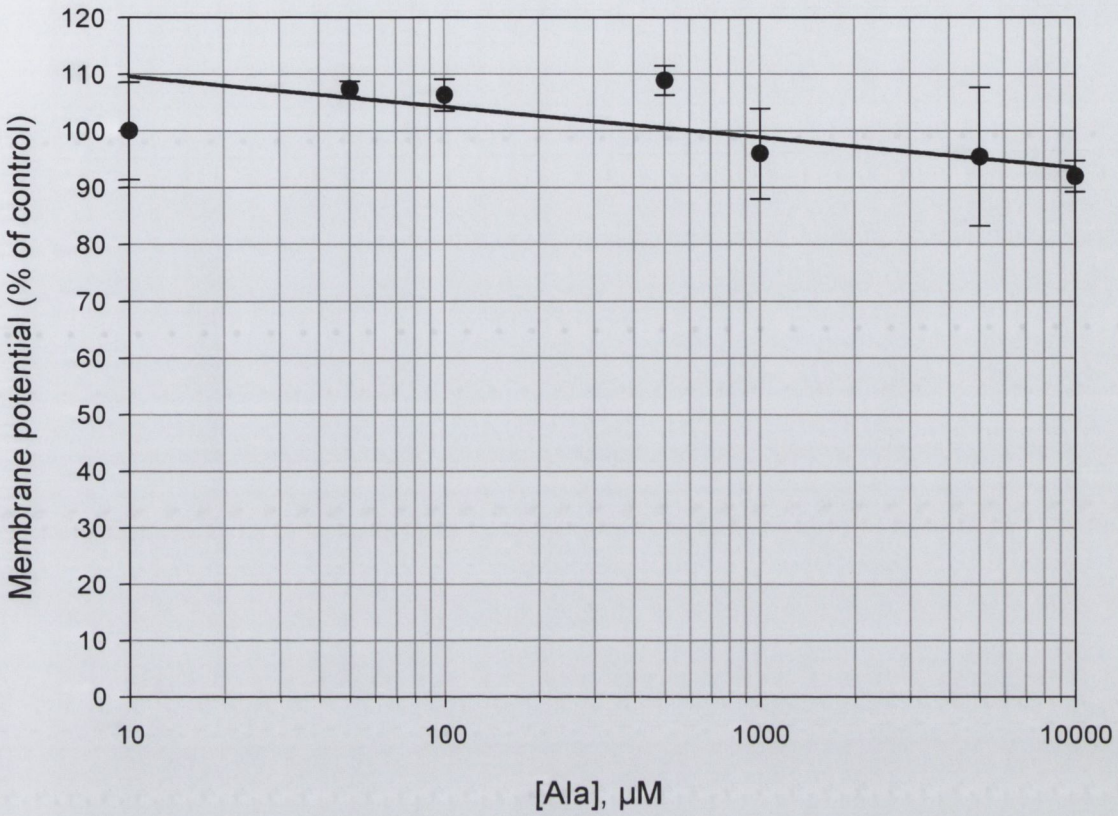


Figure 3.37: No change in the $\Delta\psi_m$ of rat cortical neurons (13 DIV) following stimulation with Ala

Primary cultures of rat cortical neurons, prepared from suspensions of dissociated cells from fetal rats (E18), were maintained in identical culture conditions for 13 days. On the day of the experiment, the neurons were exposed for 24 hours to increasing concentrations of Ala (added directly to the incubation medium) prior to measurement of the mitochondrial membrane potential. The fluorescence values were expressed as a percentage of control (untreated) neurons. Data represent mean ± s.d. values of triplicate reactions derived from three separate experiments (n = 3).

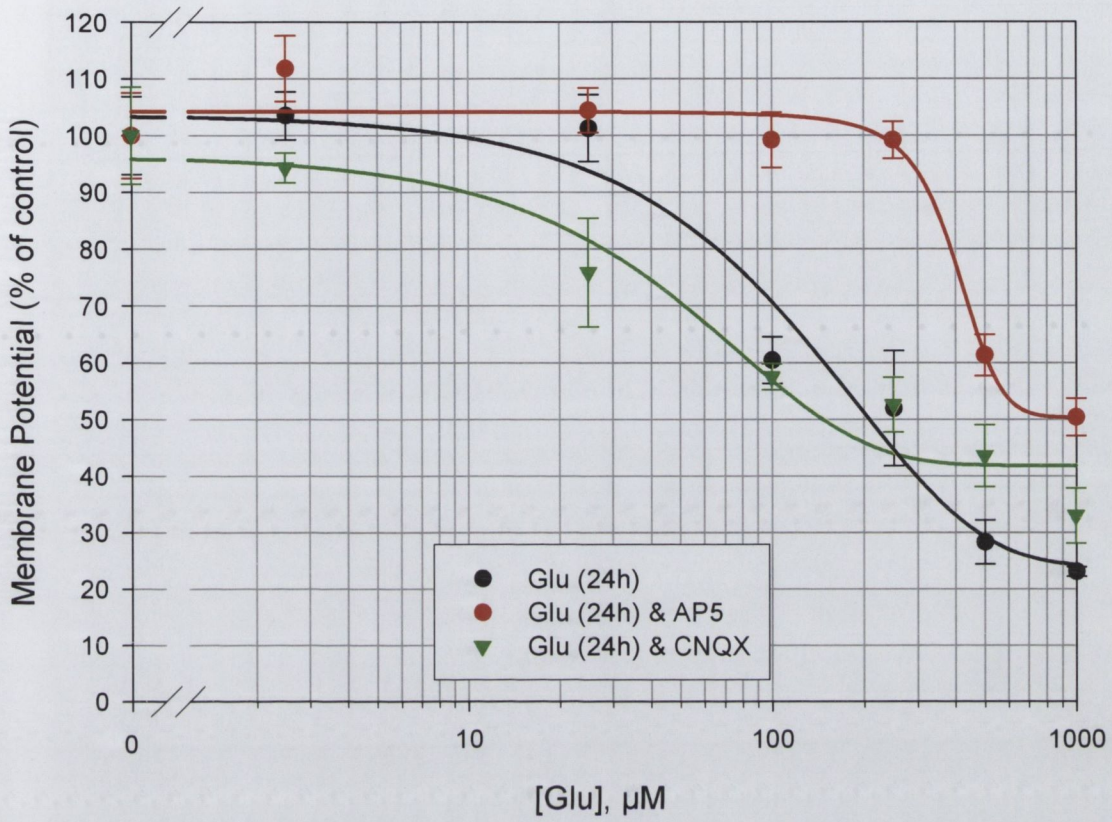


Figure 3.38: Loss of $\Delta\psi_m$ in rat cortical neurons (13 DIV), following stimulation with Glu, is mediated through the NMDA receptor subtype

Primary cultures of rat cortical neurons, prepared from suspensions of dissociated cells from fetal rats (E18), were maintained in identical culture conditions for 13 days. On the day of the experiment, cells were pre-incubated for 15 min with either AP5 (500 µM) or CNQX (10 µM) prior to co-exposure for 24 hours with increasing concentrations of Glu prior to measurement of the mitochondrial membrane potential. The fluorescence values were expressed as a percentage of control (untreated) neurons. Data represent mean ± s.d. values of triplicate reactions derived from three separate experiments (n = 3).

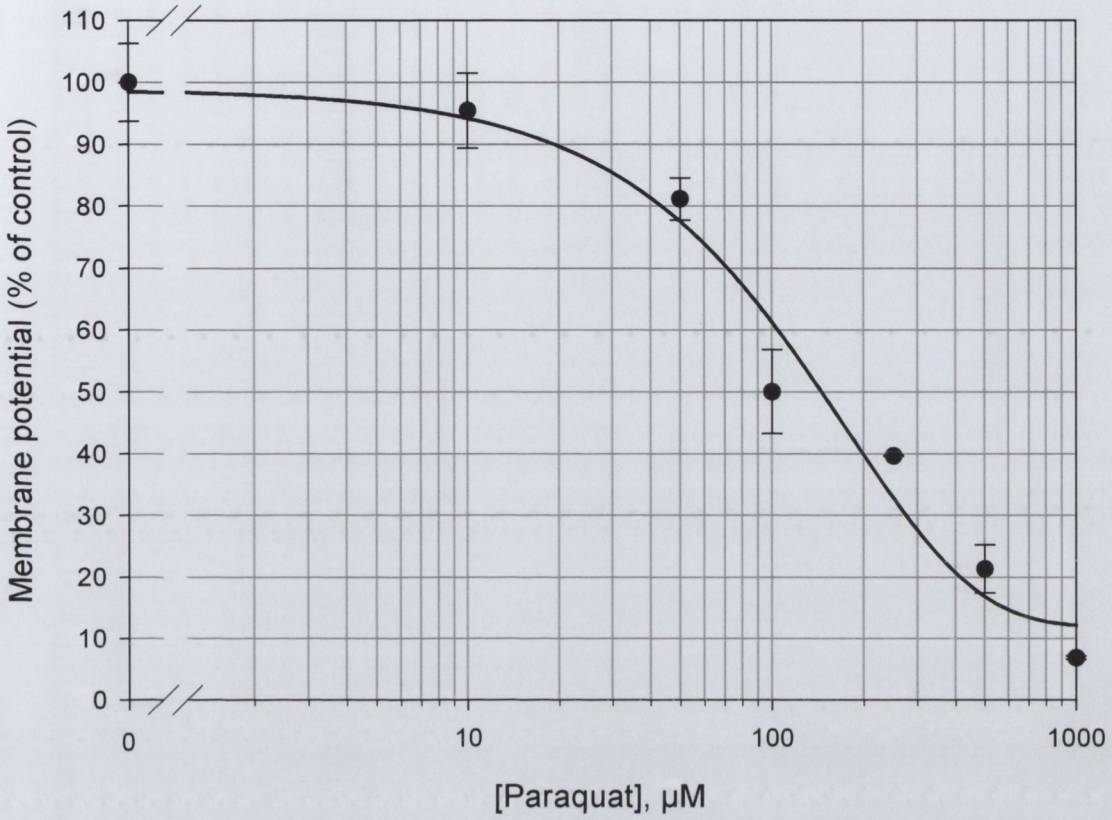


Figure 3.39: The $\Delta\psi_m$ of rat cortical neurons (13 DIV) decreases rapidly following treatment with paraquat

Primary cultures of rat cortical neurons, prepared from suspensions of dissociated cells from fetal rats (E18), were maintained in identical culture conditions for 13 days. On the day of the experiment, the neurons were exposed for 24 hours to various concentrations of paraquat (added directly to the incubation medium) prior to measurement of the mitochondrial membrane potential. The fluorescence values were expressed as a percentage of control (untreated) neurons. Data represent mean ± s.d. values of triplicate reactions derived from three separate experiments (n = 3).

Mouse Cerebellar Granule Cells (mCGCs)

Assay	DIV	Time [h]	EC_{50} [µM]		
			Glu	Asp	NMDA
MTT	7	4	80	100	>300
		24	60	70	300
ATP	7	4	37	65	90
		24	50	60	140

a)

Rat Cortical Neurons

Assay	DIV	Time [h]	EC_{50} [µM]		
			Glu	Asp	Paraquat
MTT	10	24	280	>300	160
	13		90	140	200
ATP	10	24	170	500	80
	13		140	180	100
Tetramethyl-rhodamine	13	24	160	300	100

b)

Tables 3.1 a) & b): Determination of the viability, energy status and mitochondrial membrane potential of mCGCs and rat cortical neurons.

Mouse cerebellar granule cells (7 DIV) were exposed for either 4 or 24 hours to various concentrations of the EAAs, Glu, Asp and NMDA. The effects of the EAAs on cell viability and intracellular ATP concentration, following the different exposure periods, are summarised in Table a). Rat cortical neurons (10 and 13 DIV) were exposed to various concentrations of Glu, Asp and paraquat for 24 hours and the effects of these compounds on cell viability, intracellular ATP concentration and mitochondrial membrane potential are summarised in the Table b).

3.3 Discussion

This Chapter describes the use of two different primary cell culture systems, that is, mCGCs and rat cortical neurons, to study the phenomenon of Glu neurotoxicity, a process which may contribute to the neuronal death observed in a variety of acute and chronic neurological diseases (Lipton and Rosenberg, 1994). One attractive hypothesis is that neuronal cell death is mediated by excessive activation of Glu receptor subtypes, which is defined in the classical sense as "excitotoxicity" (Olney *et al.*, 1971). In general, the molecular mechanisms involved are still poorly understood but include a role for oxidative stress, mitochondrial dysfunction (Ankarcrona *et al.*, 1995) and mitochondrial Ca^{2+} accumulation (Budd and Nicholls, 1996). A great deal of evidence implicates intracellular Ca^{2+} overload, following for example, overactivation of the NMDA receptor-channel complex or release of Ca^{2+} from intracellular stores (such as the mitochondria or endoplasmic reticulum), as a major contributor in neuronal cell death (Choi, 1988a, 1988b, 1995; Budd and Nicholls, 1996; Griffiths *et al.,* 1998). It appears that Glu-induced imbalances in Ca^{2+} ion homeostasis result in the over-activation of a number of Ca^{2+}-dependent enzymes, the consequence of which is neuronal death by either apoptotic or necrotic mechanisms.

This Chapter investigates the relationship between synaptic excitation and neuronal death in two different neuronal cultures. Primary cultures of mCGCs have been used extensively as the *in vitro* model to study the molecular mechanisms of excitotoxicity. This is, in part, due to the observations that these cultures contain predominantly glutamatergic neurons. The first aim of this Chapter was to establish cultures of primary mCGCs in our laboratory as a model to investigate excitotoxicity. It has been widely reported that both the intensity of the Glu exposure and the resulting effects on mitochondrial function are critical factors in determining which of the two pathways (apoptosis or necrosis) to neuronal cell death is followed (Ankarcrona *et al.*, 1995; Leist *et al.,* 1997; Lipton and Nicotera, 1998). Therefore, mCGCs were exposed for either 4 or 24 hours (Frandsen *et al.,* 1987) to various concentrations of the EAAs, Glu, Asp and NMDA. A non-excitatory compound, Ala, was used as a control compound in these experiments. The effect of the EAAs on cell viability following the different exposure periods was investigated by an MTT assay. It was found that the EAAs clearly demonstrated a reproducible, neurotoxic effect on the cells in a concentration-dependent manner. In addition, the results were indicative of an inverse relationship between exposure time and cell survival. It was observed that even after a 4

hour exposure to Glu and Asp, a substantial decrease was observed in cell viability. These findings are consistent with studies of Glu toxicity in similar cultures (Griffiths *et al.*, 1998, 2000). The much higher potency of Glu and Asp when compared to NMDA in our results is also in accordance with previous publications (Schousboe *et al.*, 1985). The non-excitatory compound, Ala, did not induce neuronal death in the cultures at either time-point, supporting the finding that Glu receptors mediate excitotoxic neuronal cell death.

Defects in mitochondrial ATP generation have frequently been associated with neurodegenerative diseases (Beal, 1996, 1998, 2003; Fiskum *et al.*, 2000). The ability of Glu to reduce the supply of ATP by mitochondrial depolarisation or to increase ATP demand as a result of neuronal Ca^{2+} loading could act as the main initiator of neuronal cell death. In our experiments, the exposure of mCGCs to high concentrations of Glu, Asp and NMDA, for 4 hours, induced a rapid decrease in intracellular ATP concentrations. Following 24 hours exposure, the ATP levels had decreased even further. These results suggest that the rapid decline in ATP levels in mCGCs following insult is an early event in EAA-induced neurotoxicity.

In this Chapter, it was demonstrated that the NMDA receptor plays the predominant role in mediating Glu-induced neuronal death in mCGCs. Several research groups have examined intensively the pharmacology of Glu toxicity in neuronal cultures and it has been shown that this toxicity can be attenuated by NMDA receptor antagonists (Choi *et al.*, 1988; Frandsen *et al.*, 1989; Goldberg *et al.*, 1987; Rogers *et al.*, 1997; Koh and Choi, 1991). In the present study, mCGCs were exposed to the NMDA receptor antagonist, AP5, in combination with various concentrations of Glu, Asp or NMDA for 24 hours, to investigate whether the effective blockade of NMDA receptors could eliminate all signs of Glu neurotoxicity. It was found that even at toxic concentrations of Glu, Asp and NMDA, AP5 was able to protect against ATP depletion and thus provide rescue from cell death. It was also observed that the protection of the cells from ATP loss and cytotoxicity was a function of both the concentration of the EAAs and their relative potencies.

The quinoxalinedione, CNQX was also used to investigate whether the potent, selective blockade of non-NMDA receptors could reduce Glu neurotoxicity. The selective combination of various concentrations of the EAAs with the antagonist CNQX induced loss of intracellular ATP concentrations leading to neuronal cell death. Therefore, the finding that CNQX did not attenuate Glu-induced neuronal cell death in these cultures provides additional direct support for the principle that the NMDA subtype of Glu receptors predominantly mediates neuronal injury following EAA exposure. These findings are in

accordance with previous publications (Choi *et al.*, 1988; Frandsen *et al.*, 1989; Goldberg *et al.*, 1987; Rogers *et al.*, 1997; Koh and Choi, 1991).

Following the establishment of the mCGC system as a model to investigate excitotoxicity, a second *in vitro* cell culture system, from a different species and brain region, was developed and optimised as an alternative model. The main disadvantage in using the mCGC system alone as a model to investigate excitotoxicity is the use of serum in the medium. Schramm *et al.* (1990) reported that the Glu level in serum could cause neuronal death through the activation of the NMDA receptor. Therefore, it was decided that a robust, reproducible cell system containing an apparently pure neuronal population, and ideally involving a serum-free media was also required to further investigate Glu-mediated neurotoxicity. The rat cortical neuronal system reported by Schmuck and Schlüter, (1996) and Schmuck *et al.* (2000) was chosen, as it seemed to meet the criteria required. Other advantages included the rat being the chosen rodent species in regulatory and non-regulatory toxicological investigations.

It has been observed that the efficiency of neurotoxic cell death is dependent on the length of time the neurons have been maintained in culture, an indication of the time required for the neurons to express functional ionotropic Glu receptors (Griffiths *et al.*, 1997; Lidwell *et al.,* 2000). In addition to time in culture, Glu concentration and the cell population (Schubert *et al.*, 2001) are also important factors. In order to maximise NMDA receptor-mediated neurotoxicity, rat cortical neurons were cultured for 7 to 13 DIV before exposure to Glu for 24 hours. It was found that immature embryonic cortical neurons cultured for 7 days have low sensitivity to Glu indicating non-functional ionotropic receptors. However, exposures of 10 DIV and 13 DIV neurons to Glu revealed that while substantial cell death occurred at 10 DIV, the neurons were much more sensitive following Glu stimulation at 13 DIV. The observation that the total number of living cells following Glu stimulation decreases with culture age suggests that embryonic cortical neurons cultured for 13 days (mature) express more functional Glu receptors and therefore undergo neuronal death following exposure to NMDA agonists. In order to demonstrate the efficient coupling between mature embryonic cortical neurons and sensitive Glu receptors further experiments were necessary. 10 DIV and 13 DIV cortical neurons were exposed independently for 24 hours to various concentrations of excitatory (Glu and Asp), non-excitatory (Ala) and neurotoxic but non-excitotoxic compounds (paraquat), before being assessed for effects on cell viability and ATP. It was found that (a) loss of intracellular ATP and cytotoxicity were more pronounced in 13 DIV rat cortical neurons

following exposure to Glu and Asp, (b) that Ala had no effect on energy levels nor on cell viability on either culture day and (c) that paraquat rapidly decreased energy levels and caused rapid cell death regardless of time in culture, demonstrating that its neurotoxic action is not dependent on NMDA receptor activation. On account of these results, it was decided to use 13 DIV rat cortical neurons in the subsequent experiments. When rat cortical neurons (13 DIV) were exposed for either 4 or 24 hours to various concentrations of the excitatory amino acids, Glu and Asp it was found that cytotoxicity following EAA exposure was not only concentration-dependent but also time-dependent. The non-excitatory compound, Ala, was used as a control in these experiments and did not induce neuronal death in the cultures at either time-point.

It has been reported that mitochondrial dysfunction, leading to a decrease of mitochondrial membrane potential ($\Delta\psi_m$) and release of critical (protein) factors, triggers a sequence of biochemical events resulting in cell death. Thus, it was investigated, in this Chapter, whether a loss of $\Delta\psi_m$ was an important event in EAA-induced neurotoxicity in rat cortical cultures. Rat cortical neurons (13 DIV) were exposed for 24 hours to various concentrations of Glu and Asp and it was observed that the $\Delta\psi_m$ deceased rapidly in a concentration-dependent manner. These results demonstrate that NMDA receptor activation is associated with a profound depolarisation of $\Delta\psi_m$. Given that $\Delta\psi_m$ forms the major part of the total proton motive force that drives ATP synthesis by oxidative phosphorylation (Nicholls and Budd, 1998, 2000), the loss of $\Delta\psi_m$ could seriously impede the ability of neurons to maintain their bioenergetic state.

In this study, it was demonstrated that the NMDA receptor played a predominant role in mediating Glu-induced neuronal death in mature rat cortical neurons. Rat cortical neurons were exposed to the selective NMDA receptor antagonist, AP5, in the presence of various concentrations of Glu for both 4 and 24 hours, to consider whether the effective blockade of NMDA receptors could eliminate all signs of Glu neurotoxicity. Even at high concentrations of Glu, AP5 was found to prevent ATP depletion and loss of mitochondrial membrane potential, and to provide rescue from cell death. These results demonstrate that Glu neurotoxicity in mature rat cortical neurons is mediated through NMDA receptors alone and these results are consistent with those reported by Choi *et al.* (1988).

It has also been reported that not only NMDA but also AMPA and KA can induce cytotoxicity in cultured neurons, an observation indicating that non-NMDA receptors may be involved (Frandsen and Schousboe, 1987; Sinclair et al., 2003). Therefore, the quinoxalinedione, CNQX was used to investigate whether the potent, selective blockade

of non-NMDA receptors could reduce Glu neurotoxicity in mature rat cortical neurons. The selective combination of various concentrations of Glu with the antagonist CNQX caused decreased intracellular ATP concentrations and loss of mitochondrial membrane potential leading to neuronal cell death. Frandsen *et al.* (1989) also reported that CNQX protected against toxicity induced by non-NMDA agonists but not from that induced by NMDA. Therefore, the finding that CNQX did not attenuate Glu-induced neuronal cell death in our cultures of rat cortical neurons provides additional substantiation for (a) the hypothesis that Glu-induced neurotoxicity is predominantly mediated through the NMDA subclass of Glu receptors, which in accordance with previous publications (Rogers *et al.*, 1997; Koh and Choi, 1991), and (b) that these cultures provide an appropriate model in which to study excitotoxicity.

In summary, it has been shown that both mCGCs and rat cortical neurons can be used to investigate excitotoxicity. In both systems exposure to the EAAs, Glu, Asp and NMDA, and the subsequent over-activation of the NMDA receptors resulted in a concentration-dependent loss of cell viability, intracellular ATP concentration and mitochondrial membrane potential, leading to neuronal cell death. However, further work is required to investigate the mode of neuronal cell death in excitotoxicity, that is, whether cell death is by apoptosis or necrosis.

An additional mechanism that might amplify the progression of the excitotoxic cascade is the abnormal transcription of immediate-early genes (*IEGs*). These genes encode DNA-binding proteins (transcription factors) that regulate the expression of other genes important to cell activation, survival or possibly responsible for enhancing neurotoxicity. It has been confirmed in this Chapter that *in vitro* systems can be used as models to investigate excitotoxicity. Thus, the two different *in vitro* systems, that is, mCGCs and rat cortical neurons, with be used in the next two Chapters to investigate the expression of *IEGs*, namely the *c-fos* and *c-jun* families, in excitotoxicity.

Chapter 4

Expression of Excitatory Amino Acid induced *IEGs* in Mouse Cerebellar Granule Cells.

4.1 Introduction

Many synapses in the mammalian nervous system use glutamate (Glu) as a neurotransmitter to mediate neuronal excitation. Glutamatergic neurotransmission is mediated by two types of receptors, namely ionotropic and metabotropic receptors. The ionotropic receptors mediate the fast excitatory post-synaptic responses, while the metabotropic receptors, which are linked by G-proteins to a variety of intracellular messengers, mediate much slower pre- and post-synaptic responses (Michaelis, 1998; Platenik *et al.*, 2000). Excessive NMDA receptor activation is thought to initiate the process of excitotoxicity (Olney *et al.*, 1971), whereby characteristic pathological neuronal membrane permeability changes and disturbed ion homeostasis arise following the prolonged depolarising action of Glu (and other excitatory amino acids (EAAs), for example aspartate (Asp) or N-methyl-D-aspartate (NMDA)) at post-synaptic EAA receptor sites. It is thought that excitotoxicity may underlie age-related multifactorial disorders (such as Huntington's disease, Parkinson's disease and amyotrophic lateral sclerosis; Lipton and Rosenberg, 1994) as well as acute and chronic neuropathologies (epilepsy and ischaemia). Although causative mechanisms of excitotoxic neuronal death remain to be clarified, events such as protease activation, synthesis of diffusible gases, for example nitric oxide, and free radical formation are tied to massive Ca^{2+} influx through the NMDA receptor. All have been suggested as contributing to neuronal damage (Ankarcrona *et al.*, 1995; Frandsen and Schousboe, 1993; Nicotera *et al.*, 1992). An additional mechanism that could amplify the progression of the excitotoxic cascade is the abnormal transcriptional induction of genes that alter cellular activity. EAA receptor activation and subsequent increased cytosolic Ca^{2+} are reported to co-ordinately activate a series of genes known as *immediate early genes* (*IEGs*).

When a neuronal cell responds to environmental stimuli by alteration of gene transcription, two sets of genes can be distinguished. One set consists of genes whose expression is low or undetectable in quiescent cells, but which is activated rapidly and transiently within minutes of stimulation. This transcription is independent of new protein synthesis (Morgan and Curran, 1986; Sheng and Greenberg, 1990; Hughes and Dragunow, 1995). These genes are called *IEGs*, of which some regulate the expression of a later transcribed subset of genes called d*elayed-response genes*, which function as survival or toxic factors (Tatter *et al.*, 1995). The d*elayed-response genes* are induced more slowly, via a mechanism that is generally dependent on new protein synthesis. *IEGs* function as

transcription factors that couple short-term signalling events to long-term alterations in cellular phenotype by the selective regulation of gene expression (Curran and Morgan, 1987). In general, transcription factors are proteins that bind to a specific DNA sequence in a promoter or enhancer region and, via interaction of their trans-activation domains with the transcription complex of RNA polymerase, activate or suppress transcription of a particular gene. The transcription factors are classified into several large families based on the structure of their DNA binding domains. The main groups are helix-turn-helix, zinc finger, homeodomain and leucine zipper/basic helix-loop-helix proteins (Pabo and Sauer, 1992).

IEGs encode proteins, which are closely related in structure and can substitute for one another in a number of functional assays. Most prominent among the *IEGs* are the *c-fos* and *c-jun* gene families, which encode the nuclear phosphoproteins c-Fos and c-Jun, respectively. c-Fos and c-Jun are components of the transcriptional regulatory complex, activator protein - 1 (AP-1; Curran and Franza, 1988), which is associated with the regulation of both differentiation and proliferation in various cell types (Angel and Karin, 1991; Curran and Morgan, 1991). Both c-Fos and c-Jun proteins contain a conserved structural motif and binding region, called the "*leucine zipper*", which allows strong protein-protein interactions to occur. The leucine-zipper structure is found within proteins of the b-zip family. The leucine-zipper is an α-helical domain in which four or five leucine residues occur at regular seven-residue intervals. These leucine residues locate on the same rotational position of the α-helix and, because of this regular spacing, form a linear crest of leucine residues that protrude from the side of the protein helix. Proteins that have a leucine-zipper domain bind to each other because of hydrophobic interactions between the linear leucine crests of the two molecules. There are at least 4 types of Fos proteins, c-Fos, FosB, Fra-1 (Fos related antigen - 1) and Fra-2, and three Jun proteins, namely c-Jun, JunB and JunD. All of the Fos and Jun family members contain leucine-zipper domains, which means that they can associate together to form various heterodimers (Hughes and Dragunow, 1995). In addition to heterodimerisation, the Jun, but not the Fos family of *IEG*-encoded proteins, are capable of homodimerisation (Vogt and Bos, 1990). Furthermore the Jun proteins can dimerise with transcription factors from the ATF and CREB families, that also possess the leucine zipper motif and even with other less related transcription factors (Herdegen and Leah, 1998). A highly basic stretch of amino acids is located adjacent to the leucine zipper domain of Fos and Jun and is required for the interaction of the Fos:Jun heterodimer with DNA (Neuberg *et al.*, 1989; Turner and Tjian,

1989). The resulting Fos:Jun heterodimers and Jun:Jun homodimers bind with high affinity to the DNA regulatory element named AP-1 (with a consensus sequence 5'-TGACTCA-3'), which has a binding site for the AP-1 complex, in the promoter and enhancer regions of many genes and has been shown to effect both positive and negative regulation of their expression (Sassone-Corsi *et al.*, 1988; Angel and Karin, 1991; Hughes and Dragunow, 1995). In the AP-1 complex, both Fos and Jun proteins bind directly to DNA. Therefore, the term AP-1 does not refer to a unique transcription factor but rather to a general DNA binding activity that can be constituted by various homo- and heterodimeric complexes comprising proteins encoded by *fos* and *jun* gene family members (Curran and Franza; Kerppola and Curran, 1991; Morgan and Curran, 1995). The specificity of the *IEG* response is dictated by the stoichiometry of the various members and the available target genes. Cell type- and stimulus-dependent post-translational modification of *IEG* products may contribute to their biological activity as well as adding a further level of specificity to their response (Herzog and Morgan, 1996).

The induction of *IEGs* was first examined in PC12 cells (Greene and Tischler, 1982; Curran and Morgan, 1985; Greenberg *et al.*, 1985, 1986; Milbrandt, 1986; Morgan and Curran, 1986 Hughes and Dragunow, 1995). The rat adrenal PC12 pheochromocytoma cell line has been used as an *in vitro* model for neurodevelopment, as the cells, in response to growth factors such as nerve growth factor (NGF), differentiate to a phenotype resembling sympathetic neurons. The cells are characterised by the cessation of proliferation and the promotion of neurite outgrowth (Greenberg *et al.*, 1985). PC12 cells have excitable membranes that can be depolarised by specific neurotransmitters or elevated levels of extracellular potassium chloride (KCl; Dichter *et al.*, 1977). In the PC12 cell line, *IEGs* were not only stimulated by growth factors but also by calcium influx due to depolarisation. It was found by Morgan and Curran (1986) that agents or conditions (high K^+ or the Ca^{2+} agonist BAY K8644) that provoked a voltage-dependent increased cytosolic Ca^{2+} influx in PC12 cells were potent inducers of *c-fos*. These results demonstrated that Ca^{2+} was a major second messenger regulating *IEG* expression in excitable cells and suggested that synaptic transmission in the neuronal cells might be coupled to the regulation of gene expression.

In the CNS, induction of the early gene, *c-fos*, is thought to be involved in neuronal plasticity and memory formation (Curran and Morgan, 1987; Morris *et al.*, 1986). Additionally, it has been reported (Didier *et al.*, 1992) that *c-fos* may play a role in survival and/or maturation of cerebellar granule cells *in vitro*. In most cell types, the basal level of

the proto-oncogene *c-fos* is relatively low. Greenberg *et al.* (1986), reported that within minutes of its activation by neurotransmitters, expression of the *c-fos* gene is repressed. The rapid disappearance of the *c-fos* mRNA reflects the fact that this mRNA has an extremely short half-life time (12 min; Shyu *et al.*, 1989). In addition, *c-fos* expression is a consequence of transcriptional repression, that is, the protein product c-Fos shuts off transcription of the *c-fos IEG* (Sassone-Corsi *et al.,* 1988b). It was first reported by Szekely *et al.* (1989) that *c-fos* was rapidly and transiently expressed, in a Ca^{2+}-requiring manner, in primary cultures of mouse cerebellar granule cells (mCGCs) following a brief exposure to low levels of the excitatory amino acid, Glu. This suggested that *c-fos* expression was probably mediated by activation of the NMDA subtype of Glu receptor although transcription of *c-fos* may also be triggered by Ca^{2+} influx via voltage-gated Ca^{2+} channels (Murphy *et al.*, 1991; Bading *et al.*, 1993; Ghosh *et al.*, 1994, Griffiths *et al.*, 1998). It was also reported that following excitotoxic lesion (that is, overstimulation of NMDA ionotropic receptors) *in vivo*, a continuous, rather than transient, expression of *c-fos* occurred (Pennypacker *et al.*, 1994; Shan *et al.*, 1997).

Consistent with these findings are the observations that excitotoxic cell death in primary cultures of mCGCs (Gorman *et al.*, 1995) and rat neo-cortical neurons (Meredith *et al.*, 1996) correlated with the appearance of a delayed, elevated and sustained expression of *c-fos* mRNA. Therefore, it seemed that brief exposure of neurons to low levels of the excitatory amino acid, Glu, induced rapid and transient expression of *c-fos,* while excitotoxic exposure in the same cultures induced elevated and sustained levels of *c-fos.* Griffiths *et al.* (1997) investigated this hypothesis further in mCGCs exposed to the EAAs, Glu, NMDA and KA. It was found that following exposure to non-toxic levels of the EAAs, a transient increase in *c-fos* mRNA expression occurred which peaked at 30 min but which had returned to basal levels by 240 min. In addition, exposure of the granule cells to toxic concentrations of the EAAs resulted in a delay in *c-fos* mRNA expression, which was followed by a subsequent increased and sustained expression. From these results, Griffiths *et al.* (1997) proposed that a ratio ($Q^{240/30}$) between *c-fos* mRNA levels at 30 min and 240 min following stimulation could be used as a specific test to predict excitotoxic outcome. Their results predicted that $Q^{240/30} > 1$ correlated reproducibly with excitotoxic cell death whereas a ratio of < 1 correlated with a non-excitotoxic event. So far, the investigations into *c-fos* expression, including those of Gorman *et al.* (1995), Meredith *et al.* (1996), Malcolm *et al.* (1997) and Griffiths *et al.* (1997, 2000) have been based on the method of Northern blot analysis.

Five methods are in common use for the quantification of transcription; Northern blotting and *in situ* hybridisation (Parker and Barnes, 1999), RNAse protection assays (Hod, 1992; Saccomanno *et al.*, 1992), the reverse transcription polymerase chain reaction (RT-PCR; Weis *et al.,* 1992; Zamorano *et al.,* 1996) and cDNA arrays (Bucher, 1999). Northern analysis is the only method providing information about mRNA size, alternative splicing and the integrity of RNA samples. The RNAse protection assay is most useful for mapping transcript initiation and termination sites and intron or exon boundaries, and for discriminating between related mRNAs of similar size, which would migrate at similar positions on a Northern blot. *In situ* hybridisation is the most complex method of all, but is the only one that allows localisation of transcripts to specific cells within a tissue. The main limitation of these three techniques is their comparatively low sensitivity (Melton *et al.*, 1984).

In this Chapter, the expression of *c-fos* in mCGCs was investigated using the method of quantitative, real-time reverse transcription polymerase chain reaction (RT-PCR). Real-time RT-PCR is an *in vitro* method for enzymatically amplifying defined sequences of RNA (Weis *et al.,* 1992; Zamorano *et al.,* 1996; Rappolee *et al.*, 1988) and permits the analysis of low-abundance mRNA, obtained from limited tissue samples. Polymerase chain reaction (PCR) revolutionised the study of individual gene sequences and genome organisation and is now a central tool in gene expression studies in the form of quantitative PCR. This technique records the accumulation of PCR product during the process of the reaction. PCR begins as an exponential process, with a theoretical doubling of the template concentration in each cycle. As the reaction continues, however, the cycle-to-cycle accumulation of product becomes linear, and finally a plateau is reached and no more amplification occurs. Quantitative real-time RT-PCR overcomes this limitation by evaluating product accumulation during the exponential phase of amplification and directly calculating template quantities. Real-time, RT-PCR is the most sensitive and the most flexible of the quantification methods (Wang and Brown, 1999) and can be used to compare the levels of mRNAs in different sample populations, to characterise patterns of mRNA expression, to discriminate between closely related mRNAs and to analyse RNA structure. The method of quantitative, real-time RT-PCR not only allows up to a 100-fold increase in throughput (Jordan, 2000) compared to Northern blot analysis but also has the significant benefit of reducing the number of animals used per experiment as the amount of total RNA required per sample for RT-PCR analysis (100 fg) is much reduced when compared to Northern blot analysis (15 µg).

Many excitotoxins used to activate *IEGs* are generally regarded as equivalent, with little rigorous regard to the strength and time-course of activation by each. There has not been strict demonstration of the relative abilities of different agents to activate *IEGs*. Here, we present such an analysis, showing the relative abilities of Glu and Asp to elicit *c-fos* induction. mCGCs (7 DIV) were exposed to various concentrations of Glu and Asp and the profile of *c-fos* expression was monitored by real-time RT-PCR over a period of 6 hours. In order to show that this new *in vitro* assay, based on the measurement of *c-fos* mRNA, could be used in predicting the excitotoxic potential of compounds, NMDA-receptor antagonists were employed. In this study, the isosteric Glu receptor antagonist, AP5, was used as a selective competitive antagonist at NMDA receptors and the quinoxalinedione, CNQX was used as a potent and selective competitive antagonist at non-NMDA receptors (Honoré *et al.*, 1988). In addition, the measurement of *c-fos* mRNA by RT-PCR was used to predict whether different compounds in a screen exhibited excitotoxic properties.

As discussed previously, 3 other members of the *fos* family of *IEGs*, namely, *fosB, fra-1* and *fra-2*, and 3 members of the Jun family, *junB, junD* and *c-jun* exist. It has been reported that, in general, the characteristics of induction of these other *IEGs* resemble those of *c-fos* although there are some differences in the kinetics and the magnitude of responses. Morgan and Curran reported (1991) that individual members of the *fos* and *jun* gene families can have distinctive temporal patterns of expression. It was therefore of interest, in this Chapter, to investigate the individual profiles of expression of the other members of the *fos* and *jun IEG* families in mCGCs treated with both excitotoxic and non-excitotoxic concentrations of the various EAAs.

Aims of this Chapter

The first aim of this Chapter was to investigate whether changes in *c-fos* mRNA levels could be measured in primary cultures of mCGCs with the use of real-time RT-PCR.

The second aim was to show that excitotoxicity-related changes, concentration-dependencies and receptor specificities could be quantitatively measured in primary cultures of mCGCs, using real-time RT-PCR.

The third aim was to demonstrate whether real-time RT-PCR allows for the characterisation of effects of much larger numbers of compounds, that is, whether real-time RT-PCR is suitable for screening. The levels of *c-fos* expression were investigated in mCGCs treated with 4 different groups of compounds, subdivided according to established characteristics, namely, Group 1-endogenous/synthetic excitotoxins, Group 2-neurotoxic but non-excitotoxic compounds, Group 3- neuroactive but non-toxic compounds and Group 4-compounds that are toxic to other target organelles, and to test whether a ratio between *c-fos* steady-state levels at 30 min and 240 min (Griffiths *et al.*, 1997) can be used to predict excitotoxic outcome, when measured by real-time RT-PCR.

Finally, the fourth aim was to investigate changes in the expression of other members of the *fos* (*fosB, fra-1 and fra-2*) and *jun* (*c-jun, junB and junD*) families of *IEGs* in excitotoxicity.

4.2 Results

4.2.1 Optimisation of *fos* and *jun* primers for RT-PCR gene expression analysis

NIH 3T3 mouse fibroblasts treated with 12-*o*-tetradecanoylphorbol-13-ester (TPA), are known to have induced the expression of several *IEGs* including *c-fos* (Cano e*t al.*, 1995; Soh *et al.*, 1999), and so these cells were used as a positive control to check for the sensitivity of the newly designed primers pairs. NIH 3T3 cells were grown as described in Chapter 2 (see Section 2.3). The cells were exposed to either a low (0.3 μM) or high (3 μM) concentration of TPA for 15, 30, 45, 60 or 90 min. Total RNA was isolated and cDNA prepared and the target primers were amplified by PCR. PCR products were analysed by ethidium bromide-stained agarose gel electrophoresis (see Chapter 2).

With all primers, a single PCR product of the desired length was produced (see Figures 4.1 to 4.5). Thus, all primers designed were optimal for use in real-time RT-PCR gene expression analysis.

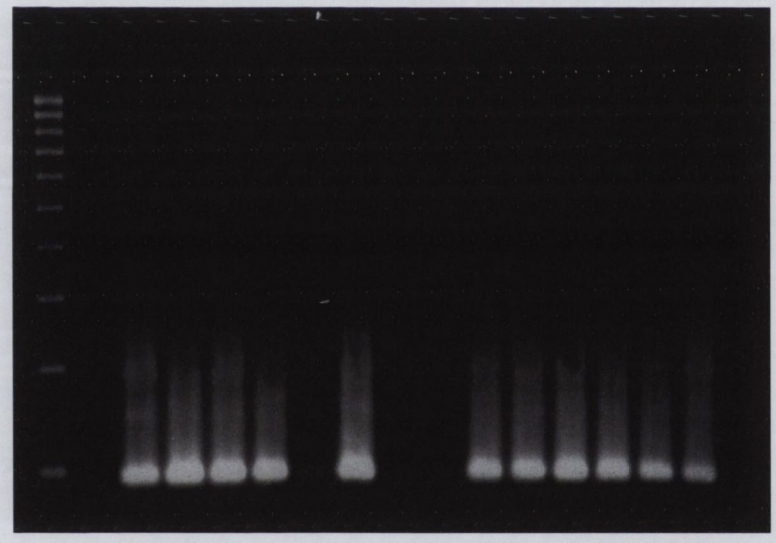


Figure 4.1: Amplification of 18S primers in 3T3 mouse fibroblasts treated with TPA

Lane 1 represents the 100 base pair ladder. Lane 2 is an empty lane. Lane 3 shows the DNA product isolated from control NIH 3T3 cells. Lanes 4, 5, 6, 7 and 8 show the DNA product following treatment of the NIH 3T3 cells with 0.3 μM TPA for 15, 30, 45, 60 and 90 min. Lanes 9 and 10 are empty. Lane 11 shows the DNA product isolated from control NIH 3T3 cells. Lanes 12, 13, 14, 15 and 16 show the DNA product following treatment of the NIH 3T3 cells with 3 μM TPA for 15, 30, 45, 60 and 90 min.

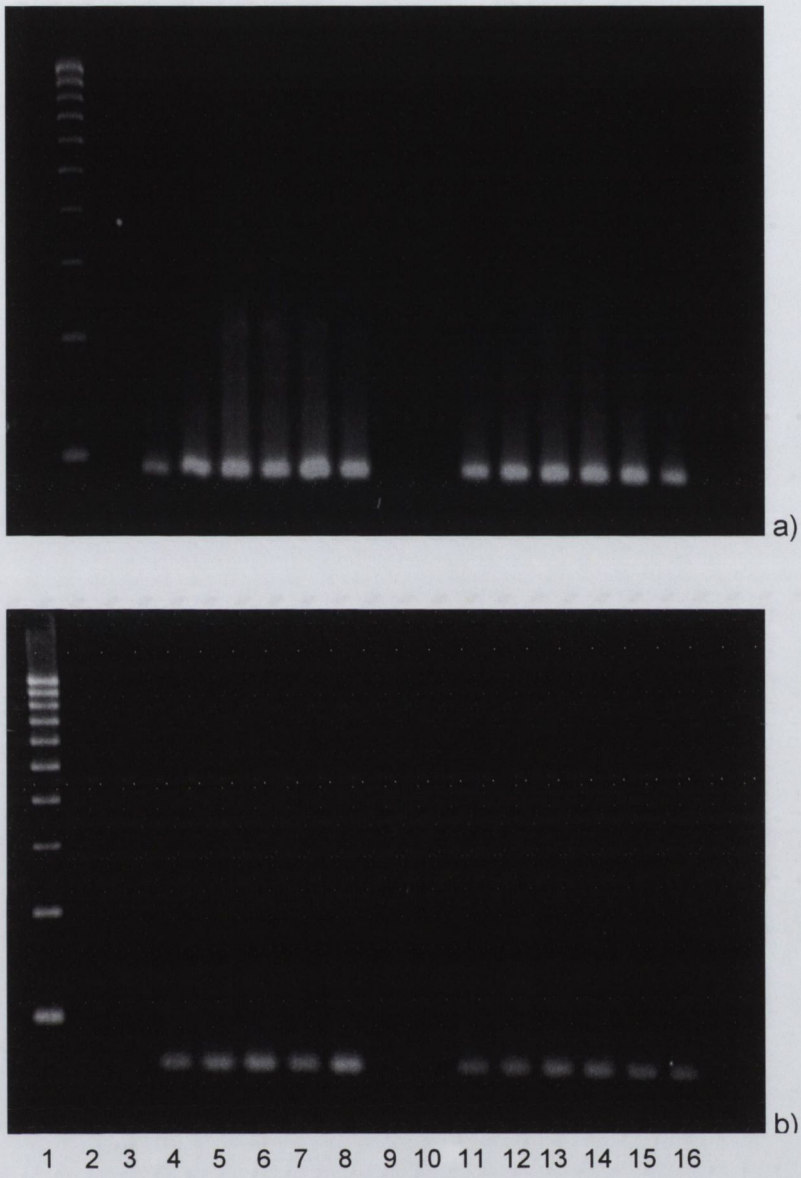


Figure 4.2: Amplification of a) *c-fos* and b) *fosB* primers in NIH 3T3 mouse fibroblasts treated with TPA

Lane 1 represents the 100 base pair ladder. Lane 2 is an empty lane. Lane 3 shows the DNA product isolated from control NIH 3T3 cells. Lanes 4, 5, 6, 7 and 8 show the DNA product following treatment of the NIH 3T3 cells with 0.3 μM TPA for 15, 30, 45, 60 and 90 min. Lanes 9 and 10 are empty. Lane 11 shows the DNA product isolated from control NIH 3T3 cells. Lanes 12, 13, 14, 15 and 16 show the DNA product following treatment of the NIH 3T3 cells with 3 μM TPA for 15, 30, 45, 60 and 90 min.

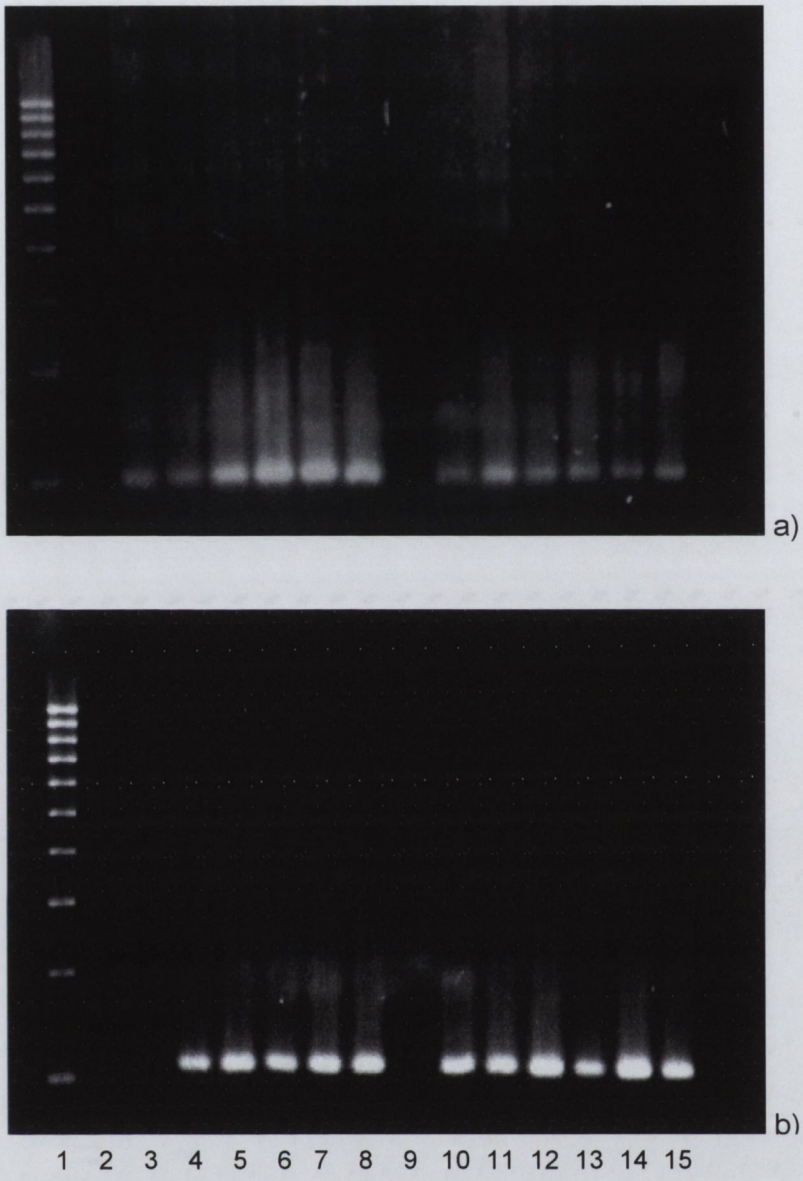


Figure 4.3: Amplification of a) *fra-1* and b) *fra-2* primers in NIH 3T3 mouse fibroblasts treated with TPA

Lane 1 represents the 100 base pair ladder. Lane 2 is an empty lane. Lane 3 shows the DNA product isolated from control NIH 3T3 cells. Lanes 4, 5, 6, 7 and 8 show the DNA product following treatment of the NIH 3T3 cells with 0.3 μM TPA for 15, 30, 45, 60 and 90 min. Lane 9 is empty. Lane 10 shows the DNA product isolated from control NIH 3T3 cells. Lanes 11, 12, 13, 14 and 15 show the DNA product following treatment of the NIH 3T3 cells with 3 μM TPA for 15, 30, 45, 60 and 90 min.

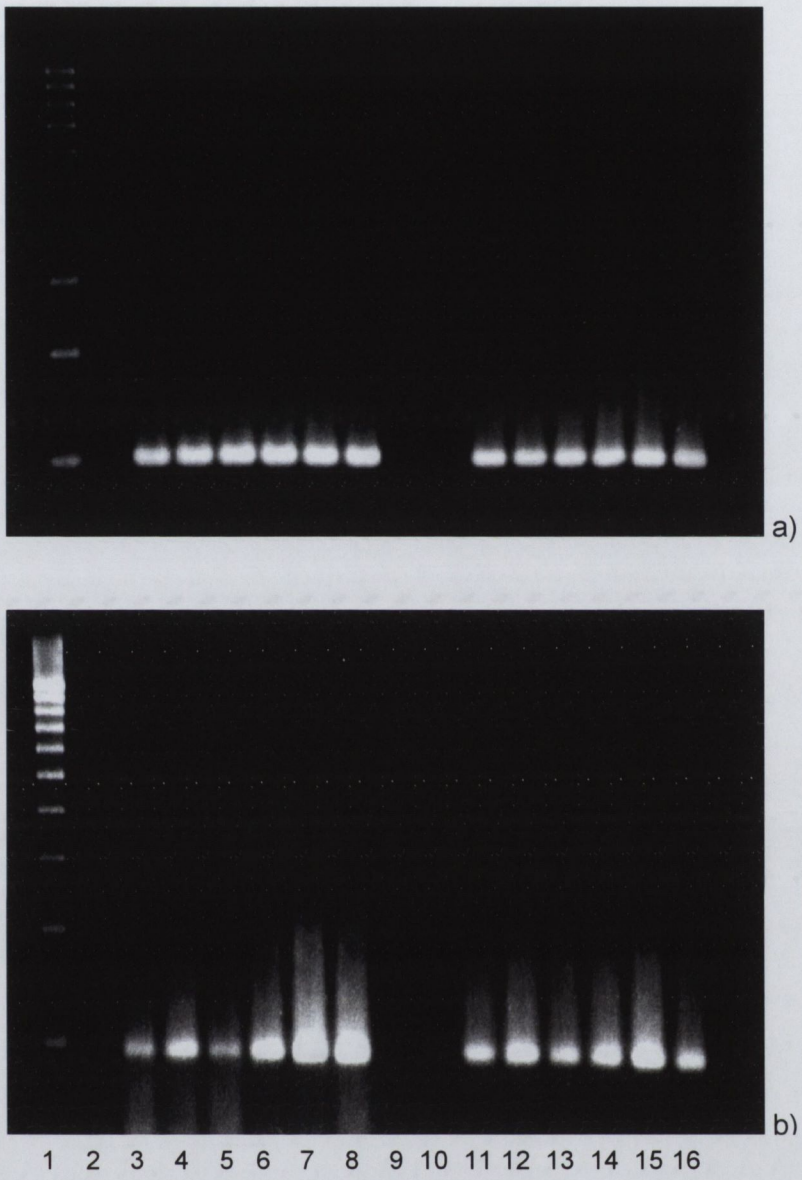


Figure 4.4: Amplification of a) *c-jun* and b) *junB* primers in NIH 3T3 mouse fibroblasts treated with TPA

Lane 1 represents the 100 base pair ladder. Lane 2 is an empty lane. Lane 3 shows the DNA product isolated from control NIH 3T3 cells. Lanes 4, 5, 6, 7 and 8 show the DNA product following treatment of the NIH 3T3 cells with 0.3 µM TPA for 15, 30, 45, 60 and 90 min. Lanes 9 and 10 are empty. Lane 11 shows the DNA product isolated from control NIH 3T3 cells. Lanes 12, 13, 14, 15 and 16 show the DNA product following treatment of the NIH 3T3 cells with 3 µM TPA for 15, 30, 45, 60 and 90 min.

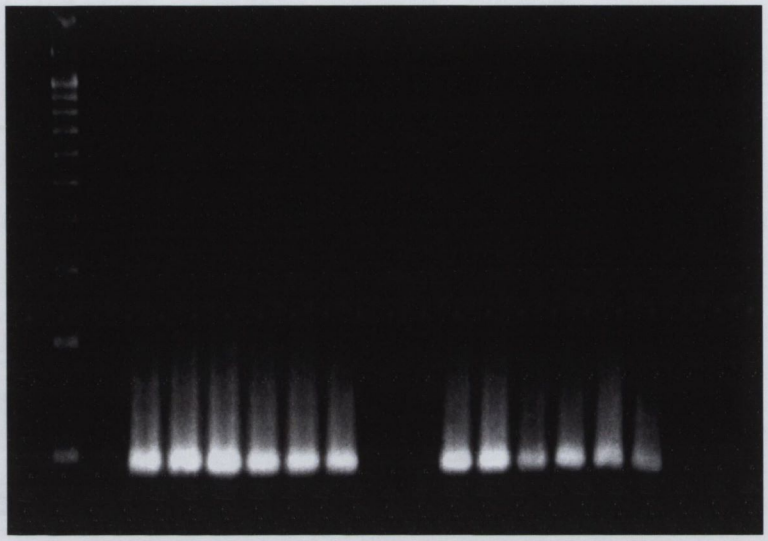


Figure 4.5: Amplification of *junD* primers in NIH 3T3 mouse fibroblasts treated with TPA

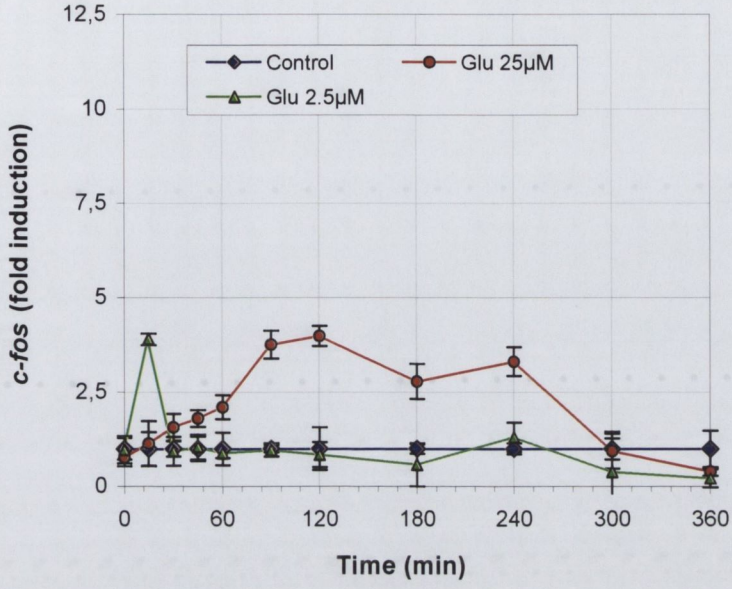
NIH 3T3 cells were grown as described in Chapter 2 (see Section 2.3). The cells were exposed to either a low (0.3 μM) or high (3 μM) concentration of TPA for 15, 30, 45, 60 or 90 min. Total RNA was isolated (Section 2.5.2) and cDNA prepared (Section 2.7) to amplify the target primers by PCR (Secion 2.12). Lane 1 represents the 100 base pair ladder. Lane 2 is an empty lane. Lane 3 shows the DNA product isolated from control NIH 3T3 cells. Lane 4 shows the DNA product following treatment of the NIH 3T3 cells with 0.3 μM TPA for 15 min. Lanes 5, 6, 7 and 8 show the DNA product following treatment of the NIH 3T3 cells with 0.3 μM TPA for 30, 45, 50 and 90 min. Lanes 9 and 10 are empty. Lane 11 shows the DNA product isolated from control NIH 3T3 cells. Lanes 12, 13, 14, 15 and 16 show the DNA product following treatment of the NIH 3T3 cells with 3 μM TPA for 15, 30, 45, 60 and 90 min.

4.2.2 *c-fos* expression profiles vary with time and Glu concentration

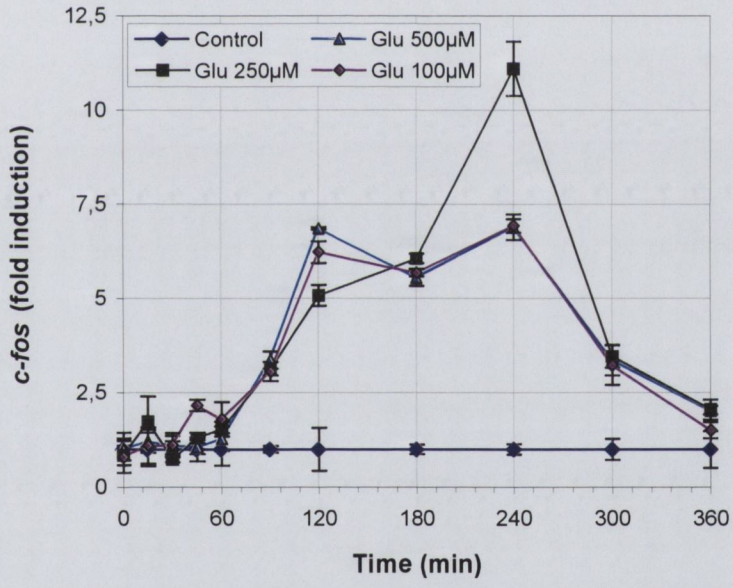
The causative mechanisms of excitotoxic cell death remain elusive. However, a number of reports suggest that a disturbance in intracellular events, leading to huge increases in Ca^{2+} and the abnormal transcriptional induction of *IEGs*, in particular *c-fos*, through the NMDA receptor may be involved (Frandsen and Schousboe, 1993; Lipton and Nicotera, 1998). Primary cultures of mCGCs were prepared from post-natal mice as described in Section 2.2.1 and by Meier and Schousboe (1982), Drejer *et al.* (1983) and Schousboe *et al.* (1989) and were routinely cultured for 7 days before exposure to the predominant EAA, Glu. Following treatment over 6 hours, the cells were lysed, total RNA was extracted and the amount of *c-fos* and 18S quantified by real-time RT-PCR. *c-fos* expression values were normalised to the internal control, 18S, prior to calculation of the fold induction of *c-fos* relative to the untreated, time matched controls (see Chapter 2). When mature mCGCs (7 DIV) were treated with various concentrations of Glu (0 - 500 μM) and *c-fos* mRNA measured using RT-PCR, different time courses of induction were obtained depending on Glu concentration. The profiles of time- and concentration-dependent Glu induced *c-fos* responses are shown in Figure 4.6 a) & b).

When mCGCs were exposed to non-toxic concentrations of Glu (2.5 μM), a 3 fold transient increase in *c-fos* mRNA induction was observed at 15 min, before returning to basal levels (see Figure 4.6 a)). Partially toxic concentrations of Glu (25 μM Glu) induced a more delayed but also increased induction of *c-fos* mRNA. At higher, toxic concentrations of Glu (namely 100, 250 and 500 μM), expression of *c-fos* was delayed in time, was sustained over 3 hours and reached maximal levels of 6 - 9 fold when compared to the untreated, time-matched control (see Figure 4.6 b)).

Thus, the transient induction of *c-fos* mRNA, detected using real-time RT-PCR, in mCGCs exposed to non-toxic concentrations of Glu is consistent with that reported previously by Szekely *et al.* (1989) using the Northern blot assay. In addition, the sustained and elevated profile of *c-fos* expression found with toxic concentrations of Glu, in the same cultures, is consistent with that reported previously by Malcolm *et al.* (1997), Meredith *et al.* (1996) and Griffiths *et al.* (1997, 2000), using the less sensitive Northern blot assay. In conclusion, real-time RT-PCR can be used as a sensitive method for the quantitative measurement of EAA induced changes in *c-fos* mRNA expression in mCGCs, which in turn can be used as a sensitive biomarker for excitotoxicity.



a)



b)

Figure 4.6: Different time-profiles of *c-fos* expression dependent on Glu concentration

Primary cultures of mCGCs (7 DIV) were exposed to various concentrations of Glu, for up to 360 min. Following treatment, the cells were lysed, total RNA was extracted and the amount of *c-fos* and 18S quantified by RT-PCR. *c-fos* expression values were normalised to 18S expression, which served as the internal control. The results above refer to the fold induction of *c-fos* expression compared to untreated, time-matched controls. Data represent mean ± s.d. values of triplicate RT-PCR reactions derived from one individual experiment. The experiments were reproduced at least three times. Figure 4.6 a) represents the *c-fos* changes with non-toxic and partially toxic concentrations of Glu while b) represents changes in *c-fos* expression with toxic concentrations.

4.2.3 NMDA receptor specificity of Glu-induced *c-fos* mRNA expression

Excitotoxicity is defined as neuronal cell death mediated by over-activation of Glu receptor subtypes. In order to investigate which Glu receptor subtype is specifically involved in the process of excitotoxicity, the degree of protection offered by the selective, competitive NMDA receptor antagonist, AP5, was assessed in the presence of various concentrations of Glu. A non-NMDA receptor antagonist, CNQX, was used for comparison.

When cultures of mCGCs (7 DIV) were treated with partially toxic concentrations of Glu (25 μM), a delayed and sustained increase in *c-fos* mRNA expression was observed, when compared to the time-matched control. In accordance with previous *in vitro* (Gorman *et al.,* 1995; Meredith *et al.,* 1996; Griffiths *et al.,* 1997, 1998, 2000) and *in vivo* (Pennypacker *et al.,* 1994; Shan *et al.,* 1997) reports, this profile was regarded as characteristic of excitotoxicity. Pre-treatment with AP5 completely inhibited the toxic *c-fos* response induced by 25 μM Glu. However, pre-treatment with CNQX had no effect (see Figure 4.7). Thus, the induction of *c-fos*, observed in mCGCs treated with a partially toxic concentration of Glu, was as a direct and specific result of over-activation of the NMDA subtype of Glu receptors.

Exposure of mCGCs to toxic concentrations of Glu (100 μM) induced an elevated and sustained increase in *c-fos* mRNA expression. It was found that pre-treatment with AP5 changed the toxic *c-fos* expression profile to that of an earlier peaking, less sustained expression, albeit not to the profile expected for complete abolition of the response. CNQX did not antagonise the toxic *c-fos* response (see Figure 4.8).

With higher, toxic concentrations of Glu (250 μM), a more delayed increase in *c-fos* mRNA expression was detected. Indeed, comparable to the profile observed with 100 μM Glu, the induction of *c-fos* was sustained over 300 min. Pre-treatment with either AP5 or CNQX did not inhibit or change the toxic profile of *c-fos* mRNA induction (see Figure 4.9).

These results suggest that the effectiveness of AP5 in inhibiting the excitotoxic *c-fos* response is inversely proportional to the concentration of Glu. Higher concentrations of AP5 are therefore required to fully compete with the very toxic concentrations of Glu (100 μM and 250 μM) used in these investigations. However, these results are consistent with Glu-induced *c-fos* mRNA expression being mediated through the NMDA receptor subtype.

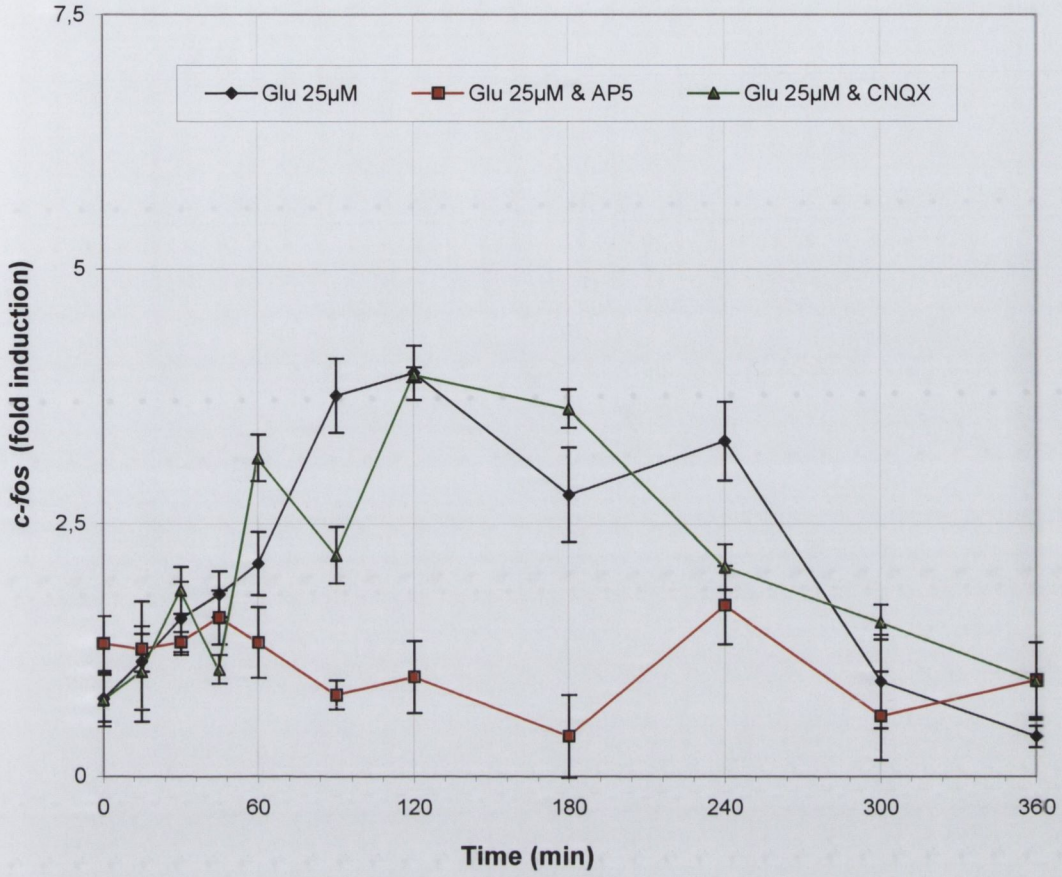


Figure 4.7: AP5 but not CNQX effectively abolishes *c-fos* mRNA expression at low Glu concentrations

Primary cultures of mCGCs (7 DIV) were pre-incubated for 15 min with either AP5 (500 µM) or CNQX (10 µM) prior to co-exposure with a fixed concentration of Glu (25 µM), for up to 360 min. Following treatment, the cells were lysed, total RNA was extracted and the amount of *c-fos* and 18S quantified by RT-PCR. The *c-fos* expression values were normalised to 18S expression, which served as the internal control. The results above refer to the fold induction of *c-fos* expression compared to untreated, time-matched controls. Data represent mean ± s.d. values of triplicate RT-PCR reactions derived from one individual experiment. The experiments were reproduced at least twice.

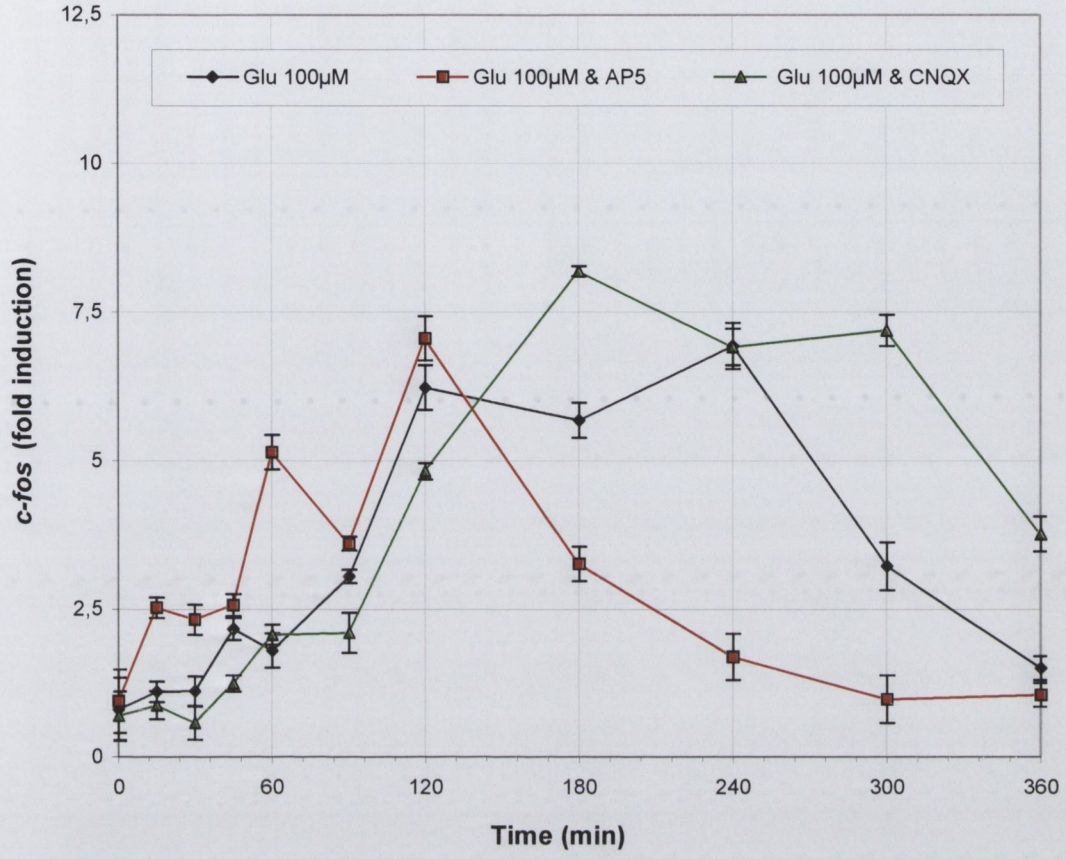


Figure 4.8: AP5 but not CNQX changes the *c-fos* mRNA expression profile at high Glu concentrations

Primary cultures of mCGCs (7 DIV) were pre-incubated with either AP5 (500 µM) or CNQX (10 µM) for 15 min prior to exposure to a fixed concentration of Glu (100 µM) for up to 360 min. Following treatment, the cells were lysed, total RNA was extracted and the amount of *c-fos* and 18S quantified by RT-PCR. The *c-fos* expression values were normalised to 18S expression, which served as the internal control. The results above refer to the fold induction of *c-fos* compared to untreated, time-matched controls. Data represent mean ± s.d. values of triplicate RT-PCR reactions derived from one individual experiment. The experiments were reproduced at least twice.

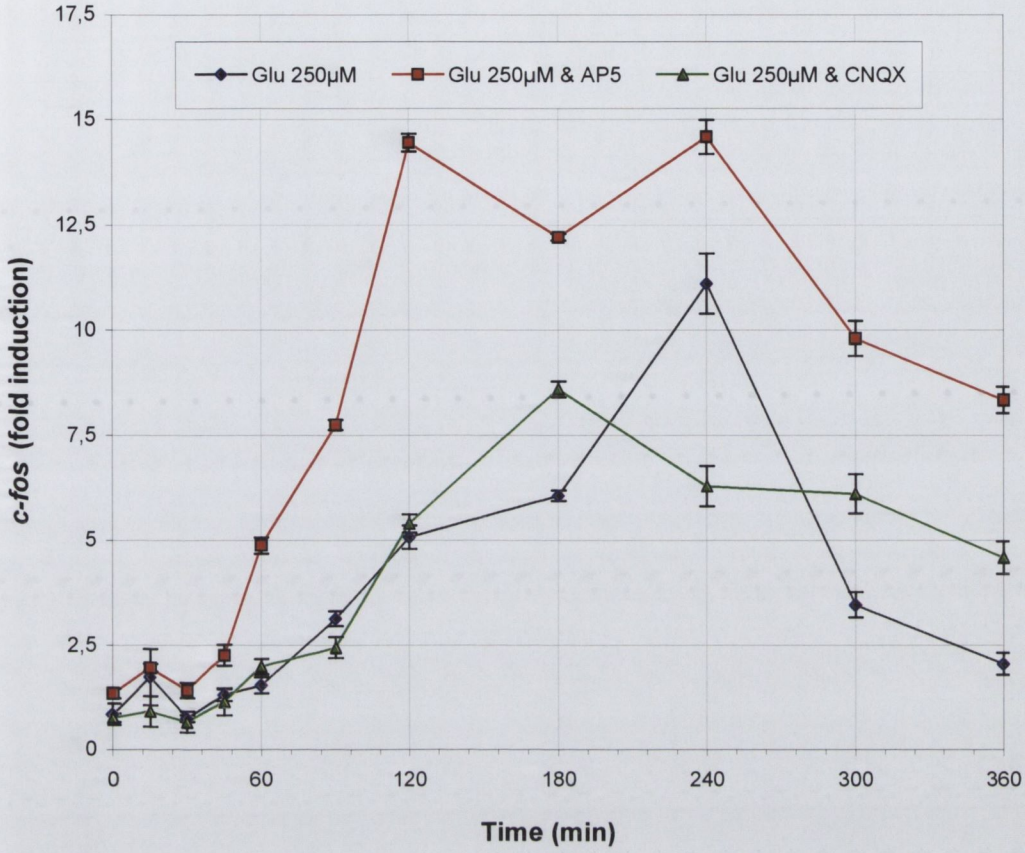


Figure 4.9: AP5 but not CNQX changes the *c-fos* mRNA expression profile at toxic concentrations of Glu

Primary cultures of mCGCs (7 DIV) were pre-incubated for 15 min with either AP5 (500 µM) or CNQX (10 µM) prior to co-exposure with a fixed concentration of Glu (250 µM), for up to 360 min. Following treatment, the cells were lysed and total RNA was extracted and the amount of *c-fos* and 18S quantified by RT-PCR. The *c-fos* expression values were normalised to 18S expression, which served as the internal control. The results above refer to the fold induction of *c-fos* expression compared to untreated, time-matched controls. Data represent mean ± s.d. values of triplicate RT-PCR reactions derived from one individual experiment. The experiments were reproduced at least twice.

4.2.4 Asp changes *c-fos* mRNA expression in a time- and concentration-dependent manner

On account of the different profiles of Glu-induced *c-fos* mRNA expression measured in mCGCs with real-time RT-PCR, the experiments were repeated with a different EAA, Asp. mCGCs (7 DIV) were stimulated with various concentrations of Asp over the same time-course of 0 to 360 min. Following treatment, the cells were lysed, total RNA was extracted and the amount of *c-fos* and 18S quantified by real-time RT-PCR. *c-fos* expression values were normalised to the internal control, 18S, prior to calculation of the fold induction of *c-fos* relative to the untreated, time matched controls (see Chapter 2). It was found that when the mCGCs were treated with various concentrations of Asp (0 - 500 µM), different time profiles of *c-fos* mRNA expression were induced depending on Asp concentration (see Figures 4.10 a) & b)).

Exposure of mCGCs to non-toxic concentrations of Asp (3.5 µM) induced a very slight increase in *c-fos* expression. With partially toxic concentrations of Asp (35 µM), an elevated, transient increase of *c-fos* mRNA expression was observed. Following exposure of mCGCs to toxic concentrations of Asp (100 - 500 µM), the kinetics of *c-fos* mRNA induction were in marked contrast. Increasing the concentration of Asp to toxic levels induced a change in the *c-fos* mRNA expression profiles from a transient increase (see Figure 4.10 a)) to that of a more delayed, elevated and sustained increase (see Figure 4.10 b)). As in the case of Glu, the elevated levels of *c-fos* induced by toxic concentrations of Asp, exhibited maximal inductions of 6 - 8 fold when compared to the non-induced time-matched controls and were sustained over 5 hours.

These results, demonstrating the involvement of increased *c-fos* mRNA expression in EAA induced excitotoxicity, are consistent with the results found for Glu in Section 4.2.2 and also with those reported by Griffiths *et al.* (1997, 2000). Thus, *c-fos* showed the same profiles of time- and concentration-dependent induction in mCGCs treated with either Asp or Glu, which means that *c-fos* mRNA expression can be used as a biomarker for excitotoxicity in EAA-stimulated mCGCs.

4.2.5 Receptor-specificity of Asp-induced changes in *c-fos* expression

In Section 4.2.3, it was shown that the selective, NMDA receptor antagonist, AP5, effectively blocked the toxic *c-fos* response induced by partially toxic concentrations of Glu

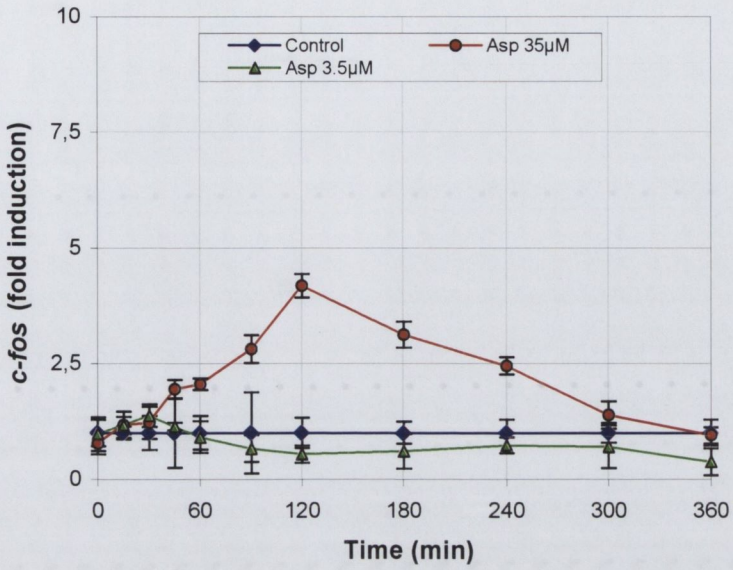
(25 μM) and also partly inhibited the *c-fos* response induced by higher toxic concentrations of Glu (100 μM). As the profiles of *c-fos* expression induced by Asp were similar to those already found for Glu, it was interesting to investigate whether AP5 antagonism was also similar. Thus, the competition of AP5 with Asp for the NMDA binding site was compared to the antagonism by CNQX. Primary cultures of mature mCGCs (7 DIV) were pre-incubated with a fixed concentration of AP5 (500 μM) or CNQX (10 μM) for 15 min, before treatment with three different concentrations of Asp. The time-course of *c-fos* mRNA expression and 18S were measured by real-time RT-PCR. Expression values of *c-fos* were normalised to the internal control, 18S, prior to calculation of the fold induction of *c-fos* relative to the untreated, time matched controls (see Chapter 2).

When cultures of mCGCs were treated with partially toxic, concentrations of Asp (35 μM), a transient increase in *c-fos* mRNA expression was observed. As for Glu, the results reveal that pre-treatment with AP5 completely inhibited the toxic *c-fos* response. Pre-treatment with CNQX did not prevent the toxic *c-fos* response (see Figure 4.11). Toxic concentrations of Asp (100 μM) induced a delayed, but substantially elevated and sustained increase in *c-fos*. It was found that pre-treatment with AP5 changed the excitotoxic profile to that of an earlier peaking, less sustained expression, meaning that AP5 partly protected against the excitotoxic *c-fos* response. Again, CNQX did not change excitotoxic *c-fos* mRNA expression from that found with Glu alone (see Figure 4.12). With higher concentrations of Asp (350 μM), a sustained and elevated increase in *c-fos* mRNA expression was detected which was not inhibited by either AP5 or CNQX (Figure 4.13).

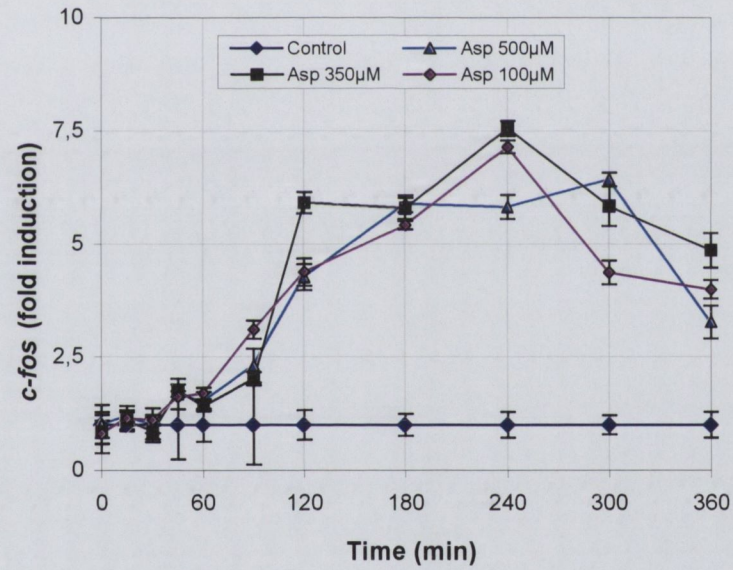
These results suggest that the effectiveness of AP5 in inhibiting the excitotoxic *c-fos* response is inversely proportional to the concentration of Asp. Thus, the results support our earlier view that higher concentrations of AP5 are required to fully compete with the very toxic concentrations of Asp (100 μM and 350 μM) used in these investigations. However, the results are consistent with Asp-induced *c-fos* mRNA expression being mediated through the NMDA receptor subtype.

4.2.6 Neither Ala nor paraquat induced *c-fos* expression in mature mCGCs

Ala, which served as a non-excitotoxic control amino acid, did not induce *c-fos* mRNA expression in mCGCs under conditions where Glu and Asp induced their effects (see Figure 4.14). Paraquat, a neurotoxic compound, which decouples mitochondria and induces oxidative stress but not excitotoxicity in mCGCs, did not induce *c-fos* mRNA expression (see Figure 4.15).



a)



b)

Figure 4.10: Asp induced *c-fos* mRNA expression is time- and concentration-dependent

Primary cultures of mCGCs (7 DIV) were exposed to various concentrations of Asp, for up to 360 min. Following treatment, the cells were lysed and total RNA was extracted and the amount of *c-fos* and 18S quantified by RT-PCR. *c-fos* expression values were normalised to 18S expression, which served as the internal control. The results above refer to the fold induction of *c-fos* expression compared to untreated, time-matched controls. Data represent mean ± s.d. values of triplicate RT-PCR reactions derived from one individual experiment. The experiments were reproduced at least three times. Figure 4.10 a) represents the *c-fos* changes with non-toxic and partially toxic concentrations of Asp while b) represents changes in *c-fos* expression with toxic concentrations.

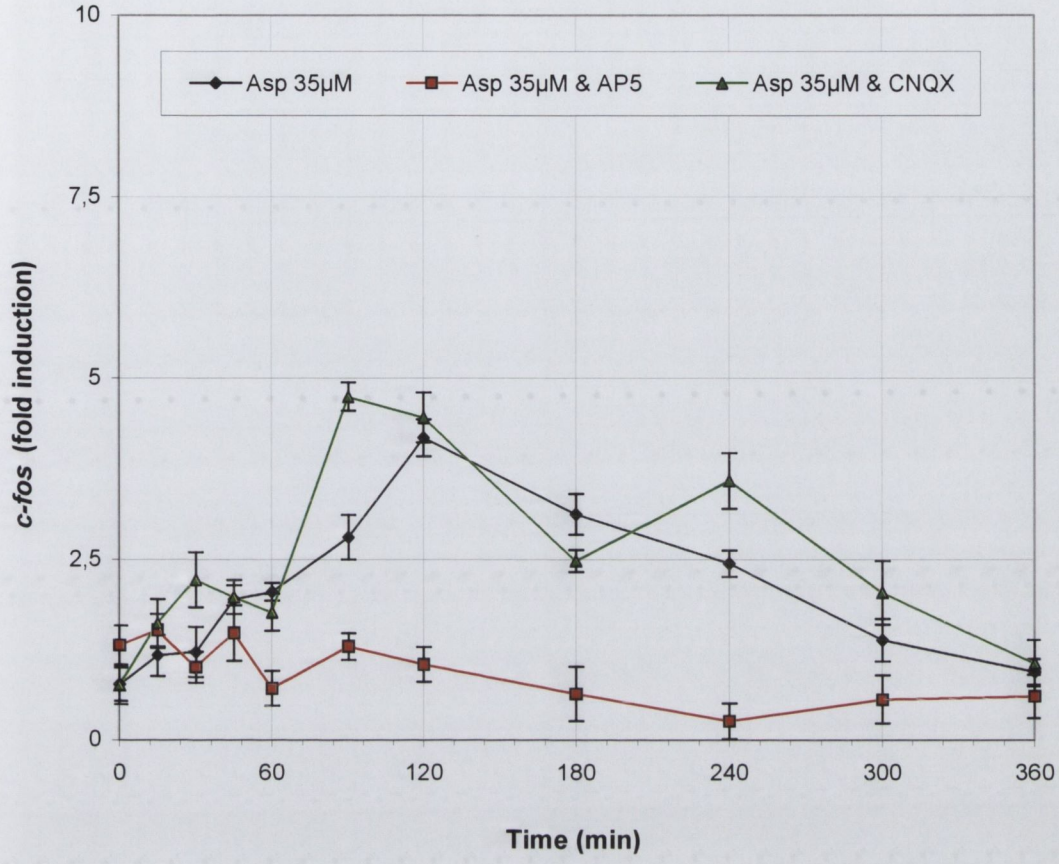


Figure 4.11: AP5 but not CNQX effectively abolishes *c-fos* mRNA expression at low Asp concentrations

Primary cultures of mCGCs (7 DIV) were pre-incubated for 15 min with either AP5 (500 µM) or CNQX (10 µM) prior to co-exposure with a fixed concentration of Asp (35 µM), for up to 360 min. Following treatment, the cells were lysed and total RNA was extracted and the amount of *c-fos* and 18S quantified by RT-PCR. The *c-fos* expression values were normalised to 18S expression, which served as the internal control. The results above refer to the fold induction of *c-fos* expression compared to untreated, time-matched controls. Data represent mean ± s.d. values of triplicate RT-PCR reactions derived from one individual experiment. The experiments were reproduced at least twice.

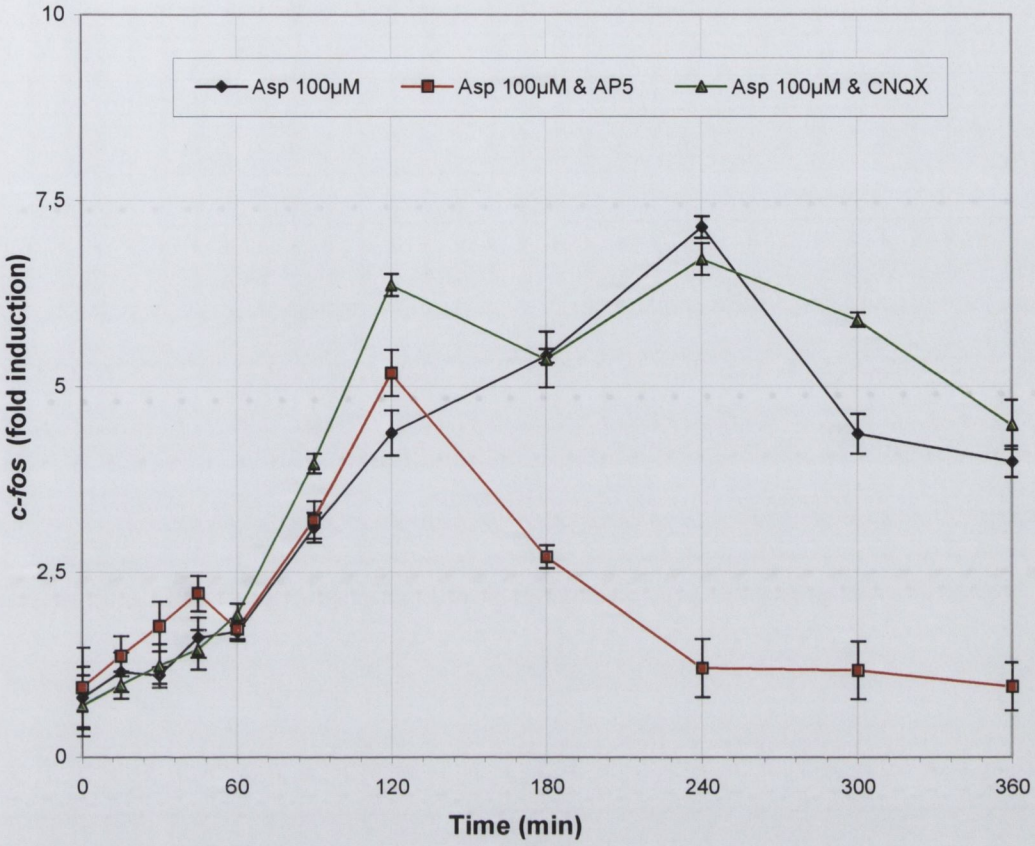


Figure 4.12: AP5 but not CNQX changes *c-fos* mRNA expression profile

Primary cultures of mCGCs (7 DIV) were pre-incubated for 15 min with either AP5 (500 µM) or CNQX (10 µM) prior to co-exposure with a fixed concentration of Asp (100 µM), for up to 360 min. Following treatment, the cells were lysed and total RNA was extracted and the amount of *c-fos* and 18S quantified by RT-PCR. The *c-fos* expression values were normalised to 18S expression, which served as the internal control. The results above refer to the fold induction of *c-fos* expression compared to untreated, time-matched controls. Data represent mean ± s.d. values of triplicate RT-PCR reactions derived from one individual experiment. The experiments were reproduced at least twice.

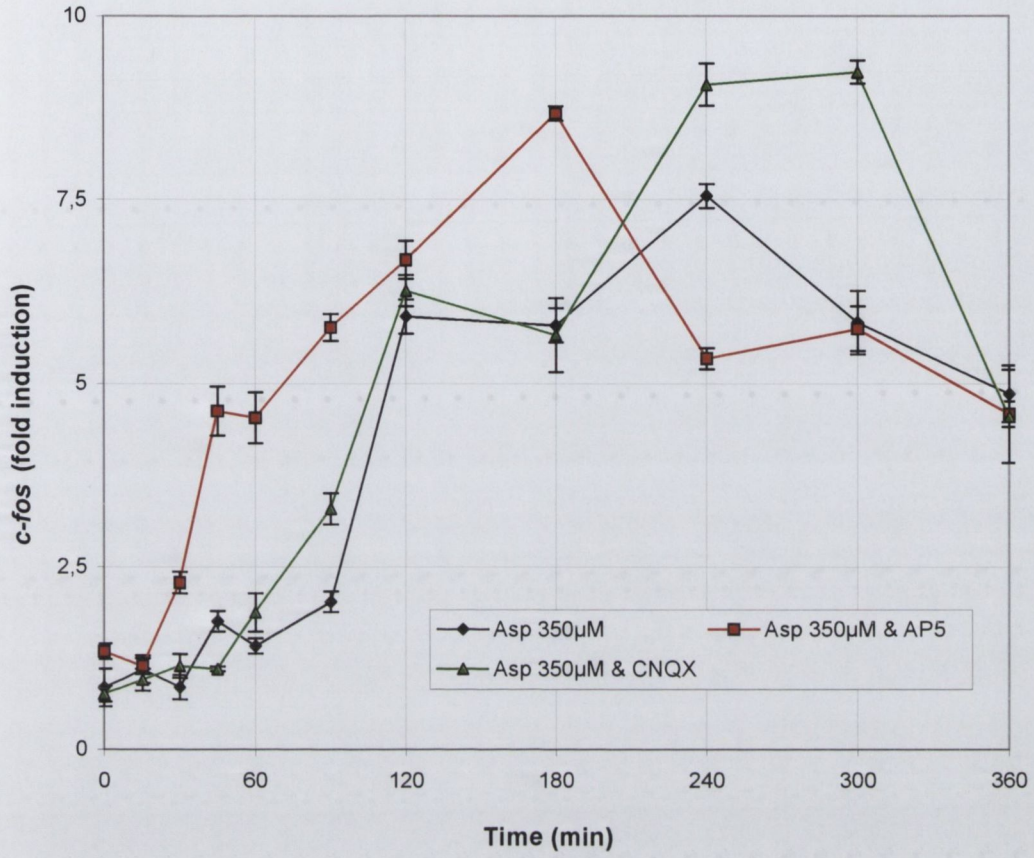
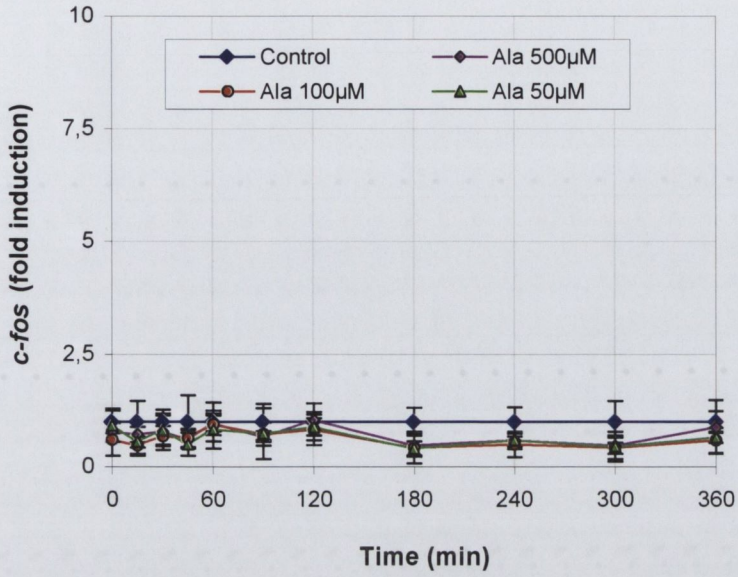
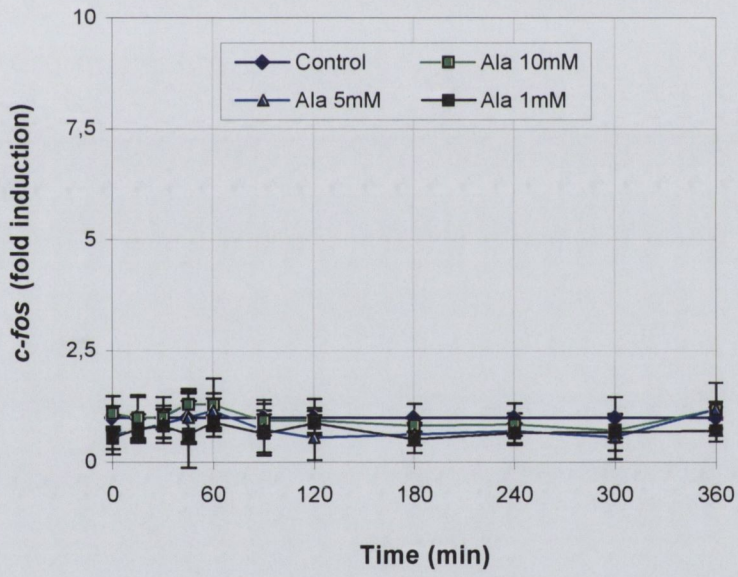


Figure 4.13: Neither AP5 nor CNQX change the *c-fos* expression profile induced by toxic concentrations of Asp

Primary cultures of mCGCs (7 DIV) were pre-incubated for 15 min with either AP5 (500 µM) or CNQX (10 µM) prior to co-exposure with a fixed concentration of Asp (350 µM), for up to 360 min. Following treatment, the cells were lysed and total RNA was extracted and the amount of *c-fos* and 18S quantified by RT-PCR. The *c-fos* expression values were normalised to 18S expression, which served as the internal control. The results above refer to the fold induction of *c-fos* expression compared to untreated, time-matched controls. Data represent mean ± s.d. values of triplicate RT-PCR reactions derived from one individual experiment. The experiments were reproduced at least twice.



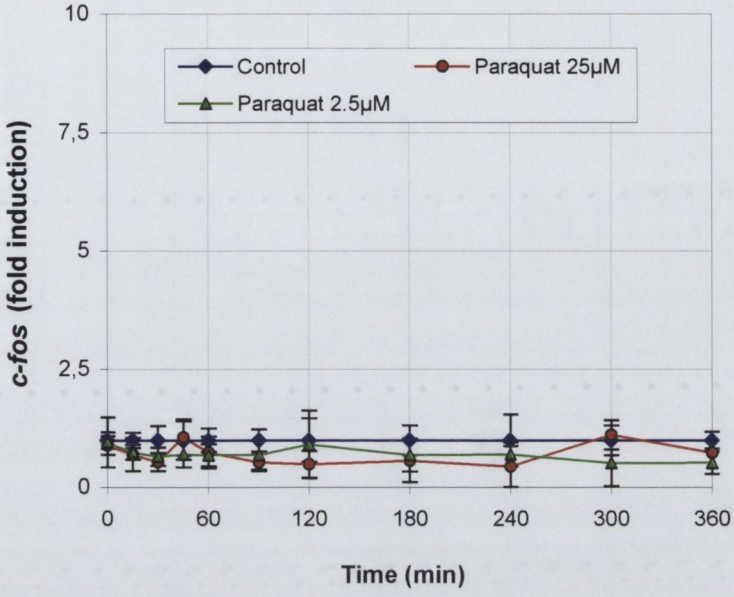
a)



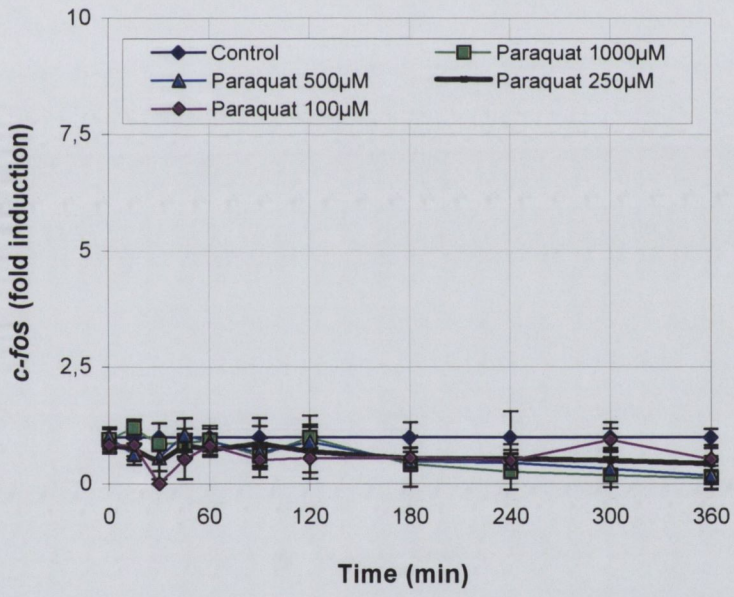
b)

Figure 4.14: No induction of c-*fos* mRNA expression in mCGCs treated with Ala

Primary cultures of mCGCs (7 DIV) were exposed to various concentrations of Ala, for up to 360 min. Following treatment, the cells were lysed and total RNA was extracted and the amount of *c-fos* and 18S quantified by RT-PCR. *c-fos* expression values were normalised to 18S expression, which served as the internal control. The results above refer to the fold induction of *c-fos* expression compared to untreated, time-matched controls. Data represent mean ± s.d. values of triplicate RT-PCR reactions derived from one individual experiment. The experiments were reproduced at least twice. Figure 4.14 a) represents the *c-fos* changes with low concentrations of Ala while b) represents changes in *c-fos* expression with high concentrations.



a)



b)

Figure 4.15: Paraquat does not induce c-*fos* mRNA expression in mCGCs

Primary cultures of mCGCs (7 DIV) were exposed to various concentrations of paraquat, for up to 360 min. Following treatment, total RNA was extracted and the amount of *c-fos* and 18S quantified by RT-PCR. *c-fos* expression values were normalised to 18S expression, which served as the internal control. The results above refer to the fold induction of *c-fos* expression compared to untreated, time-matched controls. Data represent mean ± s.d. values of triplicate RT-PCR reactions derived from one individual experiment. The experiments were reproduced at least twice. Figure 4.15 a) represents the *c-fos* changes with partially toxic concentrations of paraquat while b) represents changes in *c-fos* expression with toxic concentrations.

4.2.7 Can "toxicity-related" *c-fos* mRNA expression be used to predict excitotoxic properties of compounds?

An EU Biotech Demonstration project (Contract No. BIO4-CT98-0223), was set up to explore the potential of using a real-time RT-PCR based *in vitro* test for excitotoxicity, based on early response gene measurement, instead of the previously used Northern blot and dot-blot assays. This new method, if successful, would increase the throughput of the assays and reduce the scale, leading to a reduction in animal usage. The assay first involved the determination of "low" and "high" concentrations of compounds; low being a non-toxic concentration and high being a toxic concentration, or in the case of non-toxic compounds the highest concentration possible or relevant. These concentrations were determined from MTT-based cytotoxicity experiments, over a range of concentrations of the compound, which were performed by Griffiths and colleagues at the University of St. Andrews, Scotland. After EC_{50} values were determined, low and high concentrations were calculated with low being equivalent to one-tenth the EC_{50} value and high being equivalent to 10 times the EC_{50} value; where the EC_{50} value was the concentration found to give 50% reduction in cell viability on MTT assays. For non-toxic compounds, the low concentration was chosen as 1/100 the highest possible concentration.

Primary cultures of mCGCs (7 DIV) were exposed to low and high concentrations of various compounds and cells were lysed following 30 min or 240 min exposures; these time-points being judged optimal from previous experiments. Exposures were also performed in the absence and/or presence of the Glu receptor antagonists, AP5 and CNQX. The cell extracts following 30 and 240 min exposures were transferred to our laboratory (Bayer AG, Gemany), where total RNA was extracted and the *c-fos* and 18S mRNA levels measured by the method of real-time RT-PCR. *c-fos* expression values were normalised to the internal control, 18S, prior to calculation of the fold induction of *c-fos* relative to the untreated, time matched controls (see Chapter 2). The numerous compounds selected for the assay were representative of 4 relevant groups, namely, excitotoxins (Group 1), neurotoxic but non-excitotoxic compounds (Group 2), neuroactive but non-toxic compounds (Group 3) and compounds that were toxic to other target organelles (Group 4).

c-fos mRNA levels were used as a predictive index, based on the observation that delayed, elevated and progressively sustained *c-fos* mRNA expression is associated with

excitotoxicity, and a ratio measurement of *c-fos* mRNA expression at 240/30 min following toxic insult in mCGCs correlates with excitotoxicity.

Malcolm *et al.* (1997) and Griffiths *et al.* (1997; 2000) showed that comparison of *c-fos* mRNA expression at early and late time-points (30 and 240 min) for low and high concentrations of excitatory and non-excitatory compounds were best made using a ratio of expression levels, viz

$$Q^{240/30} = \frac{cfos\ mRNA\ {}^{240\,min}_{250\,\mu M}}{cfos\ mRNA\ {}^{30\,min}_{250\,\mu M}} \times \frac{cfos\ mRNA\ {}^{30\,min}_{2.5\,\mu M}}{cfos\ mRNA\ {}^{240\,min}_{2.5\,\mu M}}$$

The ratio method involves three criteria, namely, that the *c-fos* 240/30 min ratio must be greater than 1 to correlate with delayed, elevated and sustained *c-fos* mRNA expression and therefore excitotoxicity, while ratios must be less than 1 to correlate with a transient expression and therefore a non-excitotoxic outcome. Lastly, for a positive correlation with excitotoxicity, abrogation of the response must be observed in the presence of NMDA receptor antagonists.

4.2.8 Screening experiment using the original protocol

The *c-fos* mRNA levels found following the exposure of the mCGCs to the various compounds are shown in Tables 4.1 a), b) and c). The ratio method (see Section 4.2.7) was used to determine the excitotoxic properties of the various compounds by examining the *c-fos* mRNA expression levels according to the three criteria outlined above.

The first group, the "excitotoxins", consisted of Glu, Asp and L-cysteine sulphinate (L-CSA). For the three known excitotoxins, *c-fos* mRNA levels changed to that of a more sustained expression. In the case of Glu and Asp, the higher, toxic concentrations induced a change from a rapid, transient expression to a more sustained and slightly elevated expression of *c-fos* mRNA. However, the receptor pharmacology as defined by AP5 inhibition was uncertain. This was probably due to the lack of competition between AP5 and the toxic concentrations of Glu (250 μM) and Asp (350 μM) as we subsequently found (Figures 4.9 and 4.13). CNQX did not inhibit the excitotoxic *c-fos* response induced by Glu or Asp. In the case of L-CSA, a relatively low level of sustained *c-fos* mRNA expression was observed, which was also not blocked by AP5. However, the smaller changes in mRNA levels prevent firm conclusions from being made (Table 4.1 a)).

The second group, the "neurotoxic but non-excitotoxic" compounds, were comprised of lindane, veratridine* (antagonist of voltage-gated Ca^{2+} channels), 1-methyl-4-phenylpyridinium Iodide (MPP^+ iodide) and acrylamide (Table 4.1 a)). Low and high concentrations of lindane (Lin) induced transient increases in *c-fos* mRNA expression at 30 min, which had returned to below basal levels by 240 min. Ratios were below 1 for high concentrations in the presence of either AP5 or CNQX. Toxic concentrations of veratridine (Verat) changed the *c-fos* mRNA profile to that of a sustained one, giving *c-fos* ratios above 1. The sustained *c-fos* response induced by veratridine, which neither AP5 nor CNQX antagonised, can be expected for a membrane depolarising agent. MPP^+ iodide and acrylamide (Acryl) gave small changes in *c-fos* mRNA expression, suggestive of changes to sustained levels with antagonism by AP5. However, the relatively small changes again confuse the interpretation.

The third group of "neuroactive but non-toxic" compounds, contained taurine (Tau), Ala, nimodipine (Nimodip), GABA, pentylenetetrazole (PTZ), valproate (Vpate) and PK 11195 (Table 4.1 b)). All of these compounds gave *c-fos* mRNA 240/30 min ratios below 1 for both the low and high concentrations. Ratios were also below 1 for high concentrations in the presence of either AP5 or CNQX. Therefore, the ratio approach correctly predicted these compounds as being non-excitotoxic.

The fourth group contained "compounds that are toxic to other target organelles", namely, sodium cyanide (NaCN), paraquat* (toxic by a general mechanism, for example, inhibition of the respiratory chain and induction of oxidative stress) and thalidomide (Table 4.1 c)). Low concentrations of all 3 exhibited *c-fos* ratios below 1. NaCN and thalidomide also gave ratios below 1 at high concentrations. Although, high concentrations of paraquat gave a *c-fos* ratio above 1, this ratio was not considered as excitotoxic, as it was shown in Section 4.2.6 that paraquat has no effect on *c-fos* induction with time or concentration. Ratios were below 1 for high concentrations of all 3 compounds in the presence of either AP5 or CNQX.

On the whole, the results show that sustained *c-fos* mRNA expression correlated well with excitotoxic properties, although optimisation of compound and antagonist concentrations is required. In addition, the ratio approach correctly predicted the Group 2, 3 and 4 compounds as being non-excitotoxic.

Group 1	30 min *c-fos* fold induction	240 min *c-fos* fold induction	$Q^{240/30}$	$Q^{240/30}$ Conclusion	Correct Conclusion
Glu Low (2.5 µM)	3,14	0,96	0,31	Non-Excitotoxic	Yes
Glu High (250µM)	3,84	4,45	1,16	Excitotoxic	Yes
Glu High & AP5	4,71	3,40	0,72	Non-Excitotoxic	Yes
Glu High & CNQX	3,24	4,65	1,43	Excitotoxic	Yes
Asp Low (3.5 µM)	2,71	0,86	0,32	Non-Excitotoxic	Yes
Asp High (350µM)	3,35	4,57	1,36	Excitotoxic	Yes
Asp High & AP5	2,91	5,32	1,82	Excitotoxic	No
Asp High& CNQX	3,51	5,66	1,61	Excitotoxic	Yes
L-CSA Low (2 µM)	1,22	0,29	0,24	Non-Excitotoxic	Yes
L-CSA High (200µM)	1,17	1,30	1,11	Excitotoxic	Yes
L-CSA High & AP5	0,97	1,40	1,45	Excitotoxic	No
L-CSA High& CNQX	1,06	1,89	1,78	Excitotoxic	Yes
Group 2	**30 min *c-fos* fold induction**	**240 min *c-fos* fold induction**	**$Q^{240/30}$**	**$Q^{240/30}$ Conclusion**	**Correct Conclusion**
Lin Low (1 µM)	3,15	0,84	0,27	Non-Excitotoxic	Yes
Lin High (100 µM)	1,53	0,30	0,20	Non-Excitotoxic	Yes
Lin High & AP5	0,80	0,22	0,28	Non-Excitotoxic	Yes
Lin High & CNQX	1,40	0,29	0,21	Non-Excitotoxic	Yes
Verat (0,7 µM)	2,41	1,66	0,70	Non-Excitotoxic	Yes
Verat (70 µM)	3,75	4,73	1,26	Excitotoxic	No
Verat High & AP5	3,56	7,27	2,38	Excitotoxic	No
Verat High & CNQX	4,45	5,23	1,18	Excitotoxic	No
MPP^+ iodide(4 µM)	1,86	0,86	0,46	Non-Excitotoxic	Yes
MPP^+ iodide (400 µM)	1,94	1,55	0,80	Non-Excitotoxic	Yes
MPP^+ iodide High & AP5	1,77	0,51	0,29	Non-Excitotoxic	Yes
MPP^+ iodide High & CNQX	1,66	2,49	1,50	Excitotoxic	No
Acryl (100 µM)	2,08	1,96	0,94	Non-Excitotoxic	Yes
Acryl (10,000µM)	1,30	1,51	1,16	Excitotoxic	No
Acryl High & AP5	1,51	0,87	0,59	Non-Excitotoxic	Yes
Acryl High & CNQX	1,44	2,19	1,52	Excitotoxic	No

Table 4.1 a): Group 1 and 2 compounds were tested for excitotoxic properties

Group 3	30 min *c-fos* fold induction	240 min *c-fos* fold induction	$Q^{240/30}$	$Q^{240/30}$ Conclusion	Correct Conclusion
Tau Low (100µM)	2,75	0,70	0,25	Non-Excitotoxic	Yes
Tau High (10mM)	2,60	0,27	0,10	Non-Excitotoxic	Yes
Tau High & AP5	1,75	0,09	0,05	Non-Excitotoxic	Yes
Tau High & CNQX	3,46	0,28	0,08	Non-Excitotoxic	Yes
Ala Low (100µM)	3,30	0,73	0,22	Non-Excitotoxic	Yes
Ala High (10mM)	3,16	1,23	0,39	Non-Excitotoxic	Yes
Ala High & AP5	2,68	0,28	0,10	Non-Excitotoxic	Yes
Ala High & CNQX	3,27	1,01	0,31	Non-Excitotoxic	Yes
Nimodipine (1µM)	3,03	0,03	0,01	Non-Excitotoxic	Yes
Nimodipine (100µM)	1,73	0,05	0,03	Non-Excitotoxic	Yes
Nimodip High & AP5	1,44	0,04	0,03	Non-Excitotoxic	Yes
Nimodip High & CNQX	2,07	0,03	0,01	Non-Excitotoxic	Yes
GABA Low (100µM)	2,34	0,65	0,28	Non-Excitotoxic	Yes
GABA High (10mM)	2,33	0,44	0,19	Non-Excitotoxic	Yes
GABA High & AP5	1,88	0,25	0,13	Non-Excitotoxic	Yes
GABA High & CNQX	2,17	0,44	0,20	Non-Excitotoxic	Yes
PTZ Low (10µM)	0,97	0,44	0,45	Non-Excitotoxic	Yes
PTZ High (10mM)	0,88	0,32	0,37	Non-Excitotoxic	Yes
PTZ High & AP5	0,81	0,22	0,27	Non-Excitotoxic	Yes
PTZ High & CNQX	0,90	0,31	0,34	Non-Excitotoxic	Yes
Valproate (100µM)	7,58	1,09	0,14	Non-Excitotoxic	Yes
Valproate (10mM)	6,23	0,13	0,02	Non-Excitotoxic	Yes
Vpate High & AP5	4,07	0,11	0,03	Non-Excitotoxic	Yes
Vpate High & CNQX	7,09	0,21	0,03	Non-Excitotoxic	Yes
PK III 95 Low (1 µM)	1,81	1,24	0,68	Non-Excitotoxic	Yes
PK III 95 (100 µM)	1,06	0,27	0,26	Non-Excitotoxic	Yes
PK III 95 High & AP5	2,65	0,71	0,27	Non-Excitotoxic	Yes
PK III 95 High &CNQX	4,79	1,70	0,35	Non-Excitotoxic	Yes

Table 4.1 b): Group 3 (neuroactive but non-toxic compounds) compounds were tested for excitotoxicity with the *c-fos* mRNA ratio method ($Q^{240/30}$)

Group 4	30 min *c-fos* fold induction	240 min *c-fos* fold induction	$Q^{240/30}$	$Q^{240/30}$ Conclusion	Correct Conclusion
NaCN Low (30μM)	1,63	0,89	0,55	Non-Excitotoxic	Yes
NaCN High (3000μM)	1,49	0,66	0,44	Non-Excitotoxic	Yes
NaCN High & AP5	1,36	1,72	1,27	Excitotoxic	No
NaCN High & CNQX	1,92	0,94	0,49	Non-Excitotoxic	Yes
Paraquat (100μM)	1,45	1,25	0,86	Non-Excitotoxic	Yes
Paraquat (10mM)	0,73	1,09	1,49	Excitotoxic	No
Paraquat High & AP5	0,69	0,67	0,97	Non-Excitotoxic	Yes
Paraquat High & CNQX	1,59	0,72	0,45	Non-Excitotoxic	Yes
Thalidomide (1μM)	4,97	0,96	0,19	Non-Excitotoxic	Yes
Thalidomide (100μM)	6,13	1,74	0,28	Non-Excitotoxic	Yes
Thalidomide High & AP5	4,53	0,97	0,21	Non-Excitotoxic	Yes
Thalidomide High & CNQX	3,89	1,62	0,42	Non-Excitotoxic	Yes

Table 4.1 c): Group 4 (toxic to other target organelles) compounds were tested for excitotoxicity with the *c-fos* mRNA ratio method ($Q^{240/30}$)

Mature mCGCs were exposed by Griffiths and colleagues in the University of St. Andrews, Scotland, to low or high concentrations of 4 groups of compounds, defined by previous cell viability (MTT) experiments (see Section 4.2.7), for 30 min or 240 min. The neurons were pre-incubated for 15 min with either AP5 (500 μM) or CNQX (10 μM) prior to exposure to the high concentration of the compound. The *c-fos* mRNA ratio test ($Q^{240/30}$) was used to investigate whether *c-fos* could be used as a predictor of excitotoxicity (see Section 4.2.7). The hypothesis behind the test was that a ratio of less than 1 correlates with a non-excitotoxic outcome whereas a ratio greater than 1 correlates with an excitotoxic event. Moreover, a further criteria for acceptance is that the excitotoxin-induced elevation of the *c-fos* mRNA ratio should be prevented in the presence of an NMDA receptor antagonist. The results represent the average of triplicate cell culture wells of one experiment.

4.2.9 Screening experiment using a modified antagonist protocol in the *c-fos* assay ($Q^{240/30}$) test

It was decided following consideration of the results from the previous experiments and indeed several others, which are not shown in this thesis, to modify the original assay protocol in two ways. An increased number of excitotoxins would be included and a cocktail of an NMDA receptor antagonist (TCP) and a non-NMDA receptor antagonist (NBQX) would be used, in order to accommodate the increased throughput of the compounds.

Primary mCGCs were exposed to 19 compounds, of which 14 were excitotoxins, in the presence and absence of an antagonist cocktail, containing NBQX (100 μM) and TCP (1 μM). The antagonist cocktail was designed to give a complete block of NMDA and non-NMDA (AMPA) Glu receptor subtypes. Again, Griffiths and colleagues at the University of St. Andrews, Scotland, were responsible for the production of mCGCs and for the exposure of these cells to "high" and "low" concentrations of the various compounds for either 30 or 240 min, in the presence and absence of the antagonist cocktail. The extracts were transferred to our laboratory (Bayer AG, Germany), where real-time RT-PCR analysis of *c-fos* and 18S mRNA expression performed. *c-fos* expression values were normalised to the internal control, 18S, prior to calculation of the fold induction of *c-fos* relative to the untreated, time matched controls (see Chapter 2). The 19 compounds were representative of the same 4 classes of compounds measured earlier. The *c-fos* ratio method ($Q^{240/30}$; see Section 4.2.7) was used to predict an excitotoxic outcome, that is, a $Q^{240/30} > 1$ correlated with excitotoxicity whereas a $Q^{240/30} < 1$ correlated with a non-excitotoxic outcome, and for a positive excitotoxic response, abrogation of the elevated *c-fos* mRNA should be observed in the presence of an NMDA receptor antagonist cocktail.

The Group 1 "excitotoxins" comprised the following, Glu, Asp, L-homocysteic acid (L-HCA), D-homocysteic acid (D-HCA), kainic acid (KA), (RS)-(tetrazol-5-yl)-glycine (TG), (*S*)-CPW 399, L-CSA, zinc chloride ($ZnCl_2$), L-homocysteine sulphinate (L-HCSA), *S*-sulpho-L-cysteine (L-SSC), quisqualic acid (QA), NMDA and D-homocysteine sulphinate (D-HCSA). All 14 of the known or potential excitotoxins showed elevated and sustained *c-fos* mRNA expression with high, toxic concentrations. Apart from TG, QA, D-HCSA and L-HCSA, which showed elevated *c-fos* ratios at both low and high concentrations, all of the remaining excitotoxins gave a *c-fos* ratio which albeit above 1 for the non-toxic parameter, was less than the ratios observed with the high, toxic concentrations. High concentrations were associated with *c-fos* ratios considerably greater than 1. Antagonism was observed

for 6 of the 11 excitotoxins. Low concentrations of TG, QA and D-HCSA induced elevated *c-fos* expression at the 30 min and 240 min time-points, giving *c-fos* ratios above 1 for the non-toxic parameter. In addition, high concentrations of all 3 compounds gave *c-fos* ratios above 1, which were inhibited in the presence of the NBQX/TCP antagonist cocktail. A possible explanation for these high ratios may be that the low concentration of each of the 3 compounds was in fact toxic, due to the very potent nature of the compounds. With low concentrations of KA, a transient expression of *c-fos* was induced which changed with high concentrations to a more elevated and sustained induction at 240 min. No antagonism of the excitotoxic *c-fos* response was observed in the presence of the NBQX/TCP antagonist cocktail, which may be expected as TCP is an NMDA receptor antagonist and NBQX is an AMPA receptor antagonist. In the case of (*S*)-CPW 399, an AMPA agonist and therefore a putative excitotoxin, receptor antagonism, although expected, was not found and this result is as yet unexplained. However, the compound did produce elevated and sustained *c-fos* mRNA induction and therefore would have been predicted as an excitotoxin in the screen (Table 4.2 a)).

The second group contained the "non-excitotoxic" compound veratridine (antagonist of voltage gated Ca^{2+} channels). High concentrations of veratridine induced elevated and sustained *c-fos* mRNA expression, which was not blocked by the antagonist cocktail. Thus, this compound was correctly screened as non-excitotoxic (Table 4.2 b)). The third group comprised the "neuroactive but non-toxic" compounds, (-)-bicuculline and L-AP4 (Table 4.2 b)). Low concentrations of (-)-bicuculline gave a *c-fos* mRNA ratio below 1. Toxic concentrations were associated with *c-fos* ratios above 1, which failed to be blocked by the NBQX/TCP antagonist cocktail indicating, at face value, a non-excitotoxic compound. However, the expression levels of this compound are very low and are probably responsible for producing this artefactual ratio. L-AP4 appeared to act as an excitotoxin in this screen showing elevated *c-fos* mRNA expression with high concentrations at 240 min, which were inhibited by the antagonist cocktail. The explanation for this result is as yet unknown. The fourth group consisted of paracetamol and rotenone, both of which did not increase *c-fos* expression from a low concentration to a high concentration and which were screened as non-excitotoxic. Overall, the results show that elevated and sustained *c-fos* mRNA expression correlated well with excitotoxic properties, although conditions such as concentrations of compounds and antagonists may not be optimal. In addition, the modified protocol, including use of the antagonist cocktail showed a marked improvement in excitotoxic prediction over the original protocol.

Group 1	30 min *c-fos* fold induction	240 min *c-fos* fold induction	$Q^{240/30}$	$Q^{240/30}$ Conclusion	Correct Conclusion
Glu Low (2.5µM)	2,13	0,99	0,46	Non-Excitotoxic	Yes
Glu High (250µM)	1,65	4,01	2,42	Excitotoxic	Yes
Glu High & NBQX/TCP	4,84	2,22	0,46	Non-Excitotoxic	Yes
Asp Low (3.5µM)	1,17	1,00	0,86	Non-Excitotoxic	Yes
Asp High (350µM)	1,66	2,90	1,74	Excitotoxic	Yes
Asp High & NBQX/TCP	1,24	0,35	0,29	Non-Excitotoxic	Yes
L-HCA Low (3µM)	0,89	0,92	1,03	Excitotoxic	No
L-HCA High (300µM)	1,53	3,46	2,27	Excitotoxic	Yes
L-HCA High & NBQX/TCP	1,52	1,30	0,83	Non-Excitotoxic	Yes
D-HCA Low (15µM)	1,17	0,88	0,75	Non-Excitotoxic	Yes
D-HCA High (1500µM)	2,85	5,50	1,93	Excitotoxic	Yes
D-HCA High & NBQX/TCP	1,92	1,30	0,68	Non-Excitotoxic	Yes
KA Low (20µM)	2,35	2,97	1,27	Excitotoxic	No
KA High (2000µM)	1,70	7,42	4,37	Excitotoxic	Yes
KA High & NBQX/TCP	1,68	10,43	6,21	Excitotoxic	No
TG Low (0,2µM)	4,72	16,21	3,43	Excitotoxic	No
TG High (20µM)	2,88	8,12	2,82	Excitotoxic	Yes
TG High & NBQX/TCP	4,80	4,98	1,04	Excitotoxic	No
(*S*)-CPW 399 Low (4µM)	0,91	1,49	1,63	Excitotoxic	No
(*S*)-CPW 399 High (400µM)	0,96	6,13	6,40	Excitotoxic	Yes
(*S*)-CPW 399 High & NBQX/TCP	0,83	7,11	8,54	Excitotoxic	No
L-CSA Low (2µM)	0,59	0,86	1,45	Excitotoxic	No
L-CSA High (200µM)	1,12	4,11	3,66	Excitotoxic	Yes
L-CSA High & NBQX/TCP	1,68	2,61	1,55	Excitotoxic	No
$ZnCl_2$ Low (2.5µM)	0,67	0,47	0,70	Non-Excitotoxic	Yes
$ZnCl_2$ High (250µM)	0,70	2,32	3,33	Excitotoxic	Yes
$ZnCl_2$ High & NBQX/TCP	0,49	2,43	4,97	Excitotoxic	No
L-HCSA Low (30µM)	2,99	3,82	1,28	Excitotoxic	No
L-HCSA High (3000µM)	1,77	5,86	3,32	Excitotoxic	Yes
L-HCSA High & NBQX/TCP	3,36	4,93	1,47	Excitotoxic	No
L-SSC Low (1µM)	1,46	1,88	1,28	Excitotoxic	No
L-SSC High (100µM)	3,18	10,11	3,18	Excitotoxic	Yes
L-SSC High & NBQX/TCP	3,73	5,14	1,38	Excitotoxic	No
QA Low (30µM)	7,56	11,89	1,57	Excitotoxic	No
QA High (3000µM)	5,34	15,98	2,99	Excitotoxic	Yes
QA High & NBQX/TCP	12,59	8,99	0,71	Non-Excitotoxic	Yes
NMDA Low (3µM)	2,25	2,40	1,07	Excitotoxic	No
NMDA High (300µM)	6,56	15,06	2,29	Excitotoxic	Yes
NMDA High & NBQX/TCP	4,39	6,16	1,40	Excitotoxic	No
D-HCSA Low (2µM)	4,60	16,48	3,58	Excitotoxic	No
D-HCSA High (200µM)	3,03	12,54	4,14	Excitotoxic	Yes
D-HCSA High & NBQX/TCP	4,83	6,99	1,45	Excitotoxic	No

Table 4.2 a): Group 1 excitotoxins were tested for with the *c-fos* mRNA ratio method

Group 2	30 min *c-fos* fold induction	240 min *c-fos* fold induction	$Q^{240/30}$	$Q^{240/30}$ Conclusion	Correct Conclusion
Veratridine Low (0.7µM)	2,11	3,33	1,58	Excitotoxic	No
Veratridine High (70µM)	1,99	5,58	2,80	Excitotoxic	No
Veratridine High & NBQX/TCP	2,70	14,65	5,42	Excitotoxic	No
Group 3	**30 min *c-fos* fold induction**	**240 min *c-fos* fold induction**	**$Q^{240/30}$**	**$Q^{240/30}$ Conclusion**	**Correct Conclusion**
(-)-Bicuculline Low (10µM)	0,74	0,70	0,94	Non-Excitotoxic	Yes
(-)-Bicuculline High (1000µM)	0,11	0,25	2,41	Excitotoxic	No
(-)-Bicuc. High & NBQX/TCP	0,13	0,27	2,07	Excitotoxic	No
L-AP4 (100µM)	1,50	0,83	0,55	Non-Excitotoxic	Yes
L-AP4 (10mM)	1,59	3,29	2,07	Excitotoxic	No
L-AP4 High & NBQX/TCP	1,37	0,72	0,53	Non-Excitotoxic	Yes
Group 4	**30 min *c-fos* fold induction**	**240 min *c-fos* fold induction**	**$Q^{240/30}$**	**$Q^{240/30}$ Conclusion**	**Correct Conclusion**
Paracetamol Low (10µM)	0,76	0,66	0,87	Non-Excitotoxic	Yes
Paracetamol High (1000µM)	0,35	0,35	1,01	Excitotoxic	No
Paracet. High & NBQX/TCP	0,20	0,21	1,04	Excitotoxic	No
Rotenone (100µM)	1,85	1,74	0,94	Non-Excitotoxic	Yes
Rotenone (10mM)	1,54	1,83	1,19	Excitotoxic	No
Rotenone High & NBQX/TCP	1,12	1,44	1,29	Excitotoxic	No

Table 4.2 b): Compounds of Group 2, 3 and 4 were tested with the *c-fos* mRNA ratio method ($Q^{240/30}$)

Primary mCGCs were exposed, in St. Andrews, to low or high concentrations of 4 groups of compounds for either 30 min or 240 min (see Section 4.2.7). The cells were pre-incubated for 15 min with a cocktail containing NBQX (100 µM) and TCP (1 µM) prior to exposure to the high concentration of the compounds. The *c-fos* mRNA ratio test ($Q^{240/30}$) was used to investigate whether *c-fos* could be used as a predictor of excitotoxicity. The results represent the average of triplicate experiments and refer to *c-fos* expression levels.

4.2.10 Single laboratory experiments using the original protocol !

Having analysed the results of the original collaborative screening experiments, we then turned to analysis of the *c-fos* expression results obtained when cell culture, exposure to compounds and RT-PCR measurements were performed in a single laboratory. Data from the experiments described in Figures 4.6 to 4.14 were analysed using the 240/30 min *c-fos* ratio method and the results are shown in Table 4.3.

In the work described herein, the *c-fos* 240/30 min ratio method was applied to the *c-fos* inductions (as measured by RT-PCR) following exposure of the mCGCs, established in our laboratory, to either low or high concentrations of Glu or Asp (see Figures 4.6 and 4.10, respectively) in the presence and absence of AP5 (500 μM) or CNQX (10 μM) (see Figures 4.7 to 4.13). The ratio method was also applied to the non-excitotoxic compound, Ala (see Figure 4.14).

The results show that non-toxic concentrations of Glu, Asp and Ala exhibited *c-fos* 240/30 min ratios of 1 – 1.5, suggestive of non-excitotoxicity. Toxic concentrations, however, gave rise to *c-fos* 240/30 min ratios of 6 – 14, suggestive of excitotoxicity. High and low concentrations of Ala gave *c-fos* ratios less than 1, correctly predictive of a non-excitotoxic outcome.

With toxic concentrations of both Glu and Asp (100 μM), pre-treatment with AP5 gave *c-fos* 240/30 min ratios under 1 indicating substantial abolition of the excitotoxic *c-fos* response. Although pre-treatment with AP5 did not completely block the excitotoxic *c-fos* response induced by higher toxic concentrations of both Glu and Asp (250 μM and 350 μM, respectively), the ratios were somewhat reduced when compared to the ratios with the high concentrations alone, indicative of partial antagonism by AP5. Gorman *et al.* (1995) reported that following exposure of mCGCs to high concentrations of Glu (250 μM), the sustained *c-fos* mRNA levels were only partially reduced by 500 μM AP5, a finding that supports the partial antagonism observed in these experiments.

With all toxic concentrations, pre-treatment with CNQX failed to protect the neurons against the excitotoxic *c-fos* response, with ratios greater than 1.

These "single laboratory" results confirm the need to use a more appropriate lower concentration ratio of agonist to antagonist for the receptor pharmacology criterion in the test. The higher expression levels of *c-fos* in these latter experiments also aids in the interpretation of the 240/30 min ratio method.

Compound	30 min *c-fos* fold induction	240 min *c-fos* fold induction	$Q^{240/30}$	$Q^{240/30}$ Conclusion	Correct Conclusion
Glu Low (2.5 µM)	0,93	1,31	1,40	Non-Excitotoxic	Yes
Glu High (100µM)	1,11	6,93	6,23	Excitotoxic	Yes
Glu High & AP5	2,32	1,69	0,73	Non-Excitotoxic	Yes
Glu High & CNQX	1,10	6,92	6,26	Excitotoxic	Yes
Glu Low (2.5 µM)	0,93	1,31	1,40	Non-Excitotoxic	Yes
Glu High (250µM)	0,74	11,11	14,93	Excitotoxic	Yes
Glu High & AP5	1,42	14,59	10,29	Excitotoxic	No
Glu High & CNQX	0,66	6,29	9,58	Excitotoxic	Yes
Asp Low (3.5 µM)	1,37	0,73	0,53	Non-Excitotoxic	Yes
Asp High (100µM)	1,10	7,14	6,47	Excitotoxic	Yes
Asp High & AP5	1,77	1,21	0,68	Non-Excitotoxic	Yes
Asp High& CNQX	1,23	6,71	5,43	Excitotoxic	Yes
Asp Low (3.5 µM)	1,37	0,73	0,53	Non-Excitotoxic	Yes
Asp High (350µM)	0,86	7,55	8,82	Excitotoxic	Yes
Asp High& AP5	2,29	5,34	2,33	Excitotoxic	No
Asp High & CNQX	1,15	9,06	7,91	Excitotoxic	Yes
Ala Low (100 µM)	0,8	0,7	0,8	Non-Excitotoxic	Yes
Ala High (10 mM)	1,0	0,9	0,8	Non-Excitotoxic	Yes

Table 4.3: The *c-fos* $Q^{240/30}$ method tested in our mCGC cultures as a predictive index for excitotoxicity

Primary cultures of mCGCs were exposed to Glu, Asp and Ala for either 30 or 240 min at low, non-toxic concentrations; or at high, toxic concentrations, defined by previous cell viability (MTT) experiments (see Chapter 3, Figures 3.6, 3.7 and 3.9). The cells were pre-incubated for 15 min with either AP5 (500 µM) or CNQX (10 µM) prior to co-exposure with a high concentration of the test compound. The results represent the average of triplicate experiments and refer to *c-fos* induction values relative to the time-matched control (after normalisation to the internal control, 18S).

4.2.11 *fosB* expression profiles vary with time and Glu concentration

Lidwell *et al.* (2000) reported that the product of *fosB*, and not *c-fos*, was selectively expressed under excitotoxic conditions. Furthermore, Greenberg *et al.* (1998) reported that FosB and ΔFosB, rather than other Fos family member proteins, are up-regulated following excessive glutamatergic transmission during motor seizures. However, the *fosB* gene has been studied relatively little in *in vitro* neuronal preparations. It was of interest therefore, to investigate whether an association existed between NMDA receptor mediated excitotoxicity and the expression of *fosB*.

Primary mCGCs were prepared from post-natal mice as described in Meier and Schousboe (1982), Drejer *et al.* (1983) and Schousboe *et al.* (1989) and were cultured for 7 days before exposure to various concentrations of Glu. Following treatment from 0 to 360 min, the cells were lysed, total RNA was extracted and the amount of *fosB* and 18S quantified by real-time RT-PCR. Prior to calculation of the fold induction of *fosB* relative to the untreated, time matched controls, *fosB* expression values were normalised to the internal control, 18S (see Chapter 2). When mature mCGCs were treated with various concentrations of Glu, up to 500 μM, and *fosB* mRNA levels measured using RT-PCR, different time- and concentration-dependant profiles were obtained. The results are shown in Figures 4.16 a) & b).

Exposure to non-toxic concentrations of Glu (2.5 μM) resulted in a transient increase in *fosB*, which had returned to the basal level by 90 min. Partially toxic concentrations of Glu (25 μM) induced a progressive increase in *fosB* mRNA expression, reaching maximum levels of 15 fold and which was sustained over 240 min before returning to basal levels.

The profile of *fosB* mRNA induction changed following exposure to higher toxic concentrations of Glu (100 - 500 μM). There appeared to be a delay in the onset of *fosB* mRNA induction, which was accompanied by a progressively elevated and sustained induction. This induction was sustained over 240 min and reached maximal induction values of 25 - 35 fold (3 fold higher than maximal *c-fos* levels induced by Glu), when compared to the non-induced time-matched controls.

Therefore, the finding that highly elevated and sustained *fosB* mRNA expression changes with Glu induced toxicity in mCGCs, suggests that this gene may be used, in addition to *c-fos*, as a specific biomarker in predicting an excitotoxic outcome and may even prove a more sensitive endpoint.

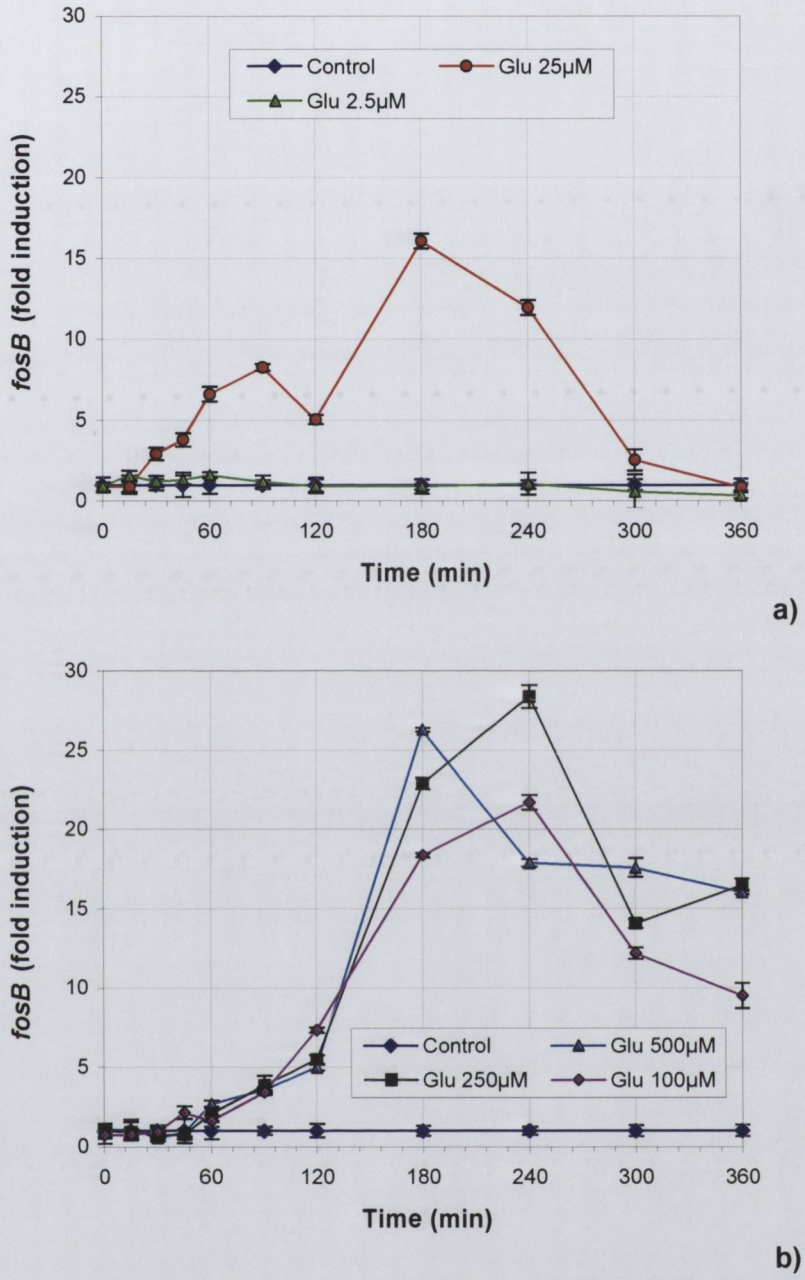


Figure 4.16: Different time-profiles of *fosB* expression dependent on Glu concentration

Primary cultures of mCGCs (7 DIV) were exposed to various concentrations of Glu, for up to 360 min. Following treatment, the cells were lysed and total RNA was extracted and the amount of *fosB* and 18S quantified by RT-PCR. *fosB* expression values were normalised to 18S expression, which served as the internal control. The results above refer to the fold induction of *fosB* expression compared to untreated, time-matched controls. Data represent mean ± s.d. values of triplicate RT-PCR reactions derived from one individual experiment. The experiments were reproduced at least three times. Figure 4.16 a) represents the *fosB* changes with non-toxic and partially toxic concentrations of Glu while b) represents changes in *fosB* expression with toxic concentrations.

4.2.12 NMDA receptor specificity of Glu-induced *fosB* mRNA expression

To further demonstrate that *fosB* can be used as a specific and additional mechanistic biomarker for NMDA receptor mediated excitotoxicity, the effect of an NMDA and non-NMDA receptor antagonist on the excitotoxic *fosB* response was compared. Mature mCGCs (7 DIV) were treated with three different concentrations of Glu and the subsequent increases in *fosB* expression levels were examined in the presence of AP5 and CNQX.

When mCGCs were treated with low, but partially toxic, concentrations of Glu (25 µM), from 0 to 360 min, a progressive increase in *fosB* expression was observed which was sustained for 240 min before gradually returning to basal levels. Pre-treatment with the NMDA receptor antagonist, AP5, completely inhibited the toxic *fosB* response, while pre-treatment with the non-NMDA receptor, CNQX, did not antagonise the response (see Figure 4.17). These results are supportive of an NMDA receptor mediated *fosB* induction.

Toxic concentrations of Glu (100 µM) also induced a progressive, but more elevated and sustained increase in *fosB* mRNA expression. It was found that while pre-treatment with AP5 changed the excitotoxic *fosB* profile, to that of an earlier peaking, less sustained expression, complete abolition of the response did not occur. CNQX did not antagonise the excitotoxic *fosB* response (see Figure 4.18).

With higher toxic concentrations of Glu (250 µM), a delayed, elevated and sustained increase in *fosB* mRNA expression was detected. However, neither AP5 nor CNQX inhibited *fosB* induction nor changed the toxic profile (see Figure 4.19).

As for the *c-fos* experiments, the concentration of the NMDA receptor antagonist, AP5, used in these investigations was obviously not sufficient to compete with the higher, toxic concentrations of Glu (100 and 250 µM). However, the pharmacology of Glu-induced *fosB* mRNA expression is indicative of an NMDA receptor mediated action.

Thus, *fosB* is induced in excitotoxic neuronal cell death and the measurement of *fosB* may be used as an early predictive indicator of the excitotoxic potential of compounds. Furthermore, these results are the first demonstration, using a new method of gene expression measurement (real-time RT-PCR) that both *c-fos* and *fosB* are specifically involved in the complex process of excitotoxicity.

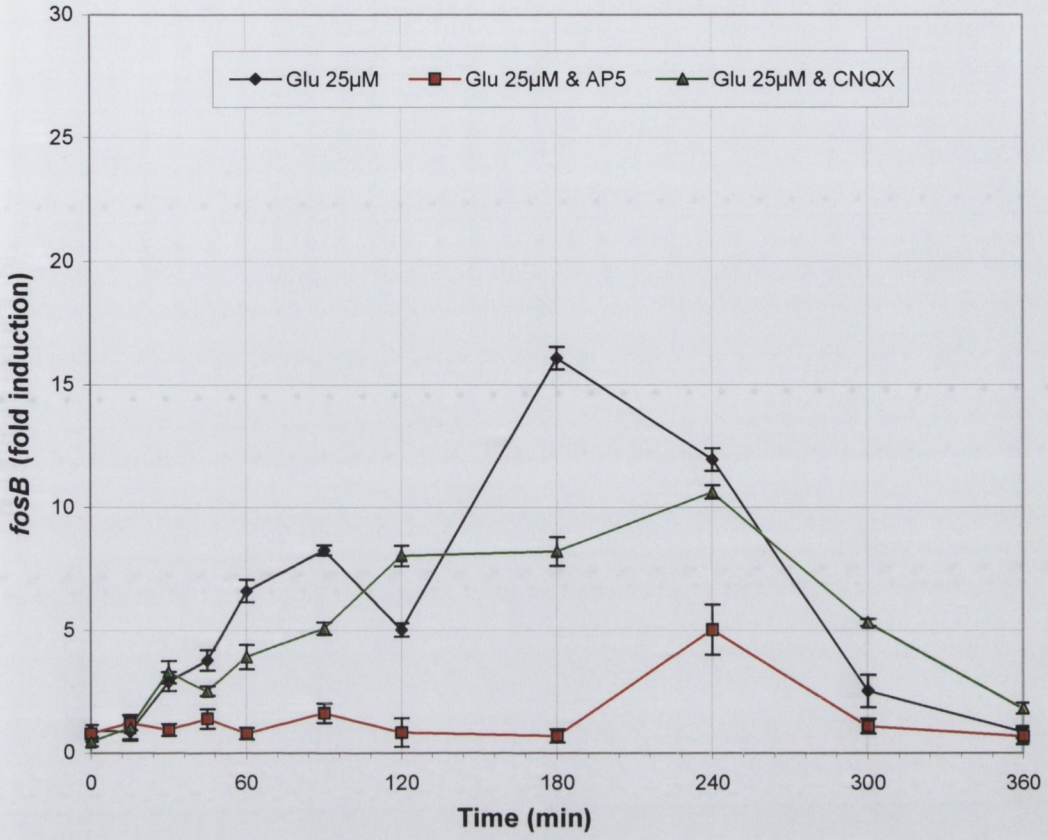


Figure 4.17: AP5 but not CNQX effectively antagonises *fosB* mRNA expression at low Glu concentrations

Primary cultures of mCGCs (7 DIV) were pre-incubated for 15 min with either AP5 (500 µM) or CNQX (10 µM) prior to co-exposure with a fixed concentration of Glu (25 µM), for up to 360 min. Following treatment, the cells were lysed and total RNA was extracted and the amount of *fosB* and 18S quantified by RT-PCR. The expression values of *fosB* were normalised to 18S expression, which served as the internal control. The results above refer to the fold induction of *fosB* expression compared to untreated, time-matched controls. Data represent mean ± s.d. values of triplicate RT-PCR reactions derived from one individual experiment. The experiments were reproduced at least twice, with similar events.

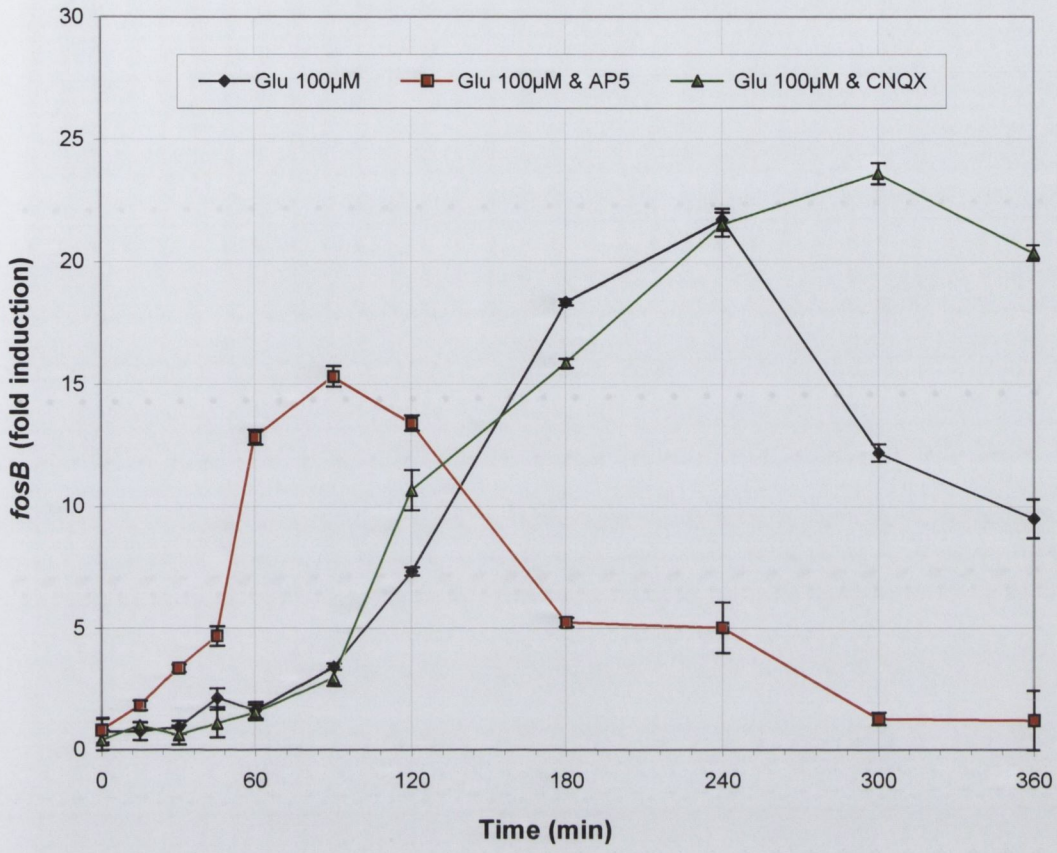


Figure 4.18: AP5 but not CNQX changes the *fosB* mRNA expression profile

Primary cultures of mCGCs (7 DIV) were pre-incubated for 15 min with either AP5 (500 µM) or CNQX (10 µM) prior to co-exposure with a fixed concentration of Glu (100 µM), for up to 360 min. Following treatment, the cells were lysed and total RNA was extracted and the amount of *fosB* and 18S quantified by RT-PCR. *fosB* expression values were normalised to 18S expression, which served as the internal control. The results above refer to the fold induction of *fosB* expression compared to untreated, time-matched controls. Data represent mean ± s.d. values of triplicate RT-PCR reactions derived from one individual experiment. The experiments were reproduced at least twice.

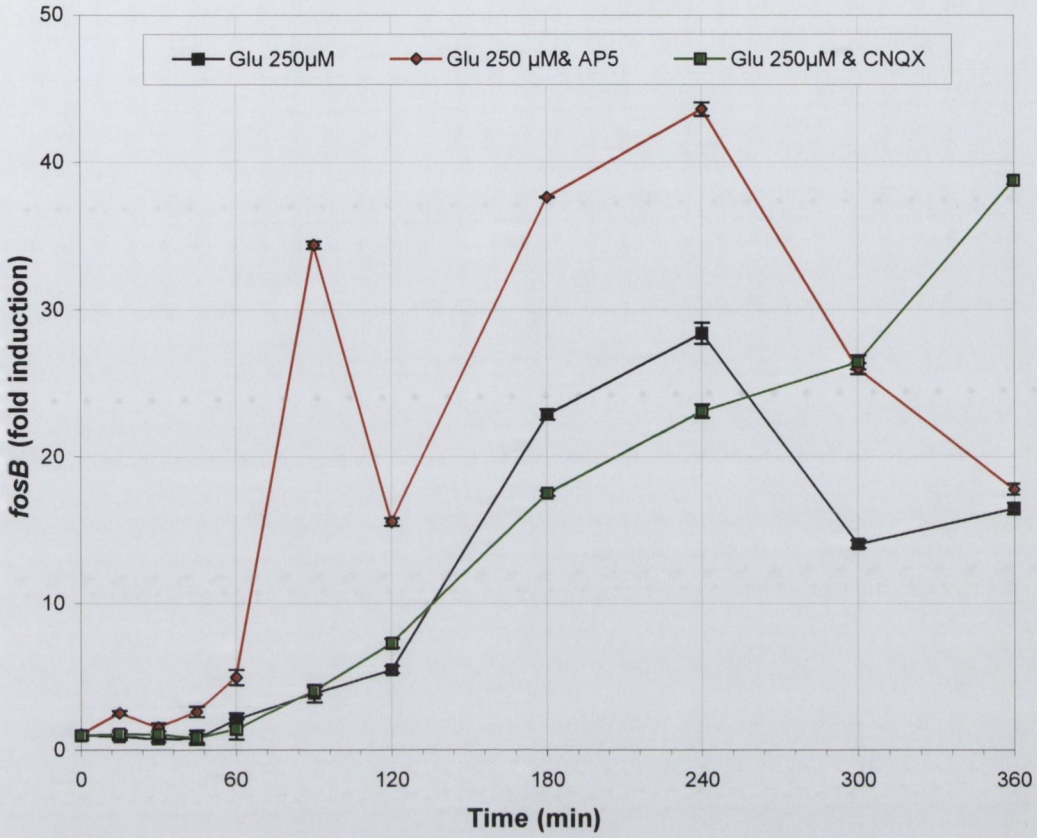


Figure 4.19: AP5 but not CNQX changes the *fosB* mRNA expression profile

Primary cultures of mCGCs (7 DIV) were pre-incubated for 15 min with either AP5 (500 µM) or CNQX (10 µM) prior to co-exposure with a fixed concentration of Glu (250 µM), for up to 360 min. Following treatment, the cells were lysed and total RNA was extracted and the amount of *fosB* and 18S quantified by RT-PCR. *fosB* expression values were normalised to 18S expression, which served as the internal control. The results above refer to the fold induction of *fosB* expression compared to untreated, time-matched controls. Data represent mean ± s.d. values of triplicate RT-PCR reactions derived from one individual experiment. The experiments were reproduced at least twice.

4.2.13 *FosB* expression profiles vary with Asp concentration

In order to confirm our findings that *fosB* can be used, in addition to *c-fos*, as a selective biomarker for excitotoxicity, the expression profiles of *fosB* were investigated with a second known excitotoxin, Asp, over the same time course.

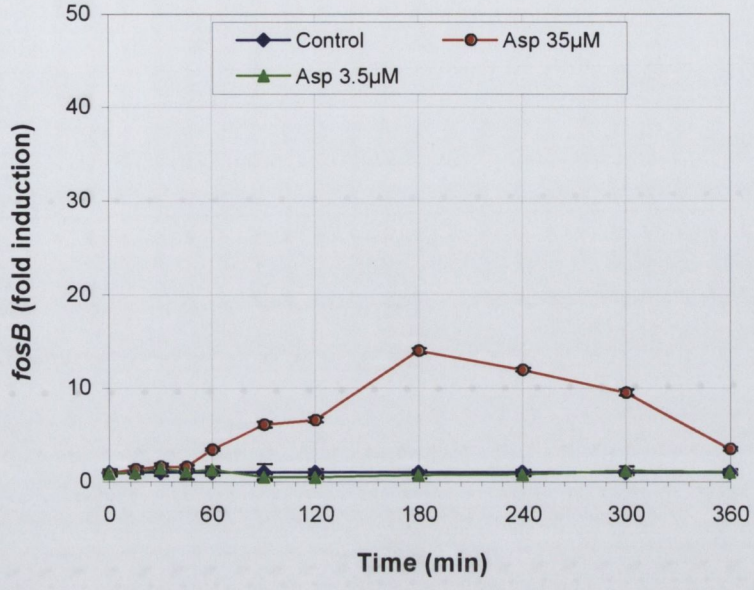
Primary cultures of mCGCs were prepared from post-natal mice as described in Meier and Schousboe (1982), Drejer *et al.* (1983) and Schousboe *et al.* (1989) and were routinely cultured for 7 days before exposure to various concentrations of the EAA, Asp. Following treatment over 0 - 360 min, the cells were lysed, total RNA was extracted and the amount of *fosB* and 18S quantified by real-time RT-PCR. The *fosB* expression values were normalised to the internal control, 18S, prior to calculation of the fold induction of *fosB* relative to the untreated, time matched controls (see Chapter 2). When mature mCGCs were treated with various concentrations of Asp (0 - 500 μM) and *fosB* mRNA levels measured using real-time RT-PCR, different time profiles of *fosB* mRNA expression were obtained depending on Asp concentration (see Figures 4.20 a) & b)).

With non-toxic concentrations of Asp (3.5 μM), no change in the expression levels of *fosB* mRNA was observed with levels remaining at the basal rate throughout the exposure period (see Figure 4.20 a)).

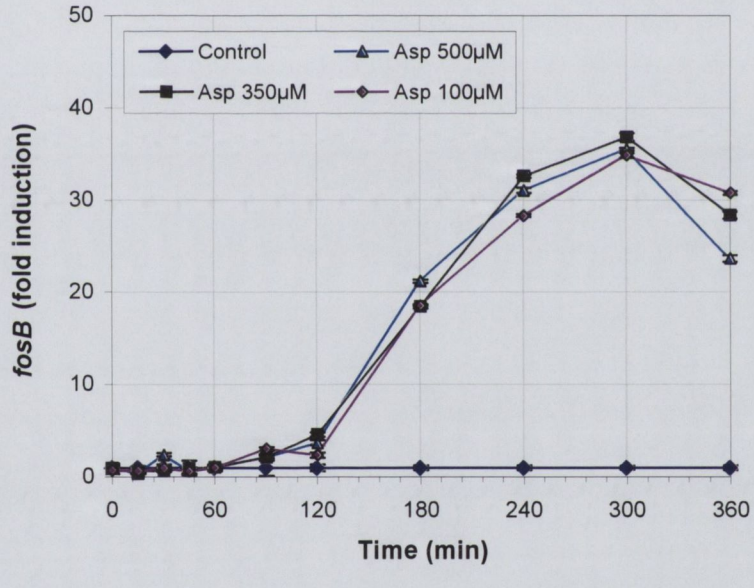
Low, partially toxic concentrations of Asp (35 μM) induced a progressive elevation in *fosB* expression, reaching maximum levels of 15 fold at 180 min before returning to basal levels (see Figure 4.20 a)).

With higher toxic concentrations of Asp (100 - 500 μM), there appeared to be a delay in the onset of *fosB* mRNA induction, which was elevated and sustained over 4 hours and which reached maximal levels of 25 - 35 fold when compared to the non-induced time-matched controls (see Figure 4.20 b)).

Therefore, elevated and sustained *fosB* expression positively correlates with excitotoxicity in mCGCs, induced by both Glu and Asp.



a)



b)

Figure 4.20: Different profiles of *fosB* expression depending on time and Asp concentration

Primary cultures of mCGCs (7 DIV) were exposed to various concentrations of Asp, for up to 360 min. Following treatment, total RNA was extracted and the amount of *fosB* and 18S quantified by RT-PCR. The *fosB* expression values were normalised to 18S expression, which served as the internal control. The results above refer to the fold induction of *fosB* expression compared to untreated, time-matched controls. Data represent mean ± s.d. values of triplicate RT-PCR reactions derived from one individual experiment. The experiments were reproduced at least three times. Figure 4.20 a) represents the *fosB* changes with non-toxic and partially toxic concentrations of Asp while b) represents changes in *fosB* expression with toxic concentrations.

4.2.14 NMDA receptor specificity of Asp-induced *fosB* mRNA expression

In order to confirm that EAA-induced *fosB* expression specifically involves NMDA receptors the degree of protection offered by AP5 was assessed in the presence of various concentrations of Asp. CNQX was used for comparison.

At low, but partially toxic, concentrations of Asp (35 μM), AP5 completely inhibited the toxic *fosB* response (see Figure 4.21). However, CNQX had no inhibitory effect on *fosB* mRNA expression.

Although AP5 did not completely inhibit *fosB* mRNA expression induced by higher concentrations of Asp (100 μM), it did shift the profiles to that of an earlier peaking, less sustained expression with reduced fold induction values. Again, CNQX did not influence the *fosB* mRNA expression profile (see Figure 4.22).

With more toxic concentrations of Asp (350 μM), AP5 again changed the exctotoxic *fosB* profile to an earlier peaking, less sustained expression while CNQX had no effect (see Figure 4.23).

As for Glu, the concentration of the antagonist, AP5, used in these investigations was not sufficient to compete totally with the higher toxic concentrations of Asp. However, these results are consistent with some or all the Asp-induced *fosB* mRNA expression being mediated through the NMDA receptor subtype.

4.2.15 Neither Ala nor paraquat induced *fosB* expression in mature mCGCs

Two control compounds were tested to demonstrate the specificity of the excitotoxic *fosB* response. Firstly Ala, a non-excitotoxic amino acid, did not induce increased *fosB* mRNA expression in mCGCs under conditions where Glu and Asp induce their effects (see Figure 4.24).

Secondly paraquat, a generally neurotoxic but non-excitotoxic compound, did not induce *fosB* mRNA expression in mCGCs (see Figure 4.25).

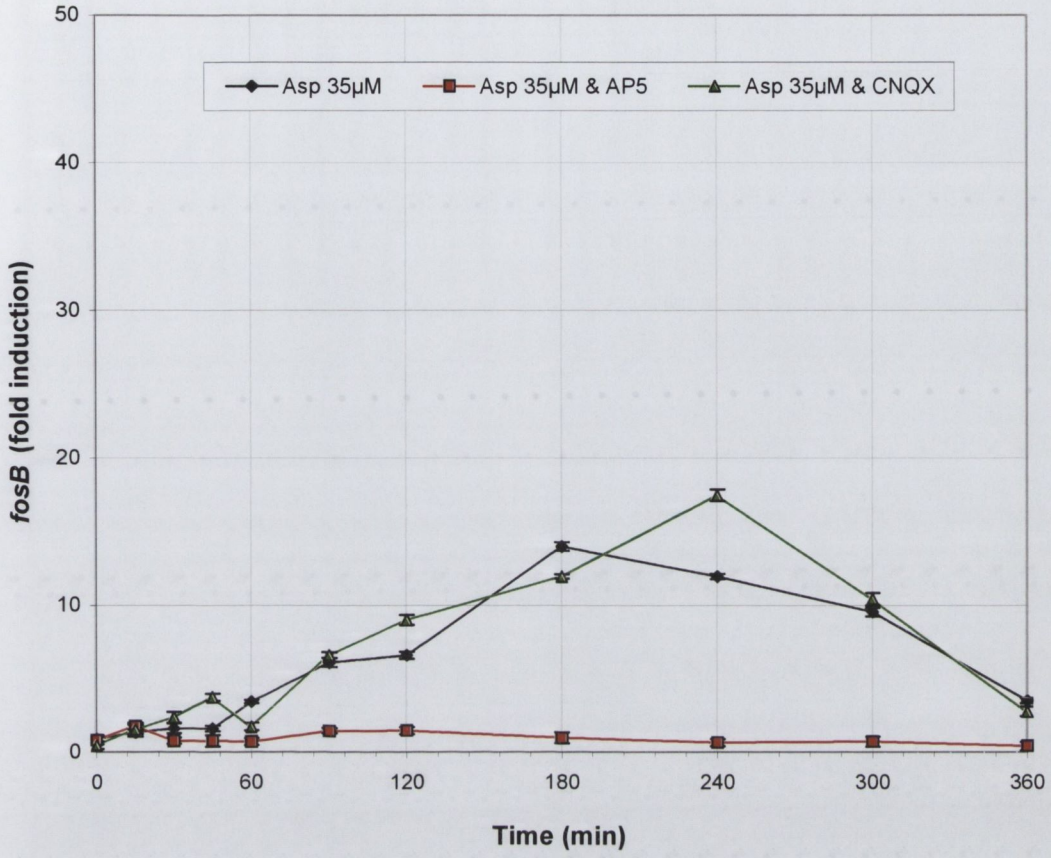


Figure 4.21: AP5 but not CNQX effectively abolishes *fosB* mRNA expression at low Asp concentrations

Primary cultures of mCGCs (7 DIV) were pre-incubated for 15 min with either AP5 (500 µM) or CNQX (10 µM) prior to co-exposure with a fixed concentration of Asp (35 µM), for up to 360 min. Following treatment, the cells were lysed and total RNA was extracted and the amount of *fosB* and 18S quantified by RT-PCR. The *fosB* expression values were normalised to 18S expression, which served as the internal control. The results above refer to the fold induction of *fosB* expression compared to untreated, time-matched controls. Data represent mean ± s.d. values of triplicate RT-PCR reactions derived from one individual experiment. The experiments were reproduced at least twice.

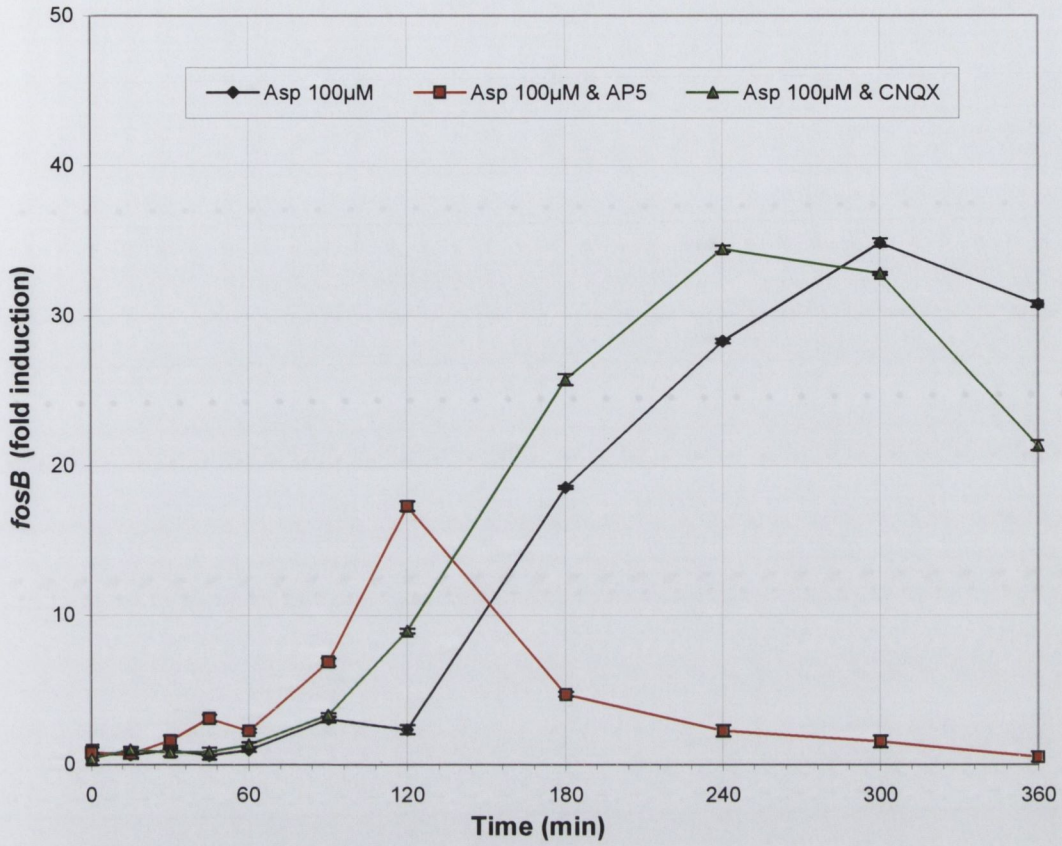


Figure 4.22: AP5 but not CNQX changes the *fosB* mRNA expression profile at higher Asp concentrations

Primary cultures of mCGCs (7 DIV) were pre-incubated for 15 min with either AP5 (500 µM) or CNQX (10 µM) prior to co-exposure with a fixed concentration of Asp (100 µM), for up to 360 min. Following treatment, the cells were lysed and total RNA was extracted and the amount of *fosB* and 18S quantified by RT-PCR. The *fosB* expression values were normalised to 18S expression, which served as the internal control. The results above refer to the fold induction of *fosB* expression compared to untreated, time-matched controls. Data represent mean ± s.d. values of triplicate RT-PCR reactions derived from one individual experiment. The experiments were reproduced at least twice.

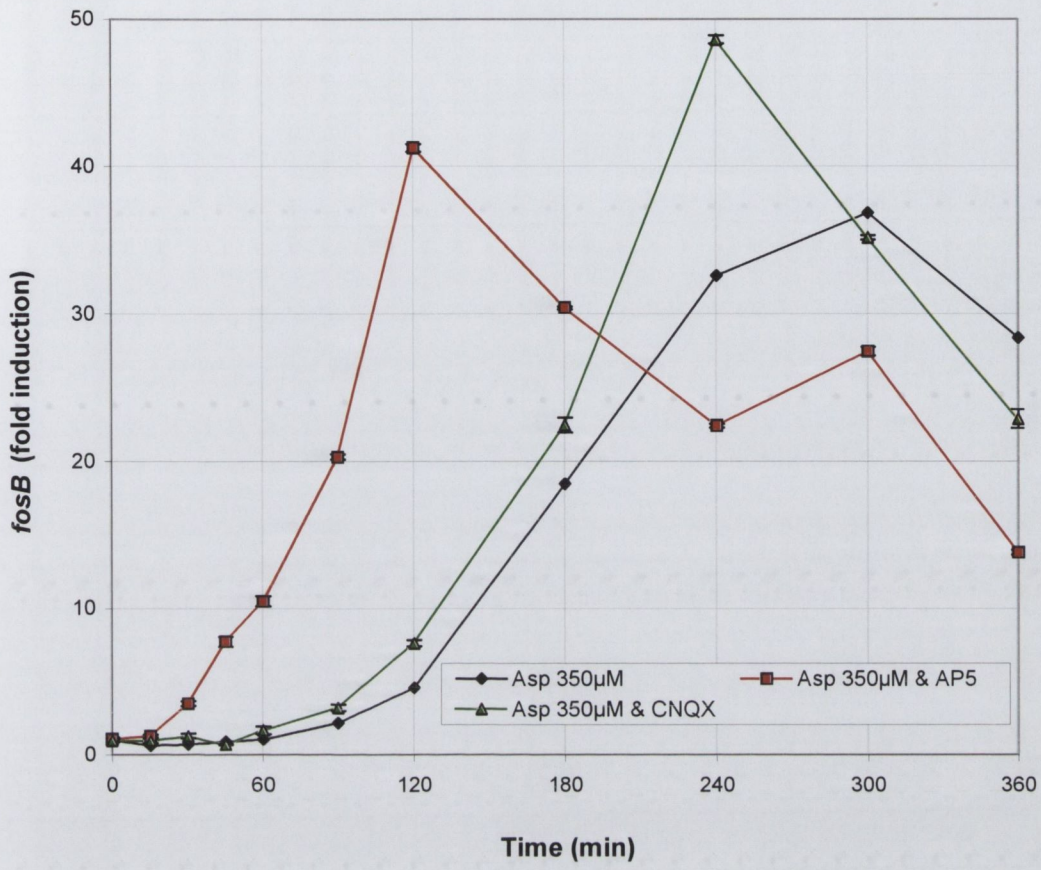
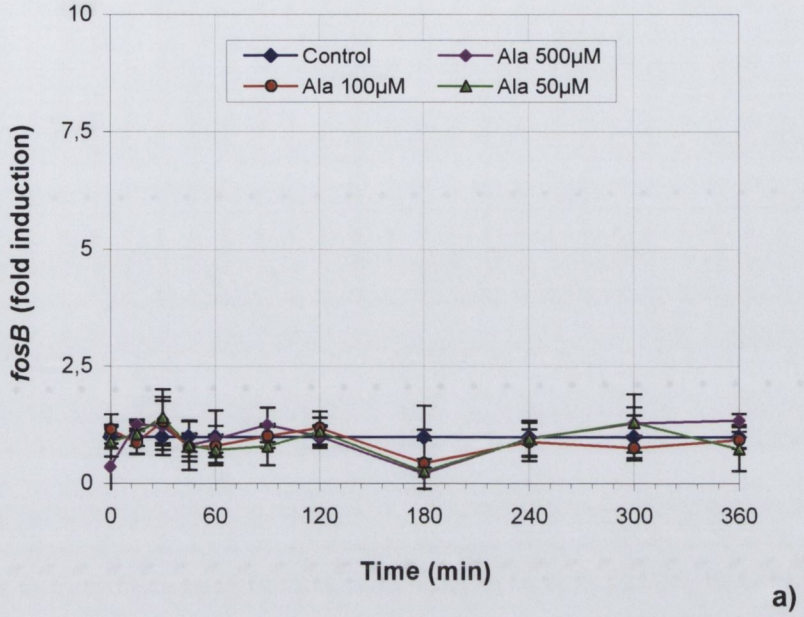


Figure 4.23: AP5 but not CNQX changes the *fosB* mRNA expression profile in response to toxic Asp concentrations

Primary cultures of mCGCs (7 DIV) were pre-incubated for 15 min with either AP5 (500 µM) or CNQX (10 µM) prior to co-exposure with a fixed concentration of Asp (350 µM), for up to 360 min. Following treatment, the cells were lysed and total RNA was extracted and the amount of *fosB* and 18S quantified by RT-PCR. The *fosB* expression values were normalised to 18S expression, which served as the internal control. The results above refer to the fold induction of *fosB* expression compared to untreated, time-matched controls. Data represent mean ± s.d. values of triplicate RT-PCR reactions derived from one individual experiment. The experiments were reproduced at least twice.



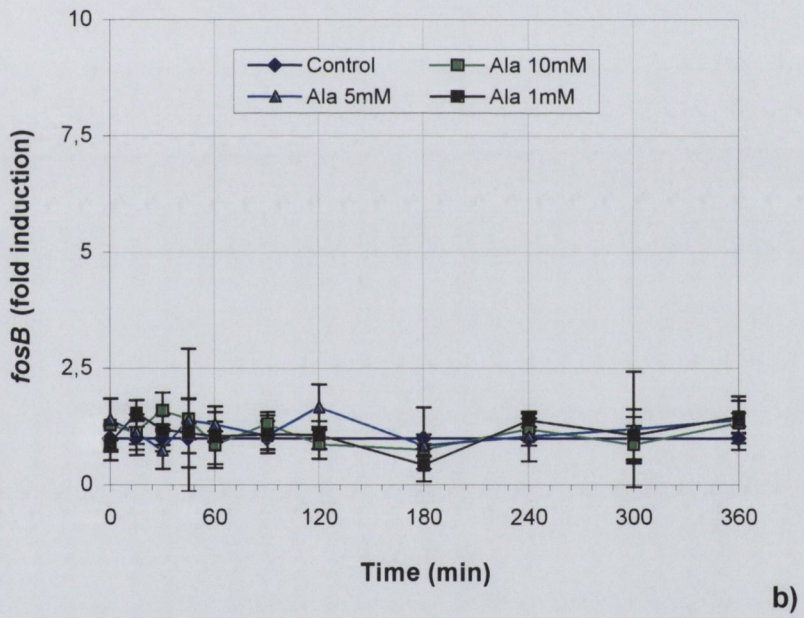
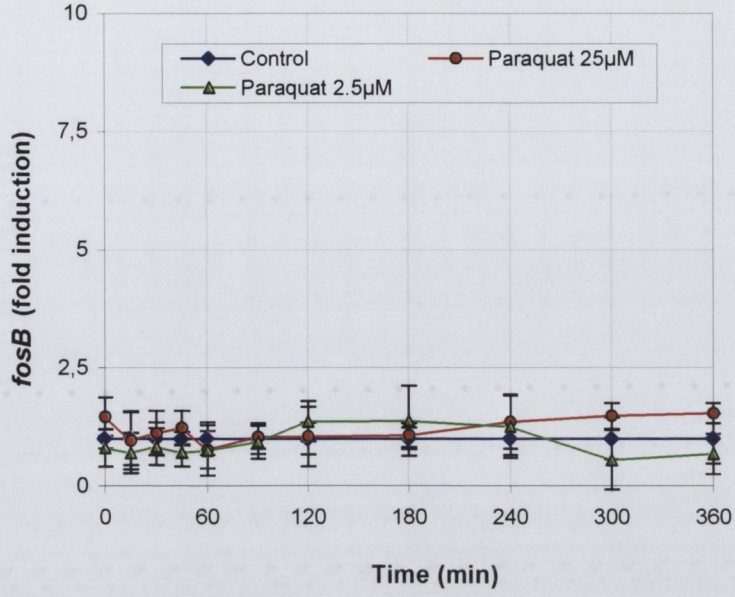
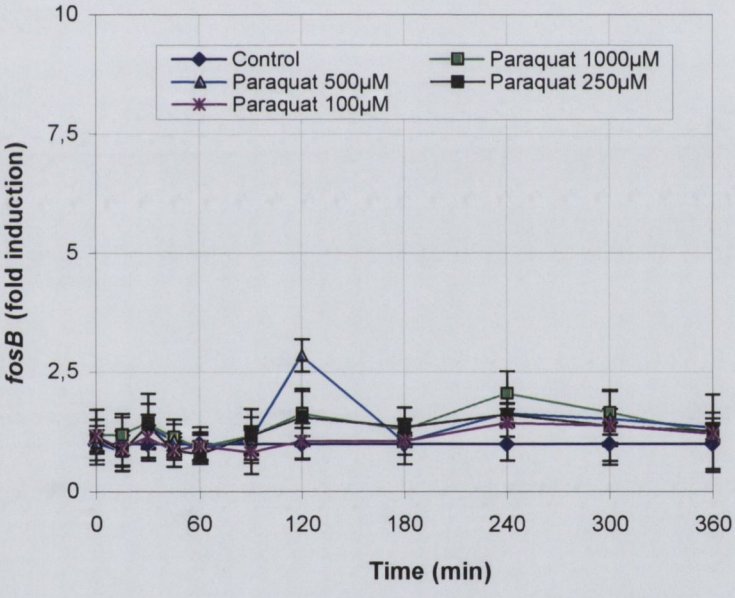


Figure 4.24: No induction of *fosB* mRNA expression in mCGCs treated with Ala

Primary cultures of mCGCs (7 DIV) were exposed to various concentrations of Ala, for up to 360 min. Following treatment, the cells were lysed and total RNA was extracted and the amount of *fosB* and 18S quantified by RT-PCR. The *fosB* expression values were normalised to 18S expression, which served as the internal control. The results above refer to the fold induction of *fosB* expression compared to untreated, time-matched controls. Data represent mean ± s.d. values of triplicate RT-PCR reactions derived from one individual experiment. The experiments were reproduced at least twice. Figure 4.24 a) represents the *fosB* changes with low concentrations of Ala while b) represents changes in *fosB* expression with high concentrations.



a)



b)

Figure 4.25: No induction of *fosB* mRNA expression in mCGCs treated with paraquat

Primary cultures of mCGCs (7 DIV) were exposed to various concentrations of paraquat, for up to 360 min. Following treatment, total RNA was extracted and the amount of *fosB* and 18S quantified by RT-PCR. The *fosB* expression values were normalised to 18S expression, which served as the internal control. The results above refer to the fold induction of *fosB* expression compared to untreated, time-matched controls. Data represent mean ± s.d. values of triplicate RT-PCR reactions derived from one individual experiment. The experiments were reproduced at least twice. Figure 4.25 a) represents the *fosB* changes with partially toxic concentrations of paraquat while b) represents changes in *fosB* expression with toxic concentrations.

4.2.16 *fra-1, fra-2* and 3 members of the *jun* family of *IEGs* are unaffected by EAAs

In an attempt to evaluate whether other members of the *fos* and *jun* families of *IEGs* are involved in the process of NMDA receptor mediated excitotoxicity, a comparative study of the time and concentration dependence of the induction of all remaining members was undertaken.

Mature mCGCs (7 DIV) were treated with the same concentrations of Glu, Asp or Ala, as used before. Following exposures from 0 - 360 min, the cells were lysed and total RNA was extracted. Real-time RT-PCR was then performed on the cell extracts with other members of the *fos* (*fra-1 and fra-2*) and *jun* (*c-jun, junB and junD*) families of *IEGs* (see Figures 4.26 to 4.39). The expression values of all genes measured were normalised to the internal control, 18S, prior to calculation of the fold induction values of all genes relative to the untreated, time matched controls (see Chapter 2).

When mCGCs were treated with either Glu (0 – 1 mM), Asp (0 – 1 mM), or Ala (0 – 10 mM), no increase in *fra-1* mRNA expression occurred (fold induction over time zero less than 1, see Figures 4.26 to 4.28).

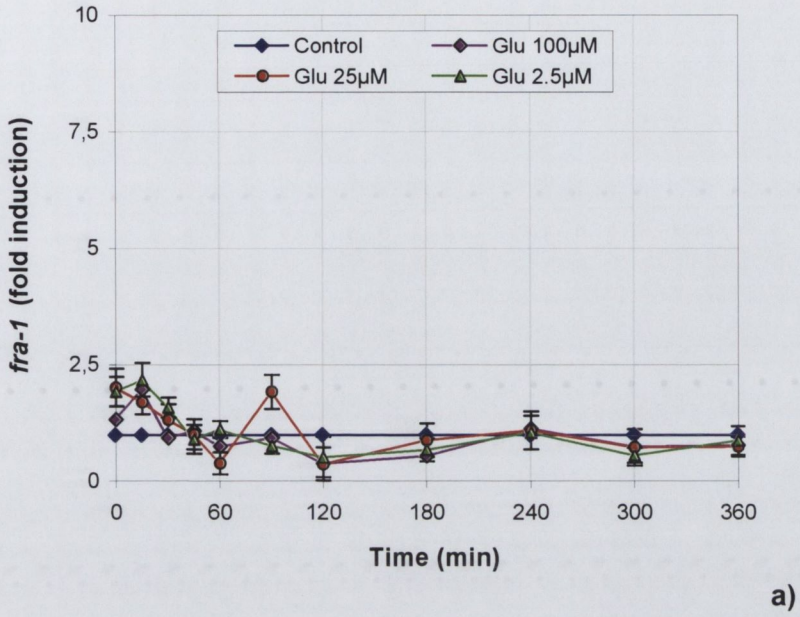
For the *fra-2 IEG*, a small increase with high concentrations of Glu occurred at later time-points. *fra-2* expression was not observed when mCGCs were treated with Ala (0 – 10 mM) over 360 min (see Figures 4.29 and 4.30).

In addition, *c-jun* mRNA expression did not increase (fold induction over time zero less than 1) over concentration ranges of Glu (0 – 1 mM), Asp (0 – 1 mM), or Ala (0 – 10 mM) (see Figures 4.31 to 4.33).

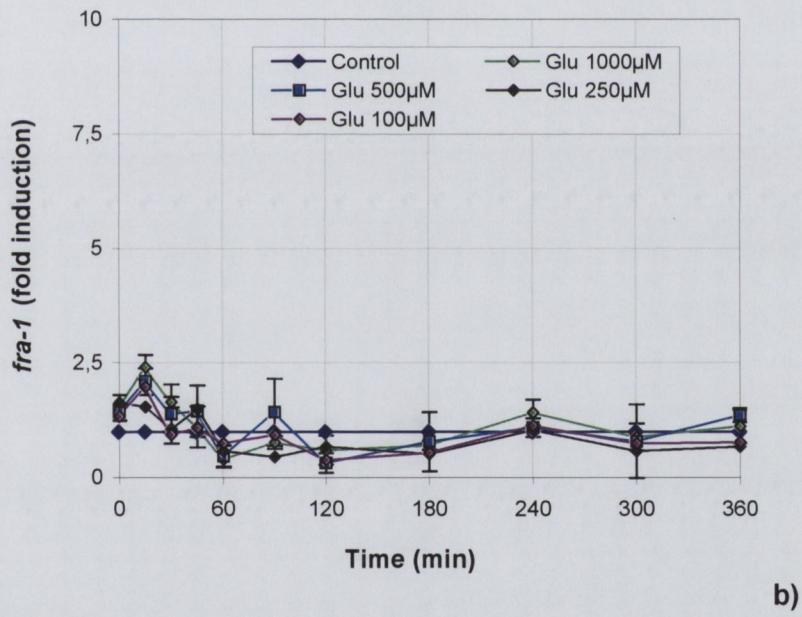
With high toxic concentrations of Glu (> 100 μM) a small increase (1 - 1.5 fold), following 2 - 3 hour exposures, in *junB* mRNA expression occurred. These increases were not found in Asp treated mCGCs, however, and so the possibility of an EAA receptor mediated response is uncertain (see Figures 4.34 to 4.36).

For *junD* there appeared again to be a small transient expression with Asp over 0 – 1 hours exposure but this expression was accompanied by high standard deviations in this range (see Figures 4.37 to 4.39)

Thus, *c-fos*, *fosB* and *fra-2 IEGs* were found, using quantitative real-time RT-PCR, to be specifically expressed in mCGCs undergoing excitotoxic cell death.



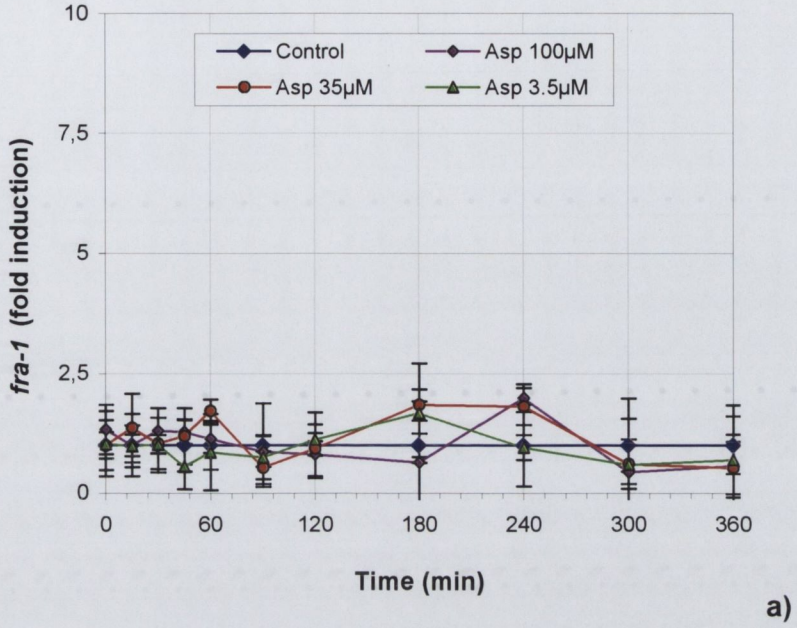
a)



b)

Figure 4.26: *fra-1* mRNA expression in mCGCs treated with various concentrations of Glu

Primary cultures of mCGCs (7 DIV) were exposed to various concentrations of Glu for up to 360 min. Following treatment, the cells were lysed and total RNA was extracted and the amount of *fra-1* and 18S quantified by RT-PCR. The *fra-1* expression values were normalised to 18S expression, which served as the internal control. The results above refer to the fold induction of *fra-1* expression compared to untreated, time-matched controls. Data represent mean ± s.d. values of triplicate RT-PCR reactions derived from one individual experiment. Figure 4.26 a) represents the *fra-1* changes with non-toxic and partially toxic concentrations of Glu while b) represents changes in *fra-1* expression with toxic concentrations.



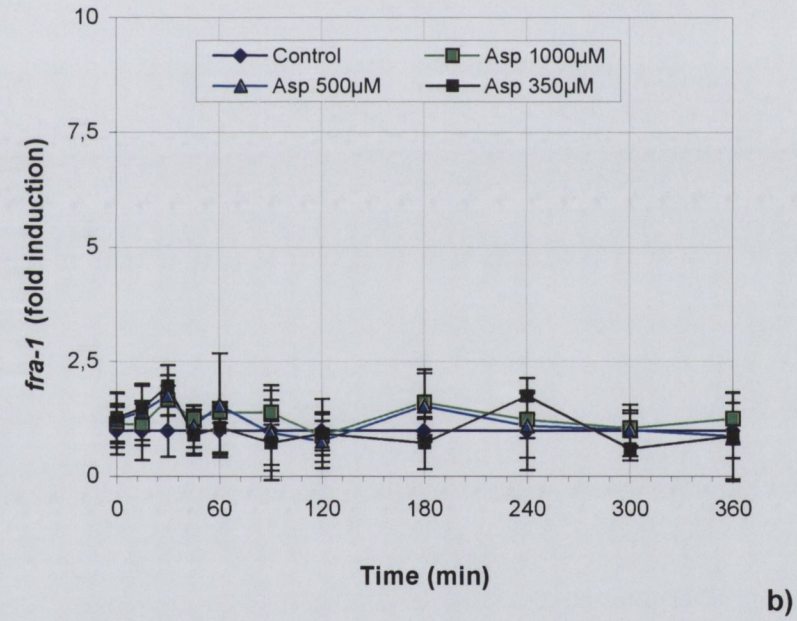


Figure 4.27: *fra-1* mRNA expression in mCGCs treated with various concentrations of Asp

Primary cultures of mCGCs (7 DIV) were exposed to various concentrations of Asp, for up to 360 min. Following treatment, the cells were lysed and total RNA was extracted and the amount of *fra-1* and 18S quantified by RT-PCR. The *fra-1* expression values were normalised to 18S expression, which served as the internal control. The results above refer to the fold induction of *fra-1* expression compared to untreated, time-matched controls. Data represent mean ± s.d. values of triplicate RT-PCR reactions derived from one individual experiment. Figure 4.27 a) represents the *fra-1* changes with non-toxic and partially toxic concentrations of Asp while b) represents changes in *fra-1*expression with toxic concentrations.

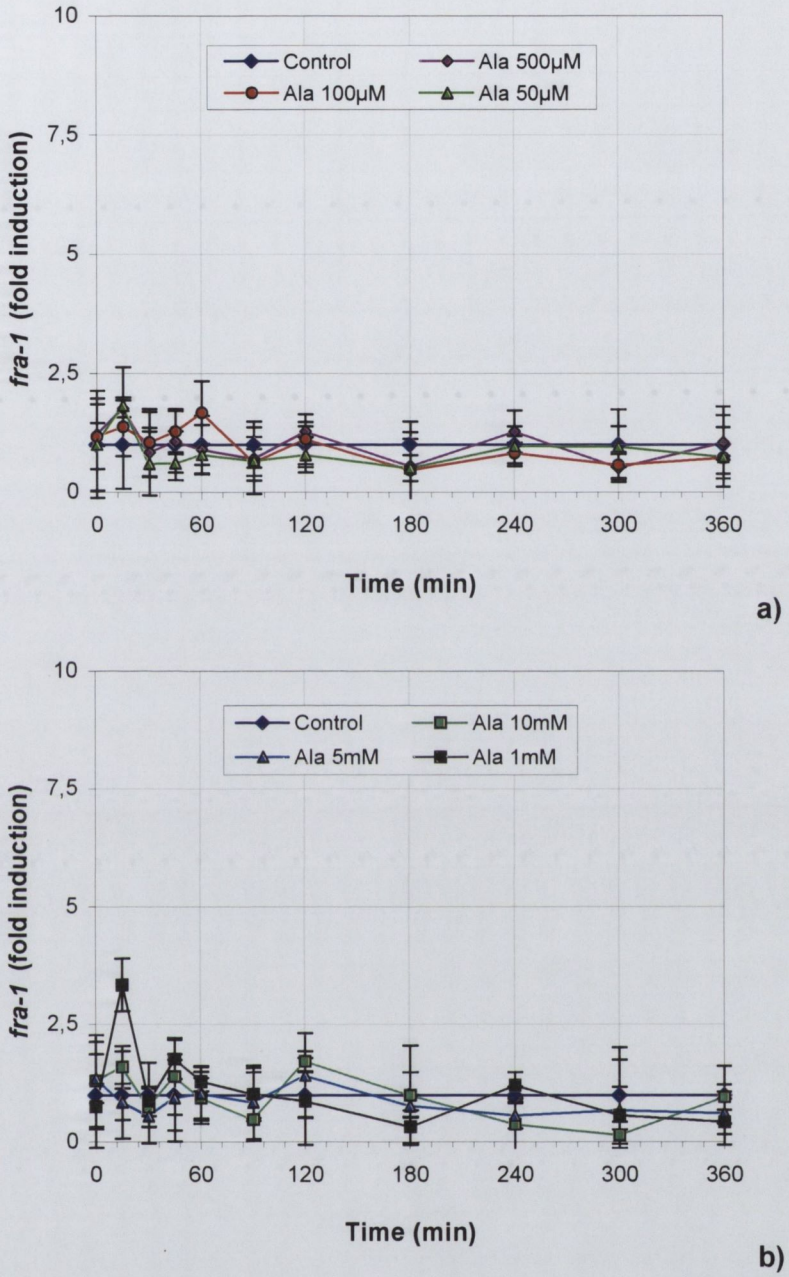


Figure 4.28: *fra-1* mRNA expression in mCGCs treated with various concentrations of Ala

Primary cultures of mCGCs (7 DIV) were exposed to various concentrations of Ala, for up to 360 min. Following treatment, the cells were lysed and total RNA was extracted and the amount of *fra-1* and 18S quantified by RT-PCR. The *fra-1* expression values were normalised to 18S expression, which served as the internal control. The results above refer to the fold induction of *fra-1* expression compared to untreated, time-matched controls. Data represent mean ± s.d. values of triplicate RT-PCR reactions derived from one individual experiment. Figure 4.28 a) represents the *fra-1* changes with low concentrations of Ala while b) represents changes in *fra-1* expression with high concentrations.

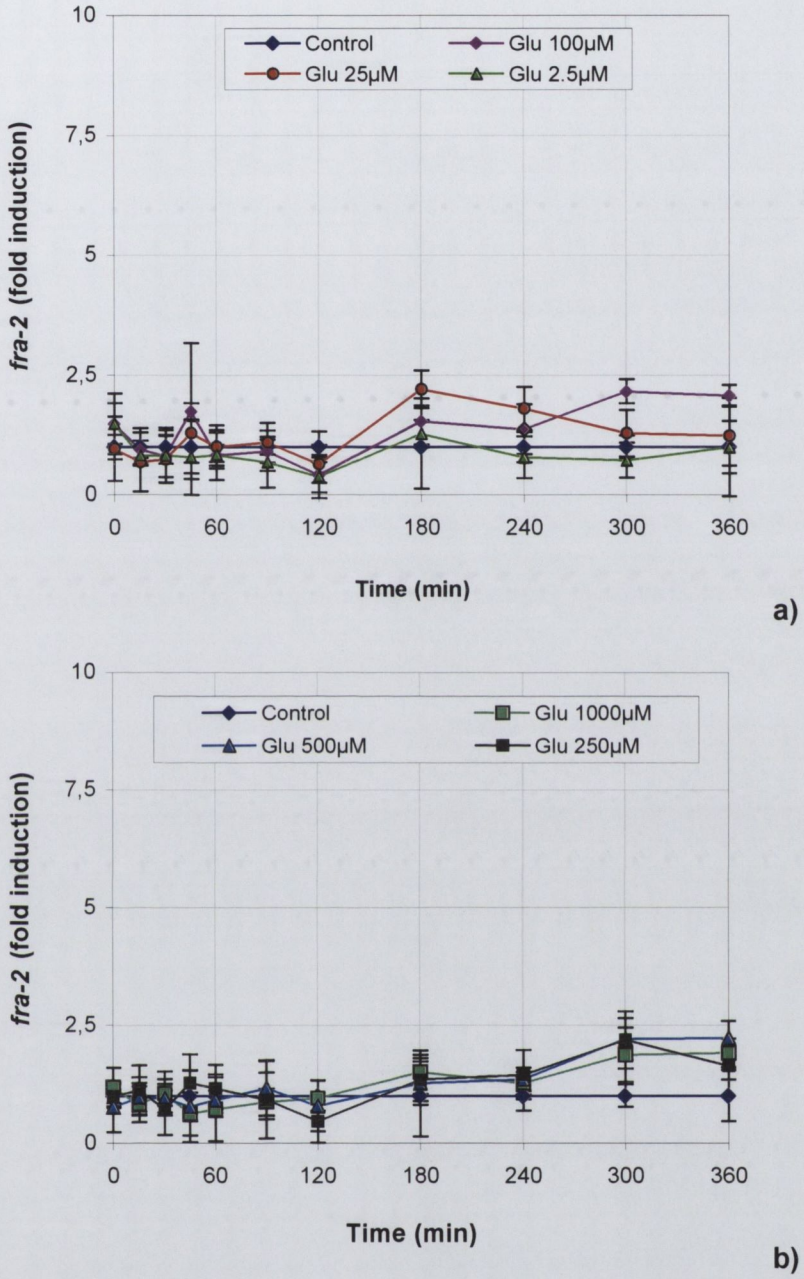


Figure 4.29: *fra-2* mRNA expression in mCGCs treated with various concentrations of Glu

Primary cultures of mCGCs (7 DIV) were exposed to various concentrations of Glu, for up to 360 min. Following treatment, the cells were lysed and total RNA was extracted and the amount of *fra-2* and 18S quantified by RT-PCR. The *fra-2* expression values were normalised to 18S expression, which served as the internal control. The results above refer to the fold induction of *fra-2* expression compared to untreated, time-matched controls. Data represent mean ± s.d. values of triplicate RT-PCR reactions derived from one individual experiment. Figure 4.29 a) represents the *fra-2* changes with non-toxic and partially toxic concentrations of Glu while b) represents changes *fra-2* expression with toxic concentrations.

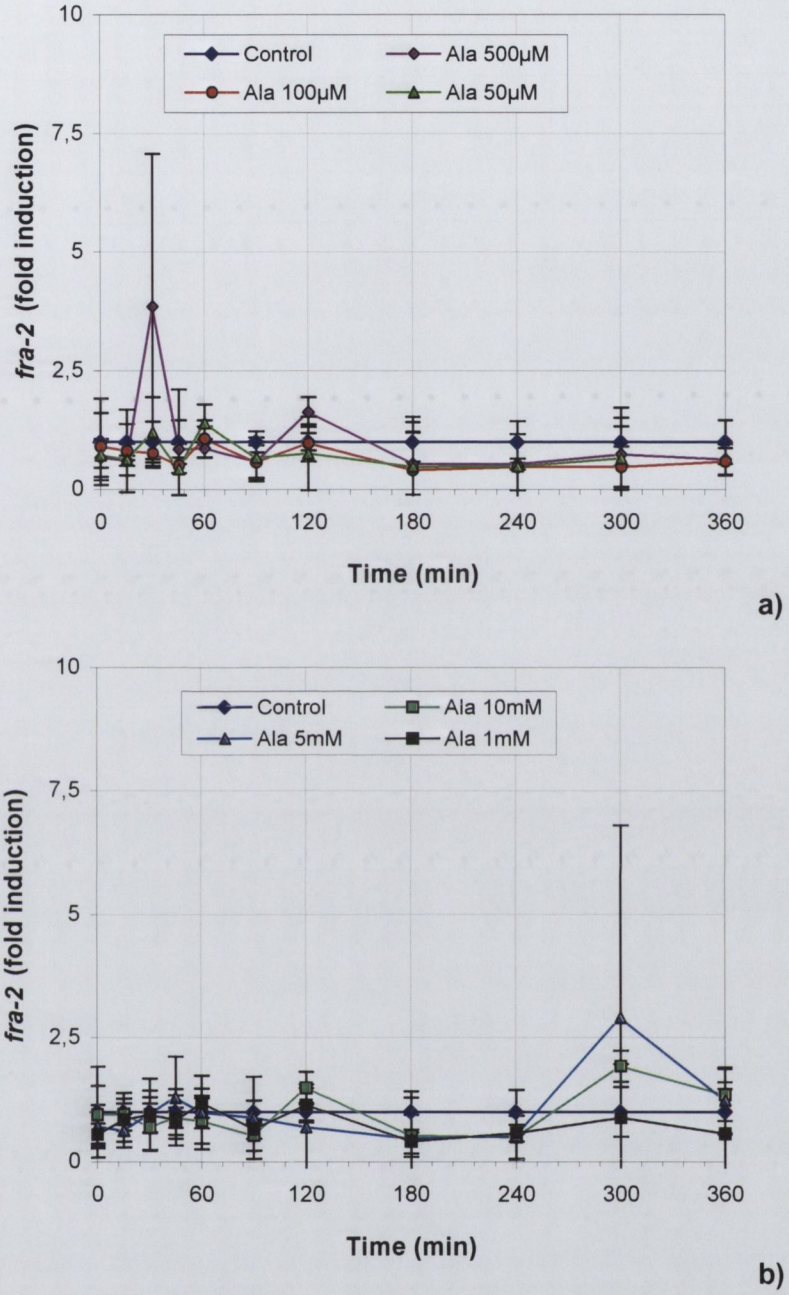
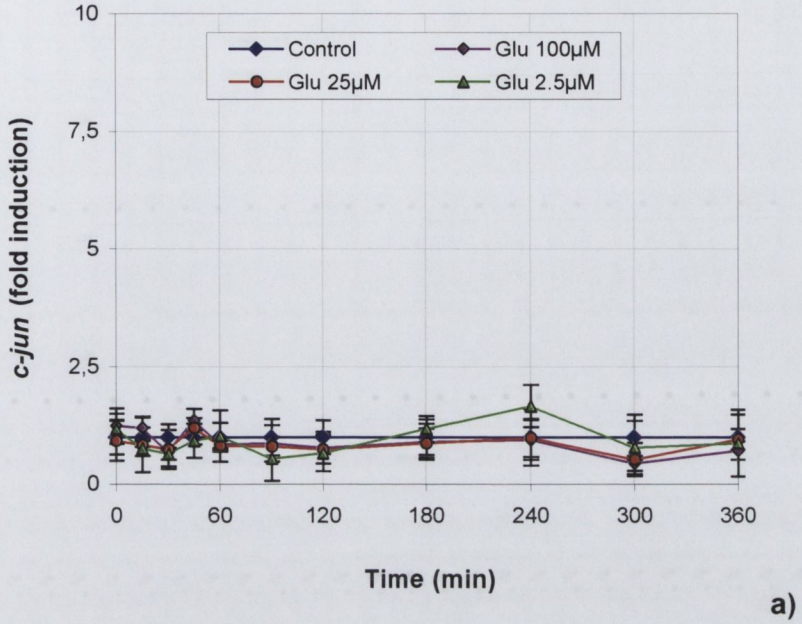
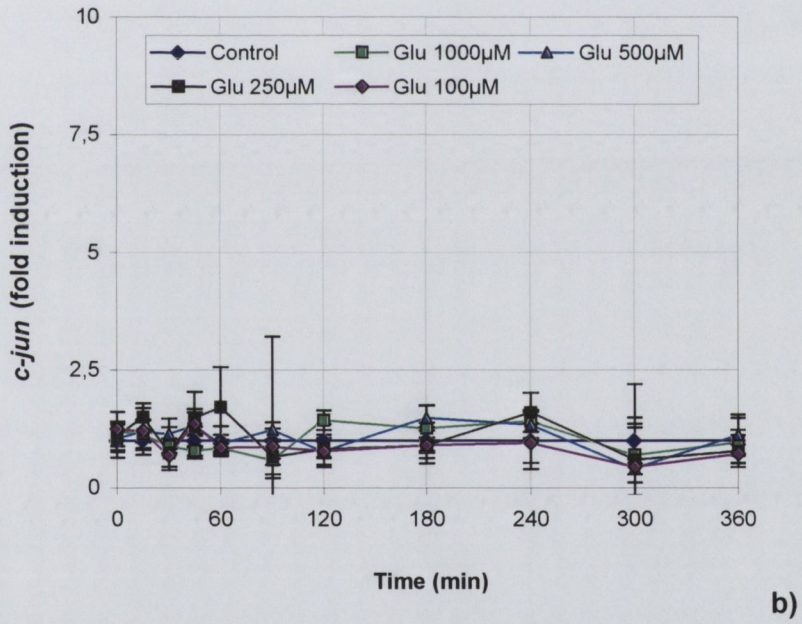


Figure 4.30: *fra-2* expression in mCGCs treated with various concentrations of Ala

Primary cultures of mCGCs (7 DIV) were exposed to various concentrations of Ala, for up to 360 min. Following treatment, total RNA was extracted and the amount of *fra-2* and 18S quantified by RT-PCR. *Fra-2* expression values were normalised to 18S expression, which served as the internal control. The results above refer to the fold induction of *fra-2* expression compared to untreated, time-matched controls. Data represent mean ± s.d. values of triplicate RT-PCR reactions derived from one individual experiment. Figure 4.30 a) represents the *fra-2* changes with low concentrations of Ala while b) represents changes in *fra-2* expression with high concentrations.



a)



b)

Figure 4.31: *c-jun* mRNA expression in mCGCs treated with various concentrations of Glu

Primary cultures of mCGCs (7 DIV) were exposed to various concentrations of Glu, for up to 360 min. Following treatment, the cells were lysed and total RNA was extracted and the amount of *c-jun* and 18S quantified by RT-PCR. The *c-jun* expression values were normalised to 18S expression, which served as the internal control. The results above refer to the fold induction of *c-jun* expression compared to untreated, time-matched controls. Data represent mean ± s.d. values of triplicate RT-PCR reactions derived from one individual experiment. Figure 4.31 a) represents the *c-jun* changes with non-toxic and partially toxic concentrations of Glu while b) represents changes in *c-jun* expression with toxic concentrations.

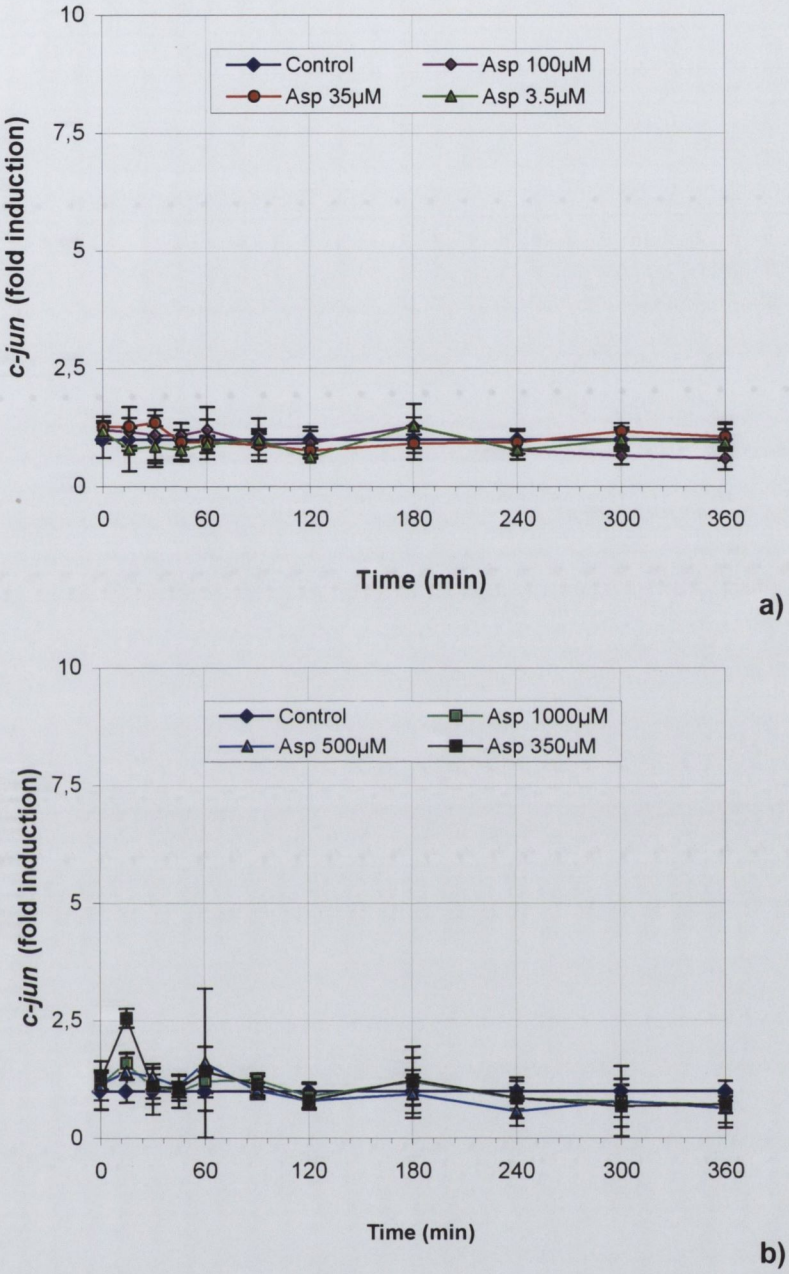


Figure 4.32: *c-jun* mRNA expression in mCGCs treated with various concentrations of Asp

Primary cultures of mCGCs (7 DIV) were exposed to various concentrations of Asp, for up to 360 min. Following treatment, the cells were lysed and total RNA was extracted and the amount of *c-jun* and 18S quantified by RT-PCR. The *c-jun* expression values were normalised to 18S expression, which served as the internal control. The results above refer to the fold induction of *c-jun* expression compared to untreated, time-matched controls. Data represent mean ± s.d. values of triplicate RT-PCR reactions derived from one individual experiment. Figure 4.32 a) represents the *c-jun* changes with non-toxic and partially toxic concentrations of Asp while b) represents changes in *c-jun* expression with toxic concentrations.

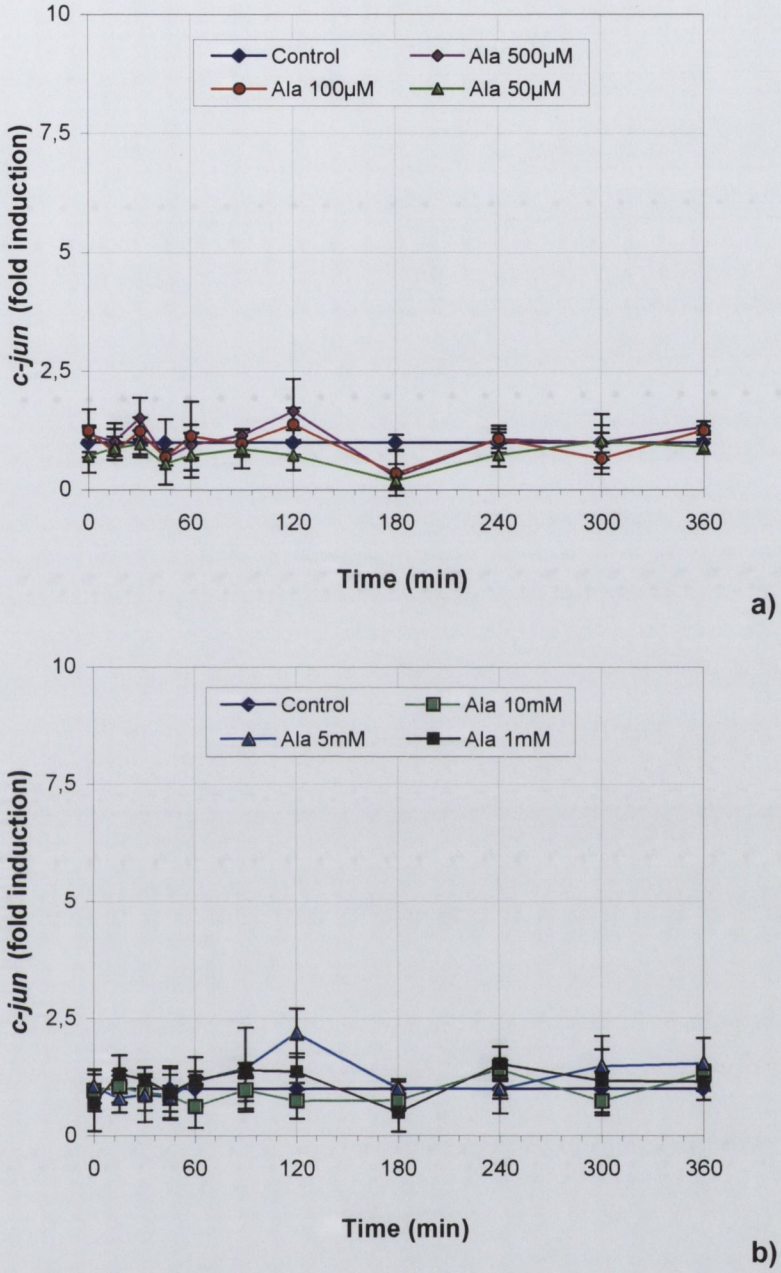
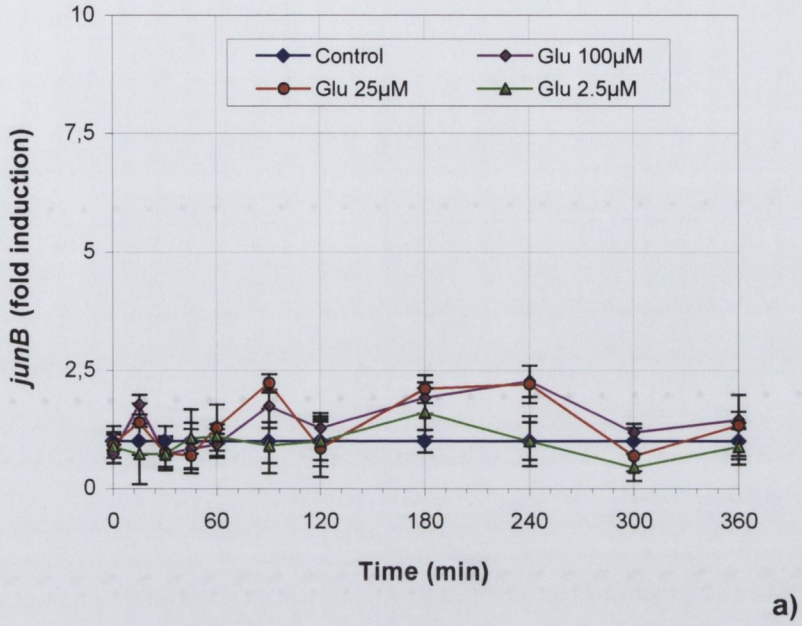
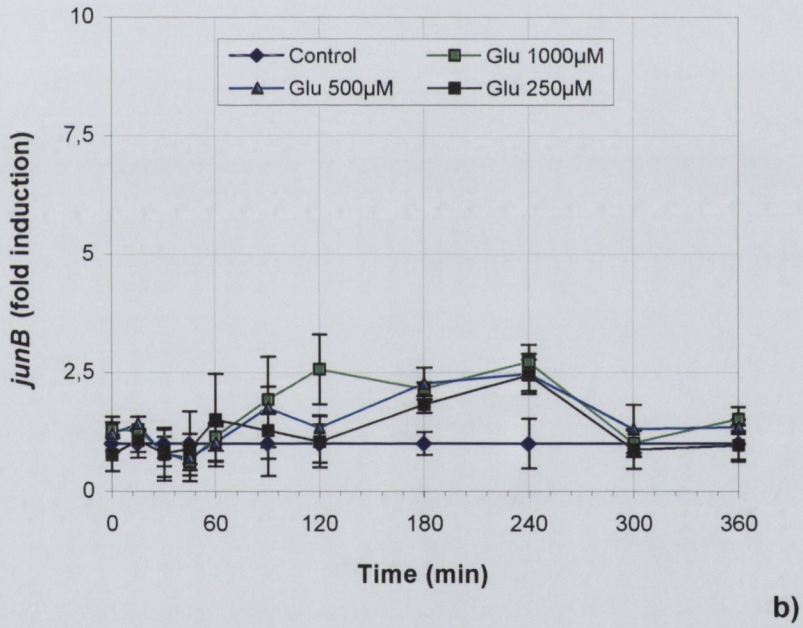


Figure 4.33: *c-jun* mRNA expression in mCGCs treated with various concentrations of Ala

Primary cultures of mCGCs (7 DIV) were exposed to various concentrations of Ala, for up to 360 min. Following treatment, the cells were lysed and total RNA was extracted and the amount of *c-jun* and 18S quantified by RT-PCR. The *c-jun* expression values were normalised to 18S expression, which served as the internal control. The results above refer to the fold induction of *c-jun* expression compared to untreated, time-matched controls. Data represent mean ± s.d. values of triplicate RT-PCR reactions derived from one individual experiment. Figure 4.33 a) represents the *c-fos* changes with low concentrations of Ala while b) represents changes in *c-jun* expression with high concentrations.



a)



b)

Figure 4.34: *junB* mRNA expression in mCGCs treated with various concentrations of Glu

Primary cultures of mCGCs (7 DIV) were exposed to various concentrations of Glu, for up to 360 min. Following treatment, the cells were lysed and total RNA was extracted and the amount of *junB* and 18S quantified by RT-PCR. The *junB* expression values were normalised to 18S expression, which served as the internal control. The results above refer to the fold induction of *junB* expression compared to untreated, time-matched controls. Data represent mean ± s.d. values of triplicate RT-PCR reactions derived from one individual experiment. Figure 4.34 a) represents the *junB* changes with non-toxic and partially toxic concentrations of Glu while b) represents changes in *junB* expression with toxic concentrations.

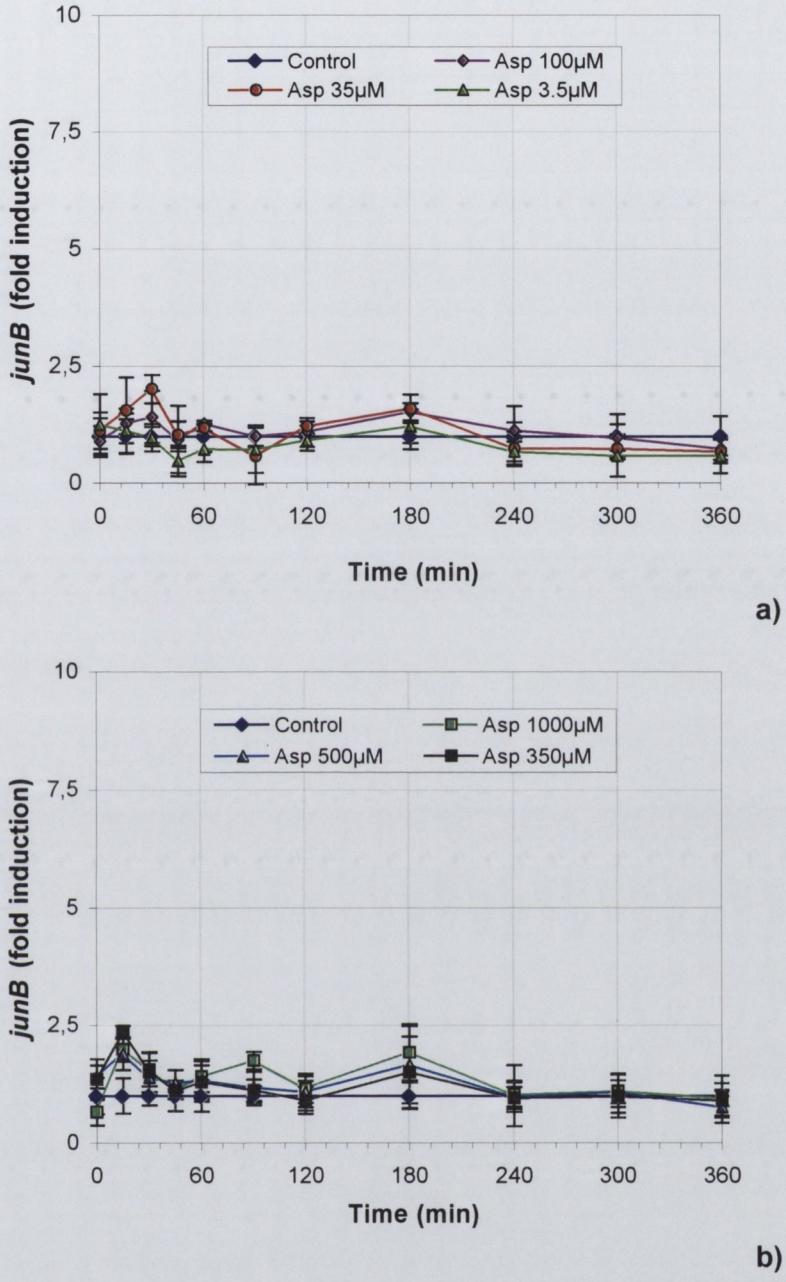


Figure 4.35: *junB* mRNA expression in mCGCs treated with various concentrations of Asp

Primary cultures of mCGCs (7 DIV) were exposed to various concentrations of Asp, for up to 360 min. Following treatment, the cells were lysed and total RNA was extracted and the amount of *junB* and 18S quantified by RT-PCR. The *junB* expression values were normalised to 18S expression, which served as the internal control. The results above refer to the fold induction of *junB* expression compared to untreated, time-matched controls. Data represent mean ± s.d. values of triplicate RT-PCR reactions derived from one individual experiment. 4.35 a) represents the *junB* changes with non-toxic and partially toxic concentrations of Asp while b) represents changes in *junB* expression with toxic concentrations.

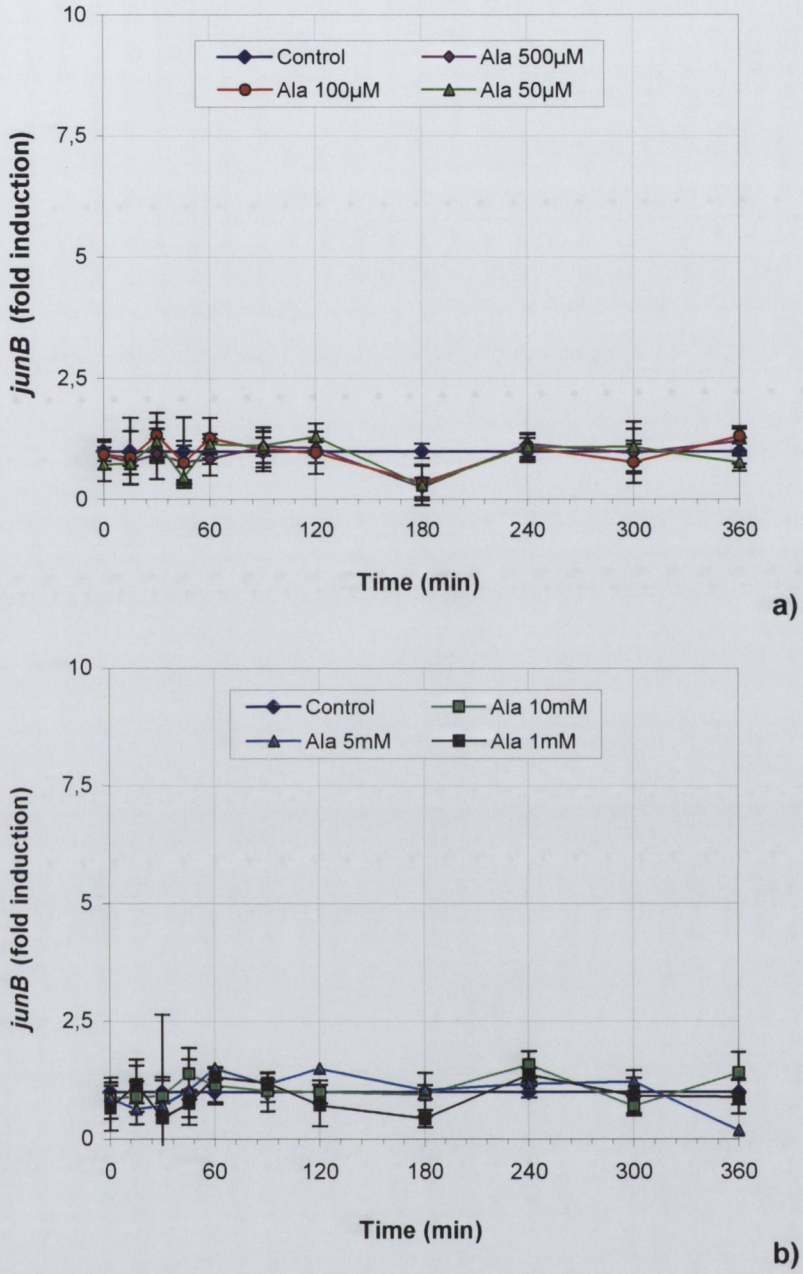


Figure 4.36: *junB* mRNA expression in mCGCs treated with various concentrations of Ala

Primary cultures of mCGCs (7 DIV) were exposed to various concentrations of Ala, for up to 360 min. Following treatment, the cells were lysed and total RNA was extracted and the amount of *junB* and 18S quantified by RT-PCR. The *junB* expression values were normalised to 18S expression, which served as the internal control. The results above refer to the fold induction of *junB* expression compared to untreated, time-matched controls. Data represent mean ± s.d. values of triplicate RT-PCR reactions derived from one individual experiment. Figure 4.36 a) represents the *junB* changes with low concentrations of Ala while b) represents changes in *junB* expression with high concentrations.

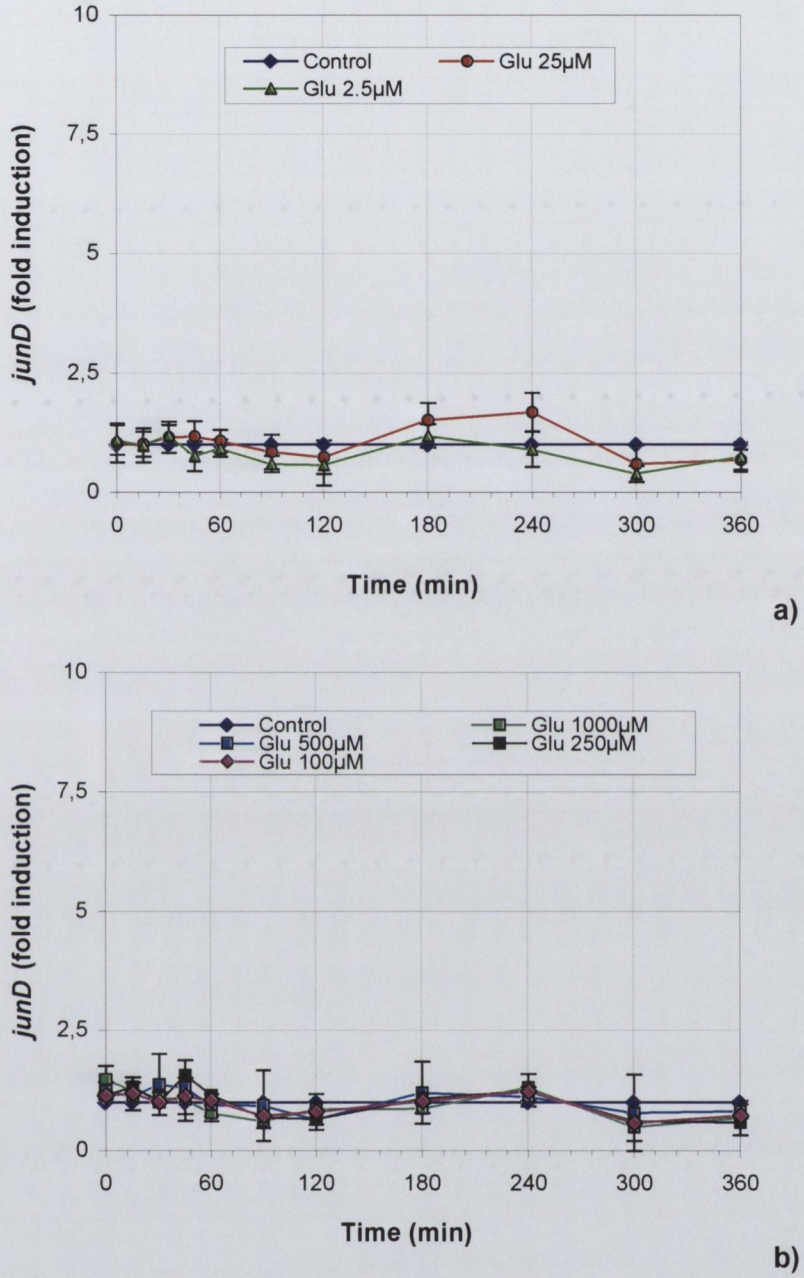
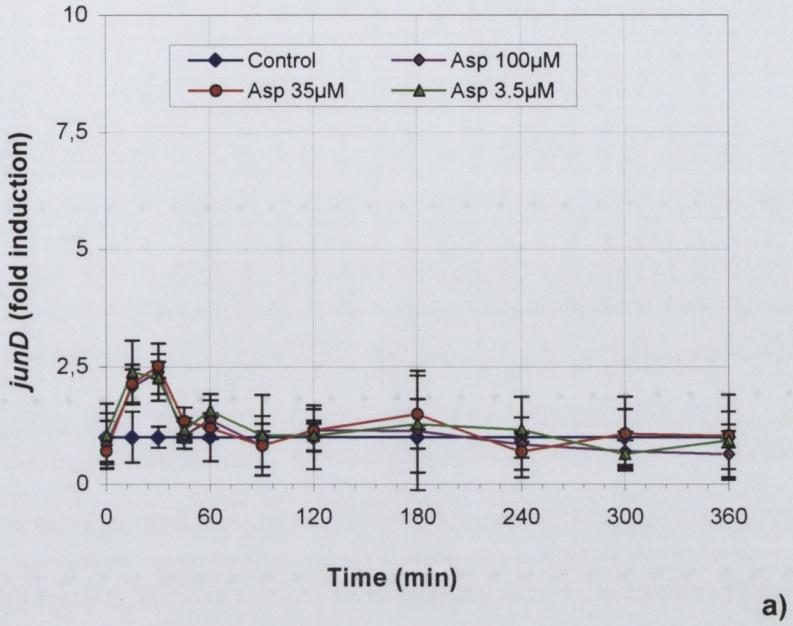


Figure 4.37: *junD* mRNA expression in mCGCs treated with various concentrations of Glu

Primary cultures of mCGCs (7 DIV) were exposed to various concentrations of Glu, for up to 360 min. Following treatment, the cells were lysed and total RNA was extracted and the amount of *junD* and 18S quantified by RT-PCR. The *junD* expression values were normalised to 18S expression, which served as the internal control. The results above refer to the fold induction of *junD* expression compared to untreated, time-matched controls. Data represent mean ± s.d. values of triplicate RT-PCR reactions derived from one individual experiment. Figure 4.37 a) represents the *junD* changes with non-toxic and partially toxic concentrations of Glu while b) represents changes in *junD* expression with toxic concentrations.



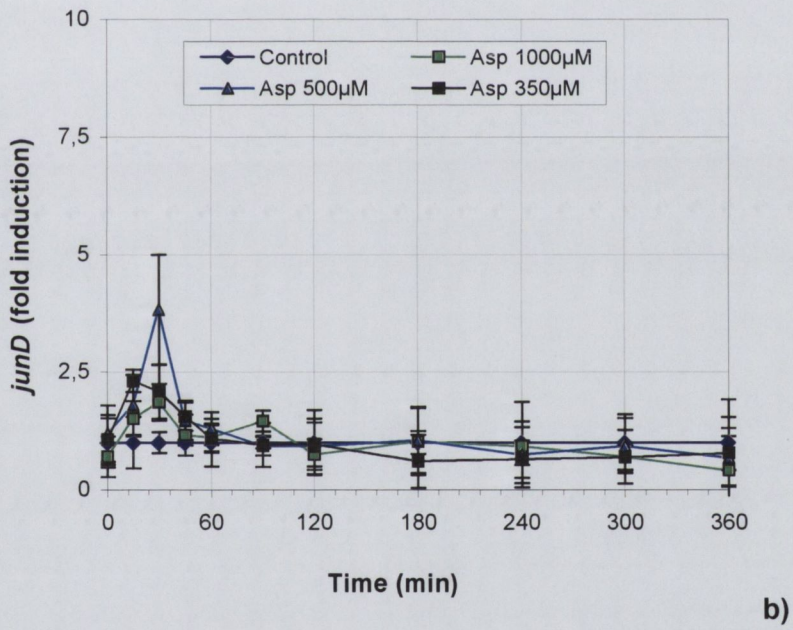
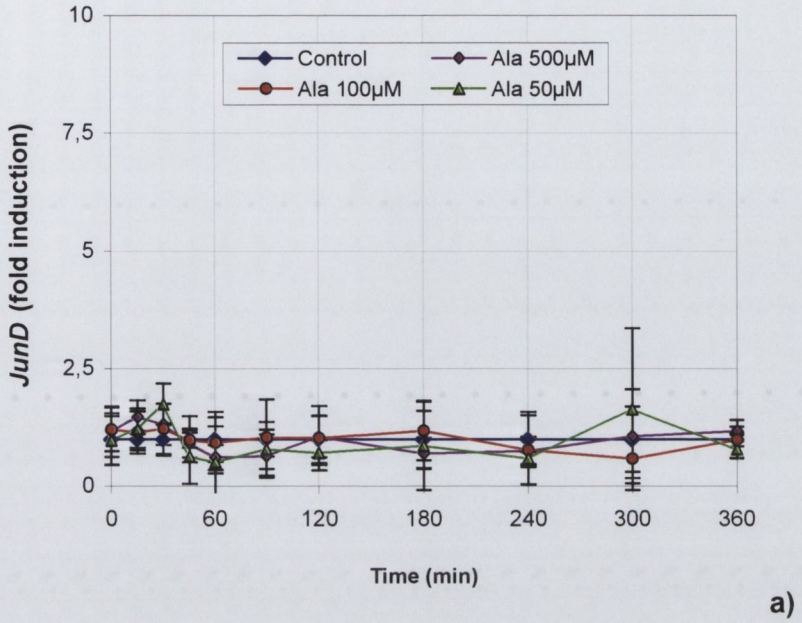
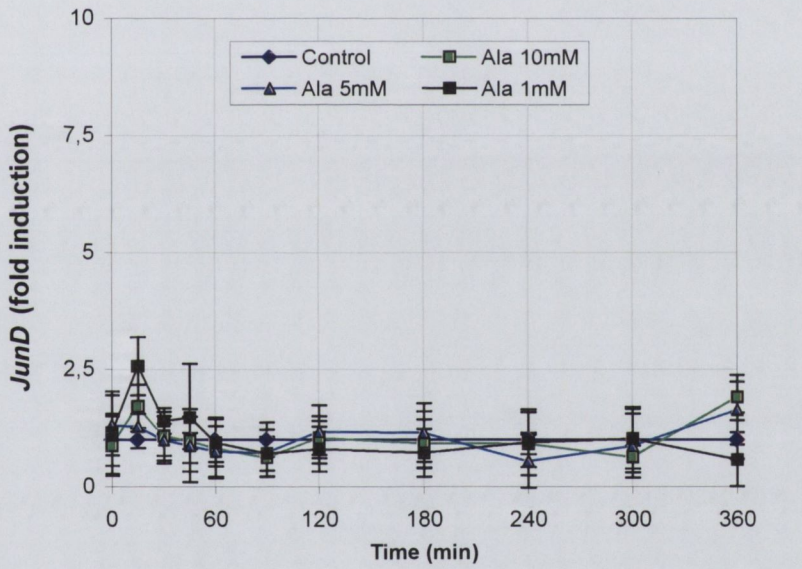


Figure 4.38: *junD* mRNA expression in mCGCs treated with various concentrations of Asp

Primary cultures of mCGCs (7 DIV) were exposed to various concentrations of Asp, for up to 360 min. Following treatment, the cells were lysed and total RNA was extracted and the amount of *junD* and 18S quantified by RT-PCR. The *junD* expression values were normalised to 18S expression, which served as the internal control. The results above refer to the fold induction of *junD* expression compared to untreated, time-matched controls. Data represent mean ± s.d. values of triplicate RT-PCR reactions derived from one individual experiment. Figure 4.38 a) represents the *junD* changes with non-toxic and partially toxic concentrations of Asp while b) represents changes in *junD* expression with toxic concentrations.



a)



b)

Figure 4.39: *junD* mRNA expression in mCGCs treated with various concentrations of Ala

Primary cultures of mCGCs (7 DIV) were exposed to various concentrations of Ala, for up to 360 min. Following treatment, the cells were lysed and total RNA was extracted and the amount of *junD* and 18S quantified by RT-PCR. The *junD* expression values were normalised to 18S expression, which served as the internal control. The results above refer to the fold induction of *junD* expression compared to untreated, time-matched controls. Data represent mean ± s.d. values of triplicate RT-PCR reactions derived from one individual experiment. Figure 4.39 a) represents the *junD* changes with low concentrations of Ala while b) represents changes in *junD* expression with high concentrations.

4.3 Discussion

In many neurological disorders, injury to neurons may be caused at least in part by over stimulation of receptors for EAAs, including Glu and Asp. Glu is the principal excitatory neurotransmitter in the brain and its interactions with specific membrane receptors are responsible for many neurological functions, including cognition, memory, movement and sensation (Gasic & Hollmann, 1992). In addition, excitatory neurotransmitters are important in influencing the developmental plasticity of synaptic connections in the nervous system. However, in a variety of pathologic conditions, including stroke and various neurodegenerative disorders, excessive activation of Glu receptors may mediate neuronal injury or death. Olney (1969) coined the term "excitotoxicity" for this condition, which may constitute a final common pathway for neuronal injury. This form of injury appears to be predominantly mediated by excessive influx of calcium ions into neurons through ionic channels, triggered by activation of Glu receptors, which in turn co-ordinately activates a series of genes known as *immediate early genes* (*IEGs*). *IEGs* encode transcription factors that serve as nuclear couplers of early cytoplasmic events to long-term changes in gene expression and cellular phenotype. Most prominent among the *IEGs* are the *fos* and *jun* gene families (Morgan and Curran, 1991; Hughes and Dragunow, 1995). The *fos* and *jun* gene families encode proteins and the interaction between these proteins forms the transcription factor, AP-1. The AP-1 complex binds with high affinity to the DNA regulatory elements (termed AP-1 sites) in the promoter and enhancer regions of many genes, and has been shown to be able to affect both positive and negative regulation of their expression.

The first aim of this study was to examine whether the time- and concentration-dependant profiles of *c-fos* mRNA induction, found by Griffiths *et al.* (2000) using the Northern blot method, could be re-produced in our laboratory (Bayer AG) using the more sensitive technology of real-time RT-PCR. Mature cultures of mCGCs were exposed to various concentrations of the EAAs, Glu and Asp, and the levels of expression of *c-fos* mRNA measured. The results revealed that different time profiles of *c-fos* mRNA expression were obtained, which were dependent on EAA concentration. It was found that following exposure of the granule cells to non-toxic concentrations of the EAAs, Glu and Asp, a rapid, transient increase in *c-fos* mRNA levels occurred. This finding is consistant with reports by Szekely *et al.* (1989). However, with toxic concentrations of the EAAs a change in the time-profile and level of *c-fos* expression was found. The profile of *c-fos* expression

changed from a rapid, transient increase to that of a delayed, elevated and sustained increase. These studies show that the application of quantitative, real-time RT-PCR methodology to the measurement of EAA-induced *c-fos* expression, provides similar time- and concentration-dependent profiles to that obtained by Gorman *et al.* (1995), Meredith *et al.* (1996) and Griffiths *et al.* (1997, 2000) using Northern blot analysis, thus encouraging further studies to employ this highly sensitive, quantifiable and reproducible technique.

Exposure of the mCGCs to the non-EAA, Ala, did not induce *c-fos* mRNA expression. Metabolically, Ala is a non-essential dietary, glucogenic amino acid, while of neurochemical interest it has been shown to be an agonist at the inhibitory glycine receptor. Additionally, the neurotoxic compound paraquat did not induce *c-fos* expression. Both can therefore be considered as negative controls in the context of this *in vitro* assay for excitotoxicity, based on early response gene measurement by real-time RT-PCR.

The mechanism of EAA-induced, sustained increases in *c-fos* mRNA levels, as measured by real-time RT-PCR, was examined using the ionotropic EAA receptor antagonists, AP5 (a selective NMDA antagonist) and CNQX (a selective antagonist at non-NMDA ionotropic receptors). The results demonstrated that AP5 completely inhibited the *c-fos* response induced by partially toxic concentrations of Glu. It was also found that the effectiveness of AP5, in blocking the excitotoxic *c-fos* response, was inversely proportional to the concentrations of EAAs used. The excitotoxic profile induced by toxic concentrations of Glu or Asp (100 μM) was partially inhibited by AP5, with the profile being shifted to that of an earlier peaking, less-sustained *c-fos* mRNA expression. With higher toxic concentrations of the EAAs, AP5 had little or no inhibitory effect. With all toxic concentrations of the EAAs, pre-treatment with CNQX did not prevent the excitotoxic *c-fos* response. Thus, elevated and sustained *c-fos* mRNA expression, induced by toxic concentrations of Glu or Asp, is prevented by selective antagonism of the NMDA receptor but not of the AMPA/Kainate receptors. It can be concluded therefore, that excitotoxicity is mediated through the specific activation of the NMDA receptor subtype in mCGCs. These results are in general agreement with the cytotoxicity profile of EAA-induced neurotoxicity, measured by the MTT assay, (see Section 3.2.2) which showed that Glu, Asp and NMDA induced neurotoxicity were inhibited by AP5 but not by CNQX.

Griffiths *et al.* (1997, 2000) devised a *c-fos* mRNA ratio test, which they proposed could be used as a valid predictive index of *in vitro* excitotoxicity. The test was based on the observation that non-toxic concentrations of EAAs induced a rapid, transient induction of

c-fos mRNA in mCGCs following 30 min treatment, while toxic concentrations induced delayed, elevated and sustained *c-fos* mRNA expression at 240 min. For a compound to be predicted as excitotoxic three criteria were required to be fulfilled, firstly, a ratio (240/30 min) of less than 1 (that is, for a transient expression) should be found with non-toxic concentrations while, secondly, toxic concentrations should give a ratio greater than 1 (that is, for sustained elevated levels). Thirdly, the excitotoxin-induced elevation of the *c-fos* mRNA ratio should be prevented in the presence of an NMDA receptor antagonist. Thus, NMDA receptor-mediated inductions of *c-fos* mRNA should be attenuated or inhibited by AP5, while CNQX should have no effect (Griffiths *et al.*, 2000).

Originally, prior to the above experiments being performed, an EU Biotech Demonstration project (Contract No. BIO4-CT98-0223) had been established to investigate whether the *c-fos* mRNA ratio test, devised by Griffiths *et al.* (1997, 2000), could be used to predict the excitotoxic properties of different compounds in a screen. As part of the validation procedure for the *c-fos* mRNA ratio test, mCGCs were cultured and exposed to 17 chemical compounds by Griffiths and colleagues at the University of St. Andrews, Scotland, at a "low" and "high" concentration, for 30 and 240 min, in the presence and absence of either AP5 or CNQX. The 17 compounds chosen were representative of 4 functionally different classes.

The first group, the excitotoxins, were comprised of Glu, Asp and L-CSA. Low concentrations of all 3 established excitotoxins induced a rapid and transient expression of *c-fos* mRNA with *c-fos* 240/30 min ratios less than 1. High concentrations, however, changed the profile of transient *c-fos* expression to that of a more sustained one giving elevated *c-fos* mRNA 240/30 min ratios. However, the receptor pharmacology, as defined by AP5 inhibition, was uncertain. Pre-treatment with CNQX offered no protection against the excitotoxic *c-fos* response induced by all 3 compounds. Overall, all 3 excitotoxins induced the sustained profile of *c-fos* expression, characteristic of excitotoxicity. Furthermore, the lack of antagonism by CNQX demonstrates the non-involvement of AMPA and/or kainate receptors in mediating the excitotoxic *c-fos* response.

The compounds included in the second group, the neurotoxic but non-excitotoxic compounds, were lindane, veratridine (a voltage gated Ca^{2+} inhibitor), MPP^+ iodide and acrylamide. Lindane had no effect on *c-fos* mRNA expression levels and was thus correctly predicted as non-excitotoxic. Veratridine showed a ratio above 1 at the high concentration and the ratio was even higher in the presence of AP5, both results being typical of a membrane depolarising agent and not of an excitotoxic compound. MPP^+

iodide and acrylamide both induced a small increase in *c-fos* mRNA expression, which was antagonised by AP5. However, the small changes make it difficult to draw firm conclusions. Therefore, the *c-fos* ratio method correctly predicted the non-excitotoxic properties of 2 members of this second group of compounds. The third group of neuroactive but non-toxic compounds were comprised of taurine, Ala, nimodipine, GABA, pentylenetetrazole, valproate and PK 11195. No induction of *c-fos* mRNA was observed in the presence of any of these compounds with *c-fos* mRNA 240/30 min ratios below 1 for both the low and high concentrations. Ratios were also below 1 for high concentrations in the presence of either AP5 or CNQX. Therefore, it can be concluded that the *c-fos* ratio test correctly predicted that all members of this group of compounds were non-excitotoxic.
The fourth group contained compounds that are toxic to other target organelles, namely, NaCN, paraquat and thalidomide. Both NaCN and thalidomide gave ratios below 1 with high concentrations. We concluded that the *c-fos* ratio predicted correctly that both NaCN and thalidomide are non-excitotoxic to mCGCs, even though they may be toxic elsewhere. Although, high concentrations of paraquat gave a *c-fos* ratio above 1, this ratio was not considered as excitotoxic, as it was shown that paraquat has no effect on *c-fos* induction with time or concentration. Ratios were below 1 for high concentrations of all 3 compounds in the presence of either AP5 or CNQX. Thus, the *c-fos* ratio test predicted correctly that all members of this group of compounds are non-excitotoxic to mCGCs.
Overall, the *c-fos* mRNA 240/30 min ratio test correctly predicted the properties of all 4 classes of chemical compounds but only provided that each result was interpreted individually to allow for such effects as low levels of expression, high initial levels of expression and lack of antagonism due to high agonist concentrations.
It was decided, following consideration of the previous experiments, to modify the original protocol in two ways. Firstly, to focus on the group of excitotoxins in the following experiment by increasing the number of excitotoxins used (from 3 to 14) and secondly, to use a modified antagonist protocol in the *c-fos* mRNA ratio test. Primary mCGCs were again cultured by the University of St. Andrews and exposed to 19 chemical compounds at a "low" and "high" concentration. Exposures were undertaken for 30 or 240 min in the presence and absence of an antagonist cocktail containing the NMDA receptor antagonist, TCP, and the non-NMDA receptor antagonist, NBQX. The 19 compounds chosen were representative of the same 4 classes of compounds measured earlier.
The excitotoxins comprised the following, Glu, Asp, L-HCA, D-HCA, KA, TG, (*S*)-CPW 399, L-CSA, $ZnCl_2$, L-HCSA, L-SSC, QA, NMDA and D-HCSA. All of the known or

potential excitotoxins induced elevated and sustained *c-fos* mRNA expression with high concentrations, with *c-fos* ratios above 1. Apart from TG, QA, D-HCSA and L-HCSA, which showed elevated *c-fos* ratios at both low and high concentrations, all of the remaining excitotoxins exhibited ratios, which although above 1 for the non-toxic parameter, were considerably less than those observed with higher, toxic concentrations. KA exhibited an elevated *c-fos* mRNA ratio with the high concentration, which was not inhibited by the NBQX/TCP antagonist cocktail. The lack of effect of the antagonist cocktail in preventing KA-induced neuronal death indicates the non-involvement of NMDA or AMPA receptors in the mechanism of KA toxicity and is in keeping with a non-NMDA receptor mediated action for KA. Indeed, the lack of antagonism in the case of KA was due to the choice of antagonists, as NBQX is a potent and highly selective antagonist of the ionotropic AMPA receptor (Suzdak *et al.*, 1993) and TCP is an antagonist of the NMDA receptor. TG, QA and D-HCSA exhibited elevated *c-fos* mRNA ratios with both low and high concentrations. However, the elevated *c-fos* responses were inhibited in the presence of the antagonist cocktail. These high ratios may be proportional to the potencies of the compounds, that is, an insufficiently low concentration may have been chosen for each of the 3 compounds to represent the non-toxic parameter. In the case of (*S*)-CPW 399, a putative AMPA agonist and therefore a putative excitotoxin, and also $ZnCl_2$, receptor antagonism, although expected, was not found and these results are as yet unexplained. However, the compounds did produce elevated and sustained *c-fos* mRNA expression and therefore would have been predicted as excitotoxins in the screen.

The second group contained the voltage-gated Ca^{2+} channel blocker, veratridine, which gave *c-fos* mRNA ratios above 1 with both low and high concentrations and also in the presence of the antagonist cocktail. Thus, according to the *c-fos* ratio method, these ratios correctly indicate a non-excitotoxic compound.

The third group comprised the "neuroactive but non-toxic" compounds, (-)-bicuculline and L-AP4. Non-toxic concentrations of (-)-bicuculline gave a *c-fos* mRNA ratio below 1. High concentrations were associated with *c-fos* ratios above 1, which failed to be blocked by the NBQX/TCP antagonist cocktail, indicating a non-excitotoxic compound. However, the expression levels of (-)-bicuculline were very low and are probably responsible for the artefactual ratio at high concentrations. L-AP4 exhibited ratios typical of an excitotoxic compound, that is, low concentrations gave a *c-fos* mRNA ratio below 1 while toxic concentrations were associated with *c-fos* ratios above 1. Additionally, the excitotoxic *c-fos* response was blocked by the NBQX/TCP antagonist cocktail giving ratios below 1.

Thus, (-)-bicuculline was correctly predicted as non-excitotoxic and the explanation behind the induction of *c-fos* by L-AP4 is as yet unknown.

The fourth group consisted of paracetamol and rotenone, which both showed *c-fos* mRNA ratios below 1 at low concentrations and ratios above 1 at high concentrations. In both cases, the ratio failed to drop below 1 in the presence of the NBQX/TCP cocktail. Therefore, using the *c-fos* ratio method, the results correctly indicate the non-excitotoxic properties of these compounds.

Tables 4.4 a) and b) summarise the predictive potential of the improved screen when using the *c-fos* ratio approach. Table 4.4 a) shows the results without consideration of the antagonism while Table 4.4 b) shows the results with such consideration. Tables 4.4 c) and d) summarise the predictive potential of the screen when an increase in *c-fos* expression from a non-toxic to a toxic parameter is examined. From the summarised results, it is clear that the *c-fos* ratio method is not an optimal assay for excitotoxicity screening. However, the tables also show that an increase in *c-fos* expression from a non-toxic to a toxic parameter can be used as a screen, obviating the need for producing 240/30 min ratios at all. Furthermore, there does not seem to be a major advantage in using antagonism as part of an initial screen. Rather, it would seem better to use a sequential approach, perhaps performing a second screen with antagonism on compounds shown positive in the original screen.

Because the collaborative screening experiments had produced results which, although in general showed a large degree of successful prediction, showed some difficulties due to factors such as choice of sub-optimal concentrations of agonists, antagonists, and also artefactual consequences for ratio determinations due to low expression levels, a ratio analysis was performed on the *c-fos* expression data obtained in the single laboratory experiments (shown in Figures 4.6 to 4.14). It was found that following treatment of the mCGCs with a non-toxic concentration of Glu, a transient increase in *c-fos* expression occurred at the 15 min time-point rather than at 30 min, as previously reported by Griffiths *et al.* (2000), leading to ratios around 1 for the non-toxic parameter. This ratio, however, serves as a predictor for the non-excitotoxic condition as toxic concentrations of the EAAs induced ratios of 6 – 14. It was also found that the protection capability of the NMDA receptor antagonist, AP5, was dependant on EAA concentration. Therefore the selection procedure of the high concentrations used may not be suitable for all compounds. For example, for both Glu and Asp, 100 μM was sufficient to induce the delayed, elevated and sustained *c-fos* excitotoxic profile, with *c-fos* 240/30 min ratios greater than 1.

	True	False
Positive	3	1
Negative	4	11

Table 4.4 a) Summary of predictive potential of the screen, using the *c-fos* ratio method, and including antagonism

The 3 true positive (excitotoxic) compounds were, Glu, Asp and D-HCA. The 1 false positive was L-AP4. The 4 true negative (non-excitotoxic) compounds were veratridine, (-)-bicuculline, paracetamol and rotenone. The 11 false negatives were L-HCA, KA, TG, (*S*)-CPW 399, L-CSA, $ZnCl_2$, L-HCSA, L-SSC, QA, NMDA and D-HCSA.

	True	False
Positive	3	1
Negative	4	11

Table 4.4 b) Summary of predictive potential of the screen, using the *c-fos* ratio method, without antagonism

The 3 true positive (excitotoxic) compounds were, Glu, Asp and D-HCA. The 1 false positive was L-AP4. The 4 true negative (non-excitotoxic) compounds were veratridine, (-)-bicuculline, paracetamol and rotenone. The 11 false negatives were L-HCA, KA, TG, (*S*)-CPW 399, L-CSA, $ZnCl_2$, L-HCSA, L-SSC, QA, NMDA and D-HCSA.

	True	False
Positive	9	1
Negative	4	5

Table 4.4 c) Predictive potential of the screen, based on the increase in *c-fos* expression from a non-toxic to a toxic parameter at 240 min, including antagonism

The 9 true positive (excitotoxic) compounds were, Glu, Asp, L-HCA, D-HCA, L-CSA, L-HCSA, L-SSC, QA and NMDA. The 1 false positive was L-AP4. The 4 true negative (non-excitotoxic) compounds were veratridine, (-)-bicuculline, paracetamol and rotenone. The 5 false negatives were KA, TG, (*S*)-CPW 399, $ZnCl_2$, and D-HCSA.

	True	False
Positive	12	3
Negative	2	2

Table 4.4 d) Predictive potential of the screen, based on the increase in *c-fos* expression from a non-toxic to a toxic parameter at 240 min, without antagonism

The 12 true positive (excitotoxic) compounds were Glu, Asp, L-HCA, D-HCA, KA, (*S*)-CPW 399, L-CSA, $ZnCl_2$, L-HCSA, L-SSC, QA and NMDA. The 3 false positives were L-AP4, rotenone and veratridine. The 2 true negative (non-excitotoxic) compounds were (-)-bicuculline and paracetamol. The 2 false negatives were TG and D-HCSA.

In addition, ratios less than 1 were observed in the presence of AP5, indicating an effective and specific antagonism of the NMDA receptor-mediated *c-fos* excitotoxic response. These results meet all criteria of the *c-fos* mRNA ratio test and correctly predict excitotoxicity. With higher toxic concentrations of both Glu and Asp (250 and 350 μM, respectively), although pre-treatment with AP5 failed to completely block the excitotoxic *c-fos* response, the ratios were somewhat reduced when compared to the ratios induced by the toxic concentrations alone, indicating partial antagonism by AP5. Conflicting reports have previously been published concerning the ability of AP5 (500 μM) to abolish the elevated and sustained *c-fos* profile induced by high, toxic concentrations of Glu (250 μM). Malcolm *et al.* (1997) and Griffiths *et al.* (1997, 2000) both found that 500 μM AP5 completely blocked the excitotoxic *c-fos* response induced by 250 μM Glu and gave *c-fos* ratios of less than 1. However, Gorman *et al.* (1995) reported that following exposure of mCGCs to 250 μM Glu, the sustained *c-fos* mRNA levels were only partially reduced by 500 μM AP5 (50% inhibition, as assessed by densitometry), a finding which correlates with the results outlined above. With all toxic concentrations, pre-treatment with CNQX failed to protect the neurons against excitotoxicity and thus ratios were greater than 1 indicating the lack of involvement of non-NMDA receptors in mediating the excitotoxic *c-fos* response.

Judging from these results it is necessary to be more explicit in the detail of the predictive *c-fos* excitotoxicity ratio test. For example, when the *c-fos* ratio method is used the early and late time-points chosen should be representative of the change in *c-fos* mRNA expression from that of the transient status to the more delayed, elevated and sustained status. Additionally, the concentrations of the NMDA receptor agonists used should be sufficient to induce the excitotoxic *c-fos* mRNA response but not so extreme that they are incapable of being blocked by a chosen fixed concentration of antagonist. Lastly, where a fixed concentration of an NMDA receptor antagonist is used it should be sufficient to block the excitotoxic responses mediated by toxic concentrations of a variety of compounds. Some of these conditions would be unachievable, of course, for screening of compounds, which being novel, would not have their Glu receptor interactions characterised. It would also seem that for this test to be useful, that is, robust and accurate in prediction, merely large differences in expression levels of *c-fos* are needed from a non-toxic to a toxic parameter, which perhaps obviates the need for producing 240/30 min ratios at all.

Finally, the last aim of this Chapter was to investigate whether other members of the *fos* (*fosB, fra-1 and fra-2*) and *jun* (*c-jun, junB and junD*) families of *IEGs* are involved in the

process of excitotoxicity. FosB was reported by Lidwell *et al.* (2000) as being selectably detectable only under excitotoxic conditions and therefore *fosB* was chosen as the first member of the *fos* family of *IEGs* to be examined. It was shown that following exposure of mCGCs to non-toxic concentrations of Glu, a transient increase in *fosB* mRNA expression was observed. However, toxic concentrations of Glu caused a change in the profile of *fosB* expression from a transient increase to that of a delayed, highly elevated and sustained increase. A similar phenomenon was observed with Asp. Our results demonstrate, therefore, that both *c-fos* and *fosB* are induced during excitotoxicity and that both exhibit different time profiles of expression depending on EAA concentration. Indeed, the levels of sustained *fosB* induction are much higher under excitotoxic conditions when compared to *c-fos*. As mentioned earlier, following exposure of the mGCCs to toxic concentrations of Glu, a delayed, sustained and elevated *c-fos* induction, of approx. 10 - fold the basal rate, occurred. Under the same excitotoxic conditions, a *fosB* mRNA induction occurred that was delayed, sustained and elevated to approx. 30 - fold that at the basal rate.

On account of these observations, it was necessary to examine whether this highly elevated and sustained *fosB* mRNA induction was a specific result of over-activation of the NMDA receptor subtype. Primary cultures of mCGCs were treated with different concentrations of Glu in the presence of AP5 or CNQX. It was found that AP5 completely inhibited the transient *fosB* expression at low, partially toxic concentrations of Glu whereas CNQX had no effect. With toxic concentrations of Glu although having no effect on the extremely elevated levels of excitotoxic *fosB* expression, AP5 did shift the profiles of *fosB* mRNA expression to that of an earlier peaking, less-sustained expression. However, with higher toxic concentrations of Glu, AP5 had no effect. In addition, CNQX, offered no protection against the delayed, elevated and sustained increases in *fosB* expression with toxic concentrations of Glu, demonstrating the specific involvement of NMDA receptors in the *fosB* excitotoxic response. As with *c-fos*, these results demonstrate that the different profiles of *fosB* expression, from an early, transient expression with low, non-toxic concentrations of Glu to that of a highly elevated and sustained expression with toxic concentrations of Glu, are mediated by over-activation of the NMDA receptor subtype in mCGCs. Similar excitotoxic *fosB* profiles were found following treatment of the mCGCs with various concentrations of Asp in the presence of AP5 or CNQX.

As shown for *c-fos*, exposure of the mCGCs to the non-EAA, Ala, or to paraquat did not induce *fosB* expression over 360 min. Both can therefore be considered as negative

controls in the context of a new *in vitro* assay for excitotoxicity, based on *c-fos* and *fosB* measurement by RT-PCR.

The expression of *fra-1* and *fra-2* and *c-jun, junB* and *junD* were also investigated in response to Glu and Asp and inductions were compared to the negative control, Ala. It was found that no significant increases in expression occurred for any of the other *fos* or *jun* family members with either the EAAs or non-EAA, Ala.

In conclusion, both *c-fos* and *fosB* give rise to a delayed, elevated and sustained increase in their respective expression levels, which is correlated in time- and concentration-dependency to EAA treatment of mature mCGCs and which is mediated specifically via the NMDA subtype of Glu receptors. Both *IEGs* can therefore be used as *in vitro* screens for predicting the potential excitotoxic properties of compounds. Furthermore, it has been shown that the *c-fos* ratio method devised by Griffiths *et al.* (1997, 2000) can be used. However, a large increase in *c-fos* expression, under excitotoxic conditions, obviates the need for the ratio method. In this Chapter, it was found that EAA-induced elevated and sustained transcription of *c-fos* and *fosB* correlates with excitotoxicity in mCGCs, using a new *in vitro* detection method based on real-time RT-PCR, and that *fosB* may be used as a more sensitive or as an additional biomarker in predicting excitotoxic outcomes. In the next Chapter, we will further our investigations into *c-fos* and *fosB* expression under both non-excitotoxic and excitotoxic conditions in rat cortical neurons, as the rat is the preferred species in regulatory and non-regulatory toxicity testing.

Chapter 5

Expression of *IEGs* in Rat Cortical Neurons.

5.1 Introduction

The stimulation of neurons by neurotransmitters or neurotropic factors elicits changes in gene expression that are critical for neuronal survival, differentiation and the adaptive responses of mature neuronal cell types (Greenberg *et al.*, 1986; Morgan and Curran, 1986). Within minutes of neurotransmitter release, the expression of a family of genes termed *immediate early genes* (*IEGs*) is induced in the post-synaptic neuron. *IEGs* are genes that are responsive to trans-synaptic stimulation and membrane electrical activity in neuronal cells. Transcription of these genes occurs rapidly and transiently, within minutes of stimulation. Many *IEGs* encode transcription factors that then induce subsequent waves of delayed response gene expression. Delayed response genes encode proteins that are likely to be determinants of neuronal plasticity. These proteins may include neurotransmitter-synthesizing enzymes, neurotransmitter receptors as well as structural components of the synapse. The prototypic *IEG*, *c-fos*, has been reported to be both rapidly and transiently transcribed in response to a variety of neurotransmitters that trigger Ca^{2+} influx in *in vitro* cell culture systems (Greenberg *et al.*, 1986; Curran and Morgan, 1995; Bading *et al.*, 1993). The *c-fos* gene encodes a transcription factor, c-Fos, which forms a heterodimer with members of the Jun family of transcription factors via a leucine zipper, forming the transcription factor complex AP-1. AP-1 regulates the expression of late response genes that contain Fos/Jun-binding sites (consensus 5'-TGAG/CTCA-3') within their promoters (Curran and Franza, 1988). The function of the AP-1 complex is therefore to activate the transcription of a variety of target genes in response to stimulation of cell surface receptors that are connected to several different signal transduction pathways (Angel and Karin, 1991). These downstream target genes mediate a variety of responses including differentiation and neuronal transduction. Thus, rather than being a specialised executor of a unique response to exogenous stimuli, the AP-1 complex plays a general role in the transduction of signals from the membrane to the nucleus. For example, Jun and Fos transcription factors exert a potent biological role by their control of gene transcription of, for example, nerve growth factors (Hengerer *et al.*, 1990) and tyrosine hydroxylase (Ginzang-Ginsberg *et al.*, 1990). Moreover, Jun and Fos proteins positively and negatively modulate the transcriptional activities of numerous other transcription factors such as CREB and ATF proteins (Sassone-Corsi *et al.*, 1991). However, reports suggest that over-expression of the proto-oncogene *c-fos* may contribute to neuronal cell death *in vivo* (Pennypacker *et al.*, 1994; Shan *et al.*, 1997) and

in vitro (Gorman *et al.*, 1995; Meredith *et al.*, 1996; Grifiths *et al.*, 1997). These findings led to the suggestion that over-expression of *c-fos* could be used as an indicator of excitotoxicity in *in vitro* neuronal systems. Grifiths *et al.* (1997, 2000) proposed that a ratio between *c-fos* mRNA expression levels at 30 min and 240 min following stimulation could be used as a specific test to predict excitotoxicity. All of their investigations employed the method of Northern blot analysis. However, this method contains many limitations, such as low sensitivity and low throughput.

The purpose of Chapter 4 was therefore to investigate the involvement of *IEGs* in excitotoxicity using the high-throughput method of real-time RT-PCR. In Chapter 4, members of the *fos* and *jun* families of *IEGs* were examined individually, over 360 min, in primary cultures of mouse cerebellar granule cells (mCGCs; 7 DIV) undergoing excitotoxic cell death. The *fos* family is comprised of 4 members, *c-fos, fosB, fra-1* and *fra-2*. It was found that the predominant EAA, Glu, and also Asp, induced the increased expression of *c-fos* and *fosB*, both of which belong to the *fos* family of genes. None of the remaining *IEGs* showed any significant signs of increased expression. The profiles of both *c-fos* and *fosB* were similar in two respects. Both *IEGs* exhibited patterns of induction that were time- and concentration-dependent, that is, a transient induction in *IEG* mRNA expression was found with low concentrations of EAAs and this profile changed to a more delayed, elevated and sustained profile with higher, toxic concentrations of the EAAs. Moreover, the expression of both *c-fos* and *fosB* was NMDA-receptor mediated. The only difference between the excitotoxic induction patterns of both *c-fos* and *fosB* was in the levels of induction. Surprisingly, *fosB* showed the highest induction levels in mCGCs undergoing EAA-induced excitotoxic cell death. Two questions arose from our investigations in mCGCs. The first was whether *fosB* was indeed the most sensitive molecular biomarker for predicting potential excitotoxic outcomes and the second was whether the profiles of *c-fos* and *fosB* induction were the same in rat cortical neurons as those observed in mCGCs.

Thus, it was found of particular interest to perform a comparative investigation with other members of the *fos* and *jun* families of *IEGs*, in particular *c-fos* and *fosB*, using primary cultures from a different species and brain area. Primary cultures of rat cortical neurons were exposed to identical concentrations of both Glu and Asp, as used in the mCGC investigations, over the same time-course (0 - 360 min). The expression levels of the *IEGs* were measured using real-time RT-PCR.

Aims of this Chapter

The first aim of this Chapter was to investigate using a second primary cell culture system from a different species and brain region, the involvement of *IEGs* in excitotoxicity, in particular whether the *IEGs c-fos* and *fosB* are induced by different EAAs in primary cultures of rat cortical neurons.

The second aim was to investigate, using real-time RT-PCR, the excitotoxicity-related changes, concentration-dependencies and receptor specificities of *c-fos* and *fosB* expression in rat cortical neurons.

The third aim was to compare the potential of *c-fos* and *fosB* in the characterisation of excitotoxic effects of much larger numbers of compounds, that is, which *IEG* is a specific biomarker for screening. The levels of *c-fos* and *fosB* expression were investigated in rat cortical neurons treated with 4 different groups of compounds, subdivided according to established characteristics, namely, Group 1- excitotoxins, Group 2-neurotoxic but non-excitotoxic compounds, Group 3- neuroactive but non-toxic compounds and Group 4- compounds that are toxic to other target organelles, at one time-point.

Finally, the fourth aim was to investigate changes in the expression of other members of the *fos* (*fra-1 and fra-2*) and *jun* (*c-jun, junB and junD*) families of *IEGs* in rat cortical neurons undergoing Glu-mediated excitotoxic cell death.

5.2 Results

5.2.1 *c-fos* mRNA expression varies with time and Glu concentration

In Chapter 4, it was demonstrated that stimulation of primary mCGCs with Glu induced changes in the profile of *c-fos* expression that were dependent on both time and concentration. It was found that toxic concentrations of Glu induced a change in *c-fos* expression from that of a transient to a more delayed, elevated and sustained expression. The delayed, elevated and sustained expression of *c-fos* mRNA, induced by toxic concentrations of Glu, is indicative of excitotoxicity. The first aim of this Chapter was to investigate whether *c-fos* was similarly induced in neurons from a different species and brain region. Experiments were performed using the same time course and concentration range as in the mCGC experiments.

Primary cultures of rat cortical neurons were prepared as described in Section 2.2.2 and cultured for 13 days before exposure to various concentrations of Glu from 0 to 360 min. Following treatment, the cells were lysed, total RNA was extracted and the amounts of *c-fos* and 18S quantified by real-time RT-PCR. *c-fos* mRNA expression levels were normalised to the internal control, 18S, before calculation of the induction values of *c-fos* when compared to the untreated control neurons. As found in the mCGCs, exposure of rat cortical neurons (13 DIV) to various concentrations of Glu induced different time courses of *c-fos* mRNA expression which were dependent on Glu concentration. The profiles of Glu-mediated *c-fos* induction are shown in Figures 5.1 a) & b).

When rat cortical neurons (13 DIV) were exposed to non-toxic concentrations of Glu (2.5 μM), a transient increase in *c-fos* mRNA levels was observed, before returning to the basal level. Exposure to a partially toxic concentration of Glu (25 μM) resulted in an early, transient increase of *c-fos* mRNA expression, which reached maximal inductions of 40 fold before gradually decreasing (see Figure 5.1 a)). Exposure to a toxic concentration of Glu (100 μM) also induced a transient profile of *c-fos* mRNA expression, which reached maximal inductions of 100 fold the basal level before gradually decreasing.

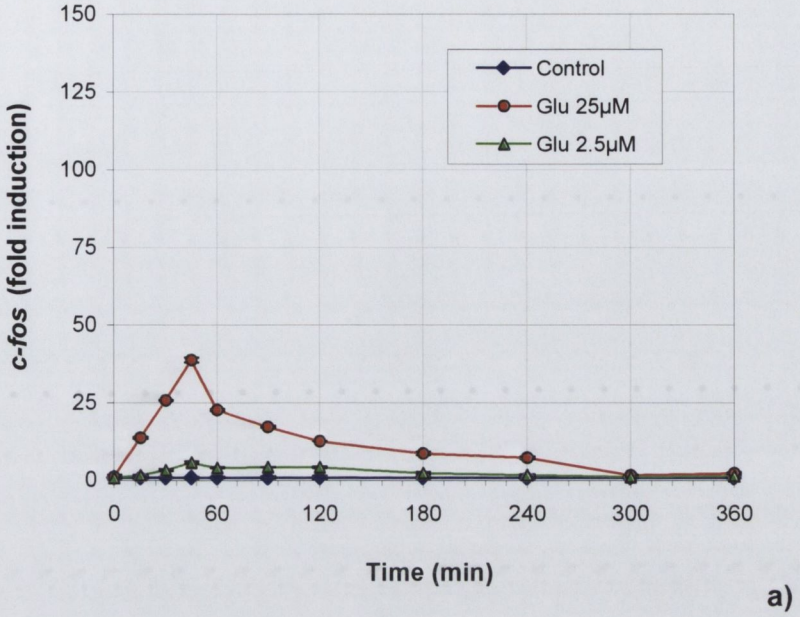
When cortical neurons were exposed to higher toxic concentrations of Glu, markedly different profiles of *c-fos* expression were observed. There appeared to be an early, rapid increase in *c-fos* mRNA expression, which remained sustained for the rest of the test period (see Figure 5.1 b)).

The transient expression of *c-fos* mRNA, detected using real-time RT-PCR, in rat cortical neurons exposed to non-toxic concentrations of Glu is consistent with that found previously in cultures of mCGCs (see Figure 4.6 a)). Furthermore, the levels of *c-fos* induction in both species were similar. With partially toxic concentrations of Glu (25 μM), a difference was observed in the expression profile of *c-fos* mRNA in mCGCs and rat cortical neurons. In primary mCGCs cultures, a delayed, elevated and sustained profile of *c-fos* expression was induced. Maximal levels of induction were reached at 120 min and were sustained for 240 min. However, in rat cortical neurons a sharp transient increase in *c-fos* mRNA expression was observed, with maximal levels reached at 45 min. After the 45 min time-point, *c-fos* mRNA expression gradually decreased. Another difference was in the levels of induction. In mCGCs, maximal inductions of 4 times the basal level were observed with partially toxic concentrations of Glu (25 μM) whereas, in rat cortical neurons maximal inductions of 40 fold the basal level were observed.

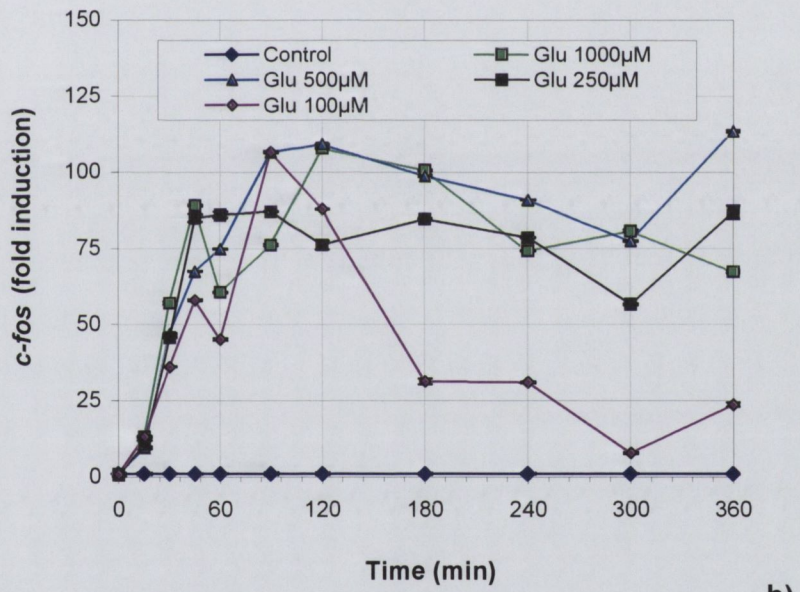
With a toxic concentration of Glu (100 μM), a transient increase in *c-fos* expression was induced in rat cortical neurons, which reached maximal inductions of 100 fold before gradually decreasing. This profile is in contrast with the *c-fos* profile observed in mCGCs with 100 μM Glu. In mCGCs, a delayed elevated and sustained increase in *c-fos* mRNA expression occurred with maximal inductions of approximately 7 fold (see Figure 4.6 b)). Differences were also observed in the *c-fos* expression profiles with higher, toxic concentrations of Glu (250 - 500 μM). In mCGCs, a delayed, elevated and sustained increase was observed with maximal inductions of 6 – 10 fold the basal level at 240 min (see Figure 4.6 b)). In rat cortical neurons, a sharp increase in *c-fos* expression values was observed with maximal inductions of 100 fold the basal level at 90 min, which remained sustained over the 360 min time course.

Despite the large differences in the levels of expression of *c-fos* mRNA between the two cell culture systems, the change in induction from the partially toxic profile of *c-fos* to that of the elevated and sustained excitotoxic profile is the same, that is, a 2.5 fold difference was observed between the profiles induced by 25 μM Glu and those induced by the higher toxic concentrations of 100 – 500 μM Glu in both cell culture systems.

In conclusion, *c-fos* can be suggested as a sensitive biomarker for EAA induced excitotoxicity, irrespective of species and brain region. Furthermore, the high levels of *c-fos* induction and the preference of the rat in regulatory and non-regulatory toxicity testing, elect the rat as a sensitive species for *in vitro* gene expression analysis.



a)



b)

Figure 5.1: *c-fos* mRNA expression is dependent on time and Glu concentration

Rat cortical neurons (13 DIV) were exposed to various concentrations of Glu, for up to 360 min. Following treatment, the cells were lysed and total RNA was extracted and the amount of *c-fos* and 18S quantified by RT-PCR. *c-fos* expression values were normalised to 18S expression, which served as the internal control. The results above refer to the fold induction of *c-fos* expression compared to untreated, time-matched controls. Data represent mean ± s.d. values of triplicate RT-PCR reactions derived from one individual experiment. The experiments were reproduced at least three times. Figure 5.1 a) represents the *c-fos* changes with non-toxic and partially toxic concentrations of Glu while b) represents changes in *c-fos* expression with toxic concentrations.

5.2.2 NMDA receptor specificity of Glu-induced *c-fos* mRNA expression

As a consequence of the different profiles of *c-fos* expression found in rat cortical neurons exposed to various concentrations of Glu, over 360 min, it was of interest to investigate whether these different responses, like in the mCGC system, were specifically NMDA receptor mediated. For this, the degree of protection offered by the selective, competitive NMDA receptor antagonist, AP5, was compared to that of the non-NMDA receptor antagonist, CNQX, in the presence of Glu. Cells were pre-treated with either AP5 or CNQX for 15 min prior to treatment with various concentrations of Glu from 0 – 360 min and the levels of *c-fos* and 18S quantified by RT-PCR. Before calculation of the induction values of *c-fos* when compared to the untreated control neurons, *c-fos* expression levels were normalised to the internal control, 18S.

When cultures of rat cortical neurons were treated with partially toxic concentrations of Glu (25 μM), a transient elevation in *c-fos* mRNA expression occurred, when compared to the time-matched control. Pre-treatment with AP5, resulted in an approximate 2 fold reduction of the peak of this transient response; after which complete abolition of the transient *c-fos* expression was observed (see Figure 5.2). Pre-treatment with CNQX failed to prevent the transient *c-fos* response. Thus, *c-fos* induction was as a direct consequence of NMDA receptor activation.

With a toxic concentration of Glu (100 μM), an elevated but transient profile of *c-fos* expression was induced in rat cortical neurons, which reached maximal inductions of 100 fold at 90 min before gradually decreasing. It was found that pre-treatment with AP5 changed the expression profile to that of an earlier peaking, transient expression. Again pre-treatment with CNQX did not inhibit the excitotoxic *c-fos* response (see Figures 5.3).

Exposure of rat cortical neurons to a higher toxic concentration of Glu (250 μM) induced an elevated and sustained increase in *c-fos* mRNA expression. Pre-treatment with either AP5 or CNQX did not inhibit the excitotoxic *c-fos* response (see Figure 5.4).

These results are in accordance with the pharmacology of Glu-induced *c-fos* expression in the mCGC culture system (see Section 4.2.3, Chapter 4), where it was shown that the NMDA subtype of Glu receptors was specifically involved. Indeed, as reported in Chapter 4, the concentration of the antagonist, AP5, used in these investigations may not have been sufficient to fully compete with the higher toxic concentrations of Glu. However, the results are consistent with Glu-induced *c-fos* mRNA expression being mediated through the NMDA subtype of Glu receptors.

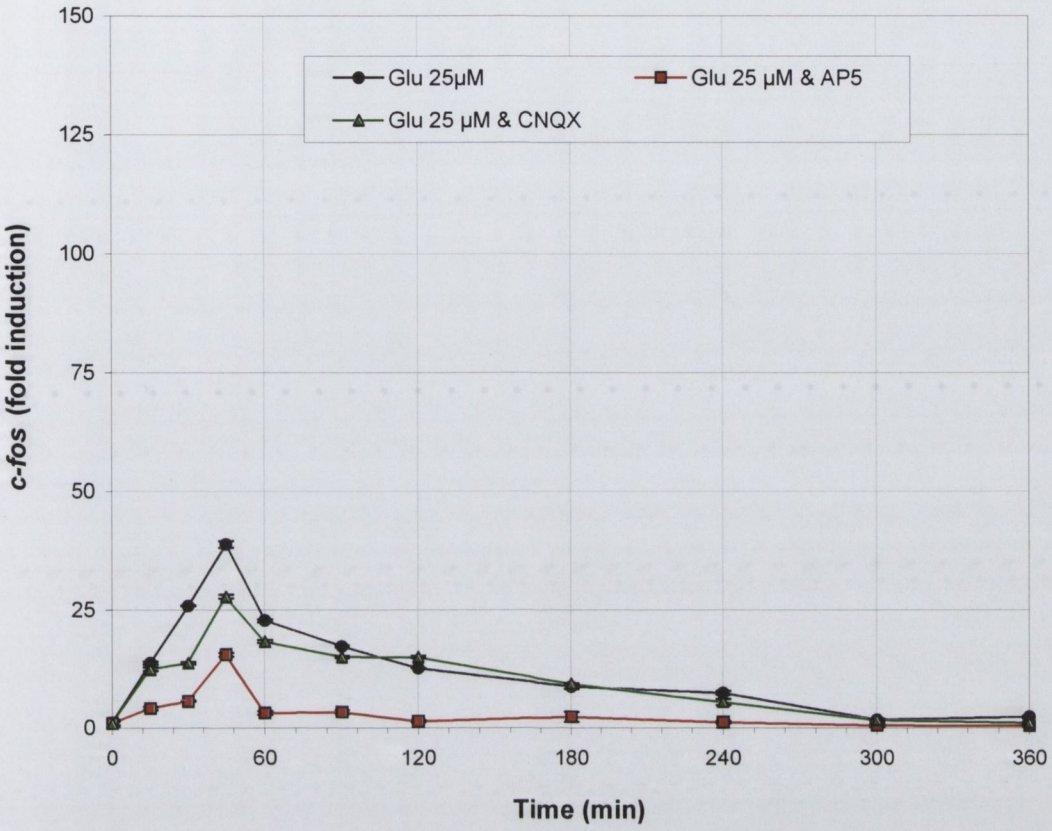


Figure 5.2: AP5 but not CNQX inhibits the *c-fos* response induced by partially toxic concentrations of Glu (25 µM)

Rat cortical neurons (13 DIV) were pre-incubated for 15 min with either AP5 (500 µM) or CNQX (10 µM) prior to co-exposure with a fixed concentration of Glu (25 µM), for up to 360 min. Following treatment, the cells were lysed and total RNA was extracted and the amount of *c-fos* and 18S quantified by RT-PCR. The *c-fos* expression values were normalised to 18S expression, which served as the internal control. The results above refer to the fold induction of *c-fos* expression compared to untreated, time-matched controls. Data represent mean ± s.d. values of triplicate RT-PCR reactions derived from one individual experiment.

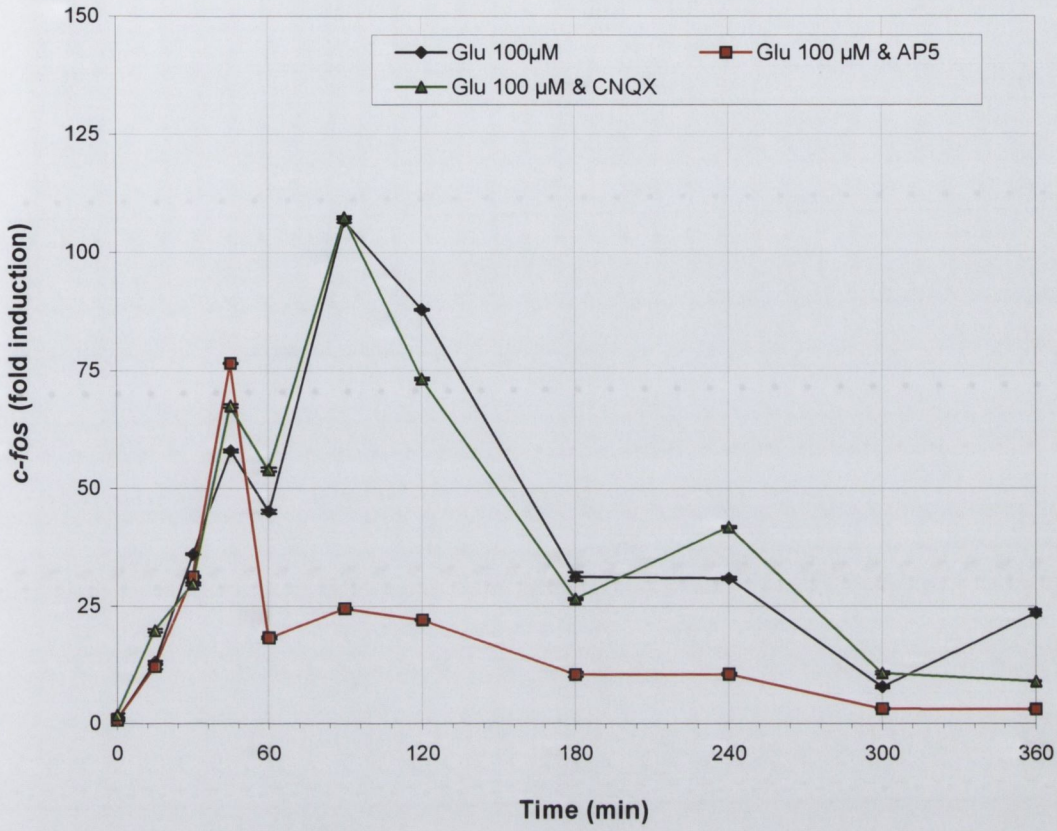


Figure 5.3: AP5 changes the *c-fos* response induced by a toxic concentration of Glu (100 µM)

Rat cortical neurons (13 DIV) were pre-incubated for 15 min with either AP5 (500 µM) or CNQX (10 µM) prior to co-exposure with a fixed concentration of Glu (100 µM), for up to 360 min. Following treatment, the cells were lysed and total RNA was extracted and the amount of *c-fos* and 18S quantified by RT-PCR. The *c-fos* expression values were normalised to 18S expression, which served as the internal control. The results above refer to the fold induction of *c-fos* expression compared to untreated, time-matched controls. Data represent mean ± s.d. values of triplicate RT-PCR reactions derived from one individual experiment.

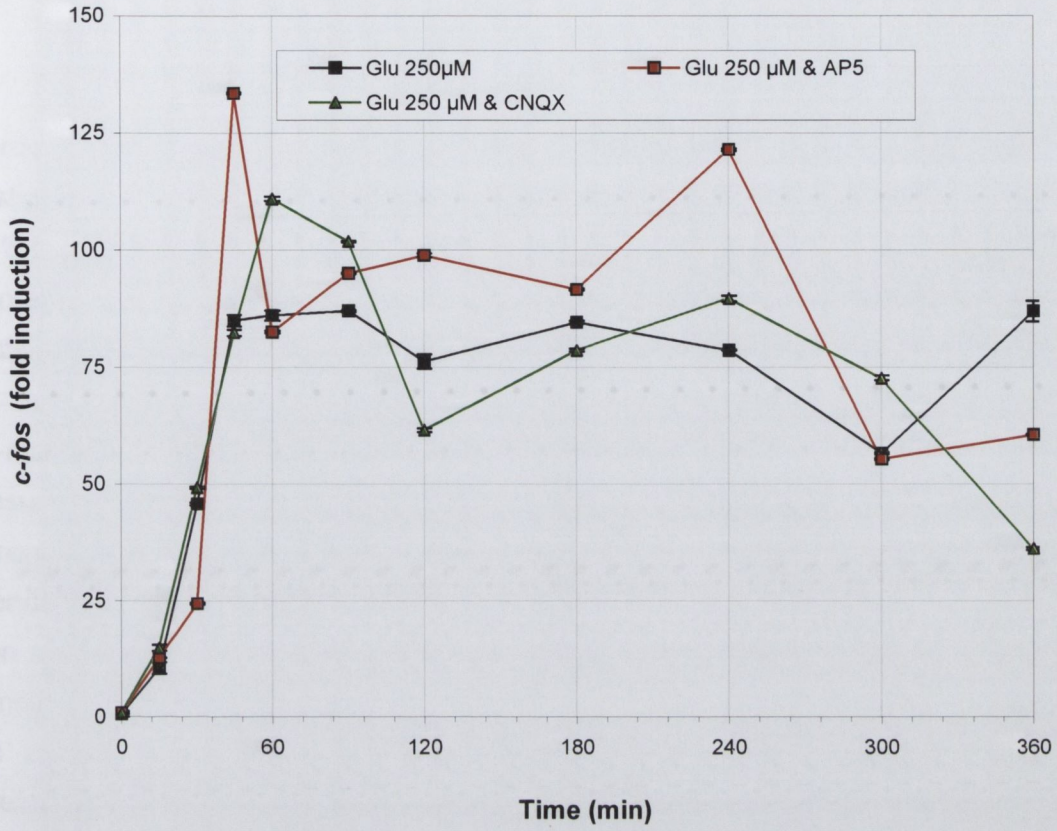


Figure 5.4: Neither AP5 nor CNQX antagonise the *c-fos* response induced by higher, toxic concentrations of Glu (250 µM)

Rat cortical neurons (13 DIV) were pre-incubated for 15 min with either AP5 (500 µM) or CNQX (10 µM) prior to co-exposure with a fixed concentration of Glu (250 µM), for up to 360 min. Following treatment, the cells were lysed and total RNA was extracted and the amount of *c-fos* and 18S quantified by RT-PCR. The *c-fos* expression values were normalised to 18S expression, which served as the internal control. The results above refer to the fold induction of *c-fos* expression compared to untreated, time-matched controls. Data represent mean ± s.d. values of triplicate RT-PCR reactions derived from one individual experiment.

5.2.3 Asp induced changes in *c-fos* expression are time and concentration-dependent

In order to confirm the *c-fos* expression profiles induced by Glu, a comparative investigation was undertaken with a second EAA, Asp. Rat cortical neurons were cultured for 13 days before exposure to various concentrations of Asp over 360 min. Following treatment the cells were lysed, total RNA was extracted and the amount of *c-fos* and 18S quantified by RT-PCR. *c-fos* expression levels were normalised to the internal control, 18S, before calculation of the induction values of *c-fos* when compared to the untreated time-matched controls. As found in the mCGCs and in the previous section with Glu, exposure of rat cortical neurons (13 DIV) to various concentrations of Asp induced different profiles of *c-fos* mRNA expression which were time- and concentration-dependent. The profiles of Asp-mediated *c-fos* induction are shown in Figures 5.5 a) & b). When rat cortical neurons were exposed to non-toxic concentrations of Asp (3.5 μM), *c-fos* mRNA expression did not increase from that at the basal level. Exposure to a partially toxic concentration of Asp (35 μM), induced a transient increase in *c-fos* mRNA expression, which reached a maximal induction of 50 fold at 120 min before returning to basal levels (see Figure 5.5 a)). This profile of *c-fos* expression is consistent with that found previously in cultures of mCGCs. Exposure of the cortical neurons to toxic concentrations of Asp (100 – 500 μM) induced a rapid increase in *c-fos* mRNA expression (125 fold the basal level), which was sustained over 4 hours (see Figure 5.5 b)). These results support and confirm the previous observations with Glu, and indeed the profiles found in mCGCs treated with Asp (see Figure 4.6 b)).

In spite of the similarity in the expression profiles of *c-fos* in mCGCs and rat cortical neurons, large differences are evident in the levels of *c-fos* induction between the two culture models. With partially toxic concentrations of Asp (35 μM), the peak induction of *c-fos* mRNA was 10 fold higher in rat cortical neurons when compared to mCGCs. Furthermore, with toxic concentrations of Asp (100 – 500 μM), the peak induction of *c-fos* mRNA was approximately 15 fold higher in rat cortical neurons. However, the change in induction from the partially toxic profile of *c-fos* to that of the elevated and sustained excitotoxic profile was the same, that is, a 2.5 fold difference was observed between the profiles induced by 35 μM Asp and those induced by the higher toxic concentrations of 100 – 500 μM Asp in both cell culture systems.

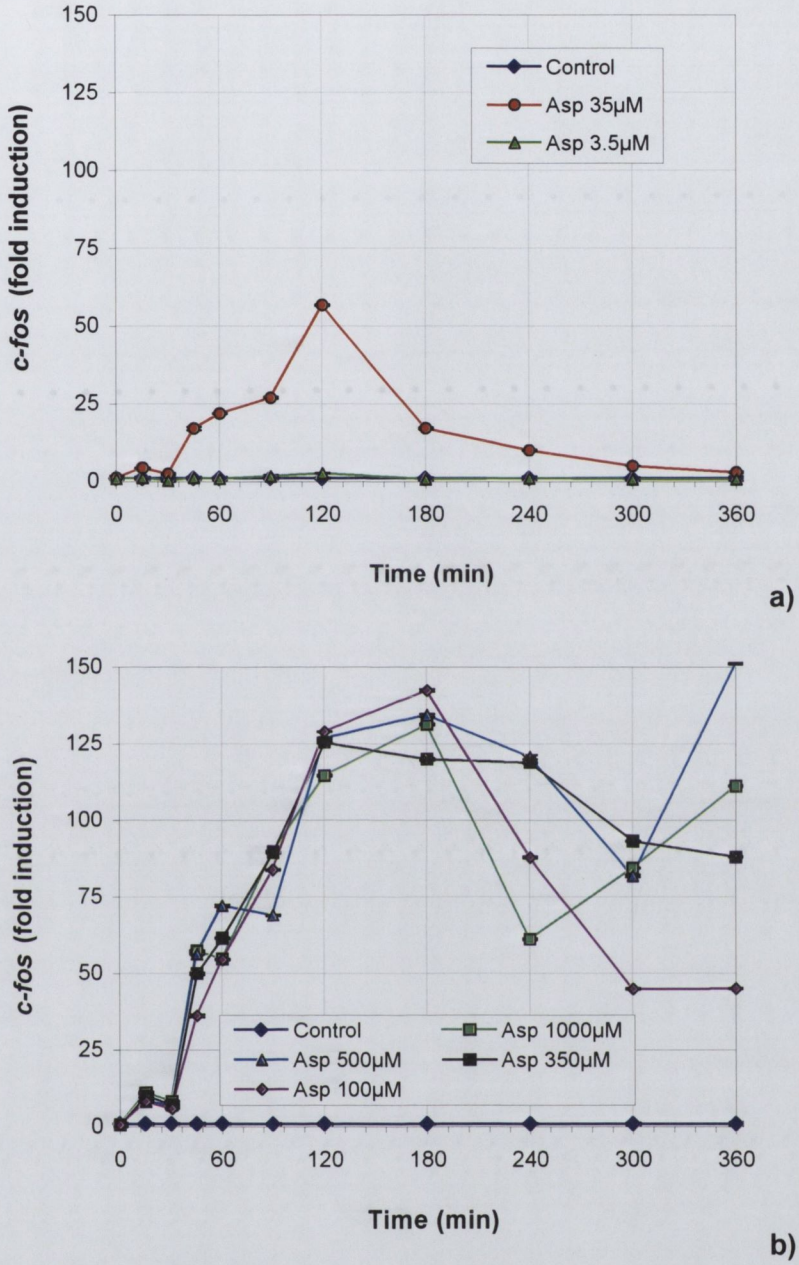


Figure 5.5: Different time profiles of *c-fos* expression dependant on Asp concentration

Rat cortical neurons (13 DIV) were exposed to various concentrations of Asp for up to 360 min. Following treatment, the cells were lysed and total RNA was extracted and the amount of *c-fos* and 18S quantified by RT-PCR. The *c-fos* expression values were normalised to 18S expression, which served as the internal control. The results above refer to the fold induction of *c-fos* expression compared to untreated, time-matched controls. Data represent mean ± s.d. values of triplicate RT-PCR reactions derived from one individual experiment. The experiments were reproduced at least three times. Figure 5.5 a) represents the *c-fos* changes with non-toxic and partially toxic concentrations of Asp while b) represents changes in *c-fos* expression with toxic concentrations.

5.2.4 Asp-induced *c-fos* mRNA expression is NMDA receptor specific

Compliant with the different profiles of *c-fos* mRNA expression in rat cortical neurons treated with Glu (Section 5.2.1) and in mCGCs treated with Asp (Section 4.2.4), different *c-fos* mRNA expression profiles, depending on time and concentration, were also found in Asp treated rat cortical neurons. Therefore, it was of interest to investigate whether these different profiles were also NMDA receptor mediated. For this, the same antagonists were used as before, that is, the selective, competitive NMDA receptor antagonist, AP5, and the non-NMDA receptor antagonist, CNQX.

When cultures of rat cortical neurons were treated with partially toxic concentrations of Asp (35 μM), an elevated, transient increase in *c-fos* mRNA expression was observed. The results reveal that pre-treatment with AP5 completely inhibited *c-fos* mRNA expression. Pre-treatment with CNQX failed to prevent the *c-fos* response (see Figure 5.6).

Exposure of the cortical neurons to toxic concentrations of Asp (100 μM) induced a rapid increase in *c-fos* mRNA expression, which was sustained over 4 hours. In the presence of AP5, the sustained expression was effectively inhibited. Pre-treatment with CNQX failed to antagonise the *c-fos* response (see Figure 5.7).

Pre-treatment of rat cortical neurons with AP5 before exposure to higher toxic concentrations of Asp (350 μM) resulted in a change of the elevated and sustained *c-fos* excitotoxic profile to that of an earlier peaking, transient expression. Although, pre-treatment with CNQX did not inhibit the excitotoxic *c-fos* response, the expression levels were lowered (see Figure 5.8).

Overall, these results demonstrate that Asp-induced *c-fos* mRNA expression is mediated through the NMDA receptor subtype.

In contrast to our earlier findings of non-inhibition by AP5 of the excitotoxic *c-fos* responses induced by high toxic concentrations of Glu in rat cortical neurons and high concentrations of Asp in mCGCs, the concentration of AP5 used in these *c-fos* investigations was sufficient to compete with the highly toxic concentrations of Asp.

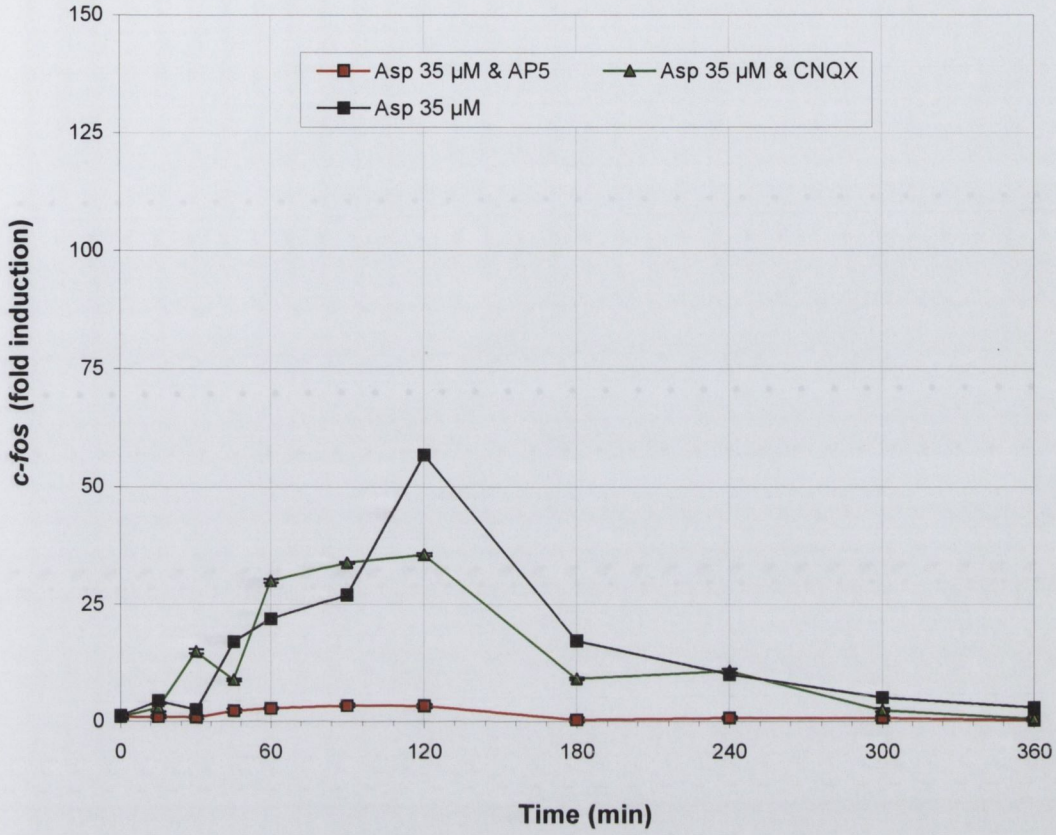


Figure 5.6: AP5 effectively abolishes the *c-fos* response induced by partially toxic concentrations of Asp

Rat cortical neurons (13 DIV) were pre-incubated for 15 min with either AP5 (500 µM) or CNQX (10 µM) prior to co-exposure with a fixed concentration Asp (35 µM), for up to 360 min. Following treatment, the cells were lysed and total RNA was extracted and the amount of *c-fos* and 18S quantified by RT-PCR. The *c-fos* expression values were normalised to 18S expression, which served as the internal control. The results above refer to the fold induction of *c-fos* expression compared to untreated, time-matched controls. Data represent mean ± s.d. values of triplicate RT-PCR reactions derived from one individual experiment. The experiments were reproduced at least twice.

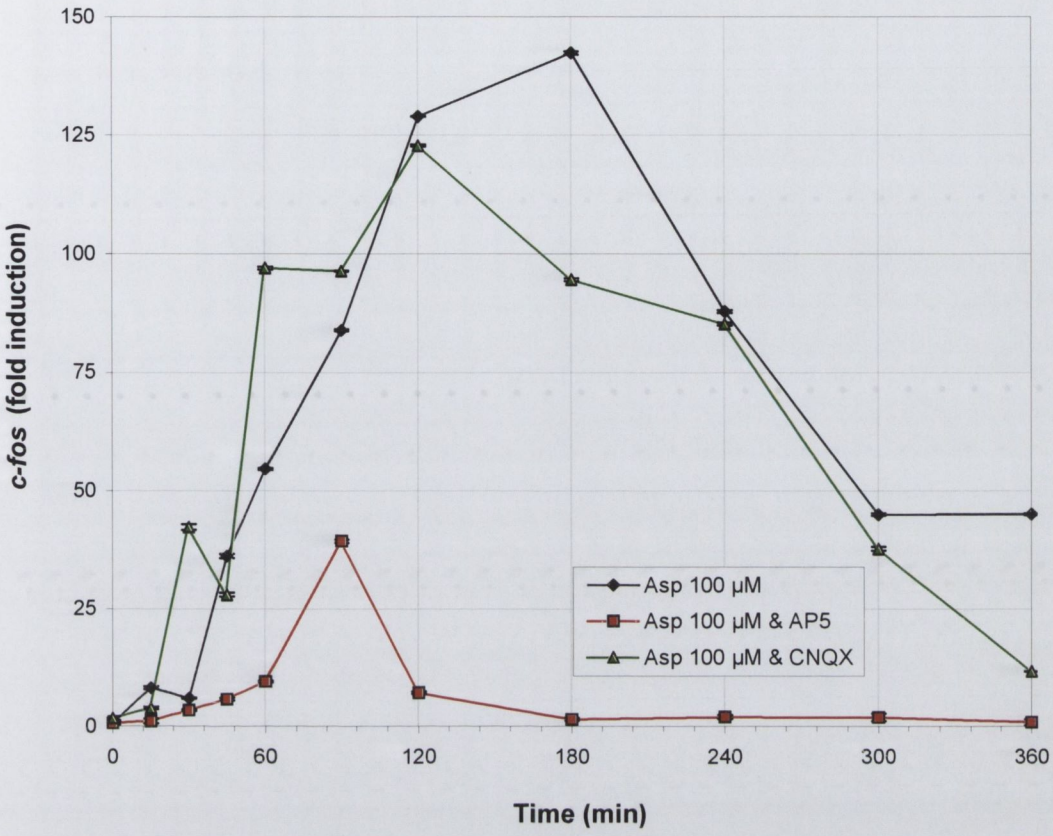


Figure 5.7: AP5 effectively antagonises the *c-fos* response induced by toxic concentrations of Asp

Rat cortical neurons (13 DIV) were pre-incubated for 15 min with either AP5 (500 µM) or CNQX (10 µM) prior to co-exposure with a fixed concentration of Asp (100 µM), for up to 360 min. Following treatment, the cells were lysed and total RNA was extracted and the amount of *c-fos* and 18S quantified by RT-PCR. The *c-fos* expression values were normalised to 18S expression, which served as the internal control. The results above refer to the fold induction of *c-fos* expression compared to untreated, time-matched controls. Data represent mean ± s.d. values of triplicate RT-PCR reactions derived from one individual experiment. The experiments were reproduced at least twice.

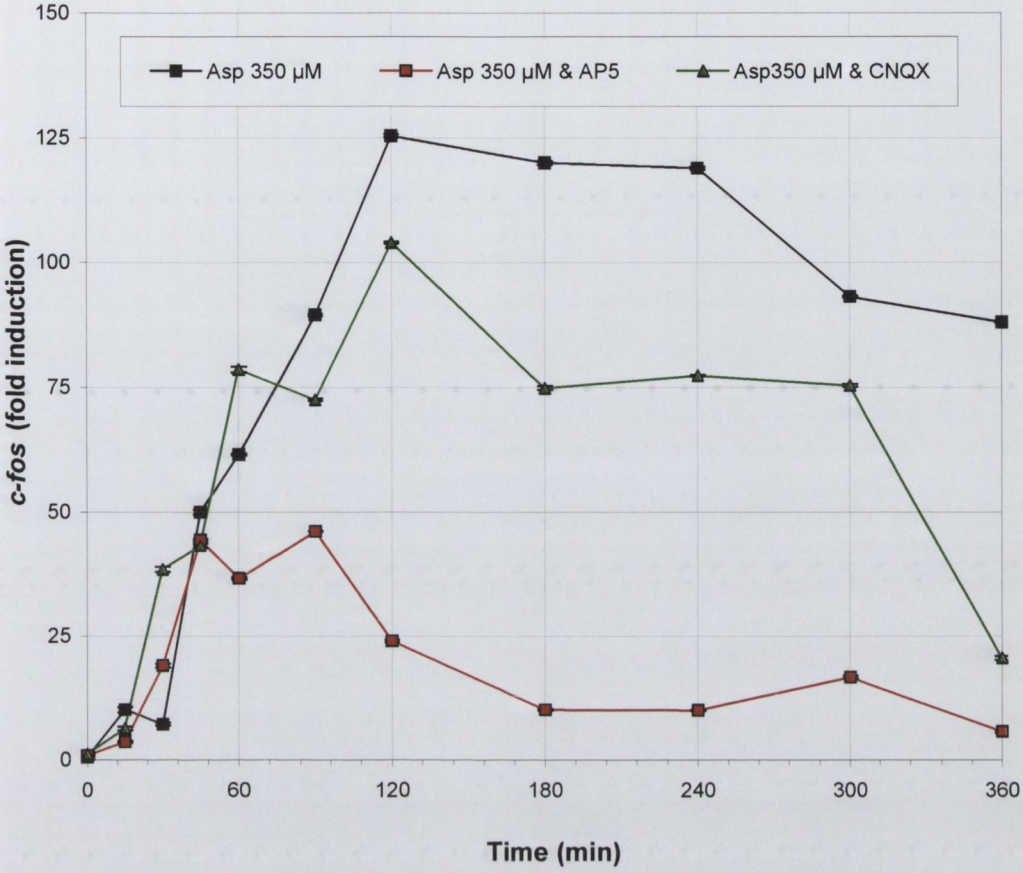


Figure 5.8: AP5 and CNQX change the *c-fos* mRNA expression profile induced by higher, toxic concentrations of Asp

Rat cortical neurons (13 DIV) were pre-incubated for 15 min with either AP5 (500 µM) or CNQX (10 µM) prior to co-exposure with a fixed concentration of Asp (350 µM), for up to 360 min. Following treatment, the cells were lysed and total RNA was extracted and the amount of *c-fos* and 18S quantified by RT-PCR. The *c-fos* expression values were normalised to 18S expression, which served as the internal control. The results above refer to the fold induction of *c-fos* expression compared to untreated, time-matched controls. Data represent mean ± s.d. values of triplicate RT-PCR reactions derived from one individual experiment. The experiments were reproduced at least twice.

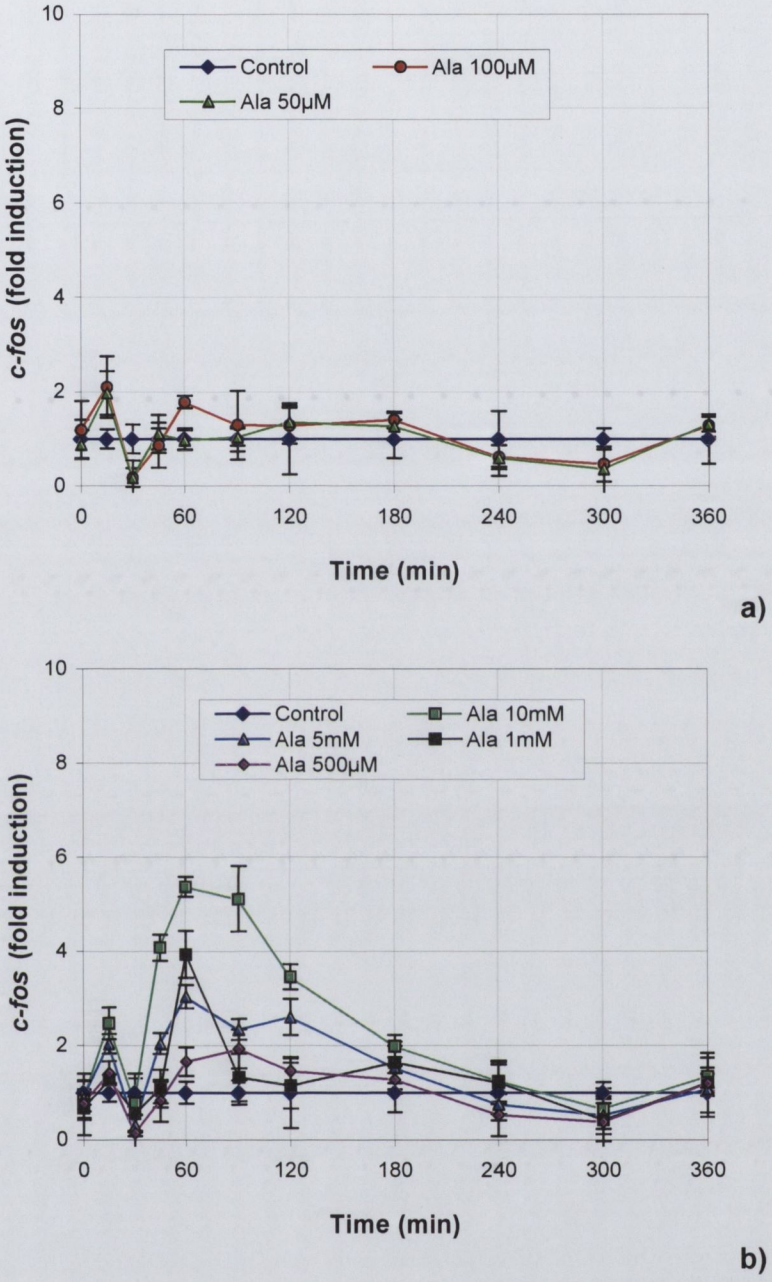


Figure 5.9: Ala does not induce c-*fos* mRNA expression in mature rat cortical neurons

Rat cortical neurons (13 DIV) were exposed to various concentrations of Ala, for up to 360 min. Following treatment, the cells were lysed and total RNA was extracted and the amount of *c-fos* and 18S quantified by RT-PCR. The *c-fos* expression values were normalised to 18S expression, which served as the internal control. The results above refer to the fold induction of *c-fos* expression compared to untreated, time-matched controls. Data represent mean ± s.d. values of triplicate RT-PCR reaction derived from one individual experiment. The experiments were reproduced at least three times. Figure 5.9 a) represents the *c-fos* changes with low concentrations of Ala while b) represents changes in *c-fos* expression with high concentrations.

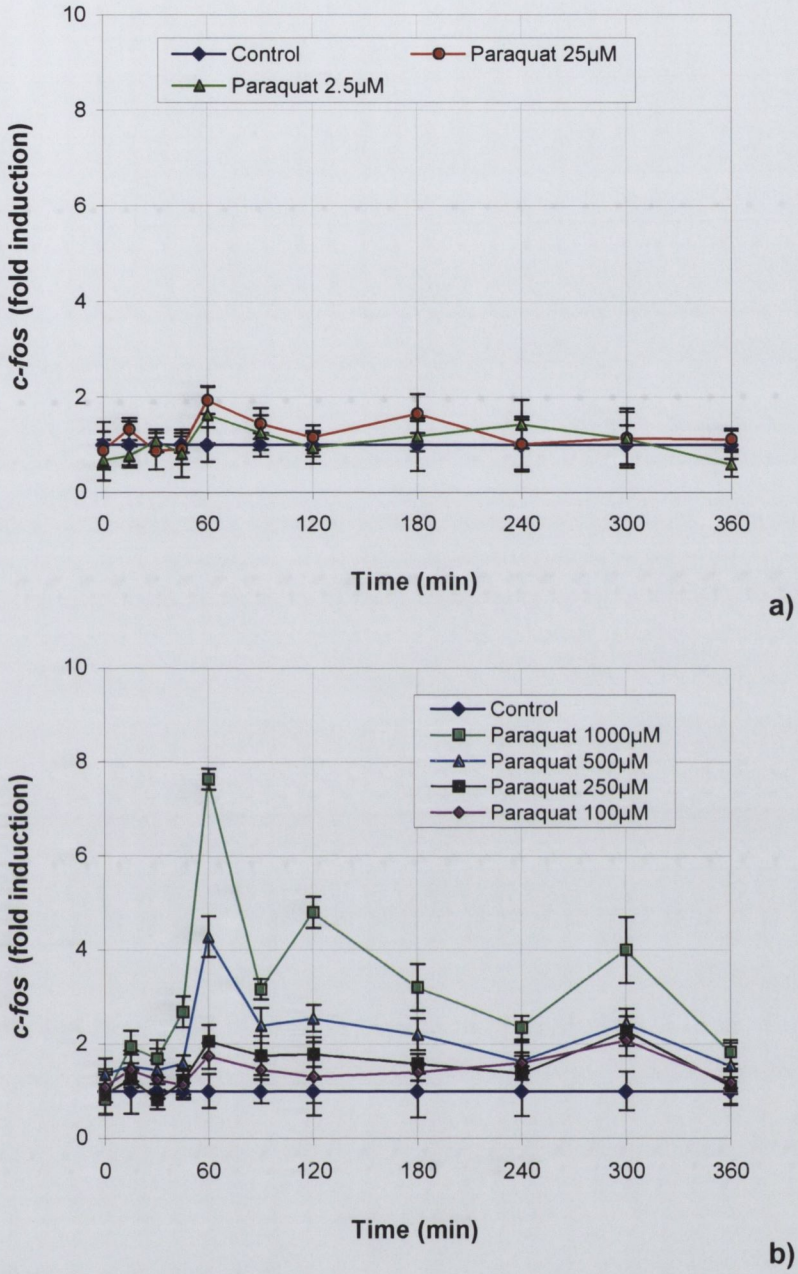


Figure 5.10: Profiles of c-*fos* induction in rat cortical neurons treated with paraquat

Rat cortical neurons (13 DIV) were exposed to various concentrations of paraquat, for up to 360 min. Following treatment, the cells were lysed and total RNA was extracted and the amount of *c-fos* and 18S quantified by RT-PCR. *c-fos* expression values were normalised to 18S expression, which served as the internal control. The results above refer to the fold induction of *c-fos* expression compared to untreated, time-matched controls. Data represent mean ± s.d. values of triplicate RT-PCR reactions derived from one individual experiment. The experiments were reproduced at least three times. Figure 5.10 a) represents the *c-fos* changes with partially toxic concentrations of paraquat while b) represents changes in *c-fos* expression with toxic concentrations.

5.2.5 Neither Ala nor paraquat induce *c-fos* expression in primary rat cortical neurons

Ala, a non-excitatory amino acid, did not induce increased levels of *c-fos* mRNA expression in rat cortical neurons under conditions where EAAs induce their effects (see Figure 5.9).

Paraquat, which induces neurotoxicity but not excitotoxicity in rat cortical neurons, did not induce increased *c-fos* mRNA expression (see Figure 5.10)

5.2.6 Changes in *fosB* expression are dependent on time and Glu concentration

The expression profiles of *fosB* were investigated in rat cortical neurons in response to treatment with the excitotoxin, Glu. Rat cortical neurons were cultured for 13 days before being exposed to various concentrations of Glu for defined periods of time (0 - 360 min). Following treatment, the cells were lysed, total RNA was extracted and the amount of *fosB* and 18S quantified by RT-PCR. Expression levels of *fosB* mRNA were normalised to the internal control, 18S, before calculation of the induction values of *fosB* when compared to the untreated control neurons. The profiles of *fosB* expression are shown in Figures 5.11 a) and b). When rat cortical neurons (13 DIV) were exposed to non-toxic concentrations of Glu (2.5 µM), a transient increase in *fosB* mRNA expression was observed.

Exposure to both partially toxic (25 µM) and toxic concentrations of Glu (100 µM) induced an early transient peak of *fosB* expression, which was sustained for 180 min.

However, higher toxic concentrations of Glu (250 – 1000 µM) changed the kinetics of the *fosB* mRNA expression profile. The response of *fosB* appeared to be biphasic. The first phase showed a progressive increase in *fosB* to a maximum induction of 125 fold at 90 – 120 min, which then dropped to almost the basal level. The second phase began at 300 min and was sustained for the remainder of the test period (see Figure 5.11 b)). Thus, the excitotoxic *fosB* response in rat cortical neurons is clearly distinguishable from that induced by lower, albeit toxic concentrations of Glu.

The transient expression of *fosB* mRNA in rat cortical neurons exposed to non-toxic concentrations of Glu is consistent with that found previously in cultures of mCGCs (see Figure 4.16 a)). With partially toxic concentrations of Glu (25 µM), a difference was observed in the onset of *fosB* mRNA expression in mCGCs and rat cortical neurons. In mCGCs, a delayed, transient profile of *fosB* mRNA expression was observed with

maximal levels of induction at 180 min. In contrast, an earlier increase in *fosB* mRNA expression was observed in rat cortical neurons, peaking at 60 min. However, levels of *fosB* induction were similar in both cell culture systems with maximal inductions of 15 fold. With toxic concentrations of Glu (100 µM), a difference was observed in the profiles of *fosB* mRNA expression, with a delayed, elevated and sustained increase observed in mCGCs and an early, elevated but transient increase observed in rat cortical neurons.

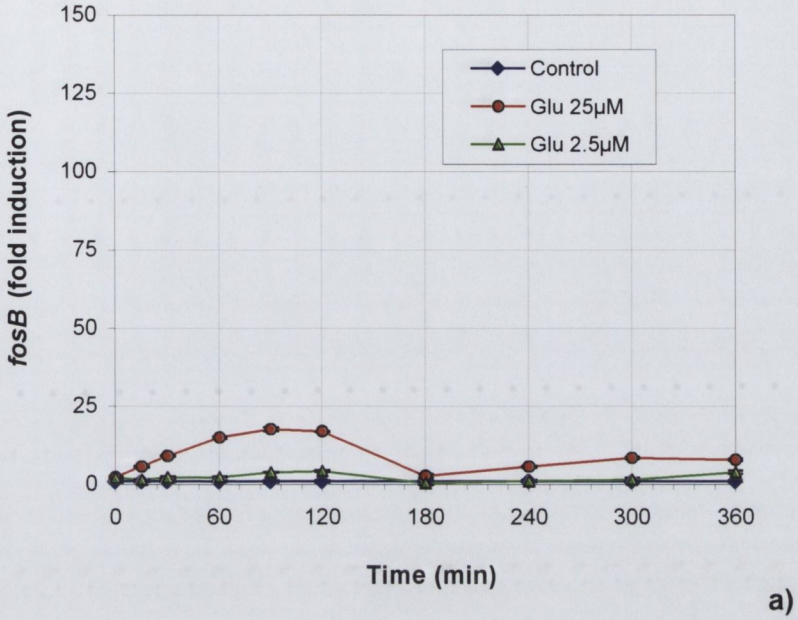
Differences were also observed in the patterns of *fosB* mRNA expression with higher toxic concentrations of Glu (250 - 500 µM). In mCGCs, a delayed, elevated and sustained increase was observed. In rat cortical neurons, a biphasic increase in *fosB* mRNA expression was observed, peaking at 90 - 120 min and 300 min, respectively.

Another difference was in the levels of induction. In mCGCs, maximal *fosB* inductions of 25 - 35 times the basal level were observed with toxic concentrations of Glu (100 - 500 µM), while in rat cortical neurons maximal inductions of 125 fold the basal level were observed.

The change in induction from the partially toxic profile of *fosB* to that of the elevated and sustained excitotoxic profile was also different between the two culture systems. A 2 fold difference was observed between the profiles induced by 25 µM Glu and those induced by the higher toxic concentrations of Glu (100 – 500 µM) in mCGCs, whereas a 6 fold difference was observed, under the same conditions, in rat cortical neurons. At this stage, it is not clear whether the different expression profiles of *fosB* are species and/or brain region specific but the results show that *fosB* can be used as a sensitive early mechanistic biomarker, in addition to *c-fos*, for excitotoxicity in both mCGCs and rat cortical neurons.

5.2.7 NMDA receptor specificity of Glu-induced *fosB* mRNA expression

In the previous section, it was shown that toxic concentrations of Glu induce different patterns of *fosB* expression in rat cortical neurons depending on concentration, that is, a transient increase in *fosB* expression was induced by 2.5 – 100 µM Glu, whereas a biphasic pattern was induced by the higher toxic concentrations of 250 – 1000 µM Glu. It can be assumed, therefore, that the biphasic pattern of *fosB* mRNA expression represents the excitotoxic condition. In addition, the biphasic profiles of *fosB* are in contrast to excitotoxic Glu-induced *c-fos* and *fosB* expression in mCGCs (see Sections 4.2.2 and 4.2.11, Chapter 4) and also to the excitotoxic *c-fos* profiles observed in rat cortical neurons treated with Glu (see Section 5.2.1).



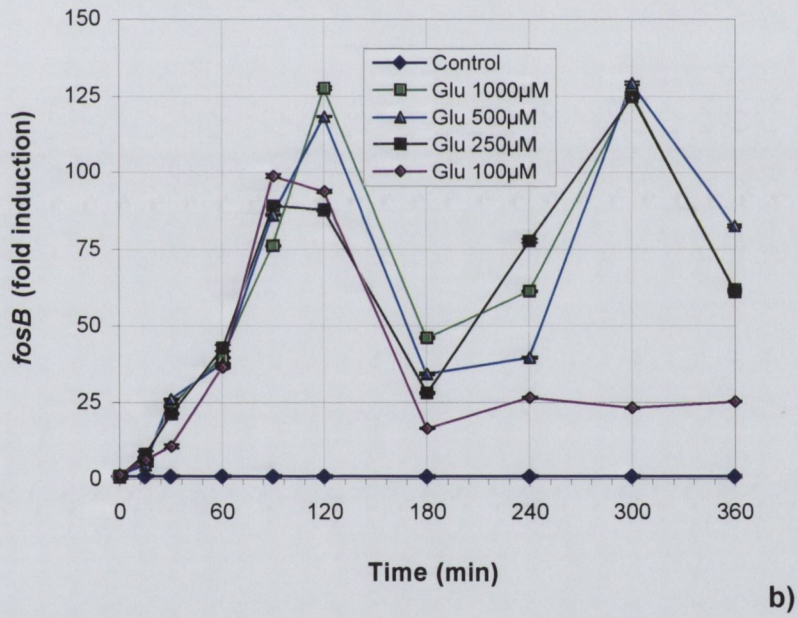


Figure 5.11: Induction of *fosB* mRNA expression as a function of time and Glu concentration

Rat cortical neurons (13 DIV) were exposed to various concentrations of Glu, for up to 360 min. Following treatment, the cells were lysed, total RNA was extracted and the amount of *fosB* and 18S quantified by RT-PCR. *fosB* expression values were normalised to 18S expression, which served as the internal control. The results above refer to the fold induction of *fosB* expression compared to untreated, time-matched controls. Data represent mean ± s.d. values of triplicate RT-PCR reactions derived from one individual experiment. The experiments were reproduced at least three times. Figure 5.11 a) represents the *fosB* changes with non-toxic and partially toxic concentrations of Glu while b) represents changes in *fosB* expression with toxic concentrations.

In order to investigate the pharmacology of these different *fosB* responses in rat cortical neurons, the inhibitory effect of the NMDA receptor antagonist, AP5, was compared to that of the non-NMDA receptor antagonist, CNQX, in the presence of various concentrations of Glu.

Rat cortical neurons were pre-treated with a fixed concentration of AP5 or CNQX before being exposed to three different toxic concentrations of Glu. Following treatment, the cells were lysed, total RNA was extracted and the amount of *fosB* and 18S quantified by real-time RT-PCR. The expression levels of *fosB* mRNA were normalised to the internal control, 18S, prior to calculation of the fold induction of *fosB,* in the presence and absence of the antagonists, relative to the untreated, time matched controls (see Chapter 2).

The transient *fosB* response, induced by low but partially toxic concentrations of Glu (25 μM), was completely inhibited by pre-treatment of the neurons with AP5. Pre-treatment with CNQX did not protect the neurons against the Glu-induced *fosB* response (see Figure 5.12). Thus, the induction of *fosB*, observed in rat cortical neurons treated with a partially toxic concentration of Glu, was as a direct and specific result of over-stimulation of the NMDA subtype of Glu receptors.

When the neurons were exposed to a toxic concentration of Glu (100 μM), pre-treatment with AP5 completely inhibited the toxic *fosB* response (see Figure 5.13) while pre-treatment with CNQX exhibited no antagonistic effect. These results are consistent with Glu-induced *fosB* mRNA expression being mediated through the NMDA receptor subtype. However, exposure of the rat cortical neurons to higher toxic concentration of Glu (250 μM) saturated the NMDA receptor and neither AP5 nor CNQX could compete effectively with the toxic concentration of Glu (see Figure 5.14).

On account of the full inhibition by AP5 of the toxic *fosB* responses induced by 25 and 100 μM Glu and the lack of antagonism by CNQX, it can be speculated that the biphasic excitotoxic *fosB* response is also NMDA receptor mediated. Indeed, consistant with the pharmacology of Glu-induced *c-fos* expression (see Section 5.2.2 and 5.2.4, respectively), the lack of inhibition by AP5 at high toxic concentrations may be due to an insufficiently high concentration of antagonist used. Overall, it can be concluded that the excitotoxic expression of *fosB* in rat cortical neurons, treated with toxic concentrations of Glu, is NMDA receptor mediated.

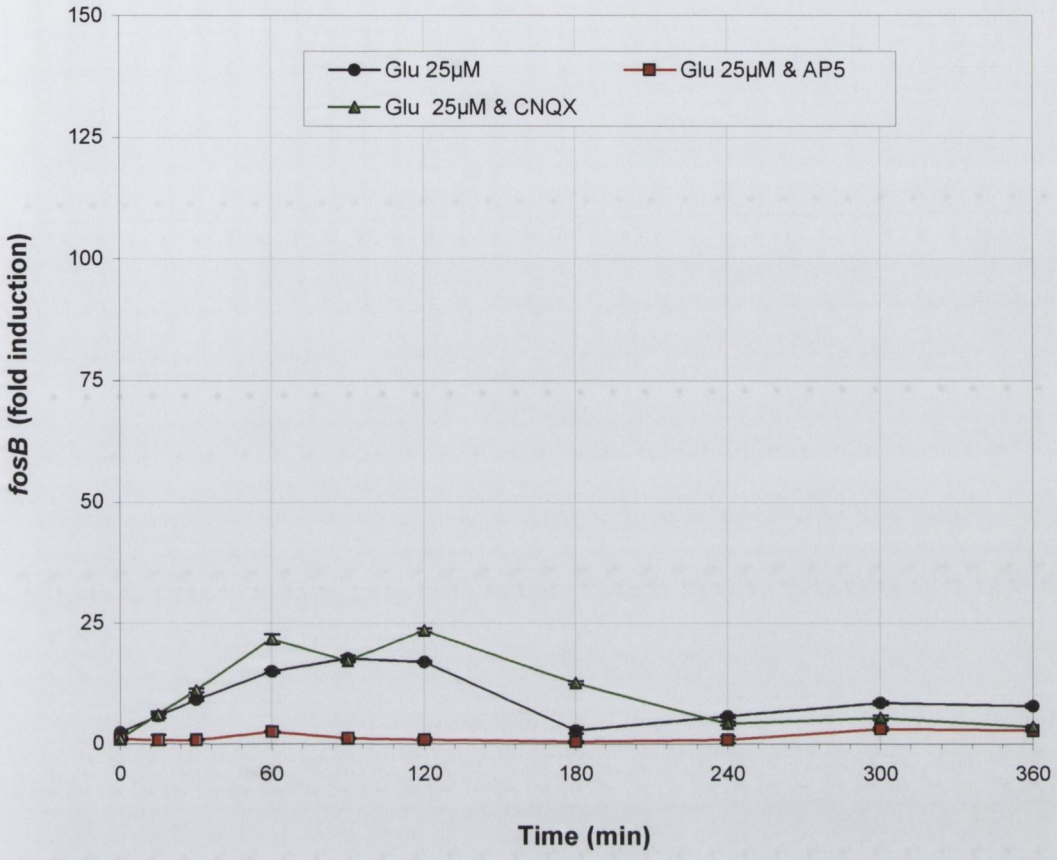


Figure 5.12: AP5 effectively antagonises *fosB* mRNA expression induced by partially toxic concentrations of Glu

Rat cortical neurons (13 DIV) were pre-incubated for 15 min with either AP5 (500 μM) or CNQX (10 μM) prior to co-exposure with a fixed concentration of Glu (25 μM), for up to 360 min. Following treatment, the cells were lysed and total RNA was extracted and the amount of *fosB* and 18S quantified by RT-PCR. The *fosB* expression values were normalised to 18S expression, which served as the internal control. The results above refer to the fold induction of *fosB* expression compared to untreated, time-matched controls. Data represent mean ± s.d. values of triplicate RT-PCR reactions derived from one individual experiment.

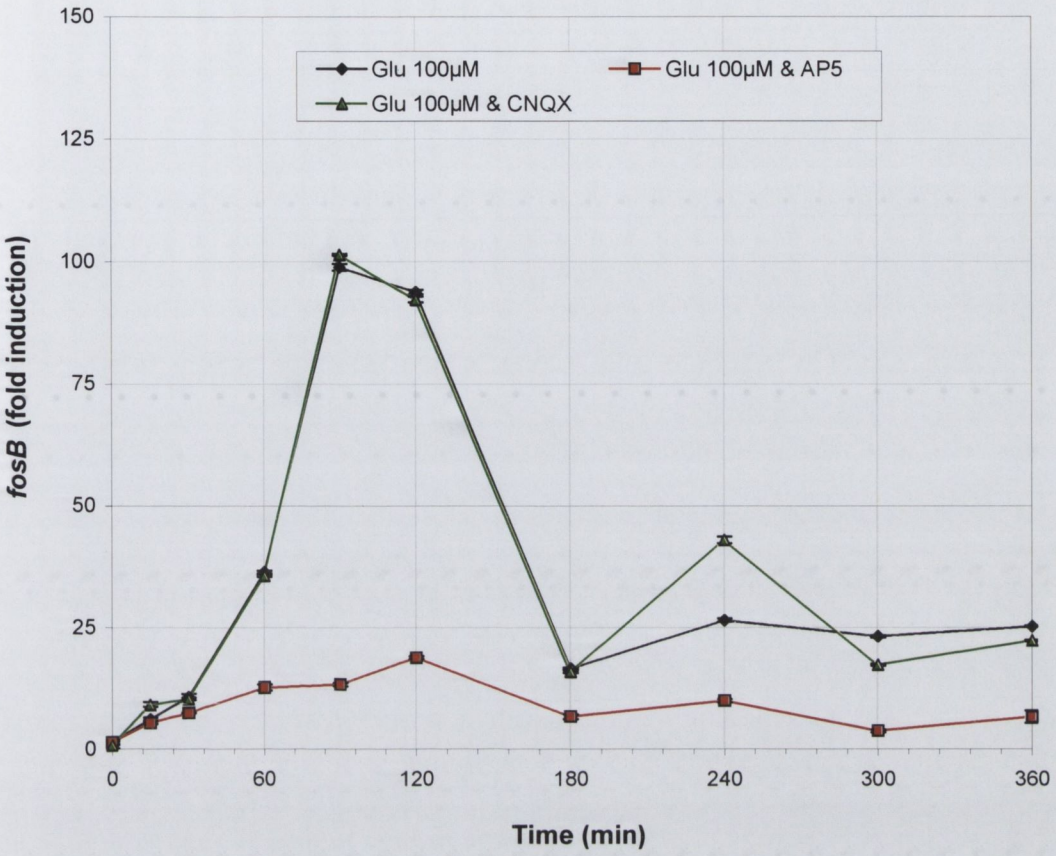


Figure 5.13: AP5 inhibits elevated *fosB* mRNA expression induced by toxic concentrations of Glu (100 µM)

Rat cortical neurons (13 DIV) were pre-incubated for 15 min with either AP5 (500 µM) or CNQX (10 µM) prior to co-exposure with a fixed concentration of Glu (100 µM), for up to 360 min. Following treatment, the cells were lysed and total RNA was extracted and the amount of *fosB* and 18S quantified by RT-PCR. The *fosB* expression values were normalised to 18S expression, which served as the internal control. The results above refer to the fold induction of *fosB* expression compared to untreated, time-matched controls. Data represent mean ± s.d. values of triplicate RT-PCR reactions derived from one individual experiment.

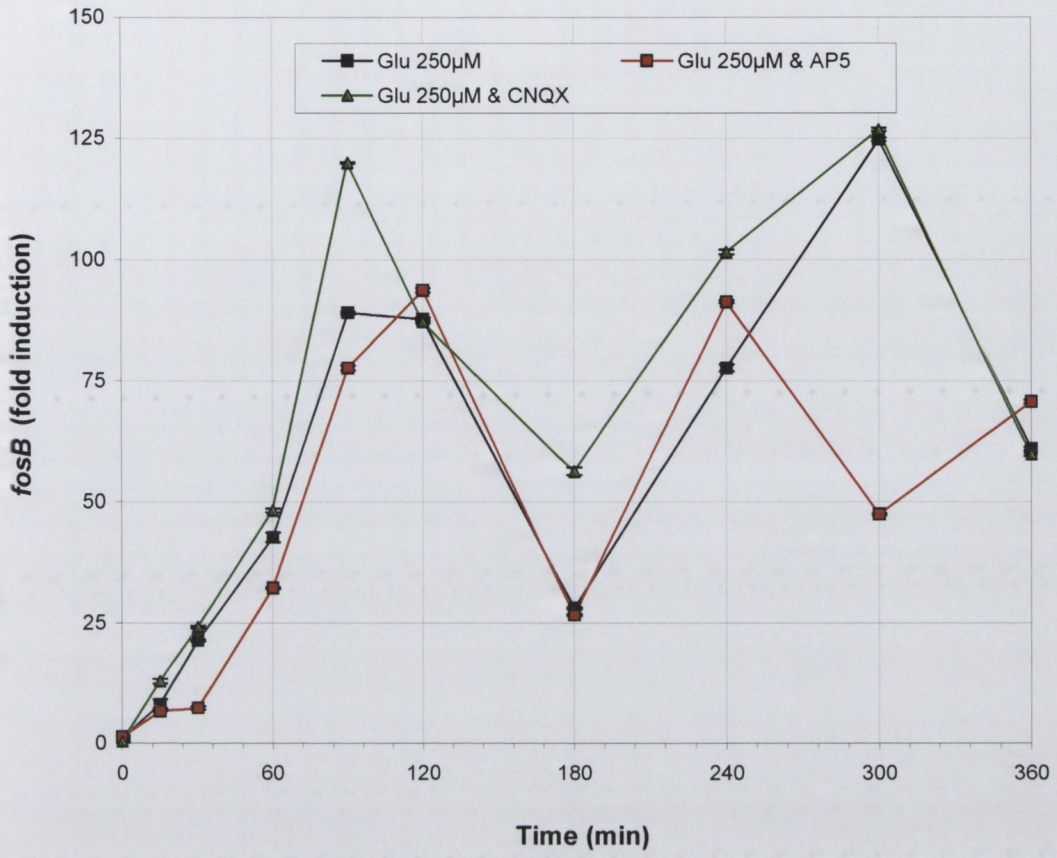


Figure 5.14: Neither AP5 nor CNQX inhibit the *fosB* response induced by higher, toxic concentrations of Glu (250 µM)

Rat cortical neurons (13 DIV) were pre-incubated for 15 min with either AP5 (500 µM) or CNQX (10 µM) prior to co-exposure with a fixed concentration of Glu (250 µM), for up to 360 min. Following treatment, the cells were lysed and total RNA was extracted and the amount of *fosB* and 18S quantified by RT-PCR. The *fosB* expression values were normalised to 18S expression, which served as the internal control. The results above refer to the fold induction of *fosB* expression compared to untreated, time-matched controls. Data represent mean ± s.d. values of triplicate RT-PCR reactions derived from one individual experiment.

5.2.8 Changes in *fosB* expression as a function of time and Asp concentration

On account of the novel biphasic expression profiles of *fosB* mRNA induced in rat cortical neurons by toxic concentrations of Glu (250 – 1000 μM), a second known excitotoxin, Asp, was investigated. Primary cultures of rat cortical neurons (13 DIV) were exposed over the same time course (0 - 360 min) to various concentrations of Asp. Following treatment, the cells were lysed, total RNA was extracted and the amount of *fosB* and 18S quantified by real-time RT-PCR. *fosB* expression levels were normalised to the internal control, 18S, before calculation of the induction values of *fosB* when compared to the untreated control neurons. The profiles of time- and concentration-dependent Asp induced *fosB* mRNA expression are shown in Figures 5.15 a) & b).

When rat cortical neurons were exposed to non-toxic concentrations of Asp (3.5 μM), a slight transient increase in *fosB* mRNA expression was observed before returning to the basal level (see Figure 5.15 a)).

Exposure to a partially toxic concentration of Asp (35 μM) induced a biphasic *fosB* response, with the first wave of *fosB* expression occurring at the 90 min time-point and the second wave occurring at the later time-point of 240 min (see Figure 5.15 a)). This profile is different from that observed in rat cortical neurons treated with Glu (25 μM), where an elevated but transient *fosB* expression profile was observed (see Figure 5.11 a)). A biphasic *fosB* response was also observed when rat cortical neurons were exposed to a toxic concentration of Asp (100 μM). Again, this profile is different from that observed in rat cortical neurons treated with Glu, where an elevated, transient *fosB* expression profile was observed (see Figure 5.11 b)). In addition, and supporting the profiles of Glu-mediated excitotoxic *fosB* expression (see Figure 5.11 b)), exposure of the cortical neurons to higher toxic concentrations of Asp (350 – 1000 μM) resulted in biphasic *fosB* mRNA expression (Figure 5.15 b)). However the levels of *fosB* induction, at both peaks, were lower than in rat cortical neurons treated with Glu (250 – 1000 μM).

Contrasting profiles of *fosB* expression were observed in mCGCs (see Section 4.2.13) and rat cortical neurons (Figure 5.15 a) and b)) exposed to Asp. In mCGCs, no increase in *fosB* mRNA expression occurred with non-toxic concentrations of Asp (3.5 μM). However, in rat cortical neurons *fosB* mRNA expression was transiently increased.

With partially toxic concentrations of Asp (35 μM), a difference was observed in the pattern of *fosB* mRNA expression in mCGCs and rat cortical neurons. In mCGCs, a delayed, elevated and sustained profile of *fosB* expression was observed. In contrast, a

biphasic pattern of *fosB* mRNA expression was observed in rat cortical neurons. However, levels of *fosB* induction were similar in both cell culture systems with maximal inductions of 15 - 20 fold.

With toxic concentrations of Asp (100 μM), the profiles of *fosB* expression were different between the two cell culture systems. A delayed, elevated and sustained profile of *fosB* mRNA expression was observed in mCGCs treated with toxic concentrations of Asp. However, a biphasic profile of *fosB* expression was observed in rat cortical neurons.

Differences were also observed in the profiles of *fosB* mRNA expression with higher toxic concentrations of Asp (350 - 500 μM). In mCGCs, a delayed, elevated and sustained increase was observed. In rat cortical neurons, a biphasic increase in *fosB* mRNA expression was observed. Another difference was in the levels of induction. In mCGCs, maximal *fosB* inductions of 35 times the basal level were observed with toxic concentrations of Asp (100 - 500 μM), while in rat cortical neurons maximal inductions of 75 fold the basal level were observed.

The change in induction from the partially toxic profile of *fosB* to that of the elevated and sustained excitotoxic profile was also different between the two culture systems. An approximate 2 fold difference was observed between the profiles induced by 35 μM Asp and those induced by the higher toxic concentrations of Asp (100 – 500 μM) in mCGCs, whereas a 4 fold difference was observed, under the same conditions, in rat cortical neurons.

At this stage, it is not clear whether the different profiles of *fosB* mRNA expression, under excitotoxic conditions, in rat cortical neurons and mCGCs are due to the differences in species and/or brain region. However, the results show that *fosB* is clearly up-regulated in the complex process of excitotoxicity and thus may be used, in addition to *c-fos,* as an early mechanistic biomarker of excitotoxicity.

5.2.9 NMDA receptor specificity of Asp-induced *fosB* mRNA expression

In the previous section, a biphasic profile of *fosB* expression was observed with excitotoxic concentrations of Asp. These concentration-dependent profiles are consistent with those found for Glu-induced *fosB* mRNA expression in rat cortical neurons. It was also shown in Section 5.2.7 that the NMDA receptor subtype mediated Glu-induced *fosB* mRNA expression. Therefore, it was of interest to determine whether Asp-induced *fosB* expression was also NMDA receptor mediated.

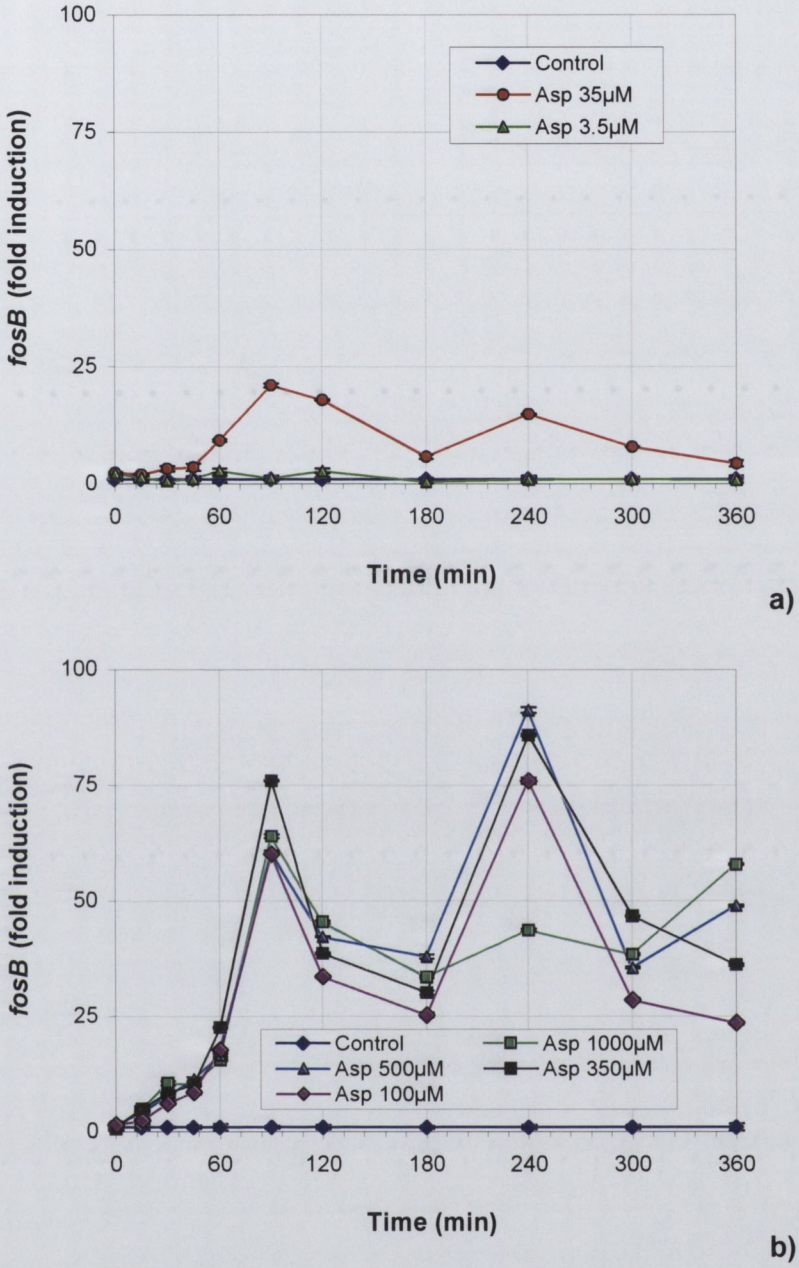


Figure 5.15: Changes in *fosB* expression as a function of time and Asp concentration

Rat cortical neurons (13 DIV) were exposed to various concentrations of Asp, for up to 360 min. Following treatment, the cells were lysed and total RNA was extracted and the amount of *fosB* and 18S quantified by RT-PCR. *FosB* expression values were normalised to 18S expression, which served as the internal control. The results above refer to the fold induction of *fosB* expression compared to untreated, time-matched controls. Data represent mean ± s.d. values of triplicate RT-PCR reactions derived from one individual experiment. The experiments were reproduced at least three times. Figure 5.15 a) represents the *fosB* changes with non-toxic and partially toxic concentrations of Asp while b) represents changes in *fosB* expression with toxic concentrations.

When rat cortical neurons were treated with partially toxic concentrations of Asp (35 μM), a biphasic increase in *fosB* mRNA expression was observed, when compared to the time-matched controls. Pre-treatment with AP5 completely inhibited the biphasic *fosB* response. In contrast, pre-treatment with CNQX had no inhibitory effect (see Figure 5.16). Thus, the induction of *fosB* in rat cortical neurons, treated with a partially toxic concentration of Asp, was as a direct and specific result of over-stimulation of the NMDA subtype of Glu receptors.

Exposure to a toxic concentration of Asp (100 μM) induced a biphasic *fosB* response. It was found that pre-treatment with AP5, effectively antagonised the excitotoxic biphasic *fosB* response by decreasing the first wave of *fosB* expression and by completely inhibiting the second wave of expression. CNQX did not antagonise the biphasic *fosB* response (see Figure 5.17).

When rat cortical neurons were treated with an even higher toxic concentration of Asp (350 μM), AP5 changed the excitotoxic *fosB* profile by decreasing the first wave of expression and by completely inhibiting the second wave of expression. CNQX, failed to inhibit the excitotoxic biphasic *fosB* response (Figure 5.18).

These results demonstrate that Asp-induced *fosB* mRNA expression is mediated through the NMDA receptor subtype. In addition, the concentration of AP5 used in these *fosB* investigations was sufficient to compete with the highly toxic concentrations of Asp (100 μM and 350 μM). A possible explanation may be the less potent nature of Asp when compared to Glu.

5.2.10 Neither Ala nor paraquat induce *fosB* expression in rat cortical neurons

Ala, a non-excitotoxic amino acid, did not induce *fosB* mRNA expression in rat cortical neurons under conditions where other EAAs induce their effects (see Figure 5.19).

Paraquat, which induces neurotoxicity, but not excitotoxicity, in rat cortical neurons caused a slight induction in *fosB* mRNA levels at the early time-points (see Figure 5.20). However, this increase was disregarded due to the high standard deviations.

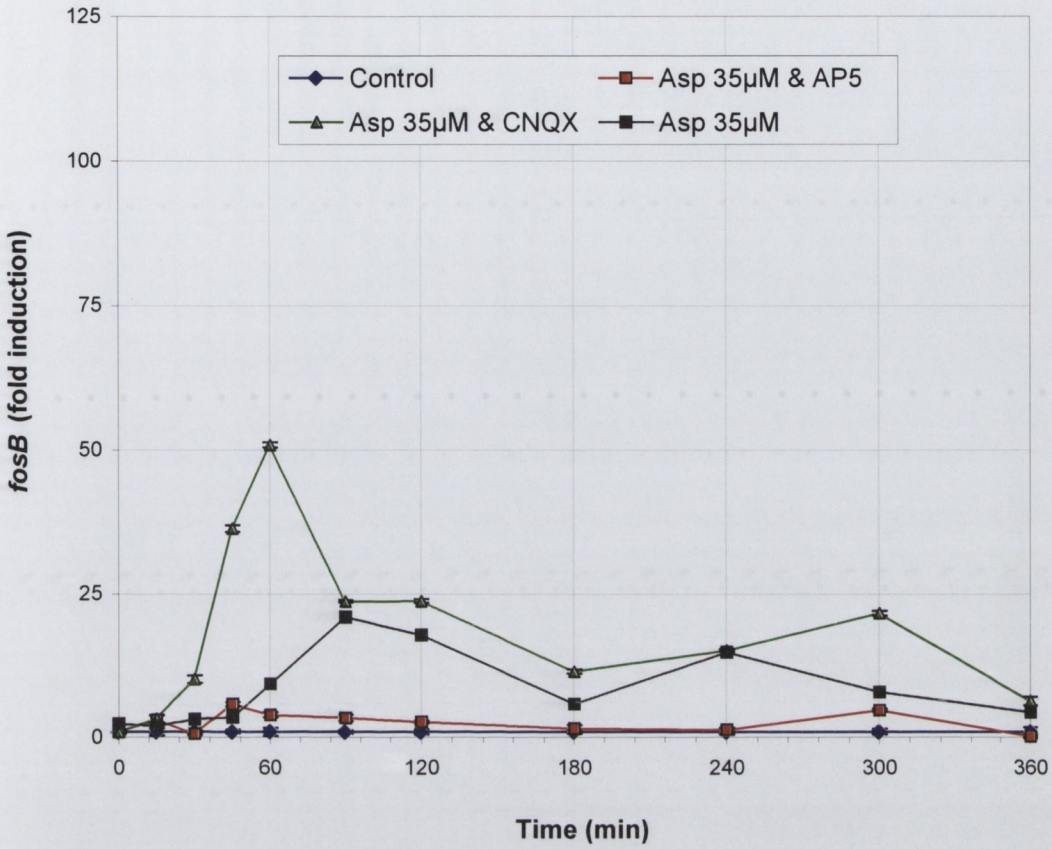


Figure 5.16: AP5 but not CNQX effectively abolishes *fosB* mRNA expression in rat cortical neurons stimulated with Asp (35 µM)

Rat cortical neurons (13 DIV) were pre-incubated for 15 min with either AP5 (500 µM) or CNQX (10 µM) prior to co-exposure with a fixed concentration of Asp (35 µM), for up to 360 min. Following treatment, the cells were lysed and total RNA was extracted and the amount of *fosB* and 18S quantified by RT-PCR. The *fosB* expression values were normalised to 18S expression, which served as the internal control. The results above refer to the fold induction of *fosB* expression compared to untreated, time-matched controls. Data represent mean ± s.d. values of triplicate RT-PCR reactions derived from one individual experiment.

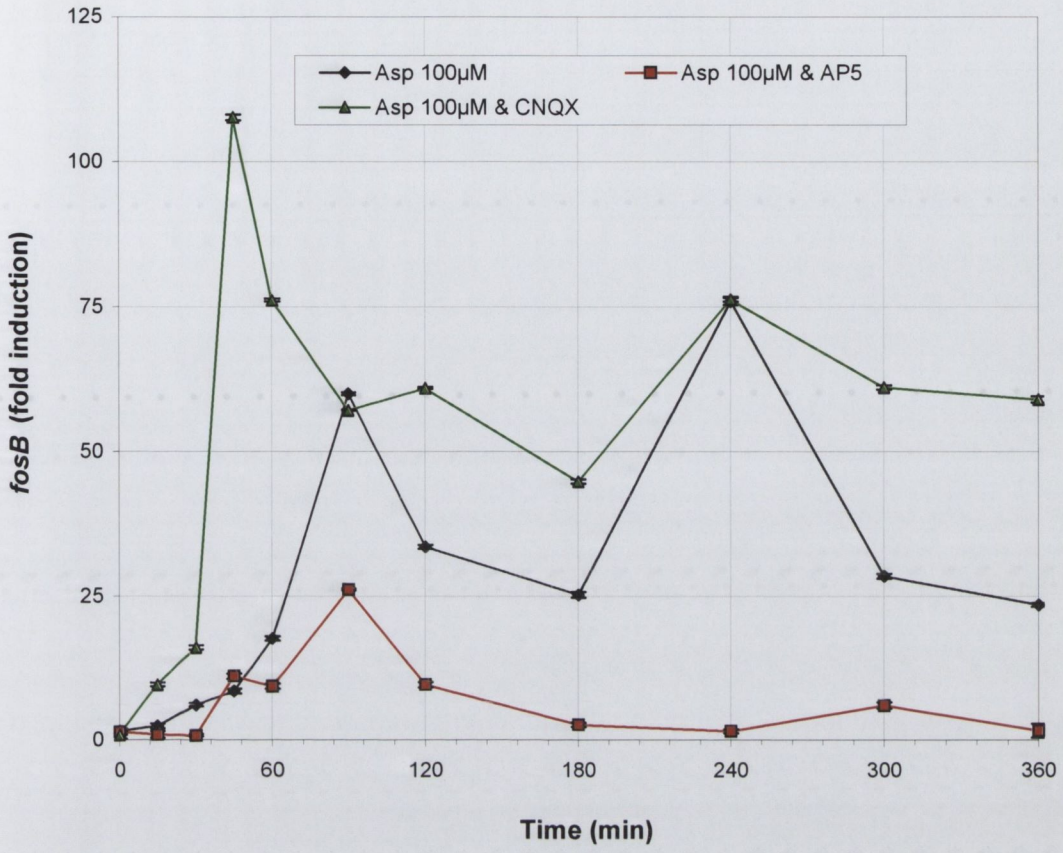


Figure 5.17: AP5 but not CNQX effectively antagonises the biphasic toxic *fosB* response induced by Asp (100 µM)

Rat cortical neurons (13 DIV) were pre-incubated for 15 min with either AP5 (500 µM) or CNQX (10 µM) prior to co-exposure with a fixed concentration of Asp (100 µM), for up to 360 min. Following treatment, the cells were lysed and total RNA was extracted and the amount of *fosB* and 18S quantified by RT-PCR. The *fosB* expression values were normalised to 18S expression, which served as the internal control. The results above refer to the fold induction of *fosB* expression compared to untreated, time-matched controls. Data represent mean ± s.d. values of triplicate RT-PCR reactions derived from one individual experiment.

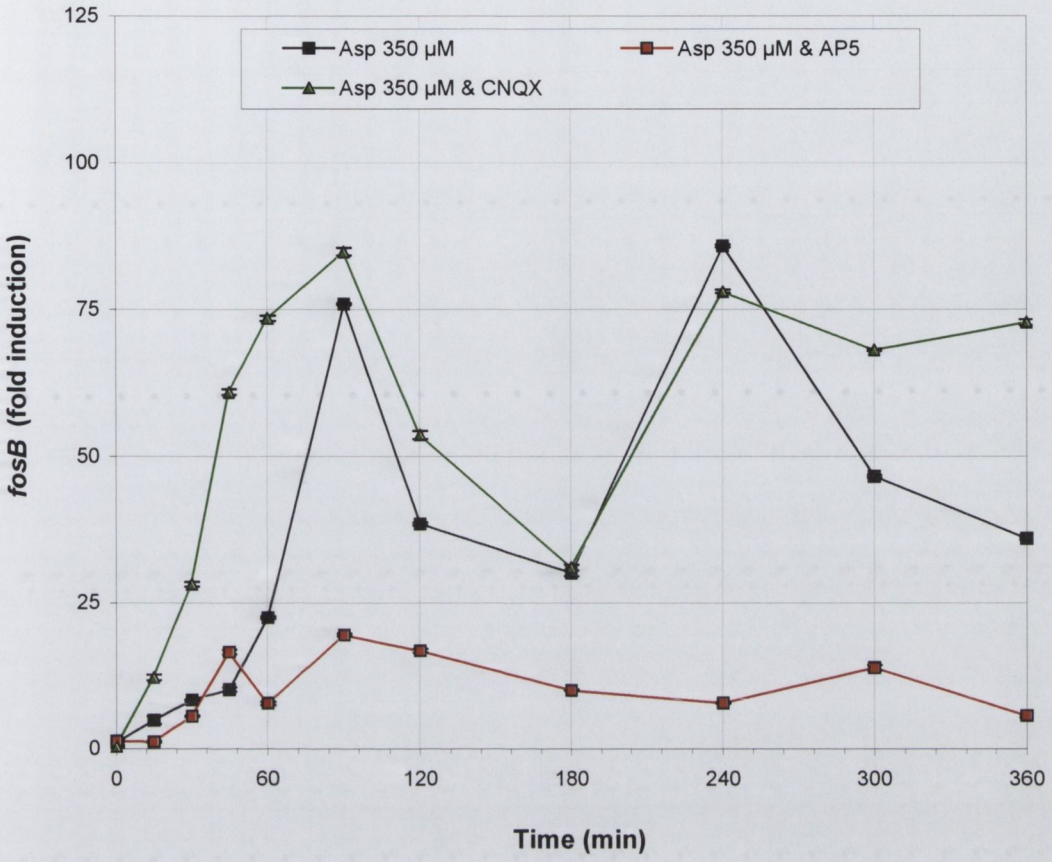
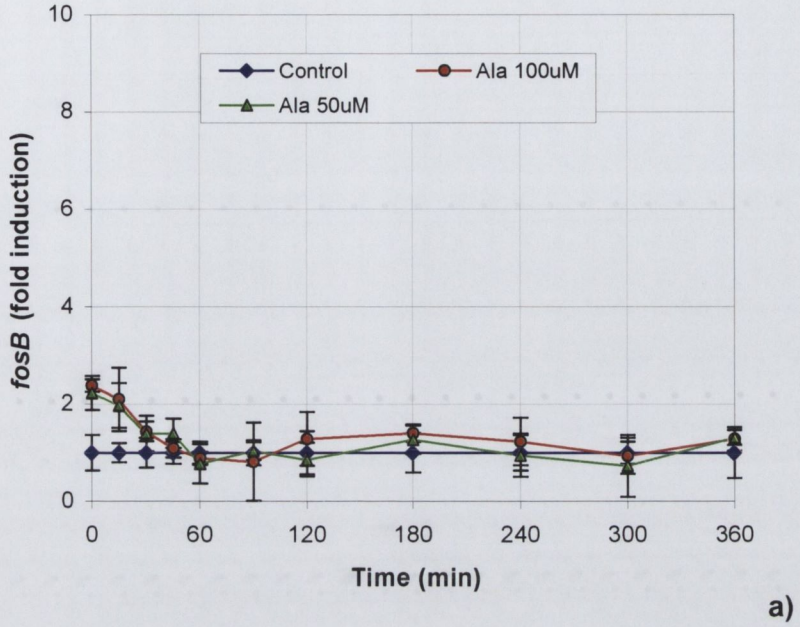


Figure 5.18: AP5 but not CNQX antagonises the biphasic excitotoxic *fosB* response induced by Asp (350 µM)

Rat cortical neurons (13 DIV) were pre-incubated for 15 min with either AP5 (500 µM) or CNQX (10 µM) prior to co-exposure with a fixed concentration of Asp (350 µM), for up to 360 min. Following treatment, the cells were lysed and total RNA was extracted and the amount of *fosB* and 18S quantified by RT-PCR. The *fosB* expression values were normalised to 18S expression, which served as the internal control. The results above refer to the fold induction of *fosB* expression compared to untreated, time-matched controls. Data represent mean ± s.d. values of triplicate RT-PCR reactions derived from one individual experiment.



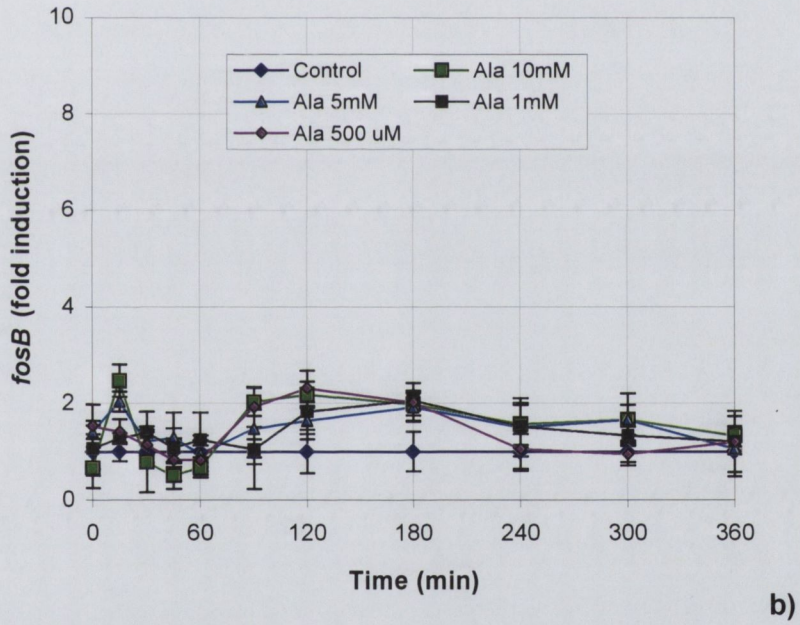
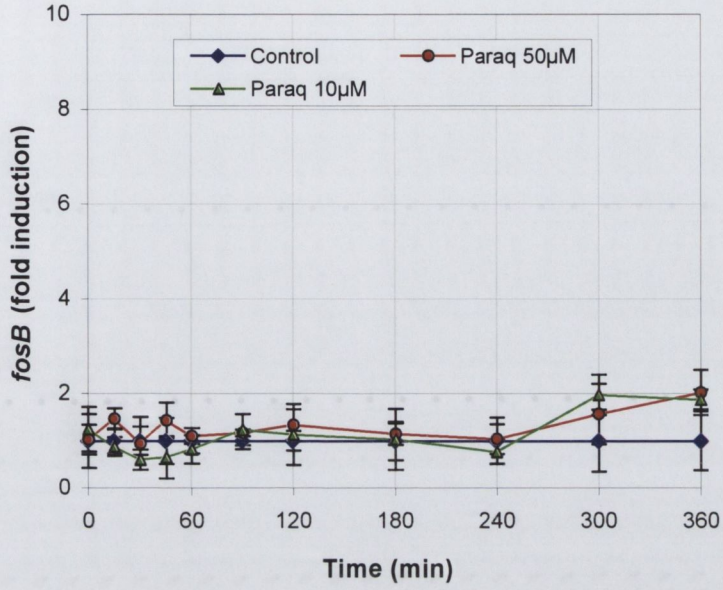
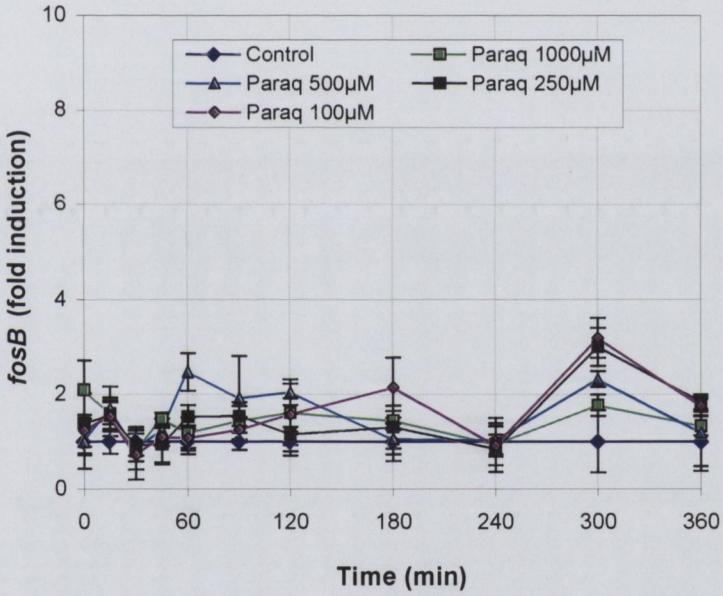


Figure 5.19: *fosB* mRNA expression is not induced in rat cortical neurons treated with Ala

Rat cortical neurons (13 DIV) were exposed to various concentrations of Ala, for up to 360 min. Following treatment, the cells were lysed and total RNA was extracted and the amount of *fosB* and 18S quantified by RT-PCR. The *fosB* expression values were normalised to 18S expression, which served as the internal control. The results above refer to the fold induction of *fosB* expression compared to untreated, time-matched controls. Data represent mean ± s.d. values of triplicate RT-PCR reactions derived from one individual experiment. The experiments were reproduced at least three times. Figure 5.19 a) represents the *fosB* changes with low concentrations of Ala while b) represents changes in *fosB* expression with high concentrations.



a)



b)

Figure 5.20: *fosB* mRNA is not induced in rat cortical neurons treated with paraquat

Rat cortical neurons (13 DIV) were exposed to various concentrations of paraquat, for up to 360 min. Following treatment, the cells were lysed and total RNA was extracted and the amount of *fosB* and 18S quantified by RT-PCR. The *fosB* expression values were normalised to 18S expression, which served as the internal control. The results above refer to the fold induction of *fosB* expression compared to untreated, time-matched controls. Data represent mean ± s.d. values of triplicate RT-PCR reactions derived from one individual experiment. The experiments were reproduced at least three times. Figure 5.20 a) represents *fosB* expression with partially toxic concentrations of paraquat while b) represents *fosB* expression with toxic concentrations.

5.2.11 Assessment of the potential of *c-fos* and *fosB* as screens for excitotoxicity

In the previous Chapter and in Sections 5.2.1/3/6/8 of this Chapter, it was shown that both *c-fos* and *fosB* are induced in mCGCs and rat cortical neurons under excitotoxic conditions. Furthermore, the levels of induction of both *IEGs* are much higher in rat cortical neurons when compared to mCGCs. From consideration of the previous results, it was decided to investigate whether the measurement of *c-fos* and *fosB* in rat cortical neurons could be used to predict the excitotoxic potential of compounds. A 60 min time-point was selected as the earliest possible time-point to reflect elevated and sustained *c-fos* and *fosB* expression, under excitotoxic conditions.

The hypothesis of this new screen was that for a compound to be classified as excitotoxic, it must induce an unambiguous elevation in *c-fos* mRNA expression from a low concentration to a high concentration at one time-point, 60 min, and the elevated *c-fos* response must be inhibited or reduced in the presence of an NMDA receptor antagonist.

The low (non-toxic) and high (toxic) concentrations used for each compound were chosen from the data obtained in the MTT cytotoxicity experiments, over a range of concentrations of the compound, performed by Griffiths and colleagues at the University of St. Andrews, Scotland, on mCGCs. It was assumed that, despite the possible differences in the EC_{50} values of the compounds in mCGCs and rat cortical neurons, the concentrations were both high enough and low enough to see a trend in an initial assessment.

Rat cortical neurons were exposed to low and high concentrations of the various compounds for 60 min. Exposures were also performed in the presence and/or absence of an antagonist cocktail containing AP5 and CNQX. The cells were lysed, total RNA was extracted and the *c-fos, fosB* and 18S mRNA levels measured by the method of real-time RT-PCR. *c-fos* and *fosB* expression values were normalised to the internal control, 18S, prior to calculation of the fold induction of both *IEGs* relative to the untreated, time matched controls (see Chapter 2). A subset of 15 compounds were selected, from the lists of compounds used in the "original" (see Section 4.2.8) and "modified" (see Section 4.2.9) mCGC screens, that were representative of the same 4 relevant groups, namely, excitotoxins (Group 1), neurotoxic but non-excitotoxic compounds (Group 2), neuroactive but non-toxic compounds (Group 3) and compounds that were toxic to other target organelles (Group 4).

5.2.12 Analysis of the effects of a wide range of compounds on *c-fos* expression

The *c-fos* mRNA levels for the 15 different compounds are shown in Tables 5.1 a) and b). The first group, the "excitotoxins", were comprised of the following 10 compounds: Glu, Asp, QA, *S*-sulpho-L-cysteine (L-SSC), KA, NMDA, L-homocysteine sulphinate (L-HCSA), L-homocysteic acid (L-HCA), D-homocysteic acid (D-HCA) and L-cysteine sulphinate (L-CSA). It was found that all 10 excitotoxins induced elevated and sustained levels of *c-fos* mRNA expression with high concentrations when compared to the low concentrations. The elevated levels of *c-fos* mRNA expression observed with low concentrations of QA and L-HCSA indicate that the low concentrations may have been toxic to the rat cortical neurons and therefore a lower concentration should have been chosen to represent the non-toxic condition. Although, pre-treatment of the neurons with the AP5/CNQX antagonist cocktail inhibited the elevated *c-fos* expression levels induced by high concentrations of 8 compounds, inhibition was not observed in the case of L-HCSA probably due to the very high concentrations of agonists used. KA also induced an increase in *c-fos* mRNA expression with the low concentration, which changed to a more elevated profile with the high concentration. However, no inhibition was observed in the presence of the antagonist cocktail which was probably due to saturation of the KA receptor (see Table 5.1 a)). Overall, the results reveal that *c-fos* expression levels correctly predicted these compounds as excitotoxic.

The second group contained one example of a "neurotoxic but non-excitotoxic" compound, namely MPP^+ iodide. As MPP^+ iodide did not induce *c-fos* mRNA expression with either low or high concentrations and also in the presence of the AP5/CNQX antagonist cocktail, this compound was predicted as non-excitotoxic (Table 5.1 b)).

The third group contained the "neuroactive but non-toxic" compounds Ala, GABA and glycine. Although GABA and glycine were correctly predicted as being non-excitotoxic, Ala seemed to meet the criteria of an excitotoxic compound. However, the small increase and the fact that Ala did not induce *c-fos* in Section 5.2.5 allow this result to be disregarded.

The fourth group contained only paraquat, a compound which was classified as being "toxic to other target organelles" (see Table 5.1 b)). Although high concentrations of paraquat gave increased *c-fos* expression, which was inhibited by the antagonist cocktail, paraquat can be considered as non-excitotoxic as it was shown in Section 5.2.10 that paraquat has no effect on *c-fos* induction with time or concentration. Overall, the results show that elevated *c-fos* mRNA expression correlates with excitotoxicity, although conditions such as concentrations of compounds and antagonists may not be optimal.

Group 1	60 min fold induction	Prediction	Correct Prediction
Glu Low (2.5 µM) Glu High (250 µM) Glu High & AP5/CNQX	3,7 71,3 57,6	Excitotoxic	Yes
Asp Low (3.5 µM) Asp High (350 µM) Asp High & AP5/CNQX	2,1 82,1 14,5	Excitotoxic	Yes
QA Low (30 µM) QA High (3000 µM) QA High & AP5/CNQX	86,0 78,3 68,0	Non-Excitotoxic	No
L-SSC Low (1 µM) L-SSC High (100 µM) L-SSC High & AP5/CNQX	8,4 63,0 42,8	Excitotoxic	Yes
KA Low (20 µM) KA High (2000 µM) KA High & AP5/CNQX	48,6 105,9 107,4	Non-Excitotoxic	No
NMDA Low (2.5 µM) NMDA High (250 µM) NMDA High & AP5/CNQX	2,0 38,8 0,6	Excitotoxic	Yes
L-HCSA Low (30 µM) L-HCSA High (3000 µM) L-HCSA High & AP5/CNQX	50,1 37,9 46,8	Non-Excitotoxic	No
L-HCA Low (3 µM) L-HCA High (300 µM) L-HCA High & AP5/CNQX	13,0 53,5 13,2	Excitotoxic	Yes
D-HCA Low (15 µM) D-HCA High (1500 µM) D-HCA High & AP5/CNQX	16,2 53,4 48,6	Excitotoxic	Yes
L-CSA Low (2 µM) L-CSA High (200 µM) L-CSA High & AP5/CNQX	1,2 52,8 12,2	Excitotoxic	Yes

Group 2	60 min fold induction	Prediction	Correct Prediction
MPP^+ iodide Low (4 µM)	1,3	Non-Excitotoxic	Yes
MPP^+ iodide High (400 µM)	1,3		
MPP^+ iodide High & AP5/CNQX	1,2		
Group 3	**60 min fold induction**	**Prediction**	**Correct Prediction**
Ala Low (100 µM)	1,3	Excitotoxic	No
Ala High (10 mM)	3,8		
Ala High & AP5/CNQX	1,5		
GABA Low (10 µM)	2,6	Non-Excitotoxic	Yes
GABA High (1000 µM)	7,6		
GABA High & AP5/CNQX	7,0		
Glycine Low (100 µM)	1,0	Non-Excitotoxic	Yes
Glycine High (10 mM)	1,0		
Glycine High & AP5/CNQX	7,7		
Group 4	**60 min fold induction**	**Prediction**	**Correct Prediction**
Paraquat Low (2.5 µM)	1,4	Excitotoxic	No
Paraquat High (250 µM)	5,2		
Paraquat High & AP5/CNQX	1,0		

Table 5.1 a) & b) *c-fos* screen of 4 different classes of compounds

Primary cultures of rat cortical neurons (13 DIV) were exposed to 4 different classes of compounds for 60 min at "low" non-toxic concentrations or at "high" toxic concentrations. The cortical neurons were pre-incubated for 15 min with an antagonist "cocktail" of AP5 (500 µM) and CNQX (10 µM) prior to exposure to the high concentration of each compound. Following treatment, the cells were lysed, total RNA was extracted and the amount of *c-fos* and 18S quantified by RT-PCR. The expression values of *c-fos* were normalised to 18S, which served as the internal control. The results above refer to the fold induction of *c-fos* expression compared to untreated, time-matched controls. Data represent mean values of triplicate RT-PCR reactions derived from one individual experiment. The experiments were reproduced at least twice.

5.2.13 Analysis of the effects of a range of compounds on *fosB* expression

The *fosB* mRNA levels for the 15 different compounds are shown in Tables 5.2 a) and b). The "excitotoxins" (Group 1) were comprised of Glu, QA, Asp, L-SSC, KA, NMDA, L-HCSA, L-HCA, D-HCA and L-CSA. It was found that all 10 compounds induced elevated *fosB* mRNA expression under excitotoxic conditions, when compared to *fosB* expression under non-toxic conditions. For 8 compounds, antagonism predicted NMDA receptor pharmacology. Surprisingly for Glu, there was no receptor antagonism. However, it has been shown in Chapter 4 and in Section 5.2.7 of this Chapter that AP5 did not antagonise the elevated *fosB* expression induced by this high concentration of Glu. For L-HCSA, no receptor antagonism of *fosB* expression was observed, probably because this compound induced high levels of expression even at the low concentrations used. These results are in accordance with the pharmacology of L-HCSA induced *c-fos* expression and thus support our earlier reasoning that the concentration chosen for this compound was too high for optimal agonist antagonist competition. Although, KA induced an increase in *fosB* mRNA expression with the non-toxic concentration, which changed to a more elevated profile with the toxic concentration, no inhibition was observed in the presence of the antagonist cocktail, again probably due to saturation of the KA receptor (see Table 5.2 a)).

The second group contained the "neurotoxic but non-excitotoxic" compound MPP^+ iodide. Induction of *fosB* mRNA was not observed in rat cortical neurons treated with non-toxic or toxic concentrations of MPP^+ iodide and also in the presence of the AP5/CNQX antagonist cocktail. Thus, measurement of *fosB* expression levels correctly predicted this compound as non-excitotoxic (see Table 5.2 b)).

The third group contained the "neuroactive but non-toxic" compounds, Ala, GABA and glycine. High concentrations of all 3 compounds induced small increases in *fosB* mRNA expression, which were inhibited in the presence of the antagonist cocktail. However, the small increases can be regarded as insubstantial when compared to the elevated levels of *fosB* expression with toxic concentrations of the excitotoxins (see Table 5.2 b)). All 3 compounds can thus be considered as non-excitotoxic.

The fourth group contained paraquat. Although high concentrations of paraquat gave increased *c-fos* expression, which was inhibited by the antagonist cocktail, the expression levels of this compound were very low and it was also shown in Section 5.2.10 that paraquat has no effect on *c-fos* induction with time or concentration (see Table 5.2 b)).

To summarise, both *c-fos* and *fosB* can be used as screens to predict the excitotoxic properties of compounds on rat cortical neurons. This study is by no means exhaustive and further work using a greater range of compounds and optimised antagonist concentrations is required. However, the results show that the levels of expression of *c-fos* and *fosB* are so high that a single time-single concentration endpoint can be used. The addition of the receptor pharmacology criterion again needs to be treated with caution for compounds with unknown Glu receptor pharmacology.

5.2.14 Effects of the excitotoxin, Glu, on the expression of other members of the *fos* and *jun* families of *IEGs*

In addition to *c-fos* and *fosB*, expression profiles were determined for other members of the *fos* (*fra-1* and *fra-2*) and *jun* (*c-jun*, *junB* and *junD*) families of *IEGs*. Mature rat cortical neurons (13 DIV) were treated with various concentrations of Glu over 360 min, and real-time RT-PCR performed on cell extracts to investigate changes in the expression of other members of the *fos* and *jun* families of genes in excitotoxicity (see Figures 5.21 to 5.25). The expression values of all genes measured were normalised to the internal control, 18S, prior to calculation of the fold induction values of all genes relative to the untreated, time matched controls (see Chapter 2).

When rat cortical neurons were treated with various concentrations of Glu (0 – 1 mM) over 360 min, no increase in *fra-1* expression was observed, when compared to the time-matched controls.

High concentrations of Glu (100 – 1000 μM) induced increases of up to 17 fold in *fra-2* expression. A similar but much smaller increase (factor of 2) was also observed in mCGCs treated with Glu. Thus, the results suggest that, although the induction of *fra-2* in rat cortical neurons is small when compared to the expression values of *c-fos* and *fosB* with high concentrations of Glu and Asp, *fra-2* mRNA expression is induced under excitotoxic conditions. Further work is therefore required to investigate the role of *fra-2* in excitotoxicity.

c-jun only induced a small increase in expression (6 fold) at one time-point (300 min) with toxic concentrations of Glu (250 – 1000 μM). No increase in either *junB* or *junD* mRNA expression was observed over 360 min with non-toxic and toxic concentrations of Glu.

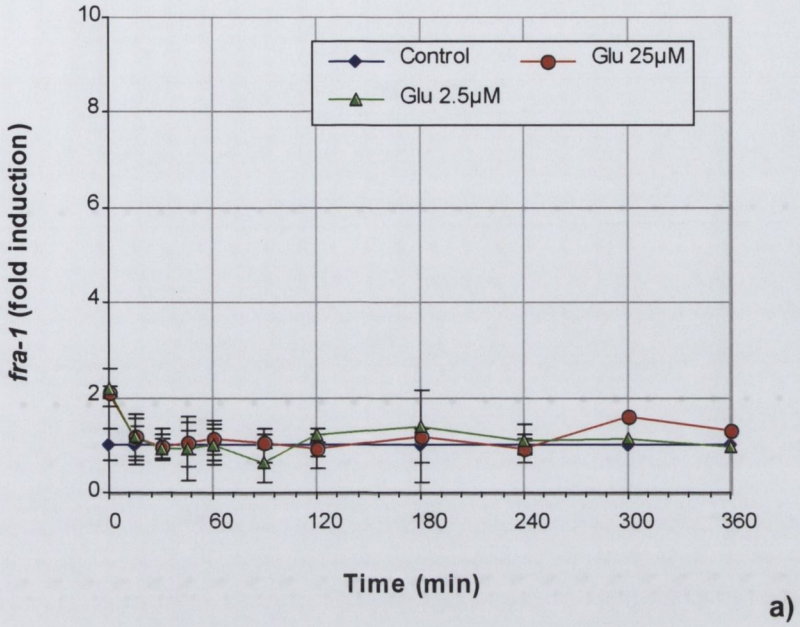
Overall, these studies have shown, in the rat, that 3 members of the *fos* family of *IEGs*, namely *c-fos*, *fosB* and *fra-2*, have increased expression under excitotoxic conditions.

Group 1	60 min fold induction	Prediction	Correct Prediction
Glu Low (2.5 µM) Glu High (250 µM) Glu High & AP5/CNQX	6,9 95,0 107,8	Non-Excitotoxic	No
Asp Low (3.5 µM) Asp High (350 µM) Asp High & AP5/CNQX	2,02 121,6 3,3	Excitotoxic	Yes
QA Low (30 µM) QA High (3000 µM) QA High & AP5/CNQX	135,9 109,6 97	Non-Excitotoxic	No
L-SSC Low (1 µM) L-SSC High (100 µM) L-SSC High & AP5/CNQX	2,1 77,5 29,6	Excitotoxic	Yes
KA Low (20 µM) KA High (2000 µM) KA High & AP5/CNQX	76,5 168,1 150,5	Excitotoxic	Yes
NMDA Low (2.5 µM) NMDA High (250 µM) NMDA High & AP5/CNQX	1,2 60,3 0,3	Excitotoxic	Yes
L-HCSA Low (30 µM) L-HCSA High (3000 µM) L-HCSA High & AP5/CNQX	51,1 31,8 32,9	Non-Excitotoxic	No
L-HCA Low (3 µM) L-HCA High (300 µM) L-HCA High & AP5/CNQX	12,7 48,5 5,7	Excitotoxic	Yes
D-HCA Low (15 µM) D-HCA High (1500 µM) D-HCA High & AP5/CNQX	11,4 72,2 58,5	Excitotoxic	Yes
L-CSA Low (2 µM) L-CSA High (200 µM) L-CSA High & AP5/CNQX	1,7 92,4 1,9	Excitotoxic	Yes

Group 2	60 min fold induction	Prediction	Correct Prediction
MPP^+ iodide Low (4 µM) MPP^+ iodide High (400 µM) MPP^+ iodide High & AP5/CNQX	0,8 1,3 0,7	Excitotoxic	No
Group 3	**60 min fold induction**	**Prediction**	**Correct Prediction**
Ala Low (100 µM) Ala High (10 mM) Ala High & AP5/CNQX	1,1 4,4 0,9	Excitotoxic	No
GABA Low (10 µM) GABA High (1000 µM) GABA High & AP5/CNQX	1,1 2,0 0,8	Excitotoxic	No
Glycine Low (100 µM) Glycine High (10 mM) Glycine High & AP5/CNQX	2,1 9,8 1,4	Excitotoxic	No
Group 4	**60 min fold induction**	**Prediction**	**Correct Prediction**
Paraquat Low (2.5 µM) Paraquat High (250 µM) Paraquat High & AP5/CNQX	0,7 2,3 0,5	Excitotoxic	No

Tables 5.2 a) & b): *fosB* screen of 4 different classes of compounds.

Primary cultures of rat cortical neurons (13 DIV) were exposed to 4 different classes of compounds for 60 min at "low" non-toxic concentrations; or at "high" toxic concentrations. The cortical neurons were pre-incubated for 15 min with an antagonist "cocktail" of AP5 (500 µM) and CNQX (10 µM) prior to exposure to the "High" concentration of each compound. Following treatment, the amount of *fosB* and 18S were quantified by RT-PCR. *The fosB* expression values were normalised to 18S, which served as the internal control. The results above refer to the fold induction of *18S* expression compared to untreated, time-matched controls. Data represent mean values of triplicate RT-PCR reactions derived from one individual experiment. The experiments were reproduced at least twice.



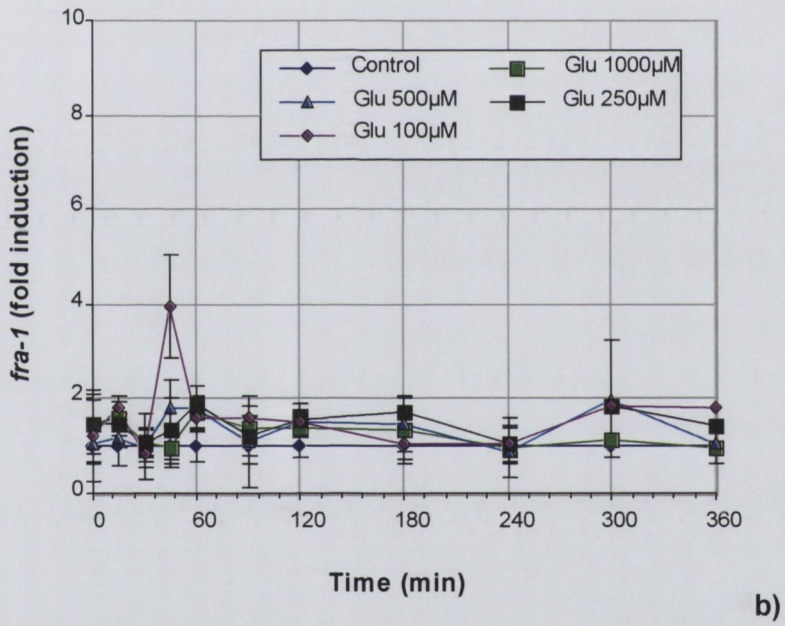
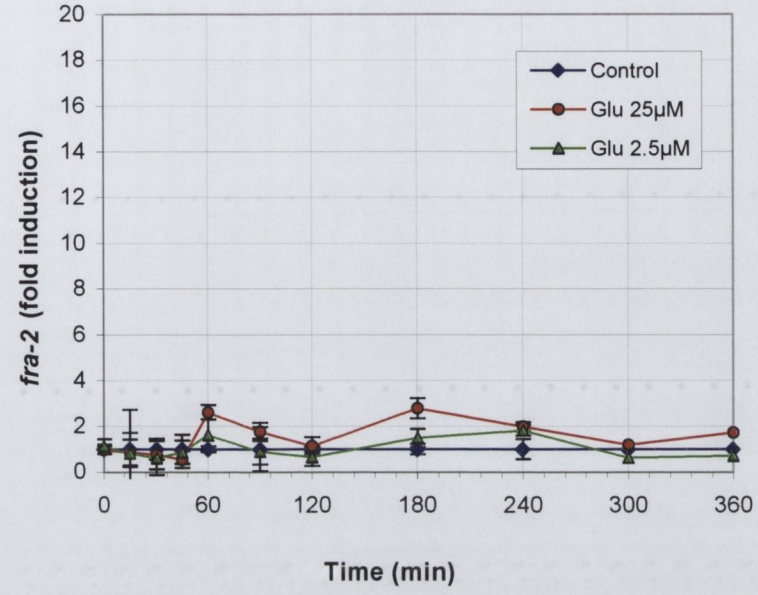
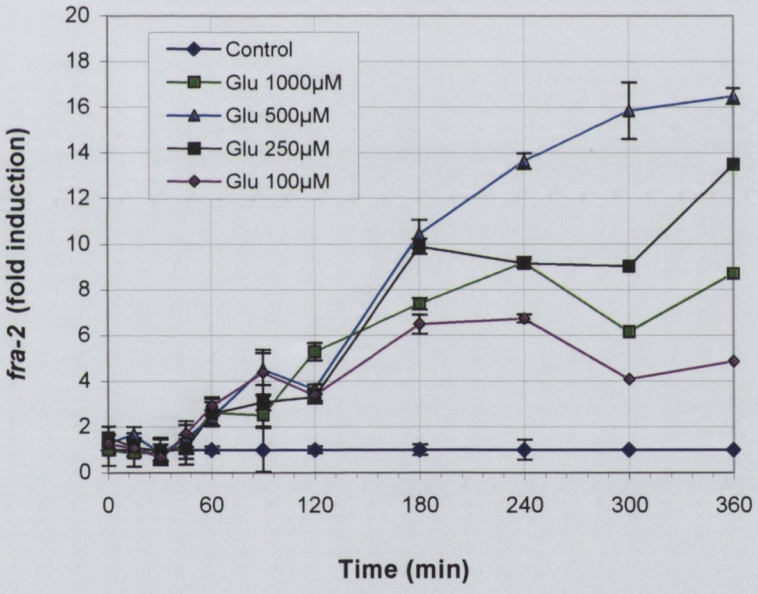


Figure 5.21: Induction of *fra-1* mRNA in rat cortical neurons treated with Glu

Rat cortical neurons (13 DIV) were exposed to various concentrations of Glu, for up to 360 min. Following treatment, the cells were lysed, total RNA was extracted and the amount of *fra-1* and 18S quantified by RT-PCR. The expression values of *fra-1* were normalised to 18S expression, which served as the internal control. The results above refer to the fold induction of *fra-1* expression compared to untreated, time-matched controls. Data represent mean ± s.d. values of triplicate RT-PCR reactions derived from one individual experiment. Figure 5.22 a) represents the *fra-1* changes with non-toxic and partially toxic concentrations of Glu while b) represents changes in *fra-1* expression with toxic concentrations.



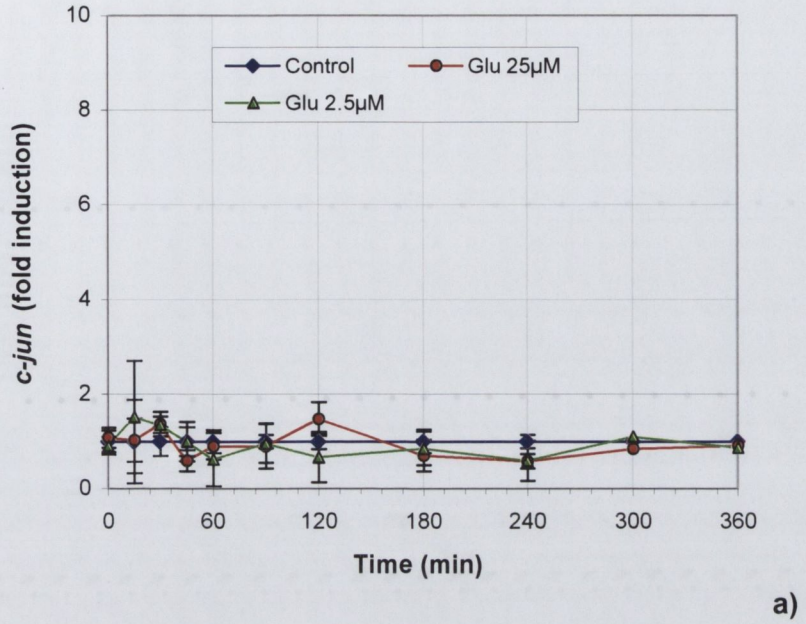
a)



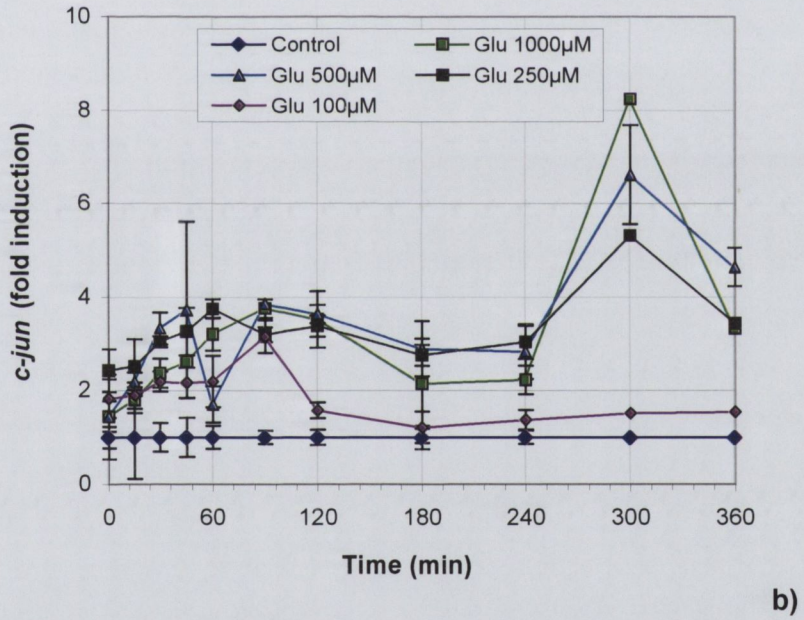
b)

Figure 5.22: Induction of *fra-2* mRNA in rat cortical neurons treated with Glu

Rat cortical neurons (13 DIV) were exposed to various concentrations of Glu, for up to 360 min. Following treatment, the cells were lysed, total RNA was extracted and the amount of *fra-2* and 18S quantified by RT-PCR. The expression values of *fra-2* were normalised to 18S expression, which served as the internal control. The results above refer to the fold induction of *fra-2* expression compared to untreated, time-matched controls. Data represent mean ± s.d. values of triplicate RT-PCR reactions derived from one individual experiment. Figure 5.22 a) represents the *fra-2* changes with non-toxic and partially toxic concentrations of Glu while b) represents changes in *fra-2* expression with toxic concentrations.



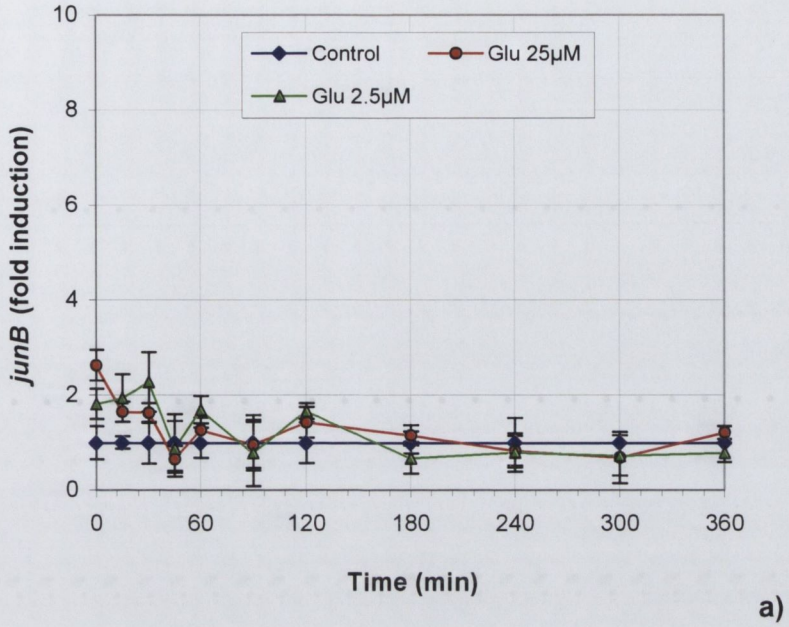
a)



b)

Figure 5.23: No induction of *c-jun* mRNA in mature rat cortical neurons treated with Glu

Rat cortical neurons (13 DIV) were exposed to various concentrations of Glu, for up to 360 min. Following treatment, the cells were lysed and total RNA was extracted and the amount of *c-jun* and 18S quantified by RT-PCR. The *c-jun* expression values were normalised to 18S expression, which served as the internal control. The results above refer to the fold induction of *c-jun* expression compared to untreated, time-matched controls. Data represent mean ± s.d. values of triplicate RT-PCR reactions derived from one individual experiment. The experiments were reproduced at least three times. Figure 5.23 a) represents the *c-jun* changes with non-toxic and partially toxic concentrations of Glu while b) represents changes in *c-jun* expression with toxic concentrations.



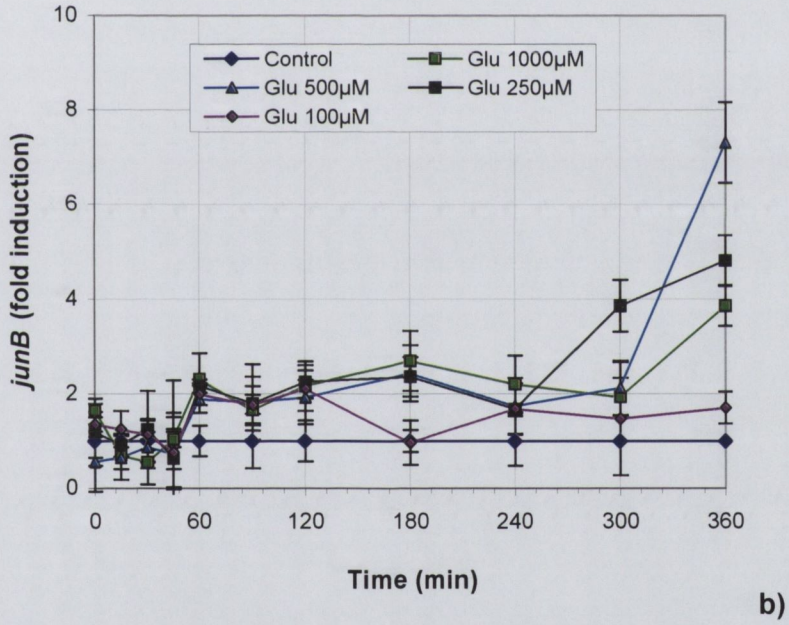


Figure 5.24: No induction of *junB* mRNA in mature rat cortical neurons treated with Glu

Rat cortical neurons (13 DIV) were exposed to various concentrations of Glu, for up to 360 min. Following treatment, total RNA was extracted and the amount of *junB* and 18S quantified by RT-PCR. The *junB* expression values were normalised to 18S expression, which served as the internal control. The results above refer to the fold induction of *junB* expression compared to untreated, time-matched controls. Data represent mean ± s.d. values of triplicate RT-PCR reactions derived from one individual experiment. The experiments were reproduced at least three times. Figure 5.24 a) represents the *junB* changes with non-toxic and partially toxic concentrations of Glu while b) represents changes in *junB* expression with toxic concentrations.

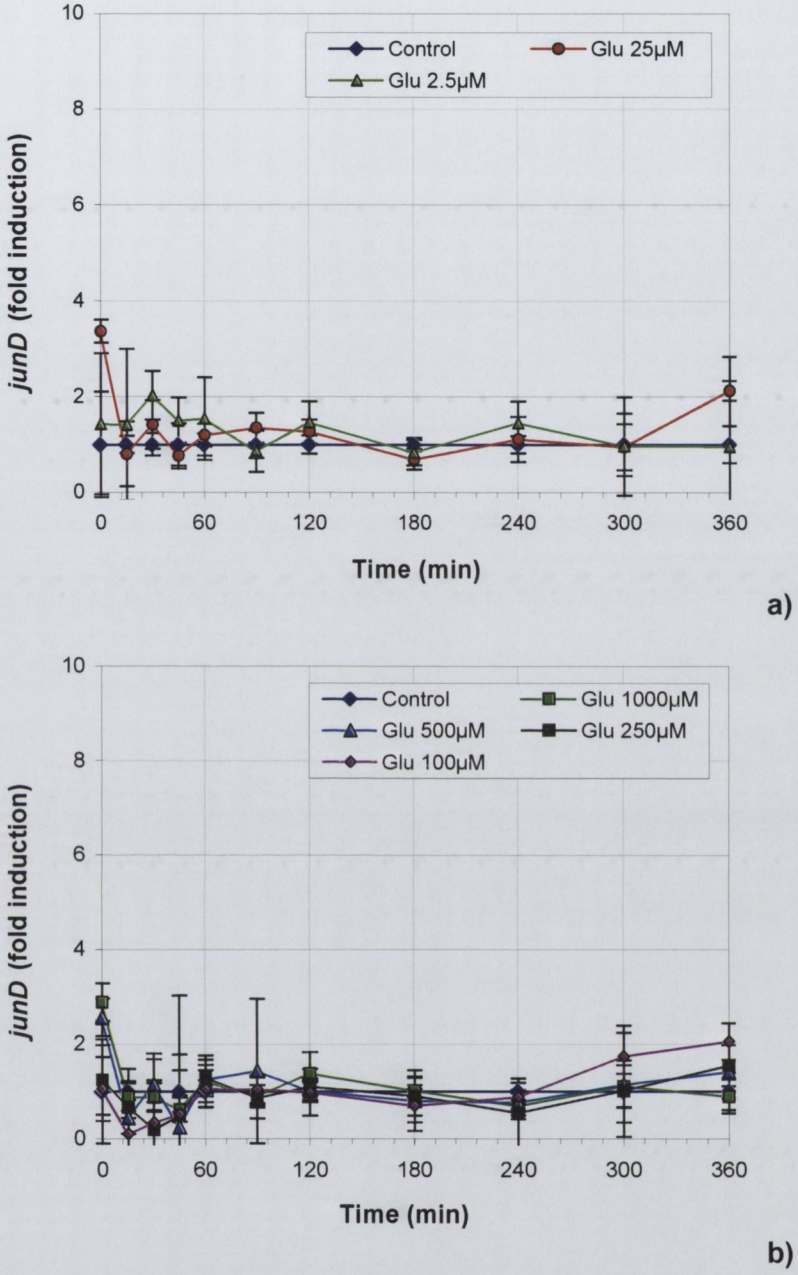


Figure 5.25: No induction of *junD* mRNA in mature rat cortical neurons treated with Glu

Rat cortical neurons (13 DIV) were exposed to various concentrations of Glu, for up to 360 min. Following treatment, the cells were lysed and total RNA was extracted and the amount of *junD* and 18S quantified by RT-PCR. The *junD* expression values were normalised to 18S expression, which served as the internal control. The results above refer to the fold induction of *junD* expression compared to untreated, time-matched controls. Data represent mean ± s.d. values of triplicate RT-PCR reactions derived from one individual experiment. The experiments were reproduced at least three times. Figure 5.25 a) represents the *junD* changes with non-toxic and partially toxic concentrations of Glu while b) represents changes in *junD* expression with toxic concentrations.

5.3 Discussion

The immediate response of the cell to external stimuli results in the induction of a select set of genes, many of which are nuclear proto-oncogenes. Prominent among these early response genes are members of the *fos* and *jun* families. In Chapter 4, it was shown that in addition to *c-fos*, *fosB* was transiently expressed in mCGCs following a brief stimulation with non-toxic concentrations of Glu. Both *fos* family members gave different expression profiles depending on EAA concentration and the length of the exposure period. Following exposure to a more toxic concentration of Glu, the transient profile of *fosB* expression changed to a more delayed, elevated and sustained profile. Moreover, the excitotoxin-induced elevation of *fosB* mRNA was prevented in the presence of the NMDA-receptor antagonist, AP5, but not in the presence of the non-NMDA receptor antagonist, CNQX. Thus, these profiles of *fosB* mRNA expression, under toxic conditions, suggested that *fosB* is also involved in the mechanism of excitotoxicity. When the expression levels of both *c-fos* and *fosB*, induced by toxic concentrations of Glu were compared, it was observed that the levels of *fosB* were higher than *c-fos*. Thus, it seemed that *fosB* may also be a more sensitive endpoint for excitotoxicity investigations.

The first aim of Chapter 5 was to investigate the profiles of *c-fos* and *fosB* expression in neuronal cells from a different species and brain region, treated with various concentrations of two known excitotoxins. Rat cortical neurons were exposed to various concentrations of Glu and Asp and the levels of expression of *c-fos* mRNA measured by real-time RT-PCR. The results revealed that different time profiles of *c-fos* mRNA expression were obtained which were dependent on EAA concentration. It was found that following exposure of the cortical cells to non-toxic concentrations of Glu, a rapid, transient increase in *c-fos* mRNA expression occurred. In contrast, exposure to toxic concentrations of Glu induced a rapid, elevated and sustained increase in *c-fos* mRNA expression. With non-toxic concentrations of Asp, no increase in *c-fos* mRNA expression was observed. However, exposure to toxic concentrations of Asp induced the same early, elevated and sustained profiles as observed with toxic concentrations of Glu. Thus, sustained profiles of *c-fos* expression, induced by toxic concentrations of EAAs, are mechanistically relevant in excitotoxicity.

The pharmacology of EAA-induced *c-fos* mRNA expression in rat cortical neurons was investigated using the NMDA receptor antagonist, AP5 and the non-NMDA receptor antagonist, CNQX. AP5 effectively inhibited the *c-fos* response induced by partially toxic

concentrations of Glu and Asp. With higher, toxic concentrations of Glu, AP5 had no inhibitory effect. However, AP5 reduced the profile of *c-fos* expression induced by toxic concentrations of Asp to an early peaking, less sustained expression. Thus, the effectiveness of AP5, in blocking the excitotoxic *c-fos* response, was inversely proportional to the potent properties and/or concentrations of EAAs used. With all toxic concentrations of the EAAs, pre-treatment with CNQX did not prevent the excitotoxic *c-fos* response. Thus, elevated and sustained expression of *c-fos* mRNA, induced by toxic concentrations of Glu or Asp, is mediated by over-activation of the NMDA receptor and not the AMPA and/or kainate receptors.

In both *in vitro* model systems used, that is mCGCs and rat cortical neurons, to investigate early gene expression in excitotoxicity, large differences were observed in the induction levels and profiles of *c-fos* mRNA. In rat cortical neurons, *c-fos* mRNA expression, under toxic conditions, occurred earlier than in mCGCs. In addition, expression levels at the toxic parameter were higher than in mCGCs. These observations suggest the rat cortical system as a sensitive model for *in vitro* investigations into gene expression analysis.

The next aim of this Chapter was to investigate whether *fosB* was induced in rat cortical neurons treated with various concentrations of Glu and Asp, and whether its expression levels correlated with either the *c-fos* or *fosB* expression profiles observed in mCGCs. It was observed that non-toxic concentrations of Glu and Asp induced a transient increase in *fosB* mRNA levels. Higher, partially toxic and also toxic concentrations of both EAAs changed the kinetics of *fosB* mRNA expression. Instead of the *fosB* expression profile found in mCGCs (see Chapter 4) an elevated, sustained and biphasic *fosB* response was observed under excitotoxic conditions. Thus, the profile of *fosB* expression in rat cortical neurons undergoing excitotoxic cell death is different from that observed in mCGCs. The differences in expression between the excitotoxic profiles of *c-fos* and *fosB* may be related to neuronal type (cortex versus cerebellum) and/or species (mouse versus rat).

In order to identify whether the biphasic excitotoxic *fosB* response was mediated by the NMDA receptor, receptor specific antagonists were used. The specific NMDA receptor antagonist, AP5, was used and the levels of inhibition were compared with the non-NMDA receptor antagonist, CNQX. AP5 completely blocked the biphasic *fosB* expression induced by partially toxic concentrations of both Glu and Asp and also toxic concentrations of both EAAs. However, it was found that with a very toxic concentration of Glu, AP5 was unable to block the elevated, sustained and biphasic *fosB* response. In contrast to Glu, AP5 was sufficient to block the effect of very toxic concentrations of Asp.

A likely reason for the difference between Glu and Asp pharmacology is the relative potencies of the excitotoxins. Indeed, the levels of *fosB* expression in response to highly toxic concentrations of Glu were higher when compared to Asp, indicating the much higher potency of Glu. Therefore, not only the concentration of EAA used dictates the level of protection offered by AP5 against the excitotoxic *IEG* response, but also the relative potencies of the compounds. With non-toxic and toxic concentrations of either Glu or Asp, CNQX offered no protection against *fosB* mRNA expression. These results demonstrate that rat cortical neurons induce a sustained, elevated and biphasic *fosB* response under excitotoxic conditions, which is NMDA receptor mediated.

Exposure of the rat cortical neurons to the non-EAA, Ala, induced neither *c-fos* nor *fosB* expression. In addition, no induction of either *c-fos* or *fosB* expression occurred with the neurotoxin paraquat. Both compounds can therefore be considered as negative controls in the context of early response gene measurement in excitotoxicity.

Following consideration of the expression profiles of *c-fos* and *fosB* with Glu and Asp, it was decided to investigate whether the extraordinarily high expression of *c-fos* and/or *fosB* under excitotoxic conditions could be used to predict the excitotoxic properties of a range of functionally different chemical compounds. The hypothesis of the *in vitro IEG* investigation in rat cortical neurons was, that for a compound to be classified as excitotoxic it must induce an unambiguous elevation in *c-fos* and/or *fosB* expression from a non-toxic concentration to a toxic concentration at a single timepoint of 60 min. A further criterion for acceptance of *c-fos* and *fosB* as potential screens for excitotoxicity was that the excitotoxin-induced elevation of the *c-fos* and/or *fosB* mRNA response should be prevented in the presence of an antagonist cocktail containing both AP5 and CNQX. Thus, NMDA receptor-mediated actions should be attenuated or inhibited by AP5, while non-NMDA receptor actions should be prevented by CNQX. The first part of the *in vitro* screen involved the exposure of mature cultures of rat cortical neurons to 15 chemical compounds at a low (non-toxic) and high (toxic) concentration, in the presence and absence of the antagonist cocktail of AP5 and CNQX, before measurement of *c-fos* and *fosB* by real-time RT-PCR. The 15 compounds chosen were representative of 4 different classes.

The first group, were comprised of 10 known "excitotoxins", that is, Glu, QA, Asp, L-SSC, KA, NMDA, L-HCSA, L-HCA, D-HCA and L-CSA. All of the excitotoxins induced elevated and sustained *c-fos* and *fosB* mRNA expression with high concentrations of the compounds, when compared to the levels of induction induced by the low concentrations.

With the exception of KA and L-HCSA, the antagonist cocktail of AP5 and CNQX inhibited the elevated levels of *c-fos* and *fosB* mRNA expression. QA and L-HCSA induced elevated expression of *c-fos* and *fosB* at both the low and high concentrations, indicative of sub-optimal concentrations for both potent compounds. On account of the excessive concentrations of QA and L-HCSA chosen, no inhibition of the elevated *c-fos* and *fosB* response occurred in the presence of the antagonist cocktail. KA, gave rise to increases in *c-fos* and *fosB* mRNA expression with the low concentration, which changed to a more elevated expression with the high concentration. The antagonist cocktail did not inhibit the *c-fos* and *fosB* mRNA expression. The high concentrations chosen and the very toxic potency of KA may be responsible for the lack of inhibition.

The second group contained the "neurotoxic but non-excitotoxic" compound MPP^+ iodide. No elevation in *c-fos* mRNA expression was observed with either concentration of this compound and also in the presence of the AP5/CNQX cocktail. MPP^+ iodide induced a slight increase in *fosB* expression, which was inhibited in the presence of the antagonist cocktail. However, the small expression levels are responsible for this artefactual prediction.

The third group contained the "neuroactive but non-toxic" compounds, Ala, GABA and glycine, none of which caused an unambiguous increase in *c-fos* or *fosB* mRNA expression with either concentration or in the presence of the CNQX/AP5 cocktail. Lastly, the fourth group contained paraquat, a compound that was classified as being "toxic to other target organelles" and which also caused no large increases in *c-fos* mRNA expression.

The conclusion of this *IEG* investigation is that both *c-fos* and *fosB* show elevated and sustained expression in rat cortical neurons following over-activation of their NMDA receptors, and, although both *IEGs* exhibit different patterns of *IEG* induction, both may be used as molecular biomarkers to predict the excitotoxic properties of compounds. The Contingency Tables (Tables 5.3 and 5.4) demonstrate that both *c-fos* and *fosB* can be used as potential screens for predicting the potential excitotoxic properties of different compounds.

The applications of this *IEG* investigation include an ability to potentially screen for excitotoxins, and indeed just as importantly, to test newly designed antagonists of EAA receptors, in the search for new pharmaceutical drugs to treat neuropathologies in which Glu receptor over-stimulation is implicated. In a future screen for excitotoxicity, based on *c-fos*, *fosB* and perhaps *fra-2* early response gene measurements in rat cortical neurons,

a single concentration, single time-point should be used initially to screen for positive compounds. The initial screen should then be followed by an investigation into the concentration dependencies and pharmacology of the positive compounds, so as to have a proper definition of the toxicities of the various compounds.

Positive	7	2
Negative	3	3
	True	False

Table 5.3: Predictive potential of *c-fos* for screening

The 7 true positive (excitotoxic) compounds were Glu, Asp, L-SSC, NMDA, L-HCSA, L-HCA, D-HCA, and L-CSA. The 3 true negative (non-excitotoxic) compounds were MPP^+ iodide, GABA and glycine. The 3 false negatives (non-excitotoxic) were QA, KA and L-HCSA. The 2 false positives were Ala and MPP^+ iodide.

Positive	7	5
Negative	0	3
	True	False

Table 5.4: Predictive potential of *fosB* for screening

The 7 true positive (excitotoxic) compounds were Asp, L-SSC, KA, NMDA, L-HCA, D-HCA and L-CSA. The 3 false negative (non-excitotoxic) compounds were Glu, QA and L-HCSA. The 5 false positives (excitotoxic) compounds were MPP^+ iodide, Ala, GABA, glycine and paraquat.

Lastly, it was of interest to investigate whether any of the remaining members of the *fos (fra-1 and fra-2*) and *jun* (*c-jun, junB and junD*) families of genes, were involved in rat cortical neurons undergoing excitotoxicity. It was found that, apart from *fra-2*, no significant increases in expression occurred for the other members of the *fos* or *jun* families with Glu. High, toxic concentrations of Glu induced significant increases in *fra-2* expression. However, this expression of *fra-2* in rat cortical neurons is small when compared to the expression values of *c-fos* and *fosB* with toxic concentrations of Glu and Asp. Further work is therefore required to investigate the role of *fra-2* in excitotoxicity.

In this Chapter, it was demonstrated, using the quantitative method of real-time RT-PCR, that both *c-fos* and *fosB* show elevated levels of expression following toxic insult. Furthermore, it has been demonstrated that different profiles and levels of expression occur, depending on cell type. To confirm and support these results, it was decided to use an additional and alternative method to investigate patterns of gene expression in excitotoxicity. Micro-array technology was employed as an independent method in Chapter 6 to simultaneously examine the expression levels of thousands of genes, including members of the *fos* and *jun* families of *IEGs* in any given sample undergoing excitotoxic cell death and thus identify additional potential markers for excitotoxicity.

Chapter 6

Gene Expression Profiling:
Potential markers for Excitotoxicity in two different *In Vitro* Models

6.1 Introduction

Only a subset of all encoded genes is expressed in any given cell, and the levels and timing of expression govern growth, development, differentiation, homeostasis, aging and the onset of diseases. Analysis of gene expression is important in many fields of biological research, since many cellular decisions and changes in the physiology of an organism or a cell are reflected in altered patterns of gene expression. Gene expression analyses not only result in assigning known functions to genes but also often identify the concerted activities and interdependence of multiple genes in a single system. Indeed, gene expression studies can elucidate cellular pathways and mechanisms involved in inflammatory diseases, tumor suppression, heat shock responses, neurodegeneration and cancer. One of the key mechanisms of gene regulation takes place at the level of mRNA transcription. Thus, the ability to quantitate transcription levels of specific genes is central to any research into gene function (Zamorano *et al.*, 1996).

Several techniques for the analysis of gene expression at the mRNA level are available such as RT-PCR (Weis *et al.*, 1992), Northern blotting (Alwine *et al.*, 1977), differential display (Liang and Pardee, 1992), cDNA sequencing (Okubo *et al.*, 1992), serial analysis of gene expression (SAGE; Velculescu *et al.*, 1995), and dotblot analysis (Lennon and Lehrach, 1991). However, each of these methods has disadvantages, which render them unsuitable for the simultaneous analysis of large numbers of expression products. With real-time RT-PCR only a limited number of different conditions can be compared. Methods such as Northern blot analysis and nuclease protection assays have the disadvantage of being inherently serial, involving the measurement of a limited number of mRNAs at a time, and of being difficult to automate. Differential display of amplified subsets of RNAs on a sequencing gel allows a broad search for expression differences, but the results are generally not quantitative, false positives are common and characterisation of positives requires additional cloning and sequencing. Sequencing of cDNA libraries is a more direct approach, but requires a great deal of sequencing and is not sensitive to the presence of less abundant messages. Finally, dotblot analysis requires a relatively large amount of material due to the size of the filters.

Fortunately, substantial improvement in the throughput of expression screening has been obtained by the introduction of DNA microarray technology, which can simultaneously monitor changes in large numbers of cellular macromolecules within a single experiment (Watson *et al.*, 1998; Duggan *et al.*, 1999 and Graves, 1999). DNA micro-arrays can be

used to measure gene expression levels and changes in gene expression for cells in culture, dissected tissue, specific small nuclei, micro-dissected tissue and even very small numbers of selected cells when combined with appropriate amplification steps (Kwoh *et al.*, 1989; Guatelli *et al.*, 1990; Van Gelder *et al.*, 1990 and Eberwine *et al.*, 1992)

Biological systems read, store and modify genetic information using the rules of molecular recognition. Every nucleic acid strand carries the capacity to recognise complementary sequences through base pairing. The process of recognition, or hybridisation, can be highly parallel in that every sequence in a complex mixture can, in principle, be interrogated simultaneously. Almost 25 years ago, Southern showed that immobilised single-stranded DNA molecules could hybridise to their complementary sequences (Southern, 1975). The method he described, later termed the "Southern Blot", has become a core technique for molecular biologists. In the typical Southern blot, a size-separated target DNA population is immobilised on a membrane and a labelled probe, normally composed of a single gene species is hybridised to it. The dot-blot was later developed as a means to probe a target population for multiple genes. Dot-blots are effectively reverse Southerns, in that gene-specific probes are immobilised on the membrane and then hybridised against the labelled target population of cDNA. Subsequent automation and miniaturisation of the dot-blot showed how hybridisation could be used on a large scale to assemble high-density DNA probe arrays which efficiently allow the simultaneous assessment of thousands of genes in a single hybridisation assay. These arrays consist of a highly ordered matrix of thousands of different DNA sequences that can be used to measure DNA and RNA variation in applications that include gene expression profiling, comparative genomics and genotyping (Lander, 1999; Brown and Botstein, 1999; Case-Green *et al.*, 1998; Ferea and Brown, 1999). However, unlike dot-blots, which are typically prepared on membranes and rarely contain more than 100 individual gene spots, DNA arrays have a much higher number and density of spots and are generally of a diameter less than 200 µm (Rockett and Dix, 2000).

A number of techniques are being developed for the manufacture of DNA microarrays. Two main approaches exist. The first approach, DNA micro-dispensing, can be performed in a regular molecular biology laboratory. "Spotted" micro-arrays are printed onto a glass surface using computer-controlled, high-speed robotics (Schena *et al.*, 1995; 1996a and 1996b; Shalon *et al.*, 1996). The cDNAs to be arrayed are first amplified in a 96-well format using the polymerase chain reaction (PCR). The PCR products are then partially

purified by precipitation, gel-filtration, or both, to remove unwanted salts, detergents, PCR primers and proteins present in the PCR cocktail. Samples (nl) of the amplified and purified cDNAs are transferred from microtiter plates onto glass microscope slides using passive dispensers or active dispensing units based on ink-jet technology. Passive dispensers apply the cDNAs with a pin (or multiple pins) that touches the solid surface. Ink-jet based devices use either piezoelectric delivery or delivery by solenoid valves, making direct surface contact redundant. The density of the spots depends on the skills of the dispensing device. However, generally a higher density can be reached when using a passive dispenser. In preparation for monitoring gene expression, the cDNAs are chemically linked to the glass surface or, alternatively, the surface of the glass is coated with a positively charged layer (for example, poly-L-lysine) to bind the negatively charged DNA fragments. The cDNAs are then denatured by heat treatment or ultraviolet irradiation. The source of cDNAs may include fully sequenced clones, collections of partially sequenced cDNAs known as expressed sequence tags (ESTs) or randomly chosen cDNAs from any library of interest. In many cases, these are chosen directly from databases including,

IMAGE (http://www-bio.llnl.gov/bbrp/image),

Genbank database (http://www.ncbi.nlm.nih.gov/Genbank/GenbankOverview),

dbEST (http://www.ncbi.nlm.nih.gov/dbEST),

and UniGene (http://www.ncbi.nlm.nih.gov/Unigene), the resource backbones of the array technologies. Amplifications can be performed using either gene-specific primers or primer pairs that recognise vector sequences present in each clone.

The second approach encompasses the direct synthesis of oligonucleotides onto a solid surface. These miroarrays, for example Affymetrix GeneChip® arrays, utilize short oligonucleotides (25 bases) which are synthesized directly *in situ*, one base at a time, on glass slides derivatized with oligoethylene glycols (Cheung *et al.*, 1999) using two techniques: photolithography and solid-phase DNA synthesis (Fodor *et al.*, 1991). Synthetic linkers modified with photochemically removable protecting groups are attached to a glass substrate and light is directed through a photolithographic mask, using a high intensity mercury lamp, to specific areas on the surface to produce localised photodeprotection. Hydroxyl-protected versions of the four DNA building blocks (the purines adenine, guanine, and the pyrimidines cytosine and thymine) are incubated with the substrate and chemical coupling occurs at those sites that have been illuminated in the preceding step. Next, light is directed onto a different region of the substrate by a new

mask, and the chemical cycle is repeated. With each round of synthesis, nucleotides are added to the growing chains until the desired length is achieved, that is, any set of probes composed of the four nucleotides can be synthesized in a maximum of 4*N* cycles, where *N* is the length of the longest probe in the array. For example, the entire set of ~ 10^{12} 20-nucleotide oligomer probes, or any desired subset, can be synthesized in only 80 coupling cycles. Photolithography allows the construction of arrays with extremely high information content and the number of different probes that can be synthesized is limited only by the physical size of the array. Because the arrays are constructed on a rigid material (glass wafers) they are inverted and mounted in a temperature-controlled hybridisation chamber (Lipshutz *et al.*, 1999). On GeneChip® oligonucleotide arrays (Affymetrix Inc.) a given gene is currently represented by 16 – 20 pairs of different 25-mer oligonucleotides, biased towards the 3' end of the gene, that serve as sensitive, unique, sequence specific detectors. Thus, multiple oligonucleotides of different sequence are designed to hybridise to different regions of the same RNA. The use of multiple independent detectors for the same molecule greatly improves signal-to-noise ratios (due to averaging of the intensities of multiple array features), improves the accuracy of RNA quantitation (averaging and outlier removal), increases the dynamic range, moderates the effects of cross-hybridisation and reduces the rate of false positives (Lipshutz *et al.*, 1999).

An additional control element on these arrays is the use of mismatch (MM) control probes that are identical to their perfect match (PM) partners except for a single base difference in a central position. The MM probes serves as specificity controls that allow the direct subtraction of both background and cross-hybridisation signals, and allow discrimination between "real" signals and those due to non-specific or semi-specific hybridisation (hybridisation of the intended RNA molecules produces more signal for the PM probes than for the MM probes) (Lipshutz *et al.*, 1999). GeneChip® arrays are thus able to specifically detect individual gene transcripts and splice variants, and differentiate among closely related members of gene families. Because oligonucleotide probes for each gene are specifically chosen and synthesized in known locations on the arrays, the hybridisation patterns and intensities can be interpreted in terms of gene identity and relative amount with no additional sequencing or characterisation. Furthermore, the use of shorter probes increases the resolution of the information from hybridisation experiments.

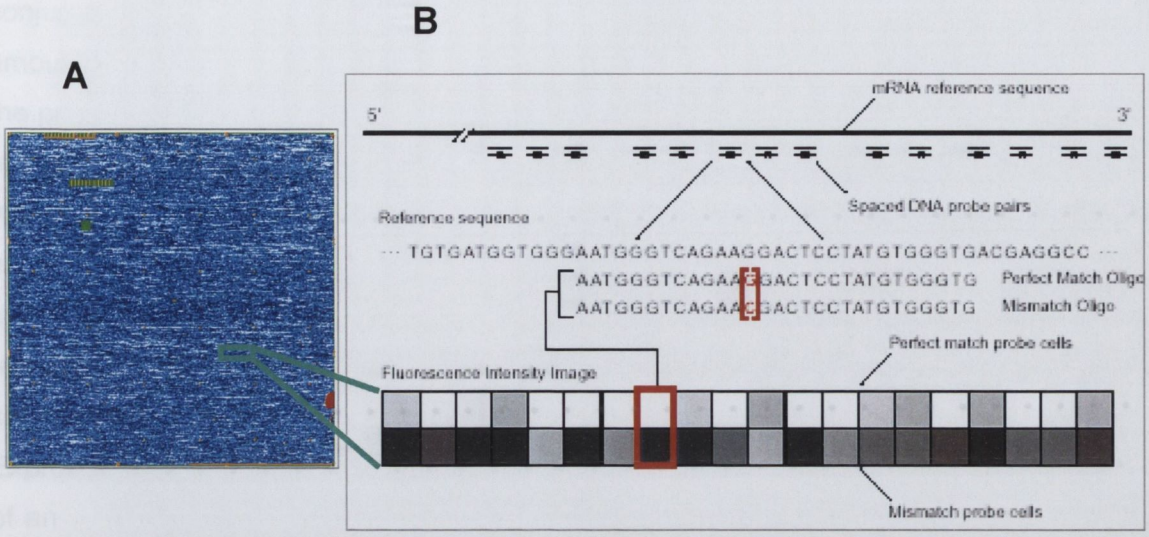


Figure 6.1: Fluorescent image of a GeneChip® Array

(A). The blue square represents the whole fluorescent image of a GeneChip® array containing approximately 9000 different probes, with each feature consisting of a 25-base oligonucleotide. (B). An enlargement of a small proportion of the array. The use of PM minus MM differences averaged across a set of probes greatly reduces the contribution of background and cross-hybridisation and increases the quantitative accuracy and reproducibility of the measurements (modified image from Lipschutz *et al.*, 1999).

On spotted arrays, single DNA fragments, greater than several hundred bases in length, generally represent genes. The DNA samples hybridised to the array are, in most cases, labelled by incorporating fluorescently tagged nucleotides during oligo-primed reverse transcription of messenger RNA (Eisen and Brown, 1999). Different fluorophores (generally Cy3- and Cy5-dUTP) are used to label cDNAs from control (reference) and experimental (test) RNAs. The labelled cDNAs are mixed together prior to hybridisation to the array and then scanned at two wavelengths following independent excitation of the two fluors (Schena *et al.*, 1995). Relative amounts of a particular gene transcript in the two samples are determined by measuring the signal intensities detected for both fluorophores and calculating signal ratios.

In the GeneChip® expression array, eukaryotic mRNA or fragmented total RNA (Lipshutz *et al.*, 1999) is labelled in a two-step linear amplification process to produce biotinylated cRNA from oligo-dT-primed cDNA. Each sample is hybridised to a separate array. After hybridisation, biotin c-RNA bound to the array is stained with steptavidin phycoerythrin

conjugate and detected by laser scanning using the GeneChip® Scanner 3000. The amount of light emitted at 570 nm is proportional to the bound target at each location on the probe array. Differentially expressed genes can be identified by informatic comparison of control and experimental hybridisation data.

Although both cDNA and oligonucleotide arrays are capable of analysing patterns of gene expression there are fundamental differences in performance and information generated by the two types of arrays due to the differences, as outlined above, in assay and gene representation. First, spotted arrays, hybridised simultaneously with two distinctly labelled samples, intrinsically normalise for noise and background in a pair-wise comparison. Expression ratios provide the transcriptional information and require that different samples of an experimental set be hybridised with the same control. However, cross-hybridisation potential between genes with significant levels of sequence similarity is high using spotted microarrays.

High-density oligonucleotide arrays (Affymetrix) allow greater flexibility in sample comparisons and provide an estimate of the levels of gene transcripts in individual samples. Additionally, the oligomer probes on high-density oligonucleotide arrays are designed to uniquely represent the cognate gene, thus minimising cross-hybridisation between similar sequences. Finally, oligonucleotide arrays require gene sequence information for specifying the de novo synthesis of the oligomers on the array, whereas spotted arrays can be produced from both known and unknown cDNA and PCR fragments. The design of micro-arrays is largely dependent on the research question that has to be answered. Diagnostic questions will often involve smaller arrays with well-defined target sequences (spotted arrays), while elucidation of metabolic pathways or identification of novel responding genes requires the use of large arrays often with undefined target sequences (high-density gene-chip arrays). However, this avalanche of genetic information does not yet provide insight into how all of the protein products of these genes interact or function within the cell. Indeed, expression data have their own limitations; mRNA levels may not reflect protein levels and expression of a protein may not always have a physiological consequence.

DNA micro-array technology typically encompasses arraying of DNA on a glass surface, hybridisation and detection methods, and software and databases that facilitate data analyses. The data format produced by a micro-array assay typically consists of a list of genes and corresponding values that represent relative RNA transcript levels. Following acquisition and processing of the fluorescent array image, there are three basic steps

required for efficient data analysis: data normalisation, data filtering and pattern identification. To compare expression values directly, it is usually necessary to apply a normalisation strategy to the data, either between paired samples or across a set of experiments. Following this, data deduction is achieved by filtering out uninformative genes; for example, genes that are expressed below a user defined threshold or genes that do not vary their expression level during the course of the experiment. The next step is to find patterns and groups in the data that can be used to assign biological meaning to the expression profiles. The methods used for data mining and interpretation are varied, ranging from straightforward lists of increased and decreased expression of genes based on user-defined thresholds to the implementation of sophisticated clustering and visualisation programs, such as hierarchical clustering (Eisen *et al.*, 1998) and K-means clustering (Tamayo *et al.*, 1999; Toronen *et al.*, 1999 and Tavazoie *et al.*, 1999). Both methods succeed in grouping the genes or samples based on their expression pattern.

Fundamental information on the time- and concentration-dependent expression of members of the *fos* and *jun* families of *IEGs* was obtained in Chapters 4 and 5 by investigating the genes individually with real-time RT-PCR, but how the genes interact and fit into the complex process of excitotoxicity is still unknown. In this Chapter, mouse and rat Affymetrix arrays were used to simultaneously investigate the expression of all the *IEGs* studied so far together with thousands of genes of interest and thereby further elucidate the associations between genes and the process of excitotoxicity.

Aims of this Chapter

The first aim of this chapter was to use Affymetrix GeneChip® technology to investigate the simultaneous expression of thousands of genes of interest under different conditions of time and concentration. In the Chapters 4 and 5, it was shown that both *c-fos* and *fosB* were specifically involved in the Glu-mediated excitotoxic cell death of mouse cerebellar granule cells and rat cortical neurons. Thus, the second aim of this Chapter was to confirm these results using an alternative method.

The third aim was to investigate whether other *IEGs* or cellular macromolecules shared similar gene expression patterns with *c-fos* or *fosB* by comparing expression profiles.

The final aim was to relate the genes most involved in excitotoxicity.

6.2 Results

6.2.1 Comparative analysis of hybridised mouse GeneChip® arrays

Szekely *et al.* (1989) reported that mCGCs exposed to low, non-toxic concentrations of Glu induced a rapid and transient expression of the immediate early gene, *c-fos*. Later, Gorman *et al.* (1995), Meredith *et al.* (1996) and Griffiths *et al.* (1997, 2000) used the method of Northern blot analysis to investigate the expression of *c-fos* in mCGCs following excitotoxic insult. It was found that the expression of *c-fos* was delayed, elevated and sustained. In Chapter 4 of this study, the method of real-time RT-PCR was used as a more sensitive technique to examine the time- and concentration-dependent profiles of *c-fos* mRNA expression, and also to investigate whether other members of the *fos* and *jun* families of *IEGs* were induced following excitotoxic insult. It was found that non-toxic concentrations of the EAAs, Glu and Asp, induced the transient *c-fos* expression as described by Szekely *et al.* (1989) while toxic concentrations induced the sustained *c-fos* described by Gorman *et al.* (1995); Meredith *et al.* (1996) and Griffiths *et al.* (1997, 1998, 2000). In addition, *fosB* was also found to show different patterns of expression depending on time and concentration, making it a second potential biomarker of excitotoxicity. In this Chapter, Affymetrix GeneChip® Technology (Mouse Genome Chip MG_U74A v2) was used to investigate whether the profile of Glu-induced *c-fos* and *fosB* expression correlated with that previously found by RT-PCR. Furthermore, it was used to identify genes that were additionally induced or co-regulated upon excitotoxic stress, and thus allow the interpretation of possible signalling pathways involved.

Primary cultures of mCGCs (7 DIV; see Section 2.2.1) were exposed to a non-toxic (2.5 μM) or toxic (250 μM) concentration of Glu for either 30 min or 240 min. RNA was extracted and purified as described in Chapter 2 (see Sections 2.5 and 2.6). The processing of RNA samples for Affymetrix chip technology encompassed the generation of biotinylated cRNA target samples. These cRNAs were generated by *in vitro* transcription of cDNA that was prepared from total RNA by using an oligo (dT) primer with a T7 polymerase promoter at its 5' end (see Section 2.18). The resulting antisense RNA was fragmented to an average size of 50 to 100 bases and was hybridised to the mouse genome oligonucleoide probe array (MG_U74Av2) containing 12488 probe sets, which were then fluorescently labelled with a phycoerythrin-conjugated streptavidin. The

intensity of the fluorescent signal within each feature was quantified by using a confocal scanner (GeneArray® scanner, Affymetrix Inc.).

Microarray Suite Version 5 of Affymetrix (MAS5) was used to analyse the fluorescence intensities of the hybridised and labelled microarrays. The expression values for 12488 features were normalised to a target intensity of 100 and were loaded into the GeneData Refiner (version 3.0.4) for bright/dark spot detection and gradient correction. Following correction, the chip data was analysed in the Analyst Software module of GeneData Expressionist (version 4.0.5). The following six groups, containing replicate experiments, were analysed:

30 min control	4 hours control
30 min 2.5 µM Glu	4 hours 2.5 µM Glu
30 min 250 µM Glu	4 hours 250 µM Glu

Initially, the distribution of gene expression values, derived from the fluorescent intensities of all individual probe sets, was displayed using a Box Plot (see Figure 6.2). It is important to note that this is not a comparative analysis, more a visual display tool of data point distribution. Since all expression values were normalised to a pre-determined target intensity, that is, all values were globally normalised to a value of 100, the median values for each chip were similar. The global distribution of expression values from each experiment was observed and each experiment checked for the presence of any obvious outliers. In this box plot, the distribution of upper and lower quartiles and also outliers were similar between the different experiments.

6.2.2 Glu induced changes in gene expression on mouse arrays

Each individual mouse array contained a total of 12488 hybridised genes, of which 5453 genes were present ($p < 0.04$) or marginally present ($0.04 < p < 0.06$). In order to extract the fundamental patterns of gene expression in excitotoxicity, it was first necessary to subject this large collection of data to different filtration procedures. The first selection involved the use of High Ratio Proportion Analysis (HRP), which filtered out uninformative genes and also genes that did not vary their expression level during the course of the experiments. A threshold of 1.8 fold was selected and genes, which were consistently more than 1.8 fold up- or down-regulated, from any of the possible pairwise comparisons between the 6 groups (see Section 6.2.1) were selected.

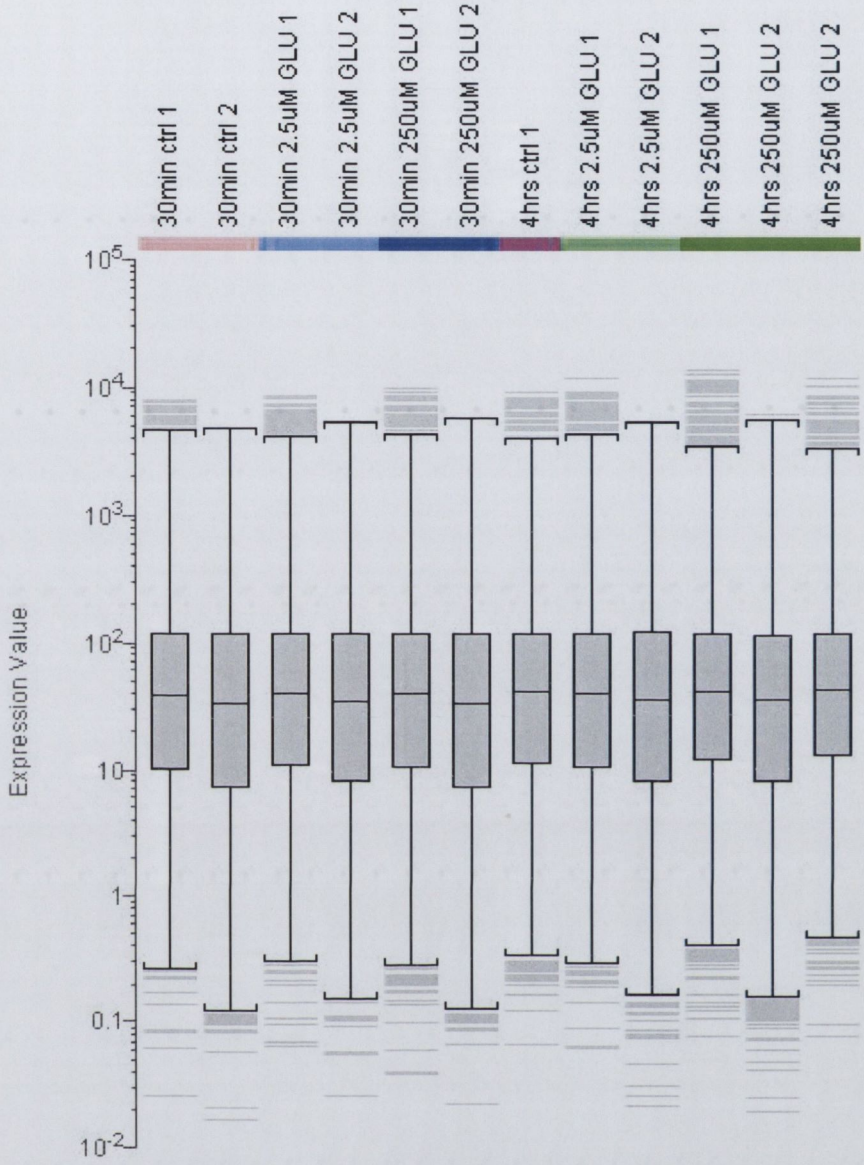


Figure 6.2: Box Plot of data obtained from the mouse MG_U74v2A array

A box plot was used to display the basic distribution of gene expression values from each experiment. The user-modifiable detection p-value cutoffs, Alpha 1(α_1) and Alpha 2(α_2), provide boundaries for defining present, marginal or absent calls. At the default settings, determined for probe sets with 16-20 probe pairs (defaults $\alpha_1 = 0.04$ and $\alpha_1 = 0.06$), any p-value that falls below α_1 is assigned a present call and above α_2 is assigned an absent call. Marginal calls are given to probe sets, which have p-values between α_1 and α_2.

The p-value was set as 1, meaning that all present ($p < 0.04$), marginally expressed genes ($0.04 < p < 0.06$) and low expressed genes with an absent call from Affymetrix MAS5 ($0.06 < p < 1$) were used.

This analysis showed 152 genes (proportion of 1, corresponding to 100%) out of the 5453 present or marginally present genes on the array were greater than 1.8 fold changed in induction or suppression. The group of 152 genes were then subject to a second more stringent selection, using N-fold regulation, and genes which had a ratio of means of more than 2.5 fold between the six experimental groups were selected. Thus, a gene list was compiled, from an initial set of 5453 genes, containing 49 genes which were more than 2.5 fold up- or down-regulated (see Figure. 6.3). Following the two different selection procedures, an initial inspection of the 49 genes indicated the presence of various *immediate early genes* and transcription factors. When the relative RNA levels obtained from the Glu-treated mCGCs were compared with those derived from a time-matched control sample, *c-fos*, *fosB* and ATF3 were selected from the group of 49 genes as the genes most induced under excitotoxic conditions. Interestingly, both *c-fos* and *fosB* were shown in Chapter 4, using the method of real-time RT-PCR, as being specifically induced under excitotoxic conditions.

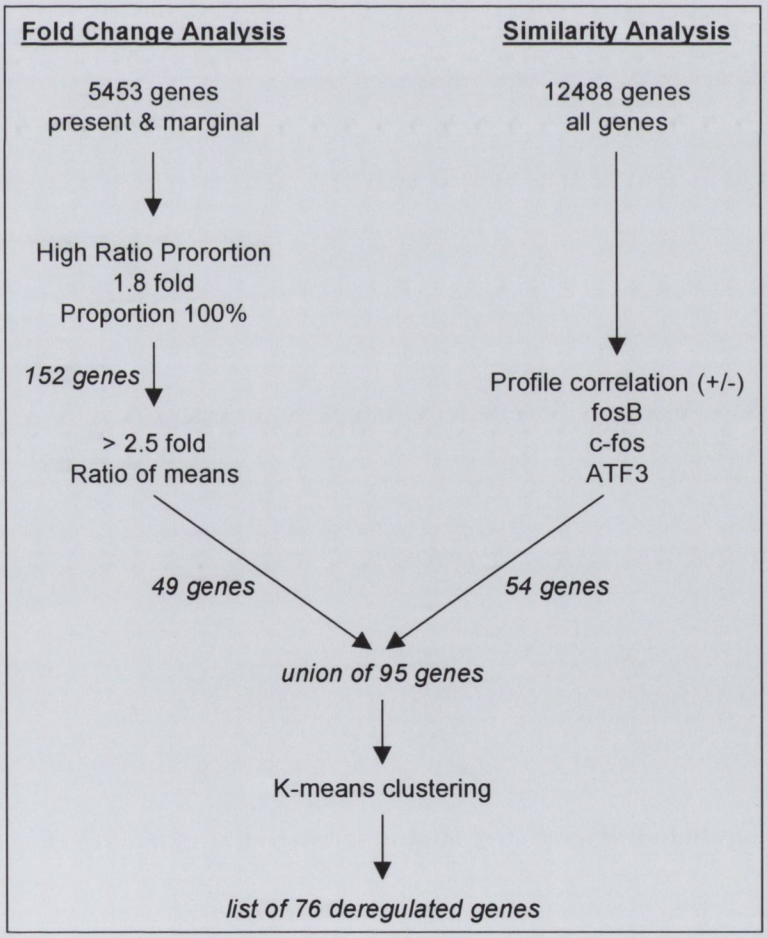


Figure 6.3: Flow chart for the identification of up- and down-regulated genes

The *IEG c-fos* (probe ID: 160901_at) was transiently induced at 30 min, when compared to the time-matched control, with non-toxic concentrations of Glu (2.5 μM). By 240 min, the levels of *c-fos* induction had decreased. With toxic concentrations of Glu (250 μM), while *c-fos* was induced at 30 min, a more elevated induction was observed at the later time-point of 240 min. These observations revealed that *c-fos* was induced in a time- and concentration-dependant manner and are in accordance with the profiles of *c-fos* expression found using real-time RT-PCR in Chapter 4 and also Northern blot analysis (Gorman *et al.*, 1995; Griffiths *et al.,* 1997, 1998, 2000). Furthermore, the characteristic delayed and sustained expression of *c-fos* mRNA under excitotoxic conditions can be used as a robust and reproducible marker for excitotoxicity (see Figure 6.4).

A similar pattern of expression was found for a second member of the *fos* family of *IEGs*, *fosB* (probe ID: 103990_at). *fosB* was induced with non-toxic concentrations of Glu at 30 min. At 240 min, the levels of *fosB* induction had decreased slightly. With toxic concentrations of Glu, no increase in expression occurred at 30 min when compared to the time-matched control. However, a 6 fold increase in *fosB* expression levels was observed at 240 min (see Figure 6.5). These observations confirm the different profiles of time- and concentration-dependent *fosB* expression found using real-time RT-PCR in Chapter 4 and thus emphasize the potential of *fosB* as an additional biomarker for excitotoxicity.

The third gene selected was ATF3. ATF3 is a constitutive transcription factor whose proteins are present in unstimulated cells bound to DNA regulatory sites. NMDA receptor activation of ATF3 enables it to interact with other *IEG*-encoded proteins, inducing the transcription of target genes. It was observed that no increase in ATF3 expression occurred with non-toxic concentrations of Glu at either 30 min or 240 min. However, with toxic concentrations of Glu, while there was no increase in expression at 30 min, a 3 fold increase in expression was observed at 240 min, when compared to the time-matched control. Two probe sets for ATF3 (probe IDs: 104155_f_at; 104156_r_at) were located on the chip and in both cases the results were the same. Thus, it can be speculated that ATF3 could be a potential and selective marker for excitotoxicity (see Figure 6.6).

To summarise, the 3 genes (*c-fos*, *fosB* and ATF3) selected were specifically induced under excitotoxic conditions and it can be speculated that all 3 genes are involved in the complex process of excitotoxicity.

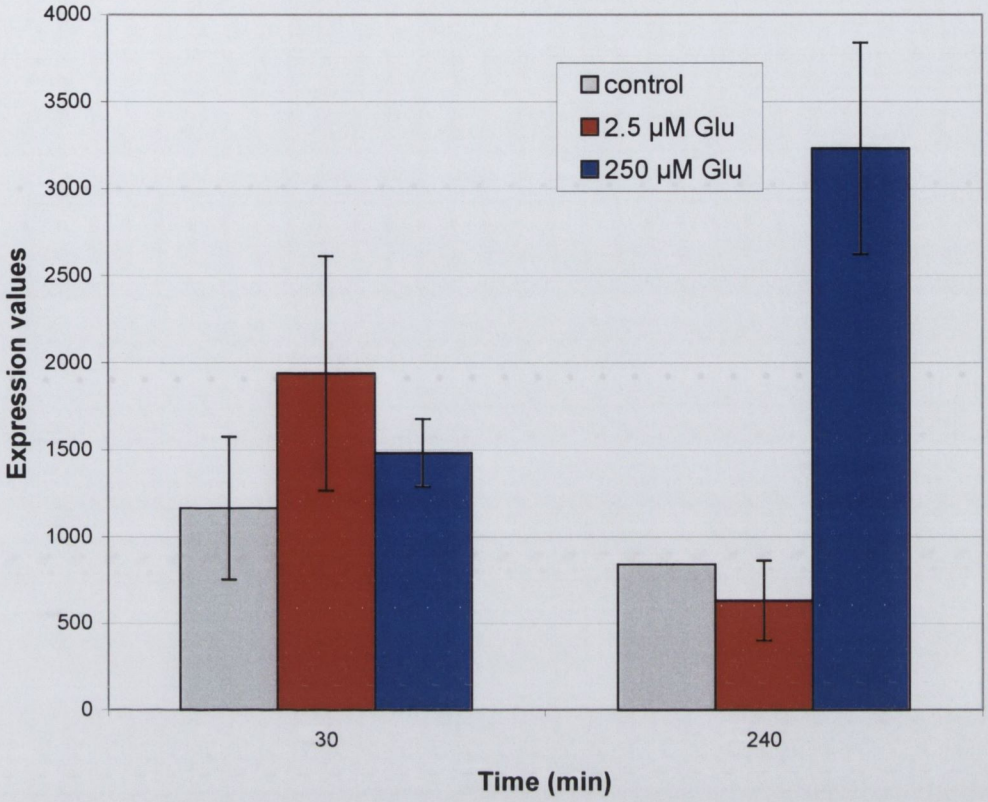


Figure 6.4: Different time-profiles of *c-fos* expression dependent on Glu concentration

Primary cultures of mCGCs (7 DIV) were exposed to a non-toxic (2.5 µM) or toxic (250 µM) concentration of Glu, for either 30 or 240 min. Following treatment, total RNA was extracted, converted to biotinylated cRNA and hybridised to separate mouse MG_U74A v2 arrays. The results above refer to the fluorescent levels of *c-fos* expression compared to untreated, time-matched controls. The levels of fluorescent signal are representative of the relative abundance of *c-fos* in the treated/untreated mCGCs. Data represent mean ± variation from the mean of the *c-fos* probe set (probe ID: 160901_at) from duplicate mouse arrays (n = 2).

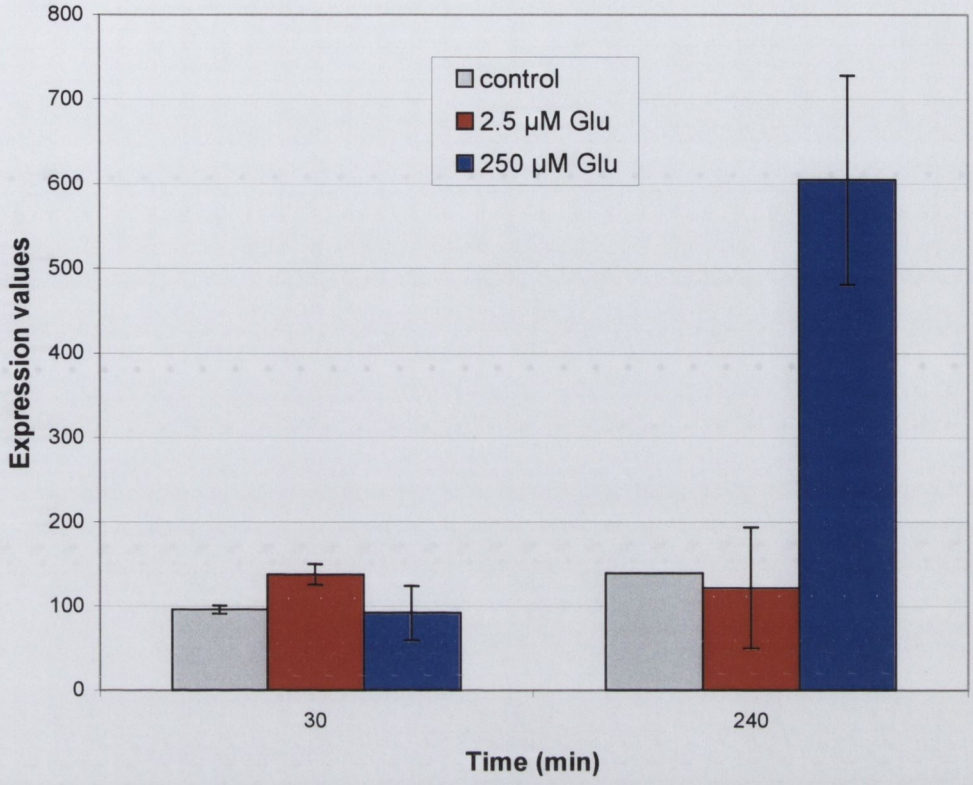


Figure 6.5: Different time- and concentration-dependent profiles of *fosB* expression

Primary cultures of mCGCs (7 DIV) were exposed to a non-toxic (2.5 µM) or toxic (250 µM) concentration of Glu, for either 30 or 240 min. Following treatment, total RNA was extracted, converted to biotinylated cRNA and hybridised to separate mouse MG_U74A v2 arrays. The results above refer to the fluorescent levels of *fosB* expression compared to untreated, time-matched controls. The levels of fluorescent signal are representative of the relative abundance of *fosB* in the treated/untreated mCGCs. Data represent mean ± variation from the mean of the *fosB* probe set (probe ID: 103990_at) from duplicate mouse arrays (n = 2).

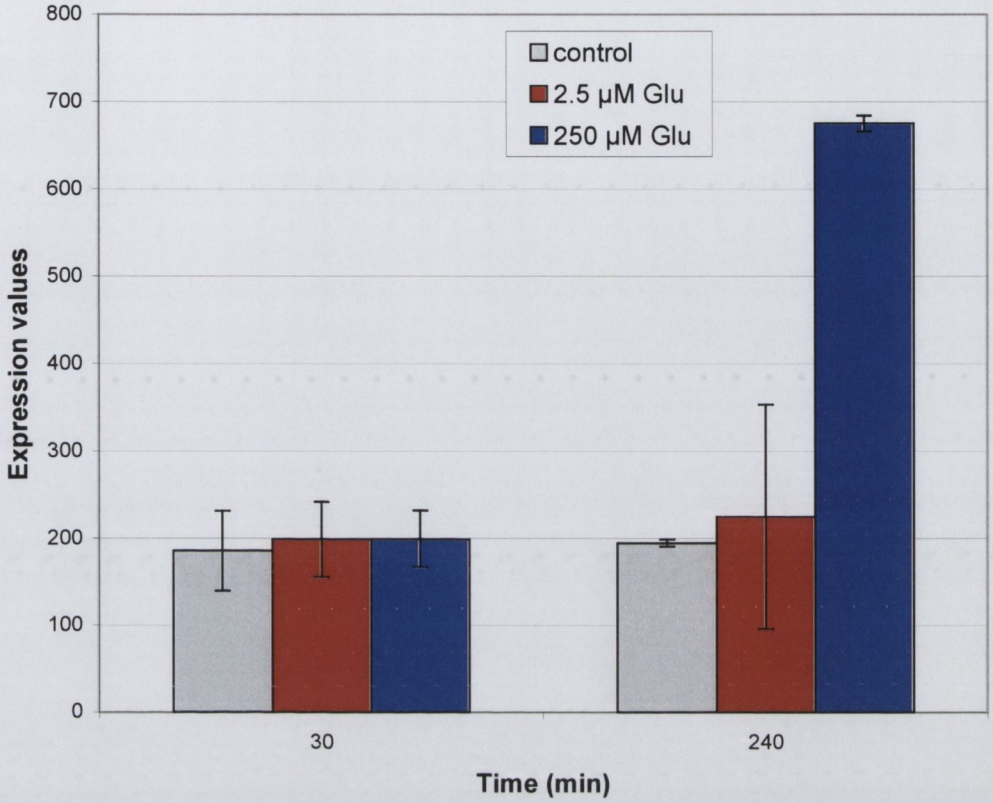


Figure 6.6: ATF3 is specifically induced under excitotoxic conditions

Primary cultures of mCGCs (7 DIV) were exposed to a non-toxic (2.5 µM) or toxic (250 µM) concentration of Glu, for either 30 or 240 min. Following treatment, total RNA was extracted, converted to biotinylated cRNA and hybridised to separate mouse MG_U74A v2 arrays. The results above refer to the fluorescent levels of ATF3 expression compared to untreated, time-matched controls. The levels of fluorescent signal are representative of the relative abundance of ATF3 in the treated/untreated mCGCs. Data represent mean ± variation from the mean of the ATF3 probe set (probe ID: 104155_f_at) from duplicate mouse arrays (n = 2).

6.2.3 Several genes share the same expression profiles as *c-fos*, *fosB* and ATF3

Using fold change analysis (HRP and ratio of means) *c-fos*, *fosB* and ATF3 were identified as possible biomarkers for excitotoxicity. However, the possibility remained that other genes could also be induced with similar expression profiles. Thus, a search was performed with all 12488 hybridised genes, in parallel to the fold change analysis, for genes that shared similar expression patterns across the 6 different experimental conditions. This analysis used the "Search by Distance" metric, which indicates the degree of similarity of an item with respect to the reference item. Lower distances reflect greater similarity. The detection p-value was set as 1, to include all present ($p < 0.04$), marginally expressed genes ($0.04 < p < 0.06$) and low expressed genes (with an absent call from Affymetrix MAS5 ($0.06 < p < 1$)), in order to identify genes that were absent in one or more of the groups and, for example, only present in response to the treatment. When *c-fos* (probe ID: 160901_at) was compared to the profiles of all genes on the array, 10 genes were selected by the Analyst Software module of GeneData Expressionist (version 4.0.5), which were similarly up-regulated under excitotoxic conditions, while 4 genes were down-regulated. An illustration of the genes similar to *c-fos* and selected from the 12488 genes is shown in Figure 6.7. The up- and down-regulated genes are shown in Table 6.2, together with their respective correlation co-efficients. The up-regulated genes consisted of a protein phosphatase, 2 *IEGs*, 2 ESTs, a transport protein, 2 non-categorised proteins and a protein involved in biosynthesis. The 4 down-regulated genes were all ESTs.

15 genes were selected that positively correlated with the expression pattern of *fosB* (probe ID: 103990_at; Figure 6.8 a)) under excitotoxic conditions while 5 genes were down-regulated. The up- and down-regulated genes are shown in Table 6.3 together with their respective correlation co-efficients. The 15 up-regulated genes consisted of 5 transcription factors, 2 apoptotic genes, a proprotein convertase, a lectin, an integral membrane protein, a plasma membrane protein, an oxidoreductase, an ATP binding factor and a protein biosynthesis inhibitor The 5 down-regulated genes were 2 non-categorised proteins, an EST, a proteasome protein and an inhibitory amino acid transporter.

For ATF3 (probe set IDs: 104155_f_at; 104156_r_at), 15 genes were positively up regulated while 6 genes were down-regulated (Figure 6.9). The list of up- and down-regulated genes is shown in Table 6.4 and 6.5 together with their respective correlation

co-efficients. The up-regulated genes of both probe sets contained transcription factors, apoptotic genes, *IEGs*, components of the complement pathway and various proteins. In both cases the down-regulated genes were ESTs.

It can be speculated, therefore, that many of the genes identified above may be mechanistically molecular biomarkers for *in vitro* excitotoxic cell death.

Gene	Affymetrix. probe ID	No. Positive Correlates	No. Negative Correlates	Total No.
fosB	103990_at	15	5	20
c-fos	160901_at	10	4	14
ATF3	104156_r_at	15	5	20
ATF3	104155_f_at	15	6	21
union		37	17	54

Genes identified by HRP and > 2.5 - fold regulation	49
union	95

Table 6.1: Summary of deregulated genes

The table above summarises the genes identified, using similarity analysis, which positively and/or negatively correlated with the expression profiles of *c-fos*, *fosB* and ATF3 across the different assay conditions. All gene groups identified by the methods of N-fold regulation and similarity analysis were merged to generate a final list of 95 deregulated genes, which were further analysed by K-Means Clustering (see Section 6.2.4).

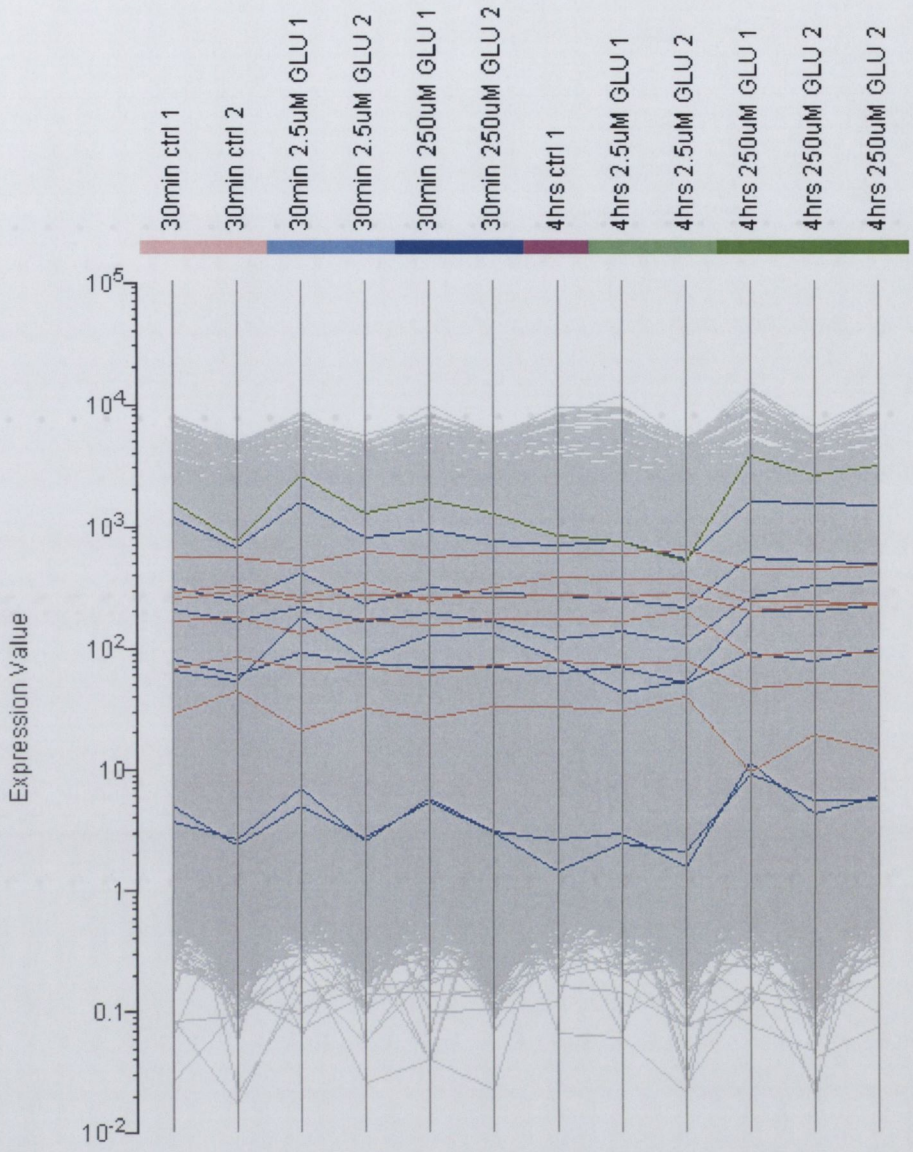


Figure 6.7: 14 genes found from a total of 12488 with a similar profile to *c-fos*

Similarity analysis was applied to the 12488 hybridised probes to identify genes similar to the *c-fos* probe set (probe ID: 160901_at), on the basis of their intensity of expression. The graph represents the expression values of all genes (grey area) on the array. The green line represents *c-fos*. Genes, whose expression patterns positively correlate with *c-fos*, across the different assay conditions are represented by the blue lines, while genes whose expression patterns negatively correlate with *c-fos* are represented by the red lines.

Gene Symbol	Gene Description	Genbank Accession	Affymetrix ID.	Correlation Coefficient
	Immediate early gene			
c-fos	FBJ osteosarcoma oncogene	160901_at	V00727	1
	Protein phosphatase			
Ptpn16	protein tyrosine phosphatase	104598_at	X61940	0.9590
	Immediate early gene			
Ier2	immediate early response 2	99109_at	M59821	0.9363
	EST			
EST	EST	96634_at	AI850090	0.9132
	Transport protein			
Aqp1	aquaporin 1	93330_at	L02914	0.9074
	Non-categorised			
Sc4mol	sterol-C4-methyl oxidase-like	160388_at	AI848668	0.9070
Cldn5	claudin 5	104516_at	U82758	0.9049
	Immediate early gene			
Egr1	early growth response 1	98579_at	M28845	0.9004
	Protein biosynthesis			
Rpl13a	ribosomal protein L13a	92834_at	X51528	0.8936
	EST			
EST	EST	94441_at	AW061237	0.8770
	Calmodulin binding factor			
Kcnn4	potassium/calcium-activated channel, subfamily N	102198_at	AF042487	0.8765
	EST			
EST	EST	161073_at	AI846304	-0.8972
EST	EST	103664_r_at	AA959648	-0.8958
EST	EST	104332_at	AI842242	-0.8841
EST	EST	101426_at	AW125333	-0.8787

Table 6.2: 14 genes found with a similar expression profile as *c-fos*

Out of 12488 hybridised probes, 10 were found whose expression profiles positively correlated (highlighted blue) with that of *c-fos* against the different assay conditions of time and concentration. 4 ESTs were negatively correlated (highlighted red) with the profile of *c-fos* expression.

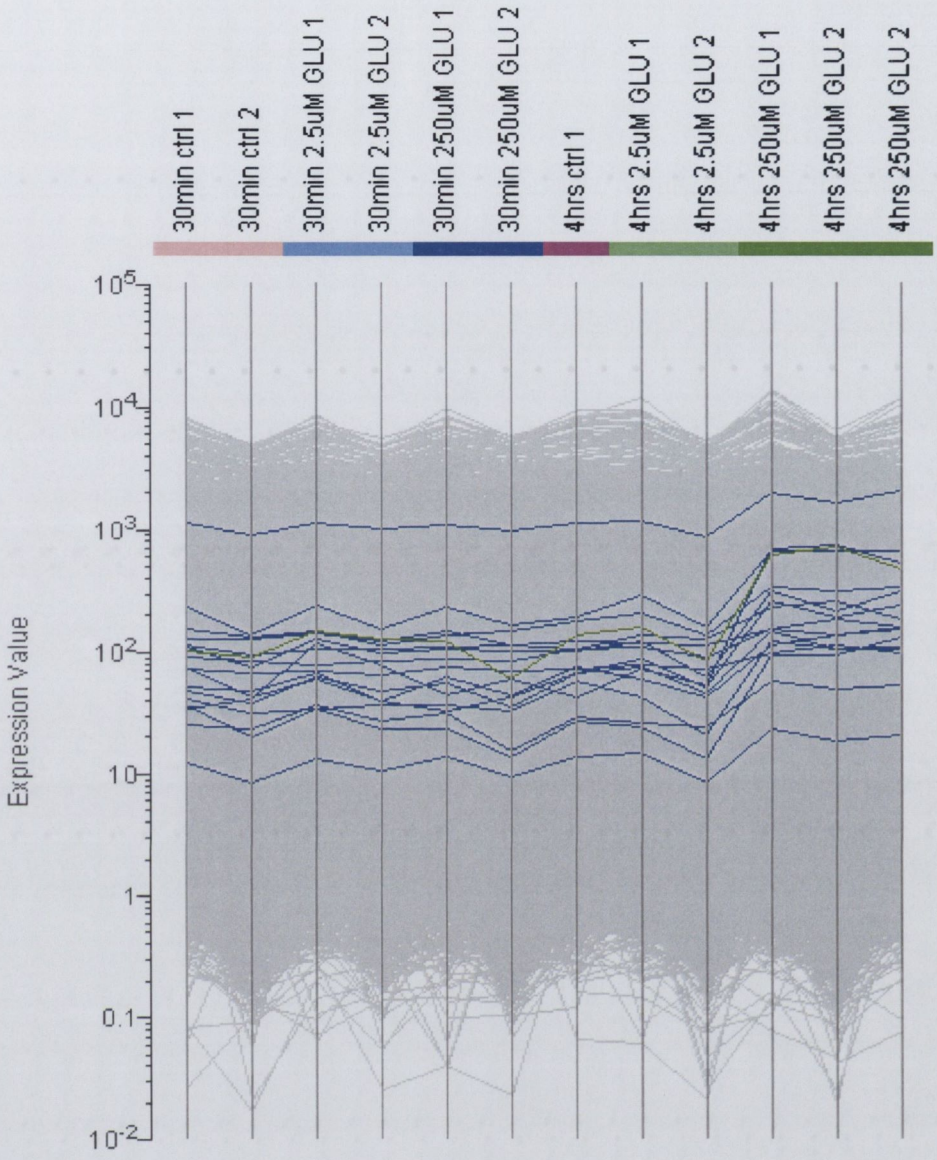


Figure 6.8 a): 15 genes found from a total of 12488 that positively correlate with *fosB*

Similarity analysis was applied to the 12488 hybridised probes to identify genes similar to the *fosB* probe set (probe ID: 103990_at), on the basis of their intensity of expression. The graph represents the expression values of all probes (grey area) on the array. The green line represents *fosB*. Genes, whose expression patterns positively correlate with *fosB*, across the different assay conditions are represented by the blue lines.

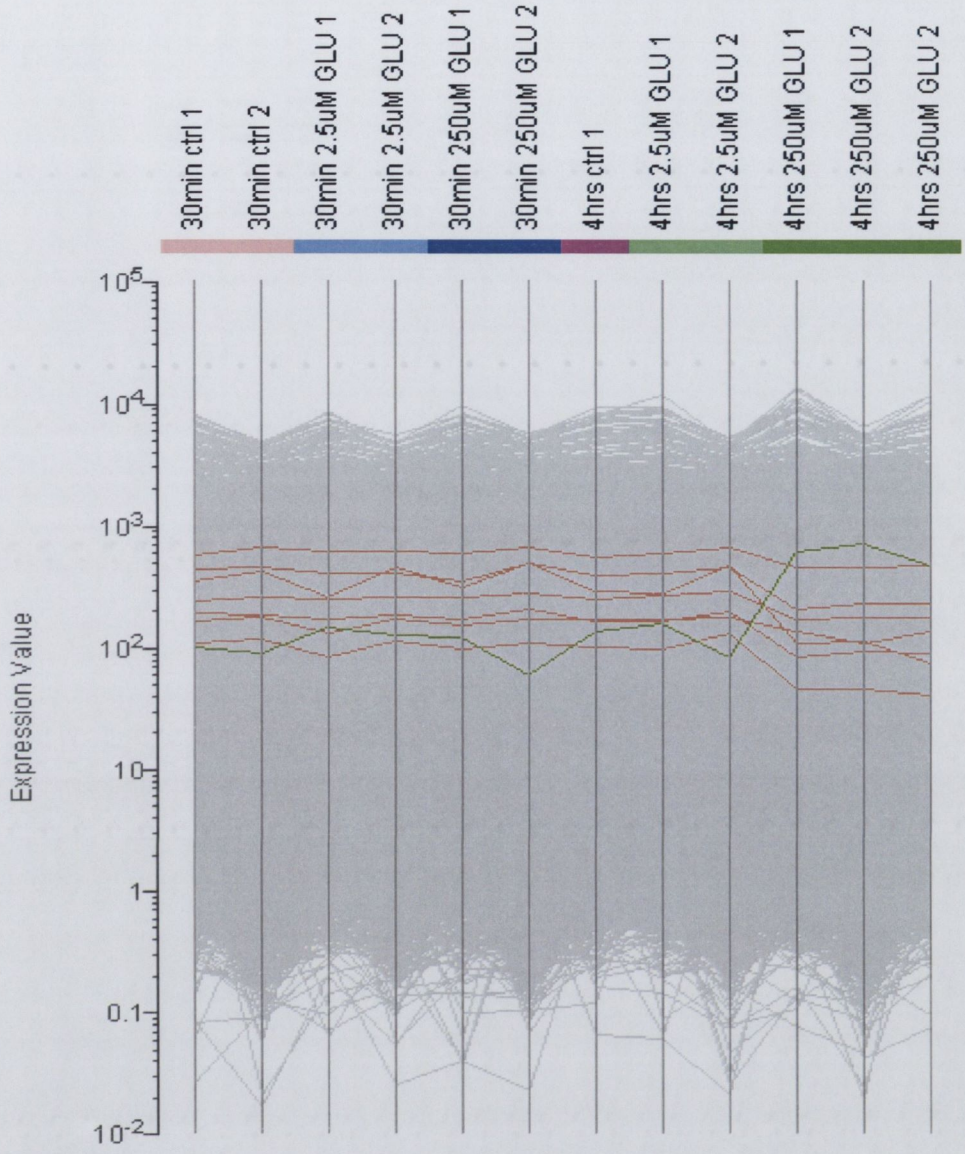


Figure 6.8 b): 5 genes found from a total of 12488 that negatively correlate with *fosB*

Similarity analysis was applied to all 12488 hybridised probes to identify genes similar to the *fosB* probe set (probe ID: 103990_at), on the basis of their intensity of expression. The graph represents the expression values of all probes (grey area) on the array. *fosB* is represented by the green line. Genes, whose expression patterns negatively correlate with *fosB*, across the different assay conditions are represented by the red lines.

Gene Symbol	Gene Description	Genbank Accession	Affymetrix ID.	Correlation Coefficient
	Immediate early gene			
fosB	FBJ osteosarcoma oncogene B	X14897	103990_at	1
	Apoptotic gene			
Gadd45b	growth arrest & DNA-damage-inducible 45 beta	X54149	102779_at	0.9503
	Transcription factor			
Atf3	activating transcription factor 3	U19118	104155_f_at	0.9492
	Proprotein convertase			
Pcsk1	proprotein convertase subtilisin/kexin type 1	M69196	94694_at	0.9387
	Transcription factor			
Nr4a1	nuclear receptor subfamily 4, group A, member 1	X16995	102371_at	0.9349
Nr4a2	nuclear receptor subfamily 4, group A, member 2	U86783	92249_g_at	0.9338
Atf4	activating transcription factor 4	M94087	100599_at	0.9329
	Lectin			
Lgals3	lectin, galactose binding, soluble 3	X16834	95706_at	0.9227
	Apoptotic gene			
Gadd45g	growth arrest & DNA-damage-inducible 45 gamma	AF055638	101979_at	0.9196
	Integral membrane protein			
Ldlr	low density lipoprotein receptor	Z19521	160832_at	0.9164
	Complement component			
C1qa	complement component 1	X58861	98562_at	0.9121
	Plasma membrane protein			
Cd36l2	thrombospondin receptor-like 2	AB008553	101389_at	0.9094
	Oxidoreductase			
Cyba	cytochrome b-245, alpha polypeptide	M31775	100059_at	0.9066
	Transcription factor			
Atf3	activating transcription factor 3	U19118	104156_r_at	0.9063
	ATP binding factor			
Uck2	uridine-cytidine kinase 2	AI850362	94367_at	0.9057
	Protein biosynthesis inhibitor			
Angl	angiogenin-like	U72672	95228_f_at	0.9023
	Non-categorised protein			
Wdr6	WD repeat domain 6	AW050287	95643_at	-0.9679
Dcra	Down syndrome critical region gene a	AV122030	162486_f_at	-0.9584
	EST			
EST	EST	AI850991	94430_at	-0.9515
	Proeasome			
Psma4	proteasome	AI851441	97459_at	-0.9472
	Inhibitory amino acid transporter			
Viaat	vesicular inhibitory amino acid transporter	AJ001598	101420_at	-0.9453

Table 6.3: 20 genes found which correlate with the expression profile of *fosB*

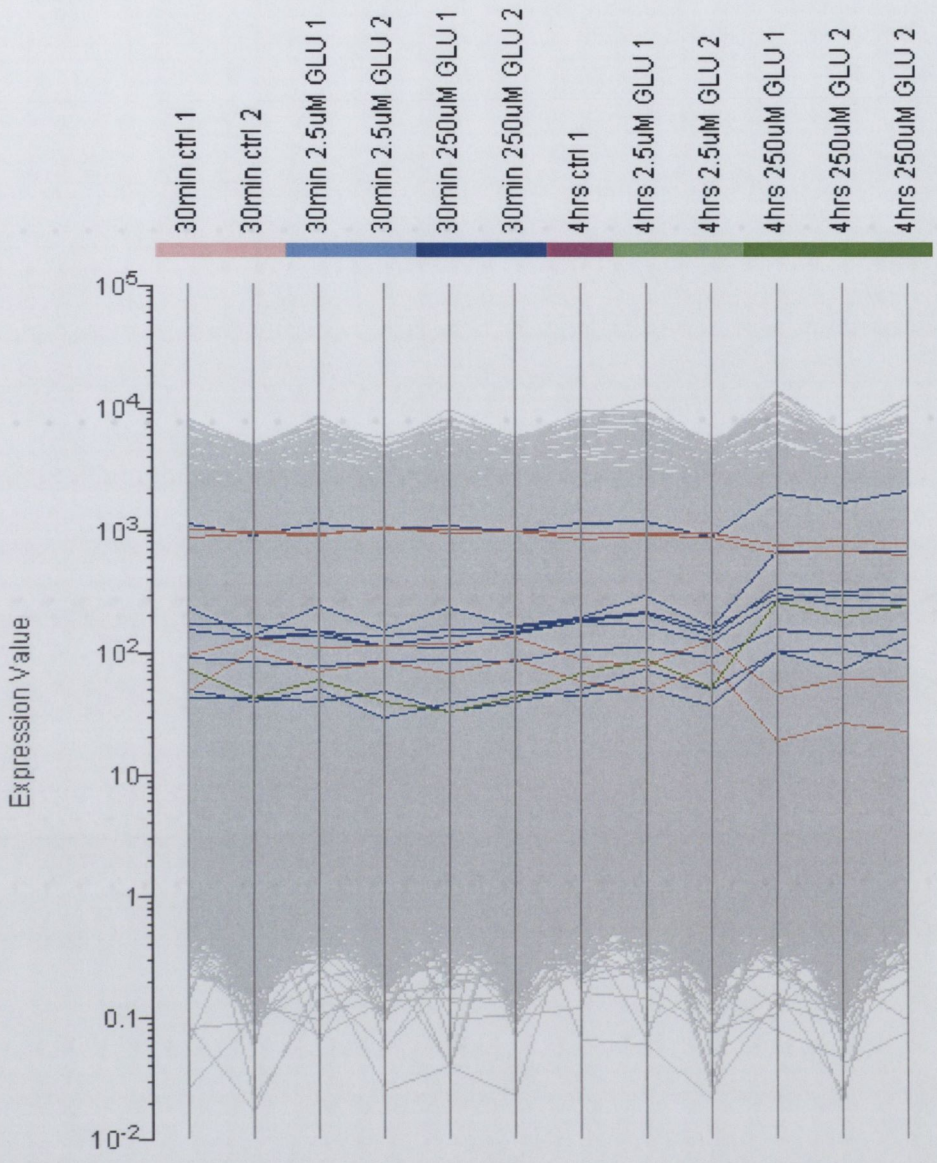


Figure 6.9: Several genes found from a total of 12488 that correlate with ATF3

A similarity search was performed with the ATF3 probe sets (probe set IDs: 104155_r_at and 104156_f_at), using correlation as a similarity measure, to identify genes similar to ATF3 on the basis of their intensity of expression. The graph represents the expression values of all genes from the individual mouse GeneChip® arrays (grey area), hybridised under different conditions of time and concentration. The green line represents ATF3. The blue lines represent genes whose expression patterns positively correlate with ATF3, across the different assay conditions, while the red lines represent genes whose expression patterns are down-regulated.

Gene Symbol	Gene Description	Affymetrix ID	Genbank Accession	Correlation Coefficient
	Transcription factor			
ATF3	activating transcription factor 3	104155_r_at	U19118	1
ATF4	activating transcription factor 4	100599_at	M94087	0.9705
	Non-categorised protein			
Rpl10	ribosomal protein 10	98342_at	M93980	0.9615
	Complement component			
C1qa	complement component 1	98562_at	X58861	0.9603
	ATP binding			
Uck2	uridine-cytidine kinase 2	94367_at	AI850362	0.9577
	Immediate early gene			
fosB	FBJ osteosarcoma oncogene B	103990_at	X14897	0.9492
	Non-categorised protein			
Cd36l2	collagen type I receptor	101389_at	AB008553	0.9490
Rpl30	ribosomal protein L30	98119_at	K02928	0.9487
	Complement component			
C1qb	complement component 1	96020_at	M22531	0.9455
	Protein			
Plp2	proteolipid protein 2	93323_at	AB031292	0.9455
	Transcription factor			
ATF3	activating transcription factor 3	104156_r_at	U19118	0.9408
	Apoptosis factor			
Gadd45g	growth arrest and DNA-damage-inducible 45 gamma	101979_at	AF055638	0.9385
	Protein biosynthesis inhibitor			
Angl	angiogenin-like	95228_f_at	U72672	0.9376
	Transcription factor			
Nr4a2	nuclear receptor subfamily 4, group A, member 2	92249_g_at	U86783	0.9363
	Ligand binding carrier			
Fth	ferritin heavy chain	94794_at	X52561	0.9353
	Apoptosis factor			
Gadd45b	growth arrest and DNA-damage-inducible 45 beta	102779_at	X54149	0.9349
	Golgi/vesicle coat			
Ap1m1	adaptor-related protein complex AP-1, mu subunit 1	94248_at	M62419	-0.9565
	ESTs			
EST	EST	104196_at	AA711908	-0.9564
EST	EST	96675_at	AW124245	-0.9532

Table 6.4: List of genes that correlate with the expression profile of ATF3 (104155_r_at)

Gene Symbol	Gene Description	Affymetrix ID	Genbank Accession	Correlation Coefficient
	Transcription factor			
ATF3	activating transcription factor 3	104156_r_at	U19118	1
	Complement component			
C1qa	complement component 1	98562_at	X58861	0.9722
	Cysteine endopeptidase			
Ctss	cathepsin S	98543_at	AJ223208	0.9636
	Oxidoreductase			
Cyba	cytochrome b-245, alpha polypeptide	100059_at	M31775	0.9444
	Transcription factor			
ATF3	activating transcription factor 3	104155_f_at	U19118	0.9408
ATF4	activating transcription factor 4	100599_at	M94087	0.9374
	Myelin protein			
Plp	proteolipid protein (myelin)	92801_at	M37335	0.9305
	Immediate early gene			
Tieg	TGFB inducible early growth response	99602_at	AF064088	0.9239
	Growth factor			
Hegfl	growth factor-like growth factor	92730_at	L07264	0.9234
	ATP binding protein			
Abcg1	ATP-binding cassette	160612_at	Z48745	0.9186
	Proteins			
Rpl3	ribosomal protein L3	100734_at	Y00225	0.9173
Plp2	proteolipid protein 2	93323_at	AB031292	0.9169
	Ligand binding carrier			
Ftl1	ferritin light chain 1	99872_s_at	L39879	0.9157
	Cell adhesion molecule			
Spp1	secreted phosphoprotein 1	97519_at	X13986	0.9146
	Proteins			
Rps3a	ribosomal protein S3a	101664_at	Z83368	0.9139
	Complement component			
C1qc	complement component	92223_at	X66295	0.9139
	ESTs			
EST	EST	96741_at	AW124129	-0.9358
EST	EST	103678_at	AI841139	-0.9350
EST	EST (Similar to G protein pathway suppressor)	102969_at	AI847369	-0.9344
EST	EST	104305_at	AW120679	-0.9341
EST	EST	93859_at	AI875598	-0.9335

Table 6.5: List of genes that correlate with the expression profile of ATF3 (104156_r_at)

6.2.4 K-Means cluster analysis of the 76 deregulated genes from the mouse arrays

K-means clustering was used to combine groups of genes selected by similarity analysis and by N fold regulation (HRP and ratio of means) into clusters representative of their distinct expression patterns.

The union of all genes similarly up-regulated more than 2.5 fold with *c-fos, fosB* and ATF3 and the union of all genes similarly down-regulated more than 2.5 fold (54 genes in total for the mouse; 45 genes in total for the rat) were merged with the group of genes ≥ 2.5 fold up/down-regulated (selected by HRP and N fold regulation) forming a final group of 95 genes. Prior to the clustering analysis, gene expression values were normalised to their respective time matched controls to yield ratios of induction (treated versus control) by pointwise division. K-means clustering selected 5 separate gene clusters of which 2 were removed following visual inspection, due to the very low expression values and also to the absence of variability in the profiles with time and concentration. The 3 clusters chosen represented 76 genes of the combined group of 95 genes (see Figure 6.10).

(c) Cluster 1

Cluster 1 was the largest cluster representing 46 genes. The expression levels of the 46 genes remained unchanged following exposure to non-toxic concentrations of Glu (2.5 μM) for either 30 min or 240 min and also to toxic concentrations of Glu (250 μM) for 30 min. However, the 46 genes were strongly up-regulated following treatment of the mCGCs with toxic concentrations of Glu for 240 min (see Figure 6.10). The change in the level of expression for any gene was considered significant if the change in expression was ≥ 2 fold. Cluster 1 contained the following groups: kinases/phosphatases (3), growth factors (2), proteins (6), an oncogene (1), DNA binding agents (3), cell adhesion factors (4), a proteolysis agent (1), cell differentiation agents (2), transcription factors (2), several ESTs (3), agents involved in cell-cell communication (2), glycolytic factors (2), integral membrane proteins (7) and non-categorised factors (9) (see Tables 6.6 a), b), and c)). The 240/30 min ratios of all members of each group were greater than 1.

(a) Cluster 2

In cluster 2, 24 genes shared a similar pattern of expression. All 24 genes remained unchanged following exposure to non-toxic concentrations of Glu (2.5 μM) for either 30

min or 240 min and also to toxic concentrations (250 μM) of Glu for 30 min. However, the 24 genes were strongly down-regulated following treatment of the mCGCs with toxic concentrations of Glu for 240 min (see Figure 6.10). This group contained a DNA binding protein (1), an inhibitory amino acid transporter (1), a proteinase (1), a cyclin-dependent protein kinase regulator (1), neurotransmitter proteins (2), a proteasome protein (1), non-categorised factors (7) and several ESTs (10) (see Tables 6.7 a) and b)). All of the 24 genes belonging to Cluster 2 displayed 240/30 min mRNA ratios less than 1, indicating their down-regulation in excitotoxicity.

(b) Cluster 3

Cluster 3 represented a group of 6 genes. Following exposure of the mCGCs to non-toxic concentrations of Glu (2.5 μM) for 30 min a small transient increase in expression of the genes was observed, with Nr4a1 expression being the highest at 30 min. By 240 min the levels of expression of all 6 genes had returned to the basal rate. While exposure to toxic concentrations of Glu (250 μM) for 30 min induced no change in expression of the 6 genes, a strong elevated expression was observed at the 240 min time-point (see Figure 6.10). This group contained the transcription factors ATF3 (represented twice on the micro-array) and Nr4a1 and the oncogenes *c-fos* and *fosB* (see Table 6.8). The 6 genes all exhibited 240/30 min mRNA ratios much greater than 1 (3 - 11) with the Nr4a1 mRNA ratio being the highest, indicating a strong up-regulation in excitotoxicity.

6.2.5 Tile display of the 76 deregulated genes following K-means clustering

The clustered tile display (see Figure 6.11) consists of large patches of colour representing groups of genes that share similar expression patterns over multiple conditions. In addition, the tile display was used to observe how the clusters were sorted by their average expression values. Each colour patch in the resulting visual map represented the expression level of the associated gene in treated mouse cerebellar granule cells, with a continuum of expression levels from *bright green* (lowest expression values) to *bright red* (highest expression values).

It was repeatedly found that genes represented by more than one array element or genes with high degrees of sequence identity were clustered next to, or in the immediate vicinity of, each other.

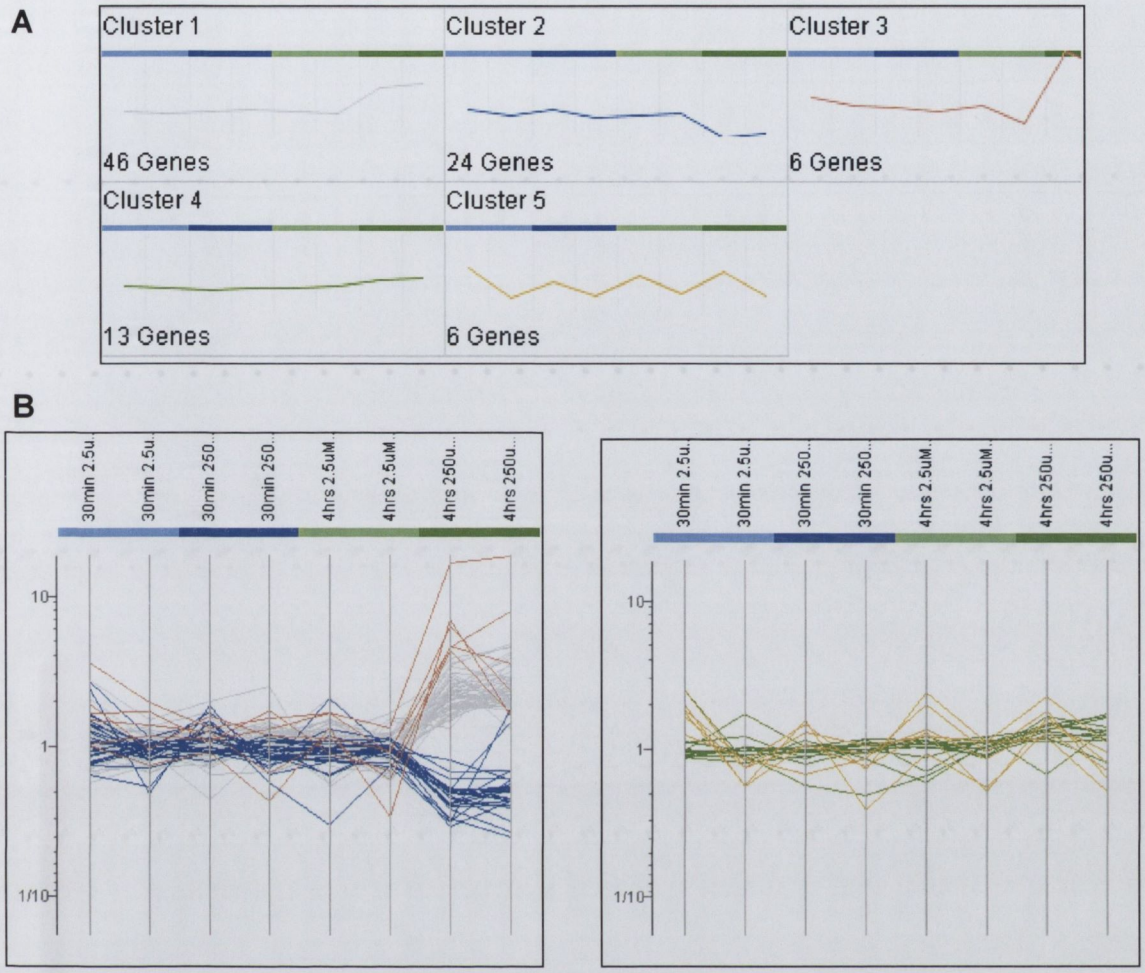


Figure 6.10: Profile display of 76 deregulated genes following K-means clustering

Cluster 1 (grey lines) represents a group of 46 genes, all of which were up-regulated following exposure of mCGCs to toxic concentrations of Glu (250 μM) for 4 hours. Cluster 2 (blue lines) represents a group of 24 genes, which were effectively down-regulated under the same excitotoxic conditions. Cluster 3 (orange lines) represents a group of 6 genes, which displayed a slight induction following exposure to non-toxic concentrations of Glu for 30 min but an even stronger induction with toxic concentrations of Glu for 4 hours. The genes belonging to Cluster numbers 4 (green lines) and 5 (yellow lines) were eliminated from the gene list, thus generating a final group of 76 genes.

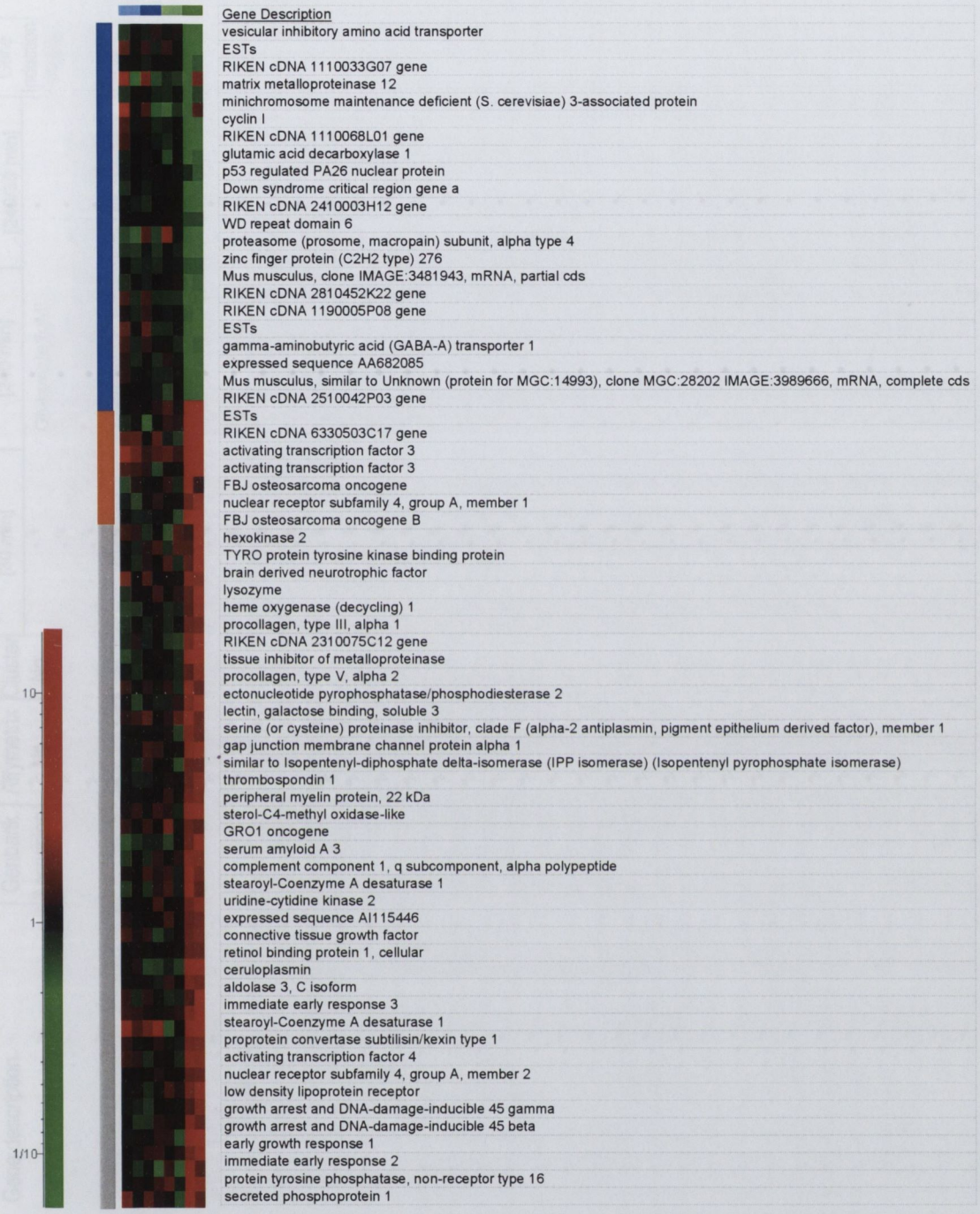


Figure 6.11: Tile display of 76 up- and down-regulated genes following K-means clustering

The tile display of K-Means clustering was used to observe how the clusters were sorted by their ratios of expression values. Each colour patch in the resulting visual map represents the expression level of the associated gene in treated mCGCs, with a continuum of expression levels from *bright green* (lowest) to *bright red* (highest). The colour map also indicates the several distinct clusters.

Gene symbol	Gene description	Genbank Accession	Affymetrix No.	Cluster No.	Ratio(treated v. cntl.) [30 min]		Ratio(treated v. cntl.) [240 min]		Ratio [240/30 min]		Excitotoxic Gene Induction Profile
					Glutamate [μM]						
					2.5	250	2.5	250	2.5	250	
	Kinase/Phosphatases										
Hmox1	heme oxygenase (decycling) 1	X56824	160101_at	1	0.93	1.33	1.09	1.96	1.18	1.47	←
Uck2	uridine-cytidine kinase 2	AI850362	94367_at	1	1.21	1.12	1.06	3.16	0.88	2.82	↑
Ptpn16	protein tyrosine phosphatase. non-receptor type 16	X61940	104598_at	1	1.30	0.90	0.93	2.28	0.72	2.52	↑
	Growth Factor										
Bdnf	brain derived neurotrophic factor	X55573	102727_at	1	0.93	0.91	0.79	2.29	0.85	2.51	↑
Ctgf	connective tissue growth factor	M70642	93294_at	1	0.69	0.87	0.83	2.32	1.21	2.68	↑
	Proteins										
Lyzs	lysozyme	M21050	100611_at	1	1.29	0.91	0.85	1.82	0.66	2.00	←
Saa3	serum amyloid A 3	X03505	102712_at	1	0.89	1.18	0.88	2.00	0.99	1.70	↑
C1qa	complement component 1	X58861	98562_at	1	0.92	0.98	1.10	2.13	1.20	2.17	↑
Pcsk1	proprotein convertase subtilisin/kexin type 1	M69196	94694_at	1	1.31	0.96	0.95	1.97	0.73	2.05	←
Plp	proteolipid protein (myelin)	M37335	92801_at	1	0.88	0.95	1.05	2.41	1.19	2.55	↑
Aqp1	aquaporin 1	L02914	93330_at	1	1.51	1.42	0.86	2.76	0.57	1.95	↑
	Oncogene										
Gro1	GRO1 oncogene	J04596	95348_at	1	0.93	1.34	0.97	2.91	1.04	2.18	↑
	IEGs										
Egr1	early growth response 1	M28845	98579_at	1	2.19	2.21	0.73	3.14	0.33	1.42	↑
Egr2	early growth response 2	M24377	102661_at	1	1.00	1.05	0.94	2.74	0.94	2.60	↑
Tieg	TGFB inducible early growth response	AF064088	99602_at	1	1.03	0.84	1.31	2.13	1.27	2.52	↑

Table 6.6 a): Normalised expression values of the 46 genes of Cluster 1 and their respective 240/30 min ratios. The ↑ represents genes which were up-regulated under excitotoxic conditions (250 μM Glu for 4 hours) and ← represents genes whose expression values were ≤ 2.

Gene symbol	Gene description	Genbank Accession	Affymetrix No.	Cluster No.	Ratio(treated v. cntl.) [30 min]		Ratio(treated v. cntl.) [240 min]		Ratio [240/30 min]		Excitotoxic Gene Induction Profile
					Glutamate [μM]						
					2.5	250	2.5	250	2.5	250	
	Cell adhesion										
Thbs1	thrombospondin 1	M62470	160469_at	1	0.76	0.88	1.10	3.01	1.45	3.41	↑
Spp1	secreted phosphoprotein 1	X13986	97519_at	1	1.05	1.13	1.02	1.94	0.97	1.72	←
Col3a1	procollagen, type III, alpha 1	X52046	98331_at	1	0.89	1.08	1.15	2.01	1.30	1.87	↑
Col5a2	procollagen, type V, alpha 2	L02918	92567_at	1	0.71	0.98	0.83	1.89	1.18	1.94	←
	Proteolysis and peptidolysis										
Ctss	cathepsin S	AJ223208	98543_at	1	0.90	0.89	0.94	1.79	1.05	2.01	←
	Cell differentiation										
Gadd45g	growth arrest and DNA-damage-inducible 45 gene	AF055638	101979_at	1	1.07	1.09	0.83	2.23	0.78	2.05	↑
Gadd45b	growth arrest and DNA-damage-inducible 45 beta	X54149	102779_at	1	1.29	1.05	1.18	2.32	0.91	2.20	↑
	Transcription factor										
Atf4	activating transcription factor 4	M94087	100599_at	1	1.04	1.01	0.99	1.88	0.95	1.86	←
Nr4a2	nuclear receptor subfamily 4, group A, member 2	U86783	92249_g_at	1	1.03	0.66	0.79	4.51	0.77	6.87	↑
	ESTs										
EST	EST	AA914105	96271_at	1	1.49	1.22	1.02	2.22	0.68	1.82	↑
EST	EST	AW061237	94441_at	1	0.91	0.72	0.64	3.26	0.70	4.51	↑
EST	EST	AW125273	94445_at	1	1.08	1.11	1.29	1.65	1.20	1.48	←
	Cell-Cell communication										
Gja1	gap junction membrane channel protein alpha 1	M63801	100064_f_at	1	0.85	1.03	0.87	1.92	1.02	1.87	←
Pmp22	peripheral myelin protein, 22 kDa	Z38110	102395_at	1	1.29	1.27	1.48	2.12	1.15	1.66	↑

Table 6.6 b): Normalised expression values of the 46 genes of Cluster 1 and their respective 240/30 min ratios. The ↑ represents genes which were up-regulated under excitotoxic conditions (250 μM Glu for 4 hours) and ← represents genes whose expression values were ≤ 2.

Gene symbol	Gene description	Genbank Accession	Affymetrix No.	Cluster No.	Ratio(treated v. cntl.) [30 min]		Ratio(treated v. cntl.) [240 min]		Ratio [240/30 min]		Excitotoxic Gene Induction Profile
					Glutamate [μM]						
					2.5	250	2.5	250	2.5	250	
	Glycolysis										
Aldo3	aldolase 3, C isoform	AW121134	160546_at	1	0.85	0.94	1.10	1.92	1.29	2.04	←
Hk2	hexokinase 2	Y11666	94375_at	1	0.82	0.99	0.98	2.00	1.20	2.02	↑
	Integral membrane proteins										
Enpp2	ectonucleotide pyrophosphatase/phosphodiesterase 2	AW122933	97317_at	1	0.92	1.05	0.98	1.82	1.07	1.73	←
Scd1	stearoyl-Coenzyme A desaturase 1	M21285	94057_g_at	1	0.97	1.00	1.00	2.11	1.03	2.10	↑
Scd1	stearoyl-Coenzyme A desaturase 1	M21285	94056_at	1	1.02	1.05	1.13	1.73	1.11	1.65	←
Cldn5	claudin 5	U82758	104516_at	1	1.07	1.16	1.18	3.51	1.10	3.02	↑
Ier3	immediate early response 3	X67644	94384_at	1	1.00	1.24	1.06	2.34	1.06	1.89	↑
Ier2	immediate early response 2	M59821	99109_at	1	1.14	1.08	0.92	2.04	0.81	1.89	↑
Tyrobp	TYRO protein tyrosine kinase binding protein	AF024637	100397_at	1	0.78	1.18	1.09	2.02	1.40	1.72	↑
	Non-categorised factors										
Timp	tissue inhibitor of metalloproteinase	V00755	101464_at	1	0.90	1.22	1.08	1.88	1.20	1.53	←
Lgals3	lectin, galactose binding, soluble 3	X16834	95706_at	1	0.98	0.97	0.70	2.53	0.72	2.62	↑
Serpinf1	serine (or cysteine) proteinase inhibitor	AF036164	93574_at	1	0.77	1.10	0.89	2.55	1.16	2.31	↑
LOC207933	similar to IPP isomerase	AA716963	96269_at	1	1.18	1.07	0.95	2.14	0.81	2.00	↑
Sc4mol	sterol-C4-methyl oxidase-like	AI848668	160388_at	1	1.03	0.97	0.87	2.22	0.85	2.30	↑
Rbp1	retinol binding protein 1, cellular	X60367	104716_at	1	0.87	1.01	1.07	2.17	1.23	2.15	↑
Cp	ceruloplasmin	U49430	92851_at	1	1.04	1.22	1.00	1.89	0.96	1.55	←
Ldlr	low density lipoprotein receptor	Z19521	160832_at	1	1.04	1.01	1.13	1.93	1.09	1.92	←
C1qb	complement component 1	M22531	96020_at	1	0.99	1.28	1.06	2.19	1.07	1.72	↑

Table 6.6 c): Normalised expression values of the 46 genes of Cluster 1 and their respective 240/30 min ratios. The ↑ represents genes which were up-regulated under excitotoxic conditions (250 μM Glu for 4 hours) and ← represents genes whose expression values were ≤ 2.

Gene symbol	Gene description	Genbank Accession	Affymetrix No.	Cluster No.	Ratio(treated v. cntl.) [30 min]		Ratio(treated v. cntl.) [240 min]		Ratio [240/30 min]		Excitotoxic Gene Induction Profile
					Glutamate [μM]						
					2.5	250	2.5	250	2.5	250	
	DNA binding										
Zfp276	zinc finger protein (C2H2 type) 276	AW125516	93432_at	2	0.57	0.96	1.38	0.40	2.41	0.41	↓
	Inhibitory amino acid transporter										
Viaat	vesicular inhibitory amino acid transporter	AJ001598	101420_at	2	0.93	1.06	1.06	0.28	1.14	0.26	↓
	Proteolysis and peptidolysis										
Mmp12	matrix metalloproteinase 12	M82831	95339_r_at	2	1.08	1.02	0.77	0.81	0.71	0.80	↓
	Cyclin-dependent protein kinase regulator										
Ccni	cyclin I	AF005886	94820_r_at	2	1.68	0.87	0.47	0.72	0.28	0.83	↓
	Neurotransmission										
Gad1	glutamic acid decarboxylase 1	Z49976	103061_at	2	1.20	0.98	0.90	0.43	0.75	0.43	↓
Gabt1	gamma-aminobutyric acid (GABA-A) transporter 1	M92378	161059_at	2	0.98	1.10	0.94	0.49	0.96	0.44	↓
	Protein degradation										
Psma4	proteasome (prosome, macropain)	AI851441	97459_at	2	1.02	1.09	1.09	0.68	1.07	0.62	↓
	Non-categorised factors										
Mcm3ap	minichromosome maintenance deficient	AJ006590	97433_at	2	0.84	0.99	0.85	0.50	1.01	0.50	↓
Pa26	p53 regulated PA26 nuclear protein	AI843106	95731_at	2	0.94	0.95	0.77	0.47	0.82	0.49	↓
Dcra	Down syndrome critical region gene a	AV122030	162486_f_at	2	0.94	1.01	0.99	0.73	1.06	0.72	↓
Wdr6	WD repeat domain 6	AW050287	95643_at	2	0.90	0.93	1.01	0.53	1.11	0.57	↓
ESTs	ESTs	AA615429	99923_at	2	0.73	0.81	0.90	0.37	1.24	0.46	↓
ESTs	ESTs	AW120679	104305_at	2	1.07	1.06	0.88	0.52	0.83	0.49	↓
ESTs	ESTs	AW124129	96741_at	2	1.23	1.15	0.89	0.47	0.72	0.41	↓

Table 6.7 a): Normalised expression values of the 24 genes of Cluster 2 and their respective 240/30 min ratios. The ↑ represents genes which were up-regulated under excitotoxic conditions (250 μM Glu for 4 hours) and ← represents genes whose expression values were ≤ 2.

Gene symbol	Gene description	Genbank Accession	Affymetrix No.	Cluster No.	Ratio(treated v. cntl.) [30 min]		Ratio(treated v. cntl.) [240 min]		Ratio [240/30 min]		Excitotoxic Gene Induction Profile
					Glutamate [μM]						
					2.5	250	2.5	250	2.5	250	
	ESTs										
ESTs	ESTs	AI839232	103685_at	2	1.19	1.01	1.17	0.48	0.98	0.47	↓
ESTs	ESTs	AA030469	104402_at	2	0.99	1.00	0.78	0.28	0.79	0.28	↓
ESTs	ESTs	AI851348	103743_at	2	1.07	0.95	0.95	0.45	0.89	0.48	↓
ESTs	ESTs	AI848025	97407_at	2	1.01	0.96	0.99	0.45	0.98	0.47	↓
ESTs	ESTs	AI848330	104717_at	2	1.13	0.96	0.94	0.41	0.83	0.43	↓
ESTs	ESTs	AI850991	94430_at	2	0.87	0.91	1.04	0.40	1.20	0.45	↓
ESTs	ESTs	AA959648	103664_r_at	2	0.90	0.86	0.93	0.60	1.03	0.70	↓
ESTs	ESTs	AI842242	104332_at	2	0.89	0.95	1.05	0.52	1.19	0.55	↓
ESTs	ESTs	AI839518	160908_r_at	2	0.98	0.87	1.01	0.36	1.03	0.42	↓
ESTs	ESTs	AA711908	104196_at	2	1.03	0.92	0.84	0.50	0.81	0.55	↓

Table 6.7 b): Cluster 2 contains 24 genes with similar expression profiles in mCGCs

Normalised expression values of the 24 genes of Cluster 2 and their respective 240/30 min ratios. The ↑ represents genes which were up-regulated under excitotoxic conditions (250 μM Glu for 4 hours) and ← represents genes whose expression values were ≤ 2.

Gene symbol	Gene description	Genbank Accession	Affymetrix No.	Cluster No.	Ratio(treated v. cntl.) [30 min]		Ratio(treated v. cntl.) [240 min]		Ratio [240/30 min]		Excitotoxic Gene Induction Profile
					Glutamate [μM]						
					2.5	250	2.5	250	2.5	250	
	Transcription factors										
Atf3	activating transcription factor 3	U19118	104155_f_at	3	1.07	1.07	1.35	4.04	1.26	3.76	↑
Atf3	activating transcription factor 3	U19118	104156_r_at	3	0.86	0.64	1.26	4.22	1.47	6.56	↑
Nr4a1	nuclear receptor subfamily 4, group A, member 1	X16995	102371_at	3	2.69	1.43	1.50	15.79	0.56	11.06	↑
	Immediate early genes										↑
c-fos	FBJ osteosarcoma oncogene	V00727	160901_at	3	1.67	1.27	0.79	4.05	0.48	3.18	↑
fosB	FBJ osteosarcoma oncogene B	X14897	103990_at	3	1.44	0.96	1.06	5.24	0.73	5.47	↑

Table 6.8: Cluster 3 contains 6 genes with similar expression profiles in mCGCs

Cluster 3 contains 6 genes with similar expression profiles in mCGCs following exposure to a toxic (250 μM) or non-toxic (2.5 μM) concentrations of Glu for either 30 min or 240 min (4 hours). Identity of the columns, from left to right: Gene symbol, Gene description with genes sorted according to biochemical properties, Genbank accession number, Affymetrix gene identification number; Cluster group, Expression levels of the 6 genes following 30 min exposure to either the non-toxic or toxic concentration of Glu, Expression levels of the 6 genes following exposure for 240 min to either the non-toxic or toxic concentration of Glu and the 240/30 min ratios of expression following non-toxic and toxic Glu stimulation, and the increase (↑), decrease (↓) or a change ≤ a ratio of 2 (↔) in the level of RNA induction. The arrow represents the pattern of expression, that is, ↑ represents genes which were up-regulated ≥ a ratio of 2 under excitotoxic conditions (exposure to 250 μM Glu for 4 hours)

6.2.6 Analysis of micro-array data from rat cortical neurons treated with Glu

In accordance with earlier reported EAA-induced time- and concentration-dependent profiles of *c-fos* and *fosB* expression in primary rat cortical neurons (see Chapter 5), 30 min and 240 min were selected as the optimal time-points for micro-array analysis. Mature rat cortical neurons (13 DIV; see Section 2.2.2) were treated with either a non-toxic concentration of Glu (2.5 µM) or a toxic concentration of Glu (250 µM). Time matched vehicle controls were used for both concentrations. Affymetrix GeneChip® Technology (Rat Genome Chip RG_U34A) was used to investigate whether the profiles of Glu-induced *c-fos* and *fosB* expression correlated with that previously found by RT-PCR and, indeed, whether other *IEGs* share similar expression profiles.

Microarray Suite Version 5 of Affymetrix (MAS5) was used to analyse the fluorescence intensities of the various hybridised and labelled microarrays. The expression values for 8799 probes were normalised to a target intensity of 100 and were loaded into the GeneData Expressionist Refiner (version 3.0.4) for bright/dark spot and gradient correction. Following correction, the microarray data was analysed in the Analyst Software module of GeneData Expressionist software package. Six groups containing replicate experiments were analysed.

30 min control	4 hours control
30 min 2.5 µM Glu	4 hours 2.5 µM Glu
30 min 250 µM Glu	4 hours 250 µM Glu

Initially, the distribution of gene expression values, derived from the fluorescent intensities of all individual probe sets, was displayed using a Box Plot (see Figure 6.12). The expression values were globally normalised to a pre-determined target intensity of 100, so that the median values for each chip were similar. The box plot demonstrated that the distribution of upper and lower quartiles and outliers were similar between the different experiments.

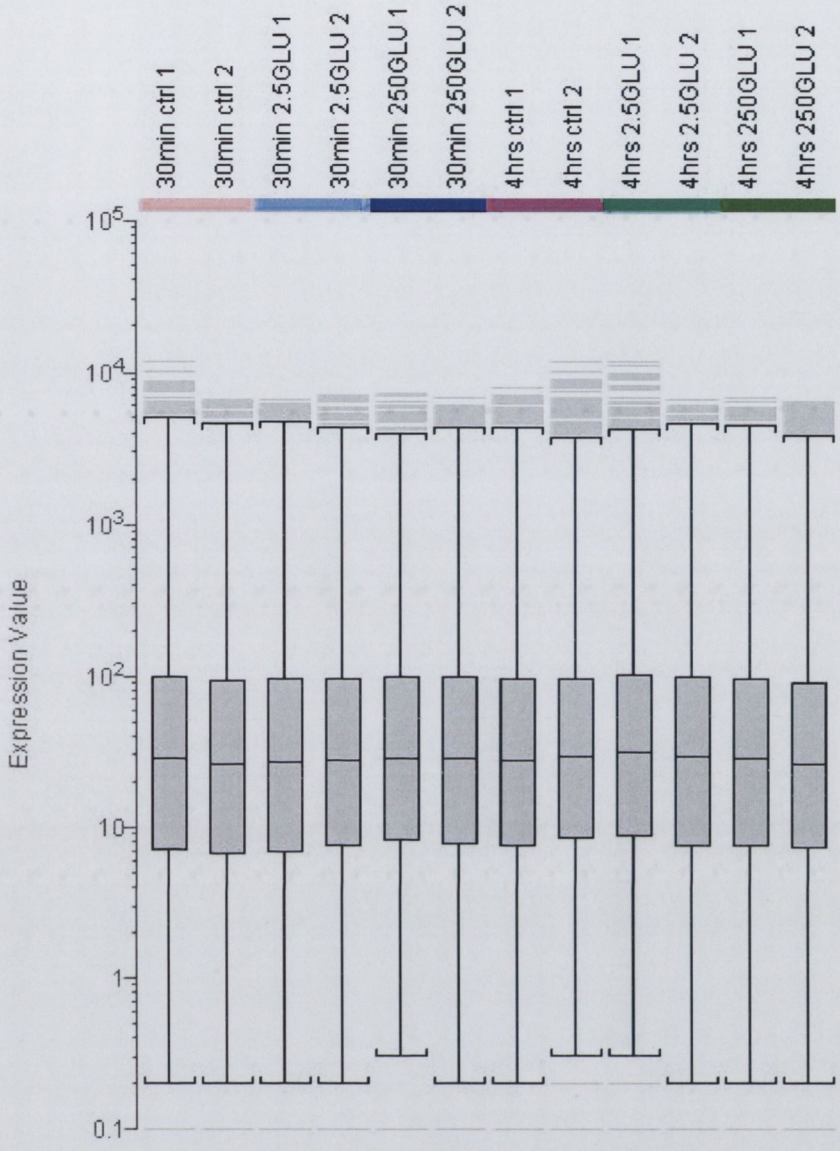


Figure 6.12: Box Plot of data obtained from hybridised rat-RG_U34A arrays

A box-plot was used to display the basic distribution of gene expression values from each individual experiment. The quality setting p-value was set as 1, meaning that all present ($p < 0.04$), marginally expressed genes ($0.04 < p < 0.06$) and low expressed genes with an absent call from Affymetrix MAS5 ($0.06 < p < 1$) were used in the analysis.

6.2.7 Gene expression changes in Glu stimulated rat cortical neurons

High Ratio Proportions (HRP) identified all genes that were regulated > 1.8 fold between any pairwise combinations of the treatments, that is, between the two time-points and between any combination of control, 2.5 µM and 250 µM Glu at a given time-point. The high ratio proportion was set as 1 (100%), meaning that any fold regulation > 1.8 was valid, if the fold induction was > 1.8 fold in all pairwise comparisons. The initial analysis resulted in a list of 132 genes. The 132 genes were then subject to a second selection, also using N fold regulation, and genes which had a ratio of means of more than 2.5 fold between the six groups were selected. Thus, a final gene list was compiled which contained 48 genes, all of which were more than 2.5 fold up- or down-regulated between the six experimental conditions (Figure 6.13).

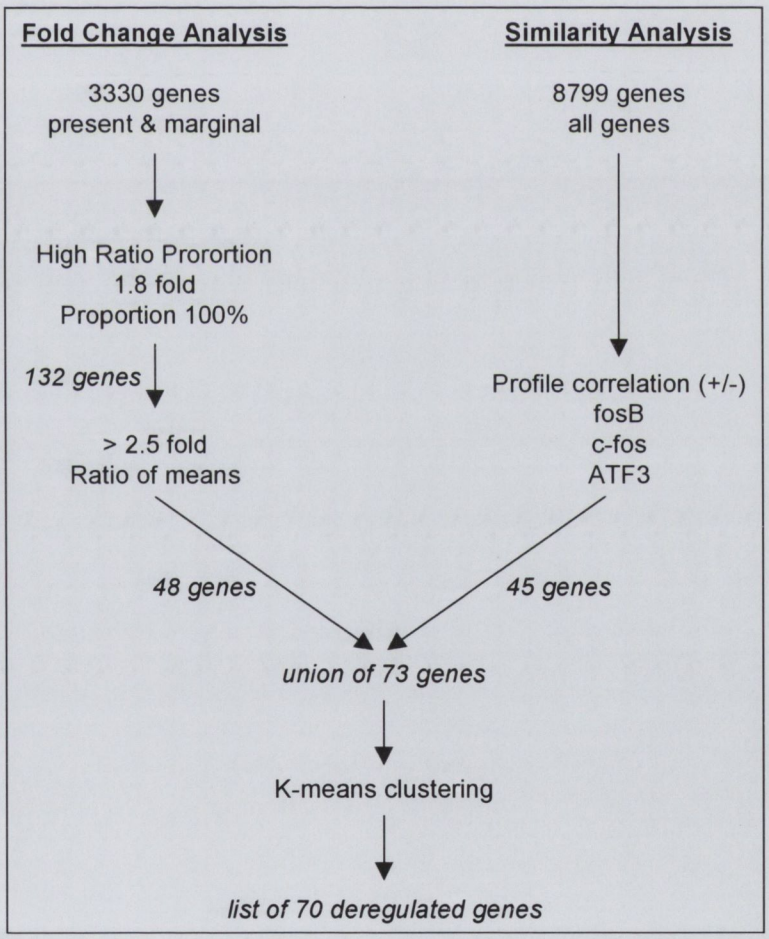


Figure 6.13: Flow chart for the identification of up- and down-regulated genes on hybridised rat RG_U34A arrays

Following the two different selection procedures, the 48 genes were initially inspected for the presence of any members of the *fos* and *jun* families of genes, in particular *c-fos*. As already mentioned, the *fosB* probe was unfortunately not present on the rat array. When the relative RNA levels obtained from the Glu-treated rat cortical neurons were compared with those derived from a time-matched control sample it was found that *c-fos*, *junB* and ATF3 were included. Furthermore the expression profiles of each of these genes may be as a result of excitotoxicity.

The prototypic *IEG*, *c-fos*, was represented two times on the rat array. From the expression values, it was observed that with non-toxic concentrations of Glu (2.5 μM) both representatives of *c-fos* (probe ID sets: X06769cds_at; X06769cds_g_at) were induced at the early time-point of 30 min. By 240 min, the levels of *c-fos* expression had decreased. With toxic concentrations of Glu (250 μM), however, while *c-fos* was induced at 30 min, a more elevated induction was observed at the later time-point of 240 min (see Figure 6.17). These observations confirm the time- and concentration-dependent profiles of *c-fos* expression found, using real-time RT-PCR (see Chapter 5). In addition, the delayed and sustained *c-fos* expression found in rat cortical neurons undergoing excitotoxic cell death was also found in mCGCs, despite the difference in species and brain region (see Chapter 4 and Section 6.2.2 of this Chapter). Thus, the results suggest that *c-fos* can be used as a marker of *in vitro* excitotoxicity, irrelevant of species and brain tissue.

A pattern of expression similar to *c-fos* was found for a member of the *jun* family of *IEGs*, *junB* (probe ID: rcAA891041_at). Non-toxic concentrations of Glu (2.5 μM) induced an increase in *junB* expression at 30 min, which had decreased to basal levels by 240 min. Likewise, while toxic concentrations of Glu (250 μM) increased *junB* expression at 30 min, a higher expression was found at the 240 min time-point (see Figure 6.18). These observations are different from those found for *junB* using real-time RT-PCR (see Chapter 5; Section 5.2.13) where no significant increases were observed.

When the profile of ATF3 expression was observed no induction was found with the non-toxic concentration of Glu at either time-point (probe ID: M63282_at). However, a 4 fold increase in expression was observed in rat cortical neurons following treatment with the toxic concentration of Glu for 240 min (see Figure 6.19). Thus, ATF3 was specifically up-regulated only under excitotxic conditions in mCGCs and rat cortical neurons.

Thus, these observations indicate that *c-fos*, *junB* and ATF3 are specifically regulated upon excitotoxic insult.

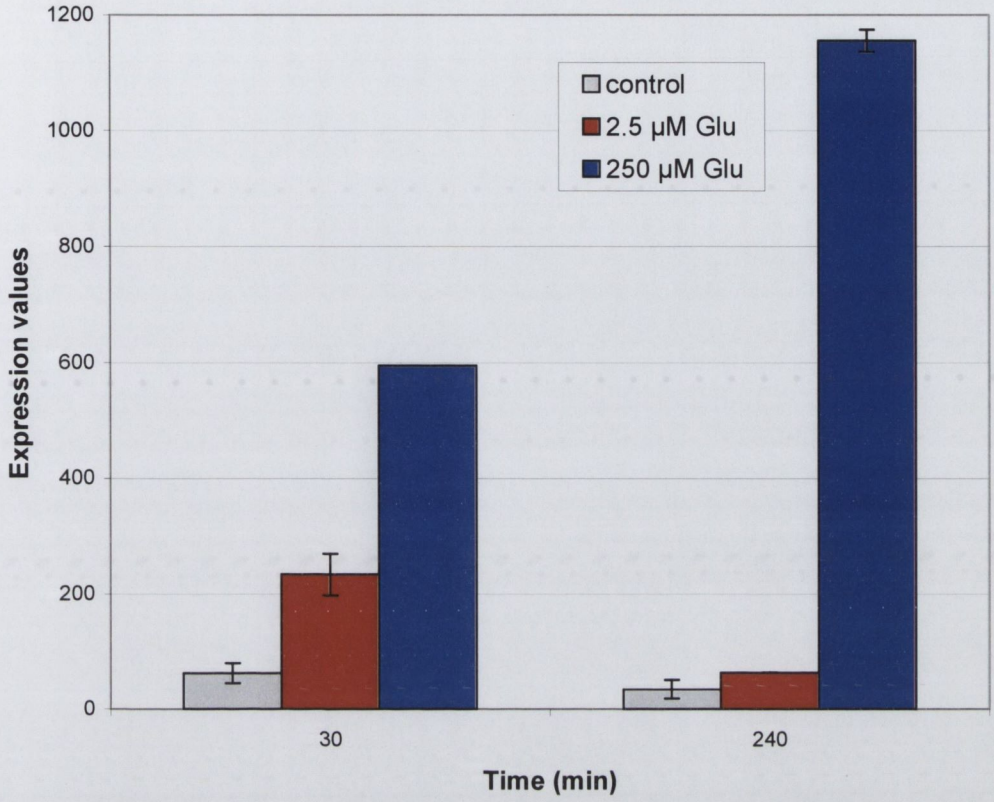


Figure 6.14: Different time-profiles of *c-fos* expression dependent on Glu concentration

Primary cultures of rat cortical neurons (13 DIV) were exposed to a non-toxic (2.5 µM) or toxic (250 µM) concentration of Glu, for either 30 or 240 min. Following treatment, total RNA was extracted, converted to biotinylated cRNA and hybridised to separate rat RG_U34A arrays. The results above refer to the fluorescent levels of *c-fos* expression compared to untreated, time-matched controls. The levels of fluorescent signal are representative of the relative abundance of *c-fos* in the treated/untreated rat cortical neurons. Data represent mean ± variation from the mean of the *c-fos* probe set (probe ID: X06769cds_g_at) from duplicate rat arrays (n = 2).

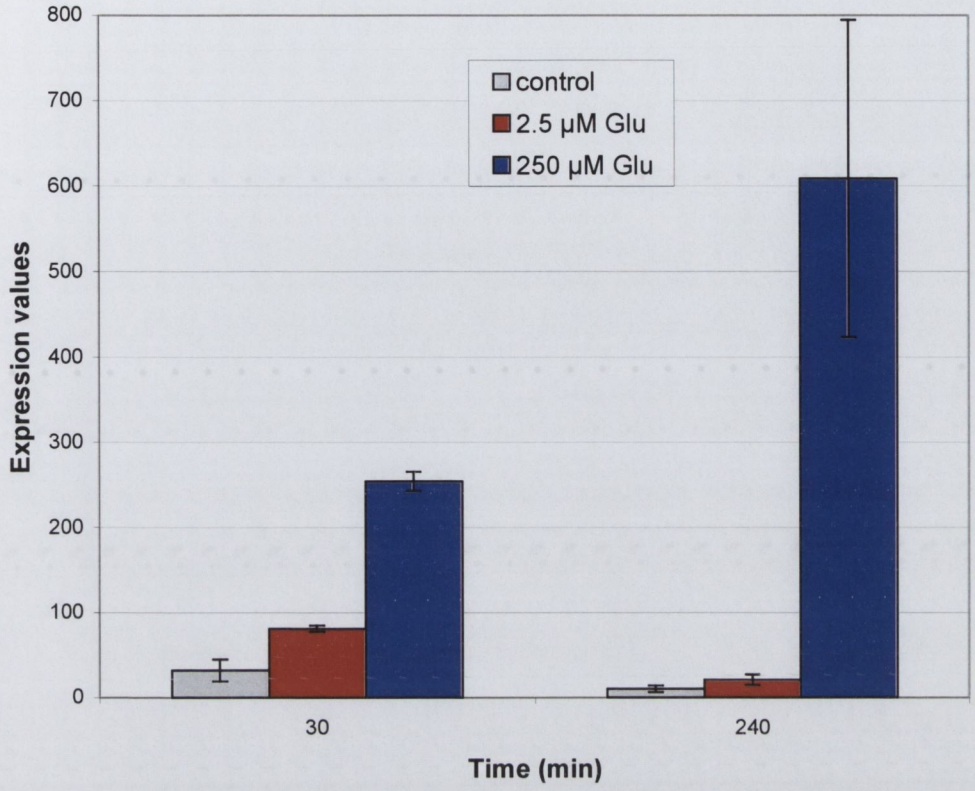


Figure 6.15: Different time-profiles of *junB* expression dependent on Glu concentration

Primary cultures of rat cortical neurons (13 DIV) were exposed to a non-toxic (2.5 µM) or toxic (250 µM) concentration of Glu, for either 30 or 240 min. Following treatment, total RNA was extracted, converted to biotinylated cRNA and hybridised to separate rat RG_U34A arrays. The results above refer to the fluorescent levels of *junB* expression compared to untreated, time-matched controls. The levels of fluorescent signal are representative of the relative abundance of *junB* in the treated/untreated rat cortical neurons. Data represent mean ± variation from the mean of the *junB* probe set (probe ID: rcAA891041_at) from duplicate rat arrays (n = 2).

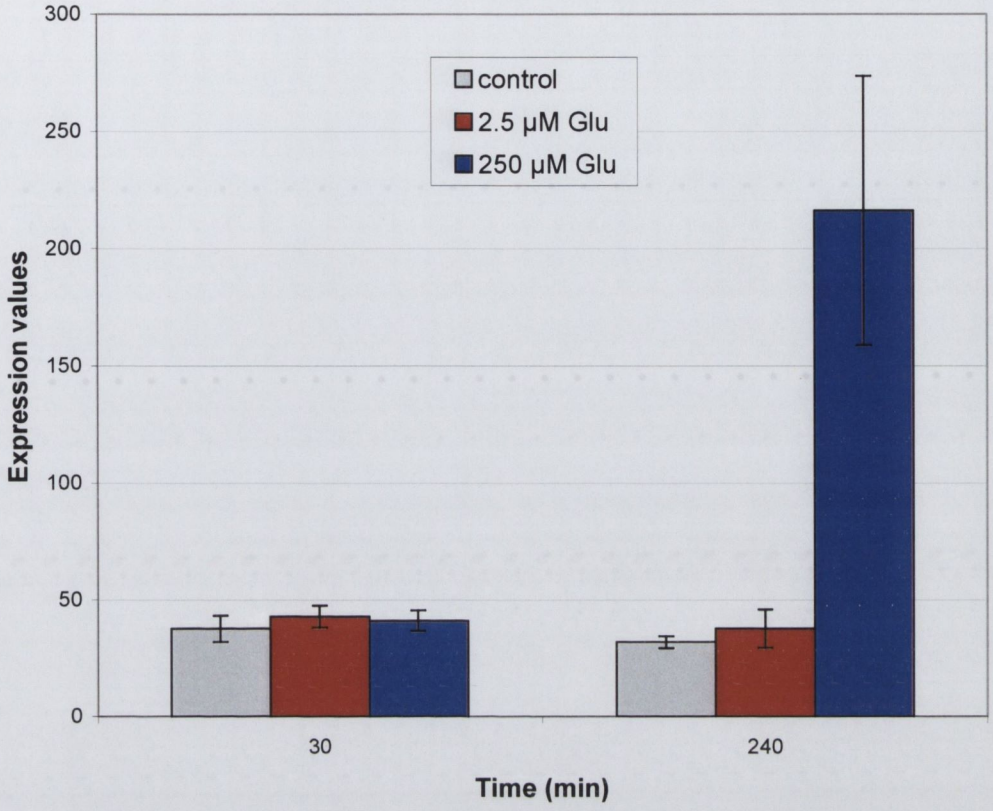


Figure 6.16: Different time-profiles of ATF3 expression dependent on Glu concentration

Primary cultures of rat cortical neurons (13 DIV) were exposed to a non-toxic (2.5 µM) or toxic (250 µM) concentration of Glu, for either 30 or 240 min. Following treatment, total RNA was extracted, converted to biotinylated cRNA and hybridised to separate rat RG_U34A arrays. The results above refer to the fluorescent levels of ATF3 expression compared to untreated, time-matched controls. The levels of fluorescent signal are representative of the relative abundance of ATF3 in the treated/untreated rat cortical neurons. Data represent mean ± variation from the mean of the ATF3 probe set (probe ID: M63282_at) from duplicate rat arrays (n = 2).

6.2.8 Search for genes with similar expression profiles to *c-fos*, *junB* and ATF3

Similarity searches were performed with each of the three genes against the complete set of 8799 genes, in parallel to the HRP and N-Fold regulation analysis. The quality setting p-value was set as 1, (to include all present ($p < 0.04$), marginally expressed genes ($0.04 < p < 0.06$) and low expressed genes with an absent call from Affymetrix MAS5 ($0.06 < p < 1$)), in order to identify genes that are absent in one or more of the groups and, for example, only present in response to the treatment. Profiles for *c-fos* and *junB* were very similar, and the highest positively correlated genes were selected. No negatively correlated genes were identified.

Two different probe sets for *c-fos* were present on the rat GeneChip® array. When both *c-fos* genes were compared to the profiles of the 8799 genes on the array, 21 genes were selected, respectively, that were similarly up-regulated across the different assay conditions. An illustration of the 21 genes, similar to one *c-fos* probe and selected from the 8799 genes is shown in Figure 6.17. The list of up-regulated genes for the two *c-fos* probe sets is shown in Tables 6.9 and 6.10, together with their respective correlation co-efficients. The up-regulated genes of both probe sets contained MAP kinase phosphatases, checkpoint genes, 11 *IEGs*, and transcription factors.

The 21 genes that positively correlated with the expression pattern of *junB* (probe ID rc_AA891041_at) are shown in Figure 6.18. The up-regulated genes included 12 *IEGs*, 4 checkpoint genes, 4 MAP kinase phosphatases and a non-categorised gene. The list of genes similar to *junB* is shown, together with their respective correlation co-efficients, in Table 6.11.

For ATF3, which was specifically up-regulated at 4 hours with toxic concentrations of Glu, 11 up-regulated and 10 down-regulated genes were selected (see Figure 6.19). The list of up- and down-regulated genes is shown in Table 6.12. The up-regulated genes consisted of 2 neurotransmitter proteins, 2 checkpoint genes, 2 transcription factors, a co-activator of gene expression, a plasmolipin, a MAP kinase phosphatase, and an apoptotic *IEG*. The 10 down-regulated genes contained 5 ESTs, a cannabinoid receptor, a transcription factor, a proteasome protein and a gene expression regulator.

It can be speculated that many of the genes identified by the similarity search above may be potential molecular biomarkers for *in vitro* excitotoxic cell death.

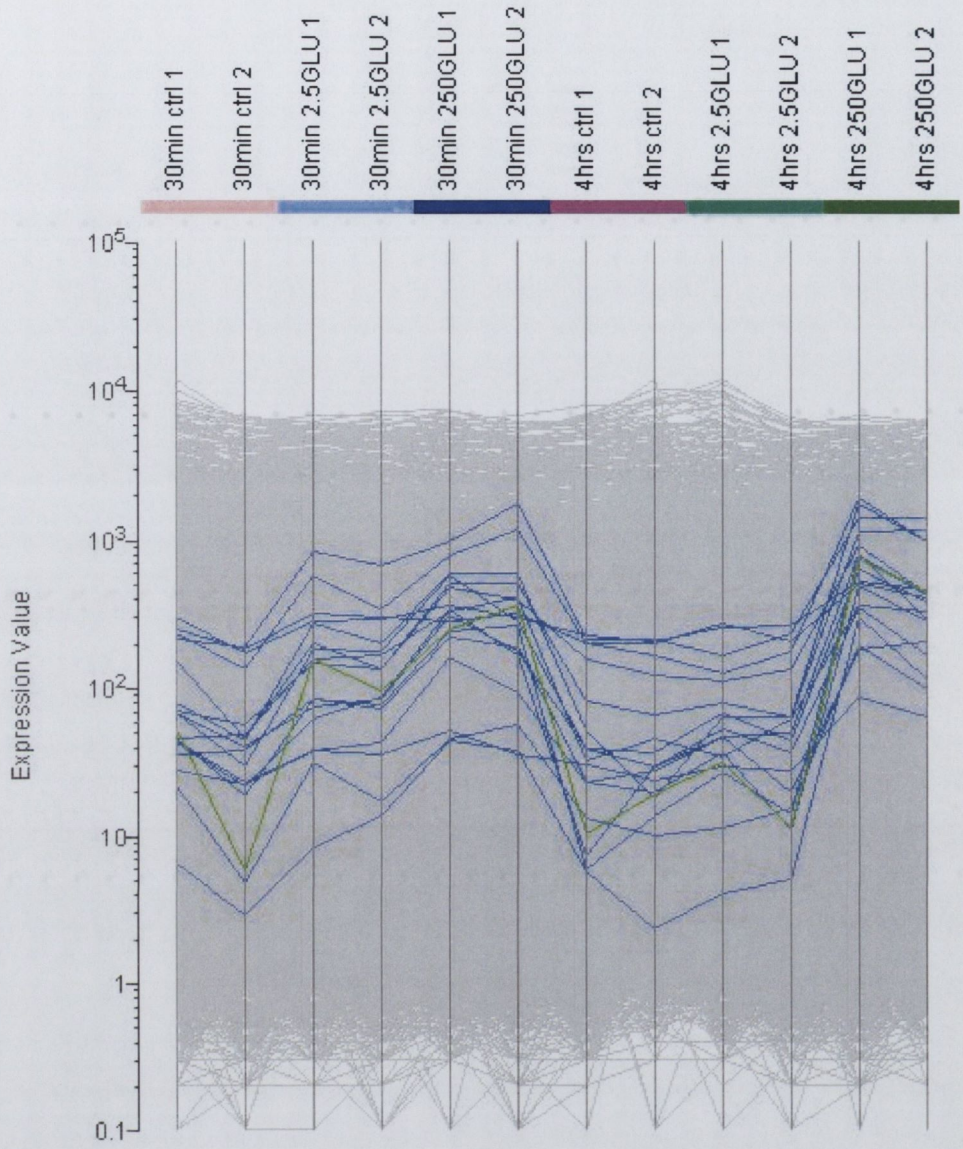


Figure 6.17: Several genes found from a total of 8799 hybridised probes that correlate with *c-fos*

A similarity search was performed with the *c-fos* probe sets (probe set ID: X06769cds_at and X06769cds_g_at), using correlation as a similarity measure, to identify genes similar to *c-fos* on the basis of their intensity of expression. The graph represents the expression values of all genes from the individual rat GeneChip® arrays (grey area), hybridised under different conditions of time and concentration. The green line represents *c-fos*. The blue lines represent genes whose expression patterns positively correlate with *c-fos*, across the different assay conditions.

Gene Symbol	Gene Description	Genbank Accession	Affymetrix ID.	Correlation Coefficient
	Immediate early genes			
egr1	Early growth response 1	M18416_at	M18416	0.9625
junB	jun B proto-oncogene	rc_AA891041_at	AA891041	0.9589
c-fos	FBJ murine osteosarcoma viral (v-fos) oncogene	X06769cds_g_at	X06769	0.9399
	Non-categorised protein			
Idi1	isopentenyl-diphosphate delta isomerase	AF003835_at	AF003835	0.9302
	Immediate early gene			
c-fos	FBR-murine osteosarcoma provirus genome	X03347cds_g_at	X03347	0.9292
	MAP Kinase phosphatase			
Ptpn16	protein tyrosine phosphatase, non-receptor 16	S81478_s_at	S81478	0.9256
	Immediate early genes			
egr1	Early growth response 1	AF023087_s_at	AF023087	0.9231
junb	jun B proto-oncogene	X54686cds_at	X54686	0.9198
Nr4a1	immediate early gene transcription factor NGFI-B	U17254_g_at	U17254	0.9093
krox 24	Rattus norvegicus Krox-24 mRNA	U75397UTR#1_s_at	U75397	0.9066
	Checkpoint gene			
Btg2	B-cell translocation gene 2	M60921_g_at	M60921	0.9051
	Immediate early genes			
Egr1	Early growth response 1	rc_AI176662_s_at	AI176662	0.8989
Nr4a1	immediate early gene transcription factor NGFI-B	U17254_at	U17254	0.8952
	Checkpoint gene			
Btg2	B-cell translocation gene 2	rc_AA944156_s_at	AA944156	0.8924
	MAP Kinase phosphatase			
Ptpn16	protein tyrosine phosphatas	S74351_s_at	S74351	0.8921
	Checkpoint gene			
Btg2	B-cell translocation gene 2	M60921_at	M60921	0.8796
	Immediate early genes			
Jun	Avian sarcoma virus 17 (v-jun) oncogene	rc_AA944014_at	AA944014	0.8663
Myd116	myeloid differentiation primary response gene 116	AF020618_at	AF020618	0.8596
	MAP Kinase phosphatase			
Ptpn16	protein tyrosine phosphatase, non-receptor 16	U02553cds_s_at	U02553	0.8546
	Transcription factor			
Nr2f2	nuclear receptor subfamily 2, group F, member 2	rc_AI012183_at	AI012183	0.8532
	Immediate early gene			
Jun	Avian sarcoma virus 17 (v-jun) oncogene	X17163cds_s_at	X17163	0.8486

Table 6.9: List of 21 genes that positively correlated with the profile of *c-fos* (X06769cds_at)

Gene Symbol	Gene Description	Genbank Accession	Affymetrix ID.	Correlation Coefficient
	Immediate early gene			
Egr1	Early growth response 1	AF023087_s_at	AF023087	0.9622
Nr4a1	immediate early gene transcription factor NGFI-B	U17254_g_at	U17254	0.9528
	MAP Kinase phosphatase			
Ptpn16	protein tyrosine phosphatase, non-receptor 16	S81478_s_at	S81478	0.9493
	Immediate early gene			
Krox 24	Rattus norvegicus Krox-24 mRNA	U75397UTR#1_s_at	U75397	0.9433
c-fos	FBR-murine osteosarcoma provirus genome	X03347cds_g_at	X03347	0.9426
c-fos	FBJ murine osteosarcoma viral (v-fos) oncogene	X06769cds_at	X06769	0.9399
	MAP Kinase phosphatase			
Ptpn16	protein tyrosine phosphatase, non-receptor 16	S74351_s_at	S74351	0.9382
	Immediate early gene			
Egr1	Early growth response 1	M18416_at	M18416	0.9349
Nr4a1	immediate early gene transcription factor NGFI-B	U17254_at	U17254	0.9292
junb	jun B proto-oncogene	rc_AA891041_at	AA891041	0.9273
	Checkpoint gene			
Btg2	B-cell translocation gene 2	rc_AA944156_s_at	AA944156	0.9247
	Immediate early gene			
junb	jun B proto-oncogene	X54686cds_at	X54686	0.9218
	EST			
EST	EST	rc_AA891054_at	AA891054	0.9151
	Anti-apoptotic protein			
Arc	activity regulated cytoskeletal-associated protein	U19866_at	U19866	0.8934
	GTP cyclohydrolase			
Gch	GTP cyclohydrolase 1	M58364_at	M58364	0.8891
	Immediate early gene			
c-jun	Avian sarcoma virus 17 (v-jun) oncogene homolog	rc_AA944014_at	AA944014	0.8880
	MAP Kinase phosphatase			
Ptpn16	protein tyrosine phosphatase, non-receptor 16	U02553cds_s_at	U02553	0.8845
Dusp6	dual specificity phosphatase 6	X94185cds_s_at	X94185	0.8783
	Non-categorised protein			
Idi1	isopentenyl-diphosphate delta isomerase	AF003835_at	AF003835	0.8694
Rph3al	rabphilin 3A-like (without C2 domains)	AF022774_at	AF022774	0.8641
	Regulator of gene expression			
Cited2	Cbp/p300-interacting transactivator	rc_AA900476_g_at	AA900476	0.8623

Table 6.10: List of genes that positively correlated with the profile of *c-fos* (X06769cds_g_at)

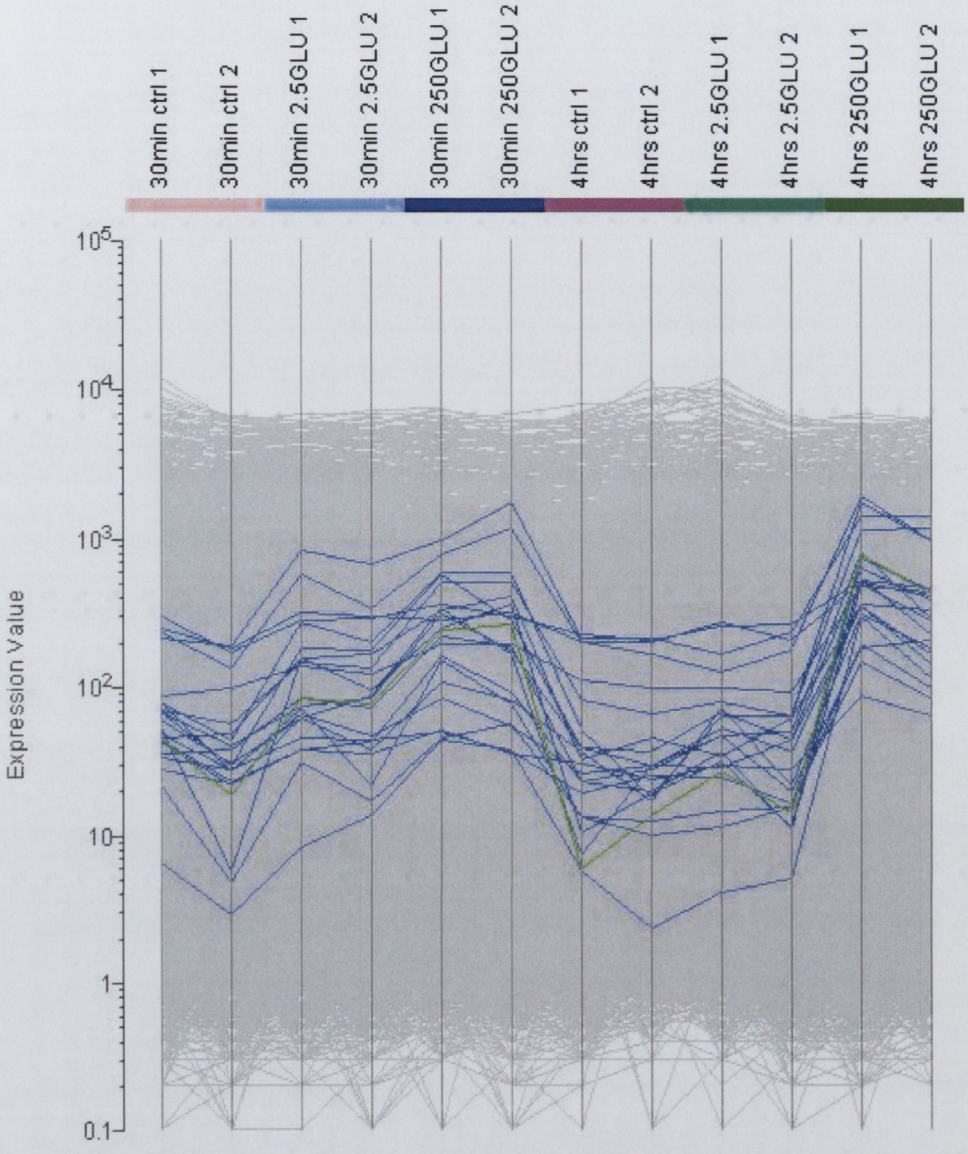


Figure 6.18: 21 genes, from a total of 8799 hybridised probes, positively correlate with *junB*

A similarity search was performed with the *junB* probe set (probe set ID: rc_AA891041_at), using correlation as a similarity measure, to identify genes similar to *junB* on the basis of their intensity of expression. The graph represents the expression values of all genes from the individual rat GeneChip® arrays (grey area), hybridised under different conditions of time and concentration. The green line represents *junB*. The blue lines represent the 21 genes whose expression patterns positively correlate with *junB*, across the different assay conditions.

Gene Symbol	Gene Description	Genbank Accession	Affymetrix ID.	Correlation Coefficient
	Immediate early genes			
c-fos	FBJ murine osteosarcoma viral (v-fos) oncogene	X06769cds_at	X06769	0.9589
junb	jun B proto-oncogene	X54686cds_at	X54686	0.9572
Egr1	Early growth response 1	M18416_at	M18416	0.9536
c-fos	FBR-murine osteosarcoma provirus genome	X03347cds_g_at	X03347	0.9476
Egr1	Early growth response 1	rc_AI176662_s_at	AI176662	0.9448
Nr4a1	immediate early gene transcription factor NGFI-B	U17254_at	U17254	0.9441
Nr4a1	immediate early gene transcription factor NGFI-B	U17254_g_at	U17254	0.9305
	Checkpoint gene			
Btg2	B-cell translocation gene 2	M60921_g_at	M60921	0.9297
	Immediate early genes			
krox 24	Rattus norvegicus Krox-24 mRNA	U75397UTR#1_s_at	U75397	0.9285
c-fos	FBJ murine osteosarcoma viral (v-fos) oncogene	X06769cds_g_at	X06769	0.9273
	MAP Kinase phosphatase			
Ptpn16	protein tyrosine phosphatase, non-receptor 16	S74351_s_at	S74351	0.9205
Ptpn16	protein tyrosine phosphatase, non-receptor 16	U02553cds_s_at	U02553	0.9121
	Immediate early genes			
Egr1	Early growth response 1	AF023087_s_at	AF023087	0.9106
	Non-categorised protein			
Idi1	isopentenyl-diphosphate delta isomerase	AF003835_at	AF003835	0.9093
	Checkpoint gene			
Myd116	myeloid differentiation primary response gene 116	AF020618_at	AF020618	0.9060
	MAP Kinase phosphatase			
Ptpn16	protein tyrosine phosphatase, non-receptor 16	S81478_s_at	S81478	0.8966
Dusp6	dual specificity phosphatase 6	X94185cds_s_at	X94185	0.8822
	Immediate early genes			
c-jun	Avian sarcoma virus 17 (v-jun) oncogene	X17163cds_s_at	X17163	0.8744
Arc	activity regulated cytoskeletal-associated protein	U19866_at	U19866	0.8712
c-jun	Avian sarcoma virus 17 (v-jun) oncogene	rc_AA944014_at	AA944014	0.8709
	Checkpoint gene			
Btg2	B-cell translocation gene 2	M60921_at	M60921	0.8656

Table 6.11: List of 21 genes that positively correlated with the profile of *junB* (rc_AA891041_at)

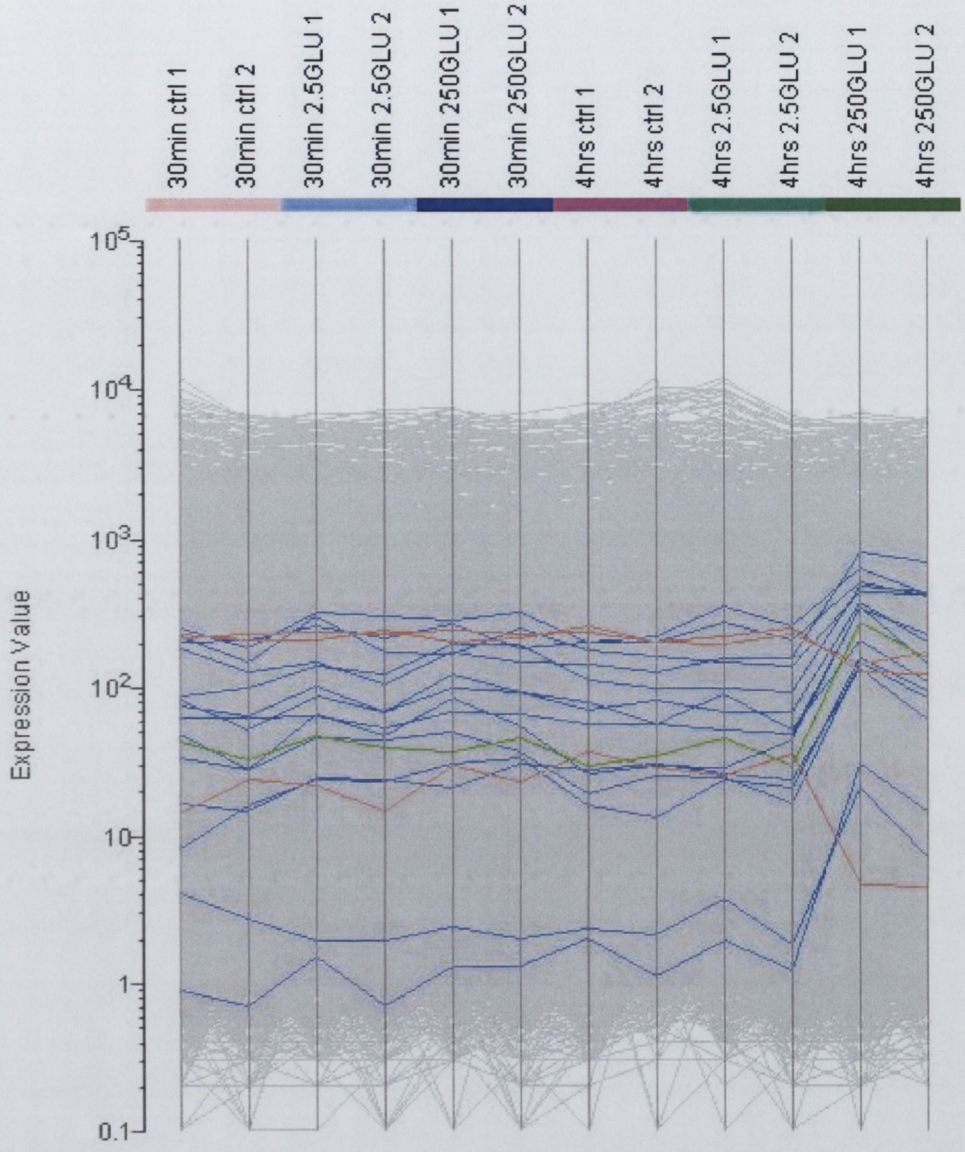


Figure 6.19: Several genes found from a total of 8799 that correlate with ATF3

A similarity search was performed with the ATF3 probe set (probe set ID: M63282_at), using correlation as a similarity measure, to identify genes similar to ATF3 on the basis of their intensity of expression. The graph represents the expression values of all genes from the individual rat GeneChip® arrays (grey area), hybridised under different conditions of time and concentration. The green line represents ATF3. The blue lines represent the 11 genes whose expression patterns positively correlate with ATF3, across the different assay conditions, while the red lines represent genes whose expression patterns are down-regulated.

Gene Symbol	Gene Description	Genbank Accession	Affymetrix ID.	Correlation Coefficient
	Neurotransmitter proteins			
Vgf	VGF nerve growth factor inducible	M74223_at	M74223	0.9534
	Transcription factor			
Crem	CAMP responsive element modulator	S66024_at	S66024	0.9401
	Neurotransmitter			
Scg2	Secretogranin II	M93669_at	M93669	0.9400
	Checkpoint protein			
Myd116	myeloid differentiation primary response gene	AF020618_g_at	AF020618	0.9317
	Co-activator of gene expression			
Cited2	Cbp/p300-interacting transactivator	rc_AA900476_g_at	AA900476	0.9249
	Plasmolipin			
Z49858	plasmolipin	Z49858_at	Z49858	0.9188
	Transcription factor			
Nr4a2	nuclear receptor subfamily 4, group A	L08595_at	L08595	0.8998
	MAP Kinase phosphatase			
Dusp6	dual specificity phosphatase 6	X94185cds_s_at	X94185	0.8966
	Apoptotic IEG			
Arc	activity regulated cytoskeletal-associated protein	U19866_at	U19866	0.8924
	Checkpoint gene			
Myd116	myeloid differentiation primary response gene	AF020618_at	AF020618	0.8923
	Cholesterol biosynthesis factor			
Idi1	isopentenyl-diphosphate delta isomerase	AF003835_at	AF003835	0.8884
	EST			
EST	ESTs	rc_AI639058_s_at	AI639058	-0.8837
EST	ESTs	rc_AA891476_at	AA891476	-0.8840
	Cannabinoid receptor			
Cnr1	Cannabinoid receptor 1	X55812complete_seq_at	X55812	-0.8861
	Transcription factor			
Foxm1	forkhead box M1	U83112_at	U83112	-0.8929
	Proteasome protein			
Psmc2	ATPase	D50694_at	D50694	-0.8976
	Gene expression regulator			
Hes5	hairy and enhancer of split 5 (Drosophila)	D12516_at	D12516	-0.8989
	EST			
EST	EST	rc_AA799481_at	AA799481	-0.8989

Table 6.12: List of genes that correlated with the expression profile of ATF3 (M63282_at)

Gene	Affymetrix probe ID	No. Positive Correlates	No. Negative Correlates	Total No.
junB	rc_AA891041_at	21	-	21
c-fos	X06769cds_at	21	-	21
c-fos	X06769cds_g_at	21	-	21
ATF3	M63282_at	11	10	21
union		35	10	45

Genes identified by HRP and > 2.5 - fold regulation	48
union	73

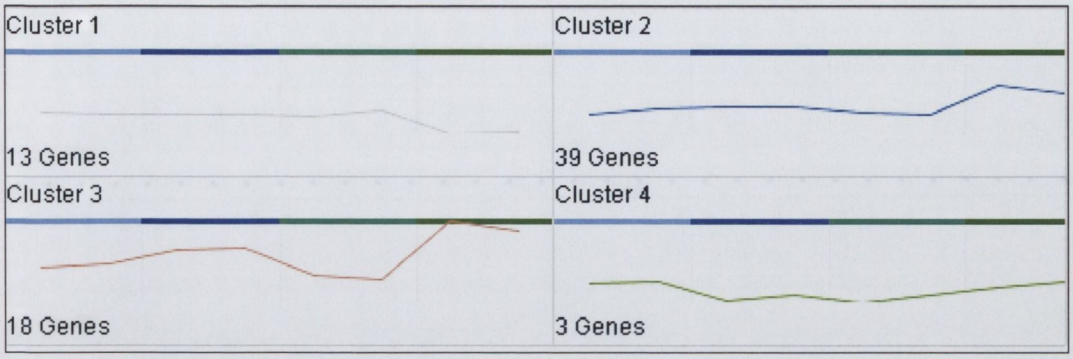
Table 6.13: Summary of deregulated genes

The Table above summarises the genes identified, using similarity analysis, which positively and/or negatively correlated with the expression profiles of *junB*, *c-fos* and ATF3 across the different assay conditions. All gene groups identified by the methods of N-fold regulation and similarity analysis were merged to generate a final list of 73 deregulated genes, which were further analysed by K-Means Clustering (Section 6.2.7).

6.2.9 K-Means cluster analysis of the 73 deregulated genes from the rat arrays

K-means clustering was used to systematically group related gene expression patterns together. A K-means clustered analysis was performed with the combined group of 73 genes from the union of all genes similarly up-regulated with *c-fos, junB* and ATF3, the genes which negatively correlated with ATF3 and the group of 49 genes ≥ 2.5 fold up/down-regulated (resulting from data filtration by HRP and N-fold regulation; see Figure 6.14). K-means clustering selected 4 separate gene clusters of which 1 was removed following visual inspection due to the very low induction values and also to the absence of variability in the profiles with time and concentration. The 3 clusters chosen represented 70 genes of the combined group of 73 genes. The clustered tile display consists of large contiguous patches of colour representing groups of genes that share similar expression patterns over multiple conditions. In addition, the tile display was used to observe how the clusters were sorted by their average expression values. Each colour patch in the resulting visual map represented the expression level of the associated gene in treated rat cortical neurons, with a continuum of expression levels from *bright green* (lowest expression values) to *bright red* (highest expression values).

A



B

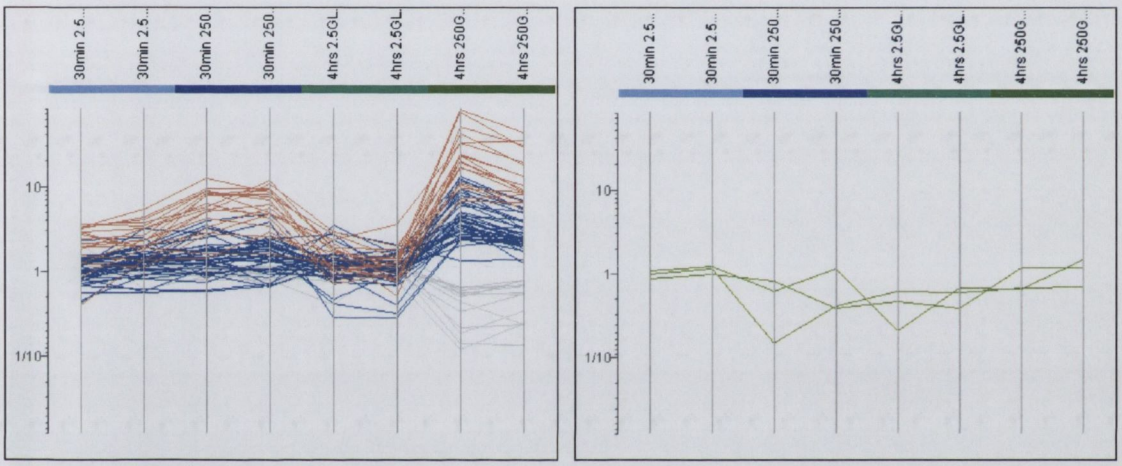


Figure 6.20: K-Means Clustering of 73 deregulated genes displayed as profile display

Cluster 1 (grey lines) represents a group of 13 genes, which were down-regulated following exposure of the rat cortical neurons to toxic concentrations of Glu (250 μM) for 4 hours. Cluster 2 (blue lines) represents a group of 39 genes that were only up-regulated following exposure to the toxic concentration of Glu (250 μM) for 4 hours. Cluster 3 (orange lines) represents a group of 18 genes which were transiently up-regulated at the 30 min time-point following exposure to a toxic concentration of Glu (250 μM) and again more strongly at 4 hours. No induction is found with the non-toxic concentration. Following K-Means Clustering, the genes representing Cluster 4 (green lines) were removed from the gene list to generate a final group of 70 genes.

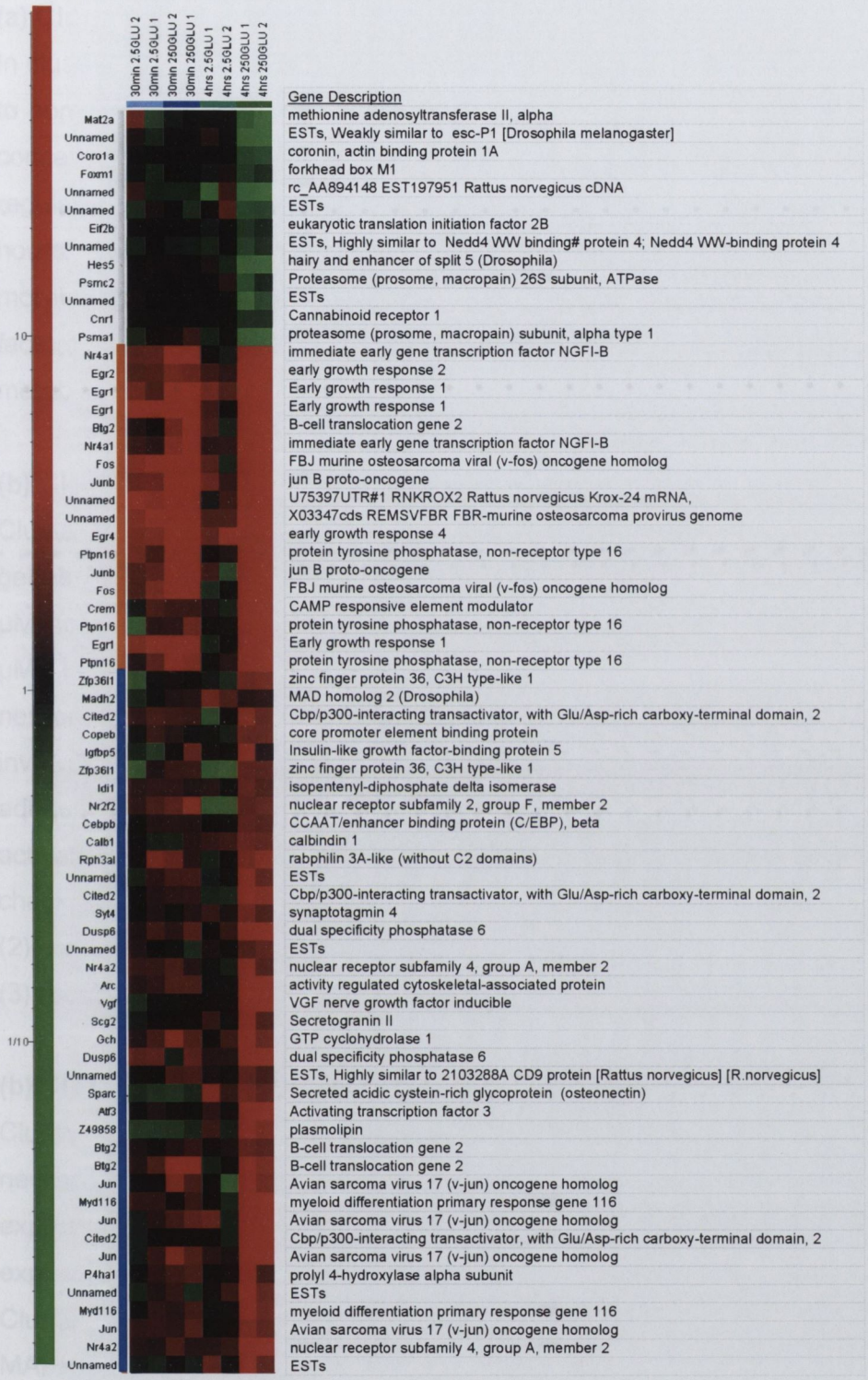


Figure 6.21: Clustered tile display of the group of 70 up- and down-regulated genes from cortical neurons, derived from clusters 1 - 3 (see Figure 6.20)

Each colour patch in the tile display represents the expression level of the associated gene in treated rat cortical neurons, with a continuum of expression levels from *bright green* (lowest) to *bright red* (highest). The colour map also indicates the several distinct clusters.

(a) Cluster 1

In cluster 1, the expression levels of all 13 genes remained unchanged following exposure to non-toxic concentrations of Glu (2.5 μM) for either 30 min or 4 hours and also to toxic concentrations of Glu (250 μM) for 30 min. However, the 13 genes were strongly down-regulated following exposure of the rat cortical neurons to toxic concentrations of Glu for 4 hours. Cluster 1 contained factors involved in amino acid metabolism (1), cell morphology/motility/regulation (1), the nervous system/GPCR pathway (1), transcription factors (1), co-repressors of gene expression (2), protein translation (1), lipoprotein metabolism (1), protein degradation (2) and several ESTs (2) (see Table 6.14).

(b) Cluster 2

Cluster 2 was the largest cluster representing 39 genes. The expression levels of the 39 genes remained unchanged following exposure to non-toxic concentrations of Glu (2.5 μM) for either 30 min or 240 min and also to toxic concentrations of Glu for 30 min (250 μM). However, the 39 genes were strongly up-regulated following treatment of the cortical neurons with toxic concentrations of Glu for 4 hours (240 min). Cluster 2 contained factors involved in cholesterol biosynthesis (1), vesicle transport (1), folic acid metabolism (1), cell adhesion/migration (1), post-translational modification (1), nervous system (1), co-activation of gene expression (3), a pro-apoptotic factor (1), an anti-apoptotic factor (1), checkpoint (4), neuronal signal transmission (3), transcription factors (6), MAPK pathway (2), oncogenes (4 representatives of *c-jun*), several ESTs (5) and miscellaneous agents (3) (see Tables 6.15 a), b) and c)).

(b) Cluster 3

Cluster 3 contained 18 genes with similar induction profiles. Exposure of the cortical neurons to toxic concentrations of Glu for 30 min or 4 hours induced a strong increase in expression of all 18 genes. In contrast, no change in expression was observed following exposure of the neurons to non-toxic concentrations of Glu for either 30 min or 4 hours. Cluster 3 contained proto-oncogenes (2), oncogenes (3), transcription factors *IEGs* (7), MAPK pathway phosphatases (3), a check-point gene (1) and pro-apoptotic *IEGs* (2) (see Table 6.16).

Gene symbol	Gene description	Genbank Accession	Affymetrix No.	Cluster No.	Ratio(treated v. cntl.) [30 min]		Ratio(treated v. cntl.) [240 min]		Ratio [240/30 min]		Excitotoxic Gene Induction Profile
					Glutamate [μM]						
					2.5	250	2.5	250	2.5	250	
	Amino acid metabolism										
Mat2a	methionine adenosyltransferase II, alpha	J05571	J05571_s_at	1	1.39	0.95	1.08	0.34	0.78	0.36	↓
	Cell morphology / motility | Regulation										
Coro1a	coronin, actin binding protein 1A	AA892506	rc_AA892506_at	1	1.05	0.96	1.02	0.54	0.98	0.57	↓
	Nervous system | GPCR pathway										
Cnr1	Cannabinoid receptor 1	X55812	X55812complete_seq_at	1	1.13	1.14	1.04	0.67	0.92	0.59	↓
	Transcription factor										
Foxm1	forkhead box M1	U83112	U83112_at	1	0.85	0.98	1.06	0.65	1.24	0.66	↓
	Corepressor of Gene expression										
Hes5	hairy and enhancer of split 5 (Drosophila)	D12516	D12516_at	1	1.13	1.16	1.01	0.18	0.89	0.16	↓
EST	Weakly similar to esc-P1 [Drosophila melanogaster]	AA799481	rc_AA799481_at	1	1.00	1.14	1.21	0.23	1.20	0.20	↓
	Protein Translation										
Eif2b	eukaryotic translation initiation factor 2B	Z48225	Z48225_at	1	1.03	1.06	0.96	0.71	0.93	0.67	↓
	Lipoprotein metabolism										
EST	rc_AA894148 EST197951 Rattus norvegicus cDNA	AA894148	rc_AA894148_s_at	1	1.14	0.79	0.98	0.26	0.85	0.33	↓
	Protein Degradation										
EST	Highly similar to Nedd4 binding protein 4;	AI639058	rc_AI639058_s_at	1	0.92	0.85	0.94	0.61	1.02	0.72	↓
Psmc2	Proteasome 26S subunit, ATPase	D50694	D50694_at	1	0.95	1.00	1.17	0.64	1.23	0.64	↓
Psma1	Proteasome subunit, alpha type 1	AI009111	rc_AI009111_at	1	0.95	1.38	0.93	0.14	0.98	0.10	↓
EST	**EST**										
EST	EST	AA892500	rc_AA892500_at	1	0.94	0.89	1.53	0.54	1.62	0.61	↓
EST	EST	AA891476	rc_AA891476_at	1	1.13	1.01	1.03	0.44	0.91	0.43	↓

Table 6.14: Cluster 1 contains 13 genes with similar expression profiles in rat cortical neurons

Gene symbol	Gene description	Genbank Accession	Affymetrix No.	Cluster No.	Ratio(treated v. cntl.) [30 min]		Ratio(treated v. cntl.) [240 min]		Ratio [240/30 min]		Excitotoxic Gene Induction Profile
					Glutamate [μM]						
					2.5	250	2.5	250	2.5	250	
	Cholesterol biosynthesis										
Idi1	isopentenyl-diphosphate delta isomerase	AF003835	AF003835_at	2	1.43	1.37	1.18	2.29	0.83	1.66	↑
	Vesicle transport										
Rph3al	rabphilin 3A-like (without C2 domains)	AF022774	AF022774_at	2	2.19	2.08	0.97	3.24	0.44	1.55	↑
	Folic Acid Metabolism										
Gch	GTP cyclohydrolase 1	M58364	M58364_at	2	1.60	2.85	1.39	3.57	0.87	1.25	↑
	Cell adhesion / migration										
Sparc	Secreted acidic cystein-rich glycoprotein	AA891204	rc_AA891204_s_at	2	0.65	0.63	2.55	2.65	3.95	4.18	↑
	Posttranslational modification										
P4ha1	prolyl 4-hydroxylase alpha subunit	X78949	X78949_at	2	1.18	1.88	1.16	2.81	0.99	1.49	↑
	Nervous system | Kidney-specific										
Z49858	plasmolipin	Z49858	Z49858_at	2	0.57	0.66	1.25	6.30	2.20	9.59	↑
	Coactivator of Gene Expression										
Cited2	Cbp/p300-interacting transactivator	AI014091	rc_AI014091_at	2	1.67	1.67	0.74	2.93	0.44	1.75	↑
Cited2	Cbp/p300-interacting transactivator	AA900476	rc_AA900476_g_at	2	1.17	1.44	0.73	4.18	0.62	2.90	↑
Cited2	Cbp/p300-interacting transactivator	AA900476	rc_AA900476_at	2	0.96	1.07	0.94	10.00	0.98	9.37	↑
	Pro-apoptotic factor										
Zfp36l1	zinc finger protein 36, C3H type-like 1	AI136891	rc_AI136891_at	2	0.86	1.67	0.37	2.36	0.43	1.42	↑

Table 6.15 a): Cluster 2 contains 39 genes with up-regulated expression profiles

Normalised expression values of the 24 genes of Cluster 2 and their respective 240/30 min ratios. The ↑ represents genes which were up-regulated under excitotoxic conditions (250 μM Glu for 4 hours) and ← represent genes whose expression values were ≤ 2.

Gene symbol	Gene description	Genbank Accession	Affymetrix No.	Cluster No.	Ratio(treated v. cntl.) [30 min]		Ratio(treated v. cntl.) [240 min]		Ratio [240/30 min]		Excitotoxic Gene Induction Profile
					Glutamate [μM]						
					2.5	250	2.5	250	2.5	250	
	Anti-apoptotic factor										
Arc	activity regulated cytoskeletal-associated protein	U19866	U19866_at	2	1.39	2.09	0.91	4.34	0.65	2.07	↑
	Checkpoint										
Btg2	B-cell translocation gene 2	M60921	M60921_at	2	1.21	1.39	1.21	2.30	1.00	1.66	↑
Btg2	B-cell translocation gene 2	AA944156	rc_AA944156_s_at	2	1.67	4.40	0.88	4.85	0.53	1.10	↑
Myd116	myeloid differentiation primary response gene	AF020618	AF020618_at	2	1.47	1.41	0.91	5.23	0.62	3.72	↑
Myd116	myeloid differentiation primary response gene	AF020618	AF020618_g_at	2	1.24	1.57	0.89	3.76	0.72	2.40	↑
	Neuronal signal transmission										
Vgf	VGF nerve growth factor inducible	M74223	M74223_at	2	0.81	1.01	1.16	5.57	1.44	5.49	↑
Scg2	Secretogranin II	M93669	M93669_at	2	0.95	1.09	1.25	2.78	1.31	2.56	↑
Syt4	synaptotagmin 4	U14398	U14398_at	2	1.17	1.11	1.43	2.49	1.22	2.25	↑
	Transcription factors										
Copeb	core promoter element binding protein	AF001417	AF001417_s_at	2	1.27	1.14	0.86	2.55	0.67	2.24	↑
Cebpb	CCAAT/enhancer binding protein (C/EBP), beta	X60769	X60769mRNA_at	2	1.18	1.34	1.03	2.28	0.87	1.71	↑
Atf3	Activating transcription factor 3	M63282	M63282_at	2	1.14	1.09	1.18	6.76	1.04	6.19	↑
Nr4a2	nuclear receptor subfamily 4, group A, member 2	L08595	L08595_at	2	1.59	1.68	0.85	3.31	0.53	1.98	↑
Nr4a2	nuclear receptor subfamily 4, group A, member 2	U01146	U01146_s_at	2	1.29	1.63	1.46	5.67	1.13	3.47	↑
Nr2f2	nuclear receptor subfamily 2, group F, member 2	AI012183	rc_AI012183_at	2	1.72	3.13	0.29	2.40	0.17	0.77	↑

Table 6.15 b): Cluster 2 contains 39 genes with up-regulated expression profiles

Normalised expression values of the 24 genes of Cluster 2 and their respective 240/30 min ratios. The ↑ represents genes which were up-regulated under excitotoxic conditions (250 μM Glu for 4 hours) and ← represent genes whose expression values were ≤ 2.

Gene symbol	Gene description	Genbank Accession	Affymetrix No.	Cluster No.	Ratio(treated v. cntl.) [30 min]		Ratio(treated v. cntl.) [240 min]		Ratio [240/30 min]		Excitotoxic Gene Induction Profile
					Glutamate [μM]						
					2.5	250	2.5	250	2.5	250	
	MAPK pathway										
Dusp6	dual specificity phosphatase 6	X94185	X94185cds_s_at	2	1.49	1.83	1.29	8.80	0.87	4.80	↑
Dusp6	dual specificity phosphatase 6	U42627	U42627_at	2	2.41	1.61	1.33	7.56	0.55	4.68	↑
	Oncogenes										
c-jun	Avian sarcoma virus 17 (v-jun) homolog	AA945867	rc_AA945867_at	2	1.05	2.59	0.71	3.59	0.67	1.39	↑
c-jun	Avian sarcoma virus 17 (v-jun) homolog	X17163	X17163cds_s_at	2	1.10	2.13	1.78	9.21	1.62	4.32	↑
c-jun	Avian sarcoma virus 17 (v-jun) homolog	AI175959	rc_AI175959_at	2	1.21	2.73	1.31	6.80	1.09	2.49	↑
c-jun	Avian sarcoma virus 17 (v-jun) homolog	AA944014	rc_AA944014_at	2	1.47	1.74	1.05	2.79	0.72	1.61	↑
	ESTs										
EST	EST	AA891054	rc_AA891054_at	2	1.08	1.81	0.87	3.15	0.81	1.74	↑
EST	EST	AA799448	rc_AA799448_g_at	2	1.14	0.79	1.17	2.22	1.02	2.82	↑
EST	EST	X76489	X76489cds_g_at	2	1.05	1.86	1.10	2.09	1.05	1.12	↑
EST	EST	AA800572	rc_AA800572_at	2	1.02	1.13	1.41	3.26	1.38	2.88	↑
EST	EST	AA800701	rc_AA800701_at	2	0.83	0.92	1.70	2.92	2.04	3.19	↑
	Miscellaneous										
Madh2	MAD homolog 2 (Drosophila)	AI228675	rc_AI228675_at	2	0.81	1.34	2.51	1.36	3.09	1.02	←
Igfbp5	Insulin-like growth factor-binding protein 5	AI029920	rc_AI029920_s_at	2	0.70	1.88	1.13	2.42	1.62	1.29	↑
Calb1	calbindin 1	AI102839	rc_AI102839_at	2	0.98	1.05	1.66	2.61	1.69	2.50	↑

Table 6.15 c): Cluster 2 contains 39 genes with up-regulated expression profiles in rat cortical neurons

Normalised expression values of the 24 genes of Cluster 2 and their respective 240/30 min ratios. The ↑ represents genes which were up-regulated under excitotoxic conditions (250 μM Glu for 4 hours) and ← represent genes whose expression values were ≤ 2.

Gene symbol	Gene description	Genbank Accession	Affymetrix No.	Cluster No.	Ratio(treated v. cntl.) [30 min]		Ratio(treated v. cntl.) [240 min]		Ratio [240/30 min]		Excitotoxic Gene Induction Profile
					Glutamate [μM]						
					2.5	250	2.5	250	2.5	250	
	Proto-oncogenes										
junb	jun B proto-oncogene	AA891041	rc_AA891041_at	3	2.56	8.02	2.09	62.09	0.82	7.74	↑
junb	jun B proto-oncogene	X54686	X54686cds_at	3	2.14	5.60	1.10	18.30	0.52	3.26	↑
	Oncogene										
c-fos	FBJ murine osteosarcoma viral (v-fos) oncogene homolog	X06769	X06769cds_at	3	4.37	10.57	1.44	40.68	0.33	3.85	↑
c-fos	X03347cds REMSVFBR FBR-murine osteosarcoma provirus genome	X03347	X03347cds_g_at	3	3.75	9.55	1.85	33.57	0.49	3.51	↑
c-fos	FBJ murine osteosarcoma viral (v-fos) oncogene homolog	X06769	X06769cds_g_at	3	2.51	5.30	0.83	8.00	0.33	1.51	↑
	Transcription factor (*IEGs*)										
Egr1	Early growth response 1	AI176662	rc_AI176662_s_at	3	2.32	7.86	2.45	14.12	1.06	1.80	↑
Egr1	Early growth response 1	M18416	M18416_at	3	3.69	8.80	1.46	13.41	0.39	1.52	↑
Egr4	early growth response 4	M92433	M92433exon#1-2_s_at	3	3.03	5.08	3.02	25.78	1.00	5.08	↑
Crem	CAMP responsive element modulator	S66024	S66024_at	3	1.38	1.63	1.00	14.48	0.73	8.91	↑
Egr1	Early growth response 1	AF023087	AF023087_s_at	3	3.69	6.80	0.94	6.57	0.26	0.97	↑
Krox24	Rattus norvegicus Krox-24 mRNA	U75397	U75397UTR#1_s_at	3	3.49	7.91	1.25	8.99	0.36	1.14	↑
Egr2	early growth response 2	U78102	U78102_at	3	1.98	2.68	1.55	8.78	0.78	3.28	↑
	MAPK pathway										
Ptpn16	protein tyrosine phosphatase, non-receptor type 16	S74351	S74351_s_at	3	2.32	8.65	1.13	51.48	0.49	5.95	↑
Ptpn16	protein tyrosine phosphatase, non-receptor type 16	U02553	U02553cds_s_at	3	0.89	2.16	1.16	30.00	1.30	13.89	↑
Ptpn16	protein tyrosine phosphatase, non-receptor type 16	S81478	S81478_s_at	3	1.83	3.86	1.16	12.69	0.63	3.29	↑
	Checkpoint										
Btg2	B-cell translocation gene 2	M60921	M60921_g_at	3	1.19	3.75	1.32	7.61	1.11	2.03	↑
	Proapoptotic IEG										
Nr4a1	immediate early gene transcription factor NGFI-B	U17254	U17254_at	3	1.46	4.44	1.40	15.87	0.96	3.58	↑
Nr4a1	immediate early gene transcription factor NGFI-B	U17254	U17254_g_at	3	2.20	7.92	0.96	18.41	0.43	2.32	↑

Table 6.16: Cluster 3 contains 13 genes with up-regulated expression profiles

6.3 Discussion

Micro-array based genomic surveys and other high-throughput approaches are becoming increasingly important in biology and chemistry. Toxicogenomics is the application of genomics to toxicology. The fundamental assumption of toxicogenomics is that there are no toxicologically relevant outcomes *in vitro* or *in vivo* that do not require differential gene expression. Differential gene expression includes differential transcription and translation, as well as message stabilisation. It also encompasses both up- and down-regulation of genes. Toxicologically relevant outcomes include all traditional endpoints, defined as quantifiable alterations in the structure and/or function of a cellular or organ level, normally considered of importance in the analysis of the adverse effects caused by chemicals, both *in vitro* and *in vivo*. The more prevalent toxicological endpoints measured include: liver weight change, endocrine levels, neuronal degeneration, lung fibrosis, vascular hypotension and hypertension, heart excitability etc. The goals of toxicogenomics are to facilitate better understanding of mechanisms of toxicity and to identify gene expression patterns that may indicate a deleterious outcome. If toxicity manifested at the organismal level is preceded by altered expression of related genes, then detection of altered gene expression can serve as a potential biomarker for subsequent deleterious outcomes and also serve as a valuable tool in the discovery of therapeutic targets and diagnostic markers. Micro-arrays may also provide insight into associations between genes in various signalling cascades. Gene expression is a multi-step process that results in an active protein. Genomics, by definition, encompasses the quantitative analysis of transcripts at the mRNA level. Expression data at the mRNA level can be produced using a set of different technologies such as real-time RT-PCR, serial analysis of gene expression (SAGE), Northern blots and DNA micro-arrays. Currently, DNA micro-arrays are very popular and promise a great potential. In this Chapter, Affymetrix GeneChip® oligonucleotide arrays were used, where each gene of interest was represented by several short oligonucleotides (20 - 30 bases) synthesized directly onto a solid support using photolithographic nucleotide chemistry (Fodor *et al.*, 1991; Chee *et al.*, 1996) making it possible to monitor, simultaneously, the expression patterns of thousands of genes.

Excitoxicity is defined as an excessive activation of the ionotropic Glu receptor, in particular the NMDA receptor subtype (Olney, 1969). In the preceding Chapters, and in accordance with published reports (Griffiths *et al.,* 1998, 2000) it was found, using real-

time RT-PCR, that a strong correlation exists between excitotoxic cell death and the appearance of a delayed, elevated and sustained increase in *c-fos* mRNA levels. In addition, it was found in Chapters 4 and 5 that another member of the *fos* family of *IEGs*, *fosB*, was involved in excitotoxicity and that its profile of expression under excitotoxic conditions differed in mCGCs and rat cortical neurons. Therefore, *c-fos* and *fosB* can be regarded as "excitotoxic" genes, that is, genes whose messages or protein levels are altered by over-stimulation and whose EAA-specific responses are NMDA receptor-mediated.

The aim of this Chapter was to use Affymetrix GeneChip® technology to investigate the differential expression of *c-fos* and *fosB* and furthermore to uncover other candidate genes relevant in the process of excitotoxicity. Mouse cerebellar granule cells and rat cortical neurons were treated with either a non-toxic or toxic concentration of Glu for either 30 or 240 min before being hybridised to their respective mouse or rat GeneChip® arrays. It should be noted here that the rat GeneChip® array did not contain oligonucleotides for *fosB* and so an investigation into the expression profile of this gene could only be performed with the mouse GeneChip® array. Exposure of mCGCs and rat cortical neurons to toxic concentrations of Glu for 240 min represented the excitotoxic condition. By comparison of the relative RNA levels obtained from stimulated cells with those derived from a time-matched control sample, it was possible to identify a collection of genes responding directly or indirectly to the stimulation by an increase or decrease in transcript levels. The main challenge was to make sense of such large collections of data sets.

In this Chapter, the data was first filtered by High Ratio Proportions (HRP) and genes, which were more than 1.8 fold up- or down-regulated, were selected. Next, the data was subjected to a second selection, also using N-fold regulation, and genes where the ratio of means was more than 2.5 fold up- or down-regulated were selected. The next challenge was to extract the fundamental patterns of gene expression inherent in the data. A search of all genes present on the arrays for similarity with *c-fos*, *fosB/junB* and ATF3 grouped genes on the basis of similarities in the up and/or down expression profiles. The union of all genes similarly up-regulated more than 2.5 fold with *c-fos, fosB/junB* and ATF3 and the union of all genes similarly down-regulated more than 2.5 fold (54 genes in total for the mouse; 45 genes in total for the rat) were merged with the group of genes ≥ 2.5 fold up/down-regulated (selected by HRP and N fold regulation) forming a group of 95 (in the case of the mouse) and 73 (in the case of the rat) deregulated genes. The mean

expression values of the genes from duplicate experiments were calculated and normalised to their respective time-matched controls. These groups were then categorised by K-means clustering into groups (clusters) representative of their distinct expression patterns.

Following normalisation, the data was applied to a ratio test derived by Griffiths *et al.* (1998) which was used to predict an excitotoxic outcome, and which was based on the observation that a toxic concentration of Glu induced increased *c-fos* mRNA expression in mCGCs at 240 min but not at the 30 min time-point. This ratio test proposed that a *c-fos* mRNA 240/30 min ratio of greater than 1 correlated with excitotoxicity, whereas a ratio of less than 1 correlated with a non-excitotoxic outcome. However, it was shown in Chapters 4 and 5 that *fosB* can also be used as an additional and specific biomarker for excitotoxicity, and indeed in this Chapter, ATF3 was shown as being induced exclusively under excitotoxic conditions. In light of these results, and on account of the ability of micro-arrays to measure the expression of thousands of genes simultaneously and in so doing uncover many potential markers for excitotoxicity, the ratio test was altered so that genes whose 240/30 min ratio was greater than 1 were potential biomarkers for excitotoxicity, while ratios of less than 1 indicated non-involvement and/or down-regulation of the genes in excitotoxicity. Thus, 240/30 min ratios of the genes belonging to all three clusters were calculated to investigate the variation in expression of other genes, in addition to *c-fos* and *fosB*, in excitotoxicity.

6.3.1 Selected genes from Mouse GeneChip® arrays

The selected genes from the mouse GeneChip® arrays were organised into three clusters. Cluster 1 was the largest cluster. The expression levels of the 46 different members remained unchanged following exposure of mCGCs to non-toxic concentrations of Glu for either 30 or 240 min and also to toxic concentrations of Glu for 30 min. However, the 46 genes were all up-regulated under excitotoxic conditions, that is, exposure to 250 μM of Glu for 240 min. Thus, all 46 up-regulated genes can be regarded as potential biomarkers for excitotoxicity. The expression of any gene in this cluster was considered significant if the expression value was ≥ 2 fold under excitotoxic conditions. Cluster 1 contained the following groups: kinases/phosphatases (3), growth factors (2), proteins (6), an oncogene (1), DNA binding factors (3), cell adhesion factors (4), a proteolytic protein (1), cell differentiation proteins (2), *IEGs* (2), several ESTs (3), proteins involved in cell-cell communication (2), glycolytic factors (2), integral membrane proteins

(7) and non-categorised proteins (9). As nothing is known of the function or regulation of the ESTs but that they are strongly up-regulated under excitotoxic conditions, they were considered as signatory for this outcome. The most inherent members of cluster 1 to excitotoxicity were the *IEGs*, *Egr1* and *Egr2,* and the transcription factors, ATF4 and Nr4a2.

Egr-1 (Krox-24, NGFI-A) and *Egr-2* (*Krox-20*) are cellular *IEGs* which encode inducible transcription factors and whose induction and cessation of expression are controlled by pre-existing transcription factors. Both Egr-1 (Krox-24) and Egr-2 (Krox-20) transcription factors have three zinc finger domains for sequence specific DNA binding. Neuronal activation via all Glu receptor subtypes can increase *Egr-1* mRNA expression through activation of the NMDA subtype of Glu receptor (Vaccarino *et al.*, 1992). *Egr-2* cannot be induced in PC12 cells (Joseph *et al.*, 1988) or by cAMP in general (Mechta *et al.*, 1989) and this may account for the lower induction values of *Egr-2.* A slight increase in the fold induction of ATF4 was observed under excitotoxic conditions. Nr4a2 showed the largest increase in induction under excitotoxic conditions. *Egr-1 (Krox-24, NGFI-A*), *Egr-2* (*Krox-20*), ATF4 and Nr4a2 all gave elevated 240/30 min ratios under excitotoxic conditions suggesting the interaction of all 4 in the process of excitotoxic cell death. 240/30 min mRNA ratios for the non-excitotoxic condition were around 1 (see Tables 6.6 a), b) and c)).

The 24 genes of cluster 2 showed a relatively steady expression level across the non-toxic conditions, except for sharing a similar pattern of down-regulation following exposure of mCGCs to toxic concentrations of Glu for 240 min. This cluster contained a DNA binding protein (1), an inhibitory amino acid transporter (1), a proteinase (1), a cyclin-dependent protein kinase regulator (1), neurotransmitter proteins (2), a proteasome protein (1), non-categorised proteins (7) and several ESTs (10). As this cluster did not show significant enrichment for function it is probable that the members of this cluster participate in multiple classically defined processes and therefore did not show significant enrichment in any one functional category. All of the 24 members of Cluster 2 had 240/30 min mRNA ratios of less than 1 indicating their down-regulation in excitotoxicity. 240/30 min mRNA ratios for the non-excitotoxic condition were around 1 (see Tables 6.7 a) and b)).

Cluster 3 represented 6 genes, that is, the transcription factors ATF3 (represented twice on the micro-array) and Nr4a1 (represented twice on the micro-array) and the oncogenes *c-fos* and *fosB*. The cluster profile showed that, like RT-PCR, exposure of the mCGCs to

non-toxic concentrations of Glu for 30 min induced a slight transient increase in the induction of *c-fos* mRNA, which had declined to the basal rate by 240 min. Following exposure of the mCGCs to toxic concentrations of Glu, maximal levels of *c-fos* mRNA were increased and the persistence of *c-fos* mRNA within the cell was prolonged. These observations, and the examination of the normalised *c-fos* expression levels over the various experimental conditions, revealed that *c-fos* was induced in a time-and concentration-dependent manner. In addition, its profiles of expression, found using GeneChip® micro-array technology, were in accordance with the profiles found using real-time RT-PCR (see Chapter 4) and also the method of Northern blot analysis (Gorman *et al.*, 1995; Griffiths *et al.*, 1997, 1998; 2000). In conclusion, *c-fos* can be regarded as an essential component in the process of excitoxicity.

The second member of the *fos* family of *IEGs*, *fosB*, also exhibited differential expression depending on time and Glu concentration. A 30 min exposure to non-toxic concentrations of Glu induced a transient increase in *fosB* expression. In contrast, toxic concentrations of Glu induced the excitotoxic profile of delayed and elevated mRNA expression. The time and concentration-dependent profiles of *fosB* induction found using GeneChip® micro-arrays thus confirm the RT-PCR findings of Chapter 4. However, although there was only a slight difference in the levels of *fosB* and *c-fos* induction under excitotoxic conditions (a factor of 1) using the micro-arrays, *fosB* expression levels were approximately 3 fold higher than *c-fos* when real-time RT-PCR was used. In summary, *fosB* can be regarded as an additional and sensitive biomarker for excitotoxicity.

The transcription factor ATF3 showed no significant induction following exposure to non-toxic concentrations of Glu for 30 min or 240 min or following exposure to toxic concentrations of Glu for 30 min. However, both representatives were strongly induced under excitotoxic conditions. ATF3 is a constitutive transcription factor whose proteins are present in quiescent or unstimulated cells bound to DNA regulatory sites, as well as in the nervous system, during the absence of any external stimulus (Herdegen & Leah, 1998). Transcription factors are proteins that control the expression of genes and as such they are the master regulators of every cell's development and function. Therefore, NMDA receptor activation of ATF3 stimulates its association with other *IEG*-encoded proteins to induce as–yet unidentified target genes important in excitotoxicity. Nr4a1, also a transcription factor, showed the same expression profiles as the oncogenes, *c-fos* and *fosB*. A 30 min exposure to non-toxic concentrations of Glu induced a slight, transient increase in Nr4a1 expression, but which had a higher induction value than both *c-fos* and

fosB. Toxic concentrations of Glu induced the excitotoxic profile of delayed and elevated expression. The level of induction of Nr4a1 under excitotoxic conditions was higher than both *c-fos* and *fosB* by a factor of 3. ATF3, *c-fos*, *fosB* and Nr4a1 all exhibited elevated 240/30 min ratios under excitotoxic conditions, indicating the up-regulation of all 4 in excitotoxicity. However, as the Nr4a1 ratio (approx. 11) was much higher than those of ATF3, *c-fos* and *fosB,* a more prominent role in excitotoxicity for this transcription factor is suggested. 240/30 min mRNA ratios for the non-excitotoxic condition were only above 1 in the case of ATF3 due to the lack of induction at the 30 min time-point (see Table 6.8).

From the cluster analysis, it can be assumed that the up-regulated members of Cluster 3 (*c-fos, fosB*, ATF3 and Nr4a1) may interact with those of Cluster 2 (*Egr-1, Egr-2,* ATF4 and Nr4a2) to regulate the genetic response to overactivation of NMDA receptors in the process of excitotoxicity. The *IEGs c-fos*, *fosB*, *Egr-1* and *Egr-2* are the first gene targets activated by the diverse intracellular messenger systems linking NMDA receptor activation and the nucleus. These genes are defined by rapid and often transient transcriptional induction, independent of *de novo* synthesis. The *IEG* encoded inducible transcription factors thus act as third messengers coupling neurotransmission to altered gene expression (Curran, 1989).

Indeed, the best-characterised *IEG*-encoded transcription factors are AP-1 and Egr. AP-1 is composed of the products of the *fos* (*c-fos, fosB, fra-1* and *fra-2*) and *jun* (*c-jun, junB* and *junD*) proto-oncogene families and also the ATF family. These Fos (c-Fos, FosB, Fra-1 and Fra-2) and Jun (c-Jun, JunB and JunD) proteins have to dimerise in order to be capable of binding to the AP-1 recognition site, also known as the TPA-responsive element (TRE; Angel and Karin, 1990). *Egr-1* (cluster 2) is the prototypical member of a family of related genes including *Egr-2* (*Krox-20*), *Egr3* and *Egr4 (NGFI-C)*. The regulatory DNA elements to which members of the Egr family bind are called Krox response elements (KRE). The members of the AP-1 and Egr transcription factor families possess different structural properties and hence are subject to different regulatory mechanisms. They also each recognise a discrete binding motif. Therefore, AP-1 and Egr transcription factors provide different "gateways" to discrete programs of late response gene expression. Each inducible transcription factor can be individually regulated in different brain regions and after different stimulations. Thus, the co-ordinated inducible transcription factor response to any given stimulation includes regulation of members of different families and discrete regulation of individual members of each family.

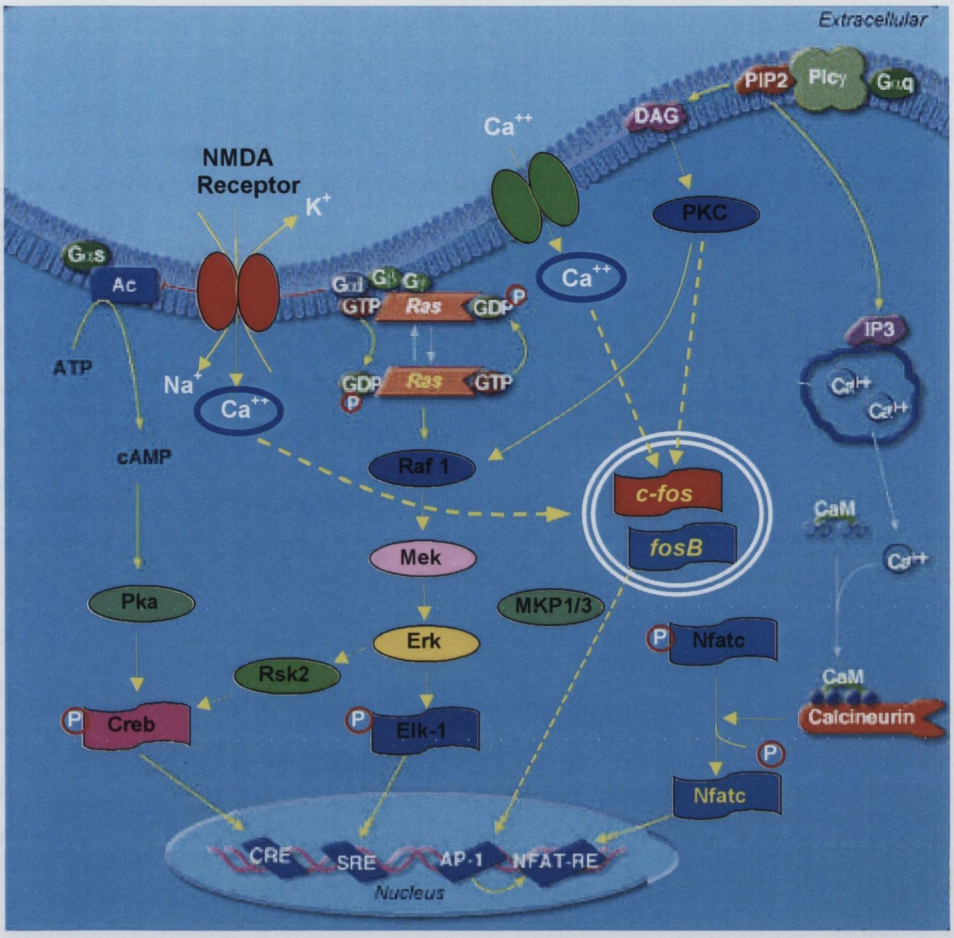


Figure 6.22: Diagram illustrating the function of third messengers in coupling neurotransmission to altered gene expression.

The *IEGs c-fos* and *fosB* are the first gene targets activated by NMDA receptor over-activation, opening of voltage gated calcium channels and diverse intracellular messenger systems, for example various kinases, DAG and IP3, linking extracellular events to the nucleus.

Because of the different structures of the leucine zipper and its flanking regions Fos cannot form homodimers (Kouzarides & Ziff, 1988) as does c-Jun, and Fos proteins cannot bind to DNA unless they dimerise. In addition, Fos does not associate with CREB, CREM or ATF-1, but it can bind to ATF4 (Hai & Curran, 1991). ATF proteins are representatives of a class of ubiquitous and constitutively expressed transcription factors (CTFs). With respect to *IEG* encoded proteins, CTFs have three principal actions (a) they activate or repress the induction of genes encoding these proteins, (b) they can form activating or repressing heterodimers with these inducible proteins and (c) they can bind, without these proteins, to many inducible transcription factor consensus sequences (Herdegen & Leah, 1998). ATF3 can homodimerise. Like Fos, FosB cannot form homodimers (Herdegen & Leah, 1998). Thus, it can be speculated that the possible AP-1 transcription factor dimers, formed under excitotoxic conditions, include Fos:ATF4, FosB:ATF4 and ATF3:ATF3 and that these AP-1 complexes, together with the transcription factors Egr1 and Egr2, are responsible for initiating the ordered expression of "target genes". Each transcription factor activates a different set of target genes, by virtue of discrete DNA recognition sites, which can then function as survival or toxic factors (Tatter *et al.*, 1995) leading to altered neurotransmitter receptor systems and signalling pathways.

6.3.2 Selected genes from Rat GeneChip® arrays

The selected genes from the rat GeneChip® arrays were also organised into three clusters. Cluster 1 contained 13 genes whose expression levels remained unchanged following exposure of the rat cortical neurons to non-toxic concentrations of Glu for either 30 min or 240 min and also to toxic concentrations of Glu for 30 min. However, the 13 genes were strongly down-regulated under excitotoxic conditions, that is, following exposure of the neurons to toxic concentrations of Glu for 240 min. Cluster 1 contained factors involved in amino acid metabolism (1), cell morphology/motility/regulation (1), the nervous system/GPCR pathway (1), transcription factors (1), co-repressors of gene expression (2), protein translation (1), lipoprotein metabolism (1), protein degradation (2) and several ESTs (2). All of the 24 genes in Cluster 1 had 240/30 min mRNA ratios of less than 1 indicating their down-regulation in excitotoxicity (see Table 6.14).

Cluster 2 was the largest cluster representing 39 genes. The genes from this group most relevant to excitotoxicity were the anti-apoptotic factor Arc, the transcription factors ATF3 and Nr4a2 and the *IEG c-jun*. The expression levels of Arc, ATF3 and Nr4a1 were

exclusively up-regulated following treatment of the neurons with toxic concentrations of Glu for 240 min, indicating a specific involvement of these genes in excitotoxicity. The 4 representatives of *c-jun* showed different levels of induction under excitotoxic conditions. It can be speculated, therefore, that in general *c-jun* expression was increased under excitotoxic conditions on micro-arrays; however, investigations into *c-jun* expression profiles using RT-PCR found only a small increase at the 5 hour time-point. The 240/30 min mRNA ratios were above 1 under excitotoxic conditions for Arc, ATF3, Nr4a1 and *c-jun* proposing these genes as potential biomarkers for excitotoxicity. Non-excitotoxic conditions gave ratios ≤ 1 (see Tables 6.15 a), b) and c)).

In cluster 3, 18 genes were found with similar expression patterns. The members most likely involved in excitotoxicity were the proto-oncogene *junB (*2 representatives), the oncogene *c-fos* (3 representatives), the transcription factors *Egr1* (4 representatives), *Egr2, Egr4*, and CREM and the pro-apoptotic *IEG*, Nr4a1 (2 representatives). The two representatives of the proto-oncogene *junB* were induced by non-toxic concentrations of Glu at 30 min, with levels slightly reduced at 4 hours. With toxic concentrations, it was observed that while both *junB* probes were increased at 30 min, an elevation in the level of induction was measured at the 4 hour time-point. However, large differences were observed between the probes in the levels of induction at the 4 hour time-point, with one representative showing an induction 3 fold greater than the other. These results are in contrast to the profiles of *junB* expression measured using the method of real-time RT-PCR (see Chapter 5; Section 5.2.13), where only slight increases in *junB* mRNA expression were found under excitotoxic conditions. Furthermore, *junB* was not induced on mouse microarrays with either non-toxic or toxic concentrations of Glu at 30 or 240 min. It is therefore difficult to conclude from these contrasting results whether *junB* is significant in excitotoxicity and further investigations are required.

The *IEG*, *c-fos*, was represented two times on the rat GeneChip® array. Both representatives were transiently induced by treatment of the neurons with non-toxic concentrations of Glu for 30 min. Treatment with a more toxic concentration of Glu for 30 min induced an increase in the expression of *c-fos* mRNA, which was even more pronounced at the 4 hour time-point. These results confirm the time-and concentration-dependant profiles of Glu-mediated *c-fos* mRNA expression found using RT-PCR and propose *c-fos* as a positive indicator of excitotoxicity in both mCGCs and rat cortical neurons. In addition, as found using RT-PCR, the levels of *c-fos* mRNA expression under excitotoxic conditions were 10 fold higher in the rat cortical system than in the mouse.

These observations suggest the rat system as being the more sensitive and robust model for gene expression studies.

3 out of the 4 representatives of the transcription factor, *Egr1*, were transiently induced at 30 min under non-excitotoxic conditions. A possible explanation why not all representatives showed the same induction may lie in the quality of the oligo that not all representatives showed the same induction. Both *Egr2* and *Egr4* were induced at 30 min with non-toxic concentrations, however *Egr2* induction remained sustained. No real induction of CREM was observed with non-toxic concentrations at either 30 min or 4 hours. Apart from CREM, expression at 30 min with toxic concentrations was more increased for all transcription factors than with non-toxic concentrations. Toxic concentrations of Glu for 4 hours stimulated even higher increases in the expression of the transcription factors. One representative of the pro-apoptotic *IEG*, Nr4a1 showed a transient expression at 30 min with non-toxic concentrations of Glu. Toxic concentrations of Glu induced a much larger increase in expression at the 30 min time-point, which was even higher at the 4 hour time-point. *JunB, c-fos, Egr1*, *Egr4*, CREM, *Egr2* and Nr4a1 all gave 240/30 mRNA ratios greater than 1 indicating their involvement in the excitotoxic cascade. Non-excitotoxic conditions gave ratios ≤ 1 (see Table 6.16).

Like in mCGCs, it is possible that the genes belonging to Clusters 2 and 3 interact with each other in the process of excitotoxicity. Stimulation of neuronal receptors activates second messenger systems whose end kinases, for example ERK and PKA translocate to the nucleus and phosphorylate CTFs such as CREB, CREM and the ATF family, already bound to DNA. This endows them with an increased DNA-binding affinity, facilitates their association with other co-induced or pre-existing transcription factors, and/or activates the general transcription machinery to initiate synthesis of *IEG* mRNA. After translation in the cytoplasm *IEG* encoded TFs, for example c-Fos, c-Jun and Krox, translocate to the nucleus and form dimers with other ITFs and/or CTFs. These then bind to specific sites in the promoters/enhancers and initiate an ordered expression of the corresponding "target" genes (as reviewed by Herdegen and Leah, 1998).

As already mentioned, all of the Jun proteins can form both homo- and heterodimers, which bind to the AP-1 site and stimulate the transcription of various *IEGs*. In contrast, Fos proteins do not associate with each other and therefore do not bind to DNA as homodimers. However, the Fos proteins can associate with any of the Jun proteins to generate stable heterodimers that have higher DNA-binding activity than the Jun homodimers (Angel and Karin, 1990).

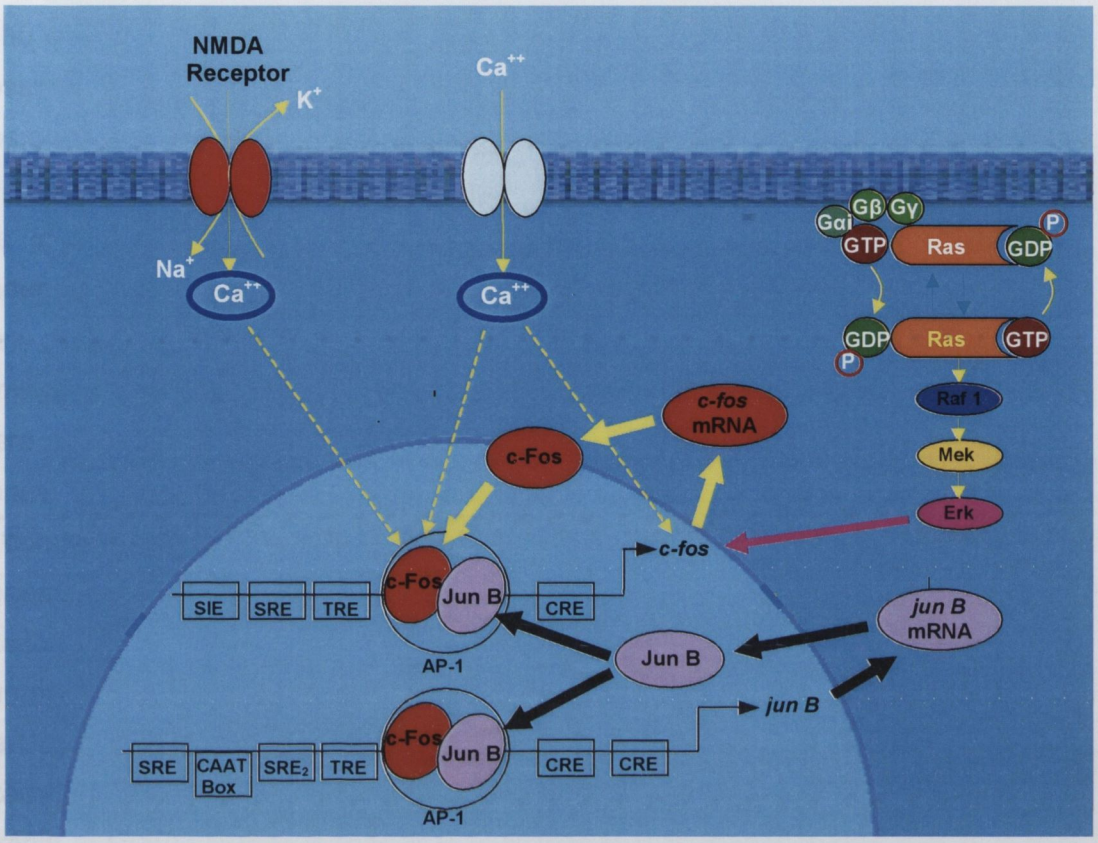


Figure 6.23: Illustration of the transcription machinery involved in the induction of *c-fos* and *junB* mRNA following overactivation of the NMDA receptor.

Stimulation of NMDA receptors and voltage gated Ca^{2+} channels activates second messenger systems whose end kinases, for example ERK, translocate to the nucleus and activate the general transcription machinery to initiate synthesis of *IEG* (in this case *c-fos* and *junB*) mRNA. Following translation in the cytoplasm, *c-fos* and/or *junB* encoded transcription factors translocate to the nucleus and form dimers with each other and/or with other inducible transcription factors and/or constitutively expressed transcription factors. These then bind to specific sites in the promoters/enhancers and initiate an ordered expression of the corresponding "target" genes

Both JunB and JunD are inefficient transcriptional activators in the absence of Fos. ATF-3 forms homodimers and heterodimers with c-jun, JunB, junD and ATF-2, but not with c-Fos (Chu *et al.*, 1994; Hsu *et al.*, 1992). In the rat, therefore, it can be speculated that the possible AP-1 transcription factor dimers formed under excitotoxic conditions include Fos:c-Jun, c-Jun:c-Jun, JunB:Fos; JunB:JunB; JunB:c-jun, ATF3:ATF3, JunB:ATF3 and c-Jun:ATF3. Interestingly, these formations suggest that the AP-1 complex c-Jun:c-Jun and the inducible:constitutive transcription complex c-jun:ATF3 are selectively expressed under excitotoxic conditions in the rat. This *in vitro* analysis of dimerisation only gives an idea about the possible interactions among the various members of the Fos and Jun families. Although the AP-1 proteins and the transcription factors Egr1, Egr2 and Egr4 were induced in parallel, each initiates the ordered activation of different sets of "target genes" on account of their distinct DNA recognition sites.

In conclusion, GeneChip® arrays are powerful tools that can be used to identify subsets of genes that might be involved in mediating complex neurotoxicological processes, such as excitotoxicity. Excitotoxicity is thought to have a pivotal role in the patho-physiology of a number of age-related neurodegenerative disorders (such as Huntington's disease and Parkinson's disease) as well as in several acute and chronic neuropathologies (for example, ischaemia, epilepsy). The causative mechanisms of excitotoxic cell death remain elusive but the evidence above and in the previous 2 Chapters suggests that the abnormal transcriptional induction of *IEGs*, such as the *fos* and *jun* families, and their respective gene products serve as master regulators.

Chapter 7

Concluding Remarks

Excitotoxicity has been considered as a major mechanism in seizure-induced neuropathology (Meldrum, 1985; 1994), and chronic neurodegeneration associated with Alzheimer's disease (Mattson *et al.*, 1999), Huntington's disease (Koh *et al.*, 1986; Alexi *et al.*, 2000) and amyotropic lateral sclerosis (Plaitakis *et al.*, 1982; Plaitakis and Caroscio, 1987; Beal *et al.*, 1986; Rothstein, 1995). Throughout the literature, the excitatory neurotransmitter, Glu, is the prevalent, speculative trigger of excitotoxicity (Olney, 1969; Budd and Nicholls, 1996; Choi, 1987, 1988, 1992; Leist and Nicotera, 1998; Michaelis, 1998). However, the biochemical events in the excitotoxic process that occur following excitatory receptor activation remain elusive. Excessive activation of the NMDA subtype of glutamate (Glu) receptors by EAAs and the subsequent increase in intracellular calcium ion (Ca^{2+}) concentration is thought to be the main initiators in a cascade of events that ultimately results in irreversible neuronal death (Bonfoco *et al.*, 1995; Frandsen and Schousboe, 1993; Nicotera *et al.*, 1992, 1996). Ca^{2+} influx is critical for activity-dependent synaptic plasticity and, if excessive, is potentially damaging because it can over-stimulate Ca^{2+}-dependent enzymes such as phospholipases and endonucleases (Lipton and Rosenberg, 1994) and irreversibly damage mitochondria. Large increases in mitochondrial matrix Ca^{2+} concentration impede mitochondrial ATP production by activating the non-selective permeability transition pore (PTP; Gunter *et al.*, 1994). Activation of the pore can result in mitochondrial depolarisation and swelling as all solutes and proteins smaller than 2 KDa can move freely through the mitochondrial membrane (Bernardi *et al.*, 1994). Mitochondrial Ca^{2+} accumulation sufficient to activate the PTP can dissipate the mitochondrial membrane potential ($\Delta\psi_m$) and therefore ADP phosphorylation irreversibly damaging the cells, even when mitochondrial respiration is stimulated initially by the Ca^{2+} uptake. In addition, transient changes in the concentration of intracellular Ca^{2+} ions can trigger alterations in gene expression. Among the Ca^{2+}-regulated processes critical for the long-term structural and functional modification of neurons are changes in gene expression. Regulation of gene expression is an important component of the cellular response to environmental cues, and involves integration of signals from many signal transduction pathways.

The first part of this study focused on establishing two different *in vitro* cell culture models, mouse cerebellar granule cells (mCGCs) and rat cortical neurons, in which to investigate excitotoxicity. The cytotoxic actions of glutamate (Glu), aspartate (Asp) and N-methyl-D-aspartate (NMDA) were investigated in mCGCs by an MTT assay following 4 and 24 hour exposures, and compared to the non-cytotoxic actions of alanine (Ala). It was observed

that all excitotoxins induced a concentration-dependent decrease in cell viability, which was inhibited by the NMDA receptor antagonist, AP5, but unchanged by the non-NMDA receptor antagonist, CNQX. In addition, it was found that all 3 excitotoxins induced concentration-dependent decreases in intracellular ATP levels, which too were inhibited by AP5 but not by CNQX. These results confirm the excitotoxin-induced neurotoxicity as being a specific result of NMDA receptor over-activation. Furthermore, these results demonstrate that the mCGC system is a suitable model for investigations into the early events underlying excitotoxicity.

Following the establishment of the mCGC system as a model to investigate excitotoxicity, a second *in vitro* cell culture system, from a different species and brain region, was developed and optimised as an additional and alternative model. The suitability of rat cortical neurons for studying excitotoxicity was demonstrated by showing Glu receptor agonist induced cytotoxicity, which could be blocked by AP5 but not by CNQX. This excitotoxicity was dependent on the length of time the neurons had been maintained in culture, presumably due to the time required for neurons to express functional ionotropic Glu receptors. In contrast, paraquat sensitivity was not dependent on fully functional ionotropic receptors, as might be expected for a Glu receptor–independent toxicity mechanism. In addition, exposure of the rat cortical neurons to the excitotoxins Glu, Asp and non-excitotoxin, paraquat, induced concentration-dependent decreases in intracellular ATP levels and mitochondrial membrane potential. These findings thus confirm the suitability of rat cortical neurons as a model in which to study excitotoxicity.

Having established two different *in vitro* models in our laboratory, the second part of this study focused on the expression of *immediate early genes* (*IEGs*) in excitotoxicity. The expression of two families of *IEGs*, that is, *fos* (*c-fos*, *fosB*, *fra-1* and *fra-2*) and *jun* (*c-jun*, *junB* and *junD*), were investigated in mCGCs stimulated with Glu and Asp. It was found that stimulation of the mCGCs with the excitotoxins induced a transient increase in *c-fos* mRNA expression at non-toxic concentrations, which changed to a more delayed, elevated and sustained expression at higher, toxic concentrations. The delayed, elevated and sustained expression of *c-fos* mRNA with toxic concentrations is indicative of excitotoxicity. *c-fos* mRNA expression was inhibited in the presence of AP5 but not in the presence of CNQX. These results thus suggest that sustained expression of *c-fos* mRNA is characteristic of excessive activation of NMDA receptors, that is, of excitotoxicity.

The question as to whether elevated and sustained *c-fos* mRNA expression could be used as a predictive index of excitotoxicity was addressed by the quantitative measurement of

c-fos induction in response to mCGCs being treated with several compounds at low (and therefore non-toxic) and high (toxic) concentrations. Exposures were performed at two time-points, representative of early and delayed expression, that is, 30 and 240 min, in the presence and absence of Glu receptor antagonists. The results suggested that the assay of delayed, elevated and sustained *c-fos* expression can be used to screen for known and potential excitotoxins at a reasonable throughput but that the test is not fully robust due to some variability in *c-fos* expression, responses to compounds and receptor antagonism. Thus, further optimisation of the *c-fos* screen is necessary. For example, when the *c-fos* 240/30 min ratio method is used the early and late time-points chosen should be clearly representative of the change in *c-fos* mRNA expression from that of a transient (that is, a non-toxic condition) to that of a more delayed, elevated and sustained expression (that is, an excitotoxic condition). However, it would seem that solely large differences in *c-fos* expression levels are required for this test to be robust and accurate in prediction, which would obviate the need for producing 240/30 min ratios at all. Thus, the concentrations of the NMDA receptor agonists used should be sufficient to induce the elevated and sustained excitotoxic *c-fos* response but also not so extreme that they are incapable of agonist-antagonist competition. Lastly, where a fixed concentration of a Glu receptor antagonist is used it should be sufficient to inhibit all potential excitotoxic *c-fos* responses mediated by toxic concentrations of a variety of compounds. Some of these conditions would be unachievable, of course, in screening of novel compounds, which would not have their Glu receptor interactions characterised.

Up to now, elevated and sustained *c-fos* expression, indicative of excitotoxicity, has been shown to be NMDA receptor mediated. However, it was found that low concentrations of kainate (KA) induced a transient induction of *c-fos* expression, which changed with higher concentrations to a delayed, elevated, and sustained expression, indicative of a KA receptor mediated excitotoxic *c-fos* response. Further work is therefore required to investigate concentration dependencies and pharmacology of the KA response.

In addition to *c-fos*, another member of the *fos* family of *IEGs* showed changes in expression which were dependent on time and concentration. Exposure of the mCGCs to non-toxic concentrations of Glu and Asp induced transient increases in *fosB* mRNA expression. With higher toxic concentrations, the profile of *fosB* expression changed to that of a delayed, elevated and sustained expression. Indeed, *fosB* expression levels were higher when compared to those of *c-fos*, under excitotoxic conditions. These findings indicate that *fosB* can be used, in addition to *c-fos*, as a selective and predictive biomarker

for excitotoxicity. The use of *fosB* in a screen of mCGCs exposed to various concentrations of functionally different chemical compounds, at early and late time-points, in the presence and absence of antagonists, remains to be determined. As for *c-fos*, EAA concentrations should be chosen which are toxic to the cells and thus excitotoxic, but also representative of the toxic potencies of the compounds. Thus, an initial screen should first be performed using a high concentration of agonist to select for positive inducers of *fosB* expression and thus excitotoxins. Following the initial screen, the positives should be tested further with pharmacological investigations.

Investigations into the expression profiles of the other members of the *fos* and *jun* families of *IEGs* , in mCGCs treated with various concentrations of Glu, revealed a slight increase in expression for *fra-2* only. Further work is therefore required to investigate the concentration-dependencies and receptor specificities of *fra-2* mRNA expression.

The third part of this study involved an investigation into the expression of *c-fos* and *fosB*, in particular, under conditions of Glu and Asp induced excitotoxicity in rat cortical neurons. It was observed that, as in mCGCs, *c-fos* mRNA expression was both time- and concentration-dependent. With non-toxic concentrations of Glu and Asp, a transient increase in *c-fos* expression was observed. However, the profile of *c-fos* expression changed to that of a more elevated and sustained expression with toxic concentrations. In contrast to the *c-fos* induction observed in mCGCs, the levels of induction were significantly higher. *c-fos* mRNA expression was also found to be NMDA receptor mediated with inhibition of the *c-fos* response observed in the presence of AP5. Thus, the results demonstrate that the rat cortical system is indeed an appropriate and sensitive model for excitotoxic investigations and furthermore *c-fos* can be used as a predictive marker for excitotoxicity.

It was also found that *fosB* is expressed in rat cortical neurons exposed to various concentrations of Glu and Asp. It was observed that non-toxic concentrations of Glu and Asp induced a transient increase in *fosB* mRNA expression. Higher, toxic concentrations of both EAAs changed the kinetics of the *fosB* response. Instead of the delayed and sustained profile of *fosB* expression found in mCGCs, a biphasic excitotoxic *fosB* response was observed. These results suggest that the excitotoxic profile of *fosB* mRNA expression in rat cortical neurons, is elevated, sustained and biphasic. The differences in expression between the excitotoxic profiles of *c-fos* and *fosB* may be related to neuronal type (cortex versus cerebellum) and/or species (mouse versus rat). In addition, the NMDA receptor antagonist, AP5, inhibited *fosB* mRNA expression under excitotoxic conditions,

demonstrating an NMDA receptor mediated response. Further work is required to investigate the different profiles of excitotoxic *fosB* expression. This would involve the investigation of *fosB* mRNA expression in rat cerebellar granule cells and mouse cortical neurons exposed to various concentrations of excitotoxins over a defined time-course.

Following consideration of the preliminary results for rat cortex with Glu and Asp, it was decided to assess a range of functionally different chemical compounds to investigate whether the change in *c-fos* and/or *fosB* expression from a low concentration to a high concentration, at one time-point, could be used to predict the potential excitotoxic properties of compounds, a method allowed by the extraordinarily high level of expression of *c-fos* and *fosB* under excitotoxic conditions. It was found that both *c-fos* and *fosB* can be used as screens to predict the excitotoxic properties of compounds. From consideration of the results, there does not seem to be major advantage is in using antagonism as part of an initial screen. Rather, it would seem better to use a sequential approach, perhaps performing a second screen with antagonism on compounds shown positive in the original screen.

In addition to *c-fos* and *fosB*, it was found that toxic concentrations of Glu induced increased expression of *fra-2* mRNA in rat cortical neurons. No changes in expression were observed for *fra-1*, *c-jun*, *junB* or *junD*. Thus, 3 members of the *fos* family of *IEGs* show increased expression under excitotoxic conditions. Further work is required to investigate the role of *fra-2* in excitotoxicity.

The final part of this study involved the use of a second independent approach, namely DNA micro-array technology, to investigate the simultaneous changes in gene expression in both mCGCs and rat cortical neurons undergoing excitotoxicity. Using conditions found optimal from RT-PCR studies, mCGCs and rat cortical neurons were treated with a non-toxic and toxic concentration of Glu for 30 and 240 min. It was found that *c-fos* and *fosB* were up-regulated in mCGCs under excitotoxic conditions, whereas, in the rat cortical system, *c-fos* and *junB* were up-regulated under excitotoxic conditions. Furthermore, a constitutive transcription factor, ATF3, was identified which was selectively expressed under excitotoxic conditions in both cell culture systems, thus an additional and potentially important biomarker for excitotoxicity. Further work, using the quantitative technique of RT-PCR, is therefore required to investigate the role of ATF3 in excitotoxicity. In addition to the genes mentioned above, other *IEGs* and transcription factors were uncovered which may be involved in the complex process of excitotoxicity. A more detailed investigation into excitotoxicity, using micro-array technology could therefore provide

further insights into the molecular mechanisms of excitotoxic neuronal cell death. This would involve the exposure of different *in vitro* models, for example cultured hippocampal neurons, striatal neurons, rat cerebellar granule cells and mouse cortical neurons, to increasing concentrations of different excitotoxins, in the presence and absence of Glu receptor antagonists, over a specified time-course. In addition, gel supershift analysis of nuclear extracts, dervived from mCGCs and rat cortical neurons treated with increasing concentrations of Glu, could be used to investigate the various transcription factor dimers speculated to be formed, in Chapter 6, under excitotoxic conditions.

In conclusion, *IEGs* play an important role in the regulation of information transmission between and within cells. *IEGs* are thought to control physiological processes of development, growth and differentiation. They are found to encode proteins that function as extracellular growth factors, cell-surface receptors, G-proteins, protein kinases, hormone receptors and transcription factors. The abnormal expression of *IEGs* is therefore critical in the processes of neuronal survival and/ or degeneration. Many *IEGs* encode transcription factors that can act as inducers and/or suppressors of gene expression. They not only interact directly with DNA and the general basal transcription factors, but they also indirectly modify transcription processes by complexing with and inducing and/or repressing other transcriptionally operating proteins. *IEG* transcription factors can also induce waves of delayed response gene expression. It is likely that the delayed response genes encode target effector proteins which decide whether the cell survives or dies, and in the latter case whether by apoptotic or necrotic mechanisms. Thus, the induction of *IEG*-encoded transcription factors and target effector proteins lies in a stream of excitation that begins with transmembrane ion fluxes and terminates with functional and morphological alterations in the affected neurons that can include synaptogenesis and neuronal cell death. Microarray analysis could therefore be used as a general and simultaneous assay for identification of overall changes in gene expression in various signalling cascades, for example the survival and/or degeneration of the cells in excitotoxicity, apoptosis and/or necrosis. Detection of altered gene expression can thus serve as a valuable tool in the discovery of therapeutic targets and diagnostic markers. Following the micro-array analysis, specific *IEG*s, constitutive transcription factors, apoptotic and necrotic agents, and effector proteins should be analysed in detail over different conditions of time and concentration, using quantitative real-time RT-PCR.

Gene expression is a multi-step process that results in an active protein. DNA micro-array technology and real-time RT-PCR encompass the respective semi-quantitative and

quantitative analysis of transcripts at the mRNA level. However, these genetic investigations do not provide insight into how all of the protein products of these genes interact or function within the cell. Further investigations, using the methods of proteomics and Western blotting, are required to quantitatively measure the relative amounts of *IEG* proteins produced under excitotoxic conditions. This would involve an initial proteomic approach, of primary neuronal cultures exposed to increasing concentrations of EAAs at a single time-point to characterise changes in the relative levels of the various *IEG* encoded proteins, for example Fos and Jun proteins, transcription factors, and apoptotic and necrotic agents. This initial screen should then be followed with a more detailed investigation, using Western blots, two-dimensional gel electrophoresis and gel supershift analysis of nuclear extracts to identifiy and validate key *IEG* protein targets (known or novel) that could aid in the clarification of the mechanism of excitotoxicity.

References

Abate, C., Rauscher, F.J.III, Gentz, R. & Curran, T. (1990). Expression and purification of the leucine zipper and the DNA-binding domains of Fos and Jun: both Fos and Jun directly contact DNA. *Proc. Natl. Acad. Sci. USA* **87,** 1032-1036.

Akaike, N., Kawai, N., Kiskin, N.I., Kijuchko, E.M., Krishtal, O.A. & Tsyndrenko, A.Y. (1987). Spider toxin blocks excitatory amino acid responses in isolated hippocampal pyramidal neurons. *Neurosci. Lett.* **79,** 326-330.

Alexi, T., Borlongan, C.V., Faull, R.L., Williams, C.E., Clark, R.G., Gluckman, P.D. & Hughes, P.E. (2000). Neuroprotective strategies for basal ganglia degeneration: Parkinson's and Huntington's diseases. *Prog. Neurobiol.* **60,** 409-470.

Alwine, J.C., Kemp, D.J. & Stark, G.R. (1977). Method for detection of specific RNAs in agarose gels by transfer to diazobenzyloxymethyl-paper and hybridisation with DNA probes. *Proc. Natl. Acad. Sci. USA* **74,** 5350-5354.

Angel, P. & Karin, M. (1991). The role of Jun, Fos and the AP-1 complex in cell-proliferation and transformation. *Biochim. Biophys. Acta.* **1072,** 129-157.

Ankarcrona, M., Dypbukt, J.M., Bonofoco, E., Zhivotovsky, B., Orrenius, S., Lipton, S.A., & Nicotera, P. (1995). Glutamate induced neuronal death: a succession of necrosis or apoptosis depending on mitochondrial function. *Neuron* **15**, 961-973.

Ankarcrona, M., Dypbukt, J.M., Orrenius, S. & Nicotera, P. (1996). Calcineurin and mitochondrial function in glutamate-induced neuronal cell death. *FEBS Letters* **394**, 321-324.

Applied Biosystems Sequence Detector User Bulletin #2, www.docs.appliedbiosystems.com/pebiodocs/04303859.pdf.

Artola, A. & Singer, W. (1987). Long-term potentiation and NMDA receptors in rat visual cortex. *Nature* **330,** 649-652.

Ascher P. & Nowak, L. (1988). The role of divalent cations in the N-methyl-D-aspartate responses of mouse central neurones in culture. *J. Physiol. (Lond.)* **399,** 247-266.

Auer, R., Wieloch, T., Olsson, Y. & Siesjo, B.K. (1984). The distribution of hypoglycemic brain damage. *Acta. Neuropathol.* **64,** 177-191.

Babcock, D.F., Herrington, J., Goodwin, P.C., Park, Y.B. & Hille, B. (1997). Mitochondrial participation in the intracellular Ca^{2+} network. *J. Cell Biol.* **136** (4), 833-844.

Bading H., Ginty, D.D. & Greenberg, M.E. (1993). Regulation of gene expression in hippocampal neurons by distinct calcium signalling pathways. *Science* **260,** 181-186.

Baird, D.H., Trenkner, E. & Mason, C.A. (1996). Arrest of afferent axon extension by target neurons *in vitro* is regulated by the NMDA receptor. *J. Neurosci.* **18** (8), 2642-2648.

Balázs, R., Dahl, D. & Harwood, J.R. (1966). Subcellular distribution of enzymes of glutamate metabolism in rat brain. *J. Neurochem.* **13,** 897-905.

Balázs, R., Jorgensen, O.S. & Hack, N. (1988). N-Methyl-D-aspartate promotes the survival of cerebellar cells in culture. *Neurosci.* **27** (2), 437-451.

Balázs, R., Resink, A., Hack, N., Van der Valk, J.B., Kumar, K.N. & Michaelis, E. (1992). NMDA treatment and K^+-induced depolarization selectively promote the expression of an NMDA-preferring class of the ionotropic glutamate receptors in cerebellar granule neurones. *Neurosci. Lett.* **137** (1), 109-13.

Balcar, V.J. & Johnston, G.A.R. (1972). The structural specificity of the high affinity uptake of L-Glutamate and L-Aspartate by rat brain slices. *J. Neurochem.* **19,** 2657-2666.

Bannister, A.G., Brown, H.G., Sutherland, J.A. & Kouzarides, T. (1994). Phosphorylation of the c-Fos and c-Jun HOB1 motif stimulates its activation capacity. *Nucleic Acids Res.* **22** (24), 5173-5176.

Beal, M.F., Kowall, N.W., Ellison, D.W., Mazurek, M.F., Swartz, K.J. & Martin, J.B. (1986). Replication of the neuro-chemical characteristics of Huntington's disease by quinolinic acid. *Nature* **321,** 168-171.

Beal, M.F. (1992). Does impairment of energy metabolism result in excitotoxic neuronal death in neurodegenerative illnesses? *Ann. Neurol.* **31,** 119-130.

Beal, M.F. (1996). Mitochondria, free radicals, and neurodegeneration. *Curr. Opin. Neurobiol.* **6** (5), 661-666.

Beal, M.F. (1998). Mitochondrial dysfunction in neurodegenerative diseases. *Biochim. Biophys. Acta.* **1366** (1-2), 211-223.

Beal, M.F. (2003). Mitochondria, oxidative damage, and inflammation in Parkinson's disease. *Ann. N. Y. Acad. Sci.* **991**, 120-131.

Bekkers, J.M. & Stevens, C.F. (1989). NMDA and non-NMDA receptors are co-localized at individual excitatory synapses in cultured rat hippocampus. *Nature* **341,** 230-233.

Bendotti, C., Vezzani, A., Tarizzo, G. & Samanin, R. (1993). Increased expression of GAP-43, somatostatin and neuropeptide Y mRNA in the hippocampus during development of hippocampal kindling in rats. *Eur. J. Neurosci.* **5,** 1312-1320.

Beretta, S., Robertson, H.A. & Graybiel, A.M. (1993). Neurochemically specialised projection neurons of the striatum respond differently to psychomotor stimulants. *Prog. Brain Res.* **99,** 201-205.

Bernardi, P., Broekemeier, K.M. & Pfeiffer, D.R. (1994). Recent progress on regulation of the mitochondrial permeability transition pore; a cyclosporin-sensitive pore in the inner mitochondrial membrane. *J. Bioenerg. Biomembr.* **26,** 509-518.

Bishop, J.M. (1983). Cellular oncogenes and retroviruses. *Ann. Rev. Biochem.* **52,** 301-354.

Bishop, J.M. (1985). Viral oncogenes. *Cell* **42,** 23-38.

Bleakman, D., Rusin, K.I., Chard, P.S., Glau, S.R. & Miller, R.J. (1992). Metabotropic glutamate receptors potentiate ionotropic glutamate responses in the rat dorsal horn. *Mol. Pharmacol.* **42,** 192-196.

Bliss, T.V.P. & Lømo, T. (1973). Long-lasting potentiation of synaptic transmission in the dentate area of the anaesthetized rabbit following stimulation of the perforant path. *J. Physiol.* **232,** 311-356.

Bliss, T.V.P., Douglas, R.M., Errington, M.L. & Lynch, M.A. (1986). Correlation between long-term potentiation and release of endogenous amino acids from dentate gyrus of anaesthetized rats. *J. Physiol.* **377,** 391-408.

Bliss, T.V.P. & Collingridge, G.L. (1993). A synaptic model of memory: long-term potentiation in the hippocampus. *Nature* **361,** 31-38.

Bonofoco, E., Ankarcrona, M., Krainc, D., Nicotera, P. & Lipton, S.A. (1995). Techniques for distinguishing apoptosis from necrosis in cerebrocortical and cerebellar neurons. In Apoptosis techniques and protocols, *Neuromethods* **29**, 237-235.

Bonofoco, E., Krainc, D., Ankarcrona, M., Nicotera, P. & Lipton, S.A. (1995). Apoptosis and necrosis: Two distinct events induced, respectively, by mild and intense insults with N-methyl-D-aspartate or nitric oxide/superoxide in cortical cell cultures. *Proc. Natl. Acad. Sci. USA* **92**, 7162-7166.

Bos, T.J., Rauscher, F.J. III, Curran, T. & Vogt, P.K. (1989). The carboxy terminus of the viral Jun oncoprotein is required for complex formation with the cellular *fos* protein. *Oncogene* **4,** 123-126.

Brewer, G.J., Torricelli, J.R., Evege, E.K. & Price, P.J. (1993). Optimised survival of Hippocampal neurons in B27-supplemented Neurobasal™, a new serum-free medium combination. *J. Neurosci. Res.* **35,** 567-576.

Brewer, G.J. & Cotman, C.W. (1989). NMDA receptor regulation of neuronal morphology in cultured hippocampal neurons. *Neurosci. Lett.* **99,** 268-273.

Brown, P.O. & Botstein, D. (1999). Exploring the new world of the genome with DNA microarrays. *Suppl. Nat. Genet.* **21,** 33-37.

Budd, S.L. & Nicholls, D.G. (1996). Mitochondria, calcium regulation and acute glutamate excitotoxicity in cultured cerebellar granule cells. *J. Neurochem.* **67,** 2282-2291.

Bucher, P. (1999). Regulatory elements and expression profiles. *Curr. Opin. Struct.* Biol. **9** (3), 400-407.

Burnashev, N., Monyer, H., Seeburg, P.H. & Sakmann, B. (1992). Divalent ion permeability of AMPA receptor channels is dominated by the edited form of a single subunit. *Neuron* **8,** 189-198.

Burnashev, N., Villarroel, A. & Sakmann, B. (1996). Dimensions and ion selectivity of recombinant AMPA and kainate receptor channels and their dependence on Q/R site residues. *J. Physiol.* **496,** 165-173.

Cano, E., Hazzalin, C.A., Kardalinou, E., Buckle, R.S. & Mahadevan, L.C. (1995). Neither ERK nor JNK/SAPK MAP kinase subtypes are essential for histone H3/HMG-14 phosphorylation or *c-fos* and *c-jun* induction. *J. Cell Sci.* **108,** 3599-3609.

Case-Green, S.C., Mir, K.U., Pritchard, C.E. & Southern, E.M. (1989). Analysing genetic information with DNA arrays. *Curr. Opin. Chem. Biol.* **2,** 404-410.

Cebers, G., Zhivtovsky, B., Ankarcrona, M. & Liljequist, S. (1997). AMPA neurotoxicity in cultured cerebellar granule neurons: mode of cell death. *Brain Res. Bull.* **43,** 393-403.

Chao, V.M. (1992). Neurotropin receptors: a window into neuronal differentiation. *Neuron* **9,** 583-593.

Chavis, P., Shinozaki, H., Bockaert, J. & Fagni, L. (1994). The metabotropic glutamate receptor types II-III inhibit L-type calcium channels via a pertussis toxic-sensitive G-protein in cultured cerebellar granule cells. *J. Neurosci.* **14,** 7067-7076.

Chee, M., Yang, R., Hubbell, E., Berno, A., Huang, X.C., Stern, D., Winkler, J., Lockhart, D.J., Mac Donald, S. & Fodor, S.P.A. (1996). Accessing genetic information with high-density DNA arrays. *Science* **274,** 610-614.

Cheung, N.S., Pascoe, C.J., Giardina, S.F., John, C.A. & Beart, P.M. (1998). Micromolar L-glutamate induces extensive apoptosis in an apoptotic-necrotic continuum of insult-dependent, excitotoxic injury in cultured cortical neurones. *Neuropharmacol.* **37,** 1419-1429.

Cheung, V.G. (1999). Making and reading microarrays. *Nature Genet.* **21,** 15-19.

Choi, D.W. (1987). Ionic dependence of glutamate neurotoxicity. *J. Neurosci.* **7**, 369-379.

Choi, D.W., Maulucci-Gedde, M. & Kriegstein, A.R. (1987). Glutamate neurotoxicity in cortical cell culture. *J. Neurosci.* **7,** 357-368.

Choi, D.W., Koh, K-Y. & Peters, S. (1998). Pharmacology of glutamate neurotoxicity in cortical cell culture: attenuation by NMDA antagonists. *J. Neurosci.* **8,** 185-196.

Choi, D.W. (1988a). Calcium-mediated neurotoxicity: relationship to specific channel types and role in ischemic damage. *Trends Neurosci.* **11**, 465-467.

Choi, D.W. (1988b). Glutamate neurotoxicity and diseases of the nervous system. *Neuron* **1**, 623-634.

Choi, D.W. (1990). Cerebral hypoxia: some new approaches and unanswered questions. *J. Neurosci.* **10,** 2493-2501.

Choi, D.W. & Rothman, S.M (1990). The role of glutamate neurotoxicity in hypoxic-ischemic neuronal death. *Ann. Rev. Neurocsi.* **13,** 171-182.

Choi, D.W. (1992). Excitotoxic cell death. *J. Neurobiol.* **23**, 1261-1276.

Choi, D.W. (1995). Calcium: still center-stage in hypoxic ischemic neuronal death. *Trends Neurosci.* **18,** 58-60.

Choi, D.W. (1996). Ischemia-induced neuronal apoptosis. *Curr. Opin. Neurobiol.* **6**, 667-672.

Chu, H.M., Tan, Y., Kobierski, L.A., Balsam, L.B. & Comb, M.J. (1994). Activating transcription factor-3 stimulates 3,5-cyclic adenosine monophosphate-dependent gene expression. *Mol. Endocrinol.* **8**, 59-68.

Cohen, D.R. & Curran, T. (1988). Fra-1 serum inducible, cellular immediate-early gene that encodes a Fos-related antigen. *Mol. Cell Biol.* **8,** 2063-2069.

Cohen, D.R., Ferreira, P.C.P., Gentz, R., Franza, B.R. & Curran, T. (1989). The product of a Fos-related gene Fra-1 binds cooperatively to the AP-1 site with Jun: transcription factor AP-1 is comprised of multiple protein complexes. *Genes Dev.* **3,** 173-184.

Cole, A.J., Saffen, D.W., Baraban, J.M. & Worley, P.F. (1989). Rapid increase of an immediate early gene messenger RNA in hippocampal neurons by synaptic NMDA receptor activation. *Nature* **340,** 474-476.

Collingridge, G.L. & Bliss, T.V.P. (1987). NMDA receptors - their role in long-term potentiation. *Trends Neurosci.* **10,** 288-293.

Cotman, C.W., Monaghan, D.T. & Ganong, A.H. (1988). Excitatory amino acid neurotransmission: NMDA receptors and Hebb-type synaptic plasticity. *Ann. Rev. Neurosci.* **11,** 61-80.

Culmsee, C., Zhu, Y., Krieglstein, J. & Mattson, M.P. (2001). Evidence for the involvement of Par-4 in ischemic neuron cell death. *J. Cereb. Blood Flow Metab.* **21,** 334-343.

Curran, T. (1989). Nobel oncogenes. *New Biologist* **1,** 229-231.

Curran, T. & Franza, B.R. (1988). Fos and Jun: The AP-1 connection. *Cell* **55,** 395-397.

Curran, T., Miller, A.D., Zokas, L. & Verma, I.M. (1984). Viral and cellular *fos* proteins: A comparative analysis. *Cell* **36,** 259-268.

Curran, T. & Morgan, J.I. (1985). Superinduction of *fos* by nerve growth factor in the presence of peripherally active benzodiazepines. *Science* **229,** 1265-1268.

Curran, T. & Morgan, J.I. (1987). Memories of *fos*. *Bioessays* **7** (6), 255-258.

Curran, T. & Morgan, J.I. (1991). The *fos* oncogene. In: Costa E., Joh T.H., editors, Fidia Research Foundation Series, **7,** New York: Thieme Medical Publishers, Inc. 9-15.

Curran, T. & Morgan, J.I. (1995). Fos: an immediate-early transcription factor in neurons. *J. Neurobiol.* **26** (3), 403-412.

Curran, T. & Teich, N.M. (1982). Candidate product of the FBJ murine osteosarcoma virus oncogene: characterisation of a 55,000-dalton phosphoprotein. *J. Virol.* **42** (1), 114-122.

Curran, T., Van Beveran, C., Ling, N. & Verma, I.M. (1985). Viral and cellular *fos* proteins: are complexed with a 39,000 dalton cellular protein. *Mol. Cell Biol.* **5,** 167-172.

Curran, T. & Verma, I.M. (1984). FBR Murine Osteosarcoma Virus. *Virol.* **135,** 218-228.

Curtis, D.R. & Watkins, J.C. (1960). The excitation and depression of spinal neurons by structurally-related amino acids. *J. Neurochem.* **6,** 117-141.

Curtis, D.R., Phillis, J.W. & Watkins, J.C. (1960). The chemical excitation of spinal neurones by certain acidic amino acids. *J. Physiol.* **150,** 656-682.

Curtis, D.R. & Watkins, J.C. (1963). Acidic amino acids with strong excitatory actions on mammalian neurones. *J. Physiol.* **166,** 1-14.

Curtis, D.R., Duggan, A.W., Felix, D., Johnston, G.A.R., Tebicis, A.K. & Watkins, J.C. (1972). Excitation of mammalian central neurones by acidic amino acids. *Brain Res.* **41,** 283-301.

Czuczwar, S.J. & Meldrum, B. (1982). Protection against chemically induced seizures by 2-amino-7-phosphonoheptanoic acid. *European J. Pharmacol.* **83,** 335-338.

Dale, N. & Grillner, S. (1986). Dual-component synaptic potentials in the lamprey mediated by excitatory amino acid receptors. *J. Neurosci.* **6** (9), 2653-2661.

Davies, J. & Watkins, J.C. (1973). Microelectrophoretic studies on the depressant action of HA-966 on chemically and synaptically excited neurones in the rat cerebral cortex and cuneate nucleus. *Brain Res.* **59,** 311-322.

Davies, J., Evans, R.H., Francis, A.A. & Watkins, J.C. (1979). Excitatory amino acid receptors and synaptic excitation in the mammalian central nervous system. *J. Physiol.* **75,** 641-645.

Davies, J. & Watkins, J.C. (1979). Selective antagonism of amino-acid induced and synaptic excitation in the cat spinal cord. *J. Physiol.* **297,** 621-635.

Davies, J., Francis, A.A., Jones, A.W. & Watkins, J.C. (1981). 2-amino-5-phosphonovalerate (2 APV), a potent and selective antagonist of amino acid-induced and synaptic excitation. *Neurosci. Lett.* **21,** 77-81.

Davies, J., Evans, R.H., Herling, P.L., Jones, A.W., Olverman, H.J. (1986). CPP, a new potent and selective NMDA antagonist. Depression of central neuron responses, affinity for D-[^{3}H]AP5 binding sites on brain membranes and anticonvulsant activity. *Brain Res.* **382,** 169-173.

Dessi, F., Charriaut-Marlangue, C., Khrestchatisky, M. & Ben-Ari, Y. (1993). Glutamate induced neuronal death is not a programmed cell death in cerebellar culture. *J. Neurochem.* **60,** 1953-1955.

Dessi, F., Charriaut-Marlangue, C. & Ben-Ari, Y. (1994). Glutamate-induced neuronal death in cerebellar culture is mediated by two distinct components: a sodium-chloride component and a calcium component. *Brain Res.* **650,** 49-55.

Dichter, M.A., Tischler, A.S. & Greene, L.A. (1977). Nerve growth factor-induced increase in electrical excitability and acetylcholine sensitivity of a rat pheochromocytoma cell line. *Nature* **268** (5620), 501-504.

Didier, M., Roux, P., Piechaczyk, M., Mangeat, P., Devilliers, G., Bockaert, J. & Pin, J. (1992). Long-term expression of the *c-fos* protein during the *in vitro* differentiation of cerebellar granule cells induced by potassium or NMDA. *Mol. Brain Res.* **12,** 249-258.

Didier, M., Bursztajn, S., Adamec, E., Passani, L., Nixon, R.A., Coyle, J.T., Wei, J.Y. & Berman, S.A. (1996). DNA strand breaks induced by sustained glutamate excitotoxicity in primary neuronal cultures. *J. Neurosci.* **16,** 2238-2250.

Didier, M., Xu, M., Berman, S.A., Saido, T.C. & Bursztajn, S. (1997). Involvement of three glutamate receptor epsilon subunits in the formation of N-methyl-D-aspartate receptors mediating excitotoxicity in primary cultures of mouse cerebellar granule cells. *Neurosci.* **78** (4), 1129-1146.

Distel, R.J., Ro, H.S., Rosen, B.S., Groves, D.L. & Spiegelman, B.M. (1987). Nucle-protein complexes that regulate gene expression in adipocyte differentiation: Direct participation of *c-fos*. *Cell* **49,** 835-844.

Donevan, S.D., Yamaguchi, S. & Rogawski, M.A. (1994). Non–N-methyl-D-aspartate receptor antagonism by 3-*N*-substituted 2,3-benzodiazepines: relationship to anticonvulsant activity. *J. Pharmacol. Exp. Ther.* **271,** 25-29.

Dragunow, M. & Robertson, H.A. (1987a). Generalised seizures induce *c-fos* protein(s) in mammalian neurons. *Neurosci. Lett.* **82,** 157-161.

Dragunow, M. & Robertson, H.A. (1987b). Kindling stimulation induces *c-fos* protein(s) in granule cells of the rat dentate gyrus. *Nature (Lond.)* **329,** 441-442.

Dragunow, M., Currie, R.W., Faull, R.L.M., Robertson, H.A. & Jansen, K. (1989). Immediate early genes, kindling and long-term potentiation. *Neurosci. Biobehav. Rev.* **13,** 301-313.

Dragunow, M., Yamada, N., Bilkey, D.K. & Lawlor, P. (1992). Induction of immediate early gene proteins in dentate granule cells and somatostatin interneurons after hippocampal seizures. *Mol. Brain Res.* **13,** 119-126.

Dragunow, M., Beilharz, E., Sirimanne, E., Lawlor, P., Williams, C., Bravo, R. & Gluckman, P. (1994). Immediate-early gene protein expression in neurons undergoing delayed death, but not necrosis, following hypoxic-ischemic injury in the young rat brain. *Mol. Brain Res.* **25,** 19-33.

Drejer, J., Larsson, O.M. & Schousboe, A. (1982). Characterization of L-glutamate uptake into and release from astrocytes and neurons cultured from different brain regions. *Exp. Brain Res.* **47,** 259-269.

Drejer, J., Larsson, O.M. & Schousboe, A. (1983). Characterization of uptake and release processes for D- and L-aspartate in primary cultures of astrocytes and cerebellar granule cells. *Neurochem. Res.* **8,** 231-243.

Drejer, J., Honoré, T., Meier, E. & Schousboe, A. (1986). Pharmacologically distinct glutamate receptors on cerebellar granule cells. *Life Sci.* **38**, 2077-2085.

Drejer, J. & Honoré, T. (1988). New quinoxalinediones show potent antagonism of quisqualate responses in cultured mouse cortical neurons. *Neurosci. Lett.* **87,** 104-108.

Duchen, M.R., Burton, N.R. & Biscoe, T.J. (1985). An intracellular study of the interactions of N-methyl-D-aspartate with ketamine in the mouse hippocampal slice. *Brain Res.* **342,** 149-153.

Duggan, D.J., Bittner, M., Chen, Y., Meltzer, P. & Trent, J.M. (1999). Expression profiling using cDNA microarrays. *Nature* **21,** 10-14.

Dugan, L.L., Sensi, S.L., Canzoniero, L.M.T., Handran, S.D., Rothman, S.M., Lin, T.S., Goldberg, M.P. & Choi, D.W. (1995). Mitochondrial production of reactive oxygen species in cortical neurons following exposure to NMDA. *J. Neurosci.* **15,** 6377-6388.

Duman, R.S., Craig, J.S., Winston, S.M., Deutch, A.Y. & Hernandez, T.D. (1992). Amygdala kindling potentiates seizure-stimulated immediate-early gene expression in rat cerebral cortex. *J. Neurochem.* **59,** 1753-1760.

Dumuis, A., Pin, J-P., Oomagari, K., Sebben, M. & Bockaert, J. (1990). Arachidonic acid released from striatal neurons by joint stimulation of ionotropic and metabotropic quisqualate receptors. *Nature* **347,** 183-184.

Dykens, J.A. (1994). Isolated cerebral and cerebella mitochondria produce free radicals when exposed to elevated Ca^{2+} and Na^{+}: Implications for neurodegeneration. *J. Neurochem.* **63,** 584-591.

Eastman, A. (1993). Apoptosis: a product of programmed and unprogrammed cell death. *Toxicol. Appl. Pharmacol.* **121,** 160-164.

Eberwine, J., Yeh, H., Miyashiro, K., Cao, Y., Nair, S., Finnell, R., Zettel, M. & Coleman, P. (1992). Analysis of gene expression in single live neurons. *Proc. Natl. Acad. Sci. USA* **89,** 3010-3014.

Eilers, A., Whitfield, J., Vekrellis, K., Neame, S.J. & Ham, J. (1999). *c-jun* and Bax: regulators of programmed cell death in developing neurons. *Biochem. Soc. Trans.* **27,** 790-797.

Eisen, M.B., Spellman, P.T., Brown, P.O. & Botstein, D. (1998). Cluster analysis and display of genome-wide expression patterns. *Proc. Natl. Acad. Sci. USA* **95,** 14863-14868.

Eisen, M.B. & Brown, P.O. (1999). DNA arrays for analysis of gene expression. *Methods in Enzymology* **303,** 179-205.

Eliasof, S. & Werblin, F. (1993). Characterisation of the glutamate transporter in retinal cones of the tiger salamander. *J. Neurosci.* **13,** 402-411.

Estus, S., Zaks, W.J., Freeman, R.S., Gruda, M., Bravo, R. & Johnson, E.M. (1994). Altered gene expression in neurons during programmed cell death: identification of *c-jun* as necessary for neuronal apoptosis. *J. Cell Biol.* **127** (6), 1717-1727.

Ferea, T.L. & Brown, P.O. (1999). Observing the living genome. *Curr. Opin. Genet. Dev.* **9,** 715-722.

Filipkowski, R.K., Hetman, M., Kaminska, B. & Kaczmarek, L., (1994). DNA fragmentation in rat brain after intraperitoneal administration of Kainate. *Neuroreport* **5,** 1538-1540.

Fiskum, G., Murphy, A.N. & Beal, M.F. (2000). Mitochondria in neurodegeneration: acute ischemia and chronic neurodegenerative diseases. *J. Cereb. Blood Flow Metab.* **19** (4), 351-369.

Fletcher, E.J., Martin, D., Aram, J.A., Honoré, L. & Honoré, T. (1988). Quinoxalinediones selectively block quisqualate and kainate receptors and synaptic events in rat neocortex and hippocampus and frog spinal cord *in vitro*. *Br. J. Pharmacol.* **95,** 585-597.

Fodor, S.P.A., Read, J.L., Pirrung, M.C., Stryer, L., Lu, A.T. & Solas, D. (1991). Light-directed, spatially addressable parallel chemical synthesis. *Science* **251,** 767-773.

Foster, A.C., Gill, R., Iverson, L.L. & Woodruff, G.W. (1987). Systemic administration of MK-801 protects against ischemia-induced hippocampal neurodegeneration in the gerbil. *Br. J. Pharmacol. Proc. Suppl.* **90,** 9P.

Frandsen, A. & Schousboe, A. (1987). Time and concentration dependency of the toxicity of excitatory amino acids on cerebral neurones in primary culture. *Neurochem. Int.* **10** (4), 583-591.

Frandsen, A., Drejer, J. & Schousboe, A. (1989). Direct evidence that excitotoxicity in cultured neurons is mediated via N-methyl-D-aspartate (NMDA) as well as non-NMDA receptors. *J. Neurochem.* **53,** 297-299.

Frandsen, A. & Schousboe, A. (1993). Excitatory amino acid-mediated cytotoxicity and calcium homeostasis in cultured neurons. *J. Neurochem.* **60** (4), 1202-1211.

Franza B.R., Rauscher, F.J., Josephs, S.F. & Curran, T. (1988). The Fos complex and Fos-related antigens recognise sequence elements that contain AP-1 sites. *Science* **239,** 1150-1153.

Garthwaite, G. & Garthwaite, J. (1986). Amino acid neurotoxicity: Intracellular sites of calcium accumulation associated with the onset of irreversible damage to rat cerebellar-neurones *in vitro*. *Neurosci. Lett.* **71,** 53-58.

Gasic, G.P. & Hollmann, M. (1992). Molecular neurobiology of glutamate receptors. *Annu. Rev. Physiol.* **54,** 507-536.

Gasull, T., DeGregorio-Rocasolano, N., Zapata, A. & Trullas, R. (2000). Choline release and inhibition of phosphatidylcholine synthesis precede excitotoxic neuronal death but not neurotoxicity induced by serum deprivation. *J. Biol. Chem.* **275,** 18350-18357.

Gentz, R., Rauscher, F.J.III, Abate, C. & Curran, T. (1989). Parallel association of Fos and Jun leucine zippers juxtaposes DNA binding domains. *Science* **243,** 1695-1699.

Ghosh A., Ginty, D.D., Bading, H. & Greenberg, M.E. (1994). Calcium regulation of gene expression in neuronal cells. *J. Neurobiol.* **25** (3), 294-303.

Ghosh, A. & Greenberg, M. (1995). Calcium signalling in neurons: molecular mechanisms and cellular consequences. *Science* **268,** 239-247.

Ginty, D.D. (1997). Calcium regulation: Isn't that spatial? *Neuron* **18,** 183-186.

Glanzmam, D.L., Kandel, E.R. & Schacher, S. (1990). Target-dependent structural changes accompanying long-term synaptic facilitation in Alpysia neurons. *Science* **249,** 799-802.

Goddard, G.V., Mc Intyre, D.C. & Leech, C.K. (1969). A permanent change in brain function resulting from daily electrical stimulation. *Exp. Neurol.* **25,** 295-330.

Goldberg, M.P., Weiss, J.H., Pham, P.C. & Choi, D.W. (1987). N-methyl-D-aspartate receptors mediate hypoxic neuronal injury in cortical culture. *J. Pharmacol. Exp. Ther.* **243** (2), 784-791.

Gorman, A.M., Scott, M.P., Rumbsy, P.C., Meredith, C. & Griffiths, R. (1995). Excitatory amino-acid induced cytotoxicity in primary cultures of mouse cerebellar granule cells correlates with elevated, sustained *c-fos* proto-oncogene expression. *Neurosci. Lett.* **191**, 116-120.

Graves, D.J. (1999). Powerful tools for genetic analysis come of age. *Trends Biotechnol.* **17,** 127-134.

Greenberg, M.E., Greene, L.A. & Ziff, E.B. (1985). Nerve growth factor and epidermal growth factor induce rapid transient changes in proto-oncogene transcription in PC12 cells. *J. Biol. Chem.* **260,** 14101-14110.

Greenberg, M.E., Ziff, E.B. & Greene, L.A. (1986). Stimulation of neuronal acetylcholine receptors induces rapid gene transcription. *Science* **234,** 80-83.

Greenberg, M.E., Thompson, M.A. & Sheng, M. (1992). Calcium regulation of immediate early gene transcription. *J. Physiol.* **86,** 99-108.

Greene, L.A. & Tischler, A. (1982). PC12 cultures in neurobiological research. *Adv. Cell. Neurobiol.* **3,** 373-414.

Griffiths, R., Malcolm, C., Ritchie, L., Frandsen, A., Schousboe, A., Scott, M., Rumbsy, P. & Meredith, C. (1997). Association of *c-fos* mRNA expression and excitotoxicity in primary cultures of mouse neocortical and cerebellar neurons. *J. Neurosci. Res.* **48,** 533-542.

Griffiths, R., Ritchie, L., Lidwell, K., Grieve, A., Malcolm, C.S., Scott, M. & Meredith, C. (1998). Calcium influx via L-type voltage-gated channels mediates the delayed, elevated increases in steady-state *c-fos* mRNA levels in cerebellar granule cells exposed to excitotoxic levels of glutamate. *J. Neurosci. Res.* **52,** 641-652.

Griffiths, R., Grieve, A., Scollon J., Scott, M., Williams, C. & Meredith, C. (2000). Preliminary evaluation of an *in vitro* test for assessment of excitotoxicity by measurement of early gene (*c-fos* mRNA) levels. *Toxicol. In Vitro* **14,** 447-458.

Griffiths,T., Evans, M.C. & Meldrum, B.S. (1983). Intracellular calcium accumulation in rat hippocampus during seizures induced by bicuculline or L-allylglycine. *Neurosci.* **10,** 385-395.

Guatelli, J.C., Whitfield, K.M., Kwoh, D.Y., Barringer, K.J., Richman, D.D. & Gingeras, T.R. (1990). Isothermal, *in vitro* amplification of nucleic acids by a multienzyme reaction modelled after retroviral replication. *Proc. Natl. Acad. Sci. USA* **87** (19), 7797

Gunter, T.E., Gunter, K.K., Sheu, S-S. & Gavin, C.E. (1994). Mitochondrial calcium transport: physiological and pathological relevance. *Am. J. Physiol.* **267,** C313-C339.

Gunter, K.K. & Gunter, T.E. (1994). Transport of calcium by mitochondria. *J. Bioenerg. Biomembr.* **26,** (5) 471-485.

Hai, T. & Curran, T. (1991). Cross-family dimerization of transcription factors Fos/Jun and ATF/CREB alters DNA binding specificity. *Proc. Natl. Acad. Sci. USA.* **88** (9), 3720-3724.

Haldeman, S. & Lennon, H. (1972). The antagonistic action of glutamic acid diethylester towards amino acid-induced and synaptic excitation of central neurones. *Brain Res.* **45,** 393-400.

Hamberger, A.C., Chiang, G.H., Nylen, E.S., Scheff, S.W. & Cotman, C.W. (1979). Glutamate as a CNS transmitter. Evaluation of glucose and glutamine as precursors for the synthesis of preferentially released glutamate. *Brain Res.* **168,** 513-530.

Hansen, A.J. (1985). Effect of anoxia on ion distribution in the brain. *Physiol. Rev.* **65** (1), 101-148.

Harrison, N.L. & Simmons, M.A. (1985). Quantitative studies on some antagonists of N-methyl-D-aspartate in slices of rat cerebral cortex. *Br. J. Pharmacol.* **84,** 381-391.

Hayashi, T. (1954). Effects of sodium glutamate on the nervous system. *Keio. J. Med.* **3,** 183-192.

Hengerer, B., Lindholm, D., Heumann, R., Ruther, U., Wagner, E.F. & Thoenen, H. (1990). Lesion-induced increase in nerve growth factor mRNA is mediated by *c-fos*. *Proc. Natl. Acad. Sci. USA.* **87** (10), 3899-3903.

Herdegen, T. & Leah, J.D. (1998). Inducible and constitutive transcription factors in the mammalian nervous system: control of gene expression by Jun, Fos and Krox, and CREB/ATF proteins. *Brain Res. Rev.* **28,** 370-490.

Hertz, L., Juurlink, B.H.J. & Szuchet, S. (1985). Cell cultures. In Lajtha A (ed) *"Handbook of Neurochemistry"*, ed. 2. New York: Plenum Press **8,** 603-661.

Herzog, K.H. & Morgan, J.I. (1996). Cellular immediate-early genes and cell death in the nervous system. *Neuropathol. Appl. Neurobiol.* **22** (6), 484-488.

Heurteaux, C., Messier, C., Destrade, C. & Lazdunski, M. (1993). Memory processing and apamin induce immediate early gene expression in mouse brain. *Mol. Brain Res.* **18,** 17-22.

Hill, D.E., Hope, I.A., Macke, J.P. & Struhl, K. (1986). Saturation mutagenesis of the yeast his3 regulatory site: Requirements for transcriptional induction and for binding by GCN4 activator protein. *Science* **234,** 451-457.

Hirai, S-I., Ryseck, R-P. & Mechta, F. (1989). Characterisation of *jun-D*: a new member of the *jun* proto-oncogene family. *EMBO. J.* **8,** 1433-1439.

Hiroi, N., Marek, G.J., Brown, J.R., Je, H., Saudou, F., Vaidya, V.A., Duman, R.S., Greenberg, M.E. & Nestler, E.J. (1998). Essential role of the *fosB* gene in molecular, cellular and behavioural actions of chronic electroconvulsive seizures. *J. Neurosci.* **18** (17), 6952-6962.

Hod, Y. (1992). A simplified ribonuclease protection assay. *Biotechniques* **13** (6), 852-854.

Honoré, T., Davies, S.N., Drejer, J., Fletcher, E.J., Jacobson, P., Lodge, D. & Nielson, F.E. (1988). Quinoxalinediones: potent competitive non-NMDA glutamate receptor antagonists. *Science* **241,** 701-703.

Hou, Y-N., Cebers, G., Terenius, L. & Liljequist, S. (1997). Characterisation of NMDA- and AMPA-induced enhancement of AP-1 DNA binding activity in rat cerebellar granule cells. *Brain Res.* **754,** 79-87.

Hsu, J.C., Bravo, R. & Taub, R. (1992). Interaction among LRF-1, JunB, c-Jun and c-Fos define a regulatory program in the G1 phase of liver regeneration. *Mol. Cell Biol.* **12,** 4654-4665.

Huettner, J.E. & Bean, B.P. (1988). Block of N-methyl-D-aspartate-activated current by the anticonvulsant MK-801: Selective binding to open channels. *Proc. Natl. Acad. Sci. USA* **85,** 1307-1311.

Hughes, P., Singleton, K. & Dragunow, M. (1994). MK-801 does not attenuate immediate-early gene expression following an amygdala afterdischarge. *Exp. Neurol.* **128,** 276-283.

Hughes, P. & Dragunow, M. (1995). Induction of immediate-early genes and the control of neurotransmitter-regulated gene expression within the nervous system. *Pharmacol. Rev.* **47** (1), 133-178.

Hughes, P., Alexi, T., Walton, M., Williams, C.E., Dragunow, M., Clark, R.G. & Gluckman, P.D. (1999). Activity and injury-dependent expression of inducible transcription factors, growth factors and apoptosis-related genes within the central nervous system. *Prog. In Neurobiol.* **57,** 421-450.

Isaacson, J.S. & Nicoll, R.A. (1993). The uptake inhibitor L-*trans*-PDC enhances responses to glutamate but fails to alter the kinetics of excitatory synaptic currents in the hippocampus. *J. Neurophysiol.* **70,** 2187-2191.

Ito, M. (1989). Long-term depression. *Ann. Rev.Neurosci.* **12,** 85-102.

Jahr, C.E. & Stevens, C.F. (1987). Glutamate activates multiple single channel conductances in hippocampal neurons. *Nature* **325,** 522-525.

Jenkins, B.G., Koroshetz, W.J., Beal, M.F. & Rosen, B.R. (1993). Evidence for impairment of energy metabolism *in vivo* in Huntington's disease using localized ^{1}H NMR spectroscopy. *Neurology* **43,** 2689-2695.

Johnson, J.W. & Ascher, P. (1987). Glycine potentiates the NMDA response in cultured mouse brain neurons. *Nature* **325,** 529-531.

Johnston, G.A.R., Curtis, D.R., Davies, J. & Mc Culloch, R.M. (1974). Spinal interneurone excitation by conformationally restricted analogues of L-glutamic acid. *Nature* **248,** 804-805.

Jones, K.A. & Baughman, R.W. (1991). Both NMDA and non-NMDA subtypes of glutamate receptors are concentrated at synapses on cerebral cortical neurons in culture. *Neuron* **7,** 593-603.

Jordan, J.A. (2000). Real-time detection of PCR products and microbiology. *Trends in Microbiology*, 61-66.

Joseph, L.J., Le Beau, G.A., Jamieson, G.A., Acharya, S., Shows, J.D., Rowley, J.D. & Sukhatme, V.P. (1988). Molecular cloning, sequencing and mapping of EGR2, a human

early growth response gene encoding a protein with zinc-binding finger structure. *Proc. Natl. Acad. Sci. USA* **85,** 7164-7168.

Kaczmarek, L. (1993a). Glutamate-receptor driven gene expression in learning. *Acta. Neurobiol. Exp.* **53,** 187-196.

Kaczmarek, L. (1993b). Molecular biology of vertebrate learning: is *c-fos* a new beginning? *J. Neurosci. Res.* **34,** 377-381.

Kaczmarek, L., Kossut, M. & Skangiel-Kramska, J. (1997). Glutamate receptors in cortical plasticity: Molecular and cellular biology. *Physiol. Rev.* **77** (1), 217-256.

Kanner, B.I. & Sharon, I. (1978). Active transport of L-glutamate by membrane vesicles isolated from rat brain. *Biochemistry* **17,** 3949-3953.

Kerppola, T.K. & Curran, T. (1991). Fos-Jun heterodimers and Jun homodimers bend DNA in opposite orientations: implications for transcription factor co-operativity. *Cell* **66,** 317-326.

Kerr, J.F.R., Wyllie, A.H. & Currie, A.R. (1972). Apoptosis: a basic biological phenomenon with wide-ranging implications in tissue kinetics. *Br. J. Cancer* **26,** 239-257.

Kerr, J.F.R. & Harmon, B.V. (1991). *Apoptosis: The molecular basis of cell death: current communications on cell and molecular biology* (Cold Spring Harbour Lab. Press, Plainview, N.Y.), **3,** 5-29.

Kessler, M., Baudry, M. & Lynch, G. (1989). Quinoxaline derivatives are high-affinity antagonists of the NMDA receptor-associated glycine sites. *Brain Res.* **489,** 377-382.

Koh, J-Y., Peters, S. & Choi, D.W. (1986). Neurons containing NADPH-diaphorase are selectively resistant to quinolinate toxicity. *Science* **243,** 73-76.

Koh, J-Y., Goldberg, M.P., Hartley, D.M. & Choi, D.W. (1990). Non-NMDA receptor-mediated neurotoxicity in cortical culture. *J. Neurosci.* **10** (2), 693-705.

Koh, J-Y. & Choi, D.W. (1991). Selective blockade of non-NMDA receptors does not block rapidly triggered glutamate-induced neuronal death. *Br. Res.* **548,** 318-321.

Koh, J-Y. & Cotman, C.W. (1992). Programmed cell death: Its possible contribution to neurotoxicity mediated by calcium channel antagonists. *Brain Res.* **587,** 233-240.

Kouzarides, T. & Ziff, E. (1988). The role of the leucine zipper in the *fos-jun* interaction. *Nature* **336,** 646-651.

Kroemer, G., Zamzami, N. & Susin, S.A. (1997). Mitochondrial control of apoptosis. *Immunol. Today* **18** (1), 44-51.

Krnjevic, K. & Phillis, J.W. (1963). Iontophoretic studies of neurones in the mammalian cerebral cortex. *J. Physiol.* **165,** 274-304.

Kwoh, D.Y., Davis, G.R., Whitfield, K.M., Chappelle, H.L., DiMichele, L.J. & Gingeras, T.R. (1989). Transcription-based amplification system and detection of amplified human immunodeficiency virus type 1 with a bead-based sandwiched hybridisation format. *Proc. Natl. Acad. Sci. USA* **86** (4), 1173-1177.

Labiner, D.M., Butler, L.S., Cao, Z., Hosford, D.A., Shin, C. & Mc Namara, J.O. (1993). Induction of *c-fos* mRNA by kindled seizures: complex relationship with neuronal burst firing. *J. Neurosci.* **13** (2), 744-751.

Lander, E. (1999). Array of hope. *Suppl. Nat. Genet.* **21,** 3-4.

Landschulz, W.H., Johnson, P.F. & Mc Knight, S.L. (1988). The leucine zipper: A hypothetical structure common to a new class of DNA binding proteins. *Science* **240,** 1759-1764.

Lau, L.F. & Nathans, D. (1987). Expression of a set of growth-related immediate early genes in BABl/c3T3 cells: co-ordinate regulation with *c-fos* or *c-myc*. *Proc. Natl. Acad. Sci. USA* **84,** 1182-1186.

Lee, W.M.F., Mitchell, P. & Tjian, R. (1987). Purified transcription factor AP-1 interacts with TPA-inducible enhancer elements. *Cell* **49,** 741-752.

Lee, W.M.F., Lin, C. & Curran, T. (1988). Activation of the transforming potential of the human *fos* proto-oncogene requires message stabilization and results in increased amounts of partially modified *fos* protein. *Mol. Cell. Biol.* **8,** 5521-5527.

Lehmann, J., Schneider, J., Mc Pherson, S., Murphy, D.E. & Bernard, P. (1987). CPP, a selective N-methyl-D-aspartate (NMDA)-type receptor antagonist: characterisation *in vivo* and *in vitro*. *J. Pharmacol. Exp. Ther.* **240,** 737-746.

Leist, M. & Nicotera, P. (1998). Apoptosis, Excitotoxicity and Neuropathology. *Exp. Cell. Res.* **239,** 183-201.

Leist, M., Single, B., Castoldi, A.F., Kühnle, S. & Nicotera, P. (1997). Intracellular adenosine triphosphate (ATP) concentration: A switch in the decision between apoptosis and necrosis. *J. Exp. Med.* **185** (8), 1481-1486.

Lennon, G.G. & Lehrach, H. (1991). Hybridization analyses of arrayed cDNA libraries. *Trends Genet.* **7,** 314-317.

Liang, P. & Pardee, A.B. (1992). Differential display of eukaryotic messenger RNA by means of the polymerase chain reaction. *Science* **257,** 967-971.

Lidwell, K. & Griffiths, R. (2000). Possible role for the FosB/JunD AP-1 transcription factor complex in glutamate-mediated excitotoxicity in cultured cerebellar granule cells. *J. Neurosci. Res.* **62,** 427-439.

Lipton, S.A. & Nicotera, P. (1998). Excitotoxicity, free radicals, necrosis and apoptosis. *Neuroscientist* **4,** 345-352.

Lipshutz., R.J., Fodor, S.P.A., Gingeras, T.R. & Lockhart, D.J. (1999). High density synthetic oligonucleotide arrays. *Nature* **21,** 20-24.

Lipton, S.A. & Rosenberg, P.A. (1994). Excitatory amino acids as a final common pathway for neurologic disorder. *N. Engl. J. Med.* **330,** 613-622.

Lodge, D., Anis, N.A. & Burton, N.R. (1982). Effects of optical isomers of ketamine on excitation of cat and rat spinal neurons by amino acids and acetylcholine. *Neurosci. Lett.* **29,** 281-286.

Lodge, D. & Johnson, G.A.R. (1985). Effect of ketamine on amino-acid evoked release of acetylcholine from rat cerebral cortex *in vitro*. *Neurosci. Lett.* **56,** 371-375.

Logan, W.J. & Synder, S.H. (1972). High affinity uptake systems for Glycine, Glutamic acid and Aspartic acids in synaptosomes of rat central nervous tissues. *Brain Res.* **42,** 413-431.

Lucas, D.R. & Newhouse, J.P. (1957). The toxic effect of sodium L-glutamate on the inner layers of the retina. *AMA Arch. Ophthalmol.* **58,** 193-201.

Lynch, G., Larson, J., Kelso, S., Barrionuevo, G. & Schottler, F. (1983). Intracellular injections of EGTA block induction of hippocampal long-term potentiation. *Nature* **305,** 716-721.

Lysko, P.G., Cox, J.A., Vigano, M.A. & Hennebery, R.C. (1994). Excitatory amino acid neurotoxicity at the N-methyl-D-aspartate receptor in cultured neurons: pharmacological characterisation. *Brain Res.* **499,** 258-266.

Mac Dermott, A.B., Mayer, M.L., Westbrook, G.L., Smith, S.J., & Baker, J.L. (1986). NMDA-receptor activation increases cytoplasmic calcium concentration in cultured spinal cord neurones. *Nature* **321,** 519-522.

Mac Dermott, A. & Dale, N. (1987). Receptors, ion channels and synaptic potentials underlying the integrative actions of excitatory amino acids. *Trends Neurosci.* **10** (7), 280-284.

Mac Donald, J.F. & Wojowicz, J.M. (1980). Two conductance mechanisms activated by applications of L-glutamate, L-aspartic, DL-homocysteic, N-methyl-D-aspartic and DL-kainic acids to cultured mammalian central neurones. *Can. J. Physiol. Pharmacol.* **58,** 1393-1397.

Maki, Y., Bos, T.J., Davies, C., Starbuck, M. & Vogt, P.K. (1987). Avian sarcoma virus 17 carries a new oncogene, *jun*. *Proc. Natl. Acad. Sci. USA* **84,** 2848-2852.

Malcolm, C., Griffiths, R., Rumbsy, P. & Meredith, C. (1997). Differential profiles of *c-fos* expression within primary cultures of mouse cerebellar granule cells stimulated with the excitatory amino acid L-glutamate: correlation with excitotoxic outcome and derivation of a predictive index. *Toxicol. in Vitro* **11,** 505-507.

Malenka, R.C., Kauer, J.A., Zucker, R.J. & Nicoll, R.A. (1988). Postsynaptic calcium is sufficient for potentiation of hippocampal synaptic transmission. *Science* **242,** 81-84.

Martin, D.P., Wallace, L. & Johnson, E.M. (1990). Cytosine arabinoside kills postmitotic neurons in a fashion resembling tropic factor deprivation: evidence that a deoxycytidine-dependent process may be required for nerve growth factor signal transduction. *J. Neurosci.* **10** (1), 184-193.

Martin, L.J., Al-Abdulla, N.A., Brambink, A.M., Kirsch, J.R., Sieber, F.E. & Portera-Cailliau, C. (1998). Neurodegeneration in excitotoxicity, global cerebral ischemia, and target deprivation: A perspective on the contributions of apoptosis and necrosis. *Brain Res. Bul.* **46** (4), 281-309.

Mattson, M.P., Guthrie, P.B. & Kater, S.B. (1988). Intracellular messengers in the generation and degeneration of hippocampal neuroarchitecture. *J. Neurosci. Res.* **21,** 464-467.

Mattson, M.P. & Kater, S.B. (1989). Excitatory and inhibitory neurotransmitters in the generation and degeneration of hippocampal neuroarchitecture. *Brain Res.* **478,** 337-348.

Mattson, M.P., Pederson, W.A., Duan, W., Culmsee, C. & Camandola, S. (1999). Cellular and molecular mechanisms underlying perturbed energy metabolism and neuronal degeneration in Alzheimer's and Parkinson's disease. *Ann. N.Y. Acad. Sci.* **893,** 154-175.

Mattson, M.P., Duan, W., Chan, S.L. & Camandola, S. (2000). Par-4: an emerging pivotal player in neuronal apoptosis and neurodegenerative disorders. *J. Mol. Neurosci.* **13,** 17-30.

Mayer, M.L., Westbrook, G.L. & Guthrie, P.B. (1984). Voltage-dependent block by Mg^{2+} of NMDA responses in spinal cord neurones. *Nature* **309,** 261-264.

Mayer, M.L., Mac Dermott, A.B., Mayer, M.L., Westbrook, G.L., Smith, S.J. & Baker, J.L. (1987). Agonist- and voltage-gated calcium entry in cultured mouse spinal cord neurons under clamp measured using arsenazo III. *J. Neurosci.* **7,** 3230-3244.

Mayer, M.L. & Westbrook, G.L. (1987). Cellular mechanisms underlying excitotoxicity. *Trends Neurosci.* **10,** 59-61.

Mayer, M.L., Vycklicky, L. & Clements, J. (1989). Regulation of NMDA receptor desensitization in mouse hippocampal neurons. *Nature* **338,** 425-427.

Mayer, M.L. & Miller, R.J. (1990). Excitatory amino acid receptors, second messengers and regulation of intracellular Ca^{2+} in mammalian neurons. *Trends Pharmacol. Sci.* **11,** 245-260.

Mc Cormack, J.G. & Denton, R.M. (1993). Mitochondrial Ca^{2+} transport and the role of intramitochondrial Ca^{2+} in the regulation of energy metabolism. *Dev. Neurosci.* **15,** 165-173.

Mc Namara, J.O. (1994). Cellular and molecular basis of epilepsy. *J. Neuosci.* **14** (6), 3413-3425.

Meberg, P.J., Gall, C.M. & Routtenberg, A. (1993). Induction of FI/GAP-43 gene: expression in hippocampal granule cells after seizures. *Mol. Brain Res.* **17,** 295-297.

Mechta, F., Piette, J., Hirai, S-I. & Yaniv, M. (1989). Stimulation of protein kinase C or protein kinase; A mediated signal transduction pathways shows three modes of response among serum inducible genes. *New Biologist* **3,** 297-304.

Meier, E. & Schousboe, A. (1982). Differences between GABA receptor binding to membranes from cerebellum during postnatal development and from cultured cerebellar granule cells. *Dev. Neurosci.* **5,** 546-553.

Meldrum, B. (1985). Possible therapeutic applications of antagonists of excitatory amino acid transmitters. *Clin. Sci.* **68,** 113-122.

Meldrum, B.S. (1994). The role of glutamate in epilepsy and other CNS disorders. *Neurology* **44,** 14-23.

Melton, D.A., Kreg, P.A., Rebaggliati, M.R., Maniatis, T., Zinn, K. & Green, M.R. 1984). Efficient *in vitro* synthesis of biologically active RNA and RNA hybridisation probes from plasmids containing a bacteriophage SP6 promoter. *Nucleic Acids Research* **12** (18), 7035-7056.

Meredith, C., Scott, M., Rumbsy, P., Frandsen, A., Schousboe, A., Gorman, A. & Griffiths, R. (1996). Sustained *c-fos* expression is associated with excitotoxicity during the development of neuronal cells *in vitro*. *Biochem. Soc. Trans.* **24,** 6S.

Mesner, P.W., Epting, C.L., Hegarty, J.L. & Green, S.H. (1995). A timetable of events during programmed cell death induced by trophic factor withdrawal from neuronal PC12 cells. *J. Neurosci.* **15,** 7357-7366.

Messer, A. (1977). The maintenance and identification of mouse cerebellar granule cells in monolayer cultures. *Brain Res.* **130,** 1-12.

Michaelis, E.K. (1998). Molecular biology of glutamate receptors in the central nervous system and their role in excitotoxicity, oxidative stress and aging. *Prog. Neurobiol.* **54,** 369-415.

Milbrandt, J. (1986). Nerve growth factor rapidly induces *c-fos* mRNA in PC12 rat pheochromocytoma cells. *Proc. Natl. Acad. Sci. USA* **83,** 4789-4793.

Mills, E.M., Gunaseker, P.G., Pavlakovic, G. & Isom, G.E. (1996). Cyanide-induced apoptosis and oxidative stress in differentiated PC12 cells. *J. Neurochem.* **67,**1039-1046.

Monaghan, D.T., Bridges, R.J. & Cotman, C.W. (1989). The excitatory amino acid receptors: their classes, pharmacology, and distinct properties in the function of the central nervous system. *Ann. Rev. Pharmacol. Toxicol.* **29,** 365-402.

Mooney, R., Madison, D.V. & Shatz, C. (1993). Enhancement of transmission at the developing retinugeniculate synapse. *Neuron* **11,** 815-825.

Moratalla, R., Vickers, E.A., Robertson, H.A, Cochran, B.H. & Graybiel, A.M. (1993). Co-ordinate expression of *c-fos* and *jun-B* is induced in the striatum by cocaine. *J. Neurosci.* **13,** 423-433.

Morgan, J.I. & Curran, T. (1986). Role of ion flux in the control of *c-fos* expression. *Nature* **322,** 552-555.

Morgan, J.I., Cohen, D. R., Hempstead, J. I. & Curran, T. (1987). Mapping patterns of *c-fos* expression in the central nervous system after seizure. *Science* **237,** 192-197.

Morgan, J.I. & Curran, T. (1991). Stimulus transcription coupling in the nervous system: involvement of the inducible proto-oncogenes *fos* and *jun*. *Ann. Rev. Neurosci.* **14,** 421-451.

Morgan, J.I. & Curran, T. (1995). The immediate-early gene response and neuronal death and regeneration. *The Neuroscientist* **1,** 68-75.

Morris, R.G.M., Anderson, E., Lynch, G.S. & Baudry, M. (1986). Selective impairment of learning and blockade of long-term potentiation by an N-methyl-D-aspartate receptor antagonist, AP5. *Nature* **319,** 774-776.

Mosmann, T. (1983). Rapid colorimetric assay for cellular growth and survival: application to proliferation and cytotoxicity assays. *Journal of Immunological Methods* **65,** 55-63.

Muller, R., Bravo, R., Burckhardt, J. & Curran, T. (1984). Induction of *c-fos* gene and protein by growth factors precedes activation of *c-myc*. *Nature* **312,** 716-720.

Mumberg, D., Lucibello, F.C., Schuermann, M. & Müller, R. (1991). Alternative splicing of *fosB* transcripts results in differentially expressed mRNAs encoding functionally antagonistic proteins. *Genes Dev.* **5,** 1212-1223.

Murphy, S.N. & Miller, R.J. (1988). A glutamate receptor regulates Ca^{2+} mobilization in hippocampal neurons. *Proc. Natl. Acad. Sci. USA* **85,** 8737-8741.

Murphy, T.H., Worley, P.F. & Baraban, J.M. (1991). L-type voltage-sensitive calcium channels mediate synaptic activation of immediate early genes. *Neuron* **7,** 625-635.

Nadler, J.V., Vaca, K.W., White, W.F., Lynch, G.S. & Cotman, C.W. (1976). Aspartate and glutamate as possible transmitters of excitatory hippocampal afferents. *Nature* **260,** 538-540.

Nadler, J.V., Perry, B.W., Gentry, C. & Cotman, C.W. (1980). Degeneration of hippocampal CA3 pyramidal cells induced by intraventricular Kainic acid. *J. Comp. Neurol.* **192,** 333-359.

Nakabeppu, Y. & Nathans, D. (1991). A naturally occurring truncated form of FosB that inhibits Fos/Jun transcriptional activity. *Cell* **64,** 751-759.

Naito, S. & Ueda, T. (1983). Adenosine triphosphate-dependent uptake of glutamate into protein I-associated vesicles. *J. Biol. Chem.* **258,** 696-699.

Nestler, E.J., Hope, B.T. & Widnell, K.L. (1993). Drug addiction: a model for the molecular basis of neural plasticity. *Neuron* **11,** 995-1006.

Neuberg, M., Adamkiewicz, J., Hunter, J.B. & Müller, R. (1989). A *fos* protein containing the *jun* leucine zipper forms a homodimer which binds to the AP-1 binding site. *Nature* **341,** 243-245.

Nguyen, P.V. & Atwood, H.L. (1994). Altered impulse activity modifies synaptic physiology and mitochondria in crayfish phasic motor neurons. *J. Neurophysiol.* **72,** 2944-2955.

Nicholls, D.G & Åkerman, K.E.O. (1982). Mitochondrial calcium transport. *Biochim. Biophys. Acta.* **683,** 57-88.

Nicholls, D.G & Atwell, D. (1990). The release and uptake of excitatory amino acids. *Trends Neurosci.* **11,** 462-468.

Nicholls, D.G & Budd, S.L. (1990). Mitochondria and neuronal glutamate excitotoxicity. *Biochim. Biophys. Acta.* **1366,** 97-112.

Nicholls, D.G & Budd, S.L. (1998). Neuronal excitotoxicity: the role of mitochondria. *Biofactors.* **8** (3-4), 287-299.

Nicholls, D.G & Budd, S.L. (2000). Mitochondria and neuronal survival. *Physiol. Rev.* **80** (1), 315-360.

Nicholls, D.G. & Scott, I.D. (1980). The regulation of brain mitochondrial calcium-ion transport: the role of ATP in the discrimination between kinetic and membrane potential-dependent Ca^{2+} efflux mechanisms. *Biochem. J.* **186,** 833-839.

Nicoletti, F., Iadarola, M.J., Wrobelwski, J.T., & Costa, E. (1986). Excitatory amino acid recognition sites coupled with inositol phospholipid metabolism. Developmental changes and interaction with alpha$_1$-adrenoceptors. *Proc. Natl. Acad. Sci. USA.* **83,** 1931-1935.

Nicoletti, F., Wrobelwski, J.T., Fadda, E. & Costa, E. (1988). Pertussis toxin inhibits signal transduction at a specific metabotropic glutamate receptor in primary cultures of cerebellar granule cells. *Neuropharmacol.* **27,** 551-556.

Nicoletti, F., Magri, G., Ingrao, F., Bruno, V., Catania, M.V., Ell'Albani, P., Conorelli, D.F. & Avola, R. (1990). Excitatory amino acids stimulate inositol phospholipid hydrolysis and reduce proliferation in cultured astrocytes. *J. Neurochem.* **27,** 771-777.

Nicotera, P., Bellomo, G. & Orrenius, S. (1992). Calcium-mediated mechanisms in chemically induced cell death. *Ann. Rev. Pharmacol. Toxicol.* **32,** 449-470.

Nicotera, P., Ankarcrona, M., Bonfoco, E., Orrenius, S. & Lipton, S.A. (1996). Neuronal apoptosis versus necrosis induced by glutamate or free radicals. *Apoptosis* **1,** 5-10.

Nishina, H., Sato, H., Suzuki, T., Sato, N. & Iba, H. (1990). Isolation and characterisation of Fra-2, an additional member of the *fos* gene family. *Proc. Natl. Acad. Sci. USA* **87,** 3619-3623.

Nowak, L., Bregestovski, P., Ascher, P., Herbet, A. & Prochiantz, A. (1986). Magnesium gates glutamate-activated channels in mouse central neurones. *Nature* **307,** 462-465.

Okubo, K., Hori, N., Matoba, R., Niiyama, T., Fukushima, A. & Kojima, Y. (1992). Large scalle cDNA sequencing for analysis of quantitative and qualitative aspects of gene expression. *Nature Genetics* **2,** 173-179.

Olney, J.W. (1969). Brain lesion, obesity and other disturbances in mice treated with monosodium glutamate. *Science* **164,** 719-721.

Olney, J.W., OL, H. & Rhee, V. (1971). Cytotoxic effects of acidic and sulphur containing amino acids on the infant mouse central nervous system. *Exp. Brain Res.* **14,** 61-76.

Olney, J.W. (1971). Glutamate induced necrosis in the infant mouse hypothalamus; an electron microscopic study. *J. Neuro-pathol. Exp. Neurol.* **30,** 75-90.

Olney, J.W. (1978). Neurotoxicity of excitatory amino acids. In: Mc Geer, E., Olney, J.W., Mc Geer, P., editors. Kainic acid as a tool in neurobiology. New York, Raven Press, 95-121.

Olney, J.W., Collins, R.C. & Sloviter, R.S. (1986). Excitotoxic mechanisms of epileptic brain damage. *Adv. Neurol.* **44,** 857-877.

Olverman, H.J., Jones, A.W. & Watkins, J.C. (1988a). [^{3}H]-2-Amino-5-phosphono-pentanoate as a ligand for N-methyl-D-aspartate receptors in the mammalian central nervous system. *Neurosci.* **26,** 1-15.

Olverman, H.J., Jones, A.W., Mewett, K.N. & Watkins, J.C. (1988b). Structure/activity relations of N-methyl-D-aspartate receptor ligands as studied by their inhibition of [^{3}H]-2-Amino-5-phosphono-pentanoic acid binding in rat brain membranes. *Neurosci.* **26,** 17-31.

Oppenheim, R.W. (1991). Cell death during development of the nervous system. *Ann. Rev. Neurosci.* **14,** 453-501.

O'Shea, E.K., Rutkowski, R., Stafford, W.F.III & Kim, P.S. (1989). Preferential heterodimer formation by isolated leucine zippers from Fos and Jun. *Science* **245,** 646-648.

Osipenko, O., Mike, A., Gyevai, A. & Vizi, E.S. (1994). Evidence that GYKI 52466, a novel non-NMDA antagonist enhances the decay of kainate-induced current in cultured chicken cortical neurons. *Develop. Brain Res.* **77,** 257-263.

Pabo, C.O. & Sauer, R.T. (1992). Transcription factors: Structural families and principles of DNA recognition. *Annu. Rev. Biochem.* **61,** 1053-1095.

Parker, R.M.C. & Barnes, N.M. (1999). MRNA: Detection by *in situ* and Northern Hybridization. *Methods in Molecular Biology* **106,** 247-283.

Partin, K.M., Patneau, D.K., Winters, C.A., Mayer, M.L. & Buonanno, A. (1993). Selective modulation of desensitisation at AMPA versus kainate receptors by cyclothiazide and concanavalin A. *Neuron* **11,** 1069-1082.

Partin, K.M. & Mayer, M.L. (1996). Negative allosteric modulation of wild-type and mutant AMPA receptors by GYKI 53655. *Mol. Pharmacol.* **49,** 142-148.

Patneau, D.K., Vyklicky, L. & Mayer, M.L. (1993). Hippocampal neurons exhibit cyclothiazide sensitive rapidly desensitising responses to kainite. *J. Neurosci.* **13,** 3496-3509.

Patneau, D.K., Wright, P.W., Winters, C., Mayer, M.L. & Gallo, V. (1994). Glial cells of the oligodendrocyte lineage express both kainate- and AMPA-preferring subtypes of glutamate receptor. *Neuron* **12,** 357-371.

Pearce, I.A., Cambray-Deakin, M.A. & Burgoyne, R.D. (1987). Glutamate acting on NMDA receptors stimulates neurite outgrowth from cerebellar granule cells. *FEBS Lett.* **223** (1), 143-147.

Peng, T-I., Jou, M-J., Sheu, S-S. & Greenamyre, J.T. (1998). Visualization of NMDA receptor-induced mitochondrial calcium accumulation in striatal neurons. *Exp. Neurol.* **149,** 1-12.

Pennypacker, K.R., Thai, L., Hong, J-S. & Mc Millian, M.K. (1994). Prolonged expression of AP-1 transcription factors in the rat hippocampus after systemic kainate treatment. *J. Neurosci.* **14** (7), 3998-4006.

Pennypacker, K.R., Hong, J-S. & Mc Millian, M.K. (1995). Implications of prolonged expression of Fos-related antigens. *Trends Pharmacol.* **16,** 317-321.

Plaitakis, A., Berl, S., & Yahr, M. (1982). Abnormal glutamate metabolism in an adult-onset degenerative neurological disorder. *Science* **216,** 193-196.

Plaitakis, A. & Caroscio, J.T. (1987). Abnormal glutamate metabolism in ALS. *Ann. Neurol.* **22,** 575-579.

Pláteník, J., Kuramoto, N. & Yoneda, Y. (2000). Molecular mechanisms associated with long-term consolidation of the NMDA signals. *Life Sciences* **67,** 335-364.

Pollard, H., Charriaut-Marlangue, C., Cantagrel, S., Represa, A., Robain, O., Moreau, J. & Ben-Ari, Y. (1994). Kainate-induced apoptotic cell death in hippocampal neurons. *Neurosci.* **63,** 7-18.

Portera-Cailliau, C., Hedreen, J.C., Price, D.L. & Koliatsos, V.E. (1995). Evidence for apoptotic cell death in Huntington's disease and excitotoxic animal models. *J. Neurosci.* **15,** 3775-3787.

Prezeau, L., Manzoni, O., Homburger, V., Sladeczek, F., Curry, K. & Bockaert, J. (1992). Characterisation of a metabotropic glutamate receptor: direct negative coupling to adenylyl cyclase and involvement of a pertussis toxin-sensitive G protein. *Proc. Natl. Acad. Sci. USA* **89,** 8040-8044.

Prezeau, L., Carrette, J., Helpap, B., Curry, K., Pin, J.P. & Bockaert, J. (1994). Pharmacological characterisation of metabotropic glutamate receptors in several types of brain cells in primary cultures. *Mol. Pharmacol.* **45,** 570-577.

Raff, M.C., Barres, B.A., Burne, J.F., Coles, H.S., Ishizaki, Y. & Jacobson, M.D. (1993). Programmed cell death and the control of cell survival: lessons from the nervous system. *Science* **262,** 695-700.

Ransone, L.J., Visvader, J., Sassone-Corsi, P. & Verma, I.M. (1989). Fos-Jun interaction: Mutational analysis of the leucine zipper domain of both proteins. *Genes Dev.* **3,** 770-781.

Rappolee, D.A., Mark, D., Banda, M.J. & Werb, Z. (1988). Wound macrophages express TGF-α and other growth factors *in vivo:* analysis by mRNA phenotyping. *Science* **241,** 708-712.

Rauscher, F.J. III, Sambucetti, L.C., Curran, T., Distel, R.J. & Spiegelman, B.M. (1988a). Common DNA binding site for Fos protein complexes and transcription factor AP-1. *Cell* **52,** 471-480.

Rauscher, F.J. III, Cohen, D.R., Curran, T., Bos, T.J., Vogt, P.K., Bohmann, D., Tjian, R. & Franza, B.R. (1988b). Fos-associated protein p39 is the product of the *jun* proto-oncogene. *Science* **240,** 1010-1016.

Rauscher, F.J. III, Voulalas, P.J., Franza, B.R. & Curran, T. (1988c). Fos and Jun bind co-operatively to the AP-1 site: reconstitution *in vitro*. *Genes Dev.* **2,** 1687-1699.

Reddy, E.P., Skalka, A.M. & Curran, T. (1988). *The Oncogene Handbook*, Elsevier, Amsterdam.

Reynolds, I.J. & Hastings, T.G. (1995). Glutamate induces the production of reactive oxygen species in cultured forebrain neurons following NMDA receptor activation. *J. Neurosci.* **15,** 3318-3327.

Reynolds, I.J. (1995). Mitochondrial membrane potential and the permeability transition in excitotoxicity. *Ann. N.Y. Acad. Sci.* **893,** 33-41.

Rockett, J.C. & Dix, D.J. (2000). DNA arrays: technology, options and toxicological applications. *Xenobiotica* **30** (2), 155-177.

Rogers, D.C. & Hunter, J. (1997). Dissociation of effects of glutamate receptor antagonists on excitotoxic and hypoxic neuronal cell death in a novel rat cortical culture system. *Brain Res.* **44** (2), 131-139.

Rozen, S. & Skaletsky, H. (1998). Primer 3 on the WWW for general users and for biologist programmers. *Methods Mol. Biol.* **132,** 365-86

Rossi, D.J. & Slater, N.T. (1993). The developmental onset of NMDA-receptor channel activity during neuronal migration. *Neuropharmacol.* **32,** 1239-1248.

Rothman, S.M. (1984). Synaptic release of excitatory amino acid neurotransmitter mediates anoxic neuronal death. *J. Neurosci.* **4,** 1884-1891.

Rothman, S.M. & Olney, J.W. (1986). Glutamate and the pathophysiology of hypoxic-ischemic brain damage. *Ann. Neurol.* **19,** 105-111.

Rothman, S.M. & Olney, J.W. (1987). Excitotoxicity and the NMDA receptor. *TINS* **10** (7), 299-302.

Rothstein, J.D. (1995). Excitotoxicity and neurodegeneration in amyotrophic lateral sclerosis. *Clin. Neurosci.* **3,** 348-359.

Ryder, K., Lau, L.F. & Nathans, D. (1988). A gene activated by growth factors is related to the oncogene v-jun. *Proc. Natl. Acad. Sci. USA* **85,** 1487-1491.

Ryder, K., Lanahan, A., Perez-Albuerne, E. & Nathans, D. (1989). Jun-D, a third member of the Jun gene family. *Proc. Natl. Acad. Sci. USA* **86,** 1500-1503.

Saccomanno, K., Gil del Alamo, P., Bassetti, M., Reza-Elahi, F. & Spada, A. (1992). *In vitro* detection of glycoprotein production and secretion by human non-functioning pituitary adenomas. *J. Endocrinol. Invest.* **16** (2), 109-115.

Saffen, D.W., Cole, A.J., Worley, P.F., Christy, B.A., Ryder, K. & Baraban, J.M. (1988). Convulsant induced increase in transcription factor messenger RNAs in rat brain. *Proc. Natl. Acad. Sci. USA* **85,** 7795-7799.

Sassone-Corsi, P., Lamph, W.W., Kamps, M. & Verma, I.M. (1988a). *fos* associated p39 is related to nuclear transcription factor AP-1. *Cell* **54,** 553-560.

Sassone-Corsi, P., Sisson, J.C. & Verma, I.M. (1988b). Transcriptional autoregulation of the proto-oncogene *fos*. *Nature* **334,** 314-319.

Sattler, R., Charlton, M.P., Hafner, M. & Tymanski, M. (1998). Distinct influx pathways, not calcium load, determine neuronal vulnerability to calcium neurotoxicity. *J. Neurochem.* **71,** 2349-2364.

Schena, M., Shalon, D., Davis, R.W. & Brown, P.O. (1995). Quantitative monitoring of gene expression patterns with a complementary DNA microarray. *Science* **270,** 467-470.

Schena, M. (1996a). Genome analysis with gene expression microarrays. *Bioessays* **18** (5), 427-431.

Schena, M., Shalon, D., Heller, R., Chai, A., Brown, P.O. & Davis, R.W. (1996b). Parallel human genome analysis: microarray-based expression monitoring of 1000 genes. *Proc. Natl. Acad. Sci. USA* **93,** 10614-10619.

Schinder, A.F., Olsen, E.C., Spitzer, N.C. & Montal, M. (1996). Mitochondrial dysfunction is a primary event in glutamate neurotoxicity. *J. Neurosci.* **16,** 6125-6133.

Schmuck, G. & Schlüter, G. (1996). An *in vitro* model for toxicological investigations of environmental neurotoxins in primary neuronal cell cultures. *Toxicology and Industrial Health* **12** (5), 683-696.

Schmuck, G., Ahr, H.J. & Schlüter, G. (2000). Rat cortical neuron cultures: An *in vitro* model for differentiating mechanisms of chemically induced neurotoxicity. *In Vitro and Molecular Toxicology* **13** (1), 37-49.

Schoepp, D.D. & Conn, P.J. (1993). Metabotropic glutamate receptors in brain function and pathology. *TiPS* **141,** 13-20.

Schousboe, A. (1981). Transport and metabolism of glutamate and GABA in neurons and glial cells. *Int. Rev. Neurobiol.* **22,** 1-45.

Schousboe, A., Drejer, J., Hansen, G.H. & Meier, E. (1985). Cultured neurons as model systems for biochemical and pharmacological studies on receptors for neurotransmitter amino acids. *Dev. Neurosci.* **7,** 252-262.

Schousboe, A., Meier, E., Drejer, J. & Hertz, L. (1989). Preparation of cultures of mouse (rat) cerebellar granule cells. In *A dissection and tissue culture manual for the nervous*

system, ed. Shahar, A., De Vellis, J.A., Vernadakis, A. & Haber, B. pp. 203-206. Liss, Alan R., New York Inc.

Schramm, M., Eimerl, S. & Costa, E. (1990). Serum and depolarizing agents cause acute neurotoxicity in cultured cerebellar granule cells: Role of the glutamate receptor responsive to *N*-methyl-D-aspartate. *Proc. Natl. Acad. Sci. USA* **87,** 1193-1197.

Schubert, D. & Piasecki, D. (2001). Oxidative glutamate toxicity can be a component of the excitotoxicity cascade. *J. Neurosci.* **21** (19), 7455-7462.

Schwartz, L.M., Smith, S.W., Jones, M.E.E. & Osborne, B.A. (1993). Do all programmed cell deaths occur via apoptosis? *Proc. Natl. Acad. Sci. USA* **90,** 980-984.

Shalon, D., Smith, S.J. & Brown, P.O. (1996). A DNA microarray system for analysing complex DNA samples using two-colour fluorescent probe hybridisation. *Genome Research* **6,** 639-645.

Shan, Y., Carlock, L.R. & Walker, P.D. (1997). NMDA receptor overstimulation triggers a prolonged wave of immediate early gene expression: relationship to excitotoxicity. *Exp. Neurol.* **144,** 406-415.

Sheardown, M.J., Nielsen, E.Ø., Hansen, A.J., Jacobsen, P. & Honoré, T. (1990). 2,3-dihydroxy-6-nitro-7-sulfamoyl-benzo(F)quinoxaline: a neuroprotectant for cerebral ischemia. *Science* **247,** 571-574.

Sheng, M. & Greenberg, M.E. (1990). The regulation and function of *c-fos* and other immediate early genes in the nervous system. *Neuron* **4,** 477-485.

Sheng, M., Mc Fadden, G. & Greenberg, M.E. (1990). Membrane depolarisation and calcium induce *c-fos* transcription via phosphorylation of transcription factor CREB. *Neuron* **4,** 571-582.

Shyu, A.B., Greenberg, M.E. & Belasco, J.G. (1989). The *c-fos* transcript is targeted for rapid decay by two distinct mRNA degradation pathways. *Genes Dev.* **3** (1), 60-72.

Siesjö, B.K. (1992). Pathophysiology and treatment of focal cerebral ischemia. *I. Pathophysiology. J. Neurosurg.* **77,** 169-184.

Siesjö, B.K., Zhao, Q., Pahlmark, K., Siesjö, P., Katsura, K. & Folbergrova, J. (1992). Glutamate, calcium, and free radicals as mediators of ischemic brain damage. *Ann. Thorac. Surg.* **59,** 1316-1320.

Simon, R.P., Swan, S.H., Griffiths, T. & Meldrum, B.S. (1984). Blockade of NMDA receptors may protect against ischemic damage in the brain. *Science* **226,** 850-852.

Sinclair, C., Reavy, H., Grieve, A., Schousboe, A., Morelli, E., Novellino, E., Campiani, G. & Griffiths, R. (2003). Inherent desensitisation-preventing properties of a novel subtype-selective AMPA receptor agonist, (S)-CPW 399, as a possible explanation for its excitotoxic action in cultured cerebellar granule cells. *Neurochem. Int.* **42,** 499-510.

Sladeczek, F., Pin, J.P., Recasens, M., Bockaert, J. & Weiss, S. (1985). Glutamate stimulates inositol phosphate formation in striatal neurones. *Nature* **317,** 717-719.

Small, D.L., Morley, P. & Buchan, A. (1999). Biology of ischemic cerebral cell death. *Progress in Cardiovascular Diseases* **42** (3), 185-207.

Smeyne, R.J., Schilling, K., Robertson, L., Luk, D., Oberdick, J., Curran, T. & Morgan, J. I. (1992). Fos-lacZ transgenic mice: mapping sites of gene induction in the central nervous system. *Neuron* **8,** 13-23.

Smeyne, R.J., Vendrell, M., Hayward, M., Baker, S.J., Miao, G.G., Schilling, K., Robertson, L.M., Curran, T. & Morgan, J.I. (1993). Continuous *c-fos* expression precedes programmed cell death in vivo. *Nature* **363,** 166-169.

Soh, J., Lee, E.H., Prywes, R. & Weinstein, I.B. (1999). Novel roles of specific isoforms of protein kinase C in activation of the c-*fos* serum response element. *Molecular and Cellular Biology* **19** (2), 1313-1324.

Somnenberg, J.L., Mac Gregor-Leon, Curran, T. & Morgan, J.I. (1989a). Dynamic alterations occur in the levels and composition of transcription factor AP-1 complexes after seizzure. *Neuron* **3,** 359-365.

Somnenberg, J.L, Mitchelmore, C., Mac Gregor-Leon, P.F., Hempstead, J., Morgan, J.I. & Currran, T. (1989b). Glutamate receptor agonists increase the expression of Fos, Fra and AP--1 DNA binding activity in the mammalian brain. *J. Neurosci. Res.* **24,** 72-80.

Southern, E.M. (1975). Detection of specific sequences among DNA fragments separated by ggel electrophoresis. *J. Mol. Biol.* **98,** 503-517.

Speerk, G. (1994). Kainic acid seizures in the rat. *Prog. Neurobiol.* **42,** 1-32.

Struhl, (1988). The *jun* oncoprotein, a vertebrate transcription factor, activates tramscription in yeast. *Nature* **332,** 649-650.

Suzzdak, P.D., Sheardown, M.J. & Honore, T. (1993). Characterisation of the metabotropic gluttamate receptor in mouse cerebellar granule cells: lack of effect of 2,3-dihydroxy-6-nitro-7-sulphsmoylbenzo(F)-quinoxaline (NBQX). *Eur. J. Pharmacol. Molec. Pharmacol.* **245,** 215-220.

Suzzuki, T., Okuno, H., Yoshida, T., Endo, T., Nishina, H. & Iba, H. (1991). Difference in tramscriptional regulatory function between c-Fos and Fra-2. *Nucleic Acid Res.* **19,** 5537-55442.

Szeekely, A.M., Barbaccia, M.L., Alho, H. & Costa, E. (1989). In primary cultures of cerebellar granule cells the activation of N-methyl-D-aspartate-sensitive glutamate receeptors induces *c-fos* mRNA expression. *Mol. Pharmacol.* **35,** 401-408.

Tamayo, P., Slonim, D., Mesirov, J., Zhu, Q., Kitareewan, S., Dmitrovsky, E., Lander, E.S. & Golub, T.R. (1999). Interpreting patterns of gene expression with self-organising maps: Methods and application to haematopoietic differentiation. *Proc. Natl. Acad. Sci. USA* **96,** 2907-2912.

Tan, S., Sagara, Y., Liu, Y., Maher, P. & Schubert, D. (1998a). The regulation of peroxide production during programmed cell death. *J. Cell Biol.* **141,** 1423-1432.

Tatter, S.B., Galpern, W.R. & Isacson, O. (1995). Neurotrophic factor protection against excitotoxic neuronal death. *Neuroscientist* **1,** 286-297.

Tavazoie, S., Hughes, J.D., Campbell, M.J., Cho, R.J. & Church, G.M. (1999). Systemic determination of genetic network architecture. *Nature* **22,** 281-285.

Teskey, G.C., Atkinson, B.G. & Cain, D.P. (1991). Expression of the proto-oncogene *c-fos* following electrical kindling in the rat. *Mol. Brain Res.* **11,** 1-10.

Thompson, M.A., Ginty, D.D., Bonni, A. & Greenberg, M.E. (1995). L-type voltage-sensitive Ca^{2+} channel activation regulates *c-fos* transcription at multiple levels. *J. Biol. Chem.* **270** (9), 4224-4235.

Turner, R. & Tjian, R. (1989). Leucine repeats and an adjacent DNA binding domain mediate the formation of functional c-Fos-c-Jun heterodimers. *Science* **243** (4899), 1689-1694.

Vaccarino, F.M., Alho, H., Santi, M.R. & Guidotti, A. (1987). Coexistence of GABA receptors and GABA-modulin in primary cultures of rat cerebellar granule cells. *J. Neurosci.* **7** (1), 65-76.

Vaccarino, F.M., Hayward, M.D., Nestler, E.J., Dumann, R.S. & Tallman, J.F. (1992). Differential induction of immediate early genes by excitatory amino acid receptor types in primary cultures of cortical and striatal neurons. *Mol. Brain Res.* **12,** 233-241.

Van Gelder, R.N., von Zastrow, M.E., Yool, A., Dement, W.C., Barchas, J.D. & Eberwine, J.H. (1990). Amplified RNA synthesized from limited quantities of heterogeneous cDNA. *Proc. Natl. Acad. Sci. USA* **87,** 1663-1667.

Van Harreveld, A. (1959). Compounds in brain extracts causing spreading depression of cerebral cortical activity and contraction of crustacean muscle. *J. Neurochem.* **3,** 300-315.

Velculescu, V.E., Zhang, L., Vogelstein, B. & Kinzler, K.W. (1995). Serial analysis of gene expression. *Science* **270,** 484-487.

Vogt, P.K., Bos, T.J. & Doolittle, R.F. (1987). Homology between the DNA-binding domain of the GCN4 regulatory protein of yeast and the carboxyl terminal region of a protein coded for by the oncogene jun. *Proc. Natl. Acad. Sci. USA* **84,** 3316-3319.

Vogt, P.K. & Bos, T.J. (1990). *Jun*: oncogene and transcription factor. *Adv. Cancer Res.* **55,** 1-35.

Watanabe, Y., Johnson, R.S., Butler, L.S., Binder, D.K., Spiegelmann, B.M., Papaioannou, V.E. & Mc Namara, J.O. (1996). Null mutation of *c-fos* impairs structural and functional plasticities in the kindling model of epilepsy. *J. Neurosci.* **16,** 3827-3836.

Watson, A., Mazumder, A., Stewart, M. & Balasubramanian, S. (1998). Technology for microarray analysis of gene expression. *Curr. Opin. Biotechnol.* **9,** 609-614.

White, R.J. & Reynolds, I.J. (1996). Mitochondrial depolarization in glutamate-stimulated neurons: an early signal specific to excitotoxin exposure. *J. Neurosci.* **16,** 5688-5697.

Weis, J.H., Tan, S.S., Martin, B.K. & Wittwer, C.T. (1992). Detection of rare mRNAs via quantitative RT-PCR. *Trends Genet.* **8** (8), 263-264.

White, R.J. & Reynolds, I.J. (1997). Mitochondria accumulate Ca^{2+} following intense glutamate stimulation of cultured rat forebrain neurones. *J. Physiol.* **498** (1), 31-47.

Wieloch, T. (1985). Hypoglycemia-induced neuronal damage prevented by an N-methyl-D-aspartate antagonist. *Science* **230,** 681-683.

Wong, E.H., Kemp, J.A., Priestly, T., Knight, A.R., Woodruff, G.N. & Iversen, I. (1986). The anticonvulsant MK-801 is a potent N-methyl-D-aspartate antagonist. *Proc. Natl. Acad. Sci. USA* **83,** 7104-7108.

Yen, J., Wisdom, R.M., Tratner, I. & Verma, I.M. (1991). An alternate spliced form of FosB is a negative regulator of transcriptional activation and transformation by Fos proteins. *Proc. Natl. Acad. Sci. USA* **88,** 5077-5081.

Zamorano, P.L., Mahesh, V.B. & Brann, D.W. (1996). Quantitative RT-PCR for neuroendocrine studies. *Neuroendocrinology* **63,** 397-407.

Zerial, M., Toschi, L., Ryseck, R.P., Schuermann, M., Muller, R. & Bravo, R. (1989). The product of a novel growth factor activated gene, *fos-B*, interacts with JUN proteins enhancing their DNA binding activity. *EMBO J.* **8,** 805-813.